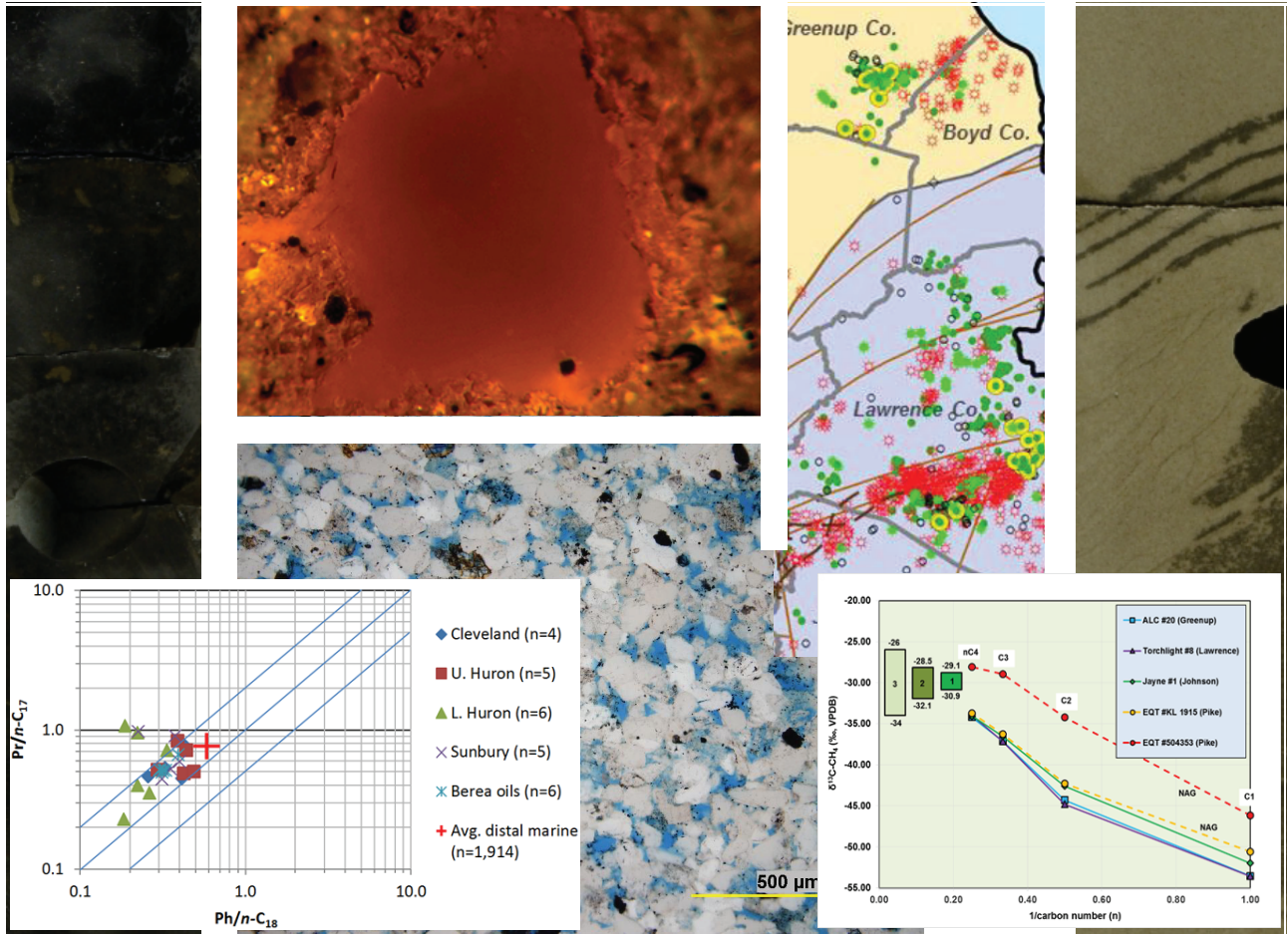


Berea Sandstone Petroleum System

T. Marty Parris, Stephen F. Greb, Cortland F. Eble, Paul C. Hackley,
and David C. Harris



Final Contract Report

Berea Consortium Project

Kentucky Geological Survey,
University of Kentucky

Primary Researchers and Chapter Authors

Cortland F. Eble, *Kentucky Geological Survey, University of Kentucky*

Stephen F. Greb, *Kentucky Geological Survey, University of Kentucky*

Paul C. Hackley, *U.S. Geological Survey, Reston, Virginia*

David C. Harris, *Kentucky Geological Survey, University of Kentucky*

T. Marty Parris, *Kentucky Geological Survey, University of Kentucky*

Other Researchers and Staff Who Assisted in Project

J. Richard Bowersox, *Kentucky Geological Survey, University of Kentucky*

Ethan Davis (student), *Kentucky Geological Survey, University of Kentucky*

Ronald A. Riley, *Ohio Geological Survey, Ohio Department of Natural Resources*

Jeffrey Deisher, *Ohio Geological Survey, Ohio Department of Natural Resources*

Brandon C. Nuttall, *Kentucky Geological Survey, University of Kentucky*

Ryan Pinkston, *Kentucky Geological Survey, University of Kentucky*

Kentucky Geological Survey
William C. Haneberg, State Geologist and Director
University of Kentucky, Lexington

Berea Sandstone Petroleum System

**T. Marty Parris, Stephen F. Greb, Cortland F. Eble, Paul C. Hackley, and
David C. Harris**

Our Mission

The Kentucky Geological Survey is a state-supported research center and public resource within the University of Kentucky. Our mission is to support sustainable prosperity of the commonwealth, the vitality of its flagship university, and the welfare of its people. We do this by conducting research and providing unbiased information about geologic resources, environmental issues, and natural hazards affecting Kentucky.

Earth Resources—Our Common Wealth

www.uky.edu/kgs

© 2019

University of Kentucky
For further information contact:
Technology Transfer Officer
Kentucky Geological Survey
228 Mining and Mineral Resources Building
University of Kentucky
Lexington, KY 40506-0107

Technical Level



Statement of Benefit to Kentucky

This report provides new insights into the geologic and geochemical factors that contributed to the emplacement of oil in the shallow Devonian Berea Sandstone in northeastern Kentucky. The results will assist companies exploring for oil and gas in thermally immature or early mature areas in Kentucky and similar basins elsewhere. These results would likely not have been possible without the collaboration among the Kentucky Geological Survey, U.S. Geological Survey, and industry partners.

Contents

Executive Summary: Berea Sandstone Petroleum System	1
Petroleum Systems	1
Reservoir Geology	2
Chapter 1. Introduction: Berea Petroleum System in Kentucky	4
Chapter 2. Geologic Framework.....	7
Stratigraphy	7
Structure and Tectonics.....	9
Thermal Maturity and Petroleum Systems	12
Chapter 3. Geochemistry Methods.....	16
Sample Material and Methods.....	16
Organic Petrography	16
Total Carbon and Sulfur	16
Programmed Pyrolysis.....	16
Bitumen Extracts and Oils: Column Chromatography, Gas Chromatography, Gas Chromatography–Mass Spectrometry, and Isotope Ratio–Mass Spectrometry	23
Natural Gas – Molecular and Isotopic Composition.....	31
Chapter 4. Geochemistry Results.....	34
Total Organic Carbon and Sulfur	34
Petrographic Composition	35
Thermal Maturity and Vitrinite/Solid-Bitumen Reflectance	36
Programmed Pyrolysis – Rock-Eval II and HAWK.....	37
Thermal-Maturity Discussion.....	37
Thermal-Maturity Summary	40
Oil and Bitumen-Extract Bulk Chemistry	41
Column Chromatography	41
Gas Chromatography (GC-FID)	41
Carbon-Isotopic Composition.....	42
Biomarker Characterization from Gas Chromatography–Mass Spectrometry (GC-MS).....	43
Oil and Bitumen-Extract Discussion	46
Oil Correlation.....	46
Sources of Organic Matter	46
Oil-Source Correlation	52
Thermal Maturity.....	53
Oil and Bitumen-Extract Summary	58
Natural-Gas Bulk and Isotopic Composition	59
Chapter 5: Discussion: Geochemistry Results and Implications for the Berea Petroleum System in Kentucky	68
Future Studies	72
Chapter 6: Reservoir Geology Methods.....	73
Thin-Section Petrography	73
Grain-Size Analysis	73
Pulse-Decay Permeability.....	73
XRD Analysis.....	73
Mercury Injection Capillary Pressure Analysis.....	73
Chapter 7: Reservoir Geology Results	75
Regional Reservoir Geology	75

Contents (Continued)

Structural Influences	75
Pay Zones in Producing Fields	77
Outcrop Analysis	78
Well and Core Analysis	80
Aristech Chemical Co. #4 Aristech Core.....	81
Ashland No. KY-4 Kelley-Watt-Bailey-Skaggs Core, Johnson County, Ky.	82
Gillespie #1 Bailey Core.....	82
Somerset Gas #1 Morlandbell Core, Leslie County, Ky.....	83
Columbia Gas #20456 Pocahontas Land (Mining) Core, Martin County, Ky.	84
Columbia Gas Trans. #20505 Margaret Simpson Well and Core, Lawrence County, Ky.....	84
Summary for Well	89
Ashland #1 Hattie Neal Well and Core, Lawrence County, Ky.	89
Summary for Well	90
KY-WV Gas #1087 Ruben Moore Well and Core, Lawrence County, Ky.	91
Summary for Well	92
KY-WV Gas #1122 Milton Moore Well and Core, Lawrence County, Ky.	92
Summary for the Two Moore Cores	94
Equitable Production Co. #504353 EQT Well and Core, Pike County, Ky.	94
Summary for the EQT Core.....	97
Porosity and Permeability Analysis.....	98
Comparisons to Bed Type	102
Comparisons to Possible Cements and XRD Results	103
Dolomite.....	106
Illite and Mica.....	107
Total Clays	107
Quartz (Quartz Grains Versus Quartz Overgrowth Cements)....	108
Siderite.....	108
Pyrite.....	108
Thin-Section Petrography.....	112
Berea Pore Types.....	112
Intergranular Porosity.....	112
Secondary Moldic Porosity	112
Microporosity.....	117
Pore-Type Distribution	117
Berea Diagenetic History	117
Quartz Overgrowths	117
Ferroan Dolomite.....	117
Pyrite.....	121
Siderite.....	121
Kaolinite	121
Mercury Injection Capillary Pressure Analysis.....	121

Contents (Continued)

Chapter 8: Reservoir Geology Discussion	132
References Cited.....	136
Appendix 1.....	linked files

Figures

1-1 Study area and geographic distribution of Berea oil and gas completions in eastern Kentucky	5
2-1 Upper Devonian and Lower Mississippian stratigraphic units in the central Appalachian Basin.....	7
2-2 A. Isopach of the combined Bedford-Berea interval in eastern Kentucky. B. Regional interpretation of depositional environments for the Bedford-Berea interval	8
2-3 Interpreted depositional systems and lateral stratigraphic relationships for elements of the Berea petroleum system	8
2-4 Major tectonic structures in eastern Kentucky. Blue shading represents area of the Rome Trough	10
2-5 Structure map on top of the Berea for part of eastern Kentucky	11
2-6 Updated isopach of the Bedford-Berea interval with superposed basement structures and areas where Berea sandstones and siltstones are thickest along a north-northwest to south-southeast elongate trend	12
2-7 Interpreted relationship between elements of the Berea petroleum system and clastic wedges of the Catskill delta	13
3-1 Location of core and cuttings samples.....	17
3-2 Locations of oil and gas samples	27
4-1 Distribution of TOC in the Ohio and Sunbury Shales.....	34
4-2 Maceral group distribution for the Skaggs-Kelly #3RS well.....	35
4-3 Vitrinite reflectance (VR_o) values.....	36
4-4 Rock-Eval thermal-maturity parameters, T_{max} ($^{\circ}C$).....	38
4-5 Rock-Eval HI indices	39
4-6 SARA results from liquid chromatography.....	42
4-7 Oil chromatograms from gas chromatography	43
4-8 Bitumen-extract chromatograms from gas chromatography of the “immature” Aristech samples	44
4-9 Pr/ n - C_{17} and Ph/ n - C_{18} discriminant plot	44
4-10 Sofer-type plot of $\delta^{13}C$ isotopic composition	45
4-11 Galimov-type plot of $\delta^{13}C$ isotopic composition	45
4-12 GC-MS m/z 191 and 217 fragmentograms for the Aristech #4 well.....	47
4-13 Normal sterane ($\alpha\beta\beta S$, m/z 218) distributions	48
4-14 Individual versus sterane concentrations in oil samples	49
4-15 Extended homohopane relative abundances in oils and bitumen extracts.....	50
4-16 Gammacerane index values for oils and extracts.....	51
4-17 Tricyclic terpane and hopane ratios	52
4-18 Sterane isomerization plot [C_{29} $\alpha\alpha$ 20S/(20S + 20R) versus C_{29} $\beta\beta S$ /($\beta\beta S$ + $\alpha\alpha R$)]	54
4-19 Diasterane/ $\alpha\alpha$ sterane ratios versus C_{27} trisnorhopane epimer ratios (Ts/Ts + Tm)	55
4-20 S content of bitumen extracts versus R_o values	56
4-21 Methylphenanthrene index (MPI) versus R_o values.....	57

Figures (Continued)

4-22	R _o equivalent values from MPI versus saturate/aromatic ratios.....	57
4-23	Gas wetness (C ₁ /C ₂ + C ₃) versus δ ¹³ C-CH ₄	60
4-24	Gas wetness (C ₁ /C ₂ + C ₃) versus δ ¹³ C-CH ₄ for gases in this study.....	61
4-25	δ ¹³ C versus δD for CH ₄	62
4-26	Gas wetness (C ₁ /C ₂ + C ₃) versus subsea depth.....	63
4-27	δ ¹³ C for CH ₄ versus measured depth.....	64
4-28	Natural gas plot showing the δ ¹³ C values C ₁ -nC ₄ gas components.....	65
4-29	Concentration and isotopic composition of N ₂	66
4-30	Concentration of He and N ₂	67
5-1	Source-rock maturation from kerogen and bitumen and the evolution of hydrocarbons.....	71
7-1	Map of producing Berea oil and gas wells showing principal tectonic structures discussed in text	76
7-2	Thickness trends across known major structures	77
7-3	Sample geophysical wells from the fields listed in Table 7-1 showing porosity zones and completed or perforated intervals	79
7-4	A. Roadcut exposure of the Berea near Garrison, Ky., showing sheet-sandstone lithofacies. B. Section through bed with irregular base (sometimes with loads), massive to parallel-laminated or parallel texture, and sometimes capped by combined-flow ripples. C. Hummocky stratification. D. Parallel-laminated bed (upper part) above low-angle, possibly hummocky bedding. E. Large flow rolls and bedding offset along shear planes associated with soft-sediment deformation.....	81
7-5	Map of cores analyzed for this project.....	82
7-6	Comparison of core intervals (and geophysical logs for cores examined in this study	83
7-7	Summary of the Columbia Pocahontas well and core	85
7-8	Cross section of wells in the vicinity of the Columbia Pocahontas Mining core.....	86
7-9	Comparison of core bedding, plug-derived porosity, and permeability with geophysical log for the Columbia Gas Transmission No. 20505 Margaret Simpson well.....	87
7-10	Correlation of logs north and south of the Columbia Gas Transmission No. 20505 Margaret Simpson well.....	88
7-11	Comparison of core bedding, plug-derived porosity, and permeability with geophysical log for the Hattie Neal well	90
7-12	Correlation of logs north and south of the Hattie Neal well.....	91
7-13	Comparison of core bedding, plug-derived porosity, and permeability with geophysical log for the Ruben Moore well	93
7-14	Correlation of logs north and south of the Ruben Moore core	94
7-15	Comparison of core bedding, plug-derived porosity, and permeability with geophysical log for the Ruben Moore well	95
7-16	Correlation of logs north and south of the Ruben Moore well	97
7-17	Comparison of core bedding, bitumen-stained intervals, with geophysical log for the EQT No. 504353 well	99
7-18	Examples of staining boundaries in soft-sediment-deformed beds in the EQT core	100
7-19	Examples of staining boundaries across bedding and scour contacts in the EQT core...101	101
7-20	Examples of bitumen staining at 3,844.5 ft, showing influences of bedding, scour or bedding contacts, and fractures on bitumen migration in the Berea.....	102

Figures (Continued)

7-21	Locations of wells with Berea porosity and permeability data used in this study	103
7-22	Historic Berea porosity and permeability data.....	104
7-23	Historic porosity versus permeability data on a logarithmic scale with all below-detection-limit data deleted	104
7-24	New porosity and permeability data collected by Chesapeake Energy from four of the Kentucky cores.....	105
7-25	Combined adjusted historic and Chesapeake datasets, and comparison of trend lines for the sum and individual datasets	105
7-26	Porosity and permeability compared to bedding in cores.....	106
7-27	Porosity and permeability compared to bedding in cores.....	107
7-28	Typical porous lithic arenite. Milton Moore #1122 well, 1,269 ft, Lawrence County	108
7-29	Porosity and permeability compared to dolomite content in cores	109
7-30	Porosity and permeability compared to dolomite content in cores, excluding all "0" values.....	109
7-31	Porosity and permeability compared to illite and mica content in cores	110
7-32	Porosity and permeability compared to illite and mica content in cores	110
7-33	Porosity and permeability compared to total clay content in cores	111
7-34	Porosity and permeability compared to total clay content in cores	111
7-35	Berea Sandstone dominated by intergranular porosity	113
7-36	Intergranular porosity filled with bitumen.....	114
7-37	Berea sandstone with well-developed secondary (moldic) porosity	115
7-38	Secondary porosity types in Berea sandstones.....	116
7-39	Microporosity in Berea sandstones	118
7-40	Quartz overgrowth cements in Berea sandstone	119
7-41	Ferroan dolomite occurrence in Berea siltstones/sandstones.....	120
7-42	Pyrite fabrics in Berea siltstones/sandstones	122
7-43	Siderite cement and replacement fabrics.....	123
7-44	Kaolinite (clay) occurrence in Berea siltstones/sandstones	124
7-45	Mercury injection capillary pressure plot and photomicrographs for sample MS1672, Columbia Nat. Resc. #20505 Margaret Simpson core, Lawrence County, Ky., 1,672 ft ..	125
7-46	Mercury injection capillary pressure plot and photomicrographs for sample HN1505, Ashland No. 1 Hattie Neal core, Lawrence County, Ky., 1,505 ft.....	126
7-47	Mercury injection capillary pressure plot and photomicrographs for sample MM1286, KY-WV Gas No. 1122 Milton Moore core, Lawrence County, Ky., 1,286 ft.....	127
7-48	Mercury injection capillary pressure plot and photomicrographs for sample MS1663, Columbia Nat. Resc. No. 20505 Margaret Simpson core, Lawrence County, Ky., 1,663 ft.....	128
7-49	Mercury injection capillary pressure plot and photomicrographs for sample HN1516, Ashland No. 1 Hattie Neal core, Lawrence County, Ky., 1,516 ft.....	129
7-50	Mercury injection capillary pressure plot and photomicrographs for sample MS1683.4, Columbia Nat. Resc. No. 20505 Margaret Simpson core, Lawrence County, Ky., 1,683.4 ft.....	130
8-1	Summary of scales of heterogeneity in Berea "tight sandstone" reservoirs	133

Tables

3-1	Sample locations, stratigraphic intervals, and sample type	18
3-2	Summary of carbon, sulfur, and reflectance analyses	19
3-3	Distribution of carbon and sulfur in the Sunbury Shale and members of the Ohio Shale	21
3-4	Summary of programmed-pyrolysis and petrographic thermal-maturity parameters	22
3-5a	Programmed-pyrolysis measurements on raw samples (analyzed by Rock-Eval II) versus solvent-extracted (shaded) samples (analyzed by HAWK)	24
3-5b	Programmed-pyrolysis measurements on raw samples (analyzed by Rock-Eval II) versus solvent-extracted (shaded) samples (analyzed by HAWK)	25
3-6	Bulk chemistry of oil and extract samples	28
3-7	Oil and extract properties from gas chromatography (GC-FID)	29
3-8	Sterane and hopane biomarker ratios for oil and extract samples	30
3-9	Extended homohopane relative abundances, hopane and tricyclic terpane ratios	31
3-10	Carbon isotopic composition of oils and bitumen extracts	32
3-11	Molecular composition of associated (OAG) and nonassociated (NAG) gases from the Berea Sandstone and Ohio Shale	32
3-12	Stable isotopic composition of associated (OAG) and nonassociated (NAG) gases from the Berea Sandstone and Ohio Shale	33
7-1	Selected features of representative Berea oil and gas fields from the KGS Oil and Gas Database	78
7-2	Berea outcrop lithofacies	80
7-3	Summary of XRD data from the Ashland No. 20505 Margaret Simpson well	89
7-4	Summary of XRD data from the Ashland No. 1 Hattie Neal well	92
7-5	Summary of XRD data from the KY-WV Ruben Moore well	96
7-6	Summary of XRD data from the KY-WV Ruben Moore well	98
7-7	Bedding types analyzed in Figures 7-26 and 7-27	106
7-8	List of wells with Berea Sandstone thin sections available for this study	112

Berea Sandstone Petroleum System

**T. Marty Parris, Stephen F. Greb,
Cortland F. Eble, Paul C. Hackley, and
David C. Harris**

Executive Summary

Since 2011, production of sweet high-gravity oil from the Upper Devonian Berea Sandstone in northeastern Kentucky has caused the region to become the leading oil producer in the state. Remarkably, Berea oil is being produced at depths of 2,200 ft or less and in an area in which the prospective source rocks—the overlying Mississippian Sunbury Shale and underlying Devonian shale—are interpreted to be immature for oil production. Farther downdip, the Berea appears to produce primarily gas in the oil window. The economic viability of Berea production is also a function of reservoir porosity and permeability. The main observations and interpretations developed from our research on petroleum systems and reservoir quality in the Berea Sandstone petroleum system are as follows:

Petroleum Systems

1. Total organic carbon measurements from Scioto County, Ohio, to Pike County, Ky., show viable source rocks in the Mississippian Sunbury Shale and Devonian Ohio Shale members (Cleveland; Upper, Middle, and Lower Huron). Petrography shows that organic matter consists primarily of oil-prone kerogen with a marine signature.
2. Proxies from gas chromatography (GC) and carbon isotope measurements on bitumen extracts and oil samples across the study area also show a marine organic signature.
3. Similar GC and key biomarker parameters and carbon isotopic composition between bitumen extracts and oils suggest that any or all of the analyzed source rocks are potential sources for Berea oil.
4. Associated gases from oil wells and a non-associated gas in northern Pike County show progressive enrichment in ^{13}C with increasing molecular weight for methane, ethane, propane, and normal-butane. Moreover, on a natural-gas plot, the samples are closely grouped, suggesting they formed from a similar source under similar thermal-maturity conditions. The $\delta^{13}\text{C}$ composition of the source (kerogen, bitumen, and/or oil) would appear to be isotopically lighter than the value suggested by a best-fit line through the higher-molecular-weight gases on the natural-gas plot.
5. Overall compositional similarities for oil and gas samples therefore suggest that Berea oils and associated wet gases, from Greenup County in the north to northern Pike County in the south, formed from a source rock with properties similar to the Sunbury and Ohio intervals and under similar thermal-maturity conditions.
6. In contrast, nonassociated gas in the EQT #540353 well in southern Pike County formed from a source enriched in ^{13}C relative to bitumen extracts in the same well. Such a source could come from a deeper, more mature part of the basin through primary (bitumen) or secondary (oil) cracking.
7. Reflectance and programmed-pyrolysis measurements show increased thermal

maturity northwest to southeast. Thermal maturities are at or below $R_o=0.50$ to 0.62 percent, the lower boundary of the oil window in Scioto, Greenup, Carter, and Lawrence Counties, and in the oil-wet gas window ($R_o=0.66$ to 1.24 percent) in Johnson, Martin, and Pike Counties. The rate at which thermal maturity increases is not uniform, and is more rapid in Pike County, possibly reflecting the influence of thrust-loading from the Pine Mountain Thrust Fault.

8. Reflectance measurements on solid bitumen were up to 0.3 percent less than those on vitrinite in the same sample, demonstrating that inclusion of solid bitumen could cause the aggregate reflectance value to be suppressed relative to the "true" reflectance value for a sample.
9. The aromatic biomarker, methylphenanthrene index, suggests that oils formed at R_o -equivalent values of 0.7 to 0.9 percent. Formation over this range of R_o equivalents is supported by enrichment in saturate and aromatic fractions relative to resins and asphaltenes in the oils. Berea oils have significantly lower sulfur concentration compared to the bitumen extracts, which may draw from organic matter affected by sulfurization. The difference in sulfur concentration suggests that Berea oils were generated as later-stage products in the mid- to late-oil window.
10. For the current thermal configuration of the study area, generation of Berea oils at R_o equivalents of 0.7 percent suggests lateral and updip migration of 5 to 20 mi into Lawrence County and 45 to 50 mi into Greenup County.
11. Rock-based thermal-maturity predictors (e.g., reflectance measurements, programmed pyrolysis) fail to predict the presence of high-gravity, low-sulfur oil in the Berea. A more complete and accurate analysis of the Berea petroleum system, including migration, is provided by the bulk composition and biomarker analysis of the oils.

12. Analysis of Berea production and gas composition in Martin and Pike Counties shows that rock-based thermal-maturity predictors are more closely aligned with production characteristics than previously thought; that is, the downdip area is characterized as an oil-wet gas zone. The paucity of oil production downdip may result from production fractionation in which lighter oils are produced preferentially over heavier oils.

Reservoir Geology

1. Berea reservoirs consist of one or more pay zones, 12 to 30 ft thick, composed of thinner porous zones (10 to 14 percent), each 1 to 6 ft thick.
2. Relative to horizontal drilling, bed dips on broad clinoforms, from small structural folds, from small faults and glide planes, and from a variety of soft-sediment features may influence lateral continuity of any pay zone.
3. Lateral transitions within beds from massive or bedded siltstone into soft-sediment-deformed beds are common and could be mistaken on horizontal gamma-ray logs for passing out of zone into a capping or underlying horizontal shale.
4. Petrographically, Berea reservoirs are lithic-rich quartz siltstone to fine-grained sandstone.
5. Berea reservoirs have a complex diagenetic history that includes quartz, ferroan dolomite, siderite, pyrite, and kaolinite cements.
6. Framework grain dissolution and moldic porosity are common in samples from Lawrence and Johnson Counties, but not from Pike County.
7. Though intergranular porosity is preserved, secondary porosity may be an important contributor to total porosity for the Berea reservoir in Lawrence and Johnson Counties.
8. Microporosity is common, and together with the small grain size, accounts for low permeability in the Berea. Microporosity

results from clay cements and matrix, and partially dissolved framework grains.

9. Core analysis shows a modest correlation between permeability and porosity ($R^2=0.75$). The correlation is better for low-permeability ($R^2=0.81$) than for high-permeability samples ($R^2=0.57$). For permeabilities greater than 0.1 md, porosities are generally greater than 10 percent. All values above 12 percent have permeability greater than 0.1 md.
10. Mercury injection capillary pressures show that high-porosity (greater than 11 percent) and high-permeability (greater than 1 md) samples have pore-throat diameters from 1 to 2 μ , which is characteristic of oil reservoirs. Meanwhile, lower-porosity (7 to 9.4 percent) and lower-permeability (0.02 to 0.2 md) samples have pore-throat diameters from 0.1 to 0.6 μ .

1. Introduction

T. Marty Parris, Stephen F. Greb, Cortland F. Eble, Paul C. Hackley, and David C. Harris

The Upper Devonian Berea Sandstone has been a major producer of natural gas and smaller amounts of oil in eastern Kentucky, starting with an 1879 discovery near Paintsville in Johnson County (B. Nuttall, Kentucky Geological Survey, personal communication, 2016). This was followed by discoveries at Beech Farm (1915) and Cordell (1917) Fields in Lawrence County (Tomastik, 1996). Production was later extended south into Pike County with development of the Canada (1942) and Nigh (1945) Fields. Infill drilling characterized the Berea play from the 1970s through the 1990s, but the play also included discoveries at Jobe Branch (1977) and Big Laurel Schools (1988) in Lawrence County, and Road Fork (1990) in Pike County. As a low-permeability reservoir, the Berea Sandstone was designated a tight formation in the early 1980s under the Federal Energy Regulatory Commission's Order 99 (Avila, 1983a, b). The tight-formation designation not only increased drilling in the Berea, but also in the underlying Ohio Shale. Conventional vertical drilling in the Berea, primarily for natural gas, remained steady through the 1980s and 1990s. During the late 2000s, horizontal drilling technology and multistage nitrogen-foam fracture stimulation was used to improve Berea gas production. During this time, at least 75 horizontal wells were completed in the Berea as gas completions in Pike County.

The historic trend of predominantly gas production in the Berea changed in 2011 and 2012 when Nyttis Exploration successfully drilled and completed horizontal oil wells in Greenup and Lawrence Counties. Those wells started a renaissance in the Berea play. Subsequently, numerous operators have used similar horizontal-well completion practices to establish Berea oil production in new areas and in infill areas that were primarily gas productive (Fig. 1-1). Low natural-gas prices accelerated the exploration focus to shallower parts of the Berea play in northeastern Kentucky, where the reservoir typically produces more oil. Since 2011, Berea oil production from horizontal wells has now been established in Greenup (n=approximately 39), Carter (n=1), Lawrence (n=approximately 71), Johnson (n=approximately 10), and Martin (n=1) Counties. In addition, liquid-

rich gases are being produced farther south in Martin and Pike Counties. Oil production in the Berea has been significant enough that counties in eastern Kentucky accounted for 58 percent of Kentucky's oil production in 2015 (Nuttall, 2016). At the time this project started, the price advantage of oil versus natural gas, along with shallow drilling depths (less than 2,100ft vertical depth) and good production rates (hundreds to thousands of barrels/month) provided strong incentives for development of the Berea in updip parts of the play.

Though currently slowed by low oil and gas prices, the resurgence in Berea drilling prompted researchers at the Kentucky Geologic Survey (KGS) to look more closely at the Berea petroleum system. The petroleum system concept includes elements that result in accumulations of oil and gas in the subsurface. The elements include the source rock and its maturity, migration pathways out of the source rock and into a reservoir, mechanisms for trapping oil and gas in a reservoir (structural and/or stratigraphic), and seals that impede migration out of the reservoir (Magoon, 1988). This examination of the Berea petroleum system has proposed and investigated a number of important scientific questions related to hydrocarbon source and migration, reservoir architecture, and the distribution of reservoir porosity and permeability.

One of the foremost questions addressed in this study is the source of hydrocarbons in the Berea. The long-held view is that the underlying Ohio Shale has sourced hydrocarbons for many petroleum systems in the Appalachian Basin (East and others, 2012, and references therein). Geochemical analysis in Ohio by Cole and others (1987) suggests, however, that oil in the Berea was sourced from the overlying Mississippian Sunbury Shale. Thus, both the Ohio and Sunbury Shales are possible sources of Berea hydrocarbons.

Closely related to the question of hydrocarbon source is the apparent mismatch between thermal-maturity levels, as determined from vitrinite-reflectance measurements, and the hydrocarbon phase produced in the Berea. Specifically, vitrinite- and bitumen-reflectance data show the Ohio Shale to be thermally immature (R_o less than 0.6 percent)

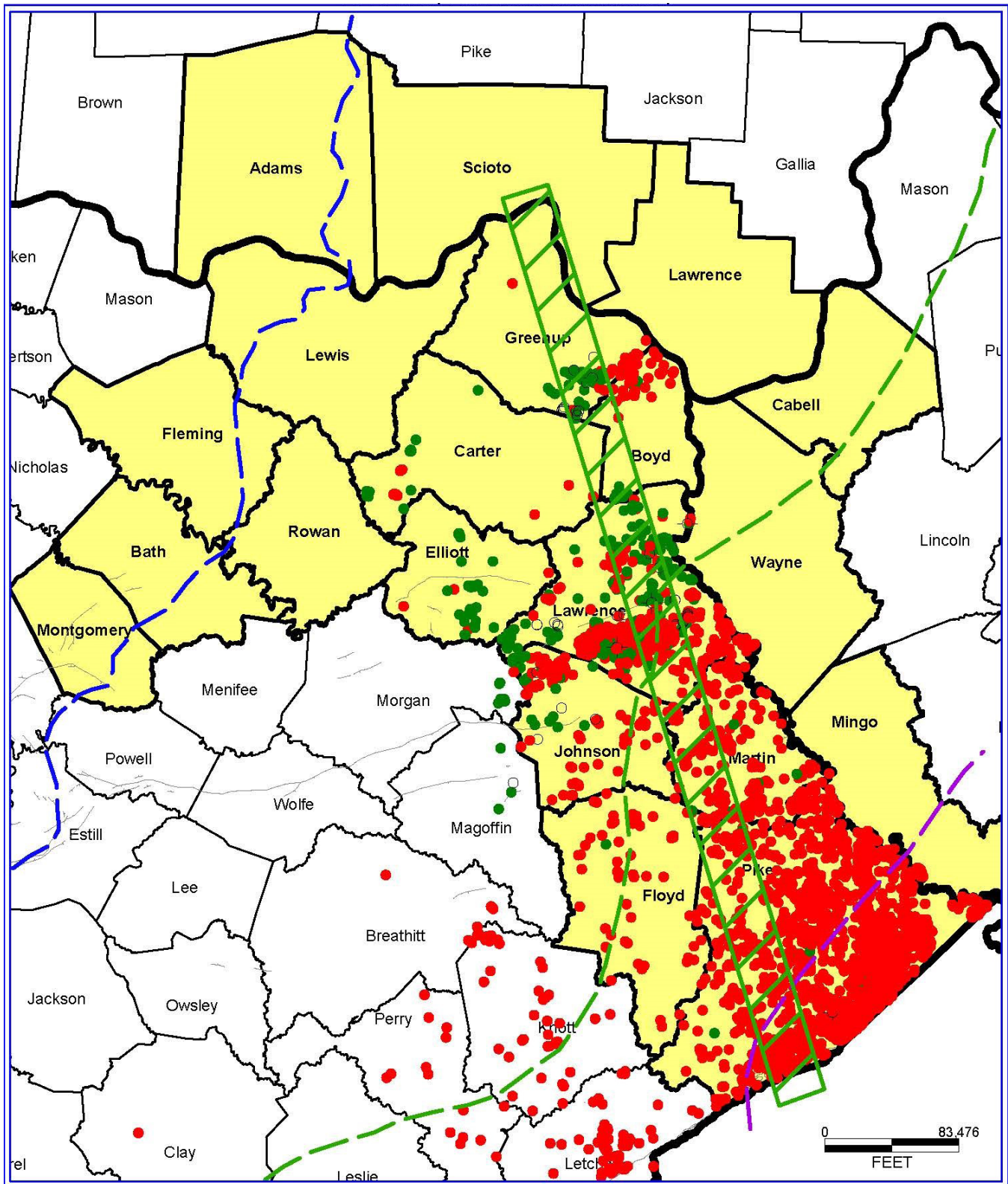


Figure 1-1. Study area and geographic distribution of Berea oil and gas completions in eastern Kentucky (2,778 wells; green for oil, red for gas). Green dashed line is the vitrinite reflectance isoline where $R_o = 0.6$ percent (approximate lower oil window boundary) and purple dashed line is $R_o = 1.3$ percent (approximate upper oil window boundary). From East and others (2012). Green hatched box is approximate location of thermal maturity sampling transect.

in areas of Berea oil and gas production and mature for oil ($R_o=0.6$ to 1.3 percent) in many areas of Berea gas production (Fig. 1-1). The mismatch could indicate that thermal-maturity indicators, such as vitrinite reflectance, do not accurately reflect the thermal-maturity history of the rocks, especially in early to mature settings. Alternatively, if the vitrinite-reflectance measurements are correct, this would suggest that hydrocarbons were either locally sourced at lower thermal-maturity levels or migrated into the shallower Berea from deeper, more thermally mature areas. The former scenario implies that hydrocarbons were generated under temperatures insufficient to generate vitrinite-reflectance values equal to or greater than 0.6 percent. Meanwhile, Cole and others (1987) argued that the presence of mature oils in many of Ohio's reservoirs implies the migration of hydrocarbons from deeper, more mature parts of the basin.

Migration of oil and gas from long distances into the Berea could be problematic, given the low-porosity and -permeability siltstone and very fine-grained sandstone that make up the reservoir. Reservoir properties not only affect migration, but defining the distribution of better reservoirs and the lithofacies in which they occur is important for optimizing drilling and completion practices.

The questions and issues broached above provide the framework for some of the specific questions proposed at the beginning of the project. To reiterate, these are:

1. Why does the Berea produce oil and gas in areas where the adjacent shales are thought to be thermally immature?
2. Is oil produced from the Berea in north-eastern Kentucky sourced from shales in the immediate area or has it migrated from deeper in the Appalachian Basin?
3. How are pay zones, porosity, and permeability distributed within the Berea?

In this report, insights into thermal maturity, hydrocarbon source, and reservoir quality are provided by integrating existing data with new measurements and observations that include:

1. Total organic content (TOC), vitrinite reflectance, and programmed pyrolysis measurements of the Ohio and Sunbury Shales.
2. Bulk chemistry and biomarker profiles of bitumen extracts from the Ohio and Sunbury Shales and of Berea oils, with a focus on evaluating the source and maturity levels in the Berea.
3. Bulk and isotopic chemistry of associated and nonassociated gases produced from the Berea and Ohio Shale, with a focus on gas source and thermal maturity.
4. An analysis of Berea structure and detailed stratigraphy using data from Berea cores and outcrops, with the goal of better understanding the reservoir architecture and distribution of porosity and permeability in the producing area.

2. Geologic Framework

Stephen F. Greb, Cortland F. Eble, T. Marty Parris, and David C. Harris

Stratigraphy

The Berea Sandstone is the uppermost Devonian unit in eastern Kentucky (Fig. 2-1). Both the Bedford Shale and Berea Sandstone were once considered part of the lowest Mississippian, but fossil plant spores from the Bedford subsequently indicated a Late Devonian age (Molyneux and others, 1984; Coleman and Clayton, 1987). Although termed "Sandstone," the Berea in eastern Kentucky is actually a siltstone across much of its extent. Berea sandstones and siltstones complexly intertongue with and grade laterally into the Bedford shales (Pepper and others, 1954; Pashin and Etensohn, 1987, 1992, 1995). Consequently, they were mapped together at the surface on many 7.5-minute geologic quadrangle maps (e.g., Morris and Pierce, 1967; McDowell, 1986).

The Berea is thickest in an elongate, northwest-southeast-oriented belt, and pinches out laterally to the west, where the combined Bedford-Berea interval is less than 30 to 40 ft thick (Fig. 2-2A). This elongate belt is interpreted as the outer part of a regional shelf deposited between coastal areas in

West Virginia and deeper basinal areas in the western part of eastern Kentucky (Fig. 2-2B) (Pashin and Etensohn, 1987, 1995). Figure 2-3 is an interpretive diagram of Bedford-Berea deposition from Pashin and Etensohn (1987), which serves to show the general stratigraphic relationships of much of the Berea petroleum system.

Members of the Ohio Shale can be divided into black, organic-rich (Lower Huron, Upper Huron, and Cleveland) and still black, but less organic-rich (Middle Huron, Three Lick Bed) shales. These black shales have traditionally been inferred to represent slow deposition in deep anoxic waters distal to Catskill clastics on the eastern margin of the continent (Rhoads and Morse, 1971; Potter and others, 1980; Etensohn and Barron, 1981; Etensohn and Elam, 1985; Etensohn and others, 1988; de Witt and others, 1993; Kepferle, 1993). Recent work has inferred that the deposition of the Devonian shales was not all under pervasive deep-water anoxic conditions. Parts of the shales are gray, rather than black, silty, and less organic-rich. These interbeds likely represent dysaerobic condi-

System	Series	Int. Stage	Central Kentucky (Cincinnati Arch)	Eastern Kentucky (Appalachian Basin)	Southeastern Ohio (Appalachian Basin)	Central West Virginia (Appalachian Basin)	
Mississippian	Lower	Tournaisian	Borden Fm (lower part)	Logana Fm	<i>undifferentiated</i>	Pocono Gp	
							Sunbury Sh Bedford Sh Berea Ss
Devonian	Upper	Famennian	Chattanooga Sh or New Albany Sh <i>in different areas</i>	Cleveland Sh Mbr <i>Three Lick Bed</i>	Cleveland Sh Mbr	Chemung Fm	
		Ohio Sh		Huron Sh Mbr	Huron Sh Mbr		Chagrín Sh
				upper middle lower	Huron Sh Mbr		
Frasnian	Upper Olenitangy Sh	Upper Olenitangy Sh	Hanover-Angola Sh				
	Rhinestreet Sh	Rhinestreet Sh	Rhinestreet Sh				

Figure 2-1. Upper Devonian and Lower Mississippian stratigraphic units in the central Appalachian Basin. The succession includes units comprising the Berea petroleum system.

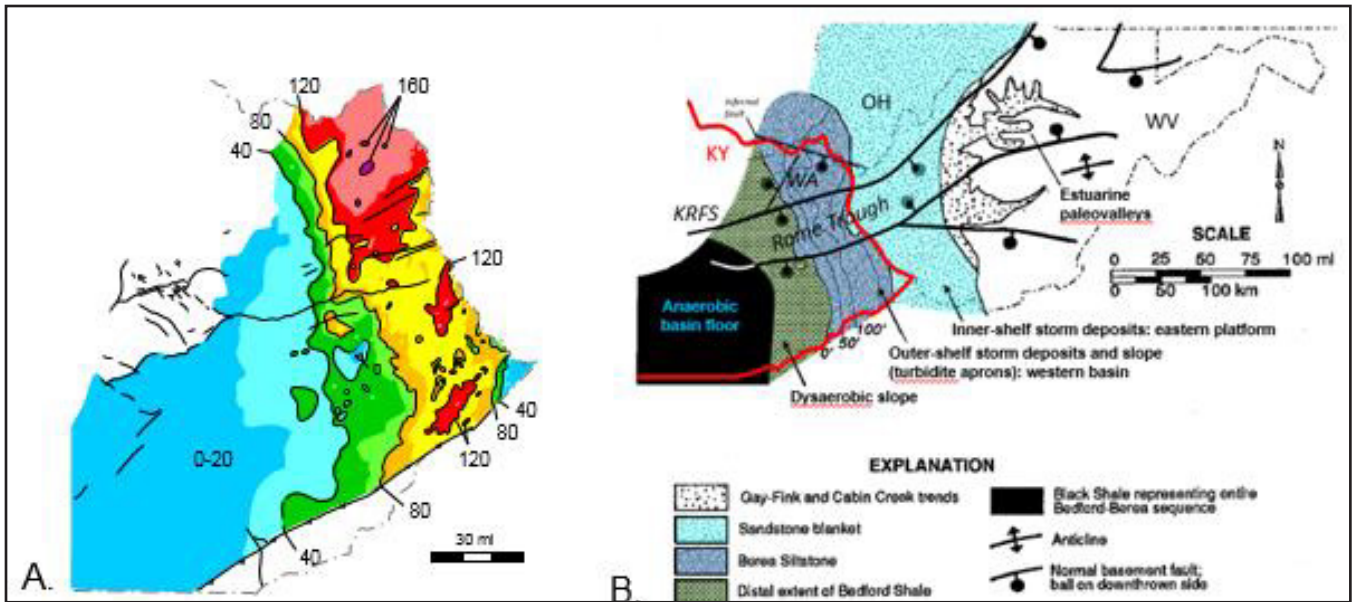


Figure 2-2. A. Isopach (ft) of the combined Bedford-Berea interval in eastern Kentucky. After Elam (1981); used with permission. B. Regional interpretation of depositional environments for the Bedford-Berea interval. After Pashin and Ettensohn (1995); used with permission of Geological Society of America..

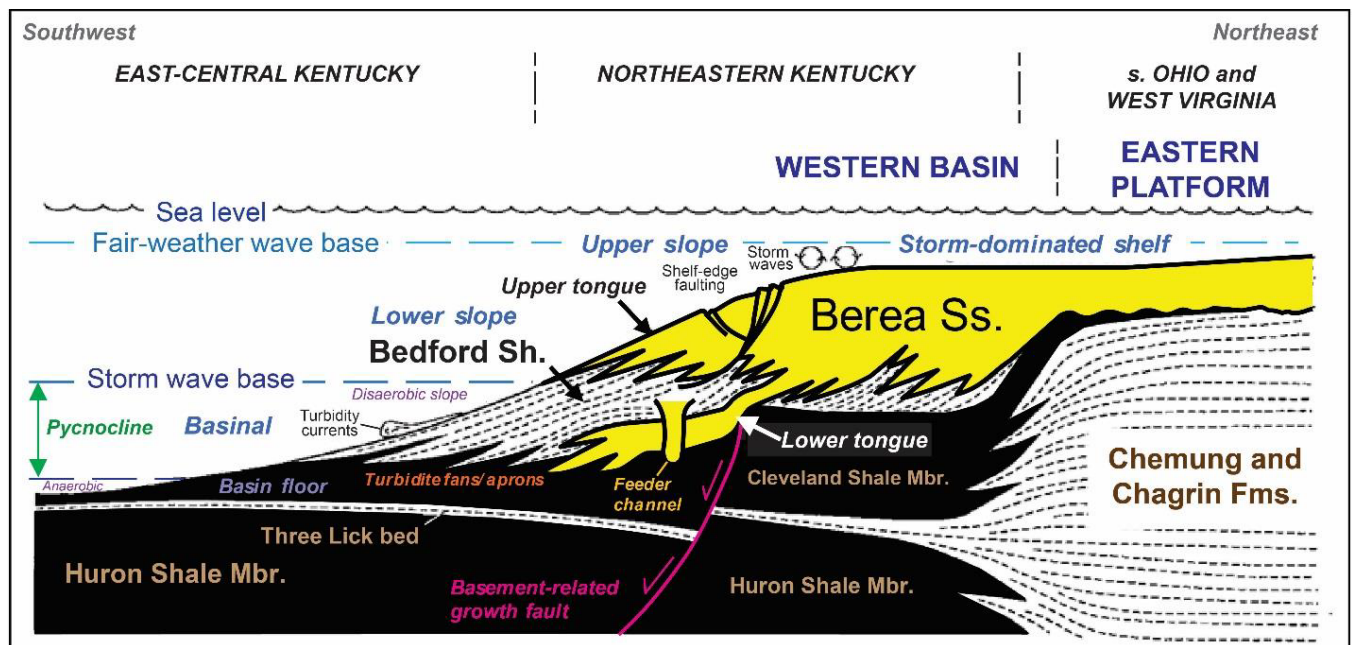


Figure 2-3. Interpreted depositional systems and lateral stratigraphic relationships for elements of the Berea petroleum system. After Pashin and Ettensohn (1995, Fig. 49), with permission of the Geological Society of America. The Sunbury Shale would cap the units shown.

tions. Studies of trace elements, carbon, oxygen, and sulfur isotopes have suggested variable oxygen conditions during deposition, from anoxic to dysaerobic to oxic (Sageman and others, 2003; Rimmer, 2004; Perkins and others, 2008). Also, the inference of deep-water environments because of anoxia has been challenged in recent years. In at least

some areas, sedimentological evidence of storm deposits and distal turbidites in the black shale, as well as sea-level change and sequence boundaries, have been used to infer shallower water depths (at least at times within or near storm wave base), as well as bottom agitation that would disrupt stratified water columns (Schieber, 1994, 1998; Schieber and Ricuputi, 2004; Alsharani and Evans, 2014).

Each of the organic-rich members of the Ohio Shale pinches out or grades laterally into progressively less organic-rich black and gray silty shales of the Chemung and Chagrin formations to the east. The Middle Huron and Three Lick Bed, which are tongues of the Chemung and Chagrin formations, were deposited in the distal parts of the Catskill deltaic clastic wedge (Wallace and others, 1977; Provo and others, 1978; Kepferle and others, 1978; Roen and others, 1978; Roen and de Witt, 1984; Kepferle, 1993). Similarly, the Bedford-Berea interval represents another part of the Catskill clastic wedge.

In eastern Kentucky, Bedford gray and green-gray shales intertongue with and grade southward and westward into black Bedford shales and then into black, organic-rich shales of the Cleveland Shale Member of the Ohio Shale (Fig. 2-3) (Ettensohn and Elam, 1985). The Bedford is interpreted to represent distal deltaic or lower-slope deposits seaward of the Berea marine shelf (Potter and others, 1983; Pashin and Ettensohn, 1987, 1992, 1995; Coates, 1988). The Bedford consists primarily of shale and siltstone interpreted to represent turbidite and distal turbidite fan deposits. The color change from black shale to gray-green shale between the Bedford and Cleveland shales and within the distal parts of the Bedford itself are interpreted as representing the position of a paleo-pycnocline between relatively deeper, downdip anoxic water and shallower, updip, dysaerobic waters (Ettensohn and Elam, 1985; Pashin and Ettensohn, 1987, 1992). Where Bedford gray shales can no longer be detected westward on the Cincinnati Arch in central and south-central Kentucky, the underlying Ohio Shale and overlying Sunbury Shale cannot be differentiated and are mapped as the Upper Devonian–Lower Mississippian New Albany Shale of the Illinois Basin.

The Berea is dominated by sheet-form sandstones and siltstones with hummocky, swaley, and massive bedding in outcrops, suggestive of storm-influenced, shallow-marine shelf environments (Pepper and others, 1954; Potter and others, 1983; Pashin and Ettensohn, 1987, 1992, 1995; Coats, 1988). In parts of the Lewis County outcrop belt, the Berea can be divided into two tongues separated by and underlain by Bedford shales (Morris and Pierce, 1967; McDowell, 1986). Southward,

upper and lower tongues of the Berea have also been recognized in some Berea oil fields in Lawrence and Johnson Counties. Pashin and Ettensohn (1987) showed this as a response to growth faulting (Fig. 2-3), although eustatic and sedimentation changes may also have influenced the stratigraphy.

The Bedford-Berea interval is sharply overlain by the Mississippian Sunbury Shale (Fig. 2-1). The contact between the Sunbury and Bedford-Berea has traditionally been interpreted as conformable, but Ettensohn (1994, 2004) considered it to be unconformable. The youngest black shale in the central Appalachian Basin, the Sunbury is inferred to have formed under depositional conditions similar to that of the underlying organic-rich members of the Ohio Shale (Elam, 1981; Van Beuren and Pryor, 1981; Ettensohn, 1985; Kepferle, 1993). Unlike the Ohio Shale, however, whose members all thicken eastward into the basin before pinching out into the Chagrin/Chemung clastic wedge, the Sunbury Shale exhibits a relatively tabular thickness distribution across eastern Kentucky (Dillman and Ettensohn, 1980; Floyd, 2015).

Structure and Tectonics

Eastern Kentucky is part of the central Appalachian Basin, and regional structures are interpreted to have influenced much of the Paleozoic section. Figure 2-4 is a map of eastern Kentucky showing the locations of major structural features. Most of the faults shown are rooted in Precambrian basement. Major fault systems are related to the Rome Trough, a Cambrian graben, which was reactivated throughout the Paleozoic (e.g., Dever, 1999; Harris and others, 2004). Relative to this study, some additional structures of potential import include the Paint Creek Uplift and Waverly Arch. The Paint Creek Uplift is a structural high above a gravity high and is likely rooted in basement structures (Ammerman and Keller, 1979). The Waverly Arch is a somewhat enigmatic structural high first delineated by a trend of thinning in the upper Knox beneath the mid-Ordovician Knox unconformity surface, and subsequently inferred to influence the thickness of younger Paleozoic strata, albeit at apparently migrating positions in northeastern Kentucky (Woodward, 1961; Ettensohn, 1980; Cable and Beardsley, 1984; Tankard, 1986; Root and Onasch, 1999).

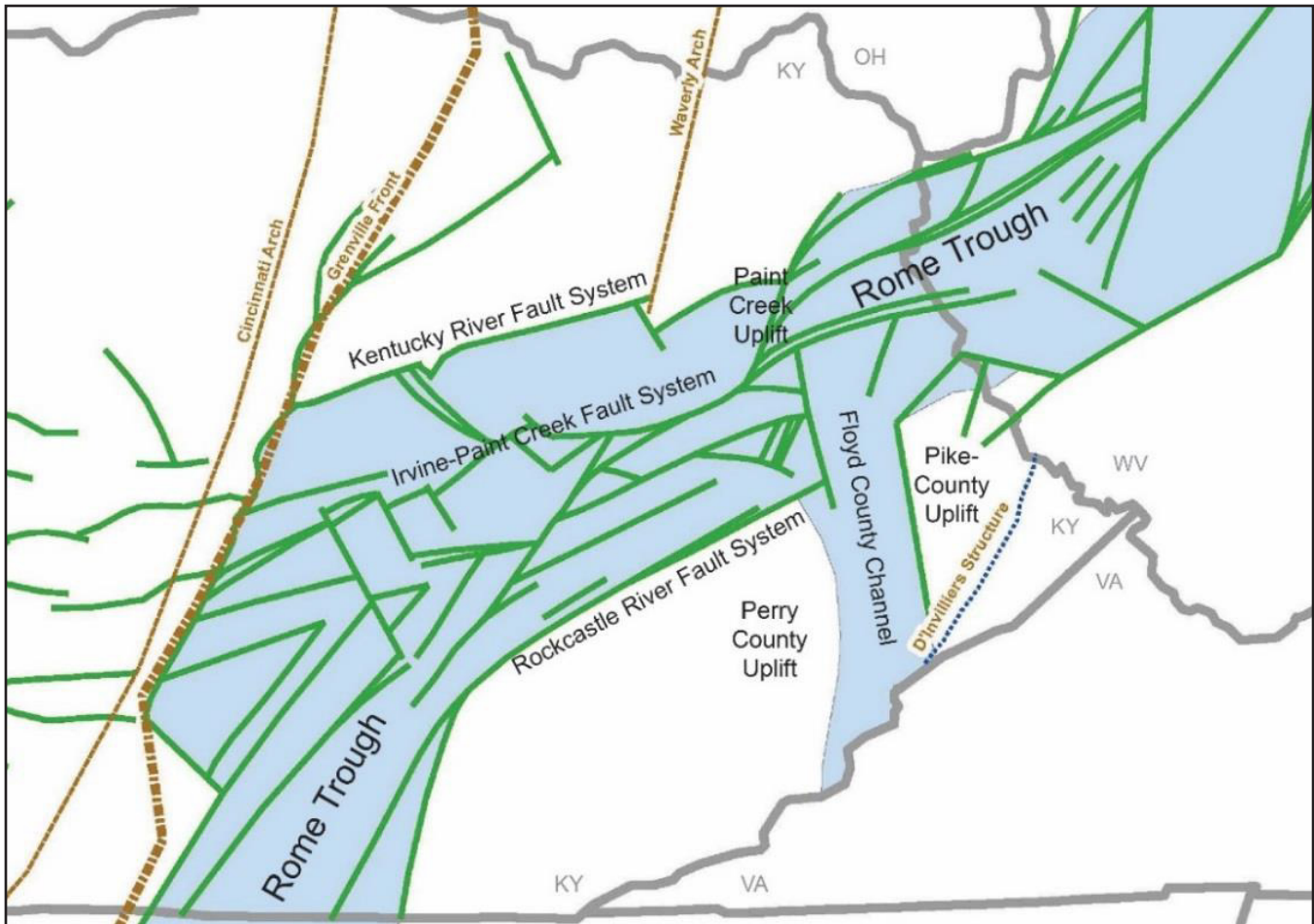


Figure 2-4. Major tectonic structures in eastern Kentucky. Blue shading represents area of the Rome Trough.

A structure map on the top of the Berea (base of the Sunbury Shale) (Fig. 2-5) for eastern Kentucky shows that, overall, the Berea dips to the southeast. This trend is interrupted by uplift across the Paint Creek Uplift, where the north-northwest/south-southeast trend of the faults associated with the Floyd County Channel intersects the east-west faults associated with the Irvine-Paint Creek Fault System. Offsets also occur along many of the major basement fault systems. See Floyd (2015) for structure maps on the various Ohio Shale members, which are similar to the Berea structure map shown in Figure 2-5.

Regional analysis of stratigraphic thickness and lithofacies shows that Bedford-Berea thickness (Fig. 2-6) does not follow regional structure (Fig. 2-5). Previous investigations have inferred structural influences on Berea thickness and lithofacies distribution (e.g., Dillman and Ettensohn, 1980; Tankard, 1986; Pashin and Ettensohn, 1987).

In a master's thesis finished concurrent with this project, Floyd (2015) found local thickness influences on members of the Ohio Shale across parts of the Kentucky River and Irvine-Paint Creek Fault Systems, within the Floyd County Channel (a basement extension of the Rome Trough), across the Pike County Uplift, and in basement faults in the western part of the basin. Floyd (2015) also noted the juxtaposition of the elongate Bedford-Berea trend with the bounding faults of the Floyd County Channel and the D'Inwilliers Structure, thicker Berea Sandstone deposition north of the Kentucky River Fault System, and locally thicker Berea Sandstone on the Pike County Uplift (Fig. 2-6).

Development of different depocenters and reactivation of basement structures during deposition of the Berea petroleum system has been interpreted as tectonic responses to the Appalachian Orogeny (Tankard, 1986; Quinlan and Beaumont, 1984; Ettensohn and others, 1988). The Ohio Shale

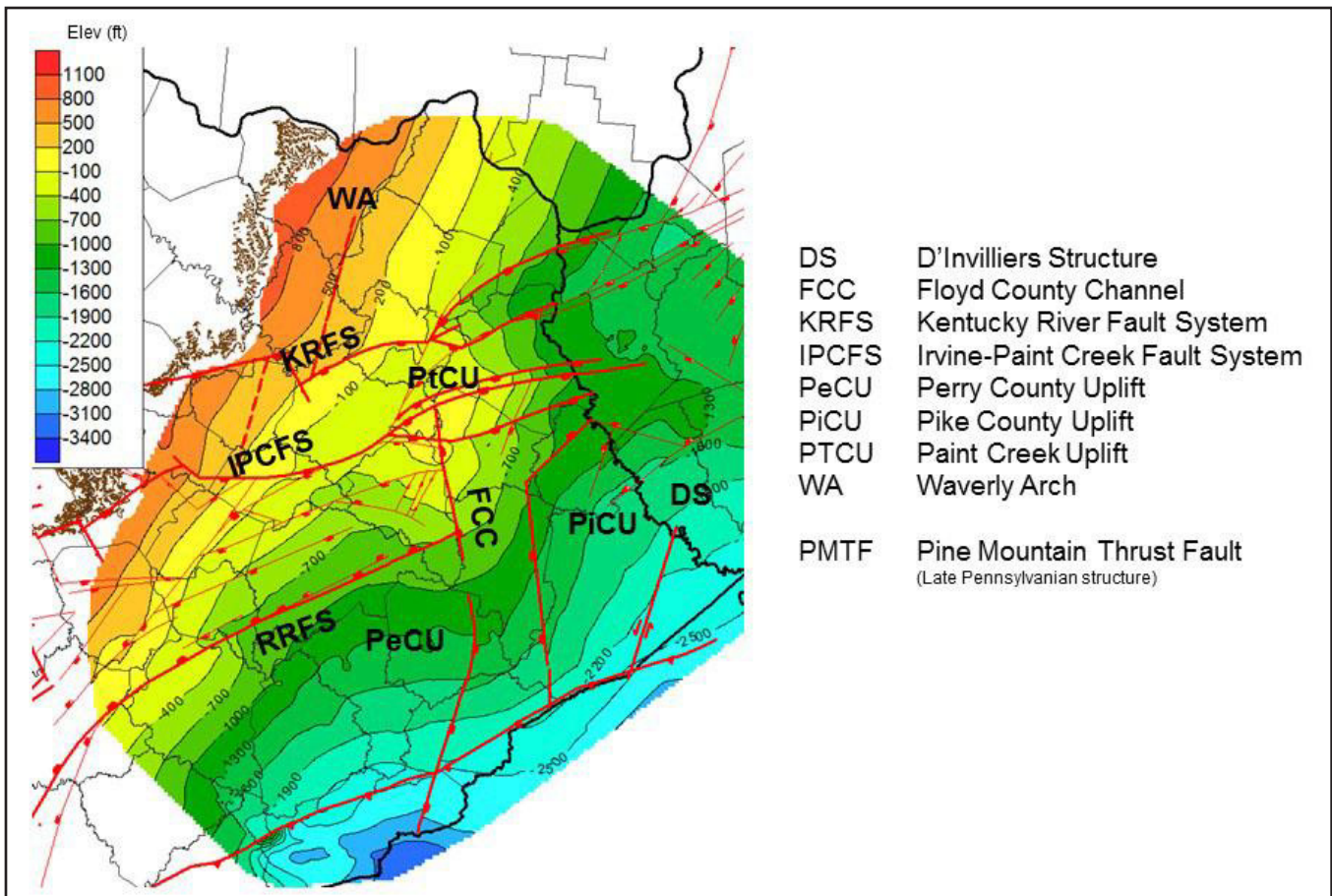


Figure 2-5. Structure map on top of the Berea for part of eastern Kentucky. From Floyd (2015); used with permission.

and Bedford-Berea interval are part of the Catskill clastic wedge (Fig. 2-7), which has been interpreted as a response to the third tectophase of the Acadian Orogeny (Ettensohn and others, 1988; Pashin and Ettensohn, 1992; Ettensohn, 2004). During this tectophase, forebulges are interpreted to have migrated westward from the orogeny, creating the accommodation space for a succession of black shales, which overlapped the Cincinnati Arch (Pashin and Ettensohn, 1987; Ettensohn and others, 1988; Ettensohn, 2004). Black shales of the Lower Huron, Upper Huron, Cleveland, and Sunbury were deposited as transgressive shales during relative deepening or sea-level rise. Less organic-rich, gray to black shales of the Middle Huron and Three Lick Bed represent “regressive” shales, which accumulated as clastics prograded outward in response to tectonic pulses (green arrows in Figure 2-7). The Bedford-Berea interval has been interpreted as a forced regression (seaward onlap) at the top of the

Catskill wedge and the end of the third tectophase (Pashin and Ettensohn, 1992; Ettensohn, 2004). Following Berea deposition, the Sunbury Shale was deposited as another transgressive black shale. It has been interpreted to represent the beginning of a fourth tectophase, which culminated in Price-Pocono-Borden deltaic progradation and deposition (Ettensohn and others, 1988; Ettensohn, 2004).

Fractures, preferentially oriented northeast-southwest, are an important contributor to porosity in Ohio Shale reservoirs in much of eastern Kentucky (Hunter and Young, 1953; Lowry and others, 1989; Hamilton-Smith, 1993; Shumaker, 1993). A regional network of planar, high-angle joints in the Lower Huron Member of the Ohio Shale appears to provide an important permeability network (Kubik, 1993; Boswell, 1996). Development of fractures has been attributed to displacement along normal faults associated with the Rome Trough (e.g., Charpentier and others, 1993). For example,

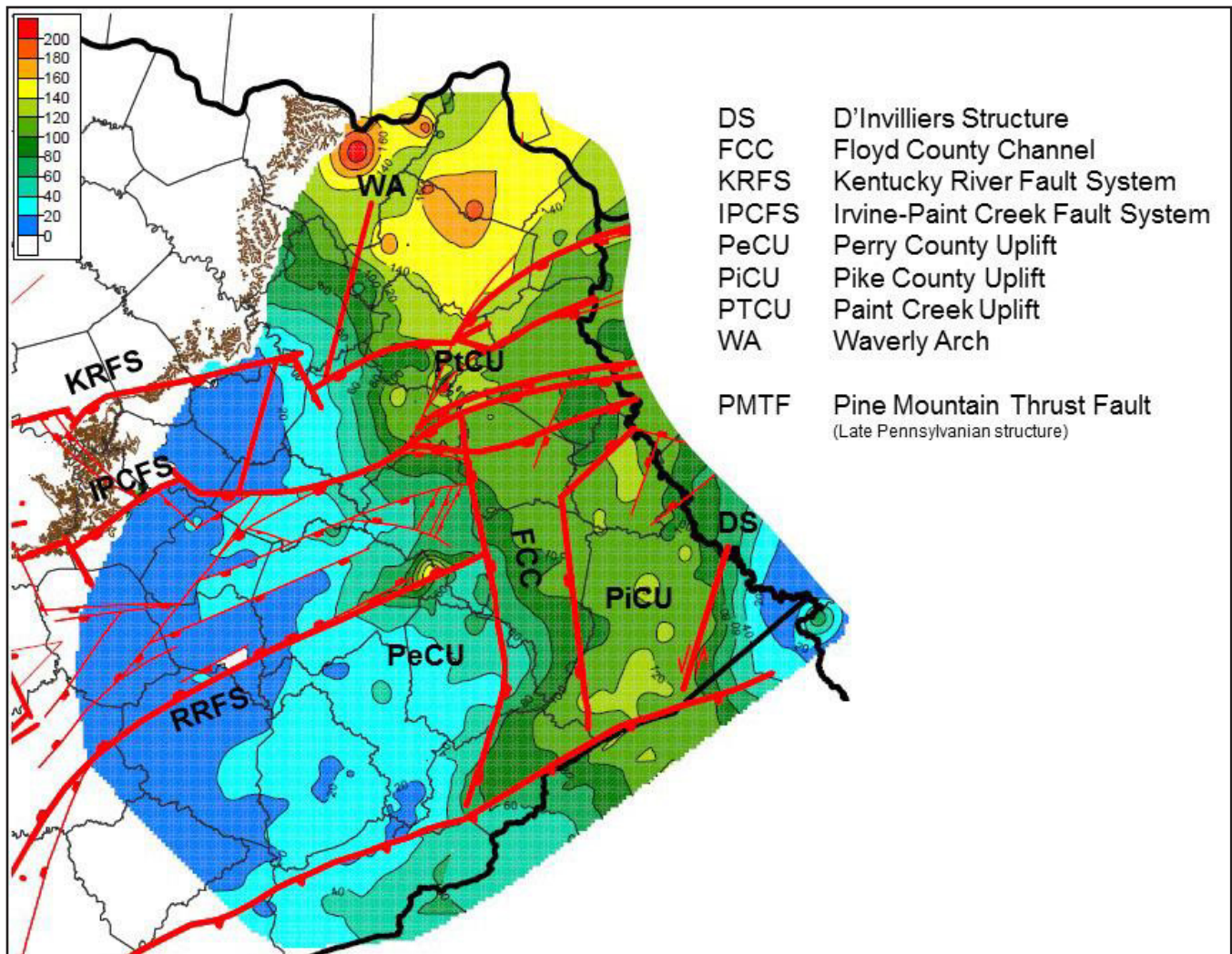


Figure 2-6. Updated isopach (ft) of the Bedford-Berea interval with superposed basement structures and areas where Berea sandstones and siltstones (yellow) are thickest along a north-northwest to south-southeast elongate trend. Modified from Floyd (2015); used with permission.

higher rates of gas production appear to follow the flanks of low-amplitude folds above basement faults and structures, especially those related to the Rome Trough and bounding basement structural highs (Shumaker, 1993). Hamilton-Smith (1993) discussed the importance of fold-related fractures to shale production. He used an example based on a seismic image from Lowry and others (1989) to show flexure in the Berea Sandstone above the Warfield Fault in West Virginia. Shumaker (1980) also suggested that development of some fracture porosity in the Ohio Shale may be related to limited decollement in the shale.

Thermal Maturity and Petroleum Systems

An analysis of more than 2,000 Devonian shale samples from the Appalachian Basin (Zielinski and McIver, 1982) showed a range of total organic carbon content (TOC) from less than 1 to 27 percent, with an average value of 2.13 percent. Curtis (1988) found total organic carbon concentrations between 3 and 6 percent for the Lower Huron Shale Member of the Ohio Shale. Zielinski and McIver (1982) showed that organic material of terrestrial origin increased in relative abundance eastward, toward the Catskill Delta. Carbon-isotope analysis also indicated an eastward increase in terrestrial components (Maynard, 1981).

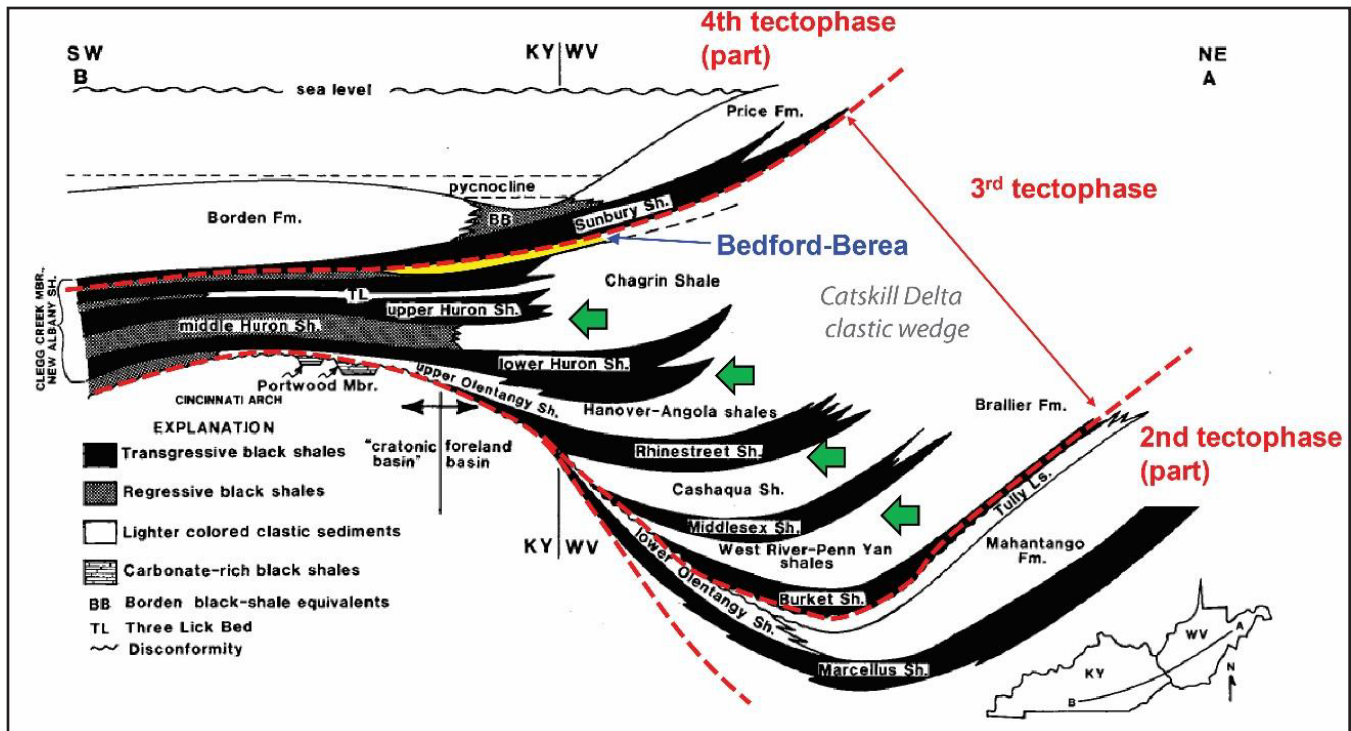


Figure 2-7. Interpreted relationship between elements of the Berea petroleum system and clastic wedges of the Catskill delta. Modified from Ettensohn and others (1988, Fig. 19), © 1988 Canadian Society of Petroleum Geologists; reprinted by permission of CSPG, whose permission is required for further use. Green arrows represent inferred tectonic pulses accompanied by deposition of transgressive black shales, followed by deposition of regressive black and gray shales.

In eastern Kentucky, TOC in Devonian black shales can exceed 25 weight percent, but dark gray shale units may be less than 0.1 weight percent TOC (Conant and Swanson, 1961; Schmoker, 1980; Boswell, 1996). Nuttall and others (2005, 2006) examined 63 samples of the Devonian Ohio Shale in an assessment of carbon storage potential and found TOC values from less than 1 to 14 percent. Rimmer and Cantrell (1989) and Rimmer and others (1993) showed that TOC in the Cleveland Member of the Ohio Shale decreases from approximately 12 percent where the Ohio Shale crops out in northeastern Kentucky to less than 2 percent in Pike County in southeastern Kentucky.

Along with TOC content, the thermal maturity of Devonian black shales is a critical factor influencing hydrocarbon generation. The decrease in TOC in the Cleveland Member cited above is in part a result of increased thermal maturity. Thermal maturity has been historically evaluated using conodont alteration indices, vitrinite reflectance, and pyrolysis measurements. For example, Rimmer and Cantrell (1989) used vitrinite-reflectance measurements in the Cleveland Member of the

Ohio Shale to show increases from 0.5 percent R_o in the outcrop belt to more than 1.0 percent in Pike County. Subsequent work by Rimmer and others (1993) used vitrinite-reflectance and pyrolysis (T_{max}) measurements to demonstrate fairly close agreement between the two techniques. T_{max} values closely followed the reflectance gradient, increasing from less than 430°C in the outcrop belt to greater than 450°C in Pike County.

More recent assessments include a revision of USGS Map I-917-E by Repetski and others (2008) in which they used conodont alteration indices and vitrinite-reflectance measurements to reinterpret the thermal maturity of Ordovician and Devonian source rocks throughout the Appalachian Basin. Overall, vitrinite-reflectance isolines trend from southwest to northeast; in northeastern Kentucky, values are close to 0.6 percent, whereas in southeastern Kentucky, values are close to 1.0 percent. East and others (2012) developed a thermal-maturity map for possible Devonian shale source rocks in the Illinois, Michigan, and Appalachian Basins. On the East and others (2012) map, most of eastern Kentucky is shown to be thermally immature

(R_o less than 0.6 percent), whereas a small southwest-northeast band of “oil window” maturation ($R_o = 0.6$ to 1.3 percent) occurs in southeastern Kentucky. A very small slice of southeasternmost Pike County is identified as gas-mature (R_o greater than 1.3 percent).

TOC and thermal-maturity studies have been important inputs for resource assessments of hydrocarbons in the Devonian shales. In 2002, the USGS conducted an assessment of technically recoverable undiscovered oil and gas resources in the Appalachian Basin (Milici and others, 2003). The assessment included the Devonian shale-middle and upper Paleozoic total petroleum system. One of the assessment units was the Greater Big Sandy Assessment Unit, most of which is located in eastern Kentucky. Estimated resources in this unit are 3.87 to 9.56 trillion cubic feet of gas and 34.1 to 104.5 million barrels of natural gas liquids.

Vitrinite reflectance has long been a standard technique for evaluating thermal maturity in source rocks, but the accuracy of the measurements is, in some geologic settings, now in question. This is especially true for source rocks that contain significant amounts of solid bitumen. Reflectance measurements of solid bitumen often yield lower values compared to vitrinite. Thus, where both are measured in the sample, the composite “vitrinite reflectance” measurement may be lower.

Recognizing this problem, investigators have turned to other measurements to assess thermal maturity. For example, Ryder and others (2013) used gas chromatography (GC) of bitumen extracts, organic matter type, spectral fluorescence of *Tasmanites*, and hydrogen index (HI) values to reassess thermal maturity in low-maturity shales in the Appalachian Basin. Their analysis included Lower Huron samples along a southern transect through southern Ohio, Kentucky (Carter, Elliott, Johnson, and Pike Counties), and West Virginia. At the western (less mature) and eastern (more mature) ends of the transect, they found moderately good agreement between R_o values in the Devonian shale and $R_{o(max)}$ values in overlying Pennsylvanian coals. In the central part of the transect, however, $R_{o(max)}$ values for the coals were greater than R_o values for the shale. They attributed the lower R_o values in the shale to measurement of solid bitumen that skewed the composite R_o measurements to lower values.

The GC data showed all the samples to be mature for oil and early-gas generation, except for one sample from southern Ohio. The GC results were consistent with the immature-mature boundary in the area defined by $R_o = 0.5$ percent for the Devonian shale and $R_{o(max)} = 0.6$ percent for Pennsylvanian coals. The immature-mature boundary based on *Tasmanites* spectral fluorescence ($\lambda_{max} = 600$ nm) and the hydrogen index (HI = 400 mg Hg/g TOC), however, was shifted to the east of the boundary based on the aforementioned R_o thresholds for shale and coal. The reason for the eastward shift remains unexplained. Moreover, HI and spectral-fluorescence measurements farther north in Ohio and Pennsylvania show the immature-mature boundary to be west of the boundary based on R_o thresholds.

Biomarkers in bitumen extracts have also been used to assess thermal maturity in Devonian shales in the region. Hackley and others (2013) investigated the thermal maturity of the Marcellus and Huron Shales in Ohio, West Virginia, and Pennsylvania using sterane and terpane biomarkers. Although vitrinite-reflectance measurements showed most of the shale samples to be immature, the biomarker data indicated that the samples were in the oil window. Compared to the reflectance measurements from the shales, the biomarker data were more consistent with the higher vitrinite-reflectance values in the coal and the production of thermogenic gas in the area.

Closer to this study area, Kroon and Castle (2011) examined biomarkers to assess the origin and thermal maturity of organic matter in the Lower Huron Member of the Ohio Shale. Cuttings samples ($n = 21$) were collected from eight wells in Kentucky (Perry, Letcher, Knott, Floyd, and Pike Counties) and West Virginia (Mingo and Logan Counties). Sterane, sterane isomer, and hopane ratios suggest that the samples are in the early to peak oil-generation window. This interpretation is consistent with vitrinite-reflectance measurements, which show the Lower Huron to be mostly in the oil window for most of the area. Kroon and Castle (2011) also used biomarkers to interpret that Lower Huron organic matter was largely derived from marine algae and bacteria deposited in conditions alternating between oxic and anoxic at water depths greater than 100 m.

In addition to the Devonian petroleum system, a deeper petroleum system associated with the Middle Cambrian Rogersville Shale has been identified in the Rome Trough of eastern Kentucky and western West Virginia (Ryder and others, 2014). This system has been the target of several deep tests, including the Bruin Exploration-S. Young #1 well in Lawrence County. Core from the Rogersville in the Exxon #1 Smith well in Wayne County,

W.Va., has TOC values ($n=4$) that range from 1.2 to 4.4 weight percent. Bitumen extracted from the Rogersville is characterized by a broad spectrum of n -alkanes from n -C₁₁ through n -C₃₀, strong odd-carbon predominance in the n -C₁₃ to n -C₁₉ range, and detectable amounts of the isoprenoids pristane and phytane. The strong odd-carbon predominance is attributed to the Ordovician alga *Gloeocapsomorpha prisca*.

3. Geochemistry Methods

T. Marty Parris, Cortland F. Eble, and Paul C. Hackley

Sample Material and Selection

Using previous thermal-maturity studies for context (e.g., Repetski and others, 2008; East and others, 2012), 12 wells were sampled along an approximately 100 mi transect extending from Scioto County, Ohio, southward to Pike County, Ky., to assess the total organic content (TOC) and thermal maturity of possible source rocks in the Ohio and Sunbury Shales (Fig. 3-1, Table 3-1). The transect, oriented orthogonal to thermal-maturity isolines defined by East and others (2012), provided the opportunity to collect samples ranging from thermally immature in the north to gas mature in the south. This effort represents one of the most comprehensive thermal-maturity assessment programs in the southern Appalachian Basin.

Where possible, samples were collected from cores, because they provided the greatest confidence in sample provenance and fewest issues with contamination (Table 3-1). Most of the sampled core material is located at the KGS Well Sample and Core Library. In addition, a core through the Sunbury and Ohio Shales in the Aristech #4 well in Scioto County, Ohio, was sampled at the Ohio Geological Survey in Columbus.

Most wells in which core was sampled typically included a gamma-ray and density log. We attempted to correlate gamma-ray maxima and minima with more organic-rich (darker) and less organic-rich (lighter) intervals, respectively. In some areas, however, the lack of core required use of cuttings. With cuttings, we attempted to assess the depth offset between the cuttings and true stratigraphic depths by using a recognizable rock type, such as the Berea Sandstone. Once the offset was estimated, the appropriate correction was made to select the depth intervals from which to sample. Within the interval of interest, cuttings containing the darkest rock were selected.

Samples selected for thermal maturity and geochemical measurements were reduced in size to approximately -4 mesh (less than 4.75 mm) using a jaw crusher. A small portion of the jaw-crushed samples was used to construct petrographic pellets for reflected-light analysis. For further geochemical measurements, the rest of the sample was fur-

ther reduced in size to -60 mesh (less than 250 μm) using a shatterbox.

Organic Petrography

Vitrinite-reflectance measurements (VR_o) were performed on 100 samples (Table 3-2). For comparison, solid bitumen reflectance (BR_o) analysis was performed on 21 of the 100 samples. Typically, 20 to 50 individual measurements of dispersed vitrinite or solid bitumen were made on separate rock fragments within each sample. Vitrinite-reflectance measurements were conducted at KGS, and solid-bitumen reflectance measurements were conducted at USGS. Petrographic pellets were constructed by combining a small amount of crushed rock material (1 to 2 g, approximately 1 mm top size; ASTM, 2015a) with either epoxy or a thermoplastic resin into 2.54- or 3.18-cm-diameter molds, and allowing the mixture to harden. Once cured, the petrographic pellets were ground and polished to produce a highly reflective, scratch-free surface. Random-reflectance measurements were obtained following ASTM International test method D7708-11 (ASTM, 2015b) on dispersed vitrinite and solid bitumen.

Total Carbon and Sulfur

Total carbon (TC) and sulfur (TS) concentrations (weight percent) were measured on 158 samples using a Leco SC-144DR carbon/sulfur analyzer, following ASTM International test method D4239-12 (ASTM, 2015c). Total inorganic carbon (TIC) concentrations were obtained using a coulometer. Total organic carbon concentrations were determined by calculating the difference between TC and TIC. Eleven additional TOC values were contributed by industry partners Hay Exploration and Cimarex Energy. Total carbon, total inorganic carbon, and total organic carbon values for analyzed samples are reported in Table 3-3.

Programmed Pyrolysis

Results from the TOC measurements were used along with geographic and stratigraphic locations to select 47 samples from nine wells for programmed-pyrolysis measurements at GeoMark Research (Tables 3-4, 3-5a, b). Approximately

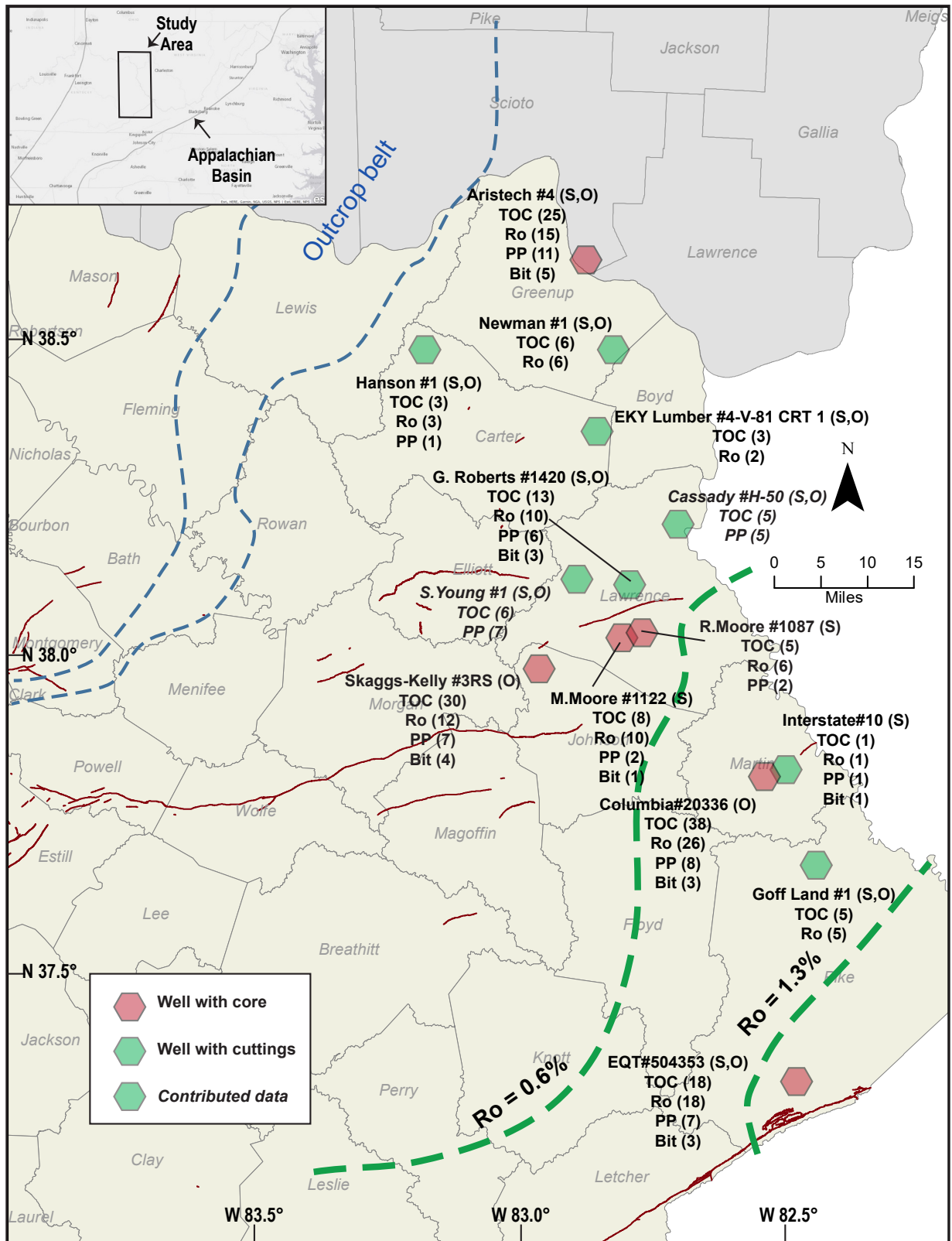


Figure 3-1. Location of core and cuttings samples. Well names are followed by sampled interval (S=Sunbury, O=Ohio Shale) and by the type and number of measurements. TOC=total organic carbon. R_o =vitrinite and/or solid bitumen reflectance. PP=programmed pyrolysis. Bit=bitumen extract analysis. The 0.6 percent and 1.3 percent R_o isolines are from East and others (2012). Kentucky and Ohio counties in tan and gray, respectively; faults in red.

Table 3-1. Sample locations, stratigraphic intervals, and sample type. Berea oil and gas samples are based on log picks from the sampled and offset wells. Gas sample depths are based on the perforated interval (Justice #KL 1915) or completed stratigraphic interval (EQT #504353). Parenthetical values are midpoints. SUN = Sunbury. Ohio Shale members: CLV = Cleveland. 3L = Three Lick Bed. UHUR = Upper Huron. MHUR = Middle Huron. LHUR = Lower Huron. OLEN = Olenotangy. Italicized samples were donated by Cimarex and Hay Exploration.

Well	County	API	Lat.	Long.	Strat. Unit	Depth (ft, sub-sea)	Sample Type
Aristech Chemical Corp. #4	Scioto	34145601410000	38.954200	-82.822119	SUN, CLV, 3L, UHUR, MHUR, LHUR	674.1 to 1,434.8	core
Magnum Drilling of Ohio—C. Newman #1	Greenup	16089000480000	38.450412	-82.769024	SUN, CLV, UHUR, LHUR	-365 to -1,015	cuttings
Kentucky Geological Survey—Hanson Aggregates #1	Carter	16043001050000	38.469552	-83.132597	SUN, "Upper" Ohio, "Lower" Ohio	326 to -154	cuttings
Chesapeake Appalachia LLC—E KY Lumber #4-V-81 CRT 1	Carter	16043001080000	38.317312	-82.801018	SUN, "Upper" Ohio, "Lower" Ohio	-514 to -914	cuttings
KY-WV Gas Co.—G. Roberts #1420	Lawrence	16127021650000	38.090954	-82.725724	SUN, CLV, UHUR, LHUR, OLEN	-821 to -1,658	cuttings
Hay Exploration—B. Cassidy #H-50	Lawrence	16127031000000	38.168043	-82.672858	SUN, CLV	-985 to -1,155	cuttings
Bruin Expl. — S. Young #1	Lawrence	16127005020000	38.087888	-82.824320	CLV, UHUR, MHUR, LHUR	-681 to -1,131	cuttings
KY-WV Gas Co.—R. Moore #1087	Lawrence	16127005020000	38.011127	-82.735469	SUN	-373 to -377	core
KY-WV Gas Co.—M. Moore #1122	Lawrence	16127005150000	38.015521	-82.762385	SUN	-328 to -333.5	core
Ashland Expl. — Skaggs-Kelly Unit #3RS	Johnson	16115001200000	37.961867	-82.937797	CLV, UHUR, MHUR, LHUR	-34.5 to -459.2	core
Interstate—Columbia Natural Resources #10	Martin	16159012300000	37.781508	-82.481060	SUN	-1,390 to -1,400	cuttings
Columbia—Columbia Gas #20336	Martin	16159002400000	37.775878	-82.494164	CLV, UHUR, MHUR, LHUR	-1,515.4 to -2,470.1	core
L&B Oil and Gas Inc.—J.B. Goff Land Co. #1	Pike	16195064260000	37.643942	-82.407774	SUN, CLV, UHUR, LHUR	-1,725 to -2,595	cuttings
Equitable—Equitable #504353	Pike	16195060410000	37.312678	-82.385750	SUN, CLV, 3L, UHUR, MHUR, LHUR	-2,351.5 to -3,148.5	core
Nyits—ALC #20	Greenup	16089002240000	38.470632	-82.842226	Berea	-338	oil and gas
Hay Expl.—R. Holbrook #HF-59	Lawrence	16127031360000	38.180148	-82.700915	Berea	-1,191	oil and gas
Nyits—Torchlight #8	Lawrence	16127030210000	38.065416	-82.639859	Berea	-1,187	oil and gas
Abarta—Jayne Heirs #H1	Johnson	16115021500000	37.940308	-82.897257	Berea	-260	oil and gas
EQT—EQT Production Co. #572356	Johnson	16115021360000	37.928550	-82.769471	Berea	-582	oil and gas
EQT—EQT Production Co. #572357	Martin	16159011757000	37.848339	-82.666424	Berea	-943	oil and gas
EQT—P. Justice #KL1915	Pike	16195020750000	37.657992	-82.401623	Ohio Sh	-1,831 to -2,597 (-2,214)	gas
EQT—EQT Production Co. #504353	Pike	16195060410000	37.312678	-82.385750	LH	-3,309 to -6,619 (-4,964)	gas

Table 3-2. Summary of carbon, sulfur, and reflectance analyses. TC=total carbon (weight percent). TIC=total inorganic carbon (weight percent). TOC=total organic carbon (weight percent). TS=total sulfur (weight percent). VR_o = vitrinite reflectance (percent), BR_o = solid bitumen reflectance (percent). Calc. VR_o Equiv. = vitrinite reflectance equivalent (percent) calculated from $BR_o \times 0.618 + 0.4$ (Jacob, 1989). * R_o calculated from T_{max} .

Well ID	TC	TIC	TOC	TS	Avg. VR_o	St. Dev.	Avg. BR_o	VR Equiv.	St. Dev.
Aristech #4									
Average	8.07	0.10	7.98	2.97	0.51	0.03	0.33	0.60	
Maximum	20.32	0.57	20.32	6.62	0.52	0.04	0.35	0.62	
Minimum	1.20	0.00	1.20	1.33	0.48	0.02	0.29	0.58	
Standard Deviation	4.45	0.13	4.50	1.33	0.01	0.01	0.02	0.01	
Number of Analyses	27	27	27	27	15	15	6	6	
G. Roberts #1420									
Average	7.15	0.05	7.10		0.58	0.04			
Maximum	8.92	0.14	8.78		0.59	0.05			
Minimum	4.86	0.00	4.81		0.57	0.03			
Standard Deviation	1.35	0.05	1.33		0.01	0.01			
Number of Analyses	7	7	7		7	7			
Newman #1									
Average	5.53	0.15	5.38		0.58	0.04			
Maximum	8.64	0.60	8.62		0.59	0.05			
Minimum	2.63	0.02	2.60		0.57	0.04			
Standard Deviation	2.15	0.23	2.11		0.01	0.00			
Number of Analyses	6	6	6		6	6			
Hanson #1									
Average	8.22	0.13	8.09		0.55	0.03	0.34	0.61	0.04
Maximum	9.54	0.37	9.53		0.56	0.03			
Minimum	7.43	0.00	7.06		0.55	0.03			
Standard Deviation	1.15	0.21	1.28		0.01	0.00			
Number of Analyses	3	3	3		3	3			
EKY Lumber #4-V-81									
Average	7.55	0.16	7.48		0.58	0.04			
Maximum	7.55	0.16	7.48		0.59	0.05			
Minimum	3.97	0.06	3.81		0.58	0.03			
Standard Deviation	1.99	0.06	2.01		0.01	0.01			
Number of Analyses	6	6	6		2	2			
B. Cassidy #50									
Average			6.13		*0.62				
Maximum			7.55		*0.70				
Minimum			2.39		*0.53				
Standard Deviation			2.16						
Number of Analyses			5		5				
S. Young #1									
Average			2.78		*0.69				
Maximum			5.21		*0.80				
Minimum			0.23		*0.63				

Table 3-2. Summary of carbon, sulfur, and reflectance analyses. TC=total carbon (weight percent). TIC=total inorganic carbon (weight percent). TOC=total organic carbon (weight percent). TS=total sulfur (weight percent). VR_o=vitrinite reflectance (percent), BR_o=solid bitumen reflectance (percent). Calc. VR_o Equiv.=vitrinite reflectance equivalent (percent) calculated from BR_o × 0.618 + 0.4 (Jacob, 1989). *R_o calculated from T_{max}.

Well ID	TC	TIC	TOC	TS	Avg. VR _o	St. Dev.	Avg. BR _o	VR Equiv.	St. Dev.
Standard Deviation			1.99						
Number of Analyses			6		6				
M. Moore #1122									
Average	9.66	0.00	9.66		0.61	0.05	0.37	0.63	0.04
Maximum	19.69	0.01	19.68		0.62	0.06	0.39	0.64	0.04
Minimum	6.72	0.00	6.72		0.60	0.05	0.34	0.61	0.04
Standard Deviation	5.62	0.00	5.62		0.01	0.00	0.04	0.02	0.00
Number of Analyses	5	5	5		5	5	2	2	2
R. Moore #1087									
Average	10.40	0.00	10.40		0.59	0.04	0.36	0.62	0.06
Maximum	21.66	0.01	21.64		0.60	0.05	0.36	0.62	0.06
Minimum	5.57	0.00	5.57		0.58	0.02	0.35	0.62	0.05
Standard Deviation	5.93	0.00	5.92		0.01	0.01	0.01	0.00	0.01
Number of Analyses	8	8	8		8	8	2	2	2
Skaggs-Kelly #3RS									
Average	7.31	0.19	7.12	2.73	0.66	0.05			
Maximum	12.25	1.23	12.18	4.00	0.67	0.06			
Minimum	3.11	0.01	2.97	1.32	0.66	0.04			
Standard Deviation	2.44	0.23	2.45	0.76	0.01	0.01			
Number of Analyses	30	30	30	30	12	12			
Columbia #20336									
Average	5.26	0.24	5.01		0.72	0.05	0.58	0.76	0.09
Maximum	13.00	2.28	12.97		0.76	0.07	0.63	0.79	0.11
Minimum	1.48	0.00	1.48		0.70	0.03	0.54	0.73	0.07
Standard Deviation	2.63	0.43	2.45		0.02	0.01	0.03	0.02	0.01
Number of Analyses	38	38	38		20	20	6	6	6
J.B. Goff Land #1									
Average	6.46	0.14	6.32		0.75	0.04			
Maximum	14.95	0.31	14.95		0.76	0.05			
Minimum	1.83	0.00	1.72		0.75	0.03			
Standard Deviation	5.15	0.11	5.19		0.01	0.01			
Number of Analyses	5	5	5		5	5			
Interstate #10									
single sample	4.56	0.21	4.36	1.59	0.74	0.07	0.44	0.67	0.05
EQT #504353									
Average	3.71	0.13	3.59	2.68	1.24	0.07	1.43	1.28	
Maximum	6.06	0.77	6.03	5.33	1.31	0.10	1.47	1.31	
Minimum	0.29	0.00	0.19	0.61	1.19	0.04	1.38	1.25	
Standard Deviation	1.72	0.19	1.71	1.24	0.04	0.02	0.05	0.03	
Number of Analyses	21	21	21	21	16	16	3	3	
*calculated R _o from Rock-Eval T _{max}									

Table 3-3. Distribution of carbon and sulfur in the Sunbury Shale and members of the Ohio Shale. TC=total carbon. TIC=total inorganic carbon. TOC=total organic carbon. TS=total sulfur.

	Stratigraphic Interval	TC	TIC	TOC	TS
Average	Sunbury	9.78	0.02	9.45	2.06
Maximum		21.66	0.21	21.64	2.80
Minimum		4.56	0.00	2.39	1.58
Analyses		30	30	32	10
Average	Cleveland	5.75	0.04	5.58	1.96
Maximum		11.22	0.18	11.21	5.33
Minimum		2.21	0.00	0.23	0.88
Analyses		24	24	29	15
Average	Three Lick	2.23	0.05	2.18	1.45
Maximum		5.21	0.10	5.16	1.90
Minimum		0.29	0.00	0.19	0.61
Analyses		3	3	3	3
Average	Upper Huron	4.16	0.17	3.86	2.72
Maximum		7.68	0.77	7.68	5.03
Minimum		0.88	0.00	0.62	2.07
Analyses		26	26	27	14
Average	Middle Huron	3.92	0.14	3.74	2.90
Maximum		6.53	0.29	6.23	3.83
Minimum		0.88	0.04	0.84	2.23
Analyses		11	11	13	5
Average	Lower Huron	6.91	0.26	6.62	3.56
Maximum		14.43	2.28	14.38	6.62
Minimum		1.48	0.00	1.48	2.07
Analyses		59	59	60	31

100 mg of washed, pre-solvent-extracted -60 mesh sample was needed for pyrolysis measurements, with smaller amounts used for samples in which TOC values exceeded 7 to 8 weight percent. Pyrolysis data (Source Rock Analyzer) for 11 additional samples from two wells were provided by Hay Exploration and Cimarex Energy.

Initially, measurements were done on raw samples using a Rock-Eval II pyrolysis instrument. Some of the samples showed shoulders on the S2 peak, which produces error in the value of S2 and T_{max} . As a result, a subset of 18 samples was solvent-extracted with a DCM methanol (9:1) mixture and remeasured with a HAWK instrument, which is a newer pyrolysis instrument with higher detec-

tion sensitivity. Results of the solvent extraction are discussed in the "Results" section.

In general, for each instrument the sample was heated in an inert atmosphere to 300°C and held for 3 min. Hydrocarbons liberated in this time yielded the first peak on the pyrogram, represented with S1, which equals free hydrocarbons in the rock that were present at the time of deposition and/or generated from kerogen since deposition (Peters, 1986). Subsequently, temperature was increased at a programmed rate of 25°C/min up to 550°C and 650°C in the Rock-Eval II and HAWK instruments, respectively. In the Rock-Eval II instrument, temperature was held at 550°C for 1 min. Hydrocarbons released during the programmed heating generated a second

peak referred to as S2. Hydrocarbons associated with S2 are produced from the cracking of kerogen, and thus S2 represents hydrocarbon generation potential of the rock. The concentrations of hydrocarbons generated in association with S1 and S2 are in milligrams of hydrocarbon (HC) per gram of rock, and are measured with a flame ionization detector (FID). In addition to hydrocarbons being generated, carbon dioxide generated during programmed heating up to 390°C was analyzed with a thermal conductivity detector (TCD) during Rock-Eval II testing and by an infrared detector in the Hawk instrument. This generated a third peak, referred to as S3, which is measured in milligrams of carbon dioxide per gram of rock.

Table 3-4. Summary of programmed-pyrolysis and petrographic thermal-maturity parameters. Conversion factors are: T_{max} factor = $(HI - 150)/50$ (Snowdon, 1995). Calculated $VR_o = (T_{max} \times 0.018) - 7.16$ (Jarvie and others, 2001). VR_o equivalent = $(BR_o \times 0.618) + 0.4$ (Jacob, 1989). ** = Data donated by industry partner, so no sample material. TOC = total organic carbon (weight percent). T_{max} (°C). HI = hydrogen index (mg hydrocarbon/g TOC), VR_o = vitrinite reflectance (percent). BR_o = solid bitumen reflectance (percent). PI = Production Index ($S1/S1 + S2$).

	TOC	T_{max}	R_o Calc.	HI	T_{max} Factor	Adj. T_{max}	Adj. R_o Calc.	VR_o Meas.	BR_o Meas.	VR_o Equiv.	PI
R. Moore #1087, Lawrence County											
Average	13.61	424	0.46	504	7.09	430.59	0.59	0.61	0.36	0.62	0.06
Maximum	19.68	426	0.49	597	8.94	433.94	0.65	0.62	0.36	0.62	0.07
Minimum	7.54	422	0.44	412	5.24	427.24	0.53	0.60	0.35	0.62	0.05
Range	12.14	4	0.05	185	3.70	6.70	0.12	0.01	0.01	0.00	0.02
Standard Deviation	8.58	2	0.04	131	2.62	4.74	0.09	0.01	0.01	0.00	0.01
Analyses	2	2	2	2	2	2	2	2	2	2	2
Skaggs-Kelley #3RS, Johnson County											
Average	8.22	432	0.62	559	8.18	440.30	0.77	0.66			0.07
Maximum	12.18	435	0.67	633	9.67	444.22	0.84	0.67			0.09
Minimum	5.39	429	0.56	476	6.51	435.51	0.68	0.66			0.06
Range	6.79	6	0.11	158	3.15	8.70	0.16	0.02			0.03
Standard Deviation	2.54	2	0.03	57	1.14	2.60	0.05	0.01			0.01
Analyses	8	8	8	8	8	8	8	6			8
Columbia 20336, Martin County											
Average	6.64	439	0.75	358	4.16	443.41	0.82	0.73	0.58	0.76	0.12
Maximum	12.97	444	0.83	490	6.81	448.81	0.92	0.75	0.63	0.79	0.17
Minimum	4.11	434	0.65	307	3.15	437.15	0.71	0.70	0.54	0.73	0.07
Range	8.86	10	0.18	183	3.66	11.66	0.21	0.06	0.09	0.06	0.09
Standard Deviation	3.11	3	0.06	61	1.22	3.73	0.07	0.02	0.03	0.02	0.03
Analyses	8	8	8	8	8	8	8	8	8	8	8
Interstate #10, Martin County											
Single sample	4.36	436	0.69	341	3.82	439.82	0.76	0.74			0.11
EQT #504353, Pike County											
Average	4.26	445	0.84	42	N/A	N/A	N/A	1.23	1.43	1.28	0.44
Maximum	6.03	456	1.05	71	N/A	N/A	N/A	1.29	1.47	1.31	0.58
Minimum	2.35	437	0.71	22	N/A	N/A	N/A	1.19	1.38	1.25	0.29
Range	3.68	19	0.34	49	N/A	N/A	N/A	0.10	0.09	0.06	0.29
Standard Deviation	1.50	9	0.16	20	N/A	N/A	N/A	0.05	0.05	0.03	0.12
Analyses	7	7	7	7	N/A	N/A	N/A	6	3	3	7

Bitumen Extracts and Oils: Column Chromatography, Gas Chromatography, Gas Chromatography–Mass Spectrometry, and Isotope Ratio–Mass Spectrometry

Based on results from the thermal-maturity analysis, along with stratigraphic and geographic location, 20 samples were selected from seven

wells for bitumen extraction and further geochemical characterization at GeoMark using gravimetric column chromatography, gas chromatography (GC-FID), gas chromatography–mass spectrometry (GC-MS), and isotope ratio mass spectrometry (IRMS) measurements. Bitumen extracts were obtained from all stratigraphic units considered to be

Table 3-5a. Programmed-pyrolysis measurements on raw samples (analyzed by Rock-Eval II) versus solvent-extracted (shaded) samples (analyzed by HAWK). TOC = total organic carbon. S1 and S2 (mg hydrocarbon/g rock). S3 (mg CO₂/g rock). T_{max} (°C). VR_o Calc. (percent) = (T_{max} × 0.018) – 7.16 (Jarvie and others, 2001).

Well	Depth (ft)	TOC	S1	S2	S3	T _{max}	R _o Calc.
EQT #504353	3,809.5	6.03	1.75	4.30	0.19	450	0.94
EQT #504353	3,809.5	6.03	0.20	2.00	0.38	456	1.05
EQT #504353	3,998.3	3.48	1.14	1.94	0.17	456	1.05
EQT #504353	3,998.3	3.48	0.12	0.69	0.36	448	0.90
EQT #504353	4,220	3.29	0.96	0.95	0.15	438	0.72
EQT #504353	4,220	3.29	0.11	0.36	0.39	443	0.81
EQT #504353	4,559.8	5.66	1.37	1.27	0.23	438	0.72
EQT #504353	4,559.8	5.66	0.17	0.68	0.33	441	0.78
Columbia #20336	2,449.4	7.52	2.99	36.88	0.73	442	0.80
Columbia #20336	2,449.4	7.52	0.46	19.00	0.32	443	0.81
Columbia #20336	3,055.3	5.07	3.10	19.41	0.43	437	0.71
Columbia #20336	3,055.3	5.07	0.47	14.55	0.41	443	0.81
Columbia #20336	3,400	4.11	1.94	12.65	0.47	439	0.74
Columbia #20336	3,400	4.11	0.34	11.59	0.21	447	0.89
Interstate #10	2,465	4.36	1.82	14.85	0.41	436	0.69
Interstate #10	2,465	4.36	0.47	8.66	0.41	443	0.81
Moore #1122	1,223	7.33	2.77	30.89	0.60	427	0.53
Moore #1122	1,223	7.33	0.25	32.22	0.35	426	0.51
Moore #1122	1,225.9	21.64	6.80	114.52	1.59	426	0.51
Moore #1122	1,225.9	21.64	0.84	112.42	0.72	424	0.47
Moore #1087	1,207.95	7.54	2.30	31.06	0.55	422	0.44
Moore #1087	1,207.95	7.54	0.44	28.62	0.33	426	0.51
Moore #1087	1,209	19.68	6.63	117.48	2.14	425	0.49
Moore #1087	1,209	19.68	0.79	100.32	0.70	424	0.47
G. Roberts #1420	1,549.5	8.00	2.41	18.07	1.26	416	0.33
G. Roberts #1420	1,549.5	8.00	2.28	22.38	1.25	417	0.35
G. Roberts #1420	1,560.5	7.25	1.79	21.20	1.08	420	0.40
G. Roberts #1420	1,560.5	7.25	1.60	23.61	1.03	419	0.38
G. Roberts #1420	1,732	6.58	1.66	28.65	0.86	428	0.54
G. Roberts #1420	1,732	6.58	1.86	30.57	0.78	431	0.60
G. Roberts #1420	1,751.5	4.81	1.81	22.76	0.66	432	0.62
G. Roberts #1420	1,751.5	4.81	1.65	21.78	0.60	434	0.65
G. Roberts #1420	2,348.5	7.98	2.38	24.04	1.10	425	0.49
G. Roberts #1420	2,348.5	7.98	1.91	27.02	1.18	429	0.56
G. Roberts #1420	2,379	8.78	3.23	49.46	1.00	430	0.58
G. Roberts #1420	2,379	8.78	2.78	51.33	0.86	430	0.58

Table 3-5b. Programmed-pyrolysis measurements on raw samples (analyzed by Rock-Eval II) versus solvent-extracted (shaded) samples (analyzed by HAWK). HI=Hydrogen Index (mg hydrocarbon/g total organic carbon, TOC). OI=Oxygen Index (mg CO₂/g TOC). PI=Production Index (S1/S1+S2). VR_o=vitrinite reflectance (percent). BR_o=solid bitumen reflectance. VR equiv. = vitrinite reflectance equivalent (percent) calculated from BR_o × 0.618 + 0.4 (Jacob, 1989).

Well	HI	OI	S2/S3	(S1/TOC) × 100	P.I.	VR _o Meas.	BR _o Meas.	VR Equiv.
EQT #504353	71	3	22.63	29.02	0.29	1.19	1.38	1.25
EQT #504353	Na	na	5.26	na	0.09	1.19	1.38	1.25
EQT #504353	56	5	11.41	32.76	0.37	1.20		
EQT #504353	Na	na	1.92	na	0.15	1.20		
EQT #504353	29	5	6.33	29.18	0.50	1.24	1.44	1.29
EQT #504353	na	na	0.92	na	0.23	1.24	1.44	1.29
EQT #504353	22	4	5.52	24.20	0.52	1.29	1.47	1.31
EQT #504353	Na	na	2.06	na	0.20	1.29	1.47	1.31
Columbia #20336	490	10	50.52	39.76	0.07	0.73		
Columbia #20336	na	Na	59.00	na	0.02	0.73		
Columbia #20336	383	8	45.14	61.14	0.14	0.70	0.55	0.74
Columbia #20336	Na	na	35.00	na	0.03	0.70	0.55	0.74
Columbia #20336	308	11	26.91	47.20	0.13	0.73	0.63	0.79
Columbia #20336	na	Na	55.00	na	0.03	0.73	0.63	0.79
Interstate #10	341	9	36.22	41.74	0.11	0.74		
Interstate #10	Na	na	36.22	na	0.05	0.74		
Moore #1122	421	8	51.48	37.79	0.08	0.59		
Moore #1122	na	na	92.00	na	0.01	0.59		
Moore #1122	529	7	72.03	31.42	0.06	0.59		
Moore #1122	na	na	156.00	na	0.01	0.59		
Moore #1087	412	7	56.47	30.50	0.07	0.60		
Moore #1087	Na	na	87.00	na	0.02	0.60		
Moore #1087	597	11	54.90	33.69	0.05	0.62		
Moore #1087	Na	na	143.00	na	0.01	0.62		
G. Roberts #1420	226	16	14.34	30.13	0.12	0.57		
G. Roberts #1420	280	16	17.90	28.50	0.09	0.57		
G. Roberts #1420	292	15	19.63	24.69	0.08	0.58		
G. Roberts #1420	326	14	22.92	22.07	0.06	0.58		
G. Roberts #1420	435	13	33.31	25.23	0.05	0.59		
G. Roberts #1420	465	12	39.19	28.27	0.06	0.59		
G. Roberts #1420	473	14	34.48	37.63	0.07	0.59		
G. Roberts #1420	453	12	36.30	34.30	0.07	0.59		
G. Roberts #1420	301	14	21.85	29.82	0.09	0.59		
G. Roberts #1420	339	15	22.90	23.93	0.07	0.59		
G. Roberts #1420	563	11	49.46	36.79	0.06	0.58		
G. Roberts #1420	585	10	59.69	31.66	0.05	0.58		

potential source rocks for Berea oils (Fig. 3-1). The units include the Sunbury (n=5), Cleveland (n=4), Upper Huron (n=5), and Lower Huron (n=6). Moreover, the extracts span the thermal-maturity range from immature (R_o less than 0.6 percent) to wet gas mature (R_o =1.1–1.4 percent). A similar suite of measurements was conducted on oils collected from six wells in Greenup, Lawrence, Johnson, and Martin Counties (Fig. 3-2). Most oil samples were sampled at the wellhead into glass vials with Teflon liners as the well was actively pumping. This was done to minimize the possible loss of lighter volatile hydrocarbons. One sample, from the EQT #572357 in Martin County, was collected at the tank battery, however.

For bitumen extraction, approximately 10 g of powdered sample was weighed into pre-cleaned 22 ml stainless-steel cells and sealed with stainless-steel caps. The cells were loaded into a Dionex ASE 350 instrument in which each cell was filled with 40 ml dichloromethane (DCM) heated at 100°C and pressurized up to 1,400 psi for 5 min. The solvent was then flushed into a collection vial. The process was repeated two more times to complete the extraction. The extract was then air-dried at room temperature and weighed after all solvent had evaporated to obtain the total extract amount (extractable organic matter; EOM).

The less-than- C_{15} fraction of the whole extracts and oils was determined by weighing an aliquot of bitumen, topping the aliquot by evaporation in a stream of nitrogen for 30 min, and reweighing. Asphaltenes were precipitated from the whole extract using *n*-hexane overnight at room temperature, followed by centrifuging for 15 min. The $C_{15}+$ deasphalted fraction was separated into saturate, aromatic, and NSO (nitrogen-sulfur-oxygen compounds or resin) hydrocarbon fractions using gravity-flow column chromatography with a 100- to 200-mesh silica gel support previously activated at 400°C. The saturate, aromatic, and NSO fractions were eluted using hexane, methylene chloride, and methylene chloride/methanol (50:50) using 50 ml solvent in a 250 ml column. The hydrocarbon fractions were dried and weighed gravimetrically (Table 3-6). The weight percent of sulfur on the whole extract was measured using the vario-ISOTOPE select elemental analyzer via the Dumas combustion process.

The isoprenoid and *n*-alkane composition of whole extracts and oils was determined using “whole oil” GC measurements using an Agilent 7890A gas chromatograph equipped with an FID detector (GC-FID; Table 3-7). The gas chromatograph was equipped with a 30 m × 0.32 mm J&W DB-5 column (0.25 μm film thickness) and temperature programmed from -60°C to 350°C at 12°C/min. Helium was used as the carrier gas at a flow rate of 2 ml/min.

GC-MS analysis of the $C_{15}+$ saturate and aromatic hydrocarbon fractions was used to determine sterane and terpane biomarker distributions and concentrations (Tables 3-8, 3-9). Measurements were done with an Agilent 7890A or 7890B gas chromatograph interfaced to a 5975C or 5977A mass spectrometer. The gas chromatograph was equipped with a 50 m × 0.2 mm J&W HP-5 column (0.11 μm film thickness) and temperature programmed from 150°C to 325°C at 2°C/min for the saturate fraction and 100°C to 325°C at 3°C/min for the aromatic fraction. Helium was used as the carrier gas at a constant flow rate of 0.5 ml/min. The mass spectrometer was run in selected ion mode (SIM) for monitoring ions with mass/charge (*m/z*) ratios of 177, 191, 205, 217, 218, 221, 223, and 259 (saturates) and *m/z* 133, 156, 170, 178, 184, 188, 192, 198, 231, 239, 245, and 253 (aromatics) (Table 3-8). Semi-quantitative measurement of absolute concentrations of individual biomarkers was done by adding 50 μl of deuterated internal standard (d4- C_{29} 20R ethylcholestane) to the $C_{15}+$ saturate fraction and 10 μl of deuterated anthracene standard (d10) to the aromatic fraction. Response factors (RF) were determined by comparing the mass spectral response at *m/z* 221 for the deuterated standard to the hopane (*m/z* 191) and sterane (*m/z* 217) authentic standards. Response factors were approximately 1.4 for terpanes and 1.0 for steranes. Sample volumes were variable in the range of 50 to 250 μl. Concentrations of individual biomarkers in the saturate fraction were determined using the equation:

$$\text{Concentration (ppm)} = \frac{[(\text{biomarker height})(\text{ng standard})]}{[(\text{standard height})(\text{RF})(\text{mg saturate fraction})]}$$

This approach assumes that all hopanes and all steranes have the same RF as the hopane and sterane authentic standards, respectively.

Table 3-6. Bulk chemistry of oil (italics>) and extract samples. Measured sample depths for extracts provided after the well name. See Table 3-1 for depths of oil samples. SUN = Sunbury. CLV = Cleveland. UHUR = Upper Huron. LHUR = Lower Huron. S = sulfur. SAT = saturate. ARO = aromatic. NSO = heteroatom components (nitrogen-, sulfur, oxygen-containing molecules). ASPH = asphaltene. Sat/Arom = saturate to aromatic ratio.

Sample ID	Type	Formation	API	%S	%SAT	%ARO	%NSO	%ASPH	Sat/Arom
<i>Addington Land Co. #20</i>	oil	Berea	40.52	0.20	47.9	40.3	11.8	0.0	1.2
<i>Torchlight #8</i>	oil	Berea	41.39	0.18	52.0	36.1	11.7	0.2	1.4
<i>Holbrook #HF-59</i>	oil	Berea	40.30	0.20	47.5	36.9	15.3	0.4	1.3
<i>EQT #572357</i>	oil	Berea	35.36	0.21	50.4	40.2	9.3	0.2	1.3
<i>Jayne Heirs #H1</i>	oil	Berea	42.43	0.21	51.9	36.8	11.3	0.0	1.4
<i>EQT #572356</i>	oil	Berea	35.54	0.17	49.1	35.7	15.2	0.0	1.4
<i>Aristech #4, 678 ft</i>	core	SUN			13.3	30.8	47.9	8.0	0.4
<i>Aristech #4, 863.8 ft</i>	core	CLV		1.73	13.5	25.7	57.4	3.4	0.5
<i>Aristech #4, 1,025 ft</i>	core	UHUR			16.7	25.8	53.8	3.8	0.7
<i>Aristech #4, 1,035 ft</i>	core	UHUR			21.9	31.5	43.0	3.6	0.7
<i>Aristech #4, 1,432 ft</i>	core	LHUR		7.53	18.1	33.2	36.7	11.9	0.6
<i>Moore #1122, 1,225.9 ft</i>	core	SUN		2.48	13.6	24.5	45.1	16.8	0.6
<i>Interstate #10, 2,460 ft</i>	core	SUN		0.79	30.2	17.6	49.3	2.9	1.7
<i>G. Roberts #1420, 1,558-1,563 ft</i>	cuttings	SUN		5.33	14.8	15.6	64.4	5.2	1.0
<i>G. Roberts #1420, 1,740-1,763 ft</i>	cuttings	CLV		1.21	18.9	17.1	63.1	0.9	1.1
<i>G. Roberts #1420, 2,339-2,358 ft</i>	cuttings	LHUR		4.76	18.8	16.3	61.3	3.8	1.2
<i>Columbia #20336, 2,449.4 ft</i>	core	CLV		0.55	29.2	31.3	37.4	2.1	0.9
<i>Columbia #20336, 2,704 ft</i>	core	UHUR			22.9	29.4	38.8	8.9	0.8
<i>Columbia #20336, 3,400 ft</i>	core	LHUR		0.83	31.3	31.7	36.7	0.4	1.0
<i>Ashland #3RS, 1,017 ft</i>	core	CLV			17.7	31.4	45.8	5.0	0.6
<i>Ashland #3RS, 1,181 ft</i>	core	UHUR			15.9	25.2	57.9	0.9	0.6
<i>Ashland #3RS, 1,183 ft</i>	core	UHUR			22.0	27.2	50.3	0.5	0.8
<i>Ashland #3RS, 1,402 ft</i>	core	LHUR			19.4	32.7	35.6	12.3	0.6
<i>EQT #504353, 3,810 ft</i>	core	SUN			42.8	22.5	34.1	0.7	1.9
<i>EQT #504353, 4,560 ft</i>	core	LHUR			44.2	10.4	44.2	1.3	4.3
<i>EQT #504353, 4,566.1 ft</i>	core	LHUR			59.2	11.7	28.3	0.8	5.1

Table 3-7. Oil (*italics*) and extract properties from gas chromatography (GC-FID). Measured sample depths for extracts provided after the well name. See Table 3-1 for depths of oil samples. Pr/Ph=pristane to phytane ratio. Pr/C17=pristane to C₁₇ n-alkane ratio. Ph/C18=phytane to C₁₈ n-alkane ratio. CPI=carbon preference index (from Hunt, 1996). TAR=terrestrial to aquatic ratio $[(n-C_{27} + n-C_{29} + n-C_{31}) / (n-C_{15} + n-C_{17} + n-C_{19})]$.

Sample ID	Pr/Ph	Pr/C17	Ph/C18	CPI	TAR
<i>Addington Land Co. #20</i>	1.97	0.51	0.33	1.03	0.10
<i>Torchlight #8</i>	2.00	0.49	0.31	1.49	0.20
<i>Holbrook #HF-59</i>	2.03	0.51	0.32	0.84	0.06
<i>EQT #572357</i>	2.12	0.66	0.39	1.04	0.10
<i>Jayne Heirs #H1</i>	2.13	0.51	0.30	1.49	0.17
<i>EQT #572356</i>	2.09	0.51	0.31	1.06	0.10
Aristech #4, 678 ft	3.08	0.90	0.37	1.06	0.24
Aristech #4, 863.8 ft	2.32	0.76	0.43	1.07	0.30
Aristech #4, 1,025 ft	4.76	0.83	0.39	1.09	0.38
Aristech #4, 1,035 ft	1.56	0.48	0.42	1.09	0.22
Aristech #4, 1,432 ft	1.56	0.23	0.18	1.03	0.17
Moore #1122, 1,225.9 ft	1.83	0.59	0.40	1.13	0.15
Interstate #10, 2,460 ft	1.92	0.52	0.35	1.06	0.14
G. Roberts #1420, 1,558–1,563 ft	1.71	0.44	0.31	0.47	0.00
G. Roberts #1420, 1,740–1,763 ft	2.03	0.53	0.33	1.13	0.16
G. Roberts #1420, 2,339–2,358 ft	2.08	0.40	0.22	0.98	0.00
Columbia #20336, 2,449.4 ft	2.13	0.46	0.26	1.07	0.11
Columbia #20336, 2,704 ft	2.02	0.51	0.29	1.06	0.15
Columbia #20336, 3,400 ft	1.39	0.35	0.26	1.07	0.16
Ashland #3RS, 1,017 ft	1.41	0.44	0.41	1.13	0.13
Ashland #3RS, 1,181 ft	2.50	0.71	0.44	1.26	0.18
Ashland #3RS, 1,183 ft	1.39	0.50	0.49	1.14	0.17
Ashland #3RS, 1,402 ft	2.92	0.71	0.33	1.05	0.07
Columbia #20336, 2,704 ft	2.02	0.51	0.29	1.06	0.15
EQT #504353, 3,810 ft	5.19	0.97	0.23	1.19	0.09
EQT #504353, 4,560 ft	14.12	1.06	0.19	1.12	0.15
EQT #504353, 4,566.1 ft	7.34	0.95	0.22	1.24	0.08

Stable carbon isotope compositions (¹³C/¹²C) of whole oil and C₁₅ + saturate and aromatic hydrocarbon fractions were measured with an Isoprime vario-ISOTOPE select elemental analyzer and a VISION isotope ratio mass spectrometer (IRMS) (Table 3-10). Results are reported on a per mil basis relative to the Vienna Pee Dee Belemnite (VPDB) standard. Stable sulfur isotope compositions (³⁴S/³²S) of whole oil and NSO fractions were measured on the same system, with results reported relative to the Vienna Canyon Diablo Troilite (VCDT).

Column chromatography, GC-FID, GC-MS, and IRMS measurements were also run on oil samples from six wells in Greenup, Lawrence, Johnson, and Martin Counties (Fig. 3-2, Tables 3-6, 3-7, 3-8, 3-9, and 3-10). All wells produced oil only from the Berea Sandstone over a depth range of -260 to -1,191 ft (subsea). The measurements provided the opportunity to assess possible source correlation between the bitumen extracts and oils and compare thermal maturity. API gravity on the oils was measured by injecting 1 to 2 ml of oil into an Anton Par DMA 500 density meter using the "API Grav-

Table 3-8. Sterane and hopane biomarker ratios for oil (italics>) and extract samples. Measured sample depths for extracts provided after the well name. See Table 3-1 for depths of oil samples. %C27, %C28, and %C29 = relative percentage of $\alpha\beta$ 20S steranes, respectively; $C_{29} \alpha\alpha S/(S+R) = 5\alpha$ -stigmastane (20S)/5 α -stigmastane (20S + 20R); $C_{29} \beta\beta S/(\beta\beta S + \alpha\alpha R) = 5\alpha$, 14 β , 17 β -stigmastane (20S)/5 α , 14 β , 17 β -stigmastane (20S) + 5 α -stigmastane (20R); Dia = diasterane, stersterane; C27 Dia/ $\alpha\alpha$ Ster = 13 β , 17 α -diacholestane (20S)/5 α -cholestane (20R); Ga/Hop-gammacerane to 17 α , 21 β -30-homohopane (22S) ratio; norhop/hop-norhopane (17 α , 21 β -30-norhopane) to hopane (17 α , 21 β -hopane) ratio; Ts/(Ts+Tm) is 18 α , 21 β -22,29,30-trisnorhopane/Ts+17 α , 21 β -22,29,30-trisnorhopane; Ster/Hop-sterane to hopane ratio = ratio of 15 most common/abundant steranes ($m/z = 217$) to 16 most common hopanes ($m/z = 191$) (Andrusevich and others, 2000; MPI = methylphenanthrene index ($1.5 \times [3MP + 2MP]/[P + 1MP + 9MPI]$), where MP = methylphenanthrene (Radke and Welte, 1983).

Sample ID	%C ₂₇ $\alpha\alpha R$	%C ₂₈ $\alpha\alpha R$	%C ₂₉ $\alpha\alpha R$	C ₂₉ $\alpha\alpha$ S/(S+R)	C ₂₉ $\beta\beta$ S/ ($\beta\beta S + \alpha\alpha R$)	C ₂₇ Dia/ $\alpha\alpha$ Ster	Ga/Hop	norhop/hop	Ts/(Ts+Tm)	Ster/Hop	MPI
Addington Land Co. #20	30.2	22.7	47.1	0.97	1.60	7.21	0.19	0.30	0.82	2.29	0.70
Torchlight #8	30.7	23.0	46.3	1.02	1.70	7.25	0.18	0.31	0.83	2.31	0.69
Holbrook #HF-59	31.6	23.1	45.3	0.94	1.66	8.09	0.24	0.32	0.83	2.34	0.66
EQT #572357	31.1	21.9	47.0	0.91	1.50	5.86	0.15	0.33	0.80	1.95	0.61
Jayne Heirs #H1	32.0	22.7	45.4	0.91	1.50	8.18	0.19	0.35	0.82	2.21	0.67
EQT #572356	31.3	22.1	46.6	0.86	1.56	8.79	0.28	0.37	0.82	2.33	0.68
Aristech #4, 678 ft	27.3	23.1	49.6	0.35	0.22	0.64	0.39	0.72	0.29	2.94	0.52
Aristech #4, 863.8 ft	28.2	21.9	49.8	0.33	0.15	0.50	0.30	0.56	0.30	2.15	0.62
Aristech #4, 1,025 ft	34.3	21.2	44.5	0.32	0.22	0.64	0.31	0.66	0.32	2.31	0.55
Aristech #4, 1,035 ft	35.2	19.5	45.3	0.33	0.22	0.69	0.25	0.74	0.31	2.52	0.53
Aristech #4, 1,432 ft	39.1	21.9	39.0	0.60	0.56	0.71	0.40	0.57	0.38	1.97	0.58
Moore #1122, 1,225.9 ft	32.7	22.8	44.5	0.63	0.34	0.69	0.44	0.60	0.37	2.82	0.53
Interstate #10, 2,460 ft	28.9	23.5	47.6	1.02	1.38	4.56	0.20	0.39	0.68	1.14	0.60
G. Roberts #1420, 1,558-1,563 ft	35.3	22.9	41.9	0.52	0.32	0.68	0.59	0.56	0.39	2.03	0.58
G. Roberts #1420, 1,740-1,763 ft	29.0	21.1	49.9	0.59	0.36	1.03	0.21	0.54	0.41	1.54	0.62
G. Roberts #1420, 2,339-2,358 ft	35.5	19.6	44.8	0.63	0.43	1.30	0.15	0.55	0.54	0.61	0.69
Columbia #20336, 2,449.4 ft	29.3	21.7	49.1	1.04	1.34	3.80	0.26	0.35	0.66	1.00	0.52
Columbia #20336, 2,704 ft	31.3	21.2	47.5	0.93	1.47	5.17	0.22	0.34	0.68	1.20	0.48
Columbia #20336, 3,400 ft	32.9	25.3	41.8	0.81	1.37	3.65	0.27	0.42	0.75	1.51	0.46
Ashland #3RS, 1,017 ft	31.2	21.5	47.2	0.53	0.38	1.19	0.38	0.66	0.36	1.93	0.47
Ashland #3RS, 1,181 ft	35.0	20.2	44.8	0.54	0.49	1.66	0.27	0.65	0.41	1.76	0.52
Ashland #3RS, 1,183 ft	31.4	21.1	47.6	0.59	0.54	1.34	0.23	0.60	0.41	2.63	0.52
Ashland #3RS, 1,402 ft	37.1	22.4	40.5	0.59	0.53	1.63	0.26	0.64	0.41	1.28	0.49
EQT #504353, 3,810 ft	47.0	24.4	28.5	0.26	0.35	0.19	1.15	0.60	0.39	1.33	0.87
EQT #504353, 4,560 ft	42.5	26.0	31.5	0.30	0.40	0.52	0.32	0.83	0.40	0.71	0.98
EQT #504353, 4,566.1 ft	43.4	26.9	29.6	0.37	0.40	0.35	0.37	0.64	0.39	0.69	1.02

Table 3-9. Extended homohopane relative abundances, hopane and tricyclic terpane ratios. Measured sample depths for extracts provided after the well name. See Table 3-1 for depths of oil samples. C_{31} - C_{35} = relative abundance of C_{31} to C_{35} homohopanes (S+R); $C_{31}R/H = 17\alpha$, 21 β -30-homohopane (22R)/17 α , 21 β -hopane; $C_{26}/C_{25} = C_{26}(R+S)/C_{25}(R+S)$ homohopanes; $C_{35}S/C_{34}S$, $C_{35}S/C_{34}S$ homohopane ratio; C_{29}/C_{30} = 17a, 21b-30-norhopane/17a, 21b-hopane; C_{24}/C_{23} , C_{24}/C_{23} tricyclic terpane ratio; C_{22}/C_{21} , C_{22}/C_{21} tricyclic terpane ratio; $O/H = \text{oleanane}/17a$, 21b-hopane.

Well	Gas Type	C_1	C_2	C_3	iC_4	nC_4	iC_5	nC_5	C_6+	He	Ar	O_2	CO_2	N_2
ALC #20	OAG	62.38	13.40	13.69	1.360	4.290	0.595	0.602	0.331	0.0667	0.0083	0.043	0.028	3.02
Torchlight #8	OAG	74.43	8.66	5.92	0.513	1.460	0.225	0.225	0.138	0.291	0.0117	0.064	0.024	7.76
Holbrook #59	OAG	62.20	19.71	11.76	0.764	2.260	0.249	0.249	0.172	0.0904	0.0059	0.042	0.044	2.36
Jayne Heits #H1	OAG	74.02	12.16	6.59	0.519	1.430	0.186	0.180	0.141	0.149	0.0122	0.210	0.020	3.82
EQT #572356	OAG	74.66	10.83	6.43	0.621	2.080	0.403	0.468	0.408	0.158	0.0071	0.073	0.031	3.30
EQT #572357	OAG	76.09	11.93	6.35	0.526	1.560	0.208	0.214	0.178	0.115	nd	0.028	0.024	2.46
EQT KL #1915	NAG	76.58	14.97	5.35	0.326	1.030	0.137	0.162	0.139	0.0229	0.0054	0.100	0.028	0.78
EQT #504353	NAG	87.76	9.45	1.53	0.104	0.155	0.022	0.015	0.008	0.0237	nd	0.041	0.062	0.67

ity @60F" method. API measurements were done in triplicate to confirm accuracy and reproducibility.

Natural Gas—Molecular and Isotopic Composition

Samples of associated natural gas (OAG) were also collected at the aforementioned six oil wells. Samples of nonassociated gas (NAG) were collected from two wells, both of which produce only from the Ohio Shale in Pike County (Fig. 3-2). The OAG samples and the NAG sample from the EQT #504353 were collected from horizontal wells, and the vertical heights and their midpoints (in parentheses) represent the true vertical depths of the reservoirs from which the samples were collected (Table 3-1). In contrast, the NAG sample from the Justice #KL 1915 was collected from a vertical well, and the vertical height and midpoint represent the actual perforated depths. Most gas samples were collected at the meter using an Isotech pressure regulator and aluminum Isotubes. The Holbrook #59 sample was collected, however, from the annulus at the wellhead. Wellhead pressures ranged from 11 to 75 psi.

Molecular and isotopic measurements were conducted at Isotech Laboratories (Tables 3-11, 3-12). The molecular composition of hydrocarbon and fixed (e.g., CO_2 , N_2) gases was measured with two Shimadzu 2010 gas chromatographs, one of which contained a thermal conductivity detector (TCD) and flame ionization detector (FID), and the second, dual TCDs. Helium was used as a carrier gas, and reference gases were used for standardization. Reference samples were used on the first run of the day and every 10th sample. Peaks on the chromatogram were labeled and integrated using GC Solutions software. Measurement precision for individual gas species equals ± 2 mole percent. Carbon isotope measurements ($\delta^{13}C$) of methane were analyzed on a Picarro cavity ring down spectrometer (model G2201-i) equipped with a custom inlet system. Hydrogen isotopes (δ^2H) of methane were also measured on a Picarro cavity ring down spectrometer (model G228-i). Precision for the Picarro equals 0.1 per mil. Carbon isotope measurements of heavier hydrocarbon gases (ethane through butane) were done using a continuous flow system that consisted of an Agilent GC combustion unit interfaced with a Finnigan Mat Delta S or a Thermo Quest Finigan Delta Plus XL mass spectrometer. Isotopes for molecular nitrogen ($\delta^{15}N$) were done with a Thermo GC Iso-link coupled to a Thermo Delta V Plus via a Thermo ConFlo IV interface. Peak detection and quantification were done with Finnigan's Isodat software. Reference gases were measured at the start of each analysis sequence and afterward to make up 10 percent of all analyzed samples. Precision for $\delta^{13}C$ measurements by online continuous-flow gas-chromatography isotope-ratio mass spectrometry equals ± 0.3 per mil.

Table 3-10. Carbon isotopic composition of oils (italics) and bitumen extracts. Measured sample depths for extracts provided after the well name. See Table 3-1 for depths of oil samples. The $\delta^{13}\text{C}$ values are in per mil (‰) and referenced to VPDB.

Sample ID	$\delta^{13}\text{C}$ Saturate	$\delta^{13}\text{C}$ Whole Oil	$\delta^{13}\text{C}$ Aromatic
<i>Addington Land Co. #20</i>	-30.4	-30.3	-29.9
<i>Torchlight #8</i>	-30.5	-30.2	-29.8
<i>Holbrook #HF-59</i>	-30.4	-30.3	-29.8
<i>EQT #572357</i>	-30.7	-30.5	-30.0
<i>Jayne Heirs #H1</i>	-30.4	-30.3	-29.9
<i>EQT #572356</i>	-30.5	-30.3	-29.9
Aristech #4, 678 ft	-30.9		-31.0
Aristech #4, 863.8 ft	-30.3	-29.6	-29.4
Aristech #4, 1,025 ft	-30.0		-29.2
Aristech #4, 1,432 ft	-30.7	-30.1	-30.4
Moore #1122, 1,225.9 ft	-30.9	-30.2	-30.4
Interstate #10, 2,460 ft	-30.0	-29.7	-29.6
G. Roberts #1420, 1,558–1,563 ft	-29.4	-29.7	-30.8
G. Roberts #1420, 1,740–1,763 ft	-28.6	-28.6	-29.2
G. Roberts #1420, 2,339–2,358 ft	-29.8	-29.0	-30.4
Columbia #20336, 2,449.4 ft	-30.4	-30.0	-29.8
Columbia #20336, 2,704 ft	-30.3		-29.1
Columbia #20336, 3,400 ft	-29.9	-29.6	-29.4
Ashland #3RS, 1,017 ft	-30.7		-30.1
Ashland #3RS, 1,181 ft	-30.4		-30.1
Ashland #3RS, 1,183 ft	-30.7		-30.2
Ashland #3RS, 1,402 ft	-30.1		-29.8
EQT #504353, 3,810 ft	-29.1		-29.1
EQT #504353, 4,560 ft			-27.8
EQT #504353, 4,566.1 ft			-27.5

Table 3-11. Molecular composition of associated (OAG) and nonassociated (NAG) gases from the Berea Sandstone and Ohio Shale. See Table 3-1 for sample locations, depths, and stratigraphic units. Concentrations are in mole percent. C_1 = methane (CH_4); C_2 = ethane (C_2H_6); C_3 = propane (C_3H_8); iC_4 = iso-butane (C_4H_{10}); nC_4 = normal butane (C_4H_{10}); iC_5 = iso-pentane (C_5H_{12}); nC_5 = normal pentane (C_5H_{12}); C_6+ = hexane (C_6H_{14}); nd = not detected.

Well	Gas Type	C_1	C_2	C_3	iC_4	nC_4	iC_5	nC_5	C_6+	He	Ar	O_2	CO_2	N_2
ALC #20	OAG	62.38	13.40	13.69	1.360	4.290	0.595	0.602	0.331	0.0667	0.0083	0.043	0.028	3.02
Torchlight #8	OAG	74.43	8.66	5.92	0.513	1.460	0.225	0.225	0.138	0.291	0.0117	0.064	0.024	7.76
Holbrook #59	OAG	62.20	19.71	11.76	0.764	2.260	0.249	0.249	0.172	0.0904	0.0059	0.042	0.044	2.36
Jayne Heirs #H1	OAG	74.02	12.16	6.59	0.519	1.430	0.186	0.180	0.141	0.149	0.0122	0.210	0.020	3.82
EQT #572356	OAG	74.66	10.83	6.43	0.621	2.080	0.403	0.468	0.408	0.158	0.0071	0.073	0.031	3.30
EQT #572357	OAG	76.09	11.93	6.35	0.526	1.560	0.208	0.214	0.178	0.115	nd	0.028	0.024	2.46
EQT KL #1915	NAG	76.58	14.97	5.35	0.326	1.030	0.137	0.162	0.139	0.0229	0.0054	0.100	0.028	0.78
EQT #504353	NAG	87.76	9.45	1.53	0.104	0.155	0.022	0.15	0.008	0.0237	nd	0.041	0.062	0.67

Table 3-12. Stable isotopic composition of associated (OAG) and nonassociated (NAG) gases from the Berea Sandstone and Ohio Shale. See Table 3-1 for sample locations, depths, and stratigraphic units. Isotopic composition is reported on a per mil basis (‰) relative to VPDB for $\delta^{13}\text{C}$, VSMOW for $\delta^2\text{H}$, and atmospheric N_2 for $\delta^{15}\text{N}$. C_1 = methane (CH_4). C_2 = ethane (C_2H_6). C_3 = propane (C_3H_8). $i\text{C}_4$ = iso-butane (C_4H_{10}). $n\text{C}_4$ = normal butane (C_4H_{10}). $i\text{C}_5$ = iso-pentane (C_5H_{12}). $n\text{C}_5$ = normal pentane (C_5H_{12}). C_6^+ = hexane (C_6H_{14}). na = not analyzed.

Well	Gas Type	$\delta^{13}\text{C}-\text{C}_1$	$\delta^2\text{H}-\text{C}_1$	$\delta^{13}\text{C}-\text{C}_2$	$\delta^{13}\text{C}-\text{C}_3$	$\delta^{13}\text{C}-i\text{C}_4$	$\delta^{13}\text{C}-n\text{C}_4$	$\delta^{15}\text{N}$
ALC #20	OAG	-53.53	-249.0	-44.29	-37.10	-34.17	-34.37	-14.1
Torchlight #8	OAG	-53.55	-269.1	-44.79	-37.14	-33.95	-34.16	-17.4
Holbrook #59	OAG	-52.27	-267.9	na	na	na	na	-16
Jayne Heirs #H1	OAG	-51.96	-269.3	-42.58	-36.52	-34.04	-33.99	-5.2
EQT #572356	OAG	-51.40	-263.3	na	na	na	na	-17.1
EQT #572357	OAG	-51.37	-260.4	na	na	na	na	-16.6
EQT KL #1915	NAG	-50.59	-245.3	-42.27	-36.24	-33.7	-33.56	-9.1
EQT #504353	NAG	-46.14	-191.1	-34.22	-28.96	-28.08	-26.73	-9.5

4. Geochemistry Results

Cortland F. Eble, Paul C. Hackley, and T. Marty Parris

Total Organic Carbon and Sulfur

Total organic carbon contents vary between 0.3 and 21.6 weight percent (n=169). Whole-core averages indicate a general northwest to southeast decrease in TOC. For example, samples from northwesternmost counties (Scioto, Greenup, and Carter) have an average TOC of 7.9 percent, whereas samples from southeasternmost counties (Martin and Pike) have an average TOC of 4.8 percent (Fig. 4-1). TOC also varies among geologic units (members and beds) within the Sunbury and Ohio Shales. In descending order, average TOC values are as follows: Sunbury (9.5 percent), Lower Huron (6.6 percent), Cleveland (5.6 percent), Upper Hu-

ron (3.9 percent), Middle Huron (3.7 percent), and Three Lick Bed (2.2 percent).

Total sulfur content, from three core locations (Aristech #4, Skaggs-Kelly #3RS, and EQT #504353) varied from 0.6 to 6.6 percent, with an average value of 2.8 percent (n=79) (Table 3-2). Although sulfur forms (sulfate, sulfide, organic) were not tested for, pyrite was found to be ubiquitous and abundant during petrographic examination. Hence, it is probable that sulfide sulfur is a dominant form within the black shale. As with TOC, total sulfur is not uniformly distributed among geologic members and beds. In descending order, average total sulfur contents are as follows: Lower Huron

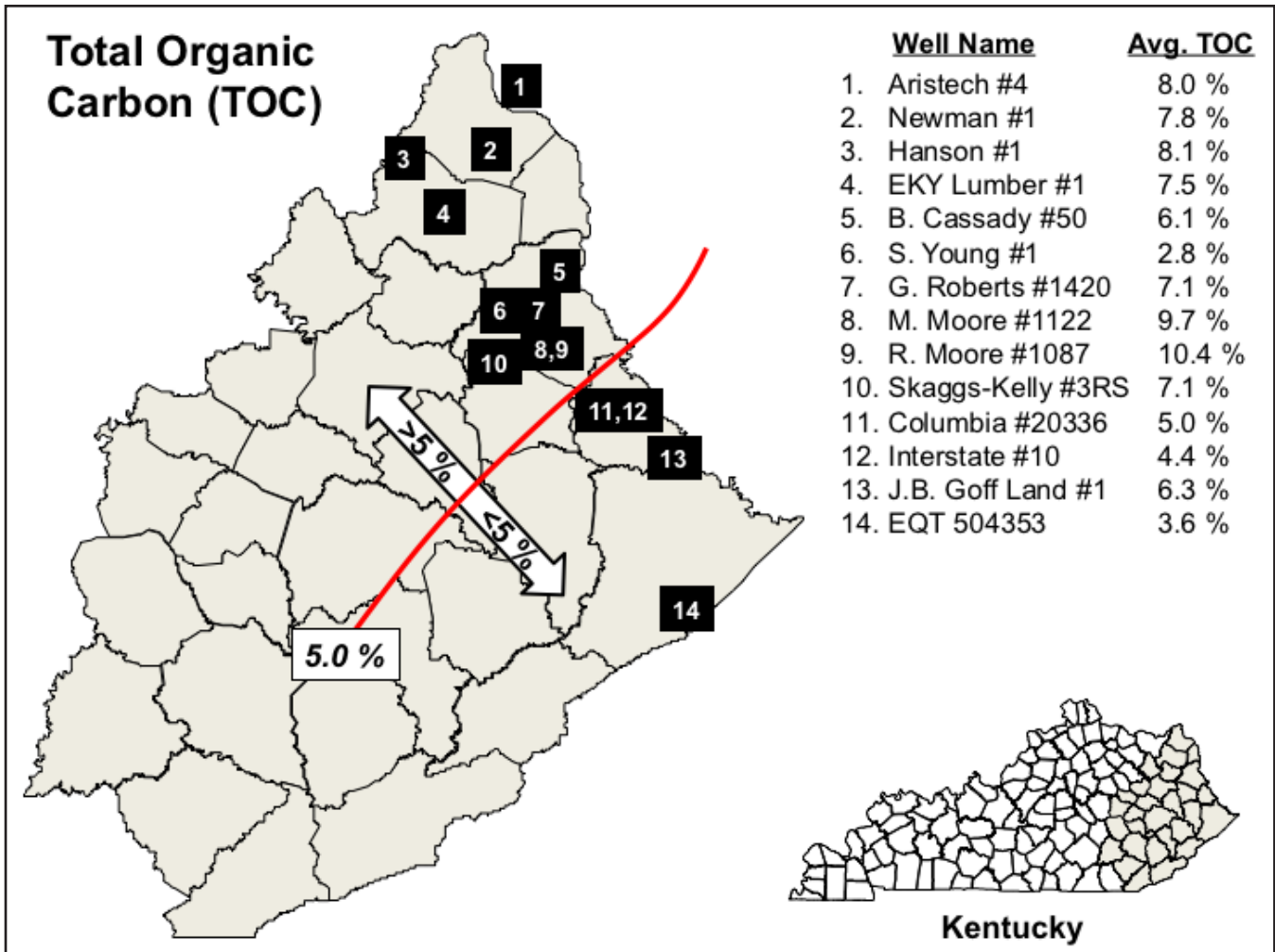


Figure 4-1. Distribution of TOC in the Ohio and Sunbury Shales. The red line is an approximate demarcation of wells with greater than 5 percent TOC and less than 5 percent average TOC.

(3.6 percent), Middle Huron (2.9 percent), Upper Huron (2.7 percent), Sunbury (2.1 percent), Cleveland (2.0 percent), and Three Lick Bed (1.5 percent) (Table 3-3).

Petrographic Composition

Collectively, the Ohio and Sunbury Shales are classified as marinites (Hutton, 1987; Rimmer and others, 1993), based on petrographic composition, which is dominantly liptinite macerals including alginite (telalginite, lamalginite, and *Tasmanites*), amorphinite, and bituminite (*sensu* Teichmüller, 1974) of marine origin. This is especially true for the Lower and Middle Huron Members of the Ohio Shale, which commonly have liptinite contents in excess of 80 percent of the organic matter by volume (Fig. 4-2). Amorphinite, in this report, describes a considerable amount of fluorescing

amorphous material associated with the inorganic (mainly clay minerals and quartz) groundmass. This type of fluorescing matrix has been described as an “organo-mineral association” or “fluorescent groundmass” by Robert (1981). Robert (1988) further noted that groundmass fluorescence disappears toward the end of the oil window, between reflectances of 0.8 and 1.2 percent. All of the macerals listed above are considered to be products, or byproducts, of algae.

Vitrinite and inertinite macerals occur throughout the Ohio and Sunbury Shales (Robl and others, 1987, 1991), and are more abundant in the Sunbury Shale and upper members of the Ohio Shale (Upper Huron, Three Lick Bed, and Cleveland) than in the Middle and Lower Huron Members (Fig. 4-2). Inertinite is more common than

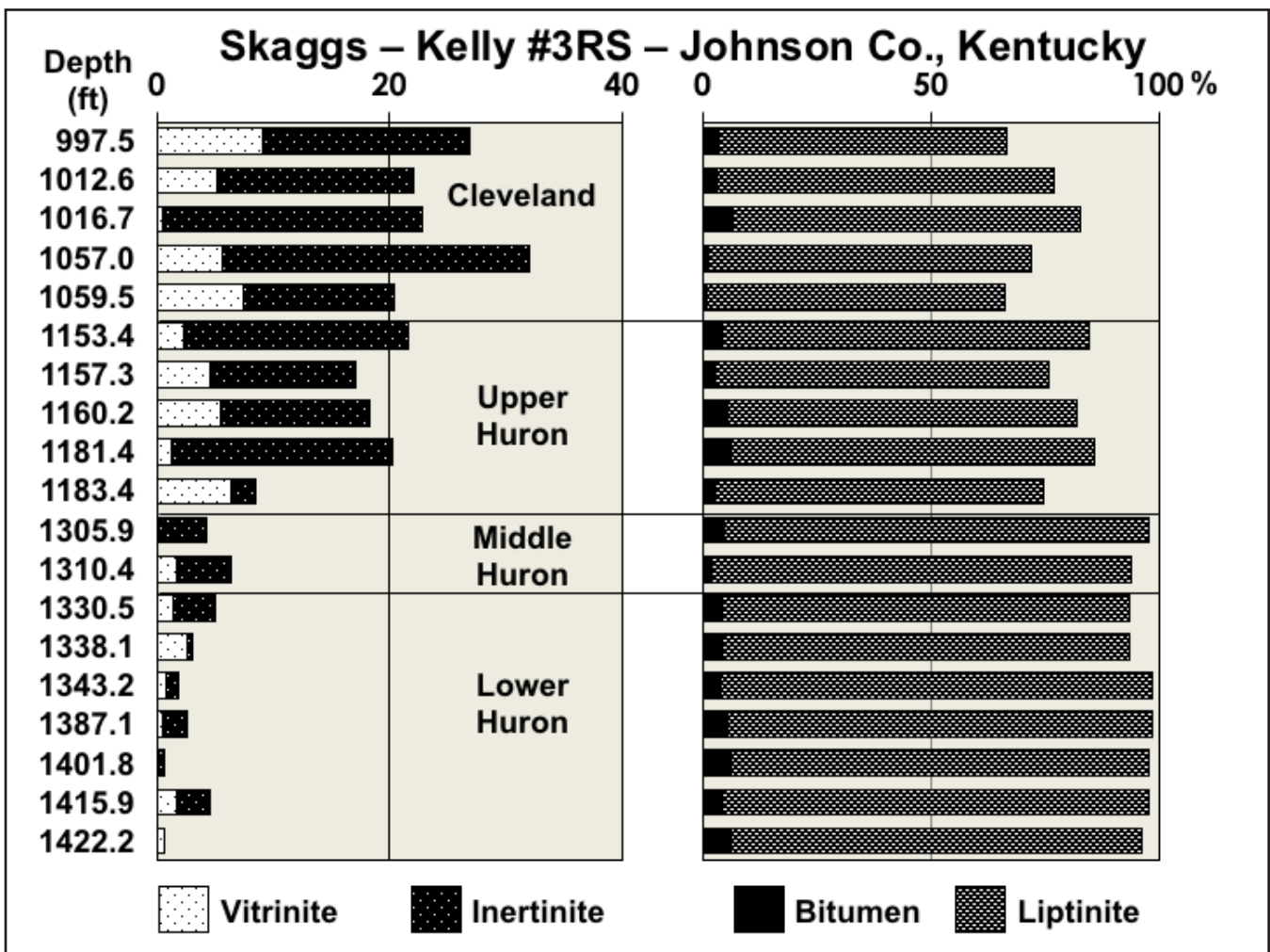


Figure 4-2. Maceral group distribution for the Skaggs-Kelly #3RS well. The Ohio Shale is dominated by liptinite macerals, with vitrinite and inertinite becoming more common in the Upper Huron and Cleveland Members.

vitrinite, and typically occurs as fusinite, semi-fusinite, and secretinite.

Vitrinite and inertinite are interpreted as “terrestrial” macerals, representing comminuted tissues of land plants. Their abundance in the Upper Huron through Sunbury Shale has been attributed to a glacial maximum, especially in the southern hemisphere, which occurred in the Late Devonian and Early Mississippian transition (Cecil and others, 2004; Ettensohn and others, 2009). The draw-down of global sea level during this time effectively provided additional land-mass area for plants to colonize (Algeo and others, 2001). As a result, more terrestrial organic detritus was introduced into the black-shale depositional system of the Ohio and Sunbury Shales. An increase in paleo-oxygen levels, and frequency of fire, toward the end of the Devonian is believed to have been a contributing

factor in the increase in inertinite observed in the youngest shale members as well (Rimmer and others, 2015).

Thermal Maturity and Vitrinite/ Solid-Bitumen Reflectance

Vitrinite-reflectance measurements (both measured VR_o and calculated equivalent VR_o from solid-bitumen reflectance measurements [Jacob, 1989]), from across the full burial and thermal-maturity spectrum in this study, range from about 0.5 to 0.6 percent at the northwest end of the transect, where samples occur at 420 to 1,830 ft, to about 1.2 to 1.3 percent at the southeast end, where samples occur between 3,705 and 4,607 ft (Table 3-2, Fig. 4-3). Other calculations to convert solid-bitumen and zooclast reflectances to vitrinite include those of Landis and Castaño (1995), Bertrand and

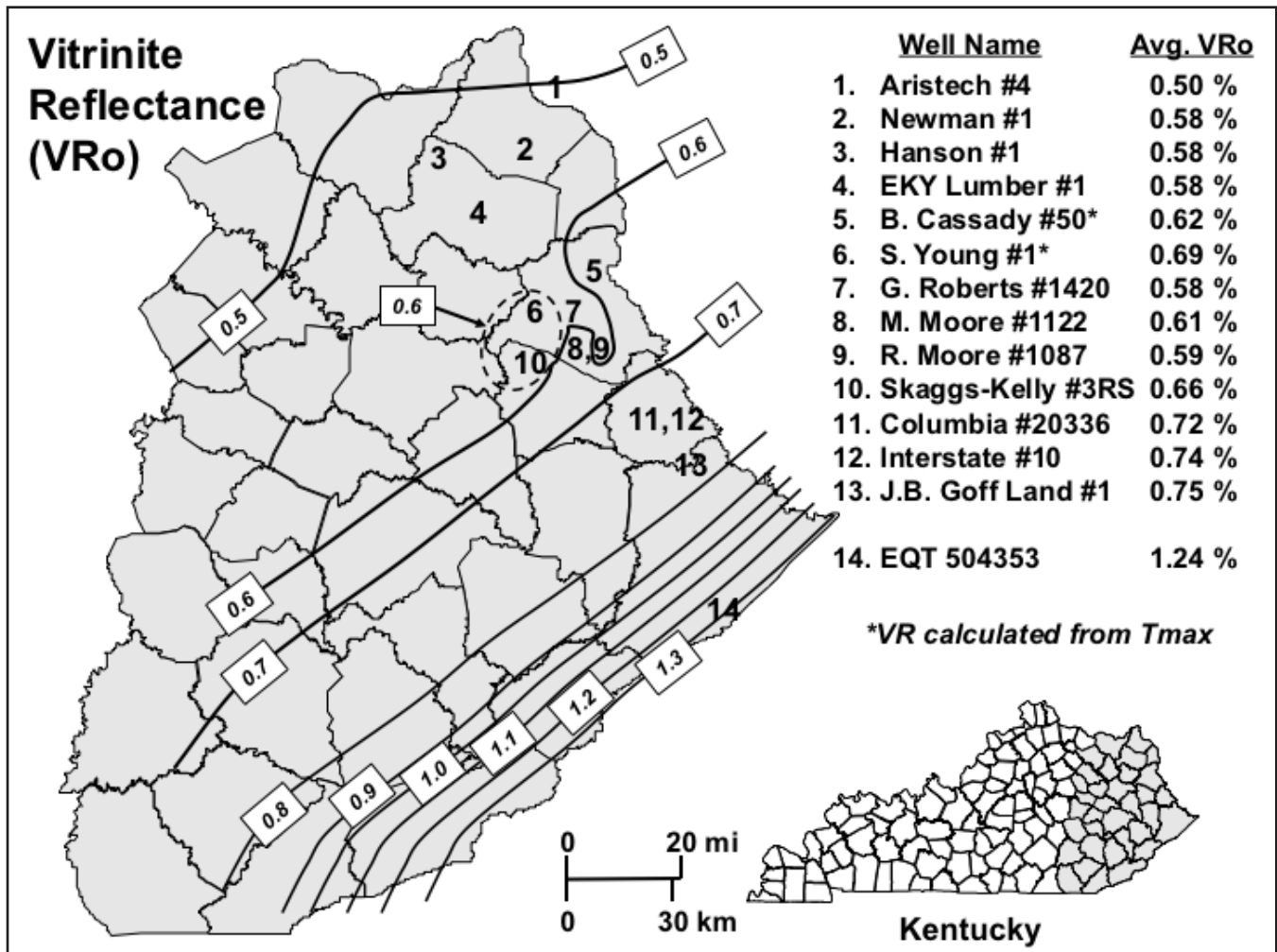


Figure 4-3. Vitrinite reflectance (VR_o) values.

Malo (2001), and Schoenherr and others (2007). An excellent summary of petrographic constituent conversion calculations is presented in Petersen and others (2013).

Programmed Pyrolysis— Rock-Eval II and HAWK

Programmed pyrolysis parameters useful for the determination of thermal maturity include T_{\max} and Production Index (PI) (Table 3-4). The use of T_{\max} as a maturation parameter has been reviewed by Tissot and Welte (1984, p. 443–447) and Tissot and others (1987). T_{\max} values of 430° to 455/460°C are generally regarded as defining the “oil window” of petroleum generation, with gas being the principal component from source rocks with T_{\max} values greater than 460°C. A commonly used T_{\max} to R_o percent conversion formula has been developed by Jarvie and others (2001), where:

$$R_o \text{ calculated} = (T_{\max} \times 0.018) - 7.16$$

(accurate if T_{\max} is greater than about 410°C)

The production index (PI), which is also referred to as the transformation ratio, is defined by the formula:

$$\text{Production Index (PI)} = S1 / (S1 + S2)$$

The threshold for oil generation occurs around a PI of 0.1 and continues through 0.4, beyond which point gas would be the main hydrocarbon phase (Peters, 1986; Peters and Cassa, 1994).

As with the reflectance measurements, T_{\max} and PI values increase in the northwest to southeast direction. Two wells (Aristech #4 and Hanson #1) from the northwestern part of the study area had average T_{\max} values of 421.6°C and 420°C, respectively, and average PI values of 0.06 for each well. Five wells from Lawrence County (G. Roberts #1420, S. Young #1, Cassady #50, M. Moore #1122, and R. Moore #1087) had average T_{\max} values of 428.9°C and an average PI of 0.08. In adjacent Johnson County, the Skaggs-Kelly #3RS well had an average T_{\max} of 432°C and average PI of 0.07. Farther to the southeast, two wells in Martin County (Columbia 20336 and Interstate #10) had an average T_{\max} value of 437.6°C and an average PI of 0.11. In Pike County, the EQT 504353 well (southeasternmost sample location) had an average T_{\max} of 444.7°C and average PI of 0.44 (Fig. 4-4).

Compared with T_{\max} and PI, hydrogen indices (HI) follow an opposite trend, decreasing from northwest to southeast. The Aristech #4 and Hanson #1 wells from the northwestern part of the study area had an average HI value of 556.1. The five wells from Lawrence County (G. Roberts #1420, S. Young #1, Cassady #50, M. Moore #1122, and R. Moore # 1087) had an average HI of 436.8. In adjacent Johnson County, the Skaggs-Kelly #3RS well had an average HI of 558.8. Farther to the southeast, two wells in Martin County (Columbia 20336 and Interstate #10) had an average HI of 349.4. In Pike County, the EQT 504353 well (southeasternmost sample location) had an average HI of 41.81 (Fig. 4-5).

Eighteen samples were analyzed by programmed pyrolysis in duplicate. One sample was analyzed in raw form and the other in solvent-extracted form. Solvent extraction is a common technique that is used to remove hydrocarbon material that may otherwise act to depress T_{\max} values (Clementz, 1979; Delvaux and others, 1990). Results were variable. Twelve samples showed a modest increase in T_{\max} temperatures of up to 8°C, five samples showed a decrease of up to 8°C, and one sample remained unchanged (Tables 3-5a, b). Some variability in the comparison of pre- and post-extracted sample data from programmed-pyrolysis analysis may result from using two different instruments; the Rock-Eval II instrument was used for pre-extracted samples, whereas the HAWK instrument was used for post-extracted samples. Because of instrumental differences, values for S1 and S3 in particular are not strictly comparable.

Thermal-Maturity Discussion

Many of the samples analyzed in this study have thermal-maturity parameters (R_o less than 0.6 percent, T_{\max} less than 430°C, PI less than 0.1) indicative of immature to marginally mature source rocks (Tissot and Welte, 1984; Peters, 1986; Tissot and others, 1987; Peters and Cassa, 1994; McCarthy and others, 2011). This is especially true for samples from the northern counties of Scioto (Ohio), Greenup, Boyd, Carter, and parts of Lawrence.

It has been suggested (Price and Barker, 1985; Barker, 1991) that vitrinite-reflectance measurements in shales rich in amorphous kerogen may be suppressed to some degree by retention of bitumen

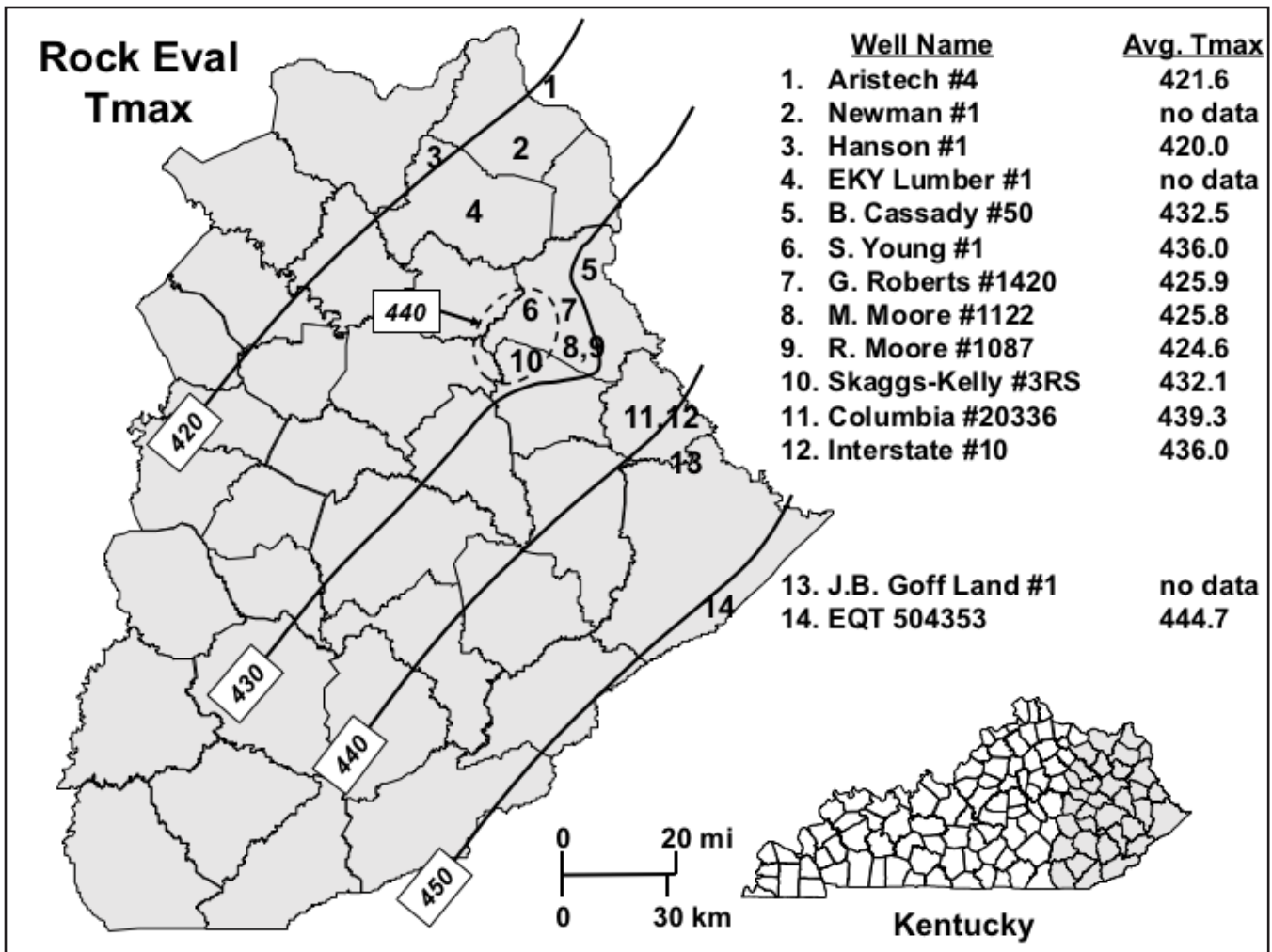


Figure 4-4. Rock-Eval thermal-maturity parameters, T_{\max} ($^{\circ}\text{C}$).

by vitrinite particles, so that the actual level of thermal maturity in the shales is higher than suggested by direct measurement. However, Barker and others (2007) examined raw and solvent-extracted samples and concluded that suppression by bitumen impregnation in the vitrinite maceral group, above the huminite stage of gelification, is typically negligible. Suppression of vitrinite reflectance has been suggested as a problem in several organic-rich shales, including the New Albany Shale in the Illinois Basin (Barrows and Cluff, 1984), organic-rich Miocene Modelo Formation of the Los Angeles Basin (Price and Barker, 1985), Mississippian-Devonian Bakken Shale of the Williston Basin (Price and others, 1984), alginite-rich coals and oil shales (Hutton and Cook, 1980; Kalkreuth and Macauley, 1987), and Pennsylvanian black shales with elevated amounts of liptinite macerals (Wenger and

Baker, 1987). Rimmer and Cantrell (1989) extrapolated an ideal conductive thermal gradient tied to measured vitrinite reflectance in Pennsylvanian coals (Hower and Rimmer, 1991), and suggested that the vitrinite reflectance of the Ohio Shale in eastern Kentucky has been suppressed by 0.3 to 0.5 percent R_o .

Reflectance suppression may be attributed to differences in organic material, different maturation pathways, or incorporation of hydrogen-rich components during accumulation, diagenesis, and maturation. It has been shown that, at the same rank, different vitrinite submacerals can have different reflectance levels (as much as 0.1–0.2 percent R_o) and chemical compositions (Brown and others, 1964; Sitler, 1979; Stach and others, 1982). In addition, Durand and others (1986) have suggested that low-reflecting vitrinite, found in marine se-

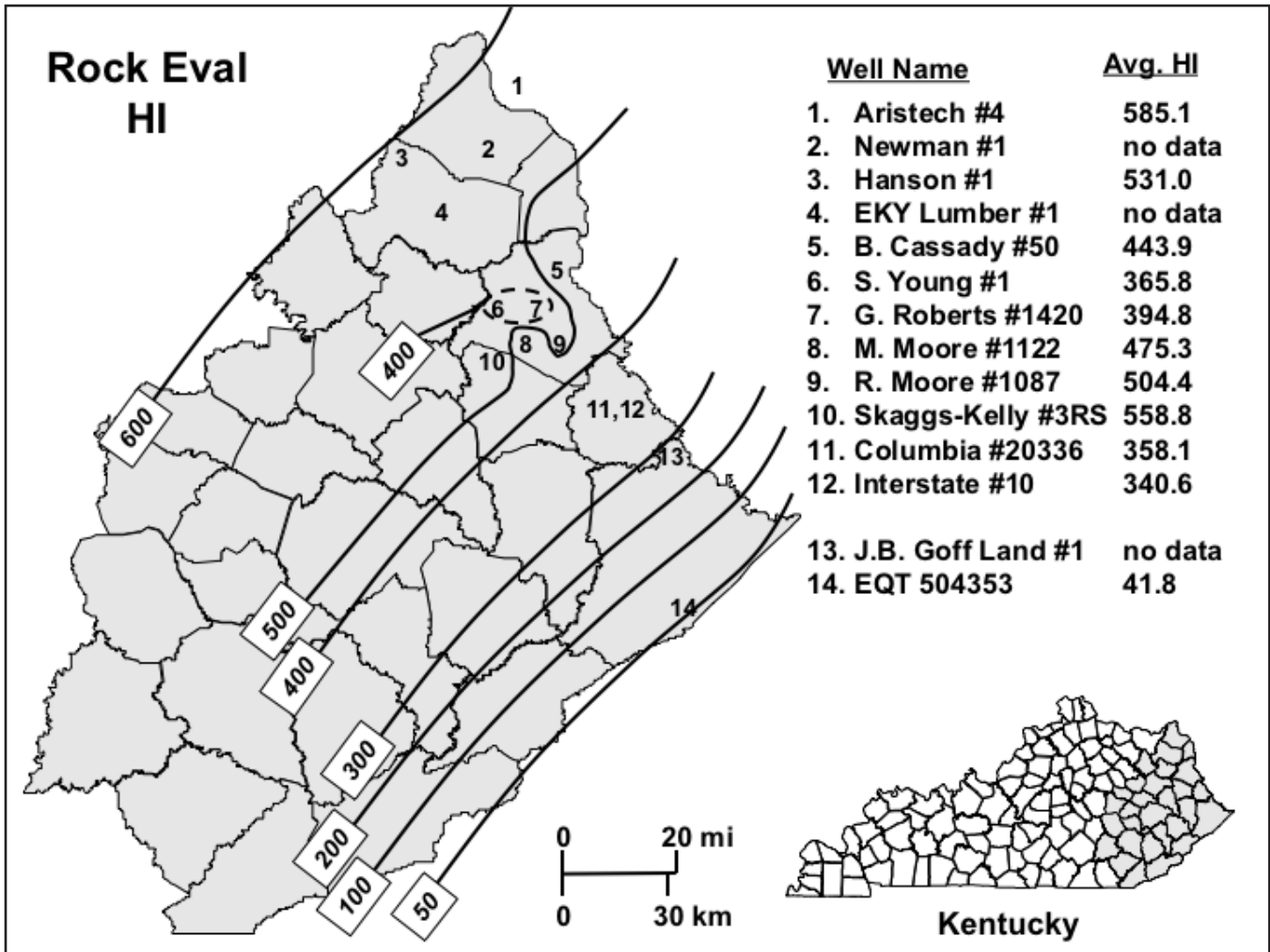


Figure 4-5. Rock-Eval HI indices.

quences associated with Type II kerogen, may not be derived from terrestrial plants.

In the present study, vitrinite-reflectance values were obtained for 100 samples at KGS, yet vitrinite is a minority component in most samples. Solid bitumen, which is more abundant in the Ohio and Sunbury Shales (collectively, “black” shales), was measured by USGS (solid-bitumen reflectance, BR_o) on 21 samples from seven wells, in which vitrinite reflectance (VR_o) was also measured (Table 3-2). Solid bitumen has a lower reflectance than vitrinite at reflectance levels of 1.05 percent and below, and attains a higher reflectance than vitrinite at reflectance levels greater than 1.05 percent. Jacob (1989) recognized this relationship and proposed the following conversion formula to convert solid-bitumen reflectance mea-

surements (BR_o) to equivalent vitrinite reflectance measurements (VR equivalent):

$$VR \text{ equivalent} = (BR_o \text{ measured} \times 0.618) + 0.4$$

(Jacob, 1989)

The comparative VR_o/BR_o data are summarized as follows:

Well ID (no. of samples)	Avg. VR _o Measured (percent)	Avg. BR _o Measured (percent)	Calculated VR Equivalent (percent)	VR _o Measured - VR Equiv.
Aristech #4 (6)	0.51	0.33	0.60	-0.09
Hanson #1 (1)	0.55	0.34	0.61	-0.06
R. Moore #1087 (2)	0.59	0.36	0.62	-0.03
M. Moore #1122 (2)	0.61	0.37	0.63	-0.02

Well ID (no. of samples)	Avg. VR _o Measured (percent)	Avg. BR _o Measured (percent)	Calculated VR Equivalent (percent)	VR _o Measured– VR Equiv.
Columbia #20336 (6)	0.72	0.58	0.76	–0.04
Interstate #10 (1)	0.74	0.44	0.67	+0.07
EQT #504353 (3)	1.23	1.43	1.28	–0.05

The average difference between the measured VR_o and calculated VR equivalent for the 21 samples is 0.05 percent, with a range of 0.02 to 0.09 percent. This indicates close agreement between the KGS and USGS laboratories using different sets of equipment. The results here contrast with a recent interlaboratory study of dispersed organics reflectance in which six samples indicated reproducibility limits (measurement difference for valid results between individual laboratories) ranging between 0.12 and 0.54 percent (Hackley and others, 2015).

Suppression of thermal-maturity indicators is not confined to vitrinite reflectance, but affects Rock-Eval T_{max} and PI as well (Price and Barker, 1985). Snowdon (1995) investigated the effects of T_{max} suppression and proposed that T_{max} is lowered 1°C for every increase in HI of 50 mg hydrocarbon/g TOC above a baseline HI of 100 to 150 for rocks with T_{max} values less than 453°C. For example, the M. Moore #1122, R. Moore #1087, and G. Roberts #1420 wells in Lawrence County have respective average T_{max} values of 425.8, 424.3, and 425.9°C, which correspond to calculated vitrinite-reflectance levels (from T_{max} values) of 0.50, 0.48, and 0.51 percent. All of these values are well below the 430°C/0.58 percent reflectance threshold for entrance to the oil window. If the hypothesis of Snowdon (1995) is correct, and T_{max} values are adjusted using the formula:

$$T_{\max} \text{ adjusted} = T_{\max} \text{ reported} + [(HI - 150)/50]$$

the M. Moore #1122, R. Moore #1087, and G. Roberts #1420 wells have adjusted T_{max} temperatures of 433, 430.6, and 429.8°C and calculated vitrinite-reflectance levels of 0.63, 0.59, and 0.58 percent, respectively. Whereas the reported T_{max} and VR calculated values for these wells indicate that they are thermally immature, the adjusted T_{max} and VR calculated values suggest placement in the lower

end of the oil window. Furthermore, the adjusted T_{max} values compare closely to the average measured vitrinite reflectance (VR_o) of 0.59, 0.61, and 0.58 percent for these wells (Table 3-4).

Two wells, located farther to the northwest, exhibit a similar relationship. The Hanson #1 well, located in Carter County, had a T_{max} of 420°C and calculated R_o of 0.40 percent, based on a single sample. The Aristech #4 well, located in Scioto County, Ohio, had an average T_{max} of 421.6°C, which corresponds to a calculated R_o of 0.43 percent. For each well, these values would suggest that organic material in the northwestern part of the study area is thermally immature. However, the adjusted T_{max} and adjusted R_o calculated values for the Hanson #1 well are 427.6°C and 0.54 percent, respectively. The measured VR_o for the Hanson #1 well is 0.58 percent. For the Aristech #4 well, the average adjusted values are 430.3°C and 0.59 percent, respectively. The average measured VR_o for the Aristech well is 0.5 percent, and the calculated VR_o equivalent from solid-bitumen reflectance (average 0.33 percent) is 0.6 percent. Collectively, these values indicate that the Hanson #1 and Aristech #4 wells may not be as thermally immature as indicated from the raw Rock-Eval II data. Collectively, thermal-maturity estimates based on adjusted HI levels and the reflectance levels indicate a closer proximity to the oil window for these wells and possibly for the northwestern portion of the study area.

Thermal-Maturity Summary

Total carbon (TC), total inorganic carbon (TIC), and total organic carbon (TOC) values were determined for 158 samples from 12 wells along a northwest-southeast transect extending from southern Ohio to southeastern Kentucky. In addition, 11 TOC measurements from two additional wells were donated by industry partners. TOC content decreases from northwest to southeast along the transect. TOC also varies among geologic units (members and beds) within the black shales. In descending order of TOC concentration, the average values are Sunbury (9.5 percent), Lower Huron (6.6 percent), Cleveland (5.6 percent), Upper Huron (3.9 percent), Middle Huron (3.7 percent), and Three Lick Bed (2.2 percent).

Vitrinite-reflectance analysis was performed on 100 samples; 21 of these samples were also ana-

lyzed for solid-bitumen reflectance. Reflectance values increase along a northwest-southeast trend, from 0.5 percent (immature) to about 1.3 percent (gas window). Vitrinite-reflectance values (VR_o) closely compare to solid-bitumen reflectance values when the latter are converted to vitrinite-equivalent values (VR_o equivalent), using the calculation of Jacob (1989).

T_{max} values from 47 Rock-Eval analyses showed an increase from 420°C to 444.7°C along the study transect, indicating an increase in thermal maturation from northwest to southeast. Production indices also increase from northwest to southeast, and vary between 0.03 and 0.34. Because of low-temperature shoulders on several S2 peaks, 18 samples were reanalyzed after solvent extraction. Twelve samples showed a modest increase in T_{max} up to 8°C, five showed a decrease of up to 8°C, and one sample was unchanged. Production indices remained the same, or were decreased by the solvent extraction process. Many T_{max} values, especially those from the northwestern part of the study area, indicate very low levels of thermal maturity. Adjusted T_{max} values, using a published formula (Snowdon, 1995) to account for excessive HI values, bring many of the T_{max} values into the lower part of the oil window. Calculated, adjusted T_{max} values were found to compare favorably with measured vitrinite-reflectance values (VR_o), and also with equivalent-vitrinite reflectance values calculated from solid-bitumen reflectance (BR_o) measurements.

Oil and Bitumen-Extract Bulk Chemistry

Berea-reservoired oils were sampled from six wells located in south-central Greenup County, south-southeast to northwest Martin County (Fig. 3-2). Bitumen extracts from 20 source-rock samples were obtained across the full thermal-maturity spectrum in the study area, ranging from immature (R_o less than 0.6 percent) in southeastern Scioto County, Ohio, to wet gas mature (R_o 1.1–1.4 percent) in south-central Pike County (Fig. 3-1, Table 3-1). Bitumen extracts were obtained from all of the black shales (Sunbury, $n=4$; Cleveland, $n=4$; Upper Huron, $n=5$; Lower Huron, $n=6$) proposed as potential source rocks for Berea oils.

Oil and extract bulk-chemistry results are compiled in Table 3-6. Overall, oil-sample API

gravity values ($n=6$) range from 35.4 to 42.4° (light crude), but occur in two sets with narrow ranges of 35.36–35.54° ($n=2$) and 40.30–42.43° ($n=4$). The two lower values of 35.35 and 35.54° are in the more-downdip, higher-maturity areas of Martin and Johnson Counties, respectively, and one was collected from the lease stock-tank in which loss of volatiles may have impacted the gravity measurement. No relationship was observed between API gravity values and sulfur concentrations.

Oil sulfur contents ($n=6$) are uniformly low, ranging from 0.17 to 0.21 weight percent (light sweet crude). Sulfur contents from bitumen extracts ($n=9$) are significantly higher, ranging from 0.50 to 7.53 weight percent. The highest extract sulfur content occurs in the Lower Huron sample from the low-maturity Aristech well.

Column Chromatography

Fractionation results from gravimetric-column chromatography of oil samples show a dominant saturate component ranging from 47.9 to 52.0 weight percent, followed by aromatics ranging from 35.7 to 40.3 weight percent, and resins plus asphaltenes ranging from 9.5 to 15.7 weight percent. Saturate to aromatic ratios range from 1.2 to 1.4. Values are tightly clustered in the bulk-composition ternary plot, whereas bitumen extract samples show a much broader range of values with a higher resins plus asphaltenes component (Fig. 4-6). Upper Huron bitumen-extract values ($n=5$) show the most uniform distribution, although these source rocks range from immature ($R_o=0.50$ percent) to early oil window ($R_o=0.75$ percent). The Lower Huron extract samples show the greatest range in composition; the most downdip high-maturity samples from Pike County contain the highest saturate proportion at 42.8–59.2 percent, which is similar to Berea oil samples.

Gas Chromatography (GC-FID)

Chromatograms of oil samples reveal similar n -alkane envelopes and acyclic isoprenoid concentrations, with minor exceptions. Distributions of n -alkanes are unimodal, with maxima toward the low carbon numbers (n -alkanes less than C_{15} equals 42.4 to 51.2 weight percent) and a steady decrease in peak height with increasing carbon number (Fig. 4-7). Peak height maxima are at n - C_5 , except for the previously mentioned wells with lower API

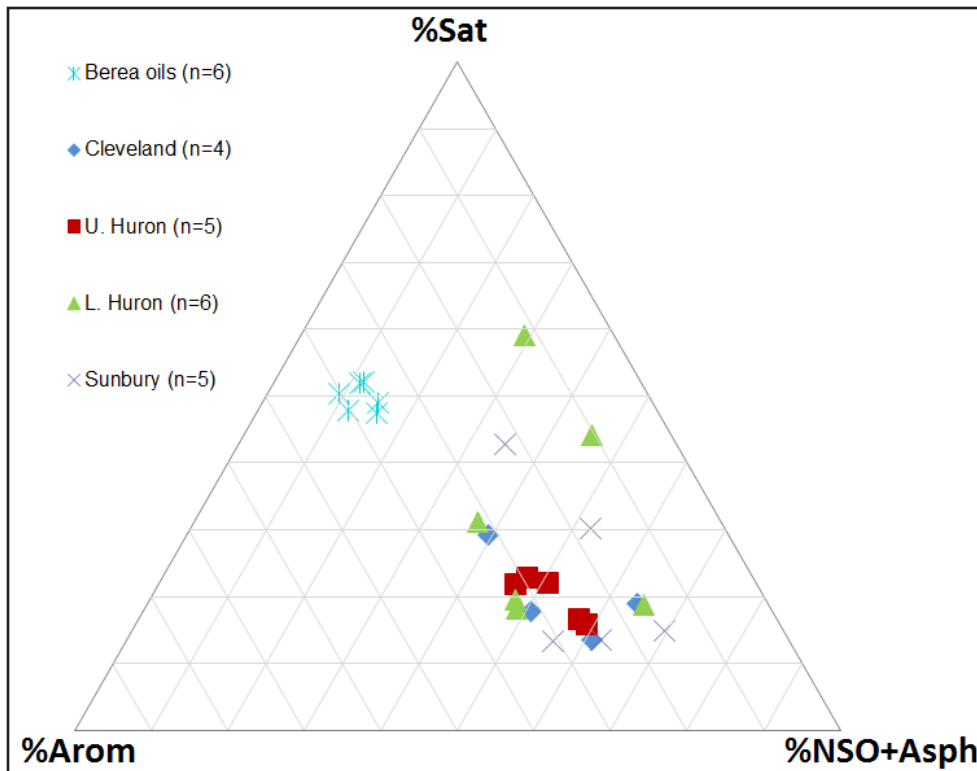


Figure 4-6. SARA results from liquid chromatography.

gravity values in which loss of light ends is apparent and maxima are at $n\text{-C}_8$. High CPI values in samples from Torchlight #8 and Jayne Heirs #H1, which both have carbon preference index (CPI) values of 1.49 (Table 3-7), may be indicative of possible contamination from high-molecular-weight phthalate plasticizers, which shows up near elution of C_{27} (Fig. 4-7). Chromatograms from bitumen extracts are more variable than for crude oils, but generally unimodal with maxima at $n\text{-C}_{15-17}$ (Fig. 4-8; showing extract chromatograms from the updip Aristech #4, which are least affected by thermal maturation). Bitumen-extract chromatograms also show possible contamination from high-molecular-weight phthalate plasticizers, as indicated by the unlabeled peaks in Figure 4-8. A slight secondary maxima may be present over an unresolved complex mixture (UCM) at $n\text{-C}_{29-31}$. Pristane to phytane ratios (Pr/Ph) for oil and bitumen extracts generally range from 1.4–3.1, with several higher outlying values greater than 4.7 from bitumen extracts (Table 3-7). The outlier Pr/Ph values are from bitumen extracts from the high-maturity EQT #504353 well in Pike County at the southernmost end of the study area. Oil samples show uni-

form Pr/Ph ratios, with all six samples ranging from 1.97 to 2.13. Isoprenoid to alkane ratios Pr/ $n\text{-C}_{17}$ and Ph/ $n\text{-C}_{18}$ for oil and bitumen extract samples plot in the mixed terrigenous-marine organic matter area of the discrimination diagram (Fig. 4-9) (Shanmugam, 1985; Hunt, 1996). Oils are tightly clustered; bitumen extracts show greater variability, but generally plot closely to oil samples. Crude-oil and bitumen-extract samples exhibit little to no evidence of biodegradation, as confirmed through absence of UCM, low Pr/ $n\text{-C}_{17}$ and Ph/ $n\text{-C}_{18}$ ratios, and the consistency of n -alkane envelopes. High Pr/ $n\text{-C}_{17}$ ratios in the three samples

from the high-maturity EQT #504353 well are suspect and may be impacted by analytical difficulties associated with the higher maturity (lower signal-to-noise) or possible co-elution of contaminant phases, as indicated by a number of unresolved minor peaks near $n\text{-C}_{17}$ and $n\text{-C}_{18}$.

Carbon-Isotopic Composition

Whole-oil and extract carbon-isotopic values are compiled in Table 3-10, along with carbon-isotope values from saturate and aromatic fractions. When the carbon-isotopic values are discriminated in a Sofer-type plot (Sofer, 1984), all values plot in the marine sector (Fig. 4-10). Berea oil samples are tightly clustered within a narrow range of about 0.28 per mil in the saturate component and 0.19 per mil in the aromatic component. Source-rock bitumen extracts show a broader range of carbon-isotopic compositions, but plot close to the Berea oils. All samples are depleted relative to an average distal marine-shale source-rock composition computed from 1,925 global saturate-aromatic carbon isotopic pairs contained in the GeoMark (2015) database (filtered by known distal marine-shale dep-

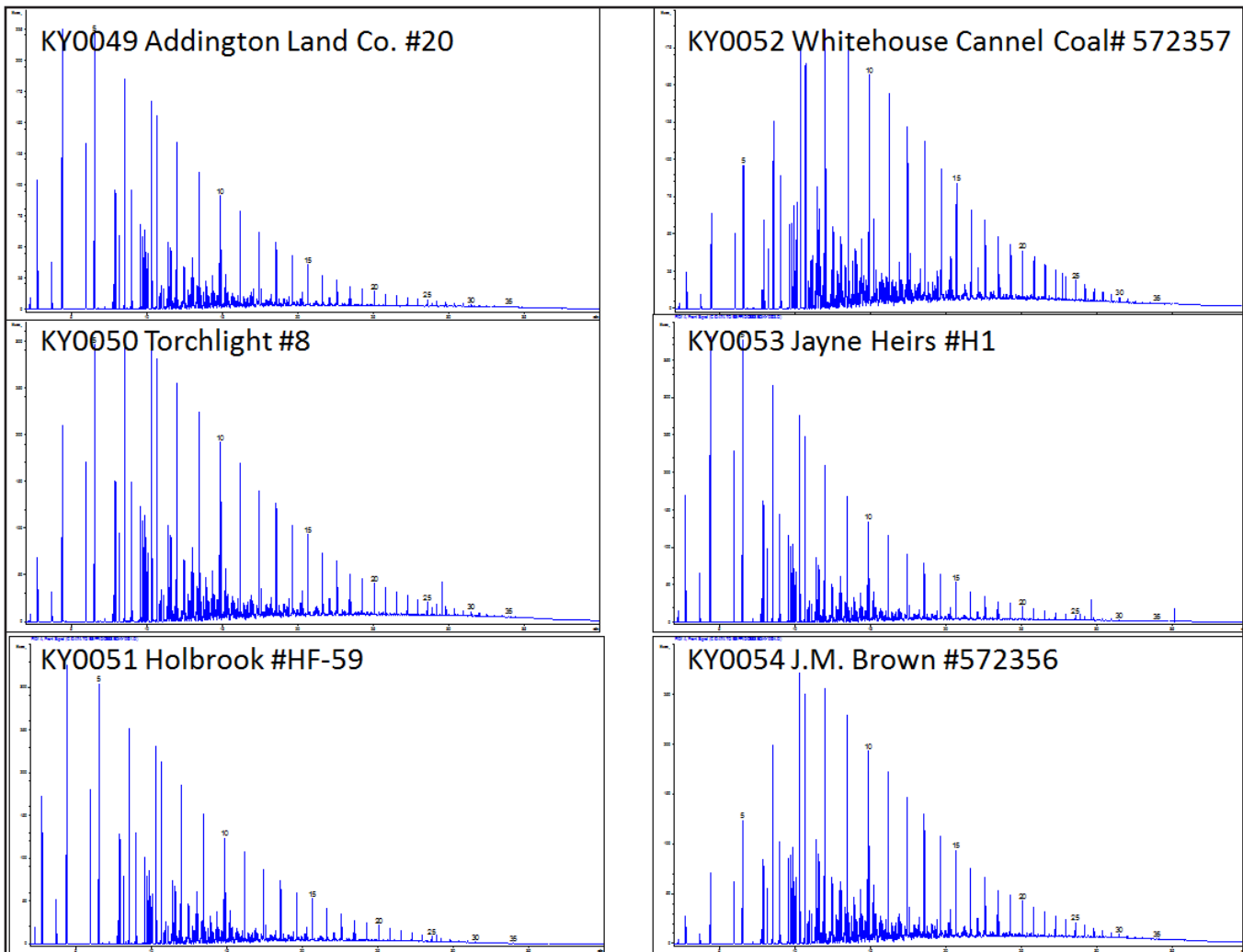


Figure 4-7. Oil chromatograms from gas chromatography. Numbers indicate number of carbon atoms. The unusual high molecular-weight peaks visible in the chromatogram from sample KY0053 Jane Heirs #H1 probably are contamination from phthalate plasticizers.

ositional environment, low to moderate thermal maturity, and nonbiodegraded). On the Galimov-type plot (Stahl, 1978), the six oil samples also are tightly clustered, showing increasing enrichment in ^{13}C with increasing fraction polarity (Fig. 4-11). Source-rock bitumen extracts show more variability; six of nine samples are enriched relative to oils in the saturate and whole-oil fraction, but three of these samples (cuttings) show relative depletion in the aromatic fraction. These three samples contain the lowest proportion of aromatics according to column-chromatography results. Saturate and aromatic fractions in two bitumen extracts (from core) are slightly depleted relative to Berea oils. Four bitumen-extract samples show similar pat-

terns to the oils, with enrichment increasing with compound polarity.

Biomarker Characterization from Gas Chromatography–Mass Spectrometry (GC-MS)

Sterane and hopane biomarker ratios from GC-MS analysis of crude oils and bitumen extracts are compiled in Table 3-8. Previous work by Cole and others (1987) did not identify sterane and hopane compounds in oil samples from eastern Ohio, which they speculated was due to advanced thermal maturity. However, more recent work by Hackley and others (2013) obtained robust biomarker results from eastern Ohio Devonian shales, and the current study obtained mass

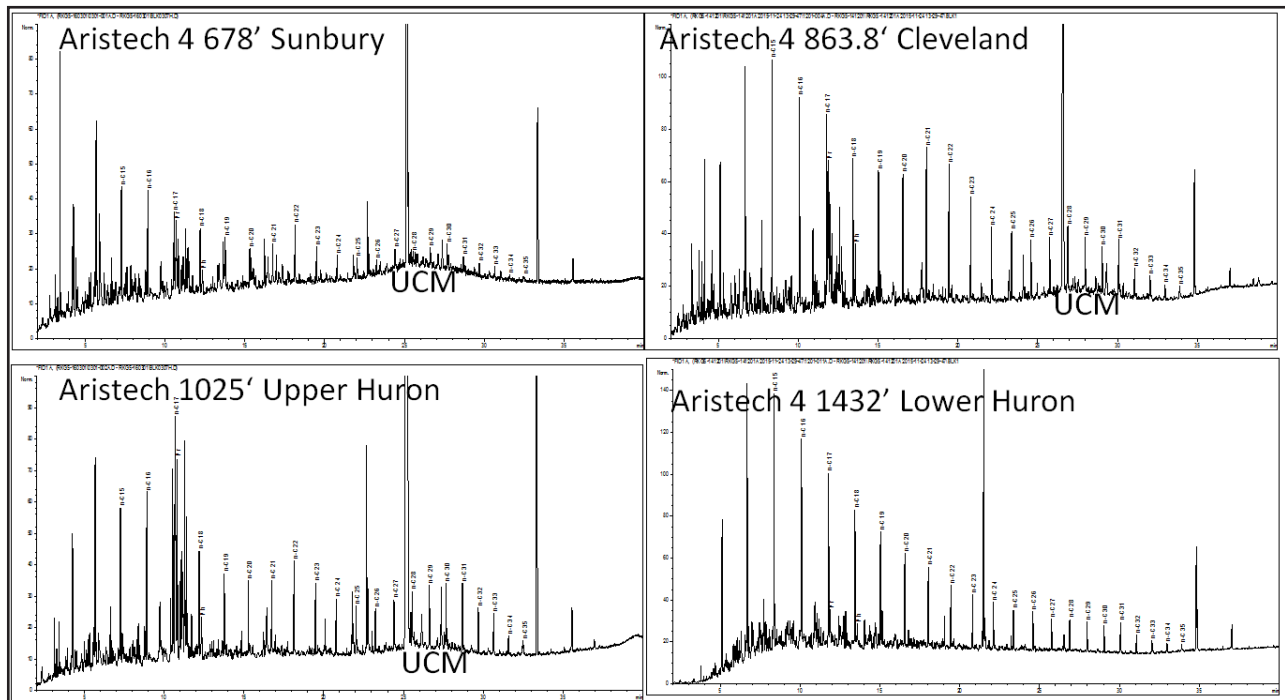


Figure 4-8. Bitumen-extract chromatograms from gas chromatography of the “immature” Aristech samples. UCM=unresolved complex mixture. The cluster of peaks near *n*-C₁₇ in the Aristech 4 at 1,025 ft Upper Huron sample is possibly from an unknown contaminant, whereas the unlabeled high-molecular-weight peaks in all four chromatograms probably are contamination from phthalate plasticizers.

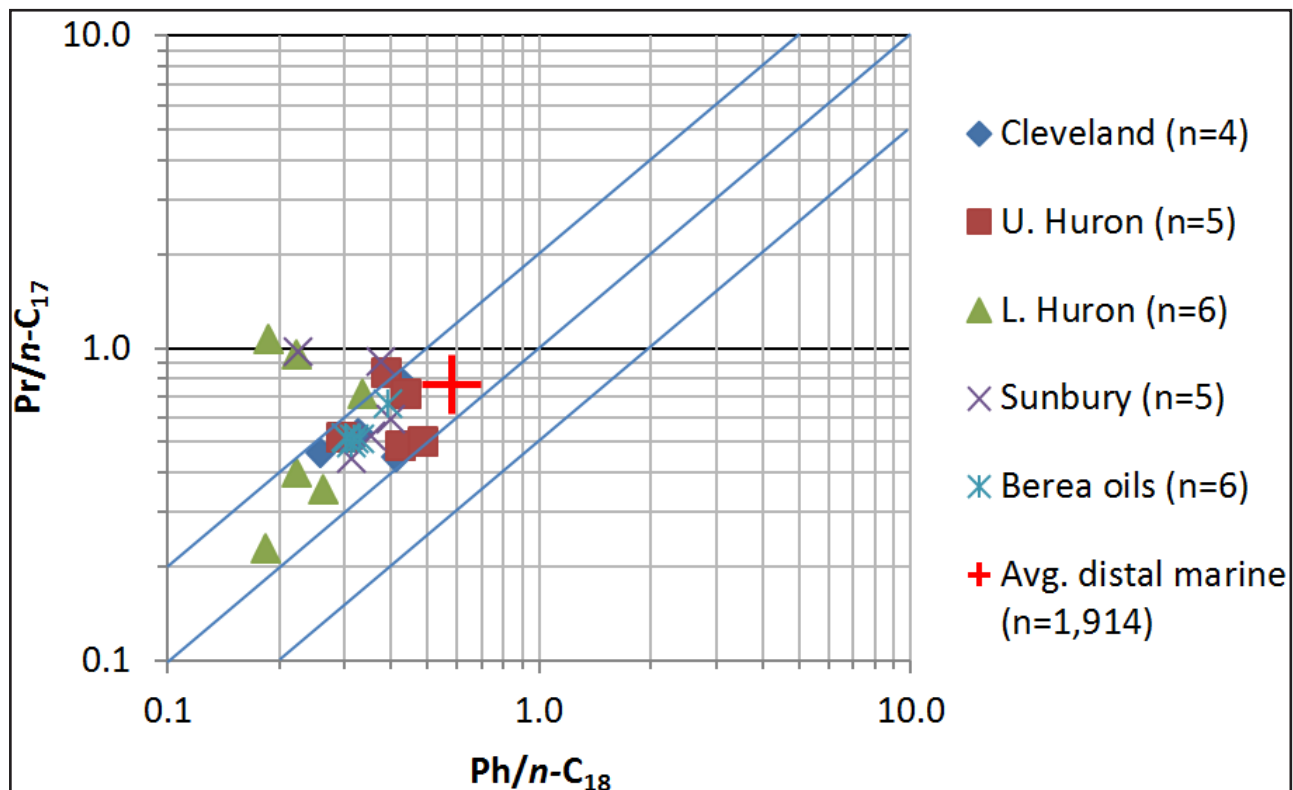


Figure 4-9. $Pr/n-C_{17}$ and $Ph/n-C_{18}$ discriminant plot. Average distal marine shale from GeoMark (2015). Organic source fields and process directions after Shanmugam (1985).

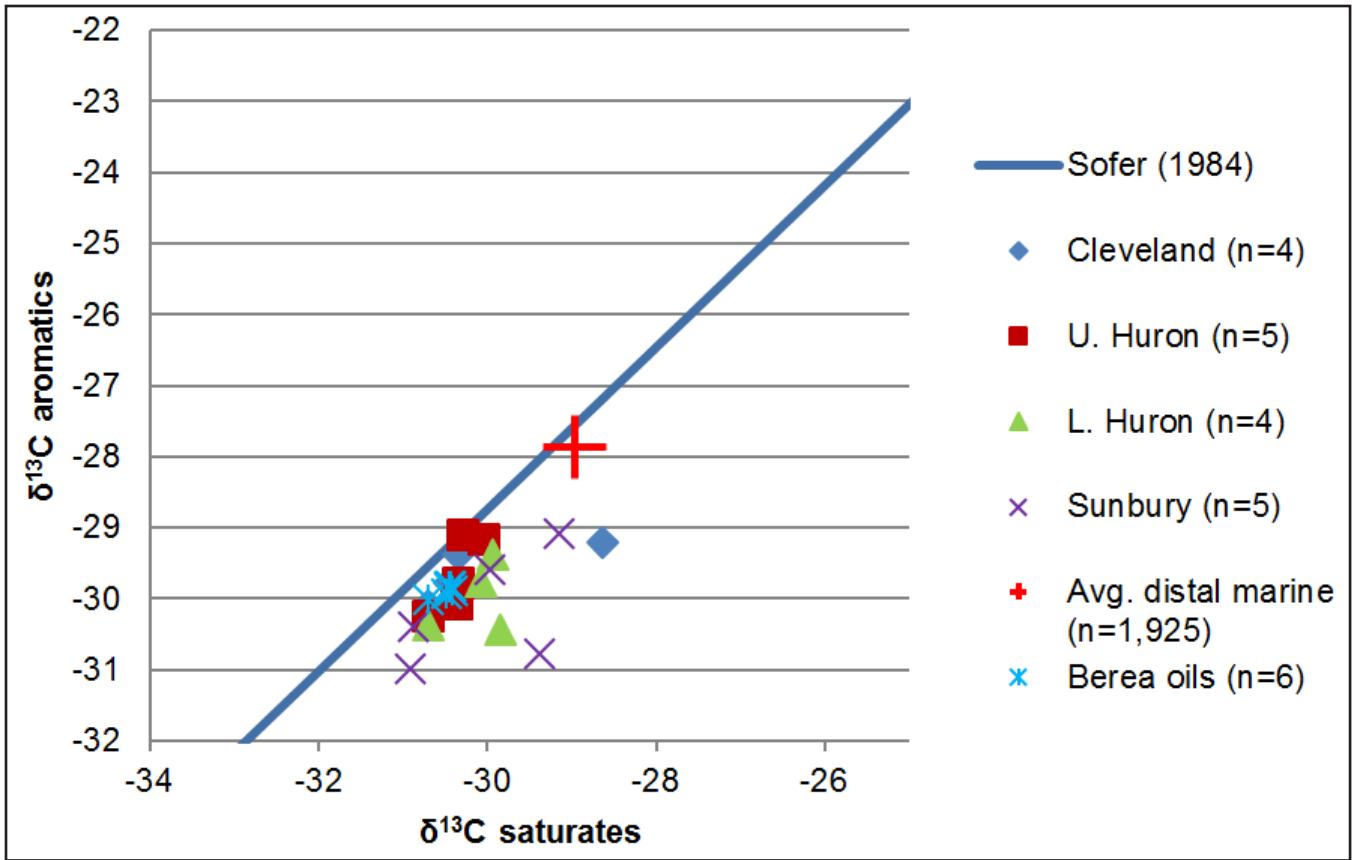


Figure 4-10. Sofer-type plot of $\delta^{13}\text{C}$ isotopic composition (Sofer, 1984). Average distal marine shale from GeoMark (2015).

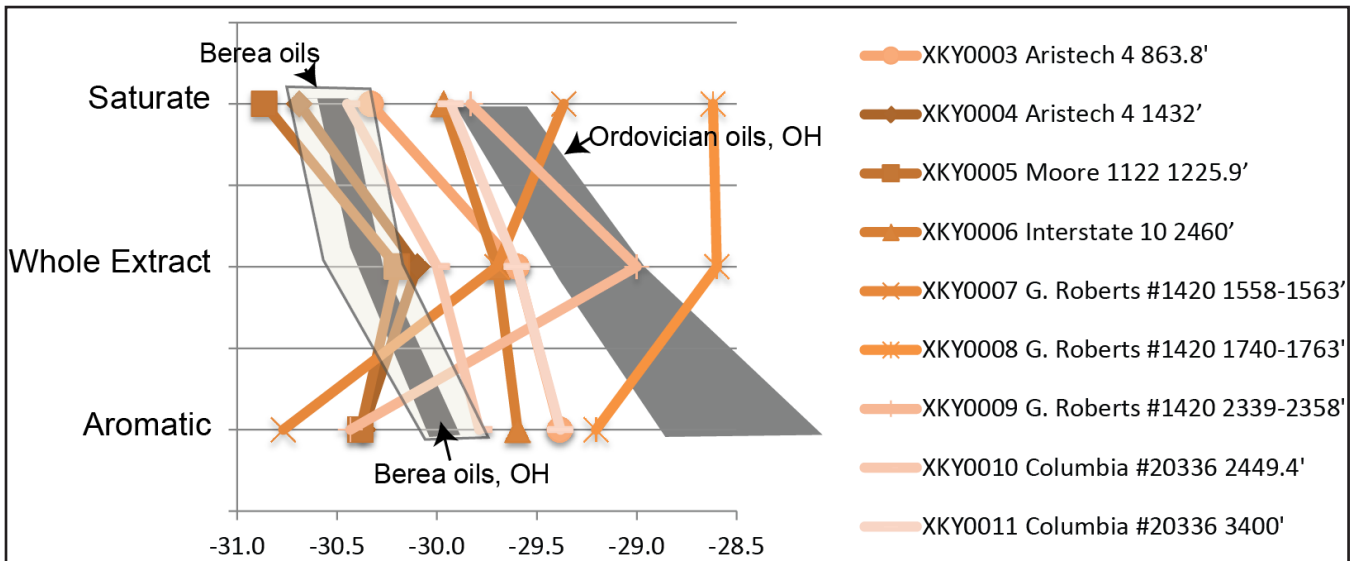


Figure 4-11. Galimov-type plot of $\delta^{13}\text{C}$ isotopic composition. Data for Berea and Ordovician oils from Ohio are from Cole and others (1987).

fragmentograms from all crude-oil and bitumen-extract samples. Bitumen-extract fragmentograms are illustrated in Figure 4-12 for the low-maturity Aristech well; chromatographic column bleed (the signal generated by column stationary phase bleeding out of the column) is suggested by rising baselines (Peters and others, 2005) in many of the m/z 191 fragmentograms. Column bleed in the m/z 191 fragmentograms is particularly evident in the high-maturity extracts from the downdip Pike County EQT #504353 well (not shown in Figure 4-12).

Normal sterane ($\alpha\beta\beta S$) distributions are shown in Figure 4-13. Crude oils and bitumen extracts are tightly clustered, with the exception of three extracts from the high-maturity EQT #504353 in Pike County. Samples are enriched in the C_{29} terrigenous component and depleted in the C_{28} marine component relative to an average distal marine shale computed from the GeoMark (2015) database ($n=1,924$; see above for description of data filtering).

Crude oils show a strong relationship between concentrations of individual sterane and hopane compounds (Table 3-9). For example, concentrations of $C_{30}H(17\alpha, 21\beta\text{-hopane})$ are strongly correlated to $5\alpha, 14\beta, 17\beta\text{-cholestane (20R)} + 13\beta, 17\alpha\text{-diastigmastane (20S)}$ ($R^2=0.96$; Fig. 4-14), $17\alpha, 21\beta\text{-30-homohopane (22S+22R)}$ to $13\beta, 17\alpha\text{-diacholestane (20S+20R)}$ ($R^2=0.94$; Fig. 4-14), and $Tm\ 17\alpha, 21\beta\text{-22,29,30-trisnorhopane}$ to $5\alpha\text{-stigmastane (20S)}$ ($R^2=0.92$; Fig. 4-14). These relationships are consistent with the Berea oil samples being from a single family of oils, with slight variations in thermal maturity (Peters and others, 2005). Figure 4-14 shows only a subset of individual correlated sterane and hopane compounds; other sterane and hopane molecules show similar strong correlations. The strong correlations present in their concentrations also suggests that ratios of individual hopanes and steranes will remain relatively constant among Berea oils.

$C_{31}\text{-}C_{35}$ homohopane distributions also are very similar among the oil samples (Fig. 4-15, Table 3-11), also implying a genetic relationship (Peters and others, 2005). C_{35} hopane was not detected in the EQT #572356 or Jayne Heirs #H1 wells in Johnson County. Compared to Berea oils, homohopane distributions in source-rock bitumen extracts

generally show higher concentrations of C_{31} , lower concentrations of $C_{32\text{-}33}$, lower to similar concentrations of C_{34} , and similar concentrations of C_{35} . With minor exceptions as illustrated in Figure 4-15, the average values of homohopane relative abundances are very similar for the different source-rock candidate bitumen extracts and also similar to the Berea oils.

Oil and Bitumen-Extract Discussion

Oil Correlation. The crude-oil samples are essentially identical in bulk composition, with very narrow ranges of values for API gravity, sulfur, SARA fractions (Fig. 4-6), and the carbon-isotopic compositions of the whole oil and its fractions (Fig. 4-11). The similarity in oil properties suggests all crude-oil samples came from the same or a similar source. Further supporting this interpretation is the strong positive correlation between individual sterane and hopane concentrations (Fig. 4-14) and similarity in extended hopane concentrations (Fig. 4-15). Based on these observations, we conclude oils reservoirized in Berea siltstones from Greenup County southeast to Martin County originated from the same or from similar source rocks. The Berea oils studied herein are identical in carbon-isotopic composition to Berea-reservoirized crude oils in eastern Ohio (Fig. 4-11) studied by Cole and others (1987).

Sources of Organic Matter. Unimodal n -alkane distributions in oils with predominance of less than C_{15} components are consistent with a marine organic-matter source (Blumer and others, 1971), as known from the geology of the Devonian-Mississippian section in the study area (e.g., Ettensohn and Elam, 1985; Pashin and Ettensohn, 1987). Pr/Ph ratios of 1.97-2.13 are consistent with a marine oil source and with low terrestrial-aquatic ratios $[(n-C_{27} + n-C_{29} + n-C_{31}) / (n-C_{15} + n-C_{17} + n-C_{19})]$ (Bourbonniere and Meyers, 1996) of 0.06-0.20. CPI values of about 1 in immature bitumen extracts from the Aristech well, and the n -alkane maxima centered at C_{15-17} also are consistent with a dominant marine component to the organic matter, as these characteristics would otherwise be suggestive of higher-maturity organic matter. Overall, the CPI values generally range from 1.0 to 1.15 for most bitumen extracts, also consistent with a marine organic-matter source. Minor C_{27-31} peaks in bitumen extracts may be contaminants or may reflect the

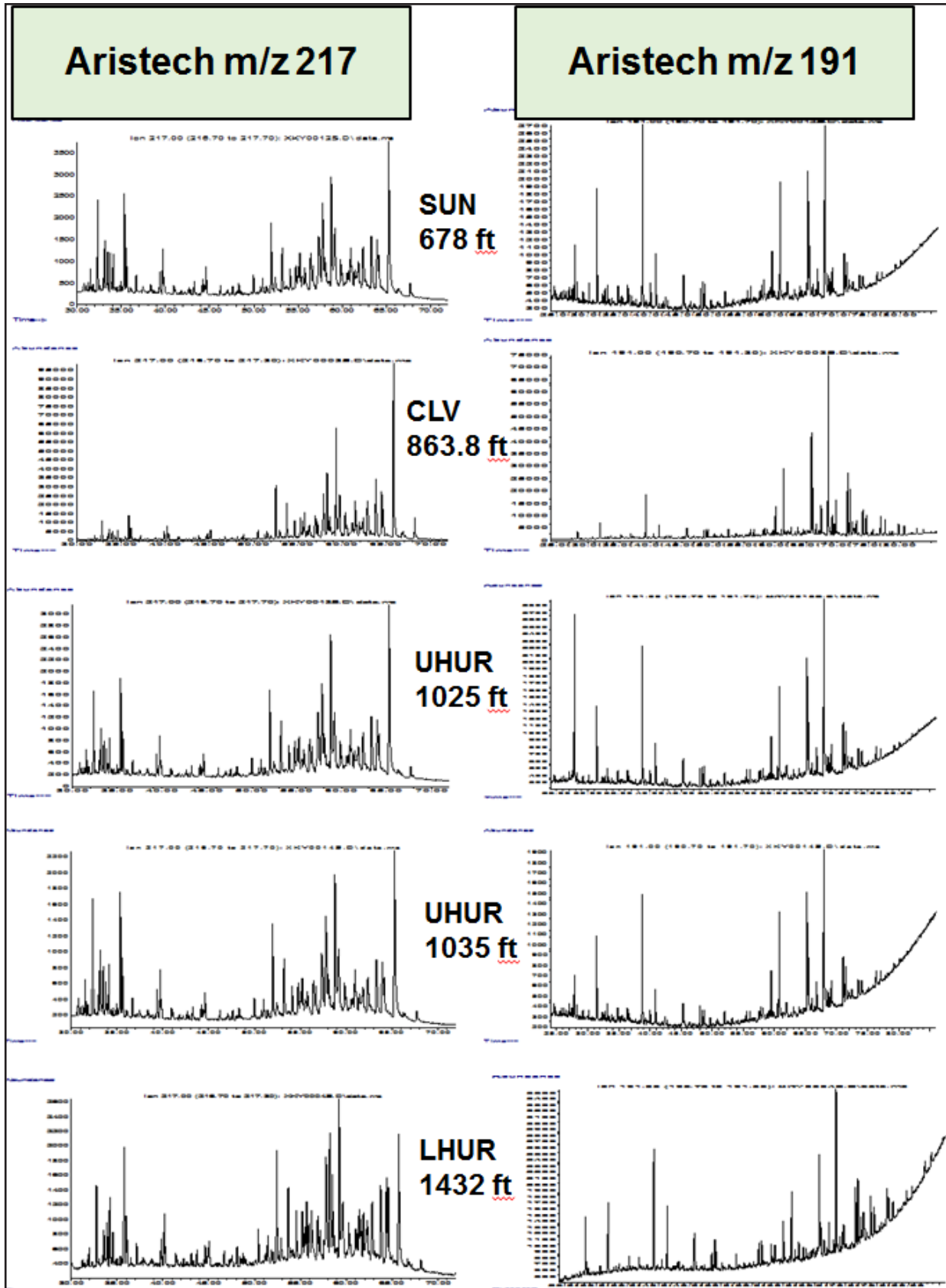


Figure 4-12. GC-MS *m/z* 191 and 217 fragmentograms for the Aristech #4 well. See Table 4-1 for key to peak labels.

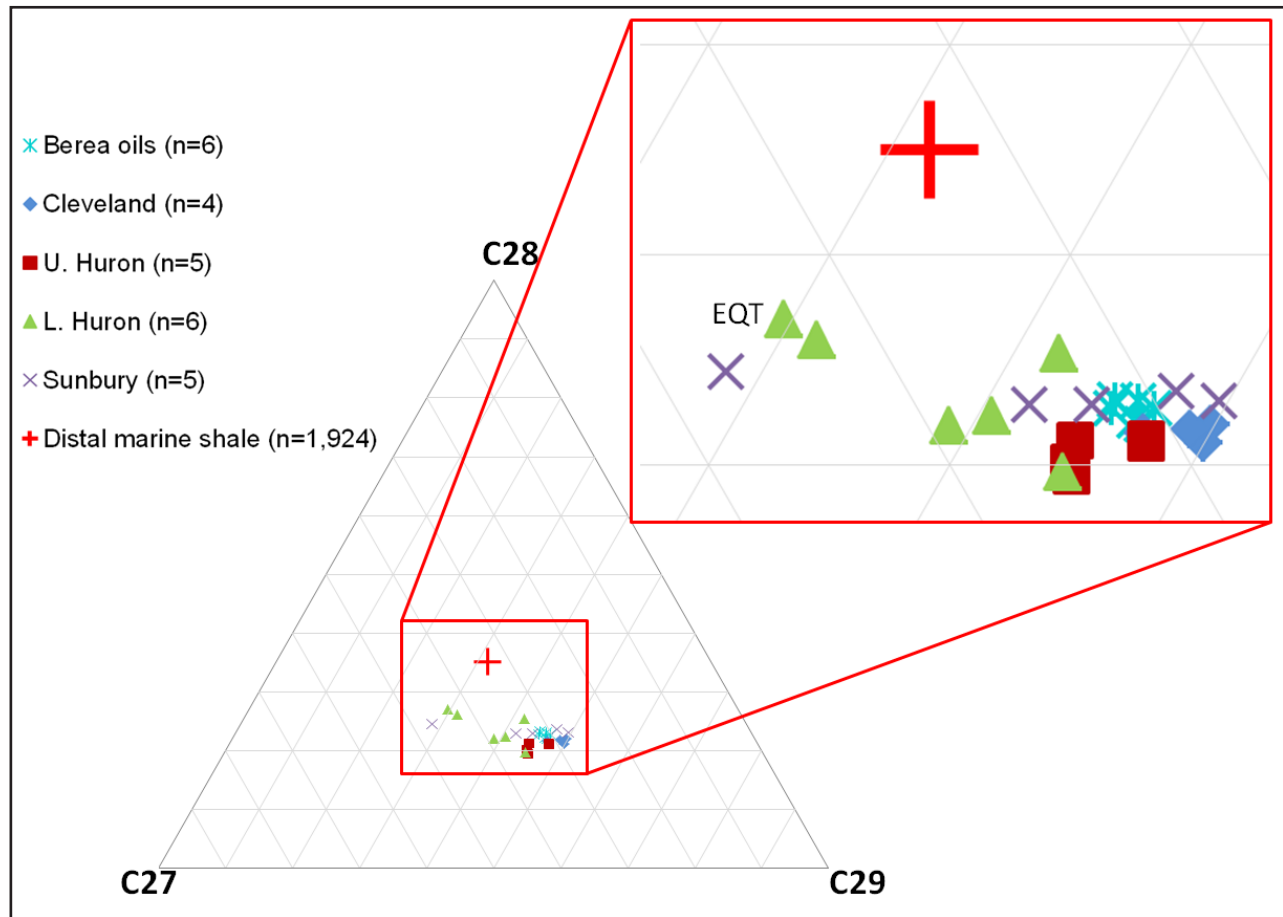


Figure 4-13. Normal sterane ($\alpha\beta$ BS, m/z 218) distributions. The EQT label refers to the three analyses from the downdip EQT Production Co. #504353 well.

presence of scattered terrigenous organic matter, as revealed through petrography, primarily in the form of inertinite with lesser amounts of vitrinite. The $Pr/n-C_{17}$ versus $Ph/n-C_{18}$ discriminant plot also indicates a mixed terrigenous-marine organic-matter source, possibly reflecting the minor terrigenous organic component.

Carbon-isotopic compositions from the extracts and Berea oils are consistent with a marine source, as shown on the Sofer-type discriminant diagram (Fig. 4-10), although values in this study are about 1 per mil lighter than the computed average distal marine shale (GeoMark, 2015). Lighter isotopic compositions in Berea oils and Devonian source-rock extracts may result from a model similar to that proposed by Lewan (1986), where light $\delta^{13}C$ values were thought to be derived from organisms fixing a dissolved CO_2 source influenced by recycled organic CO_2 sourced from bacterial breakdown of organic matter in a shallow, strati-

fied, epeiric sea. Lighter $\delta^{13}C$ values would be present because of contributions of respired organic matter to the stratified-surface ocean-dissolved inorganic-carbon pool, as opposed to isotopically heavier $\delta^{13}C$ in deeper, well-mixed waters where the dissolved photic-zone CO_2 is in equilibrium with the atmosphere. This model is consistent with previous work that described the geologic environment as a shallow epeiric sea (Ettensohn and Elam, 1985; Pashin and Ettensohn, 1987) and the presence of amorphous organic matter (bituminite) is interpreted as relict from the bacterial breakdown of marine organic matter. However, there are alternative explanations for a 1 per mil difference from the distal marine average—e.g., the average value could be weighted toward Mesozoic oils or another time interval in which CO_2 concentrations, and organic productivity and community, differed substantially from the Devonian to Mississippian samples of this study. Future work should limit the

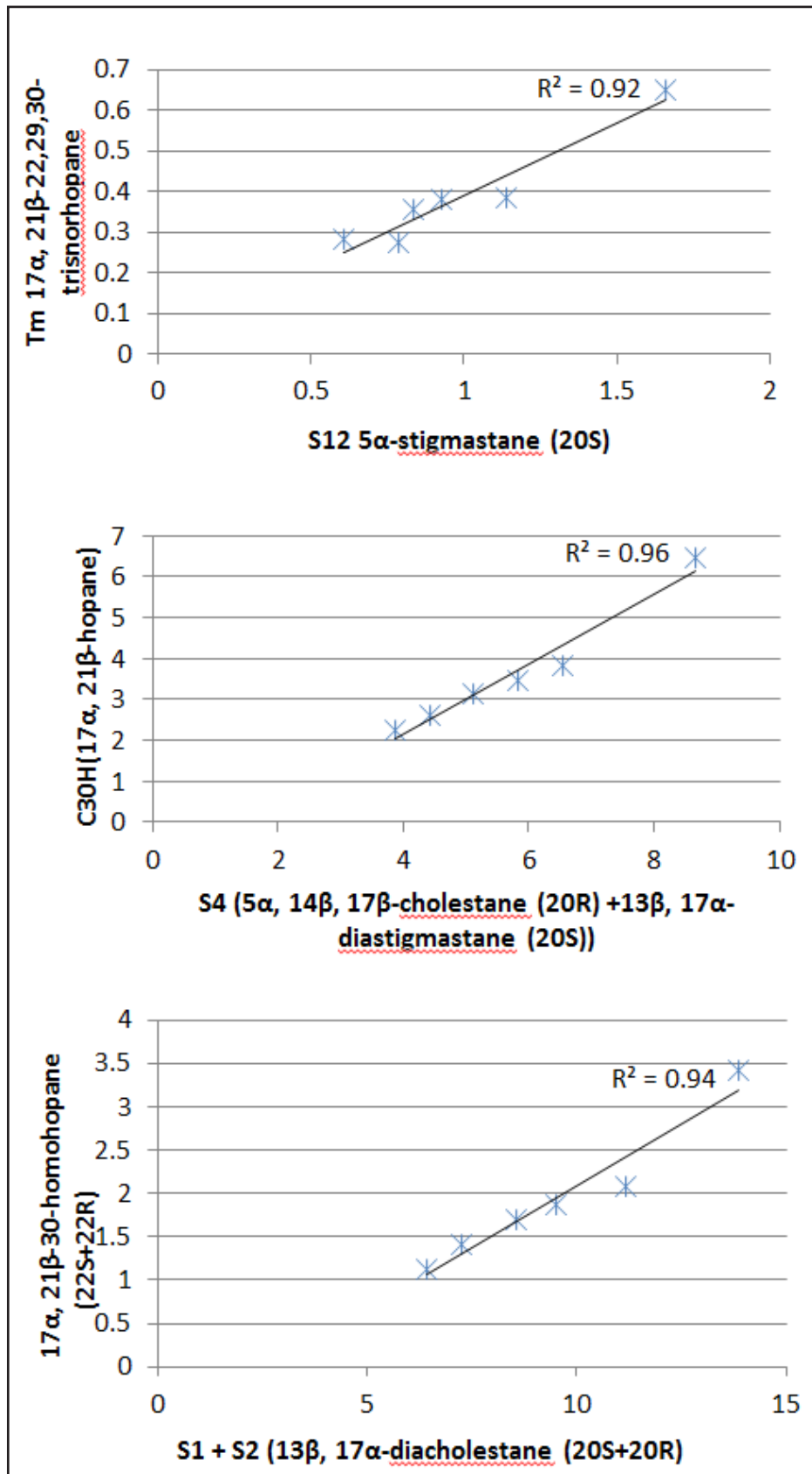


Figure 4-14. Individual versus sterane concentrations in oil samples, in parts per million.

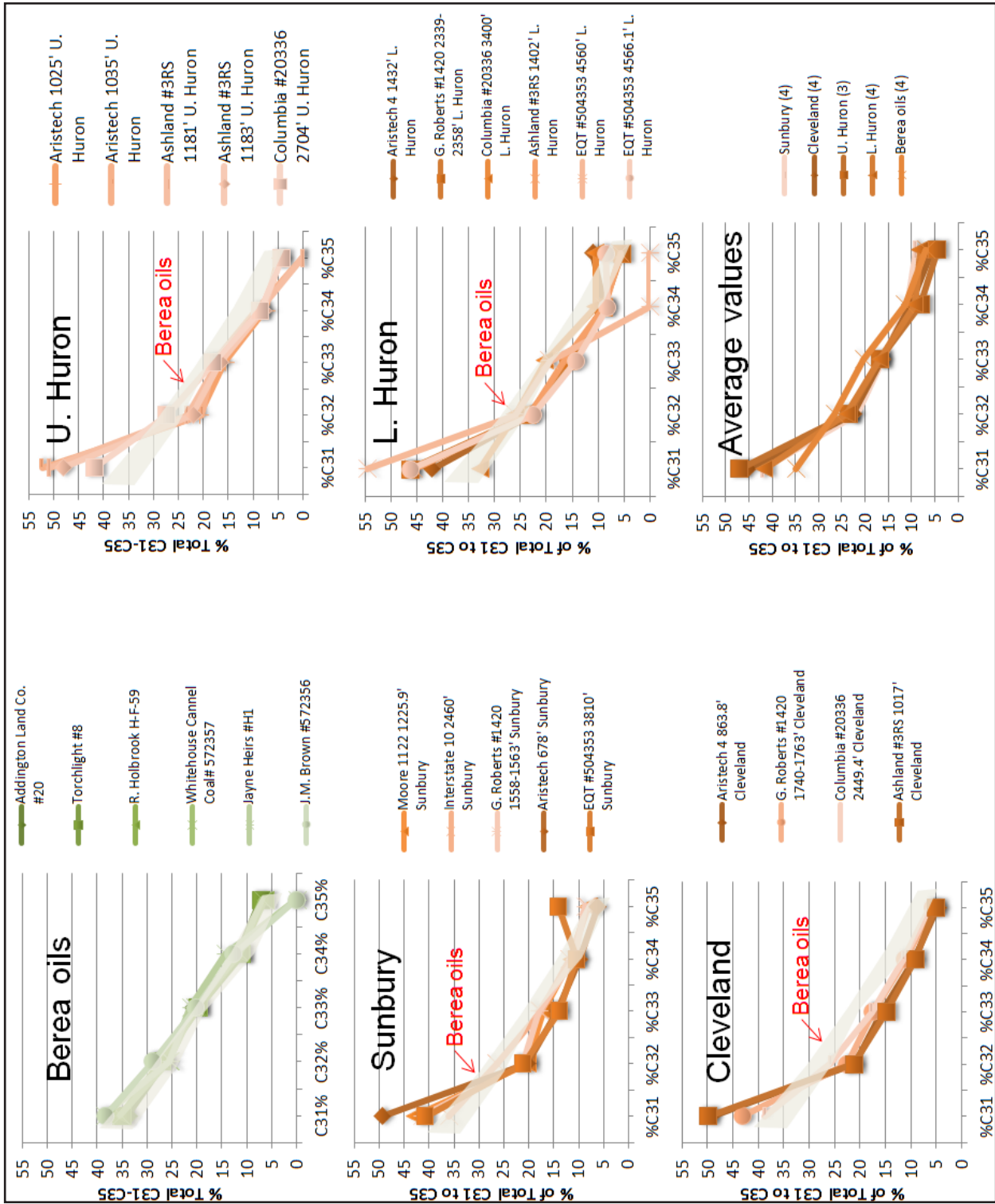


Figure 4-15. Extended homohopane relative abundances in oils and bitumen extracts. The gray swath in the plots showing the Sunbury, Cleveland, Upper and Lower Huron homohopane abundances represents the range of extended homohopane abundances present in the Berea oils (it does not reflect the absence of C₃₅ homohopane in the Jayne Heirs #H1 and J.M. Brown #572356 oil samples).

computed average distal-marine shale value exclusively to the Devonian-Mississippian for comparison.

Sterane distributions may suggest a terrigenous C_{29} contribution to the organic matter (Fig. 4-13) relative to a computed average distal-marine shale (GeoMark, 2015) and minor terrestrial organic matter (Type III kerogens vitrinite and inertinite) is present in the source rocks, as documented via organic petrography. Type III kerogen is, however, a minor component relative to constituents representing or derived from marine algae (*Tasmanites*, unidentified algal material [telalginite, lamalginite], and biodegradation products [amorphinite, bituminite]). Because we have direct proxies indicating a dominantly marine organic-matter source from organic petrography, we suggest the observed sterane distributions are representative of marine organic matter – in particular photosynthetic green algae – which may synthesize precursors to C_{29} steranes (Volkman, 1986). Peters and others (2005) also acknowledged that due to overlapping compositions, normal sterane distribu-

tions are seldom used to discriminate depositional environment and/or organic source.

Gammacerane index values of Berea oils and bitumen extracts plot similarly to the average distal-marine shale (GeoMark, 2015) and show that normal mesohaline (nonstratified, low to normal marine salinity) conditions predominated (Fig. 4-16). High diasterane to sterane ratios (0.2 to 5.2) in source-rock bitumen extracts are consistent with the clay-mineral-rich mineralogy of the Devonian-Mississippian black shales (Peters and others, 2005). Very slight concentrations of oleanane, a biomarker for terrestrial angiosperms present in the Cretaceous and earlier (Ekweozor and others, 1979), are present in Berea oils and the majority of bitumen extracts (Table 3-9). It is unlikely this compound originated in the Devonian oil or bitumen-extract samples, and it may represent minor contamination or co-elution of another compound.

Tricyclic terpanes (Table 3-11, Fig. 4-17), present in all crude oils and bitumen extracts, may originate from *Tasmanites* algae (Azevedo and others, 1992) or from prokaryotic (bacterial) membranes

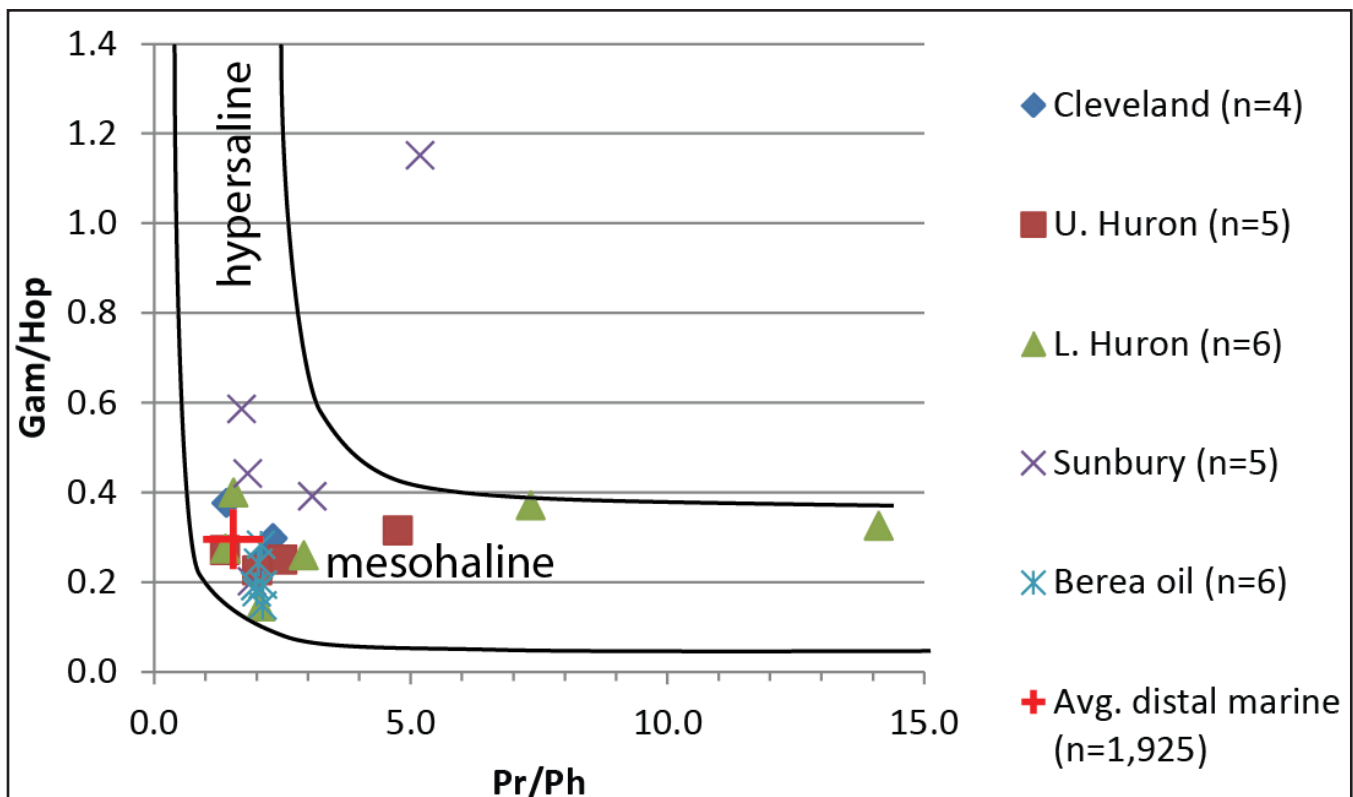


Figure 4-16. Gammacerane index values for oils and extracts. Hypersaline and mesohaline fields. Adapted with permission from Lu and others (2015), © 2015 American Chemical Society.

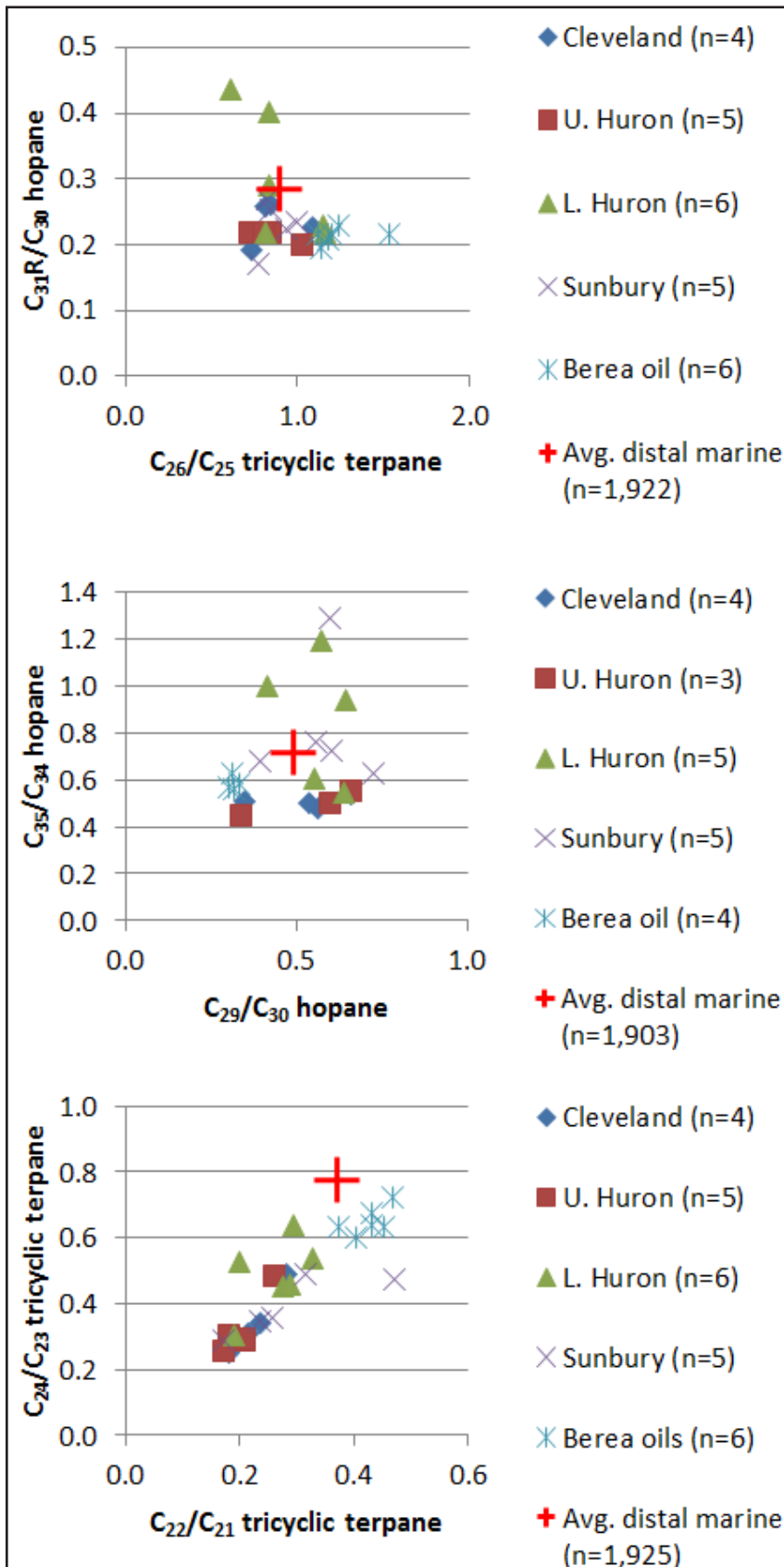


Figure 4-17. Tricyclic terpene and hopane ratios.

(Ourisson and others, 1982). *Tasmanites* is present in all of the immature samples. Also present is amorphous organic matter that may include some component of bacterial biomass. Tricyclic terpene ratios are consistent with a marine source of organic matter in the Berea petroleum system when compared to the average distal-marine shale computed from the GeoMark (2015) database. C_{24}/C_{23} ratios lower than 0.5 may reflect a minor carbonate influence in some of the Devonian shales analyzed in this study. Last, total sterane to hopane ratios greater than 1.0 (Table 3-8) suggest eukaryotic organic matter (marine algae) dominates the organic source input (Volkman, 1986).

Oil-Source Correlation. Close correspondence between normal sterane distributions of crude oils and potential source-rock extracts (Fig. 4-13) is consistent with Berea oils coming from the analyzed source rocks. However, similar sterane distributions in each of the potential source-rock extracts prohibits making a definitive correlation between the oils and source rocks. According to Peters and others (2005), sterane distributions do not change significantly through the oil-generation window. Therefore, the significantly lower C_{29} sterane component in the three bitumen extracts from the EQT #504353 suggests these are an unlikely source for Berea oils. High diasterane to sterane ratios (Table 3-8) in Berea oils (5.9–8.8) are consistent with a source in the clay-mineral-rich Devonian-Mississippian black shales.

High Pr/Ph ratios and lighter carbon-isotopic compositions in the Berea oils appear to rule out a lower Paleozoic source. Cole and others (1987) showed that the Ordovician-sourced oils of eastern Ohio con-

tained Pr/Ph ratios generally lower than 1.8 and aromatic-fraction isotopic compositions as heavy as -28 per mil. Berea oils from this study instead show strong similarity to Berea-reservoired oils in Ohio studied by Cole and others (1987). In particular, the carbon-isotopic compositions are very similar between the two areas (Fig. 4-11). Cole and others (1987) used carbon-isotopic compositions of Berea oils relative to kerogen and kerogen pyrolyzate of Sunbury source rocks to select the Sunbury as the most likely source of Berea oils in eastern Ohio. This decision appears to have been based on the Sunbury's proximity (immediately overlying the Berea). However, Cole and others (1987) also indicated that the underlying Ohio or Olentangy Shales could have sourced the Berea-reservoired oils. In Figure 4-11, bitumen extracts from the Sunbury, Cleveland, and Lower Huron are slightly heavier (up to about 0.75 per mil) than Berea oils and show similar carbon-isotopic distributions among the saturate, whole extract, and aromatic fractions. Thus, any of these intervals is a potential source for Berea oils, and the isotopic similarity precludes selecting a preferred source. Similarity in tricyclic terpane ratios (Fig. 4-17) between bitumen extracts and Berea oils also precludes selecting a preferred source rock. Total sterane to hopane ratios in Sunbury and Upper Huron bitumen extracts show more similarity to Berea oils than either of the Cleveland or Lower Huron extracts; however, this observation does not rule out the Cleveland or Lower Huron as sources.

Thermal Maturity. Sterane isomerization ratios from bitumen extracts can be used to predict thermal maturity of source-rock organic matter, although cautions are suggested, including calibration of isomerization ratios for individual basins and source rocks (Peters and others, 2005). North of our study area in eastern Ohio, Hackley and others (2013) used sterane isomerization ratios to show equivalent Devonian-shale source rocks (Huron) were mature for oil generation although "vitrinite"-reflectance values suggested immature conditions. The $\alpha\alpha\alpha$ 20S/(20S+20R) isomer ratios of C_{29} steranes are known to approach an empirical thermal-equilibrium value of 0.52–0.55 (Seifert and Moldowan, 1986), as exhibited by Berea oils and some of the bitumen extracts of this study (Table 3-8,

Fig. 4-18). This may suggest equivalent VR_o values of about 0.8 percent (Peters and others, 2005, p. 612) for these samples, although caution is suggested, as stated above, for the VR_o values are inferred from observations outside of the Berea petroleum system. Average values of measured VR_o are about 0.73–0.74 percent for samples from the same wells as the aforementioned bitumen extracts. This may suggest Berea oils were generated at thermal maturities of about 0.7–0.8 percent VR_o . Isomer ratios for C_{29} $\beta\beta$ S/($\beta\beta$ S+ $\alpha\alpha$ R) steranes reach an empirical thermal equilibrium at about 0.70 (equivalent to a VR_o value of about 0.9 percent (Peters and others, 2005, p. 612). C_{29} $\beta\beta$ S/($\beta\beta$ S+ $\alpha\alpha$ R) ratios from samples in this study that are at the approximate $\alpha\alpha\alpha$ 20S/(20S+20R) equilibrium do not quite reach the 0.7 equilibrium value for C_{29} $\beta\beta$ S/($\beta\beta$ S+ $\alpha\alpha$ R), and instead cluster at about 0.60.

Nonequilibrium values in three high-maturity extract samples from the EQT #504353 well may reflect signal-to-noise or other analytical issues. Sterane isomerization ratios for the remaining extracts and oil samples show a strong positive correlation ($R^2=0.90$), confirming the validity of the two thermal-maturity parameters. Excluding the three EQT samples, sterane isomerization ratios also show moderate correlations with average measured VR_o values from each well ($R^2=0.75$ for C_{29} $\beta\beta$ S/[$\beta\beta$ S+ $\alpha\alpha$ R] and 0.71 for $\alpha\alpha\alpha$ 20S/[20S+20R]). In summary, $\alpha\alpha\alpha$ 20S/(20S+20R) sterane isomerization ratios suggest VR_o equivalent values of 0.7–0.8 percent for oil generation in the Berea system and possibly as high as about 0.9 percent if $\beta\beta$ S/($\beta\beta$ S+ $\alpha\alpha$ R) values are at equilibrium.

Excluding the three samples from the high-maturity EQT #504353 well, C_{27} trisnorhopane epimer ratios (Ts/Ts+Tm; Table 3-8) show a moderate positive relationship ($R^2=0.66$), with average measured VR_o values from each well and strong correlations to sterane isomerization ratios ($R^2=0.81$ for 20S/[20S+20R] and 0.93 for $\beta\beta$ S/[$\beta\beta$ S+ $\alpha\alpha$ R]), indicating the utility of this thermal-maturity parameter in the Berea petroleum system. Ts/Ts+Tm also shows a strong relationship to diasterane/sterane ratios (Fig. 4-19). Because both of these ratios are in part dependent on organic source and depositional environment (Moldowan and others, 1986; Mello and others, 1998), in addition to thermal maturity, their correspondence is additional

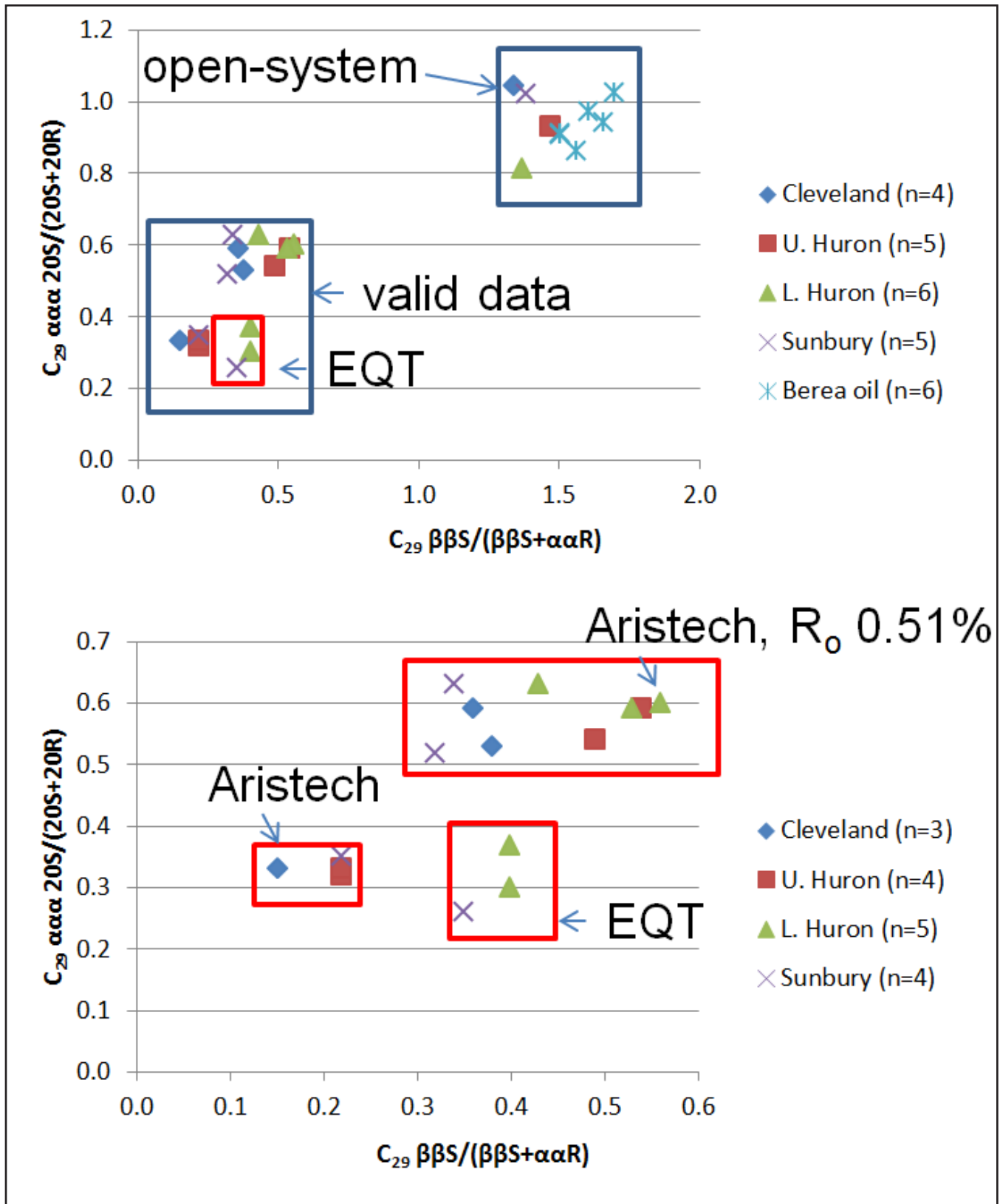


Figure 4-18. Sterane isomerization plot [$C_{29} \alpha\alpha 20S/(20S + 20R)$] versus $C_{29} \beta S/(\beta S + \alpha R)$. The EQT label refers to the three analyses from the downdip EQT Production Co. #504353 well.

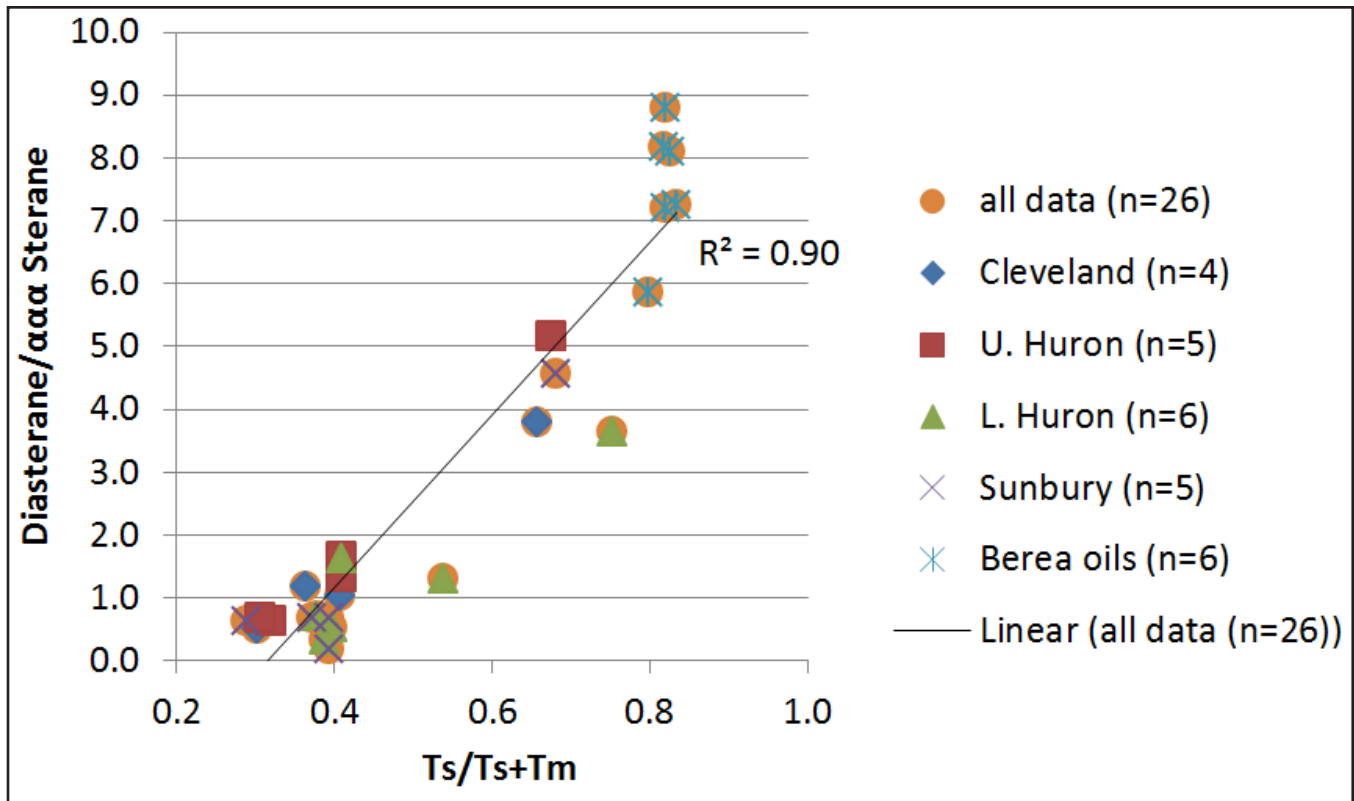


Figure 4-19. Diasterane/ $\alpha\alpha$ sterane ratios versus C_{27} trisnorhopane epimer ratios ($Ts/Ts + Tm$).

evidence suggesting oils and bitumen extracts are related and from a similar organic-matter source. The $Ts/(Ts + Tm)$ ratio reaches thermal equilibrium at 1.0 (which is not reached in our dataset), equivalent to about 1.4 percent R_o (Peters and others, 2005, p. 612). Oil samples show a moderate correlation between $Ts/Ts + Tm$ and $\beta\beta S/(\beta\beta S + \alpha\alpha R)$ ($R^2=0.67$), suggesting a slight difference in thermal maturity among the samples, as pointed out earlier from correlations between individual hopane and sterane abundances. However, no relationship is observed between $20S/(20S + 20R)$ and $Ts/Ts + Tm$ ratios in oil samples ($R^2=0.30$).

A poor negative correlation is observed between sulfur content in bitumen extracts and R_o values (correlation coefficient, $R^2=0.42$) (Fig. 4-20). However, when Cleveland samples are excluded, R^2 improves to 0.85 (the Cleveland samples define a separate, lower-sulfur trend that also shows a strong inverse correlation to thermal maturity with $R^2=0.99$). The inverse correlations observed between organic sulfur content and R_o suggest that cracking of sulfur-containing functional groups may occur during early maturation. The residual

organic matter, at higher maturity, has lower sulfur content. Accordingly, the low sulfur content in Berea oils may suggest generation from cracking of kerogen of moderate thermal-maturity level. There are several cautions with this idea, however; diagenetic sulfurization of organic matter is suggested (though not demonstrated) by high C_{35} hopane (the C_{35} hopane is preferentially sulfurized relative to lower carbon-number homohopanes, according to Köster and others, 1997) in high-maturity Sunbury and Lower Huron bitumen extracts from the EQT #504353 well (S content is not available). Preferential sulfurization of phytane precursors (Kohnen and others, 1991; de Graaf and others, 1992; Kenig and others, 1995) and their subsequent loss during thermal cracking may be responsible for the low $Ph/n-C_{18}$ and high Pr/Ph ratios in these same samples. At this maturity we would expect low S content in the remaining organic matter. However, the high-S bitumen extracts from the Sunbury and Lower Huron samples in the G. Roberts #1420 well do not show elevated C_{35} hopane, and it is possible that elevated C_{35} hopane in bitumen extracts from the EQT #504353 is a function

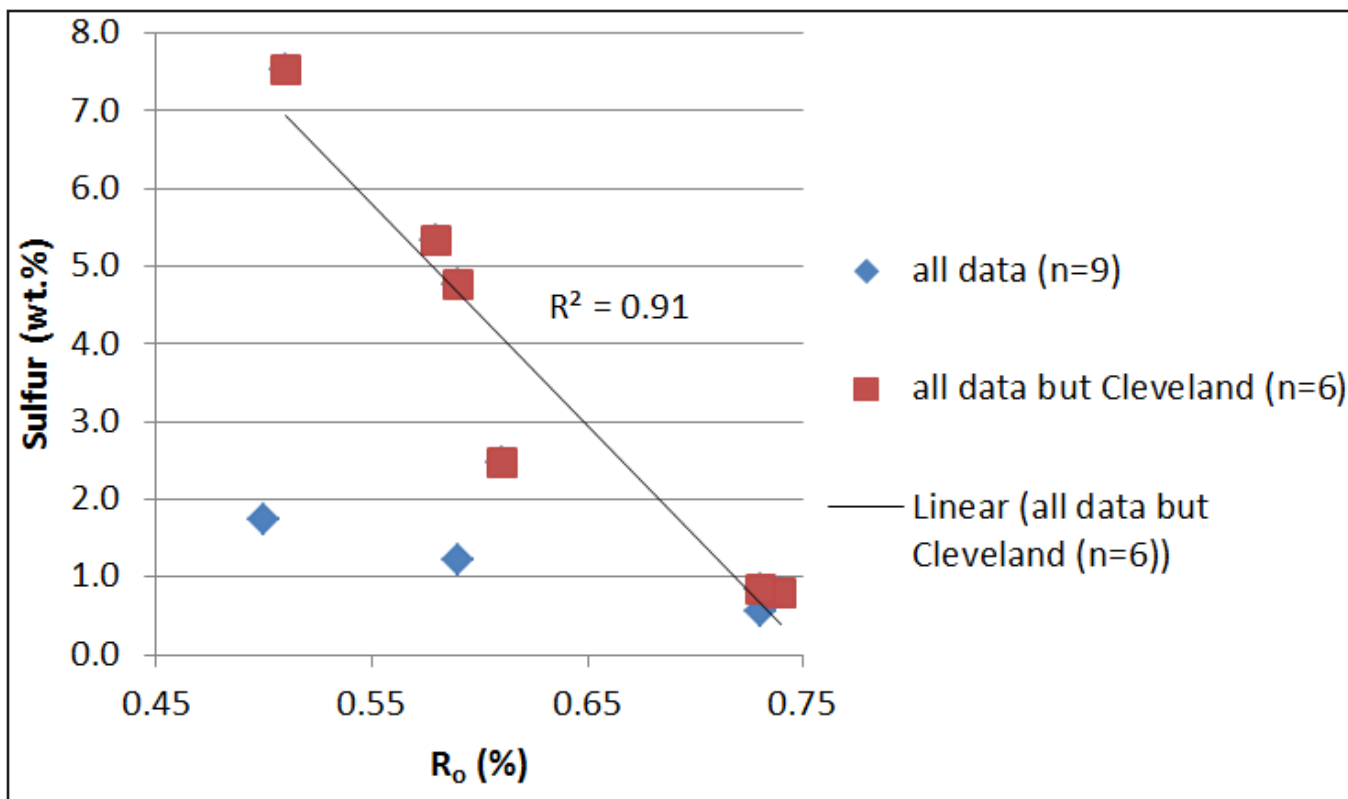


Figure 4-20. S content of bitumen extracts versus R_o values.

of a highly reducing depositional environment (Peters and others, 2005, p. 566).

Absence of C₃₅ and higher C₃₁ hopane in crude oils from the EQT #572356 or Jayne Heirs #H1 wells in Johnson County may reflect higher thermal maturity of these oils and cracking from an originally sulfur-rich kerogen. Sulfurization of organic matter increases from the C₃₁ through C₃₅ homohopanes (Köster and others, 1997). These sulfur-bound homohopanes are lost during early cracking of sulfur-rich kerogen, leading to later increase in the C₃₁ homolog (Peters and others, 2005). Sulfurization of kerogen in the Lower Huron sample from 1,432 ft in the Aristech well may be the reason for elevated C₃₅ hopane (Fig. 4-15), although, as before, this could be due to depositional anoxia. This sample contains total sulfur content of 7.53 percent in the bitumen extract, the highest value of the nine samples analyzed, although some sulfur in the bitumen extract may be elemental rather than organic.

For all three of the tricyclic terpane ratios considered above, oils show higher values than do bitumen extracts (Fig. 4-17). Considering bitumen extracts as representative of potential Berea

oil sources, this observation is counterintuitive to considerations arising from primary migration and expulsion fractionation during oil generation from bitumen, both of which should favor the lighter tricyclic terpane molecules. We therefore assume oils may show higher tricyclic terpane ratios due to phase separation during migration and loss of the lighter tricyclics into associated gases.

The methylphenanthrene index (MPI) (Radke and Welte, 1983) from aromatic biomarker analysis in the extracts shows a moderate positive correlation with thermal maturity as determined from vitrinite R_o (R²=0.69) and solid-bitumen BR_o (R²=0.81) reflectance measurements (Fig. 4-21), although these relationships are skewed by clusters of data at high and low thermal maturity. Nevertheless, based on these data, an R_o equivalent value can be computed for any sample, including Berea oils. In Figure 4-22 we show R_o equivalent values from MPI relative to saturate/aromatic ratios from all samples, oils and bitumen extracts. A strong positive relationship (R²=0.79) is consistent with oils and extracts being from the same organic-matter source and suggests that the saturate/aromatic

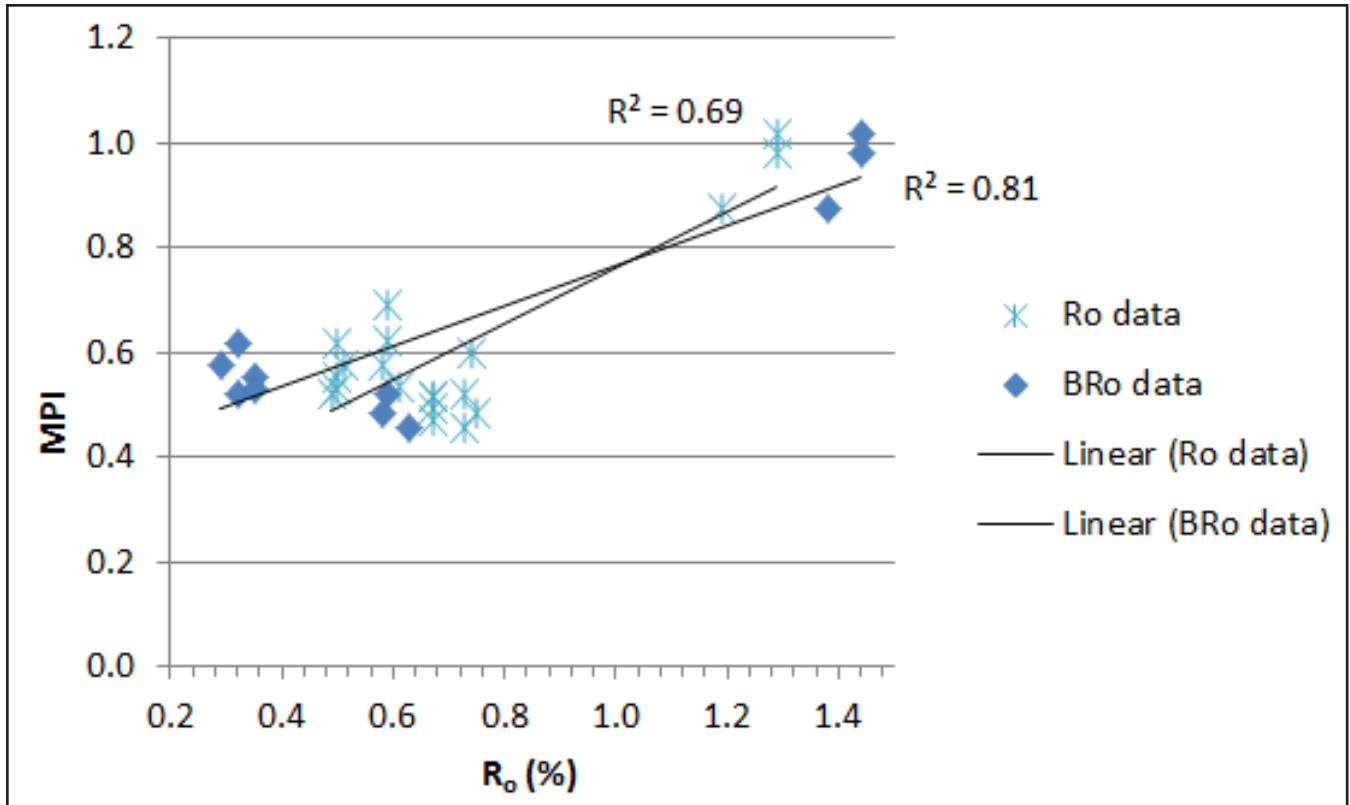


Figure 4-21. Methylphenanthrene index (MPI) versus R_o values.

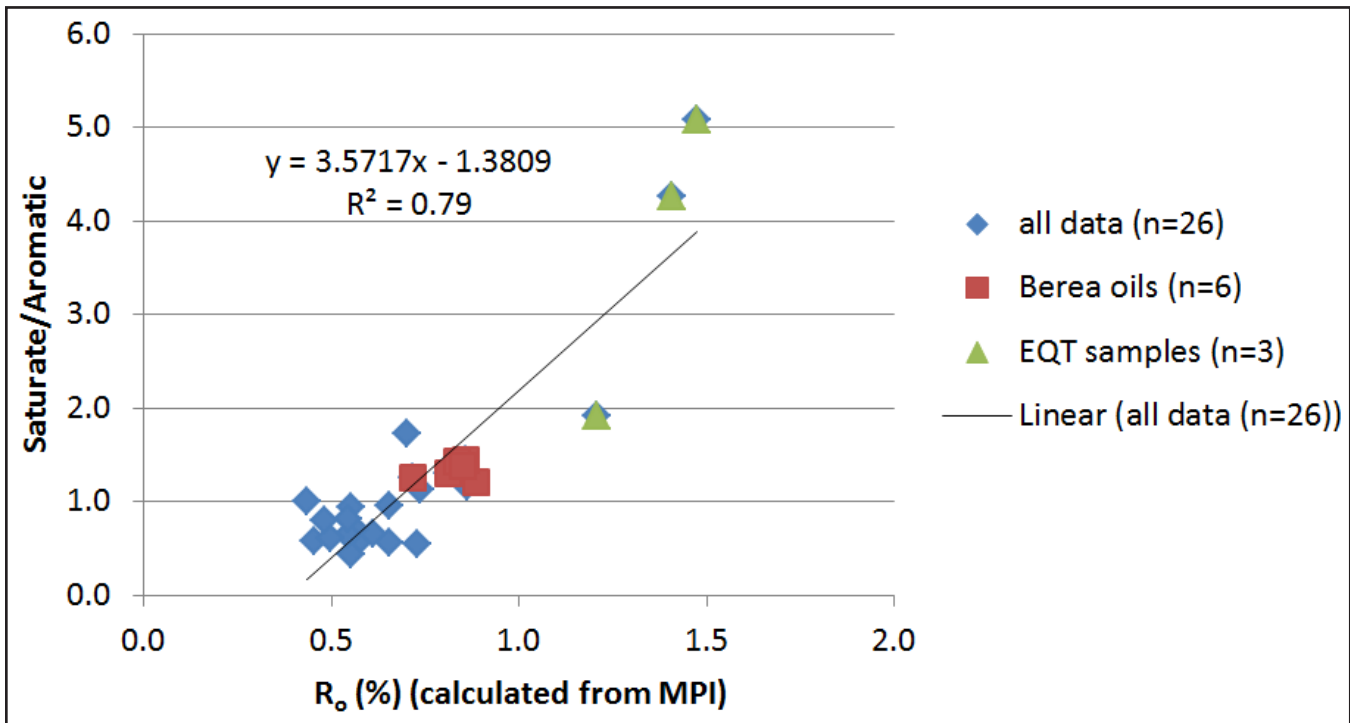


Figure 4-22. R_o equivalent values from MPI versus saturate/aromatic ratios.

ratio can be predicted from MPI values. (A similar robust relationship [$R^2=0.75$] is found using measured VR_o values for bitumen-extract samples and VR_o equivalent values from oil MPI.) Moreover, this relationship also suggests the sampled Berea oils cracked from bitumens at mid-oil-window thermal-maturity conditions of about 0.7–0.9 percent R_o (Radke, 1988), consistent with the interpretation presented above from sterane isomerization ratios. This idea is based on the position of oil samples in Figure 4-22 and would be consistent with low sulfur content in oils, which also suggests they are not formed from early cracking. As some oils were sampled from updip reservoirs in Greenup County where thermal maturity is less than 0.6 percent R_o , significant updip lateral migration of 30–50 mi from a downdip Devonian black-shale source kitchen is required.

Primary expulsion and migration of Berea oils from Devonian source rocks may explain why diasterane/sterane ratios are much higher in oils than in bitumen extracts, with the larger, more polar sterane molecule preferentially retained in the source bitumen (Peters and others, 1990). The oil sample collected farthest downdip (closest to a source kitchen) contains the lowest diasterane/sterane ratios, which may suggest it has migrated the shortest distance in Berea carrier beds, if all oil samples were generated from the same source at the same time. However, samples collected updip show no systematic increase in diasterane/sterane ratios, and the two highest diasterane/sterane ratios correspond to absence of the C_{35} homohopane, suggesting a thermal-maturity effect is present, with the two highest thermal-maturity oils containing the highest diasterane/sterane ratios. Partially corroborating this idea is that one of these two oil samples has the highest measured API value and the other appears to have lost light ends. Moreover, despite the strong contrast between diasterane/sterane ratios in oils and bitumen extracts, no similar relationship is observed for tricyclic terpane/hopane ratios, which should show a corresponding primary migration relationship with hopanes retained in bitumens. Based on these observations, we suggest the oils collected from Jayne Heirs #H1 and EQT #572356 may be slightly higher maturity than the other oil samples, even the most downdip EQT #572357. This is partially

corroborated by R_o -equivalent values calculated from MPI, which show a low value of 0.72 percent in the EQT #572357 oil. However, updip oils from ALC #20 and Torchlight #8 show higher R_o -equivalent values from MPI than do the Jayne Heirs #H1 and EQT #572356.

Oil and Bitumen-Extract Summary

1. Berea oils are of one family and all from a similar source rock, based on API gravity, sulfur, SARA fractions, *n*-alkane envelopes, carbon-isotopic compositions, normal sterane distributions, correlation between individual sterane and hopane concentrations, and similarity in extended hopane concentrations. Berea oils are identical in carbon-isotopic composition to Berea-reservoired crude oils in eastern Ohio and dissimilar to oils reservoired in lower Paleozoic eastern Ohio strata.
2. Berea oils and organic matter in the potential source rocks are from a marine source, based on multiple proxies including Pr/Ph and TAR ratios, CPI values, *n*-alkane maxima, carbon-isotopic composition, presence of tricyclic terpanes (from *Tasmanites* and/or bacterial biomass), and the positions of oil and extract samples in tricyclic terpane and hopane ratio discriminant plots.
3. The current dataset suggests any or all of the Devonian–Mississippian black-shale source rocks studied herein could be potential source rocks for Berea oils. This conclusion is based on similarities in oil and bitumen extract Pr/*n*- C_{17} and Ph/*n*- C_{18} ratios, sterane distributions (with the exception of high-maturity samples from EQT #504353), carbon-isotopic values (from Sunbury, Cleveland, and Lower Huron), and sterane/hopane and tricyclic terpane ratios.
4. Sterane isomers and C_{27} (Ts/Ts+Tm) hopanes can be used to predict thermal maturity in the Berea system and suggest oils formed at a thermal maturity of about 0.7 to 0.9 percent VR_o . A strong relationship between C_{27} (Ts/Ts+Tm) hopanes and diasterane to sterane ratios is consis-

tent with oils and bitumen extracts being from the same organic-matter source. Sulfurization of organic matter may explain high sulfur concentrations in some bitumen extracts and may suggest generation of low-sulfur Berea oils occurred in the mid to peak oil window. Consistent with sterane isomerization ratios, R_o equivalent values from MPI suggest generation of Berea oils occurred at about 0.7–0.9 percent R_o and allow prediction of saturate/aromatic ratios based on thermal maturity in the Berea petroleum system. Significant updip lateral migration of 30–50 mi from a downdip Devonian black-shale source kitchen is required to emplace low-sulfur oils in the updip oil-play areas in Lawrence and Greenup Counties.

Natural-Gas Bulk and Isotopic Composition

The ratio of methane (C_1) to ethane plus propane ($C_2 + C_3$) provides a measure of gas wetness. The $C_1/C_2 + C_3$ ratios for OAG and NAG samples in this study range from 1.9 to 7.9, which define the samples as wet gases and well below the ratio of 100 used to define dry gas (Bernard and others, 1976). When gas wetness is plotted versus $\delta^{13}C\text{-CH}_4$, the samples define a positive linear trend of decreasing wetness with increasing $\delta^{13}C$ values (Fig. 4-23). This trend, as demonstrated with empirical data from other basins, represents increased thermal maturity from the lower left to the upper right in Figure 4-23 (Bernard and others, 1976). The sample from the Torchlight #8, located just north of the Wahlbridge Fault, is slightly drier and plots off the trend. Departure from the trend suggests that the bulk hydrocarbon and/or the $\delta^{13}C\text{-CH}_4$ composition in the Torchlight #8 is being influenced by the fault. Though the data are more scattered, a similar thermal-maturity trend characterizes NAG samples collected from a variety of Cambrian–Mississippian reservoirs in eastern Kentucky (Fig. 4-24). The scatter is not surprising since the data include gases likely derived from different sources (e.g., Ordovician or Cambrian) and with different burial histories.

Schoell (1983) evaluated the origin of approximately 500 natural gases using the δD composition

of CH_4 and the $\delta^{13}C$ composition of ethane (C_2H_6), along with gas wetness and the $\delta^{13}C$ composition of CH_4 . In a strictly empirical analysis, Schoell (1983) defined fields for thermogenic (associated and nonassociated) and biogenic gases. When plotted on a Schoell-style plot (Fig. 4-25), all gases in this study and other eastern Kentucky gases show a positive trend of progressively more positive $\delta^{13}C$ and δD values for CH_4 . The trend reflects increasing thermal maturity as predicted by empirical data and theoretical fractionation models (James, 1983; Chung and others, 1988). Moreover, all samples in this study, except from the ALC #20, plot in the “thermogenic gas with oil” field. The ALC #20 sample, located in Greenup County, plots just inside the mixed-gas field, suggesting a mixture of thermogenic and biogenic gas. Given that the other Berea samples show no biogenic influence, location of the ALC #20 sample in the mixed-gas field may reflect natural variation in the CH_4 isotopic composition rather than an actual microbial influence.

When gas wetness and $\delta^{13}C$ values for CH_4 are plotted versus depth, an overall trend of increased gas dryness and $\delta^{13}C$ values with depth is observed (Figs. 4-26, 4-27). The trends agree with the above discussion about the thermal-maturity effect on these gas properties. In both plots, however, data from Johnson County and Martin County plot off the trends. That is, the Johnson and Martin County samples appear to be anomalously dry and enriched in ^{13}C for their current burial depths. Previously, we noted that vitrinite reflectance and T_{max} values in Johnson County Ohio Shale samples also appeared to be anomalously high.

Following the methods described by James (1983) and Chung and others (1988), the $\delta^{13}C$ values of methane and higher-molecular-weight hydrocarbon gases were used to further investigate the potential sources of the gases and the thermal maturity at which they were generated. The inverse carbon number for methane (C_1), ethane (C_2), propane (C_3), and normal butane (nC_4) are plotted versus the $\delta^{13}C$ values for each of these compounds for each well in what Chung and others (1988) termed a natural-gas plot (Fig. 4-28). The plots discriminate two populations. The OAG samples along with the NAG sample from the EQT #KL 1915 form a group that is depleted in ^{13}C relative to the NAG sample from the EQT #504353. As demonstrated by reflectance

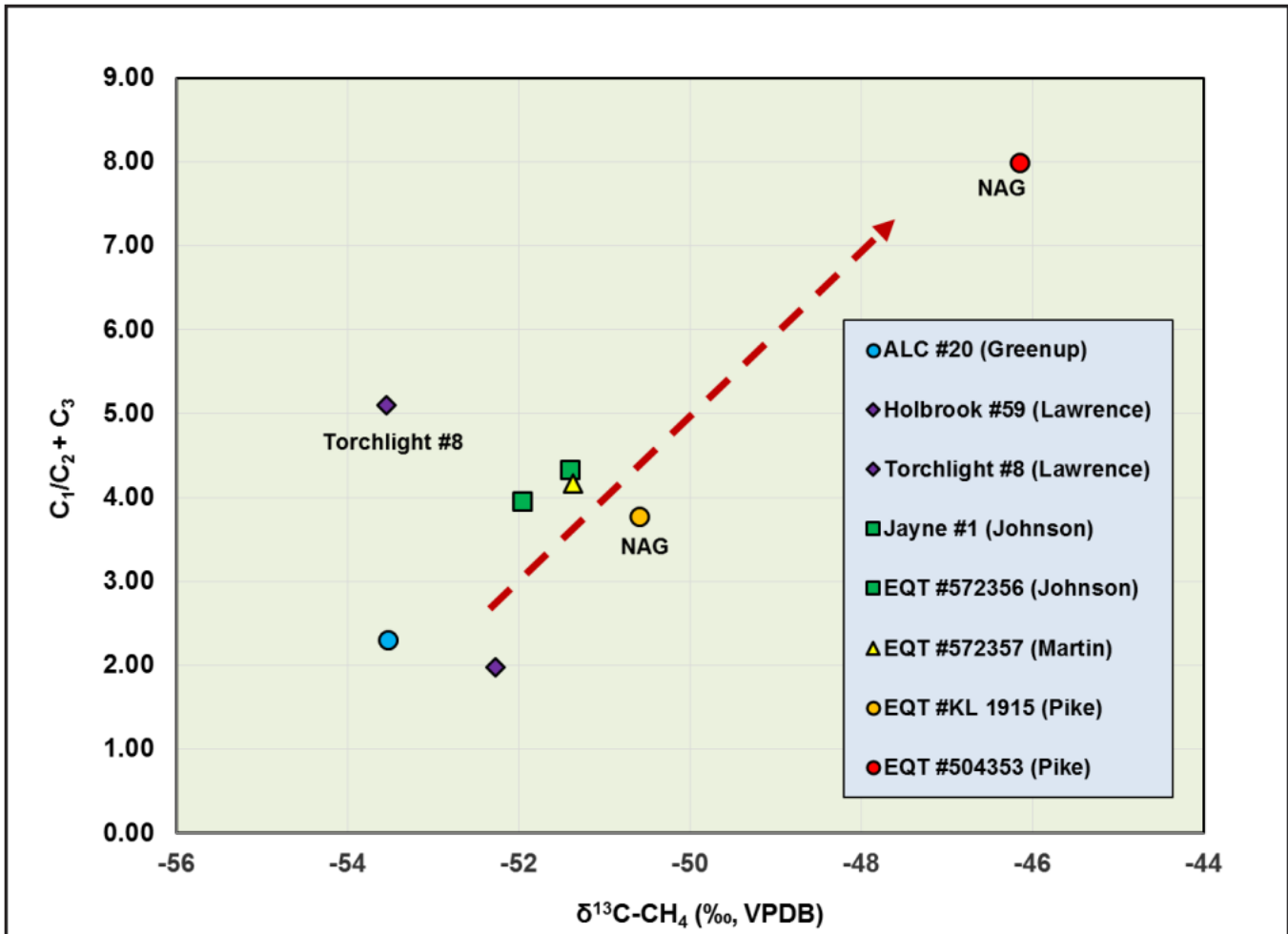


Figure 4-23. Gas wetness ($\text{C}_1/\text{C}_2 + \text{C}_3$) versus $\delta^{13}\text{C-CH}_4$. Samples are associated gases except for two nonassociated gases (NAG) from Pike County. Arrow indicates direction of increasing thermal maturity. The Torchlight #8 is near the Wahlbridge Fault (see text for further discussion).

tance and programmed-pyrolysis measurements in previous sections, samples in the isotopically lighter group come from wells in less mature and shallower settings compared to the isotopically heavier sample from the EQT #504353 (Figs. 3-1, 3-2). The latter is the most thermally mature well analyzed in this study.

All of the samples show a “normal” enrichment pattern, which, for any given sample, is characterized by progressive enrichment in ^{13}C with progressively higher molecular weight (Tang and others, 2000). The orderly enrichment results from the kinetic isotope effect (James, 1983). The similarity in composition among samples in the isotopically lighter group suggests they were derived from a similar source under similar thermal-maturity conditions. The corollary to this interpretation

is that the EQT #504353 sample was derived from a different source under different thermal-maturity conditions.

A closer look at samples in the isotopically lighter group shows a trajectory (Fig. 4-28) in which the $\delta^{13}\text{C}$ values depart from “ideal linearity” as defined by Chung and others (1988). Specifically, the gases least impacted by migration (i.e., C_2 , C_3 , and $n\text{C}_4$) depart from a best-fit line and C_1 departs significantly. Chung and others (1988) noted that such departures likely reflect contributions from structurally and isotopically different functional groups in the source rock. As a result, the precursor for C_1 may be different than for C_2 , C_3 , and $n\text{C}_4$. Another potential influence is mixing. The best-fit line projects to a $\delta^{13}\text{C}$ value for C_1 that is 8 to 10 per mil lighter compared to the measured C_1 values.

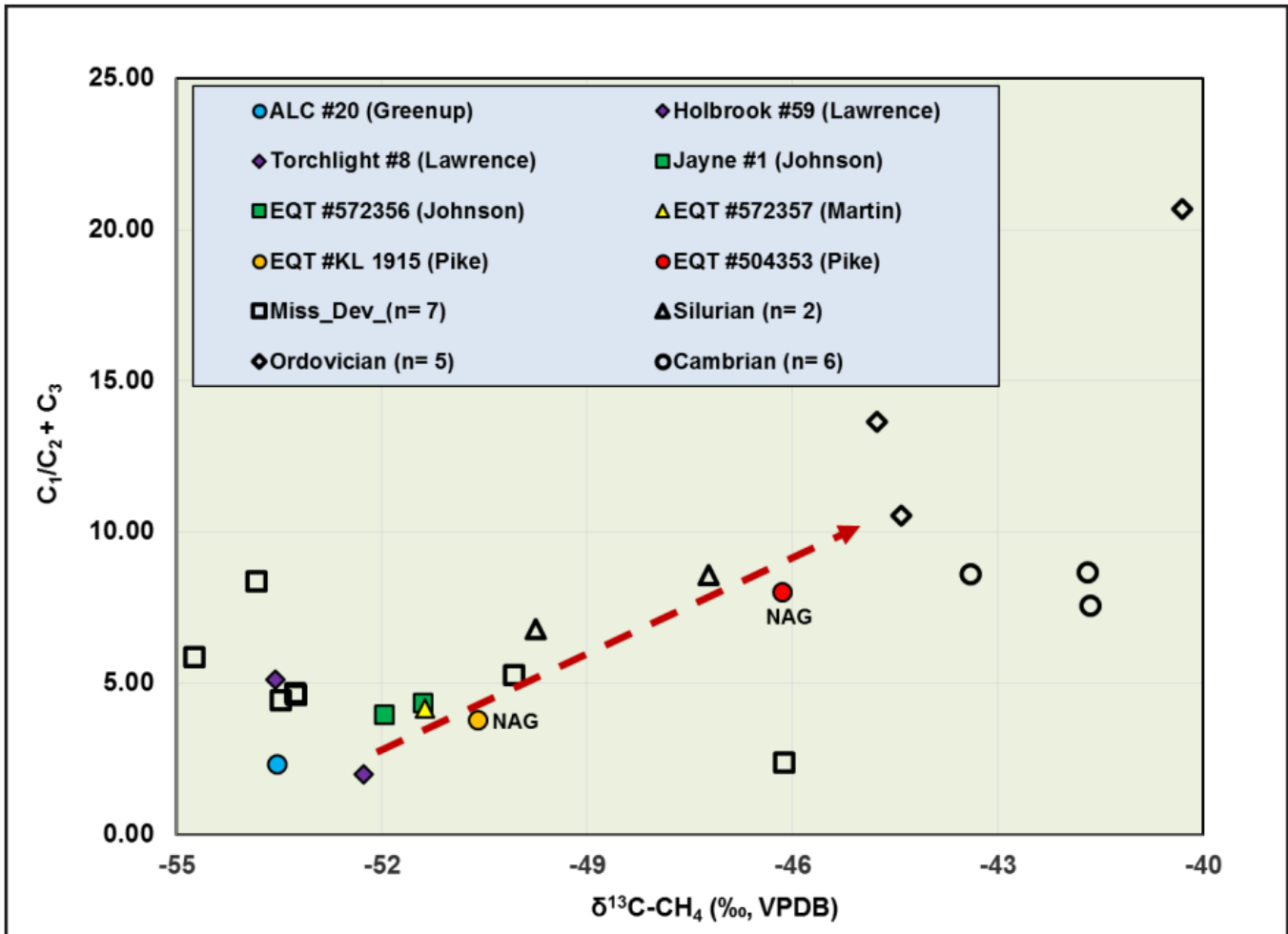


Figure 4-24. Gas wetness ($C_1/C_2 + C_3$) versus $\delta^{13}C-CH_4$ for gases in this study. Gases from Burruss and Laughrey (2010) and KGS data. With the exception of OAGs sampled in this study, all of the gases are NAGs. Arrow indicates direction of increasing thermal maturity.

This difference may reflect the later migration of isotopically heavier and more mature C_1 into the reservoir.

Chung and others (1988) further postulated that the y-intercept ($1/n=0$) of the best-fit line on the natural-gas plot provides an estimate of the $\delta^{13}C$ value of "the largest fragment molecule formed by thermal decomposition of kerogen" and therefore the possible source of higher molecular-weight gases. For the isotopically lighter group shown in Figure 4-28, the intercept occurs at a $\delta^{13}C$ value of about 25 per mil, which is more enriched in ^{13}C compared to the extracts and oils measured in this study and other regional data (Cole and others, 1987; Burruss and Laughrey, 2010). Moreover, the 8 to 9 per mil difference between the intercept value and nC_4 would appear to be incon-

gruent with organic matter at the y-intercept being a source for gas in the isotopically lighter group. Chung and others (1988) noted, however, that in nature, oils are often isotopically lighter than the $\delta^{13}C$ value provided by the y-intercept. They further stated that the source of gases, be it from kerogen or oil, might be a parent molecule having a smaller number of carbon atoms (n) than indicated by the y-intercept. This would appear to be the situation in the isotopically lighter group, where nC_4 is 3 to 5 per mil lighter than the bitumen extracts or oils. In terms of kinetic fractionation, up to 3 per mil can occur between kerogen and oil (Peters and Moldowan, 1993, p.126), with potential additional fractionation to nC_4 . Moreover, the isotopic difference between nC_4 and the oils might even be less, because the oils were not topped prior to isotope

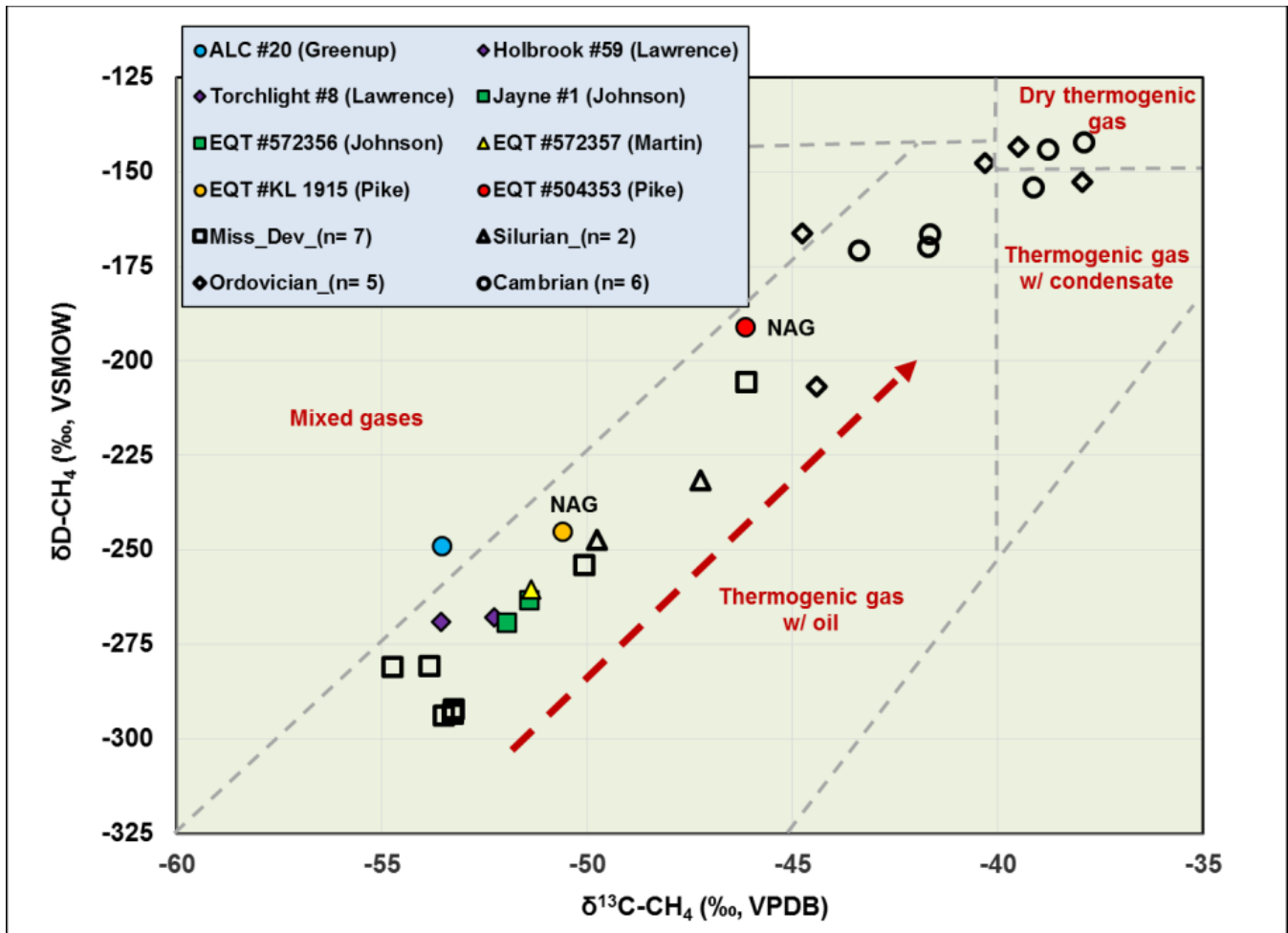


Figure 4-25. $\delta^{13}\text{C}$ versus δD for CH_4 (after Schoell, 1983). Plot includes data from this study and sources cited in Figure 4-24. With the exception of the ALC #20, which plots just inside the “mixed gas” field, all gases sampled in this study plot in the “thermogenic gas with oil” field. Arrow indicates direction of increasing thermal maturity.

measurements (GeoMark, personal communication, 2017). This means that gasoline-range hydrocarbons (C_5 - C_{10}) and other components below about $n\text{C}_{15}$, enriched in ^{13}C , were included in the whole-oil measurements (Peters and Moldowan, 1993, p. 127).

By comparison with the isotopically lighter group, gas components in the EQT #504353 more closely form a straight line on the natural-gas plot. As a result, a best-fit line through the higher-molecular-weight gases intersects the C_1 axis close to the measured value for C_1 (Fig. 4-28). This suggests that most of the C_1 was cogenetic with the higher-molecular-weight gases. Similar to the isotopically lighter group, intersection of the best-fit line with the y-intercept in the EQT #504353 shows a $\delta^{13}\text{C}$ value (approximately -20 per mil) for a possible

gas source that is heavier than the bitumen extracts (-30.2 to -27.5 per mil) in the well and about 7 per mil heavier than $n\text{C}_4$ (-26.7 per mil). What is notably different, however, is that the $\delta^{13}\text{C}$ value for $n\text{C}_4$ is slightly heavier than the bitumen extracts. This isotope relation suggests that gas in the EQT #504353 was derived from a source more isotopically heavy than the well-documented bitumen in the well (Figs. 7-17, 7-18, 7-19). Such a source could come from a deeper, more mature part of the basin.

Along with the heavier $\delta^{13}\text{C}$ values for all gas components, the slope of the best-fit line provides evidence for a higher level of thermal maturity in the EQT #504353. James (1983) and Chung and others (1988) demonstrated that with increasing thermal maturity, the difference in $\delta^{13}\text{C}$ values among the gas components decreases, resulting in a de-

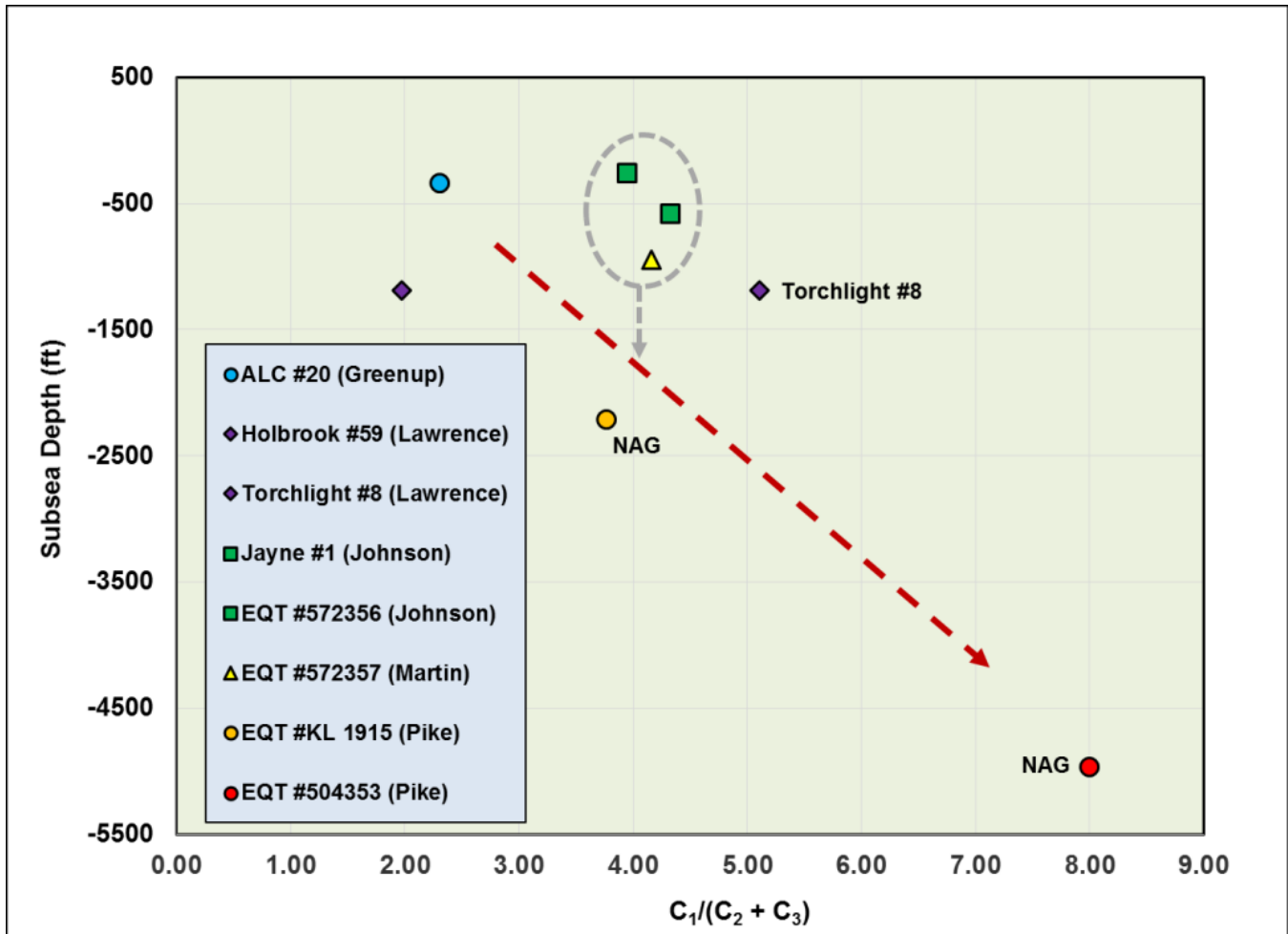


Figure 4-26. Gas wetness ($C_1/C_2 + C_3$) versus subsea depth (ft). Red arrow indicates direction of increasing thermal maturity, and gray circle and arrow represent Johnson and Martin County data (see text for further discussion).

creased slope of the natural-gas plot. James (1983) noted that the isotopic separation (i.e., slope) between C_2 and C_3 components is particularly useful, and in the EQT #504353 the separation equals 5.3, whereas in the updip wells it ranges from 6.0 to 7.9.

Nonhydrocarbon gases made up less than 10 mole percent of the total gas composition for all samples (Table 3-12). Concentrations of CO_2 were sufficiently low (0.02 to 0.062 mole percent) that isotopes could not be measured. The paucity of CO_2 likely reflects the low amounts of terrestrial-derived humic organic matter in the source rock and the paucity of inorganic carbonate rocks (Hunt, 1996). Inorganic carbonates can generate CO_2 by reactions with kaolinite at temperatures greater than $100^\circ C$ (Hutcheon and Abercrombie, 1989).

Molecular nitrogen (N_2), the dominant nonhydrocarbon gas, has concentrations in the OAG

samples consistently equal to 2 to 3 mole percent, and $\delta^{15}N$ values define a small range equal to -14.1 to -17.4 per mil (Fig. 4-29). Exceptions to the grouping of OAG samples include the heavier $\delta^{15}N$ value associated with the Jayne #1 (-5.2 per mil) and the higher concentration of N_2 in the Torchlight #8 (7.76 mole percent). In contrast, the N_2 concentrations in the NAG samples are an order of magnitude less than the OAG samples, and the former are more enriched in ^{15}N . Overall, the lighter $\delta^{15}N$ values for samples in this study suggest that N_2 was derived from sedimentary organic matter (Zhu and others, 2000). Other possible sources of N_2 , such as the deep crust, mantle, metamorphic rocks, and evaporates, tend to be more enriched in ^{15}N (-5 to 10 per mil) (Hoefs, 2004).

Concentrations of N_2 for all samples are strongly correlated with concentrations of helium

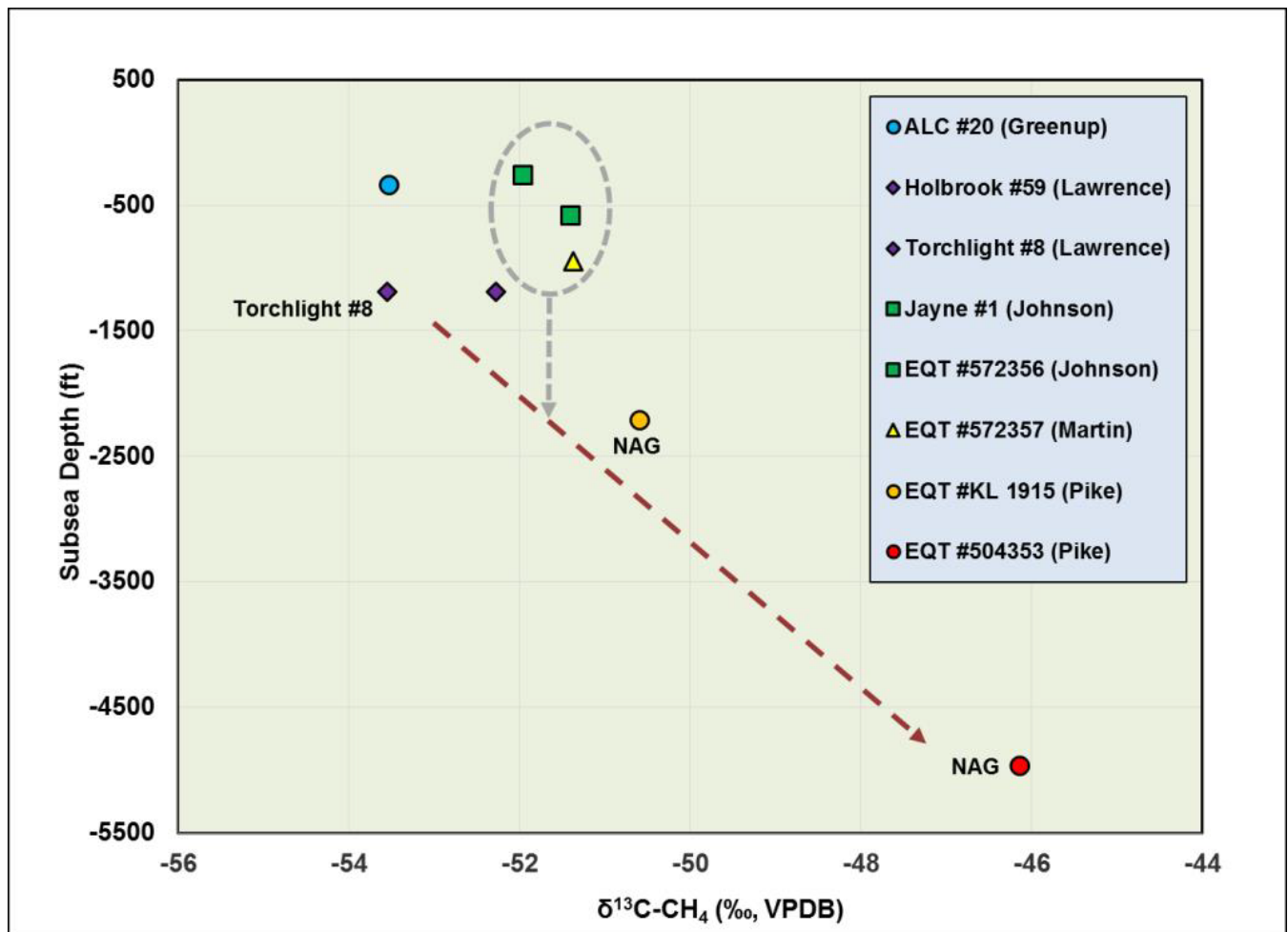


Figure 4-27. $\delta^{13}\text{C}$ for CH_4 versus measured depth (ft). Red arrow indicates direction of increasing thermal maturity, and gray circle and arrow represent Johnson and Martin County data (see text for further discussion).

(He) (Fig. 4-30). Helium produced by the radioactive decay of elements in crustal sedimentary rocks produces the isotope ^4He , whereas He derived from mantle sources is enriched in ^3He (Hunt, 1996, p. 232). Distinction between the two sources requires measurement of the isotopes and analyzing their ratios. The strong correlation between N_2 and He suggests they have similar origins, and it

is certainly plausible they were both derived from the same or similar source rock. What is not clear, however, is why concentrations of He and N_2 are so much lower in the NAG versus the OAG samples. Like the concentration of N_2 , the concentration of He in the Torchlight #8 is higher compared to all other samples. This suggests that gas composition in the Torchlight #8 is being influenced by some processes tied to the Wahlbridge Fault.

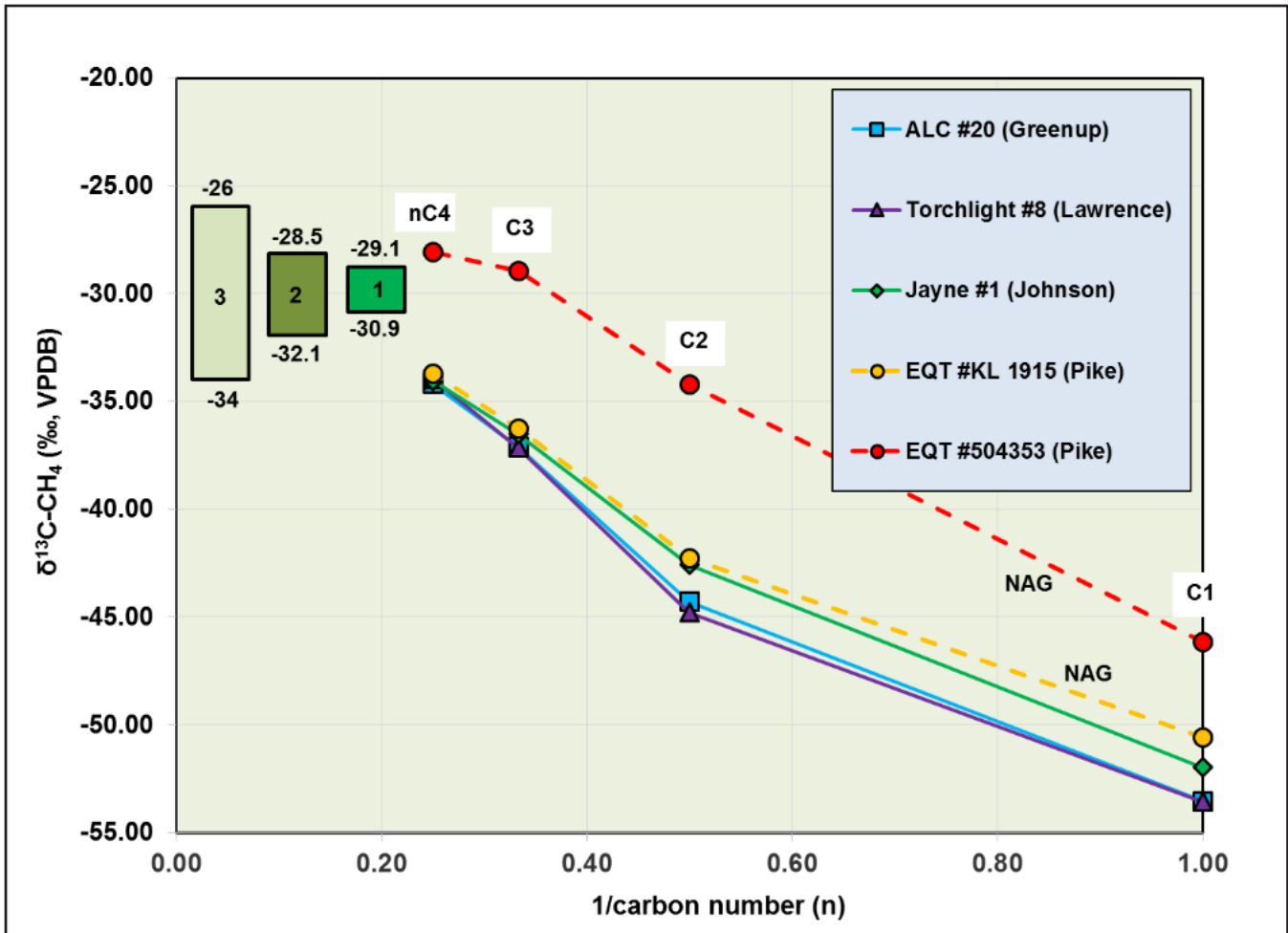


Figure 4-28. Natural gas plot showing the $\delta^{13}\text{C}$ values C_1 - $n\text{C}_4$ gas components. Barbells on left side of the plot are shifted off the $1/n=0$ axis for visualization. Barbells represent ranges of possible source organic matter that include (1) saturate, aromatic, and whole-oil components from bitumen extracts in this study from the SUN, CLV, UHUR, LHUR, and OLEN intervals in (a) updip wells and (b) the downdip EQT #504353; (2) bitumen pyrolyzates from the SUN, Ohio, OLEN, and Point Pleasant in Ohio (from Cole and others, 1987); and (3) Middle Ordovician organic matter from the Utica, Point Pleasant, and Antes in the Appalachian Basin (from Hatch and others, 1987; Burruss and Laughrey, 2010). Green ellipse represents $\delta^{13}\text{C}$ values for Berea oils. Dashed line represents best-fit line through C_2 - $n\text{C}_4$ components.

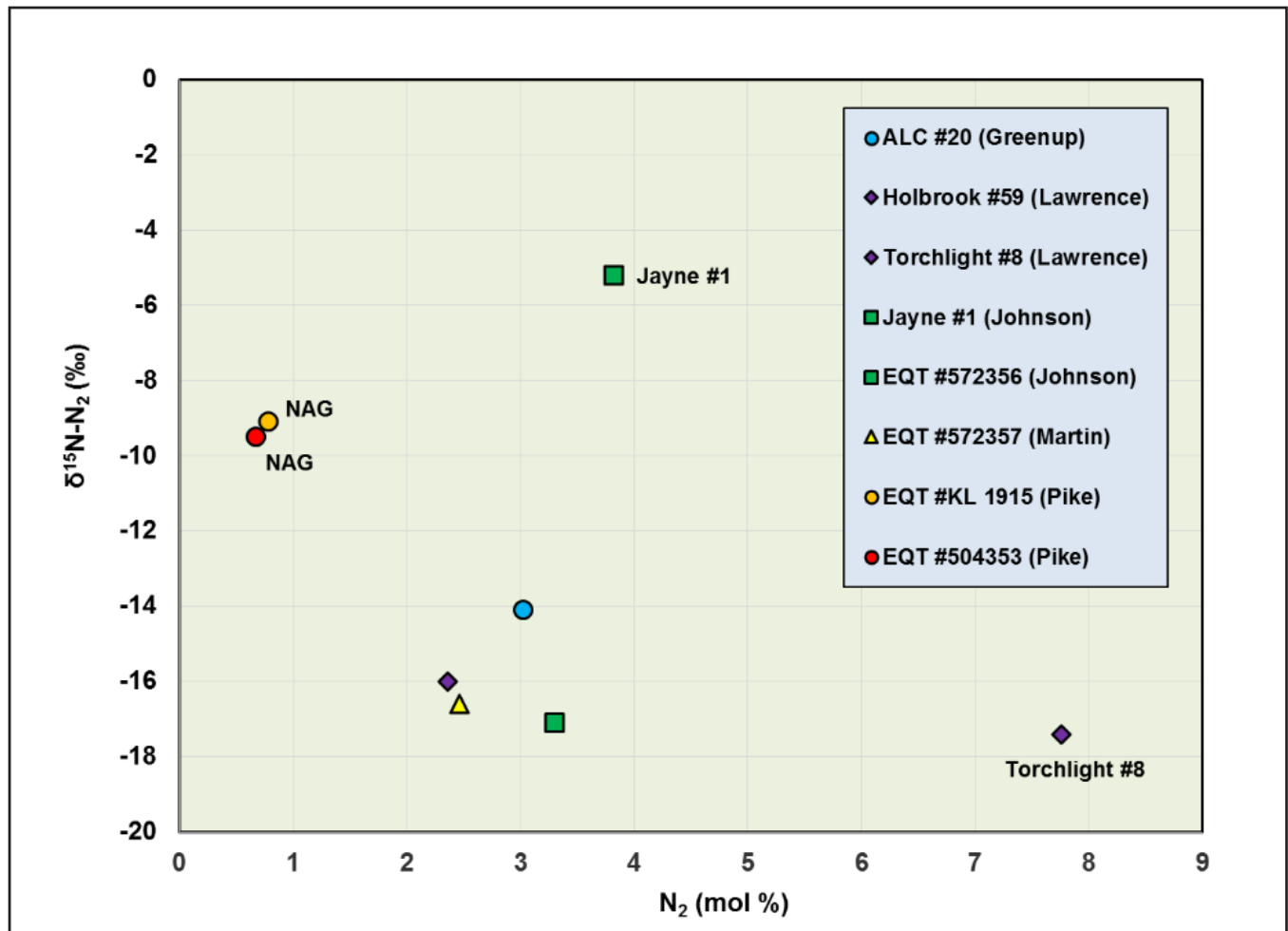


Figure 4-29. Concentration and isotopic composition of N₂.

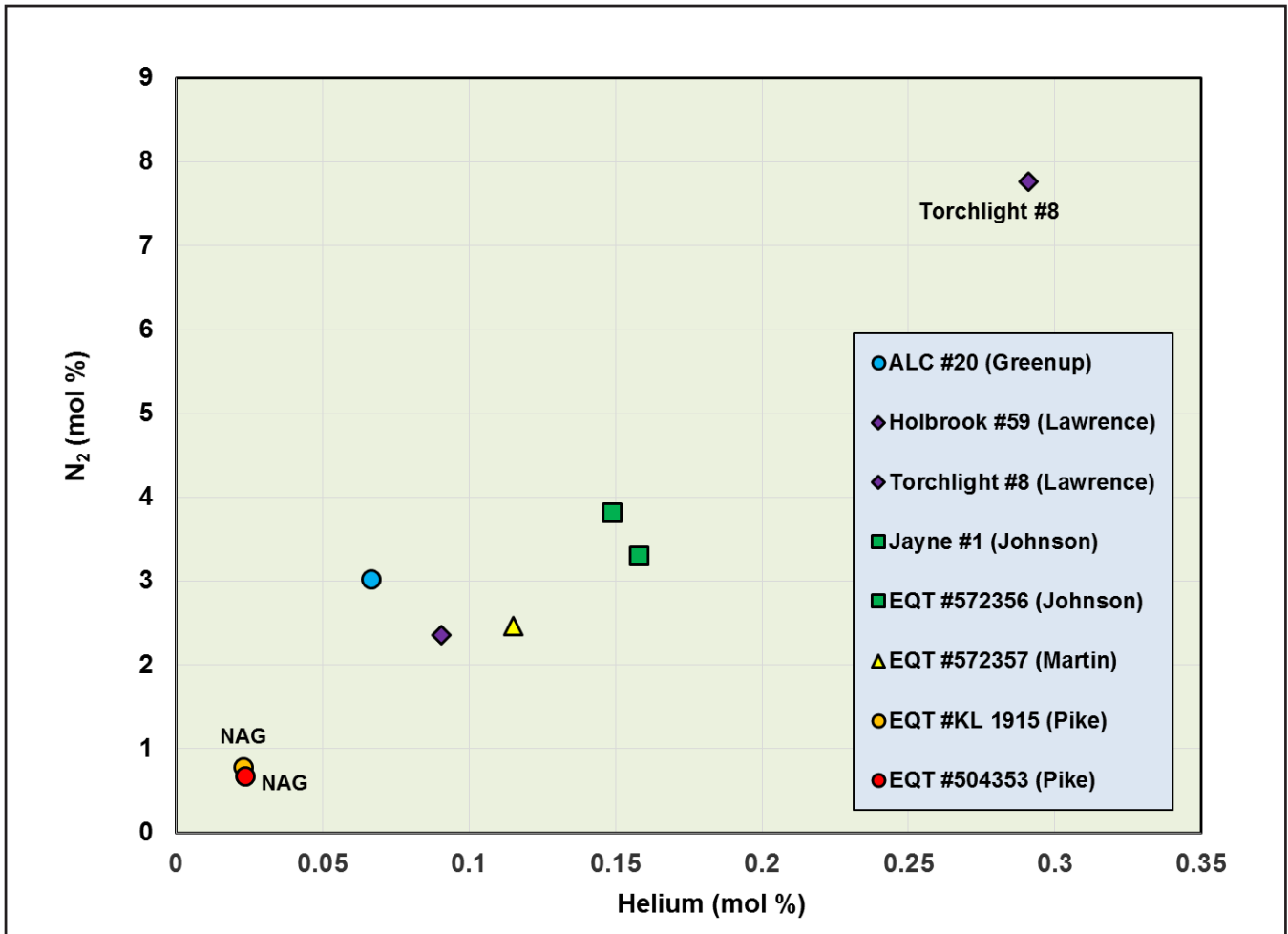


Figure 4-30. Concentration of He and N₂.

5. Discussion: Geochemistry Results and Implications for the Berea Petroleum System in Kentucky

T. Marty Parris, Paul C. Hackley, and Cortland F. Eble

The presence of oil and gas in the Berea Sandstone reservoir reflects the collective influences of source-rock composition, maturation, and migration. Production from the Berea is not only influenced by reservoir porosity and permeability and trapping mechanisms, but also by the physical and chemical properties of the hydrocarbons. The collective measurements and analyses in this study have developed new information regarding the formation and migration of oil and gas in the Berea petroleum system. Returning to the geochemical questions posed at the outset, measurements and analyses in this study provide new information on:

1. Why the Berea reservoir produces oil in areas thermally immature and gas in areas primarily oil mature and
2. Whether oil and gas in the Berea is sourced from shales in the immediate area of production or migrated from deeper in the Appalachian Basin.

Sampled along an approximately 85-mi linear transect orthogonal to regional dip and over measured depths ranging from 1,002 to 4,720 ft, six OAG and two NAG samples (Fig. 3-2) show a general increase in $\delta^{13}\text{C}$ values for C_1 and dryness ($\text{C}_1/\text{C}_2 + \text{C}_3$) with greater sample depth. The increase reflects increased thermal maturity and is consistent with rock-based thermal-maturity measurements discussed in Chapter 4 (e.g., vitrinite and solid-bitumen reflectance, programmed pyrolysis). Within the transect, however, the OAG samples and oils collected from the same wells and the NAG sample from the Justice #KL 1915 sample have remarkably similar physical and geochemical properties. For the oils, these include uniform API gravity, sulfur concentrations, SARA fractions, *n*-alkane envelopes, carbon-isotopic compositions, normal sterane distributions, correlation between individual sterane and hopane concentrations, and similarity in extended hopane concentrations (see Chapter 4). Similarly, the gases—except from the EQT #504353—show a narrow range of $\delta^{13}\text{C}-\text{C}_1$ values (-50.6 to -53.5 per mil) and gas dryness (2.3 to 5.1).

A subset of the gas samples ($n=4$) likewise shows similar carbon-isotope profiles among the C_2-nC_4 components on a natural-gas plot (Fig. 4-28). The collective uniformity among the data suggests that oil and gas in the Berea Sandstone over an approximately 60-mi distance from northern Pike County northward into Greenup County were derived from a similar source under similar thermal-maturity conditions.

Multiple proxies suggest that Berea oils were largely derived from algal material deposited in a normal marine setting. The proxies include Pr/Ph and TAR ratios, CPI values, *n*-alkane maxima, carbon-isotopic composition (Sofer analysis), and the presence of tricyclic terpanes (from *Tasmanites* and/or bacterial biomass). Petrography shows the presence of minor terrestrial organic matter, such as vitrinite and inertinite (Type III kerogen), and C_{29} sterane distributions may suggest a terrigenous contribution (although C_{29} sterane could also be sourced from photosynthetic marine plankton). The overall contribution of terrestrial organic material to the Berea oils is considered to be minor.

The distribution of steranes in Berea oils and bitumen extracts from the Sunbury, Cleveland, Upper Huron, and Lower Huron is sufficiently similar that any of the intervals could be a potential source (Fig. 4-13). Likewise, the carbon-isotopic composition of oils and bitumen extracts is similar. Slight differences in the total sterane to hopane ratios suggest greater similarity between oils and the Sunbury and Upper Huron extracts, but this single observation does not preclude possible contributions from Cleveland and Lower Huron intervals.

From a regional perspective, the carbon-isotopic compositions of Berea oils in this study are similar to those of Berea oils in Ohio, where Cole and others (1987) interpreted the source rock to be the Sunbury Shale. They acknowledged, however, that the Ohio and Olentangy could also be sources. In this study, isotopic analysis using the natural-gas plot of the OAGs and the NAG from the Justice #KL 1915 suggests a source that is isotopically heavier than the bitumen extracts or oils (Fig. 4-28,

intercept at $1/n=0$). Reconciliation of this apparent incongruence requires that higher-molecular-weight hydrocarbon gases, such as nC_4 , come from a parent molecule having a smaller number of carbon atoms (n), as suggested by Chung and others (1988), or from an isotopically heavier source not recognized in this or earlier studies.

Other potential source rocks in the region include the Ordovician Utica and its equivalents and the Middle Cambrian Rogersville Shale. When compared to Ordovician-sourced oils studied by Cole and others (1987) in eastern Ohio, the Berea oils in this study have higher Pr/Ph ratios and lighter carbon-isotopic compositions. Bitumen extracts from the Rogersville Shale show a broad spectrum of n -alkanes from $n-C_{11}$ through $n-C_{30}$, strong odd-carbon predominance in the $n-C_{13}$ to $n-C_{19}$ range, and detectable amounts of the isoprenoids pristane and phytane (Ryder and others, 2014). The strong odd-carbon predominance, attributed to the Ordovician alga *Gloeocapsomorpha prisca*, is not observed in the Berea oils or bitumen extracts in this study.

Previously, we showed that similarity in the normal sterane ratios provided evidence that most of the sampled bitumen extracts could be a source for Berea oils (Fig. 4-13). In contrast, bitumen extracts from the deeper EQT #504353 well in southern Pike County show lower proportions of the C_{29} sterane component compared to the shallower updip bitumen extracts and the oils. This difference would appear to preclude bitumen extracts in the EQT #504353 from being a source for Berea oils.

Isotopically, the $\delta^{13}C$ values for extracts in the updip wells and the downdip EQT #504353 are similar to Berea oils (Fig. 4-28). If, as discussed above, Berea oils were derived from a parent molecule with a smaller number of carbon atoms than suggested by the $1/n=0$ intercept, then extracts in the updip and downdip position could be a source. Though showing a broader range of $\delta^{13}C$ values compared to extracts in this study, Ordovician rocks are an unlikely source, for reasons discussed above (Fig. 4-28). The isotopically heavy $\delta^{13}C$ value for nC_4 (-26.7 per mil) in the EQT #504353 does require a parent molecule isotopically heavier than any organic matter measured in this or other studies in the area. Considering kinetic effects, this would seemingly require a more mature downdip source. Given the higher thermal

maturity at the position of the EQT #504353 (average $VR_o=1.24$ percent; Table 3-2), then gas derived from a downdip source could come from primary cracking or secondary cracking of oil. Organic matter in the Berea Sandstone that could participate in these processes is demonstrated by bitumen staining and oil and gas inclusions in fracture cement in the EQT #504353 (Figs. 7-17, 7-18, 7-19).

Not surprisingly, vitrinite-reflectance measurements along the northwest-southeast transect show a progression indicative of increasing thermal maturity (Fig. 4-3). This increase agrees with numerous other studies (Rimmer and others, 1993; Repetski and others, 2008; Ruppert and others, 2010; East and others, 2012; Hackley and others, 2013; Ryder and others, 2013; Araujo and others, 2014; Riley, 2016). Also reflecting the northwest to southeast increase in thermal maturity are increases in T_{max} and a decrease in HI values (Figs. 4-4, 4-5). The rate at which thermal maturity increases is mostly constant along the transect; however, in Pike County, R_o values begin to increase at a more rapid rate. The increase is also somewhat reflected in the T_{max} and HI gradients. We are not aware of any thermal anomalies that would have increased the geothermal gradient in Pike County. Consequently, the increased thermal-maturity gradient may reflect a "hinge effect" in which basin downwarping was accentuated. One possible mechanism for the downwarping is crustal loading associated with emplacement of the Pine Mountain Thrust, located along the southern border of Pike County.

One of the main goals in performing reflectance measurements was to assess the potential presence of vitrinite-reflectance suppression in areas where thermal maturity was previously characterized (e.g., Repetski and others, 2008; East and others, 2012). The results in this study consistently show that reflectance measurements for vitrinite are higher than measurements for solid bitumen, especially at thermal-maturity values less than 1.0 percent R_o (see page 39). Potential suppression of vitrinite-reflectance values is especially of concern in areas where those values are at or close to the immature-mature boundary. This is the situation in Lawrence County, which is in the heart of the Berea oil play. In this study, we carefully distinguished measurements of vitrinite versus solid

bitumen and, consequently, see no evidence for suppression of vitrinite values. Therefore, reports of vitrinite suppression are likely to be from studies in which reflectance measurements on vitrinite and solid bitumen were mixed, such as suggested by Hackley and others (2013). For pre-Pennsylvanian organic-rich mudstones and shales, this mixing may happen more frequently because of the paucity of true vitrinitic material. As stated earlier, the potential of suppression not only affects reflectance measurements, but also pyrolysis measurements, such as T_{\max} . To get around the suppression problem, corrections have been developed for reflectance and T_{\max} measurements (Lo, 1993; Snowden, 1995). Even when corrections are applied to the various data in this study (see page 39), thermal-maturity conditions still appear to be immature or early-mature in areas where high-gravity, low-sulfur oil is being produced, suggesting hydrocarbon migration into these areas.

The high concentration of aromatics and saturates relative to asphaltenes and resins, and low sulfur content, is consistent with Berea oils forming at higher thermal maturities than shown by the local source rocks in the production area (Fig. 4-6). However, this observation alone is not demonstrative of migration and emplacement of the Berea oils from a higher-maturity source, because oils always have higher proportions of aromatics and saturate molecules than their correlative source-rock bitumen extracts (e.g., Lewan, 1997). On the other hand, a previously discussed proxy for oil thermal maturity was the methylphenanthrene index (MPI) from aromatic biomarkers (Radke and Welte, 1983). Correlation of the MPI with reflectance measurements (Fig. 4-21) and saturate/aromatic ratios (Fig. 4-22) may suggest that Berea oils cracked from bitumens at thermal-maturity conditions equivalent to 0.7 to 0.9 percent R_o , again consistent with updip hydrocarbon migration in the Berea petroleum system.

Jarvie and others (2015) used the proportions of saturate, aromatic, resin, and asphaltene fractions to assess the thermal maturity at which oils were generated. Their analysis, based on GeoMark's Rock-Fluid Database (2015) and experimental work (Behar and others, 2008; Behar and Jarvie, 2013), is summarized in Figure 5-1. These authors demonstrated that thermal degradation of most kerogens yields bitumen, which consists

primarily of resins and asphaltenes and minor amounts of hydrocarbons. With increased thermal maturation through the oil window, products derived from the cracking of kerogen (primary) and bitumen (secondary) produce increased amounts of hydrocarbons. It is important to note that Jarvie and others (2015) and the other authors cited in this discussion viewed products derived from kerogen (e.g., NSO compounds) as secondary products that are important generators of hydrocarbons through secondary cracking. When viewed in the context of this evolution, Berea oils, enriched in saturate and aromatic fractions (Table 3-6), are compositionally on the boundary of black and volatile oil. The former develops at thermal maturities equivalent to 0.7 to 0.95 percent R_o and the latter at 0.95 to 1.2 percent R_o . If Berea oils formed by secondary cracking at the higher end of this thermal-maturity range, this would imply a greater distance of migration compared to formation at lower thermal maturity. It is important to note the use of secondary cracking in this context differs from the classic definition in which gas is generated from the cracking of oil, typically at higher thermal maturity (Hunt, 1996, p. 186).

Considered collectively, sterane isomerization ratios and analysis of MPI and SARA data suggest that Berea oils formed at a thermal maturity equivalent to R_o values of 0.7 to 0.9 percent. The implication of this interpretation is that Berea oils, likely derived from secondary cracking, have migrated from a deeper, more thermally mature source rock into updip Berea reservoirs. Based on mapping of vitrinite reflectance in this study (Fig. 4-3), the 0.7 percent VR_o contour runs southwest-northeast through northern Martin County and the 0.9 percent VR_o contour follows a similar trend through central Pike County. The overall trend of the reflectance contours is subparallel to the structural contours on top of the Berea (Fig. 2-5). Thus, possible distances for migration from the 0.7 percent VR_o contour into Lawrence County are on the order of 5 to 20 mi, and that distance increases to 45 to 50 mi into Greenup County. Generation from yet higher maturity levels suggests even greater migration distances.

The mechanism of oil formation by secondary cracking followed by migration into the updip areas of the Berea is also consistent with the distri-

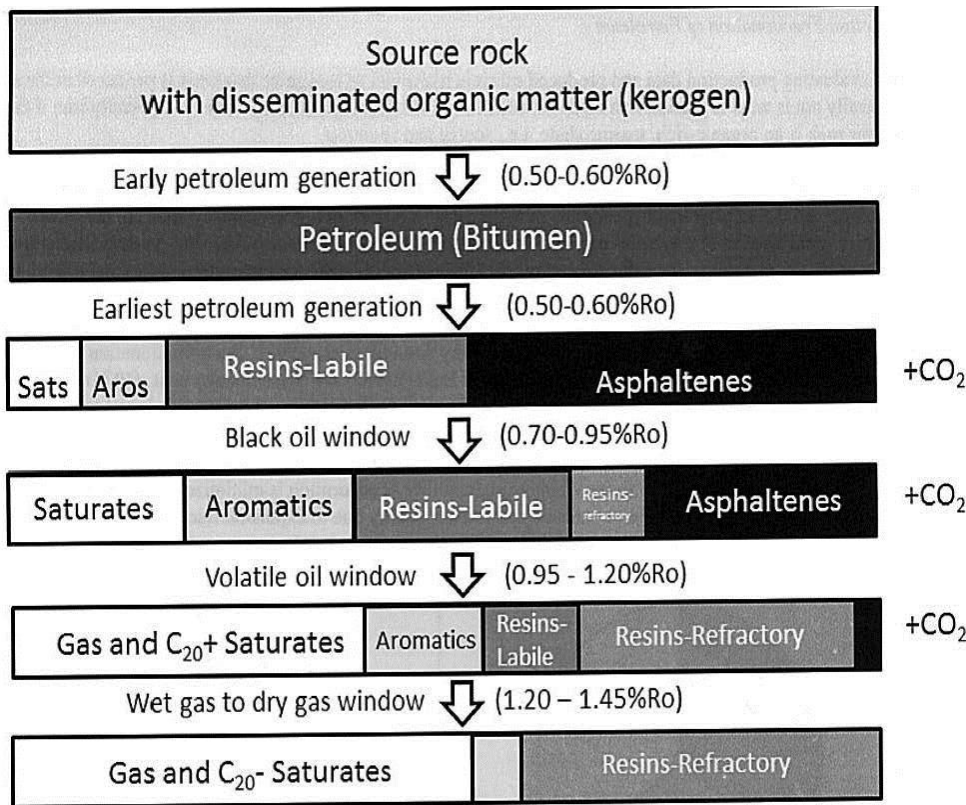


Figure 5-1. Source-rock maturation from kerogen and bitumen and the evolution of hydrocarbons. The distribution of saturates, aromatic, resin, and asphaltene compounds in oils varies systematically with increasing thermal maturity (Jarvie and others, 2015; used with permission). Note that the relative proportions of SARA components listed in this diagram are from work by Jarvie and others (2015), and were not systematically evaluated against a database of oil or bitumen extract SARA compositions for our study.

bution of sulfur in the bitumen extracts and oils. As discussed above, the sulfur content in the oils is low (0.17 to 0.21 percent), which contrasts with the higher values (0.55 to 7.53 percent) in the bitumen extracts (Table 3-6). If derived from a local source, then the oils might also be expected to have higher sulfur concentrations. Baskin and Jones (1993) found sulfur contents in reservoir bitumens to be similar to sulfur content in associated oils. We are comparing source-rock bitumen to associated oils, and we are unaware of published work comparing source-rock bitumen sulfur to sulfur in oils produced locally from the same source rock. Other workers (Pomerantz and others, 2014; Hackley and SanFilipo, 2016) have reported sulfur contents from source-rock bitumen similar to sulfur contents reported here. This is from source rocks of similar immature to early-mature conditions. However, there is no associated saturate-rich oil production. This observation may suggest low sulfur values in

Berea oils are due to sourcing from a more mature intermediate secondary product low in sulfur, followed by updip migration into the Berea reservoirs. Meanwhile, the elevated sulfur concentrations in the bitumen extracts may be sequestered in polar compounds such as the resins and asphaltenes.

The analysis of oil samples has provided important insights into the accumulation of oil in the updip portion of the Berea petroleum system that probably would not have been possible with rock-based data only. Farther south in Martin and Pike Counties, the predominance of gas production versus oil production appears to be incongruent with thermal-maturity parameters that indicate the area to be mostly in the oil window. Despite this, insights provided by Nuttall’s (2016) production analysis and gas measurements in this study suggest that thermal maturity and hydrocarbon phase being produced are more aligned than previously thought. In Nuttall’s (2016) analysis, company production reports showed that some oil is being produced from the Berea and Ohio intervals even into southern Pike County. Both gas samples from Pike County are classified as nonassociated gases (NAGs) because no liquids are being produced at the wellhead. Compositionally, however, both samples are wet gases (Fig. 4-26), and the EQT-Justice #KL1915 showed a carbon-isotope profile on the natural-gas plot (Fig. 4-28) very similar to the updip OAG samples. With this perspective, it is thus probably more accurate to view the more thermally mature areas in Martin and Pike Counties as a combined oil and wet-gas province.

The paucity of oil production in Martin and Pike Counties may reflect a difference in the petroleum produced at the wellhead versus petroleum that resides in the reservoir or source rock. Jarvie and others (2015) have noted that in low-permeability unconventional reservoirs, nonpolar compounds (i.e., saturates, aromatics) will be selectively produced over polar compounds (i.e., resins, asphaltenes). This production fractionation also affects producibility because hydrocarbon composition affects API gravity and the gas:oil ratio (GOR). Thus, in a tight source rock (e.g., Sunbury and Ohio Shale) and/or a tight reservoir (e.g., Berea Sandstone), it is likely that lighter oils will be preferentially produced over heavier oils enriched in polar compounds.

Future Studies

Analyses done in this study provide little information on the timing of hydrocarbon generation and migration in the Berea petroleum system. Some evidence for relative timing is provided by gas-composition data from wells in Johnson and Martin Counties. Here it appears that associated gas was in the Berea reservoir prior to complete uplift of the Paint Creek Uplift (Figs. 4-26, 4-27). More accurate estimates of the timing of hydrocarbon generation in a broader geologic context, however, require development of a burial-history model for the area. For example, Ryder and others (2014) used data from the Exxon Smith #1 well in Wayne County, W.Va., to model the burial and temperature history of Cambrian petroleum source rocks. The Smith #1 is located on strike with rocks in northern Lawrence County. Their analysis suggested that Mississippian-Devonian source rocks barely make it into the oil window, if at all. This agrees with our thermal-maturity measurements in the Lawrence County area. What is not clear, however, is why maximum burial followed by uplift occurs in the Jurassic, which is significantly later than the Late Pennsylvanian–Early Permian Alleghenian Orogeny (Shumaker, 1996). Thus, de-

velopment of a burial-history model specific to this part of the Appalachian Basin would better define the timing of tectonic events affecting the depositional history of source rocks in the Sunbury and Ohio Shales.

The importance of developing a burial-history model closer to the study area is underscored by the nonuniform increase in thermal maturity as depicted by the isolines on the vitrinite-reflectance map (Fig. 4-3). Specifically, the isolines in Pike County represent a rapid increase in thermal maturity compared to the rest of the study area. The cause for the increase is not clear, but it is possible that it accelerated source-rock maturation in this part of the basin.

Previously, we argued that oils were generated downdip in a more thermally mature part of the basin and migrated into the updip portion of the Berea. Part of the argument was based on the higher concentration of sulfur in the bitumen extracts versus the concentration in the oils. The presence of migrated oil does not, however, preclude the possibility of local generation. Previous studies have documented generation of oil from sulfur-rich source rocks at thermal maturities less than 0.6 percent R_o (Baskin and Peters, 1992). If the presence of sulfur similarly influenced source rocks in the Sunbury and Ohio intervals, then the 0.6 percent R_o threshold for the onset of oil generation might be too high. To test this hypothesis we intend to resample and measure the sulfur concentrations in the kerogen analyzed in this study in the Aristech #4. Some of the sample would be submitted to the USGS for hydrous-pyrolysis analysis, a technique that simulates oil generation in source rocks (Lewan, 1985). The technique involves heating a source rock in a closed system in the presence of water and measuring the extractable bitumen and expelled oil. Even if oils are being generated at lower thermal maturity, it is likely they are not being produced, for reasons described in the previous section and outlined in Figure 5-1.

6. Reservoir Geology Methods

Stephen F. Greb and David C. Harris

Reservoir geology and quality for the Berea was assessed by several different methods. First, a regional assessment was made of well and field locations using the KGS oil and gas field database. Porosity and permeability data from the database were compiled, as were selected geophysical logs. Outcrop data from previous field guides and theses were compiled, and new outcrops were measured and described. Available public cores through the interval at the KGS Well Sample and Core Library, and one core from the Ohio Geological Survey's core facility, were photographed and described. Structure maps, isopach maps, and cross sections were used from Julie Floyd's (2015) master's thesis, a project that ran concurrent with this project. Data, cross sections, and maps were compiled in Petra.

Thin-Section Petrography

Twenty-eight thin sections were made of selected samples from the Kentucky outcrops and cores to analyze grains and cements using standard procedures. All thin sections were made by Wagner Petrographic. Blue epoxy was used in thin sections to show porosity. Thin sections were stained with a dual carbonate stain (potassium ferricyanide and alizarin red) to aid in identification of calcite and dolomite, and ferroan (iron-rich) carbonates. Sections were examined at the Kentucky Geological Survey with an Olympus petrographic microscope equipped with epifluorescence (UV) illumination and a digital camera.

Grain-Size Analysis

The very fine grain size of Berea sandstones makes accurate determination of grain size difficult. In order to quantify grain size and determine any control on porosity or permeability, approximately 100 grains were measured on digital photomicrographs for selected thin sections of the Berea. The image-analysis program JMicroVision was used to manually measure the grains and compile the data. The longest apparent dimension of each grain was measured, which on average gives results close to standard mechanical grain-size analysis.

Chesapeake Energy sampled several key cores from the KGS Well Sample and Core Library and submitted those data to KGS during this study. The Chesapeake data included new porosity and permeability measurements, as well as XRD data from Chesapeake's labs.

Pulse-Decay Permeability

Chesapeake's permeability data were measured using a pulse-decay method at 400 psi and 1,000 psi NES pressure. Pulse-decay permeameters are generally used in caprock studies and in tight reservoirs because the method is capable of measuring much lower permeabilities (to nanoDarcys) in a shorter amount of time than standard gas permeameter methods. In the pulse-decay method, samples are saturated to a set pore pressure, then a pressure pulse is transmitted through the sample. The change in pressure across the sample and time of the change is measured. Permeability is calculated from a linear regression of the pressure versus time data. In chapter 7, permeability measured using this technique is differentiated from historic porosity and permeability data (generally, core analysis reports from Oilfield Research Inc.).

XRD Analysis

We do not have specific information on the machine or methods used for XRD in Chesapeake's labs, but presume they used typical XRD analyzers and standard methods. XRD analysis uses X-rays to identify mineral grains and cements. X-rays are generated, filtered, and concentrated on a prepared, powdered sample. Constructed interference patterns result from the interaction of the X-ray with the lattice spacing of crystalline minerals in the sample. Different minerals have characteristic diffraction patterns (wavelengths and peaks), which allows minerals in a sample to be identified. The Chesapeake Energy data were normalized to sum to 100 weight percent.

Mercury Injection Capillary Pressure Analysis

MICP data are used to collect information on pore-throat size, pore-throat distribution, and an-

anticipated capillary-pressure behavior in seals and tight reservoirs. MICP data in this study were analyzed at Weatherford Laboratories. Weatherford uses an Autopore IV 9520 instrument for MICP analysis, which is capable of measuring pore diameters to $0.003\ \mu\text{m}$, at a resolution of $0.1\ \mu\text{l}$ and accuracy of ± 1 percent of maximum penetrometer stem. For MICP, samples are batch Soxhlet-cleaned. Grain density and ambient porosity are measured, and samples are vacuum-dried at 180°F for 24 hr. Samples are then weighed, loaded into the selected penetrometers, and installed into the low-pressure ports of the instrument. Air is then evacuated from the penetrometers to a pressure equivalent

to $50\ \mu\text{m Hg}$ for 15 min, after which the penetrometers are backfilled with mercury. Pressure is then increased, following defined pressure tables, up to the last low-pressure point specified. The penetrometers are then removed, weighed, and loaded into the high-pressure ports. The pressure is then increased to approximately 60,000 psia, following selected pressure steps. Mercury saturation corresponding to each pressure step is collected by determining the volume of mercury remaining in the penetrometer stem. From the data collected, permeability, porosity, and various attributes of capillary entry pressures and pore-throat aperture sizes can be calculated analytically.

7. Reservoir Geology Results

Stephen F. Greb and David C. Harris

Analysis of Berea reservoirs in eastern Kentucky was made in several steps, corresponding to the following subsections: (1) "Regional Reservoir Geology," which examines the distribution of Berea oil and gas fields relative to major structures and Bedford-Berea thickness trends, (2) "Outcrop Analysis," which examined facies and bedding exposed in outcrop for comparison to available cores and subsurface data, (3) "Well and Core Analysis," which summarizes core bedding and available geophysical-log data relative to porosity and permeability data, (4) "Porosity and Permeability Analysis," which summarizes available porosity and permeability data and compares those data to XRD data from four cores and thin sections from those cores to better understand diagenetic influences on porosity and permeability, (5) "Thin-Section Petrography," which summarizes cements and analyses from thin sections, and (6) "MICP Analysis," which summarizes the results of MICP tests from six selected samples.

Regional Reservoir Geology

Structural Influences. Berea reservoirs in eastern Kentucky are generally low-permeability, heterogeneous, "tight sands" (less than 1 md permeability), which in many cases may be coarse siltstones rather than sandstones. The reservoirs have been reported as stratigraphic traps (e.g., Tomastik, 1996), but structural influences have also been reported (e.g., Lee, 1980). Heterogeneity in Berea reservoirs is thought to be dominated by facies changes and diagenetic influences such as cementation, compaction, and feldspar dissolution (e.g., Tomastik, 1996). Figure 7-1 shows the distribution of eastern Kentucky Berea oil and gas wells and fields superimposed against tectonic structures. There are several trends of production that correspond to structure. The east-west belt of fields in Lawrence and Johnson Counties is south of and parallel to the trend of the Wahlbridge Fault and a parallel fault in the Irvine-Paint Creek Fault System. Production decreases westward onto the flanks of the Paint Creek Uplift.

In Pike County, any trends that might exist between Berea fields and structure are likely masked

by the fact that most of the wells shown commingle Ohio Shale and Berea production. More Ohio Shale wells are developed to the southeast in the deeper part of the Ohio Shale (Lower Huron Member). However, in southwestern Pike County there has also been significant recent development along the D'Inwilliers Structure (bright green circles in Figure 7-1). This may be a drilling strategy or it may indicate importance of structure for gas migration in that area.

The Berea itself has been inferred to be partly structurally controlled in parts of eastern Kentucky. Several reports have suggested the Waverly Arch was a primary control on sand distribution and a possible shelf break between Berea sands and Bedford shales to the west (Tankard, 1986; Pashin and Ettensohn, 1992, 1995). Lee (1980) showed that southward, local thickness changes in the subsurface Berea-Bedford interval across small faults in Martin County. Floyd (2015) investigated structural influences on Berea thickness and facies in the subsurface of eastern Kentucky and found several examples of thickness and gross lithology changes across structures.

As previously mentioned, the Bedford-Berea interval is thick along an elongate northwest-southeast trend (Figs. 2-2, 2-6), subparallel to the eastern fault bounding the Perry County Uplift and possibly the D'Inwilliers Structure in Pike County. The total interval is thickest north of the Kentucky River Fault System, and may thin across the Waverly Arch near the Lewis-Greenup County line. Figure 7-2 shows the distribution of net Berea thickness based on a 101 API unit cutoff on subsurface gamma logs. This API limit slightly overestimates thickness along the outcrop belt (shows 0-10ft thickness where the Berea is absent), but was a best fit to subsurface data (with some variation). The map shows net Berea is thickest north of the Kentucky River Fault System (KRFS in Figure 7-2). This area defines a northern depocenter in Greenup, Carter, Boyd, and part of Lewis Counties (Figs. 7-1, 7-2). Local thickness changes in the Berea also occur on the eastern side of the Paint Creek Uplift (PtCu in Figure 7-2), where the Irvine-Paint Creek Fault System (IPCFS in Figure 7-2) splays

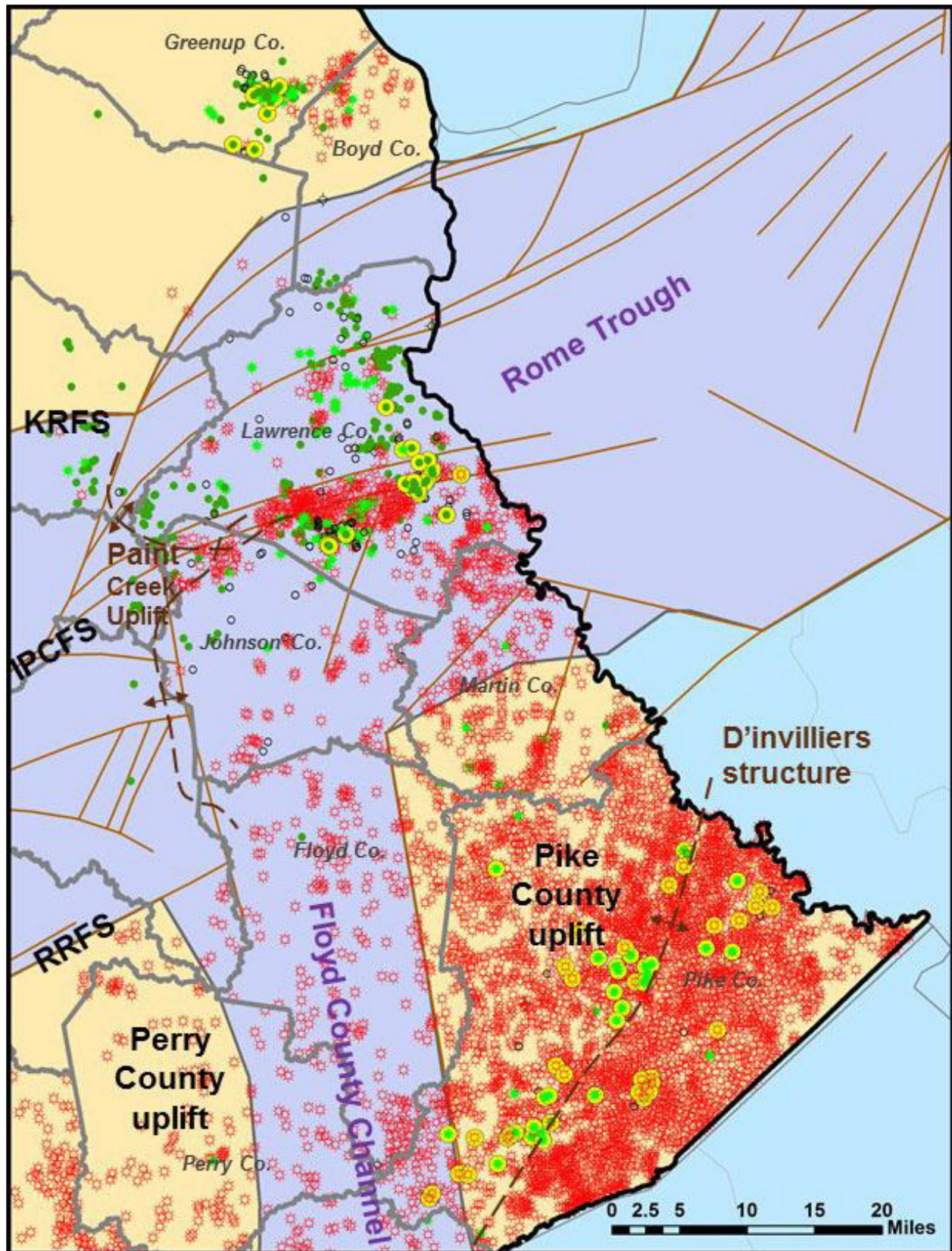


Figure 7-1. Map of producing Berea oil and gas wells showing principal tectonic structures discussed in text. Bright green circles with yellow outlines are recent horizontal wells. Those in Pike County are mostly horizontal wells in the Ohio Shale.

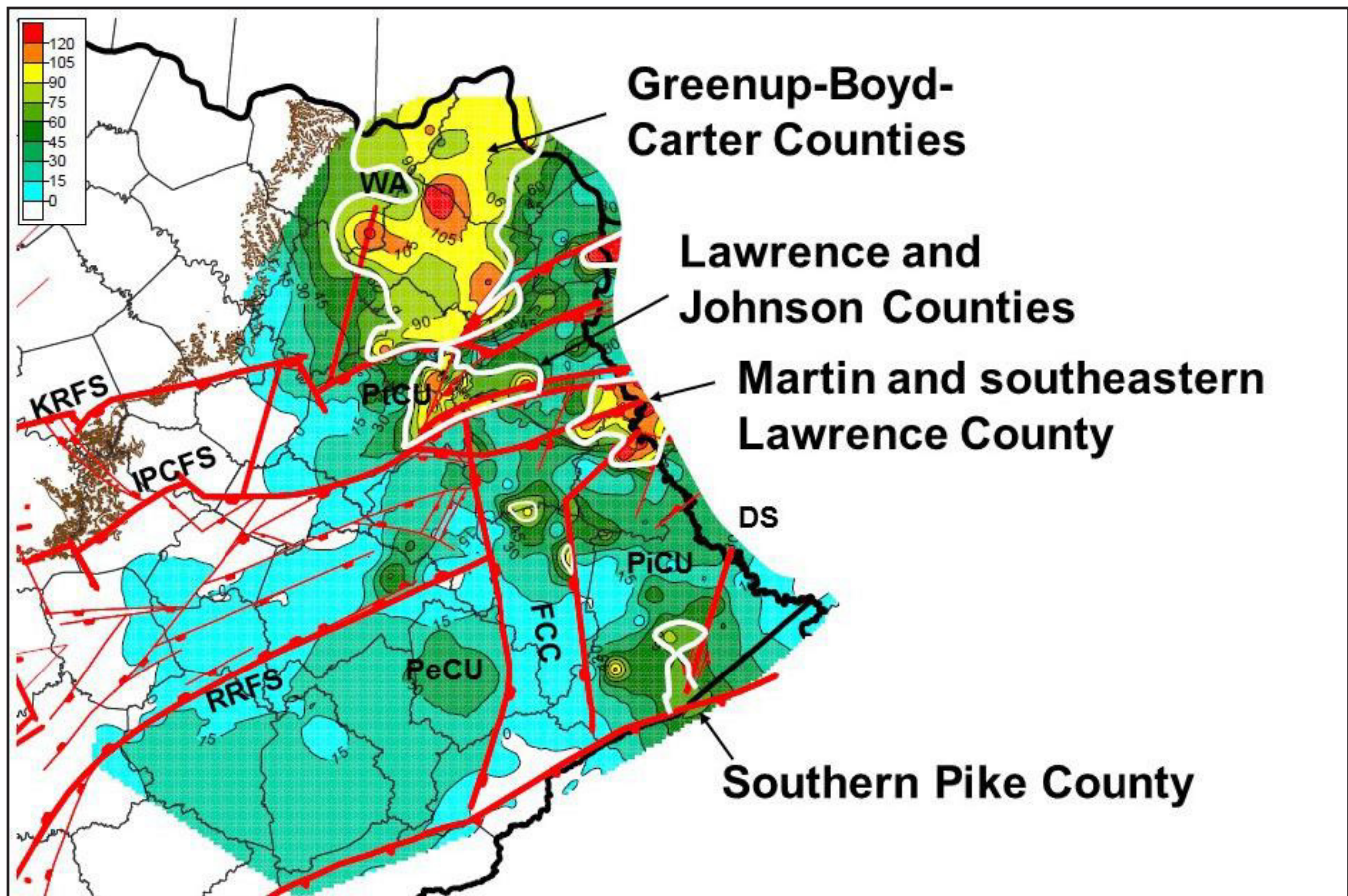


Figure 7-2. Thickness trends across known major structures. Net Berea thickness (based on a 101 API unit limit on gamma logs). Note examples of local structural influences across major fault trends. Map modified from Floyd (2015); used with permission. See Figure 7-1 for structure names. Areas outlined in white are greater than 75 ft net Berea thickness.

or is cut by northeast-southwest-oriented faults along the Floyd County Channel trend (FCC in Figure 7-2). A narrow, thick trend of net Berea sand extends eastward from the Paint Creek Uplift parallel to the Walbridge Fault, and corresponds to the area of production in Lawrence and eastern Johnson Counties (Figs. 7-1, 7-2). A small area of increased thickness occurs in Martin County (Fig. 7-2), near the West Virginia state line. This is the area in which Lee (1980) noted structural controls across several small faults. Net Berea thins south of that trend. Also, the trend of wells along the D'Inwilliers Structure (DS in Figure 7-2) in Pike County appears to correspond to another locus of sand deposition, or "southern shelf," on the southern margin of the Pike County Uplift (PiCu in Figure 7-2). More details on structural influences can be found in Floyd (2015).

Pay Zones in Producing Fields. Summaries of Berea fields in eastern Kentucky, derived from the TORIS database, Gas Atlas (Tomastik, 1996), and updates for this report (Table 7-1) show average porosities in Berea fields range from 11 to 14 percent from pay zones 12 to 30 ft thick. Figure 7-3 shows geophysical log data from representative wells in the representative fields listed in Table 7-1. In Figure 7-3, porosity intervals greater than 10 percent are highlighted in blue for fields that have a well with a density-porosity log. Perforated or reported completion zones are shown in green (oil) and red (gas). The profiles show that many wells were historically completed across the whole Berea or an upper (uBR) or lower Berea (lBr) interval. Although many operators divide the interval into an upper and lower Berea (separated by shales), there are often middle Berea sandstone tongues. Also, these informal designations may not correlate from

Table 7-1. Selected features of representative Berea oil and gas fields from the KGS Oil and Gas Database (updated from the TORIS database and as shown in the Appalachian Gas Atlas [Tomastik, 1996]).

Well No. on Figure 7-2	Field Name	County	Bedford-Berea Thickness (ft)	Net Porosity >10% (ft)	Mean Pay Porosity (%)	Mean Production Depth (ft)	KGS Record No. for Well on Figure 7-2
1	Naples CONS	Greenup	150	22	30	1,000	74276
2	Ross Chapel CONS	Boyd	134	18		1,827	2347
3	Trinity	Lawrence	116	22			28539
4	Fallsburg	Lawrence	123	28	15	1,750	11672
5	Daniels Ck. School	Lawrence	78	23	24	1,390	37868
6	Jobe Branch	Lawrence	118	25			121813
7	Yatesville	Lawrence	104	18	10	1,502	83175
8	Burgess Branch	Lawrence	60+	12+		1,718	85492
9	Redbush	Lawrence	117	23			62968
10	Tarklin	Lawrence	113	19		862	134455
11	Cordell	Lawrence	114	23			128936
12	Beech Farm	Lawrence	103	18	13	1,275	10246
13	Canada DBS	Pike	92	19	15	3,000	114172
14	Nigh DBS	Pike	94	26	20	3,200	136005

field to field if the existing prograding clinof orm model of the Berea is valid.

Pay intervals listed in Table 7-1 are reported as 12 to 30 ft thick. The current Berea play utilizes horizontal drilling in a single pay zone. Example wells from these fields (Fig. 7-3) show that pay zones consist of multiple, thinner porosity intervals. Understanding individual porosity intervals, and parts of those pay zones, is critical for successful horizontal drilling.

Outcrop Analysis

Outcrops of the Berea are limited to a few locations in northeastern Kentucky, between Vanceburg and Garrison, and northward into Ohio. Several papers and field guides have highlighted some of these outcrops (Potter and others, 1983; Pashin, 1985; Pashin and Ettensohn, 1987; Ettensohn and others, 2009). The accompanying field guide provides measured sections, photos, and descriptions of some of the key outcrops along Ky. 10 and Ky. 9 (AA Highway). Pashin (1985) and Pashin and Ettensohn (1987) divided the Berea into four sandstone/siltstone lithofacies and one interbedded shale and siltstone facies. The interbedded Bedford Shale was divided into two shale facies (Table 7-2). Of the siltstone/sandstone facies, the sheet sand-

stone facies is most widespread. The two sheet sandstone lithofacies are mostly differentiated based on the occurrence of ripples, but even in the upper facies, ripple bedding only occurs as single ripple trains capping beds or in interbedded shales, so accounts for less than 5 percent of the total Berea thickness. The upper sheet sandstone is widely exposed around Garrison, Ky. (Fig. 7-4A). Bedding is sheet-form and consists of coarse siltstone to very fine sandstone with interbedded shales. Bedding structures include massive, hummocky, parallel-laminated, and ripple-bedded types (Figs. 7-4B, C, D). Bioturbation occurs, but is uncommon.

The swaley-bedded lithofacies differs from the sheet-sandstone lithofacies in the occurrence of swaley bedding and lack of soft-sediment deformation. Relative to core, swaley and hummocky bedding have similar low- to moderate-angle dipping laminae and would be difficult to differentiate. Hence, in core, these three facies would be mostly similar, save for the soft-sediment deformation. Soft-sediment deformation is pervasive in all cores, and in most of the outcrops (Fig. 7-4E). Flow rolls and soft-sediment deformation in the Berea have been the focus of at least one report on the Berea (Cooper, 1943). In outcrop, individual sandstone/

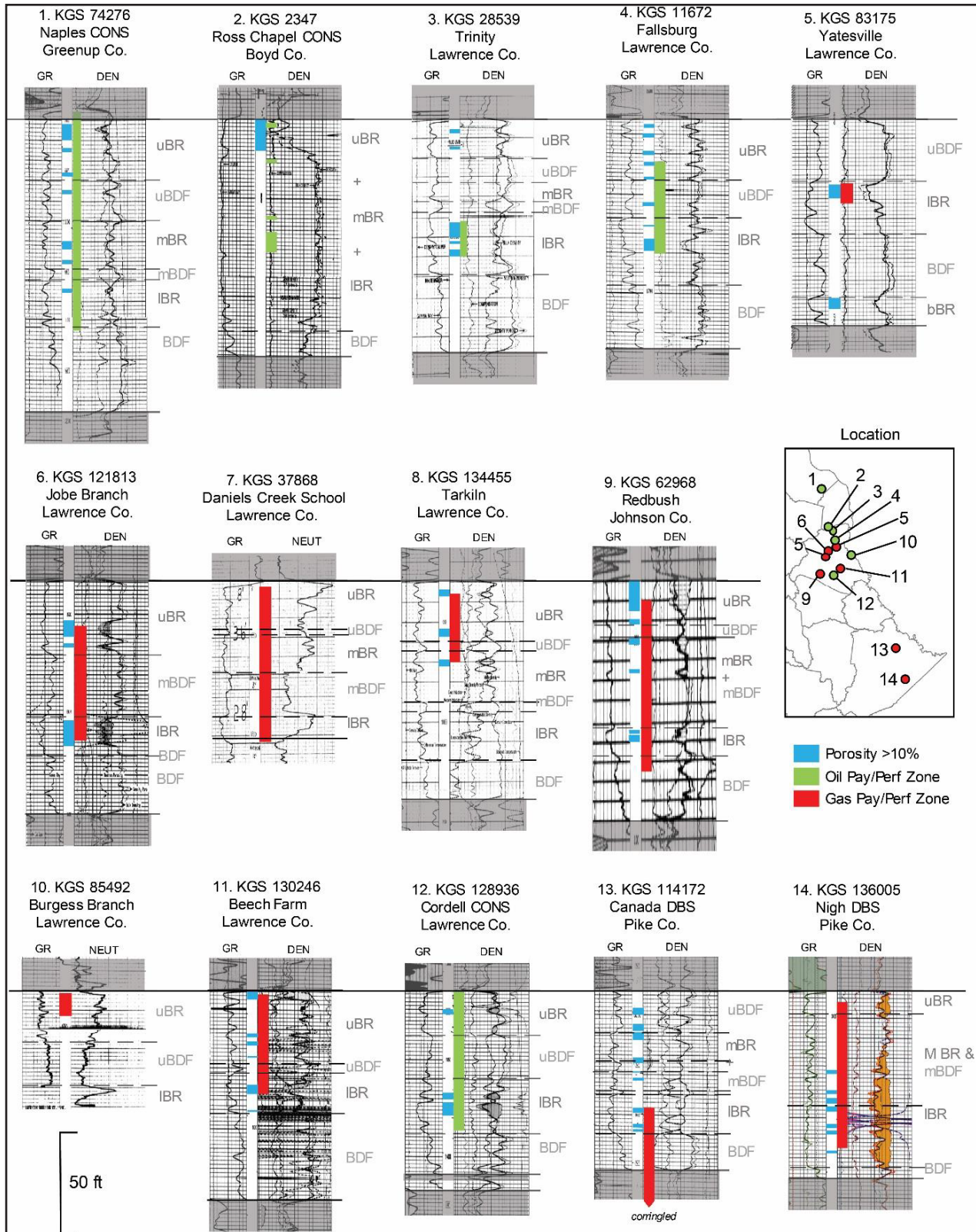


Figure 7-3. Sample geophysical wells from the fields listed in Table 7-1 showing porosity zones and completed or perforated intervals. The Bedford-Berea interval occurs between the Sunbury and Cleveland Shales (darker gray shading). Informal subdivisions of the interval are shown as basal Berea (bBR), lower Berea (IBR), middle Berea (mBR), upper Berea (uBR), main Bedford (BDF), middle Bedford (mBDF), and upper Bedford (uBDF). These subdivisions are not meant to be correlated.

Table 7-2. Berea outcrop lithofacies from Pashin (1985) and Pashin and Ettensohn (1987). Compare to Figure 2-3.

Berea Lithofacies	Description	Interpretation
Upper Sheet Sandstone (ST)	Cliff-forming siltstones and sandstones, comprised of at least 25 percent rippled, medium- to thick-bedded, tabular siltstone and sandstone. Flow rolls are common.	Outer marine shelf with proximal tempestites.
Swaley Sandstone (SW)	Similar to the ST lithofacies, but lacks flow rolls and exhibits swaley bedding. Forms much of the upper tongue of the Berea near Vanceburg, Ky.	Outer marine shelf edge, possibly sand ridge.
Shale and Siltstone (ST)	Interbedded green-gray shale and rippled, laminated, and thin-bedded siltstone and sandstone	Marine upper slope distal tempestites above storm wave base.
Lower Sheet Sandstone (LSS)	Unrippled, medium- to thick-bedded siltstone and sandstone (> 33 percent), interbedded with Bedford lithofacies. Equals the lower tongue of the Berea in Lewis County.	Marine dysaerobic toe-of-slope turbidite fans.
Massive Siltstone	Thick, scour-based, channel-form massive siltstone.	Submarine channel.
Bedford Lithofacies	Description	Interpretation
Gray-Green Shale (GG)	Most common Bedford shale, commonly silty and interbedded with thin, unrippled siltstones and black shales.	Marine dysaerobic slope below storm wave base, with turbidites.
Black Shale (BL)	Black to brownish black, silty shales commonly interbedded with gray-green shales.	Marine anaerobic basinal.

siltstone beds are generally less than 3 ft thick unless intervening shales or interbedded shales and siltstones are removed beneath the succeeding bed. This is similar to what is seen in cores.

The massive siltstone channel facies along Ky. 59 at milepost 19.1, south of Vanceburg, has been shown in several reports (e.g., Ettensohn and others, 2009). The channel is at the base of the Bedford-Berea section and cuts into the underlying Cleveland Shale. It is approximately 400 ft wide. More information is included in the accompanying field guide. None of the cores appears to cut similar channel facies, although several wells have been located in which thick, sharp-based, blocky to fining-upward gamma-ray signatures are noted near the base of the Berea, which may indicate similar channels (see Floyd, 2015). Submarine channels feeding fans would be expected on the interpreted slope environments distal to the Berea shelf.

Well and Core Analysis

Cores were examined to determine common reservoir characteristics of Berea reservoirs in eastern Kentucky. Figure 7-5 shows where publicly available cores were drilled. Figure 7-6 shows the relative position of cores next to geophysical logs from the core well or nearby wells to show the distribution of cores within the Bedford-Berea interval. Some cores are incomplete or provide little additional data. The University of Kentucky Institute for Mining and Minerals Research (IMMR) cores are thin (1 in.), near-surface cores along the outcrop belt and are not described further. Five key cores are summarized in this section (shown in bold text in Figs. 7-5, 7-6). These cores have porosity and permeability data, XRD data, and/or thin sections, which can be used to examine different aspects of heterogeneity in the Berea reservoirs of eastern Kentucky. Photographs and descriptions of all of the conventional core are provided in the accompanying Bedford-Berea core book.

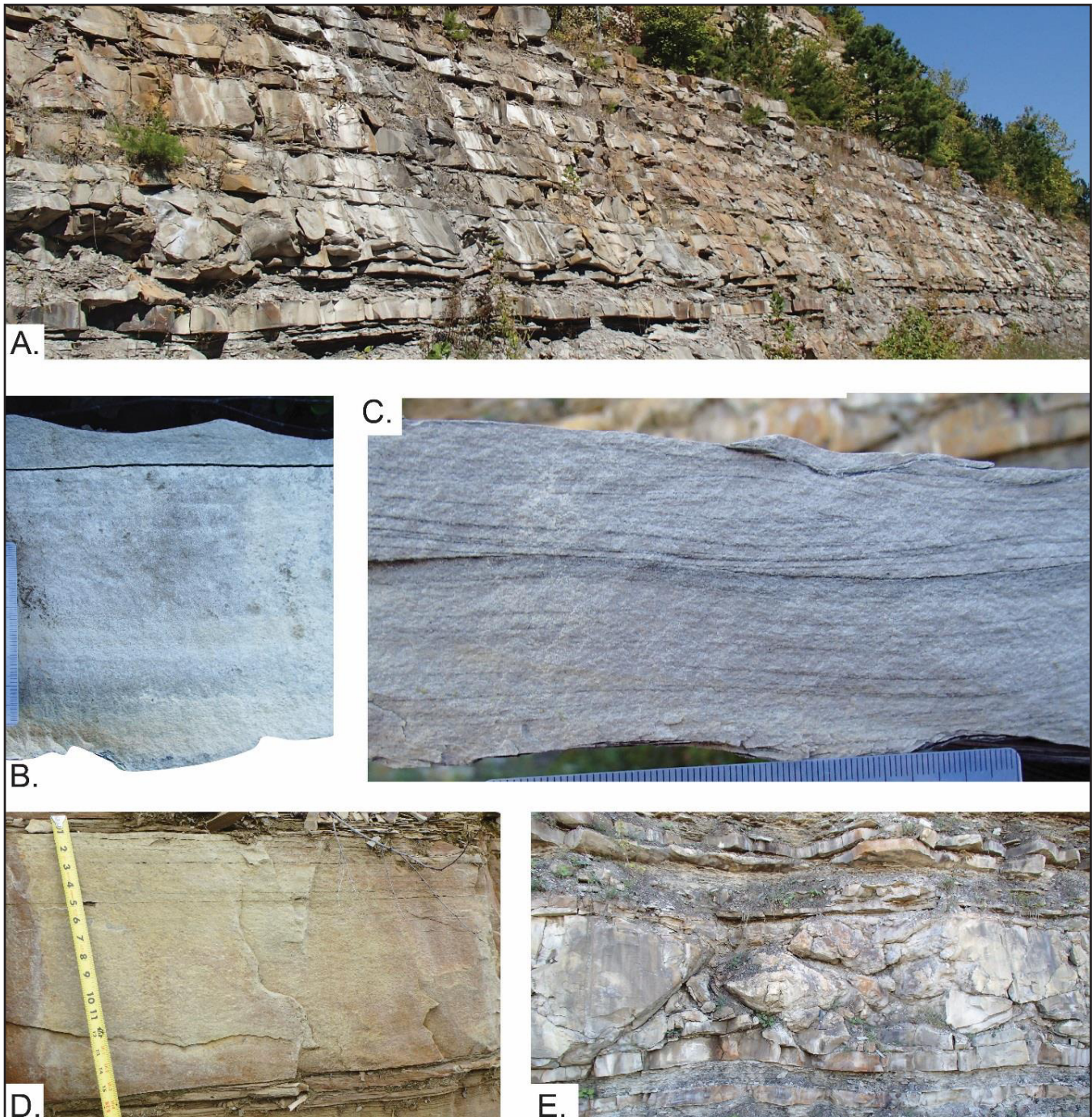


Figure 7-4. A. Roadcut exposure of the Berea near Garrison, Ky., showing sheet-sandstone lithofacies. B. Section through bed with irregular base (sometimes with loads), massive to parallel-laminated or parallel texture, and sometimes capped by combined-flow ripples. C. Hummocky stratification. D. Parallel-laminated bed (upper part) above low-angle, possibly hummocky bedding. E. Large flow rolls and bedding offset along shear planes associated with soft-sediment deformation.

Aristech Chemical Co. #4 Aristech Core, Scioto County, Ohio. The Aristech core was the only non-Kentucky core examined in the study. It is a complete core through the Bedford-Berea and also includes the Sunbury and underlying Ohio Shales.

Black shales were sampled for the thermal-maturity part of this study. No porosity or permeability data are available for the core, and no further data were collected from the Berea. The Bedford-Berea interval is 157.9 ft thick at a depth of 679.1 ft. Coars-

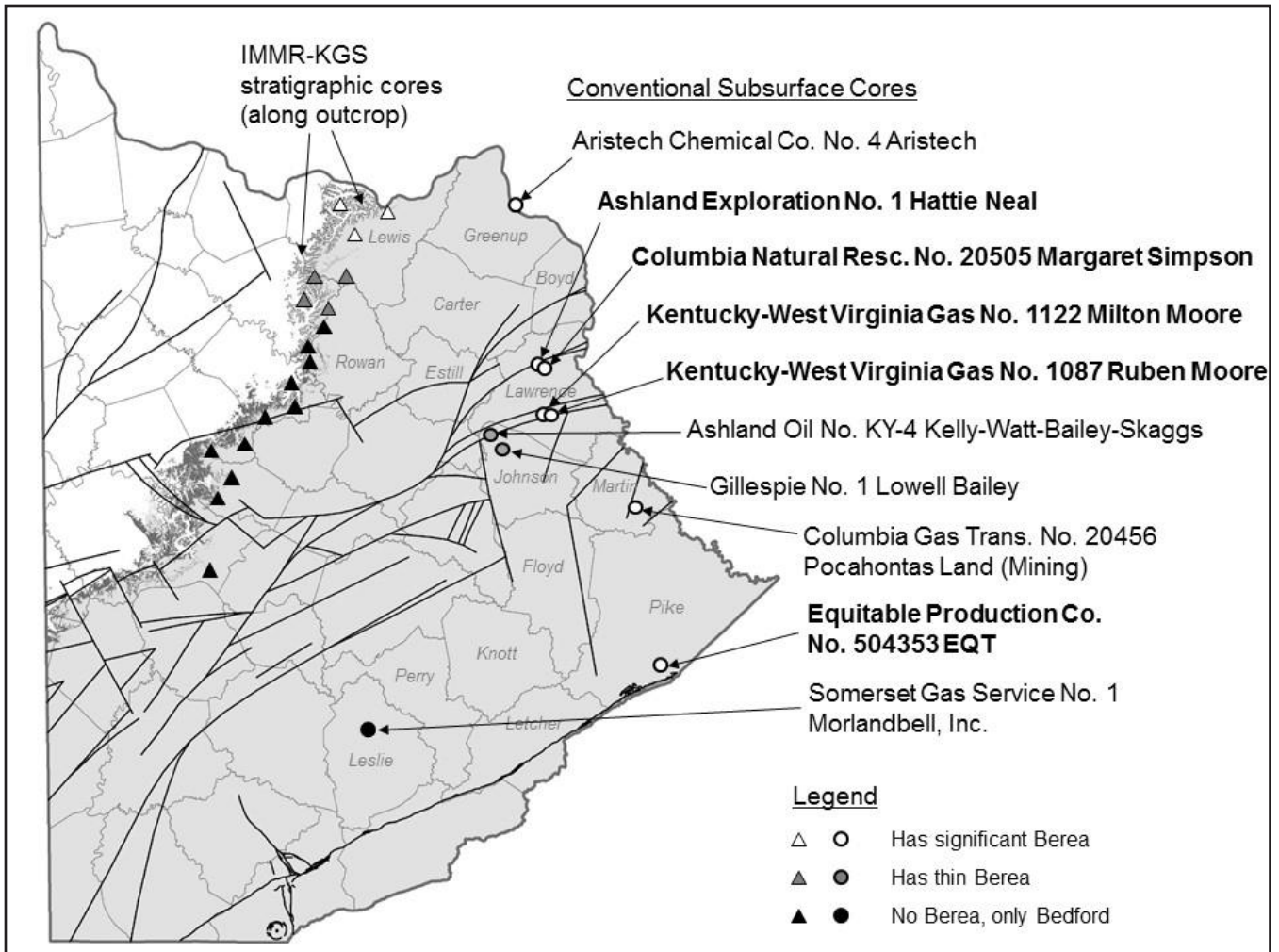


Figure 7-5. Map of cores analyzed for this project. Well names in bold black text are the primary cores used in this report.

er bedding in the core (coarse siltstone to very fine sandstone) consists of thin beds of parallel lamination; massive, low-angle (possibly hummocky or swaley) bedding; and soft-sediment deformation. Coarser beds are arranged in 5- to 15-ft-thick intervals separated by shales with laminated siltstones. Shaly intervals contain common ripples, pseudo-ripples, low-angle or undulating bedding, and soft-sediment deformation. The scale of bedding and many of the features in this core are similar to the outcrops in the Garrison, Ky., area. In general, the core contains more coarse siltstone/sandstone beds than the cores to the south, and more ripple-laminated and ripple-capped beds than cores to the south. See core description and photographs in the core workbook.

Ashland Oil No. KY-4 Kelly-Watt-Bailey-Skaggs Core, Johnson County, Ky. The Kelly-Watt-Bailey-Skaggs core contains the lower 27 ft of the Bedford-Berea interval (Fig. 7-6). The core continues into the underlying Ohio Shale and was sampled for shale chemistry and thermal-maturity analysis. There are a few coarser Berea beds near the top of the core, mostly consisting of soft-sediment deformation, but the core is dominated by Bedford shales, which are silty and gray near the top, but become increasingly darker toward the base. Because the core does not contain much Berea section, no further Berea data were collected. See core description and photographs in the core workbook.

Gillespie #1 Bailey Core, Johnson County, Ky. The preserved Bailey core is not a continuous core. The Bailey core is stored in two boxes, and is repre-

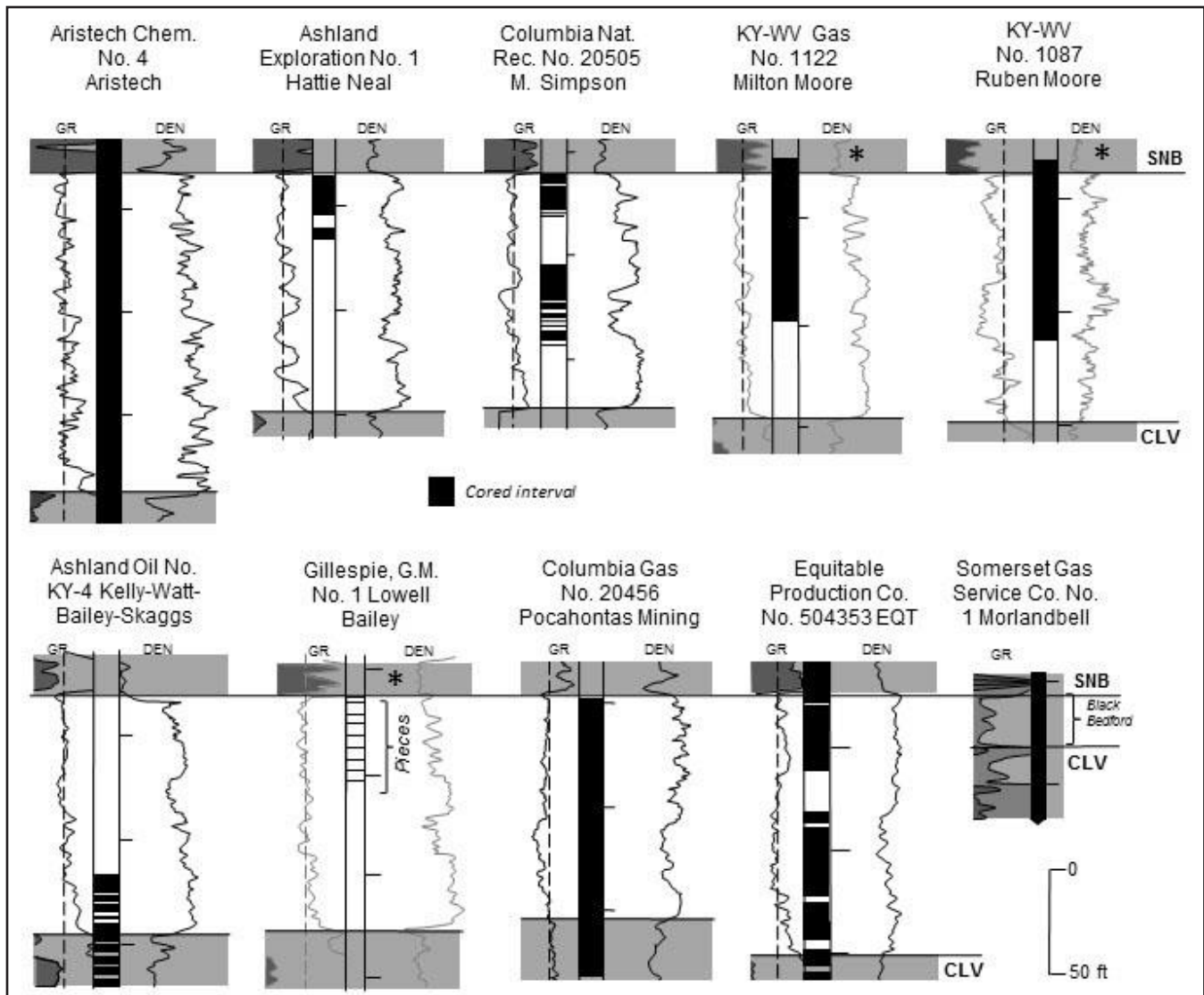


Figure 7-6. Comparison of core intervals (black-filled bars) and geophysical logs for cores examined in this study. See Figure 7-5 for locations. Well logs with asterisks did not have geophysical logs in the cored well, so logs from nearby wells were used as proxies. CLV=Cleveland Shale Member of the Ohio Shale. SNB=Sunbury Shale.

sentative of a 46-ft-thick (787–833 ft) Bedford-Berea interval. Pieces of core, each 1 to 4 inches in length, were preserved, and presumably are representative of the 1-ft interval they were taken from. A report of the original porosity and permeability data from this core contains 32 analyses; this report is available through the KGS Oil and Gas Database. The Berea has good porosity across much of the core (less than 10 percent), averaging 11.5 percent, but the upper part of the core is impermeable. A zone from 818.5–820.5 ft has permeabilities averaging 0.51 md. The pieces from which core plugs were taken were not the pieces preserved, so plug data

cannot be matched directly to bedding, but beds across the permeable interval appear to be scour-based, massive siltstone with a parallel-laminated texture and slightly dipping base (probably from loading on the underlying shale). Because of the fragmentary nature of the core, no additional data were collected, but the porosity and permeability data were used for overall analysis. See core description and photographs in the core workbook.

Somerset Gas #1 Morlandbell Core, Leslie County, Ky. The Morlandbell core is from west of the main study area, but was examined as an example of what happens to the Bedford-Berea interval

west of the main north-south thickness trend. The Bedford-Berea interval is only 25 ft thick, at 2,705 ft, and contains no Berea Sandstone. The Bedford is a black shale with thin siltstone laminae, similar to the “black Bedford” of Elam (1981). Because there was no Berea in this core, no further data were collected. See core description and photographs in the core workbook.

Columbia Gas #20456 Pocahontas Land (Mining) Core, Martin County, Ky. The Pocahontas core is 125.9 ft thick and encompasses the entire thickness of the Berea-Bedford interval, except for the uppermost contact (Fig. 7-7). The top of the core box is marked as 2,298 ft. Original core records provide data at 2,296.5 ft. Potter and others (1983) noted at least 1 ft of fine sandstone at the top of the core, which is no longer present. The well was completed in the Big Lime and Cleveland Shale. Gas from the Cleveland was noted below 2,400 ft. The Berea was cored, and oil was found, but not produced. Oil was mostly in thin beds in the lower main sandstone below 2,357.5 ft. The highest saturation was 30.5 percent at 2,381.5 ft (Fig. 7-7).

The base of the upper “coarser” interval on the gamma log is 2,298 ft; in core it is at 2,299 ft. The top of the lower coarse interval is 2,256 ft in both core and log. The base of the lower coarse interval in core is 2,390 ft; on the gamma log it is 2,392 ft. Hence, core depths are probably within 2 ft of the log depths, and may be close to log depths for parts of the core. The upper part of the core (2,298–2,355.5 ft) is dominated by deformed (convoluted) gray shale, with a few thin siltstone interbeds, typical of the Bedford Shale. Siltstones show evidence of soft-sediment deformation. More typical “Berea” lithologies are found in the lower core from 2,355.5–2,390 ft (Fig. 7-8). The lower Berea section in the well consists of two broadly coarsening-up intervals. Typical beds in the lower Berea are sharp-based, massive to massive with faint parallel-laminated texture, capped by thin, argillaceous siltstone. Soft-sediment deformation also is common in the lower core interval, but not as common as in the upper part.

Porosity and permeability data were provided with the original core records. These data are available online through the Kentucky Geological Survey Oil and Gas Database. Core porosities

are less than 3.0 (the detection limit) to 8.7 percent. The highest porosity occurs in a thin bed of siltstone with red and dark shale below the main sandstone at 2,383.5 ft. Red color is common in several of the lower shale interbeds and in several of the siltstones. In the main lower sandstone (coarse siltstone), the highest porosity is 8.1 percent in soft-sediment-deformed or massive beds with low-angle texture at 2,362.5 ft. All permeabilities were less than detection limits at the time of analysis (less than 0.10 md). No further porosity and permeability data were collected for this core because of the low permeabilities in the original dataset. This porosity zone correlates into nearby wells (Fig. 7-9).

Previous grain-size analysis of this core (Potter and others, 1983) shows a modal grain size of coarse silt (0.046+0.010 mm). The main lower “sandstone,” in which the pay was reported on drillers’ records, also has a modal grain size of coarse silt (0.04+0.01 mm).

Columbia Gas Trans. #20505 Margaret Simpson Well and Core, Lawrence County, Ky. For this well, data consist of a gamma-density/density-porosity log, two cores (with missing pieces, especially in the lower core), 12 plug samples with porosity and permeability data, XRD analyses from plug data, and thin sections from some of the plugs.

The Bedford-Berea interval is 118 ft thick, at a depth of 1,658 ft. On the geophysical log (Fig. 7-10), the Bedford-Berea interval can be divided into an upper and lower Berea siltstone/sandstone separated by gray shale. Overall, the lower Berea has a more pronounced upward-coarsening trend than the upper Berea. The overall upward-coarsening trends consist of stratigraphic intervals with smaller (4 to 10 ft) blocky to coarsening-upward gamma signatures, which likely represent individual parasequences. In core, these consist of sharp-based, thin-bedded, very fine-grained sandstones and siltstones, separated by medium to dark gray shales and interbedded shales and sandstones. Descriptions and photographs of the core are in the accompanying core book, and a generalized core section is scaled to the geophysical log for comparison in Figure 7-10. Berea siltstones and sandstones in the core are co-dominated by massive and soft-sediment-deformed beds. Approximately 20 per-

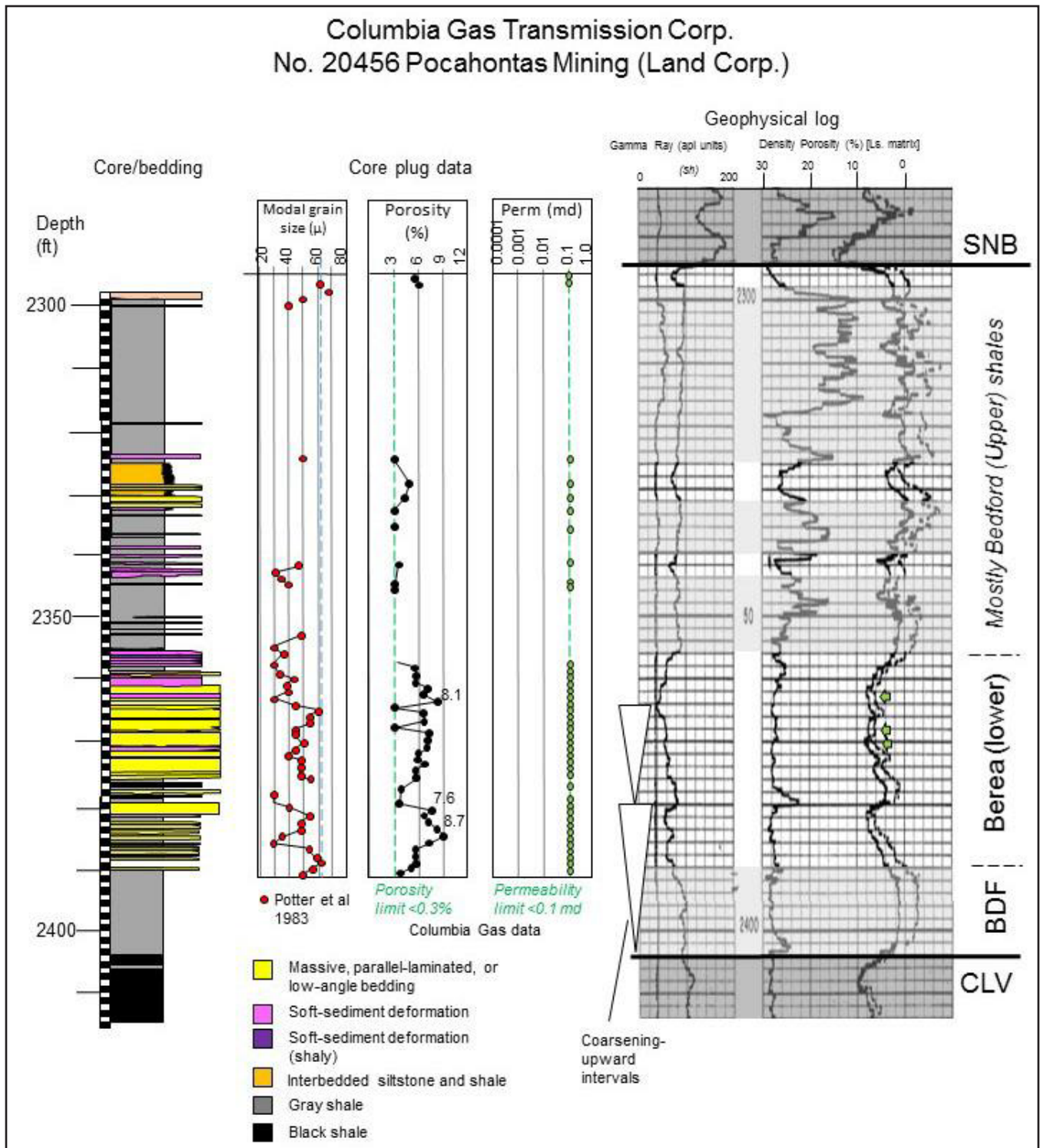


Figure 7-7. Summary of the Columbia Pocahontas well and core. Generalized core description with color-coded bedding can be compared to gamma-density log at same scale. Gray shading in log indicates shale. BDF = Bedford. CLV = Cleveland. SNB = Sunbury. Also shown are existing porosity and permeability data. Note limits to porosity and permeability measurement in green on graphs. Modal grain-size estimates are from Potter and others (1983). Blue dashed line shows very fine sandstone limit.

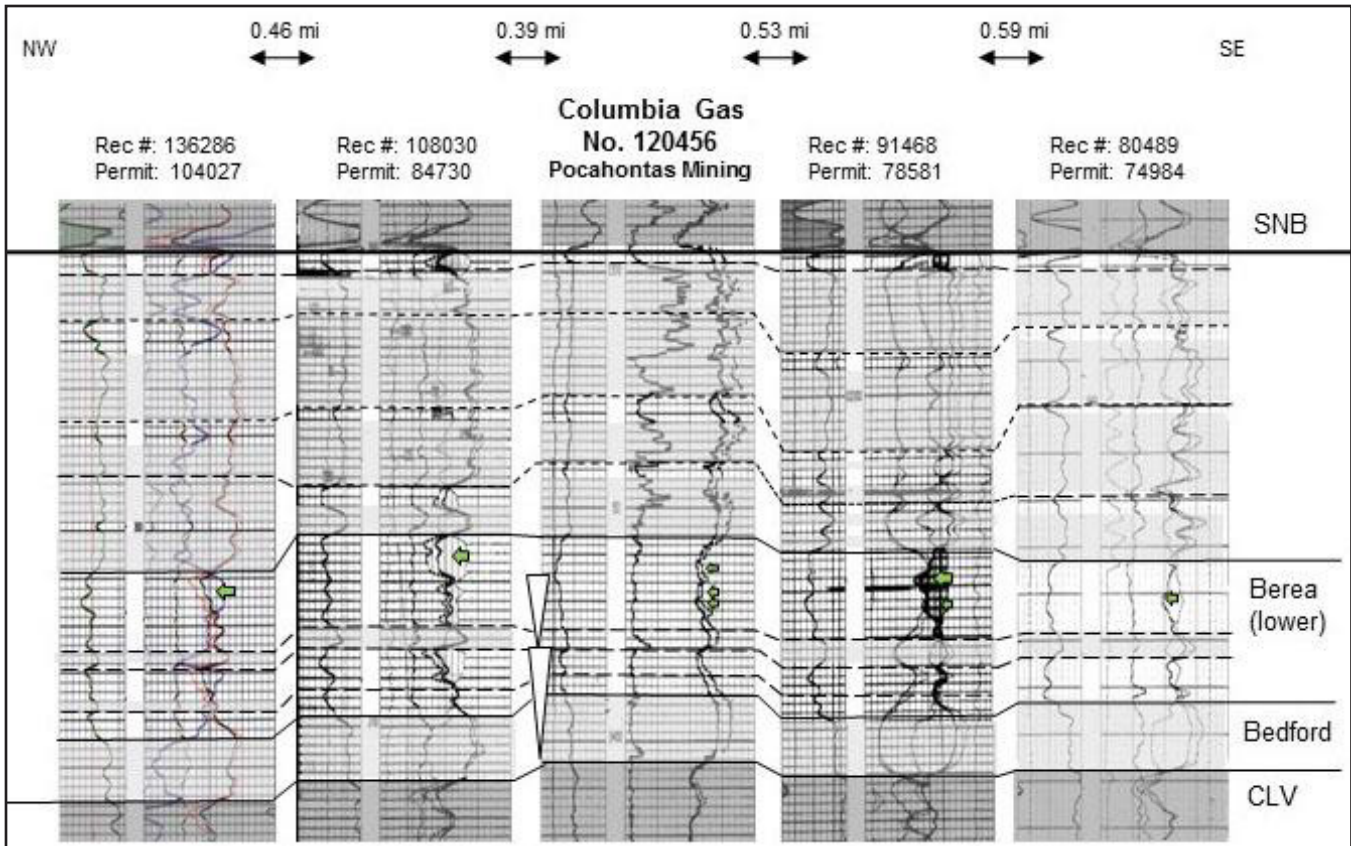


Figure 7-8. Cross section of wells in the vicinity of the Columbia Pocahontas Mining core. Green arrows point to porosity zones. Gray shading in log indicates shale. BDF = Bedford. CLV = Cleveland. SNB = Sunbury.

cent of the massive beds show faint low-angle or parallel texture or lamination.

Five porosity zones can be identified on the log: three in the upper and two in the lower part of the Berea. The top of the Berea is porous immediately beneath the contact with the Sunbury Shale (PZ1 in Figure 7-10). This interval consists of massive low-angle and soft-sediment-deformed beds. Modal grain sizes from Potter and others (1983) range from medium silt to very fine sand. Analysis of one thin section for this study shows a range from medium silt (0.073 mm) to very fine sand (0.123 mm), with a mean of coarse silt (0.045 + 0.018 mm) and a mode of finer medium silt (0.022 mm). Four plugs through the zone have porosities of 10.18 to 11.4 percent and permeabilities of 0.07 to 0.48 md. Laterally, PZ1 splits into two smaller intervals in which an intervening shale increases in thickness or merges with the underlying PZ2 zone, where the intervening shale thins (Fig. 7-10). The lower subzone is more extensive, occurring 4 to 10 ft beneath the Sunbury Shale.

The second porosity zone in the upper Berea is 12 to 18 ft beneath the Sunbury (PZ2 in Figure 7-9). It splits into two thinner zones northward and merges with PZ1 to the south (Fig. 7-10). Core through the interval in this well consists of relatively thin beds of massive low-angle bedding (possibly hummocky crossbedding) and soft-sediment deformation (including relatively argillaceous deformed beds). Potter and others (1983) indicated a general coarsening trend in this interval, from medium silt to fine sandstone. Three sandstone plugs through the zone have porosities of 9.78 to 11.53 percent and permeabilities of 0.13 to 0.70 md. The cap on the porous zone is a thin, medium to dark gray siltstone (0.9 ft) overlain by a thin gray shale (0.7 ft) in core. The siltstone has a permeability of 0.00017 md.

The third porosity zone (1,688–1,692 ft) in the upper Berea (PZ3 in Figure 7-8) in this well is thin, and no core is available through the interval.

The uppermost porosity zone in the lower half of the Berea (PZ4 in Figure 7-9) is just beneath

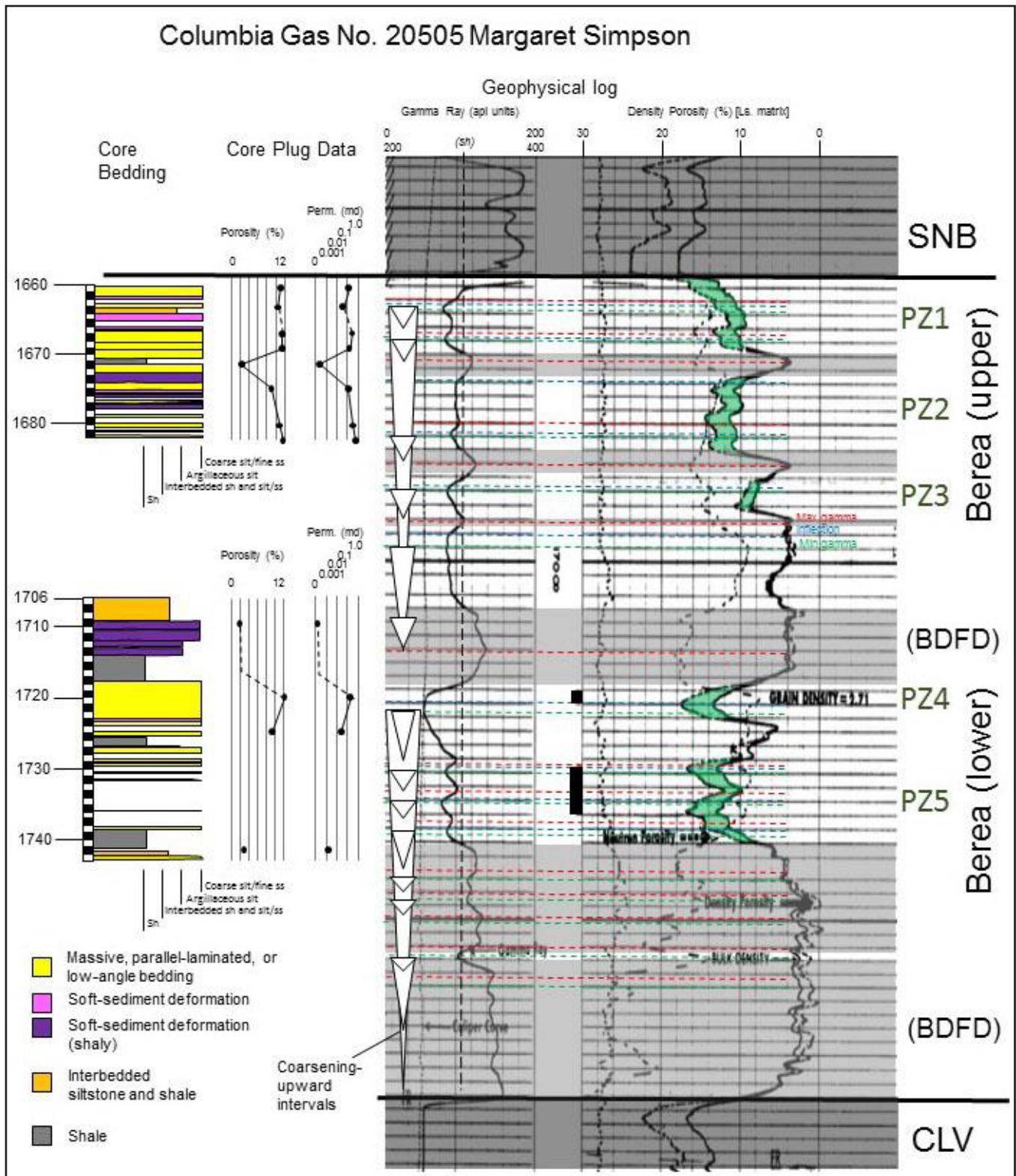


Figure 7-9. Comparison of core bedding, plug-derived porosity, and permeability with geophysical log for the Columbia Gas Transmission No. 20505 Margaret Simpson well. Gray shaded zones on the log are shales. CLV=Cleveland Shale Member of the Ohio Shale. SNB=Sunbury Shale. BDFD=Bedford Shale. Green shading on the log is porosity less than 10 percent. Porosity zones (PZ1–5) are discussed in text.

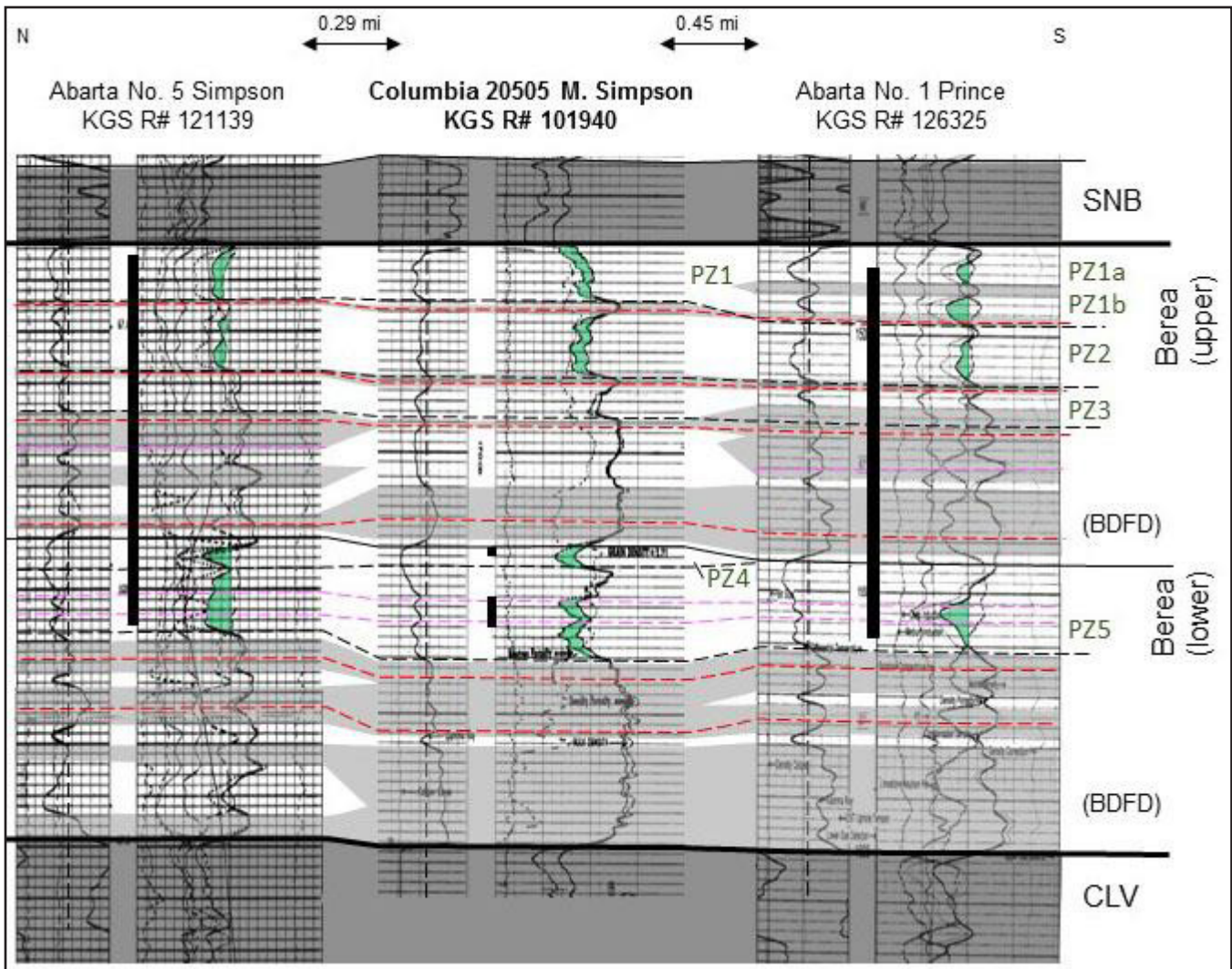


Figure 7-10. Correlation of logs north and south of the Columbia Gas Transmission #20505 Margaret Simpson well. Gray shaded zones are shales. Green shaded intervals on the log are porosity greater than 10 percent. Porosity zones (PZ1–5) are discussed in text.

a middle tongue of shale, which consists of 12 ft of gray shale and interbedded dark gray, argillaceous siltstone in core. Argillaceous siltstones in this tongue have a permeability of 0.00051 md. The porosity zone is 4 ft thick and occurs in the uppermost part of a 10-ft-thick interval with coarsening-upward to blocky gamma signatures. Potter and others (1983) indicated medium silt to fine sandstone grain sizes for this interval. This is one of two intervals completed in the well. One plug from the interval has a porosity of 12.38 percent and permeability of 0.23 md. To the south, this interval either pinches out or is truncated beneath the middle Bedford tongue (Fig. 7-10).

The second porosity zone in the lower Berea appears to consist of at least three stacked coarsening-upward intervals on the gamma log (PZ5 in Figure 7-9). Much of PZ5 in core consists of pieces of uncertain position, but the base and top of the interval are gray shales. The porous rock in this interval consists of siltstone to very fine sandstone in thin massive, massive with faint low-angle lamination or texture, and soft-sediment-deformed beds. No plugs were taken from this interval. This was the main interval completed in the well, and is the base of the completion zones in surrounding wells (Fig. 7-10).

XRD analysis of major constituents from 17 samples in the core is summarized in Ta-

ble 7-3. Quartz is the dominant framework grain (71+11 percent quartz). Dolomite is as much as 10 percent in the lowest plug sampled (1,742 ft), but was absent in many samples. Siderite makes up as much as 3.5 percent of reddish zones. Total clay content is variable, with a mean of 16.8+12.6 percent (primarily illite and mica).

Summary for Well – Porosity zones are developed in both the lower and upper Berea (informal terms) in the well. The immediate cap of each is a gray shale or dense argillaceous siltstone. Porous intervals are in thin beds of gray siltstone to very fine sandstone. Porous zones are 4 to 10 ft thick in surrounding wells. Where shales between beds are thin or not well developed, thicker, stacked, porous intervals are developed. Where shales thicken, porous zones split or thin laterally.

Ashland #1 Hattie Neal Well and Core, Lawrence County, Ky. The Hattie Neal core is 27 ft thick, representing the upper 33 ft of the Berea (Figs. 7-6, 7-11, 7-12). The density log shows two porosity zones (PZ1=1,500–1,510 ft; PZ2=1,514–1,520 ft) with greater than 10 percent porosity in the upper part of the Berea. Both were perforated for completion. Original core-measured oil saturations from

these intervals were 4.6–12.7 and 1.1–19.1, respectively.

The Hattie Neal core is dominated (approximately 70 percent) by massive bedding or massive with faint low-angle lamination (possibly hummocky stratification) and faint parallel laminae. These beds are scour-based and often have a thin, argillaceous top. Soft-sediment-deformed beds, including several apparently isoclinally folded beds, account for approximately 25 percent of the core. Many soft-sediment-deformed beds are truncated by the overlying bed. Some flow rolls are offset by post-depositional microfaults.

Across the PZ1 porosity interval, plug data show variable porosity and permeability (Fig. 7-11). Variation appears to be somewhat independent of bed type; both deformed and undeformed beds have similar variability in porosity and permeability. Although much of the core across the porosity intervals looks like sandstone, Potter and others' (1983) analysis shows modal grain sizes are in the fine- to coarse-silt size. Grain-size analysis of four thin sections for this study shows grain size ranges from medium silt (0.018 mm) to fine sand (0.173 mm), with a mean of coarse silt (0.057+0.024 mm) and a mode of coarse silt (0.035 mm).

Table 7-3. Summary of XRD data from the Ashland No. 20505 Margaret Simpson well. See Appendix 1 for data.				
XRD Analyses, n=12	Maximum	Minimum	Mean	Standard Deviation
NONCLAY FRACTION				
Quartz	79.8	38.9	71.17	11.38
K-feldspar	2.5	0.6	1.36	0.52
Plagioclase	9.7	3.3	7.36	1.89
Organic carbon (TOC)	0.3	0.0	0.20	0.11
Apatite	0.7	0.0	0.06	0.21
Pyrite	3.8	0.0	0.67	1.08
Calcite	0.1	0.0	0.01	0.02
Dolomite	10.1	0.0	1.70	3.46
Siderite	3.5	0.0	0.69	1.22
TOTAL	90.4	46.4	83.22	12.59
CLAY FRACTION				
Mixed-layer illite/smectite (includes R3)	3.3	0.4	0.97	0.87
Illite + mica	37.9	4.8	10.29	9.49
Chlorite	4.8	0.0	1.04	1.24
Kaolinite	8.6	2.1	4.48	1.93
TOTAL	53.6	9.6	16.78	12.59

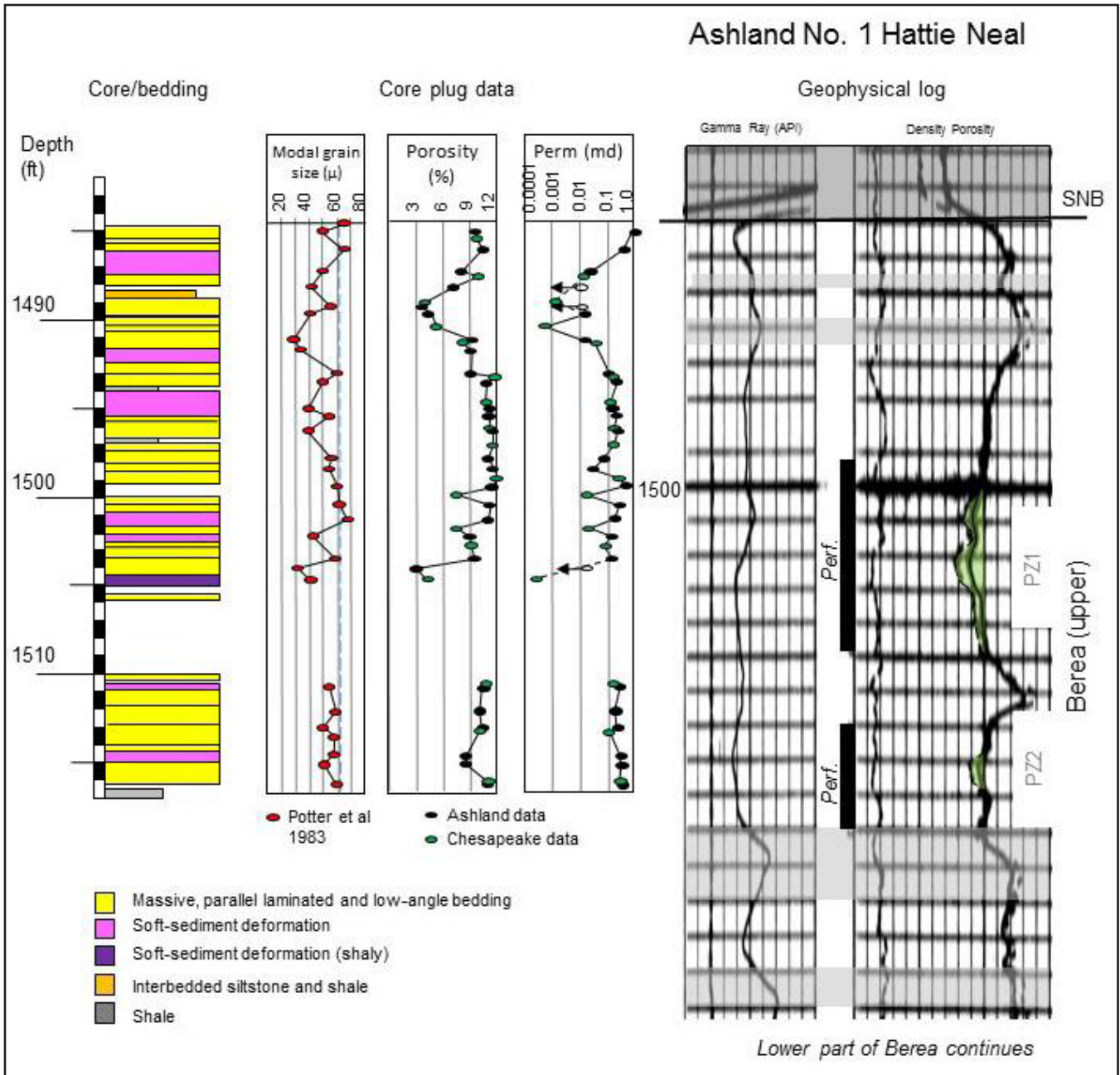


Figure 7-11. Comparison of core bedding, plug-derived porosity, and permeability with geophysical log for the Hattie Neal well. Gray shaded zones on the log are shales. CLV=Cleveland Shale Member of the Ohio Shale. SNB=Sunbury Shale. Green shading on the log is porosity greater than 10 percent (yellow porosity is greater than 8 percent). Porosity zones are discussed in the text. Note: The core is only in the upper part of the Berea in this well. For modal grain-size chart, blue-dashed line is limit of very fine sandstone.

XRD analysis of major constituents from 17 samples in the core is summarized in Table 7-4. Quartz is the dominant framework grain (71+11 percent quartz). Dolomite is as much as 39 percent near the top of the Berea, but is quite variable, and was absent in many samples. Similarly, pyrite was not a dominant component of the

XRD analysis, but is relatively common in parts of the core. Clays account for 14.3+3.7 percent (primarily illite and mica).

Summary for Well – Porosity zones are developed in both the lower and upper Berea (informal designation) in the well (Figs. 7-11, 7-12), but the core is only through the upper Berea. The porous

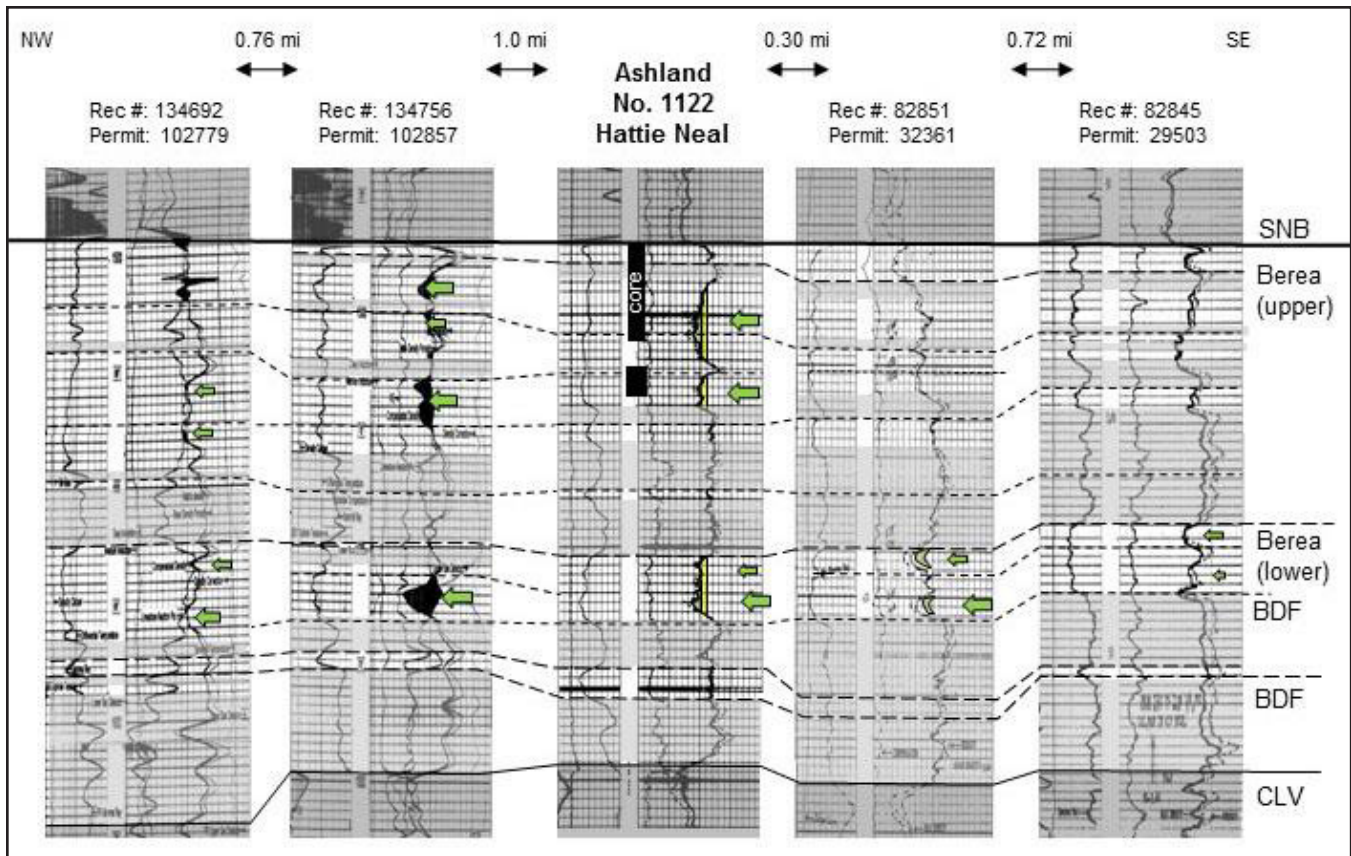


Figure 7-12. Correlation of logs north and south of the Hattie Neal well. Gray shaded zones are shales. Green shaded intervals and arrows on the logs are porosity greater than 10 percent. Porosity zones are discussed in text. CLV = Cleveland Shale Member of the Ohio Shale. BDF = Bedford shales. SNB = Sunbury Shale.

zone in the upper Berea is 14ft beneath the Sunbury, thin-bedded, massive to soft-sediment-deformed, gray siltstone to very fine sandstone. A thicker porosity interval (10–12ft) at the top of the lower Berea appears to represent merging of two smaller porosity intervals (each 4 to 6ft) laterally.

KY-WV Gas #1087 Ruben Moore Well and Core, Lawrence County, Ky. Two cores drilled by KY-WV Gas are only 1.49mi apart. Both are in the northern part of the Cordell Field. The Ruben Moore well is east of the location of the Milton Moore core. Neither core has a geophysical log with it, but the logs in nearby wells can be used to correlate the cores and data to porosity zones in the surrounding field. The Ruben Moore core penetrates the upper and lower Berea (informal designations). The upper Berea is thicker and has thicker porosity intervals than the lower Berea in this well. The upper Berea is approximately 23ft thick and composed of thin beds of massive, parallel-laminated, and soft-

sediment-deformed beds. Soft-sediment deformation dominates the upper half of the upper Berea.

Three porosity zones above 10 percent occur in the upper Berea (PZ1, PZ2, PZ3 in Figure 7-13); each porosity interval is 2 to 3ft thick. The highest porosity and permeability in the core is in the uppermost sandy interval (PZ1), just beneath the contact with the Sunbury Shale. Porosity in this interval is 16.5 percent and permeability is 0.3 md. The main porosity interval is 15 to 30ft beneath the Sunbury Shale (Fig. 7-14). It appears to consist of two porosity intervals that have merged laterally (Figs. 7-13, 7-14). The upper and lower porosity intervals thicken to the southwest, where the overall interval thickens, and thin to the northeast, where the Berea parts of the interval thin (Fig. 7-15). Berea coarse siltstones and sandstones below the upper porosity interval appear to dip (possibly along clinofolds) to the southwest, and the porosity intervals within them follow dip at 8 to 10ft/mi.

Table 7-4. Summary of XRD data from the Ashland No. 1 Hattie Neal well. See Appendix 1 for data.

XRD Analyses, n=7	Maximum	Minimum	Mean	Standard Deviation
NONCLAY FRACTION				
Quartz	80.1	41.1	71.06	11.37
K-feldspar	2.3	1.1	1.76	0.36
Plagioclase	9.8	4.2	7.34	1.44
Organic carbon (TOC)	0.3	0.0	0.13	0.08
Apatite	0.0	0.0	0.00	0.00
Pyrite	1.9	0.0	0.54	0.54
Calcite	0.2	0.0	0.03	0.06
Dolomite	39.2	0.0	4.26	11.75
Siderite	1.0	0.0	0.20	0.30
Gypsum	0.4	0.0	0.09	0.13
Halite	0.2	0.0	0.05	0.06
Anatase	0.4	0.0	0.23	0.14
TOTAL	89.7	76.0	85.68	3.67
CLAY FRACTION				
Mixed-layer illite/smectite (includes R3)	2.4	0.1	1.01	0.59
Illite + mica	16.7	4.2	8.35	3.06
Chlorite	1.1	0.3	0.74	0.23
Kaolinite	7.1	2.3	4.22	1.40
TOTAL	24.0	10.3	14.32	3.67

Two thinner sandstone (or coarse siltstone) intervals representing the lower Berea in this field also dip to the southwest and have porosity greater than 10 percent (PZ4 and PZ5 in Figures 7-13 and 7-14). The two intervals appear to merge updip to the northeast (Fig. 7-14).

XRD analysis of major constituents from 23 samples in the core is summarized in Table 7-5. Quartz is the dominant framework grain (64+18 percent quartz). Dolomite is as much as 33 percent in the lower part of the core (three samples between 1,271.5 and 1,282 ft), but is quite variable, and was absent in many samples. Pyrite and siderite are minor constituents. Pyrite is most abundant in the upper 10 ft of the core. Clays are variable and account for 22.5+18 percent (primarily illite and mica, although two samples had greater than 10 percent kaolinite).

Summary for Well – The two KY-WV Moore cores are summarized together following the Milton Moore description and results.

KY-WV Gas #1122 Milton Moore Well and Core, Lawrence County, Ky. The Milton Moore well is

1.49 mi west of the Ruben Moore well. Both are in the northern part of the Cordell Field. Neither core has a geophysical log with it, but the logs in nearby wells can be used to correlate the cores and data to porosity zones in the surrounding field.

The Milton Moore core also includes an upper and lower Berea (informal designations), just as in the Ruben Moore core, but the upper Berea is thicker than in the Ruben Moore core. Here, the upper Berea is 40 ft thick and composed of thin beds of massive, parallel-laminated, and soft-sediment-deformed beds. The upper half of the upper Berea contains common soft-sediment deformation. Three porosity zones above 10 percent are identified in the nearby log (PZ1, PZ2, PZ3); the upper two can be correlated to the core (Figs. 7-15, 7-16). Each porosity interval is 2- to 3 ft thick.

The highest porosity and permeability in the core is actually in the uppermost Berea interval, just beneath the contact with the Sunbury Shale (PZ1 in Figures 7-15 and 7-16). Porosity in this interval is 16.5 percent and permeability is 0.3 md. This zone does not show up on the nearest geo-

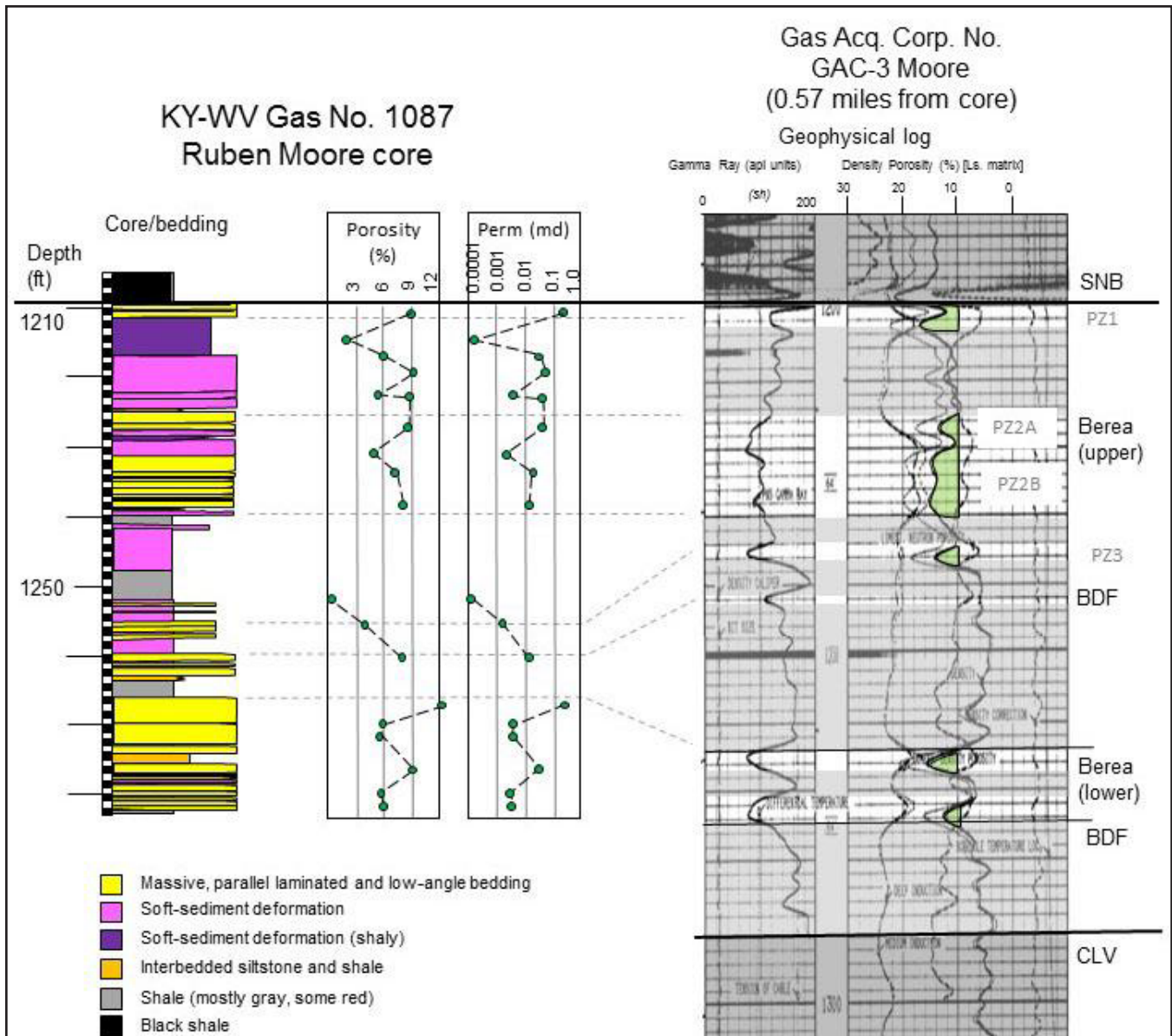


Figure 7-13. Comparison of core bedding, plug-derived porosity, and permeability with geophysical log for the Ruben Moore well. Gray shaded zones on the log are shales. Green shading on the log is porosity greater than 10 percent. Porosity zones are discussed in the text. CLV=Cleveland Shale Member of the Ohio Shale. BDF=Bedford Shale. SNB=Sunbury Shale.

physical log (from 0.36 mi away), but does occur in the next log to the south (from 1 mi away). This may indicate that the upper porosity interval has variable distribution, or that there is local truncation of the uppermost sandstone/siltstone beneath the Sunbury Shale. The underlying PZ1b, PZ2, and PZ3 intervals all correlate laterally. PZ3 is the thickest interval (8–10 ft), but splits into three thinner intervals on the south end of the cross section shown in Figure 7-16.

The lower Berea in the vicinity of this well contains three coarse siltstone/very fine sandstone intervals, which have porosities less than 10 percent on logs, although PZ5 in the core has a porosity of 12 percent and permeability greater than 0.1 md. The lower porosity zones are thin (2 to 3 ft) and do not appear to have significant porosity laterally (Fig. 7-16).

XRD analysis of major constituents from 25 samples in the core are summarized in Table 7-6. Overall results are similar to those of the Ruben

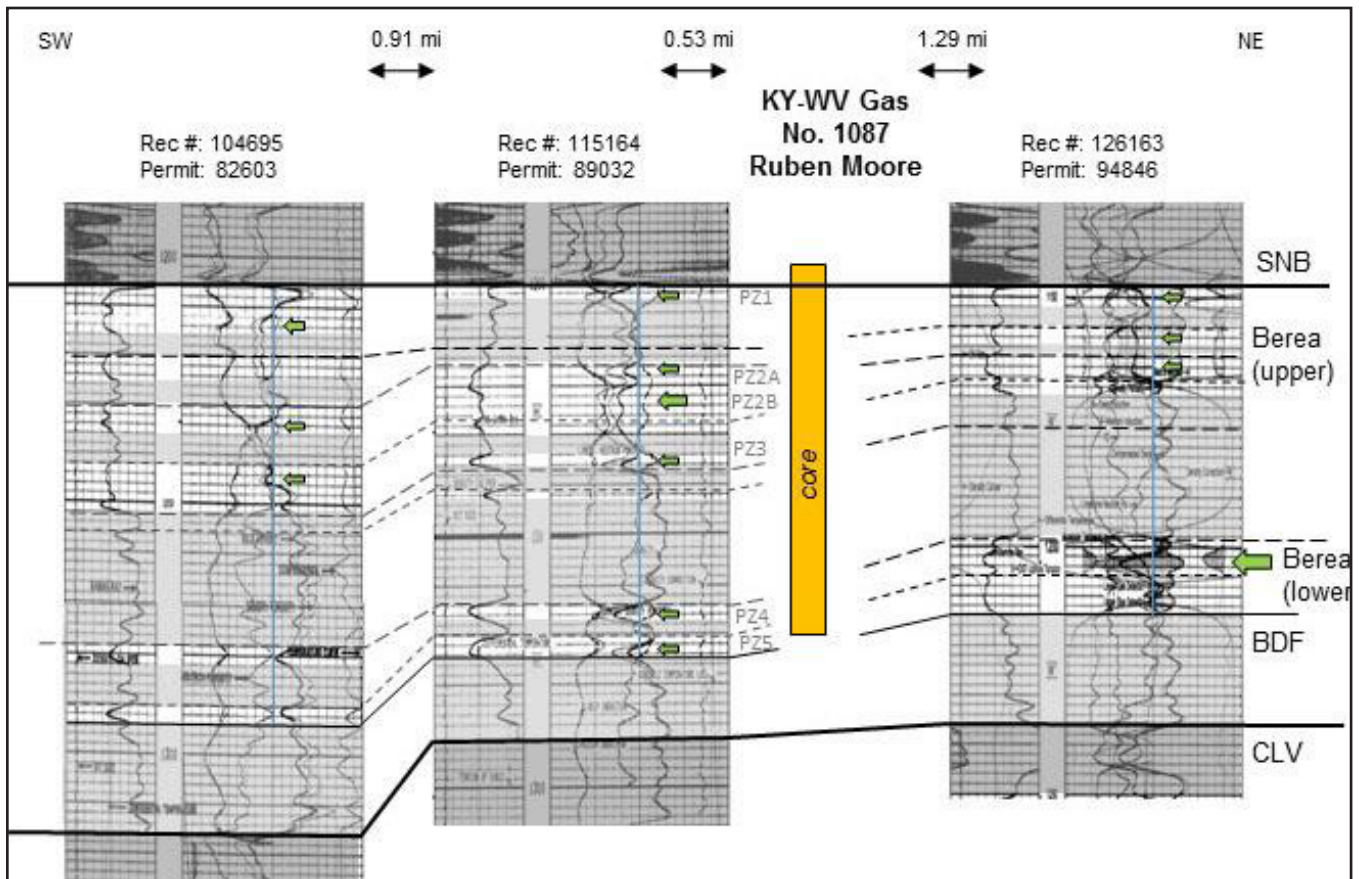


Figure 7-14. Correlation of logs north and south of the Ruben Moore core. Gray shaded zones are shales. Green arrows point to porosity zones discussed in the text. CLV = Cleveland Shale Member of the Ohio Shale. BDF = Bedford Shale. SNB = Sunbury Shale.

Moore well (Table 7-5). Quartz is the dominant framework grain (66+17 percent quartz). Dolomite is as much as 18 percent in the upper 8ft of the Berea, but is quite variable and was absent in many samples. Marcasite and pyrite were concentrated near the top of the core. Scattered pinpoint pyrite occurs throughout the core. Siderite occurs in red-stained parts of the core. Clays are variable and account for 21.2+17 percent (primarily illite and mica, although two samples had greater than 10 percent kaolinite).

Summary for the Two Moore Cores – The two KY-WV Gas Moore cores are summarized together. Both cores are from the Cordell Field and have similar bedding and general log profiles. In both cores, the upper Berea is better developed than the lower Berea. Porosity zones in the upper Berea occur in coarse siltstones to very fine sandstones with massive, parallel-laminated, and soft-sediment-deformed bedding. Porosity is thickest where mul-

iple intervals merge together. An upper zone just beneath the Sunbury Shale is locally developed near both cores. The next zone in the upper Berea is 10 to 30ft beneath the Sunbury and dips to the south and west. The two cores correlate well, and there appears to be progressive dip in many of the intervals, suggesting the general slope-like clinoforms interpreted by Pashin and Ettensohn (1995) for the Bedford-Berea interval.

Equitable Production Co. #504353 EQT Well and Core, Pike County, Ky. This core is the southernmost Berea core in Kentucky (Fig. 7-5), and is the southern end of the thermal-maturity transect of the project. The well was completed as a gas well in the underlying Ohio Shale. It is unique among the core examined because it contains in-place bitumen. The staining provides insight into the internal heterogeneity of a Berea reservoir. For this well, data consist of gamma, density, density-porosity,

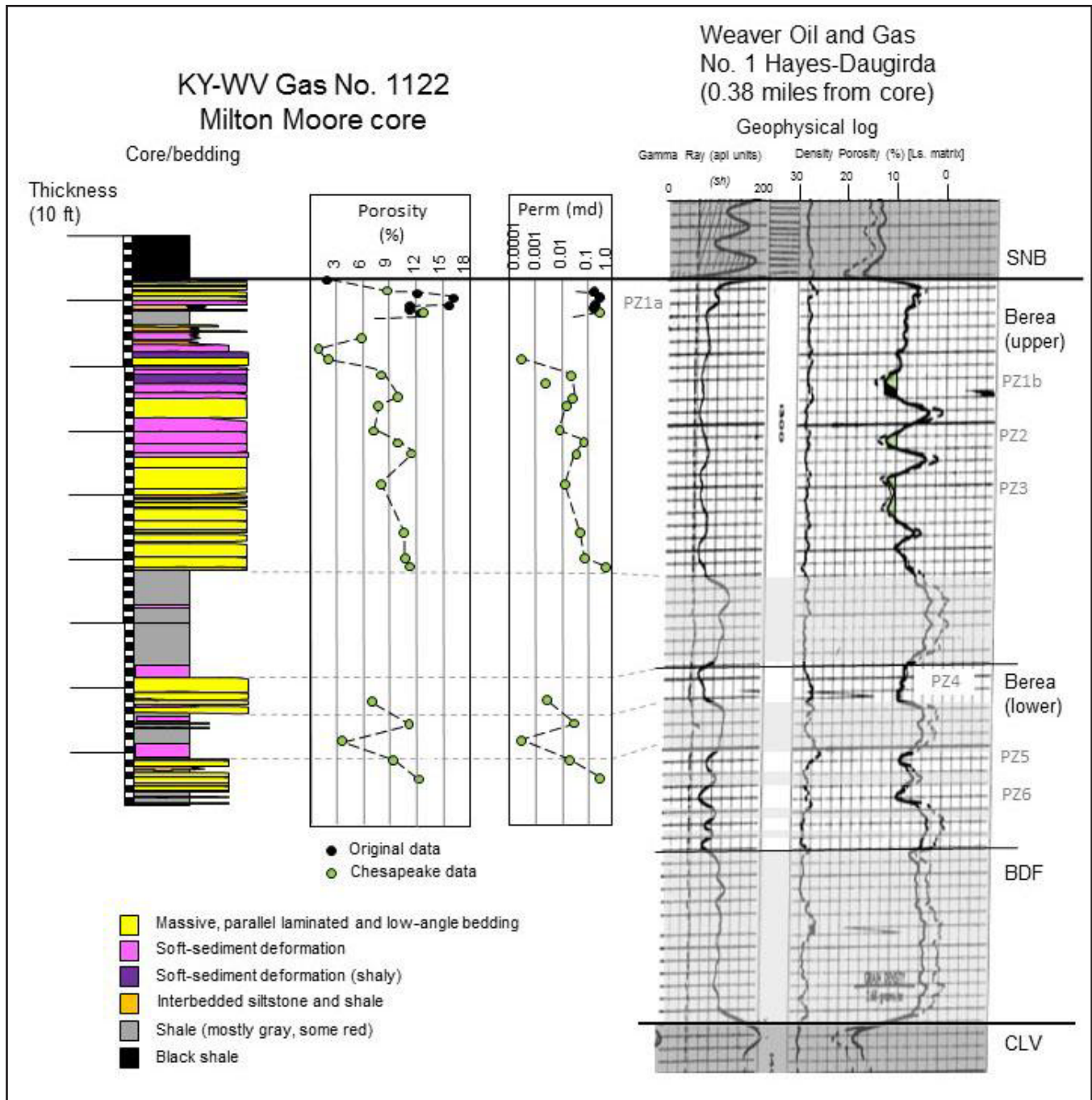


Figure 7-15. Comparison of core bedding, plug-derived porosity, and permeability with geophysical log for the Ruben Moore well. Gray shaded zones on the log are shales. Green shading on the log is porosity greater than 10 percent. Porosity zones are discussed in the text. CLV=Cleveland Shale Member of the Ohio Shale. BDF=Bedford Shale. SNB=Sunbury Shale.

neutron-porosity, and PE logs, seven cores, and thin sections from some of the plugs. Plugs were cut from this core prior to it being donated to KGS, so the data from the plugs are not available for analysis. No further porosity or permeability data were collected from this well as part of the project.

The Bedford-Berea interval is 125 ft thick, at a depth of 3,884 ft. On the geophysical log (Fig. 7-17), the Bedford-Berea interval can be divided into an upper and lower Berea siltstone/sandstone (informal designation) separated by a tongue of gray shale, but the lower Berea is much thicker (85 ft)

Table 7-5. Summary of XRD data from the KY-WV Ruben Moore well. See Appendix 1 for data.

XRD Analyses, n=23	Maximum	Minimum	Mean	Standard Deviation
NONCLAY FRACTION				
Quartz	83.0	22.9	63.65	17.54
K-feldspar	2.0	0.0	1.05	0.51
Plagioclase	10.1	2.1	6.43	2.50
Organic carbon (TOC)	9.6	0.0	0.59	1.96
Apatite	0.0	0.0	0.00	0.00
Pyrite	3.2	0.0	0.47	0.84
Calcite	0.3	0.0	0.01	0.06
Dolomite	32.9	0.0	4.69	9.36
Siderite	3.1	0.0	0.65	0.78
TOTAL	93.7	37.6	77.53	18.40
CLAY FRACTION				
Mixed-layer illite/smectite (includes R3)	8.4	0.0	1.61	1.96
Illite + mica	51.5	1.9	14.08	15.18
Chlorite	4.1	0.3	1.30	1.16
Kaolinite	12.2	0.4	5.47	2.60
TOTAL	62.4	6.3	22.47	18.40

than the upper Berea (40 ft), and does not necessarily correlate to upper and lower Berea intervals in Lawrence and Johnson Counties. In comparison to the cores to the north, this core is most similar to the Columbia Pocahontas core in Martin County, because it is very argillaceous and is dominated by soft-sediment-deformed bedding. Core photos and descriptions are included in the accompanying core book.

Three porosity intervals (greater than 8 percent log porosity) are noted in the Berea at 3,883.5–3,889, 3,892–3,894, and 3,900–3,903 ft depths. All three intervals have maximum log porosity at or slightly higher than 10 percent. Berea siltstones contain bitumen (dead oil) across these zones. Beds are most completely stained at log-porosity values of 8 to 10 percent. Beneath the three main porosity intervals, staining occurs in thinner beds, sometimes only in parts of the beds, at log porosities above 6 percent (Fig. 7-17).

Figures 7-18A, B, C, and D show examples of core with darker (bitumen) and lighter (unstained) rock. Soft-sediment-deformed beds may be completely stained or more commonly show breaks in staining along deformation contacts including diapiric dewatering structures (Figs. 7-18A, B), glide planes, internal shear planes, and flow-roll

boundaries (Figs. 7-18B, C), or along internal bedding (Fig. 7-18D). Massive to graded beds may also be completely stained, but some show distinct stain boundaries. Horizontal to low-angle bitumen fronts and thin lines of bitumen staining mark faint low-angle or parallel texture (Fig. 7-19A), which are difficult to see in unstained samples. Staining in massive (structureless) beds, in contrast, is more uniform. In some cases in massive beds, the transition is almost dendritic in pattern, with no obvious laminae boundary (Fig. 7-19B). The staining itself shows the bed or lamination texture.

Lower in the core, bed contacts and scours mark boundaries between stained and unstained core (Figs. 7-19C, D). Beds and scours separated by thin shales commonly show a lack of staining on either side of the shale contact, or are stained directly above the upper contact. Lastly, boundaries between stained and unstained core can be seen along fractures and microfractures in the core (Fig. 7-20). The combination of these apparent flow boundaries in thin-bedded strata demonstrates the small-scale heterogeneity in permeability within a Berea reservoir. Many of these microfractures, especially in massive beds or where there is no mineral staining, might not be visible.

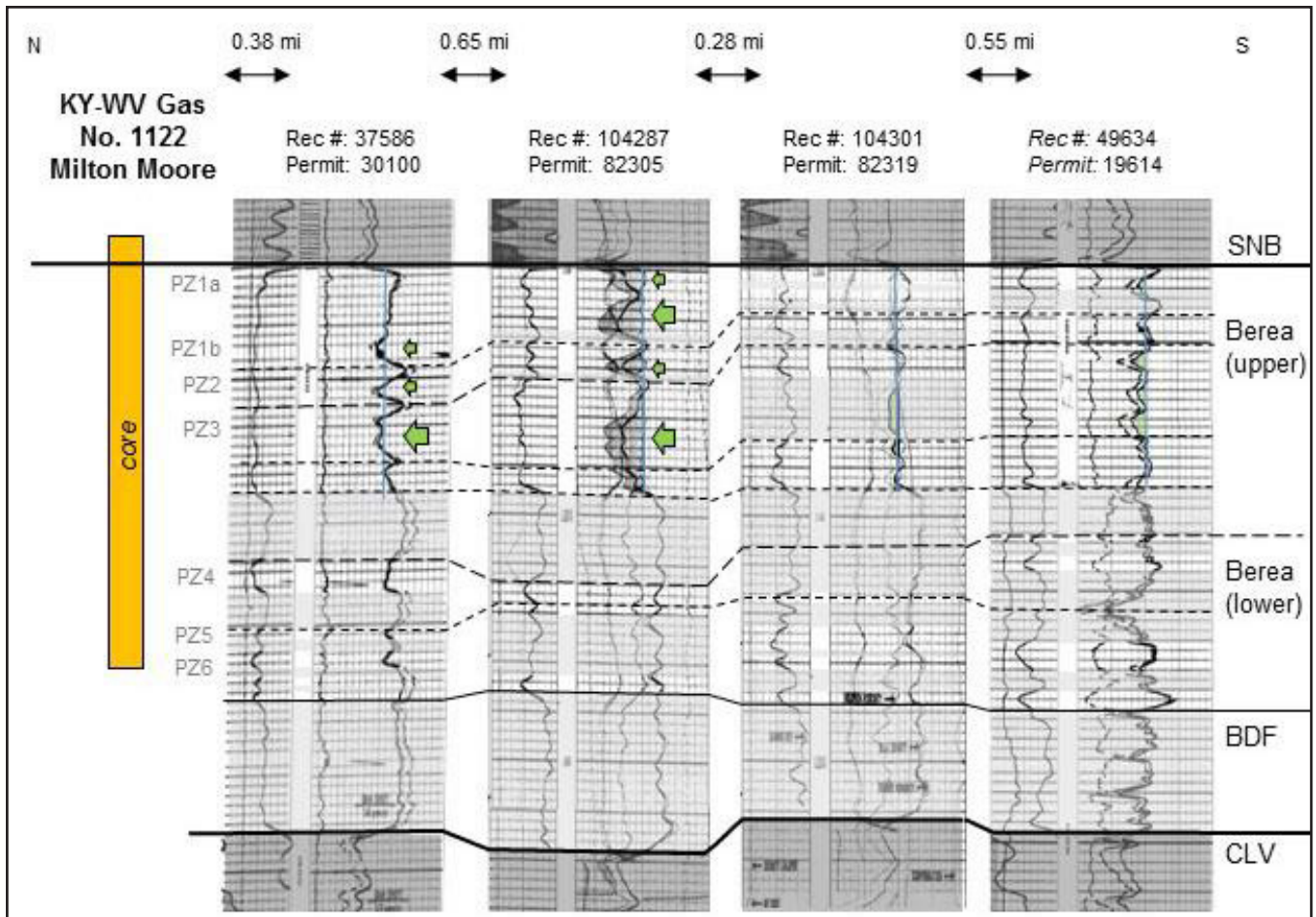


Figure 7-16. Correlation of logs north and south of the Ruben Moore well. Gray shaded zones are shales. Green shaded intervals on the log are porosity. Porosity zones are discussed in the text. The well is on the north end of the Cordell Field, with no close wells with logs any farther to the north.

In the upper part of the Bedford coarsening-upward section at the base of the Berea, and in some of the interbedded shales in the lower part of the Berea, many of the shales are red-colored. Red color was also noted in shale and parts of some of the other Kentucky cores (see core book). Red mudstone is common in the Berea in northern Ohio. It has been interpreted as red color from a northern source (Pepper and others, 1954) or from marine oxidation during times of reduced organic matter (Mausser, 1982) or from diagenetic alteration (Lewis, 1988). If the red color in the Bedford in this core were from a northern source, we would expect to see more of it in the other Kentucky cores (which have a more northerly position). The red color is likely diagenetic. At least in this core, it may be related to fluid migration since it occurs in

association with the bitumen-impregnated parts of the core.

The lowest part of the Bedford in the core, based on the accompanying geophysical logs, is a black Bedford Shale. It is similar in appearance to the underlying Cleveland Shale Member. Comparisons can be made to the black Bedford Shale in the Somerset Morlandbell core.

Summary of the EQT Core – For the other cores examined in this study, porosity intervals can be defined at bed scale or as sets of beds separated by gray shales. In this core, the staining provides direct evidence of fluid migration within beds and highlights internal heterogeneities that can create flow barriers laterally and vertically within beds. Lack of staining (bitumen impregnation) along flow rolls, ball-and-pillow structures, fractures, and at the base of beds may be caused by early

Table 7-6. Summary of XRD data from the KY-WV Ruben Moore well. See Appendix 1 for data.

XRD Analyses, n=25	Maximum	Minimum	Mean	Standard Deviation
NONCLAY FRACTION				
Quartz	83.1	25.9	66.27	17.43
K-feldspar	2.1	0.8	1.50	0.40
Plagioclase	11.7	2.2	7.15	2.34
Organic carbon (TOC)	6.8	0.0	0.69	1.81
Apatite	0.5	0.0	0.03	0.12
Pyrite	5.0	0.0	0.75	1.24
Marcasite	0.8	0.0	0.06	0.22
Dolomite	18.4	0.0	1.61	3.98
Siderite	3.8	0.0	0.64	0.93
Gypsum	0.3	0.0	0.05	0.11
TOTAL	3.8	0.0	0.64	0.93
CLAY FRACTION				
Mixed-layer illite/smectite (includes R3)	6.9	0.0	1.41	1.84
Illite + mica	49.8	2.6	13.42	14.81
Chlorite	4.3	0.4	1.25	1.05
Kaolinite	11.3	0.0	5.17	2.37
TOTAL	4.3	0.4	21.24	17.06

compaction and consolidation from syndimentary movement and dewatering of sediment. Secondary infilling of pores by clays may also occur along shale contacts. Secondary cementation along fractures and some glide planes (mostly pyrite) also appears to inhibit porosity and staining. The timing of pyrite staining is discussed in the Thin-Section Petrography section.

Porosity and Permeability Analysis

Currently, there are no published datasets of porosity and permeability for the Berea of Kentucky. For this project, we assembled all of the historic data in the KGS Oil and Gas Database (n=583 from 18 wells) and a recent collection of new data from Chesapeake Energy (n=91 from four wells). The historic data are mostly from company cores that were not available for study. The Chesapeake data were from four cores at the KGS Well Sample and Core Library, so could be compared to other data as part of this project. Figure 7-21 shows the locations of wells with porosity and permeability data. Data are compiled in Appendix 1.

The historic Berea data are problematic at low permeabilities (Fig. 7-22). A variety of lower measuring limits (impermeable, 0, less than 0.1, less

than 0.2md) reflects the capacity of the available equipment at the time of sampling. Unfortunately, these limited data tend to mask any potential relationship between porosity and permeability in the overall dataset. If data points with lower limits are deleted in an adjusted historic dataset, a weak relationship ($R^2=0.57$) is apparent on a logarithmic scale (Fig. 7-23). Mean porosity for the adjusted data is $12.8+2.7$ percent, ranging from 2.8 to 19.5 percent. Mean permeability is $2.0+3.4$ md, ranging from 0.02 to 25.0md. This adjusted dataset is not representative of the true range of Berea porosity and permeability since the low-permeability samples have been removed. It should only be used to characterize the relationship between permeability and porosity for better-quality Berea reservoirs.

The new data (Fig. 7-24) collected by Chesapeake Energy from four Berea cores in the KGS Well Sample and Core Library used pulsed-neutron permeability methods, which are capable of measuring much lower permeabilities than older techniques. The lowest permeability in the new Berea dataset (excluding shale) is 0.00005md. Mean permeability is $0.2+0.4$ md, ranging from

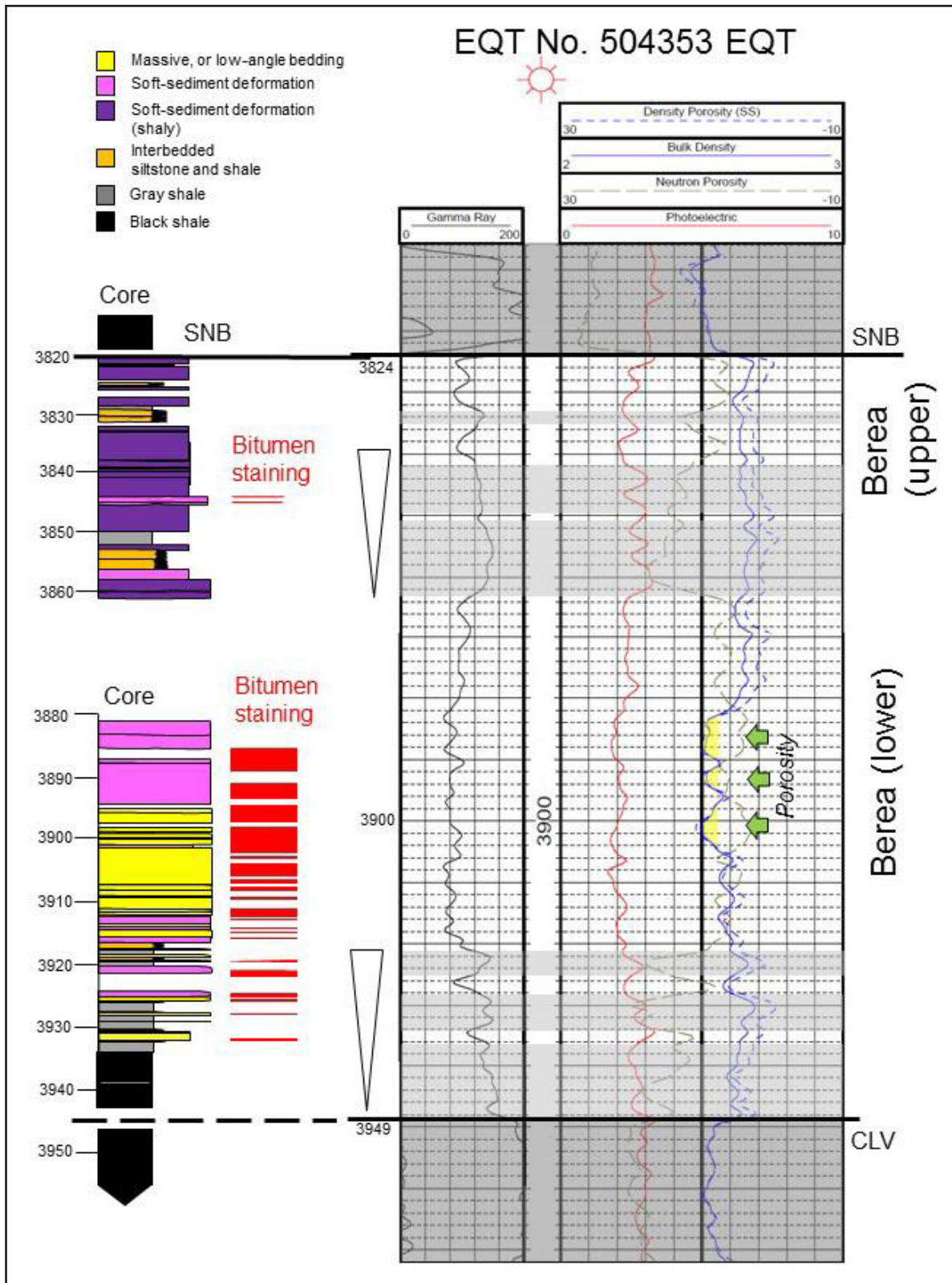


Figure 7-17. Comparison of core bedding, bitumen-stained intervals (red), with geophysical log for the EQT No.504353 well. Gray shaded zones on the log are shales. CLV=Cleveland Shale Member of the Ohio Shale. SNB=Sunbury Shale. Green arrows point to three porosity zones discussed in the text. Note: The lower part of the Bedford (based on the density and gamma signatures) in this core is a black shale.

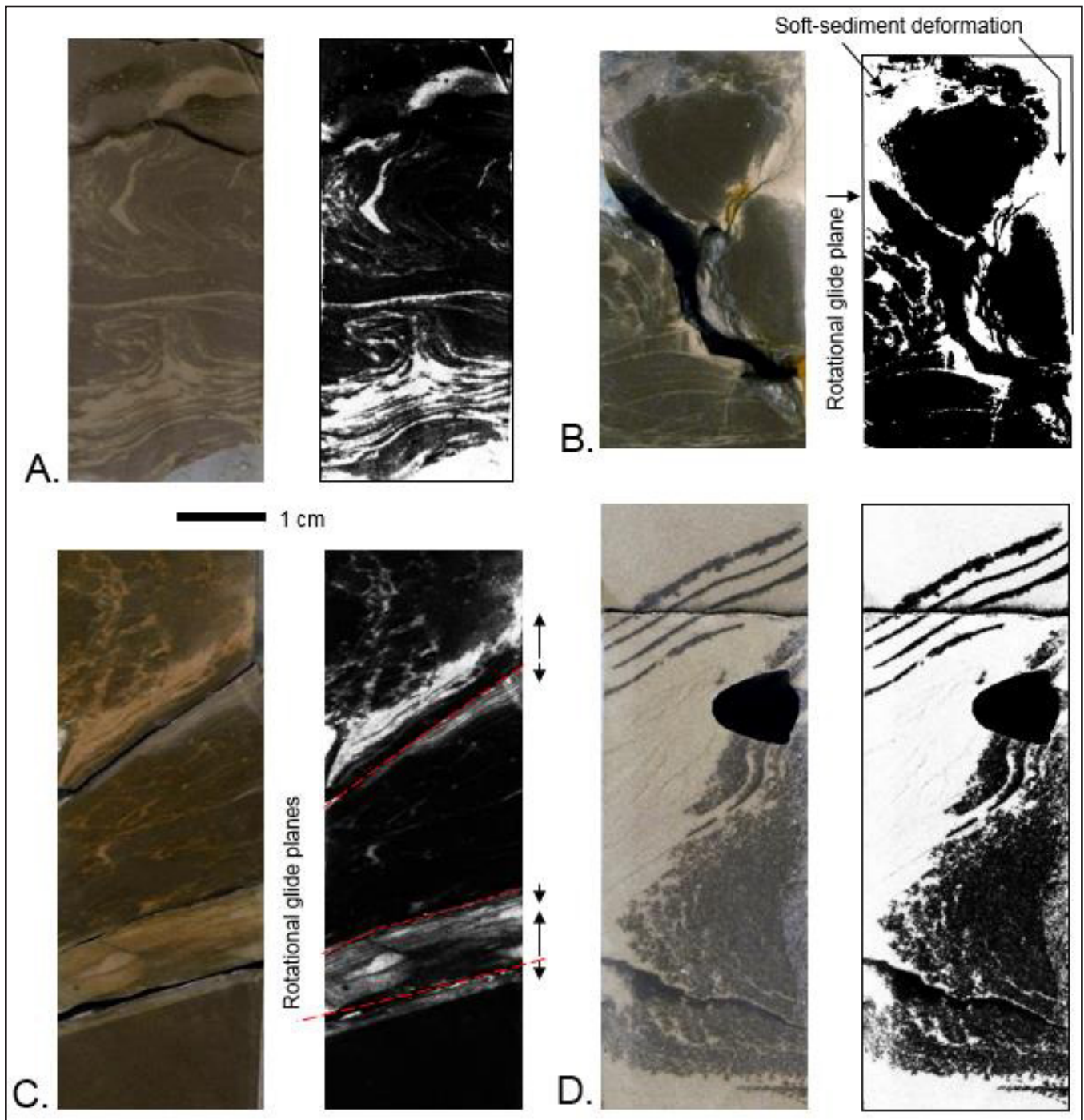


Figure 7-18. Examples of staining boundaries in soft-sediment-deformed beds in the EQT core. Core photos are juxtaposed against high-contrast black and white copies of the same image to highlight bitumen. A. Dewatering structure at 3,889 ft. B. Dewatering structure at 3,883 ft. Note lack of staining along margins. C. Multiple shear zones (red dashed lines) in larger flow roll at 3,891 ft. D. Nose of overturned flow roll at 3,912.5 ft.

0.00005 to 2.5 md. Most of the permeability values are between 1 and 0.01 md. Mean porosity is 8.9 ± 2.9 percent, ranging from 2.0 to 16.1 percent. The lower-permeability data extend the overall re-

gion in which a relationship between porosity and permeability can be tested in the Berea, resulting in a much better relationship ($R^2=0.81$) than was found in the historic (higher-permeability) data.

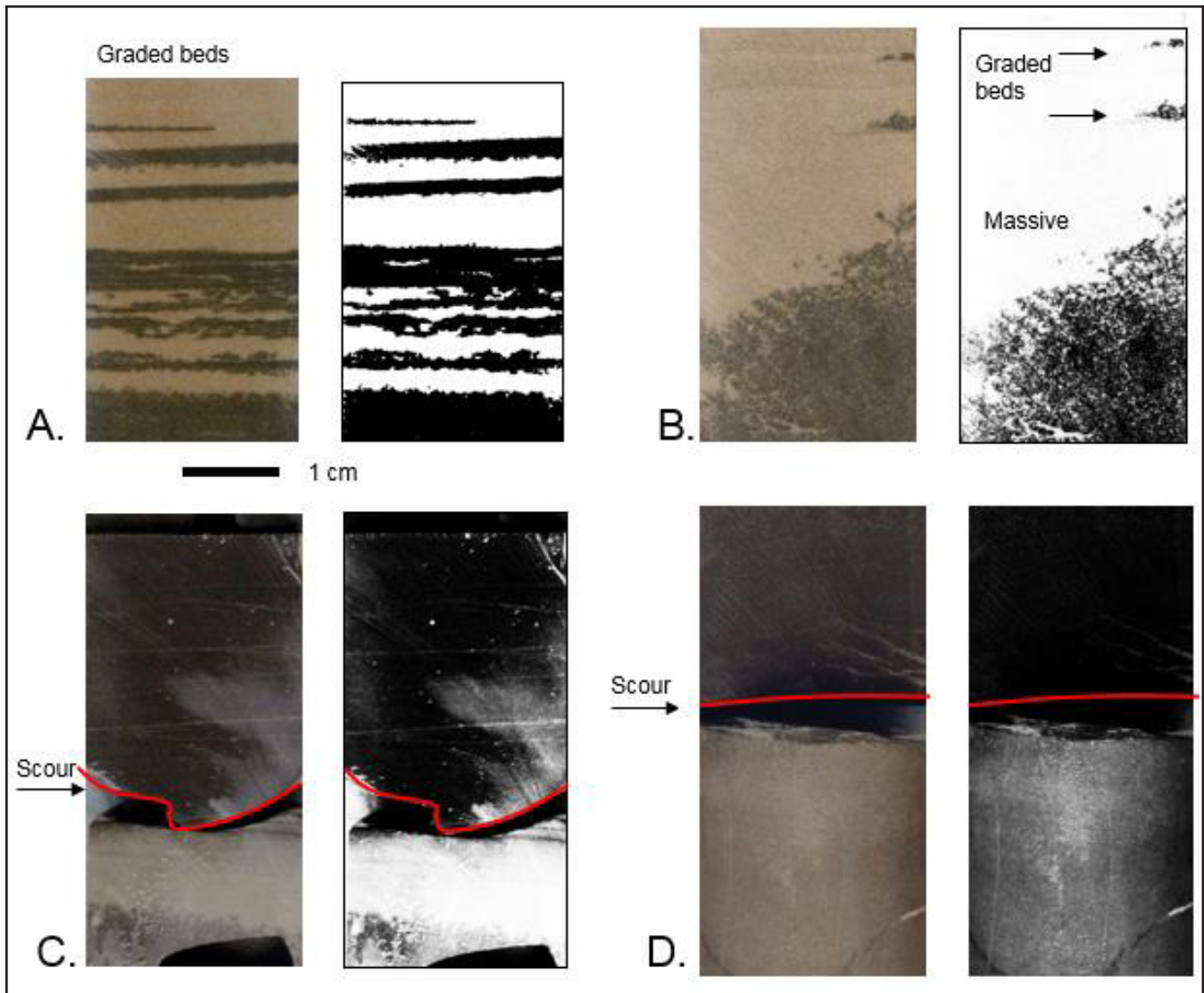


Figure 7-19. Examples of staining boundaries across bedding and scour contacts in the EQT core. Core photos are juxtaposed against high-contrast black-and-white copies of the same image to highlight bitumen. A. Straight-line to parallel gradational staining highlighting otherwise hard-to-see graded or parallel-laminated bedding at 3,907.5 ft. B. Dendritic staining in massive bed (possibly from soft-sediment deformation) at 3,913 ft. C. Sharp boundary between stained and unstained core across scour surface at 3,910.7 ft. D. Sharp boundary between stained and unstained core across scour surface at 3,913.5 ft (red lines).

When the new dataset is combined with the historic (adjusted) data, the trend has an $R^2=0.75$ (Fig. 7-25). For the combined data, mean porosity is $11.6+3.3$ percent, ranging from 2.0 to 19.5 percent. Mean permeability is $1.4+2.9$ md, ranging from 0.00005 to 25 md. For permeabilities greater than 0.1 md, porosities are generally greater than 10 percent. All porosity values above 12 percent have permeabilities greater than 0.1 md. A comparison of trend lines from the different datasets shows a steeper-sloping trend line in the low-permeability Chesapeake data, and a shallower slope

in the higher-permeability data in the historic data (Fig. 7-25). It is possible that there are multiple relationships between permeability and porosity in the Berea of Kentucky: one governing low-permeability/low-porosity (below approximately 0.1 md permeability and 10 percent porosity) siltstone and sandstone and one governing siltstone and sandstone with higher permeabilities and porosities (above approximately 0.1 md permeability and 10 percent porosity). More variability is associated with higher permeabilities.

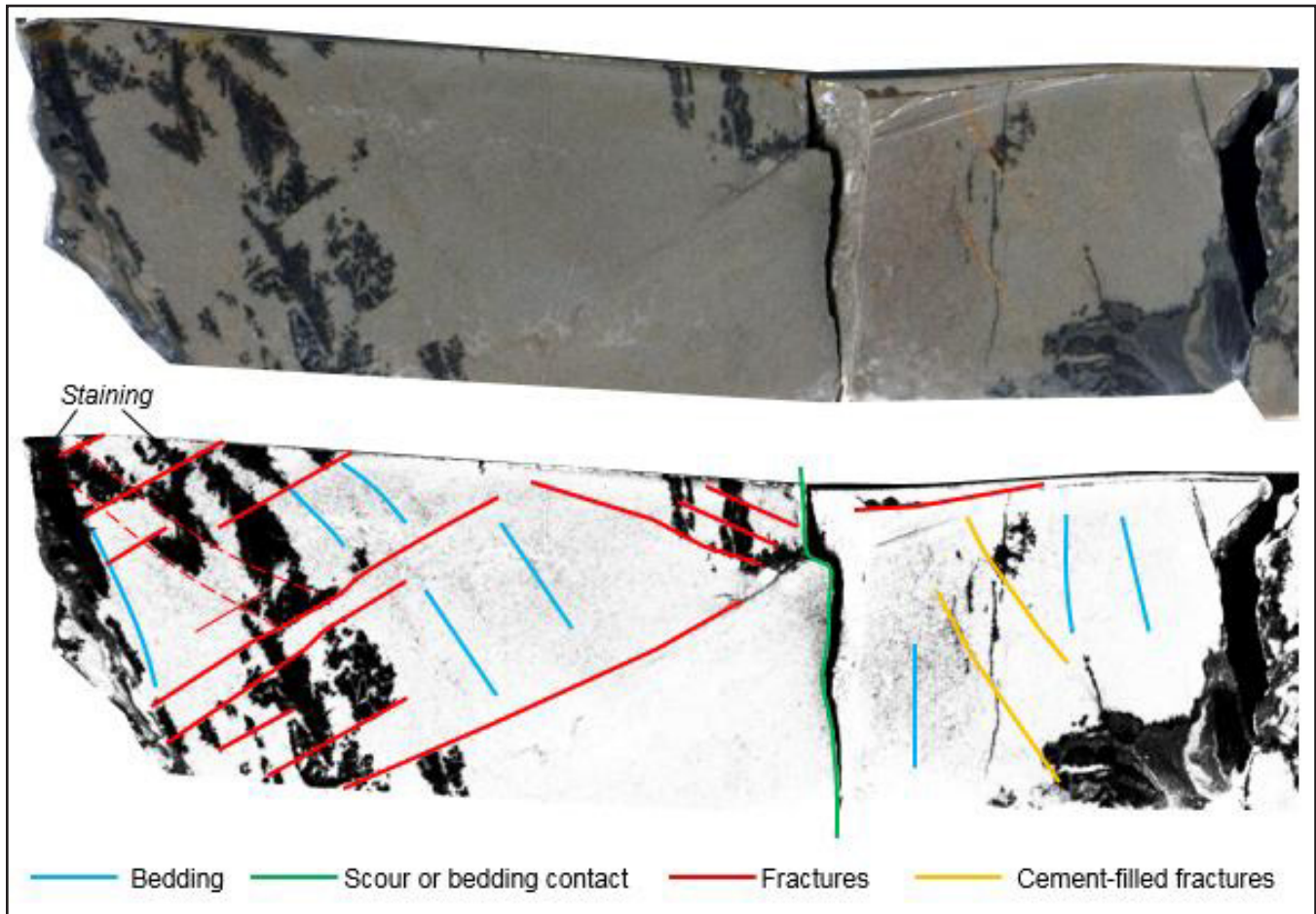


Figure 7-20. Examples of bitumen staining at 3,844.5 ft, showing influences of bedding, scour or bedding contacts, and fractures on bitumen migration in the Berea.

Comparisons to Bed Type. Bed type was compared to porosity and permeability for historic data and new data collected by Chesapeake Energy for four cores in the KGS Well Sample and Core Library (green text in Figure 7-21). Bed types and their corresponding bedding are shown in Table 7-7. In general, the relationship between porosity and permeability appears to be independent of bed type (Figs. 7-26, 7-27). However, the best permeabilities and porosities are in the low-angle bed types (possibly hummocky bedding) and the lowest permeability and porosity is in the dense, gray, massive bed (only one sample), which appears to be a finer-grained or more argillaceous siltstone (Fig. 7-27). If we examine only the highest permeabilities in each bed type, then $S_{la} > S_m \sim S_{ml} > S_{sd} \sim S_{sd}(sh)$. For the best potential reservoir rock (greater than 10 percent porosity and greater than 0.1 md), most of the data are from S_{la} , S_m , and S_{ml} beds. De-

formed beds (S_{sd} , $S_{sd}(sh)$) are less common in better reservoir rock, although there is considerable range and overlap of bed types relative to porosity and permeability (Fig. 7-27). This is partly true in the EQT core from Pike County. The most-stained intervals are generally in massive beds or beds with poorly developed grading or faint parallel laminae, with variability. Soft-sediment beds also are bitumen impregnated, but have many internal discontinuities (Fig. 7-18). Interestingly, there is not a significant difference in the porosity and permeability values for deformed beds with and without significant shale (Figs. 7-26, 7-27). The two bed types were separated during analysis because it seemed likely that more shale would lead to less porosity and permeability. However, it appears that aspects of grain fabric and possibly compaction in the deformed beds are more important than their lithology.

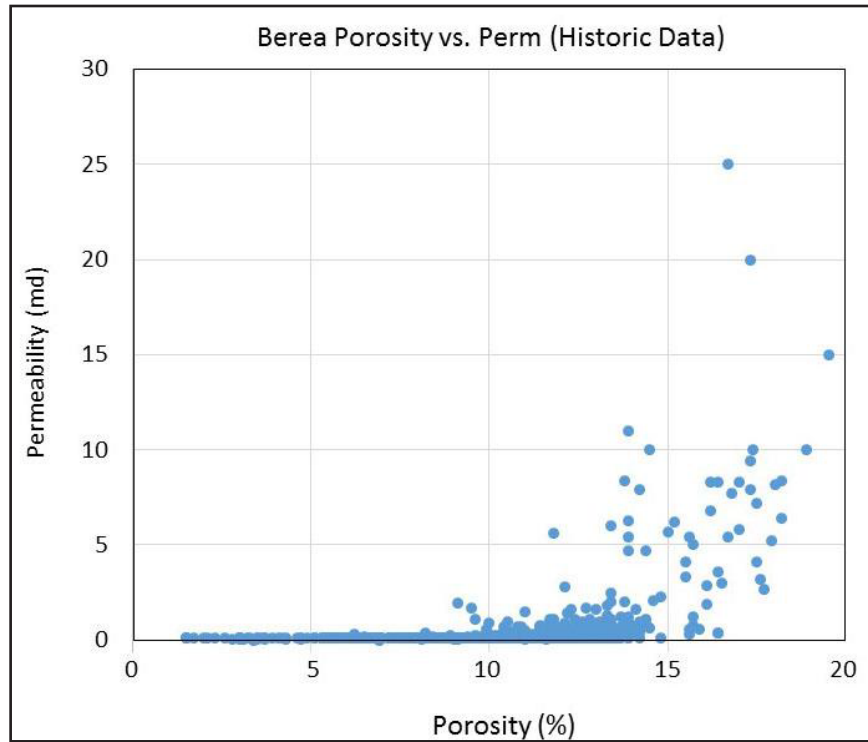


Figure 7-22. Historic Berea porosity and permeability data. The large number of points at “0” permeability reflects permeability data below detection limits at the time of measurement and plotting on a normal scale.

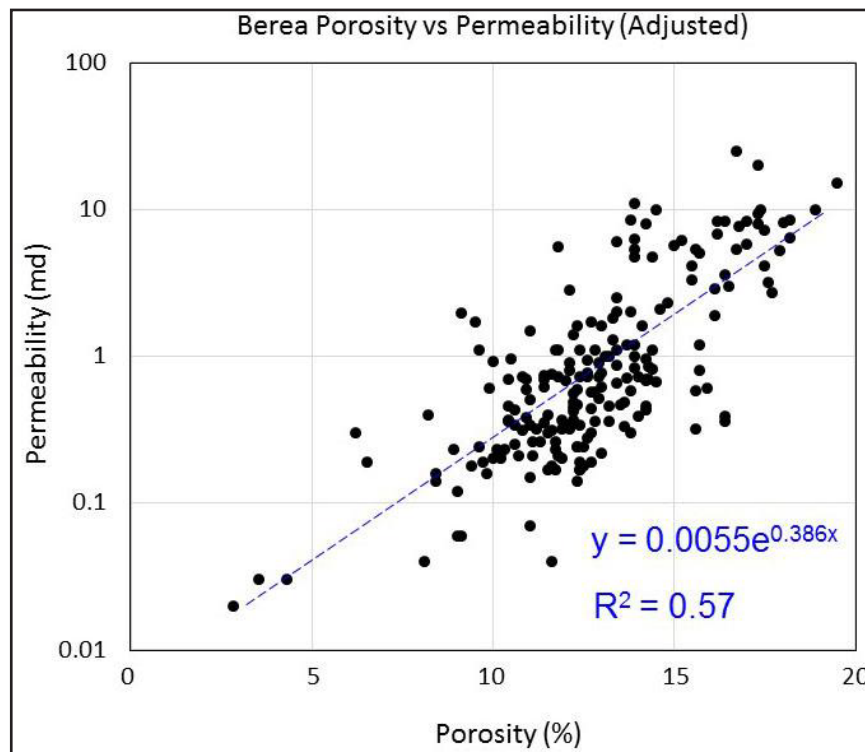


Figure 7-23. Historic porosity versus permeability data on a logarithmic scale with all below-detection-limit data deleted.

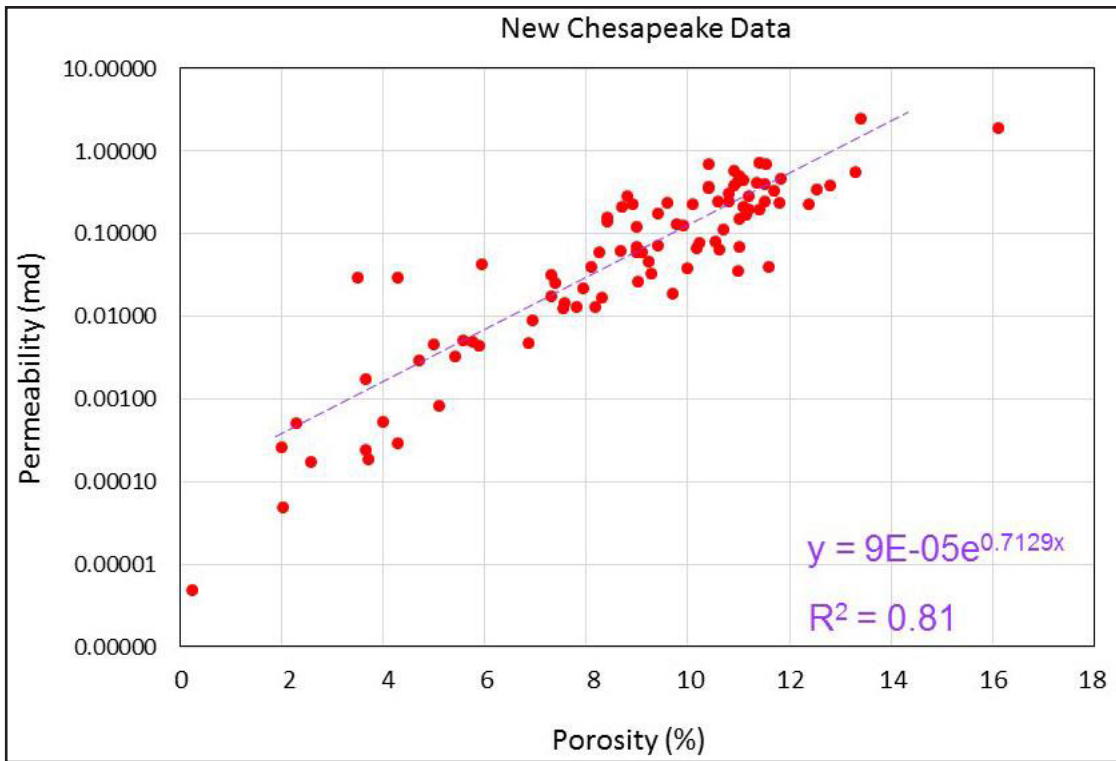


Figure 7-24. New porosity and permeability data collected by Chesapeake Energy from four of the Kentucky cores.

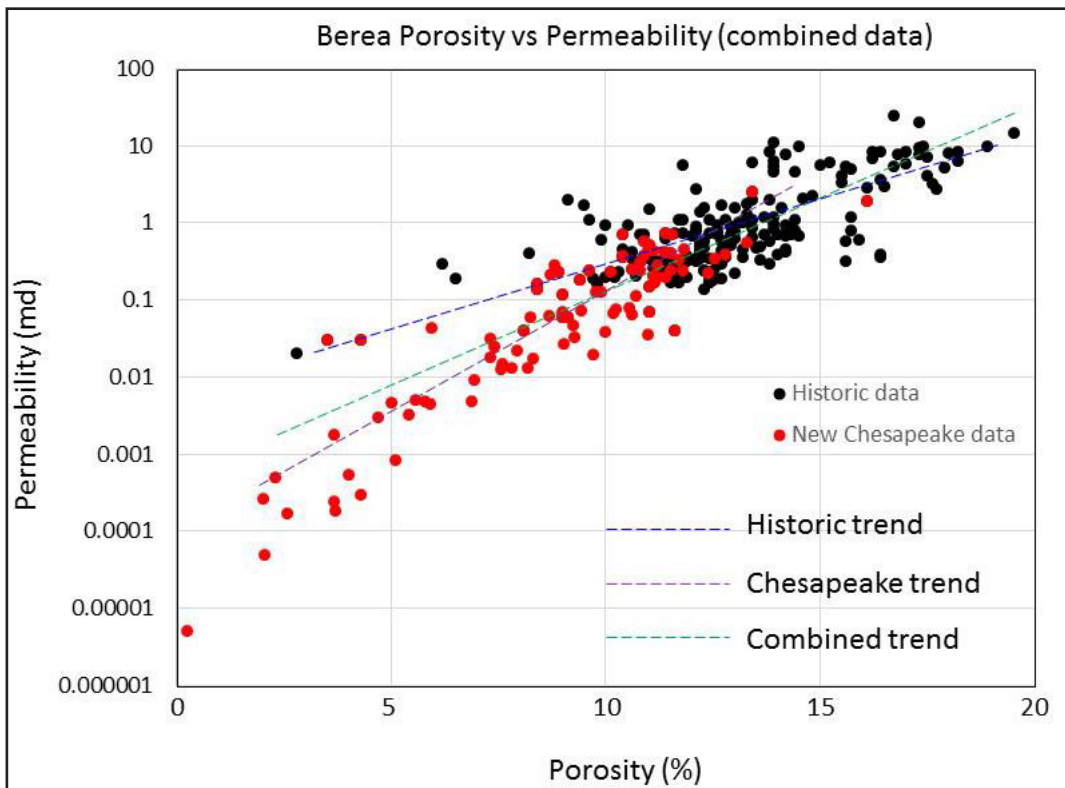


Figure 7-25. Combined adjusted historic and Chesapeake datasets, and comparison of trend lines for the sum and individual datasets.

Symbol	Bed Type
Sm	Massive (structureless) bedding in coarse siltstone to very fine-grained sandstone.
Sml	Massive bedding with faint laminated texture or laminae in c. slt to vfg. ss.
Smg	Massive, argillaceous, dark gray siltstone.
Ssd	Soft-sediment-deformed coarse siltstone to very fine-grained sandstone.
Ssd (sh)	Soft-sediment-deformed, argillaceous coarse siltstone to very fine-grained sandstone.
Sla	Low-angle laminated coarse siltstone to very fine-grained sandstone (may represent hummocky or swaley bedding, or soft-sediment loading and bed dip).
Sr	Ripple-bedded or laminated coarse siltstone to very fine-grained sandstone.
Sl	Parallel-laminated coarse siltstone to very fine-grained sandstone (may include graded to faintly graded beds).

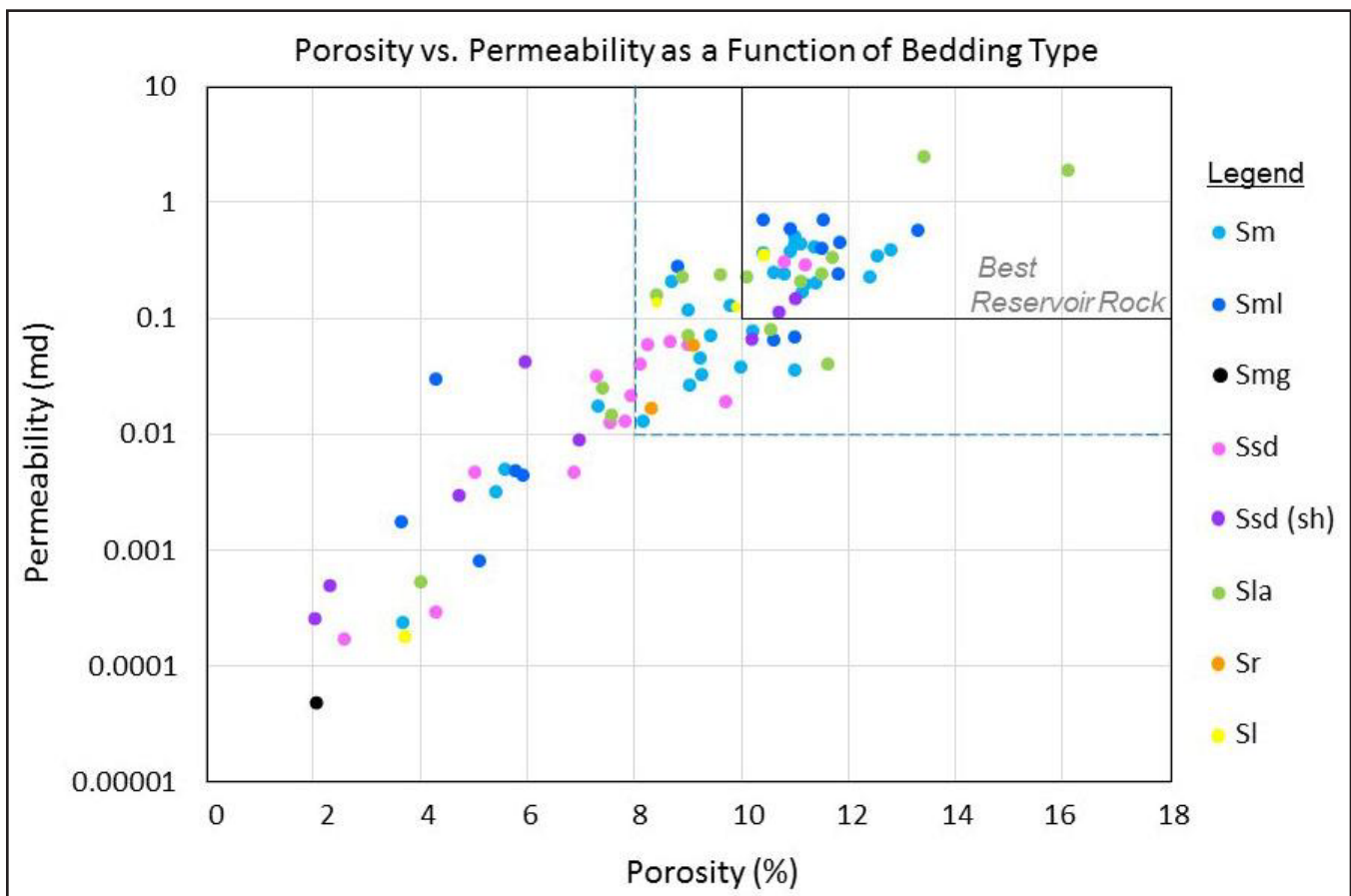


Figure 7-26. Porosity and permeability compared to bedding in cores. See Table 7-7 for explanation of bedding types. The best reservoir rock field is defined as greater than 0.1 md and greater than 10 percent porosity. The dashed-line box represents a field with greater than 0.01 md permeability and greater than 8 percent porosity.

A comparison of porosity and permeability in the Berea to XRD results follows for each of the major cement constituents:

Dolomite – XRD analysis of the Berea shows that dolomite varies from 0 to 39 percent in 74 sam-

ples from the four study cores. When the percentage of dolomite is compared to porosity and permeability, there does not appear to be a significant relationship (Fig. 7-29). However, if “0” values are separated from the 0–5 percent dolomite category,

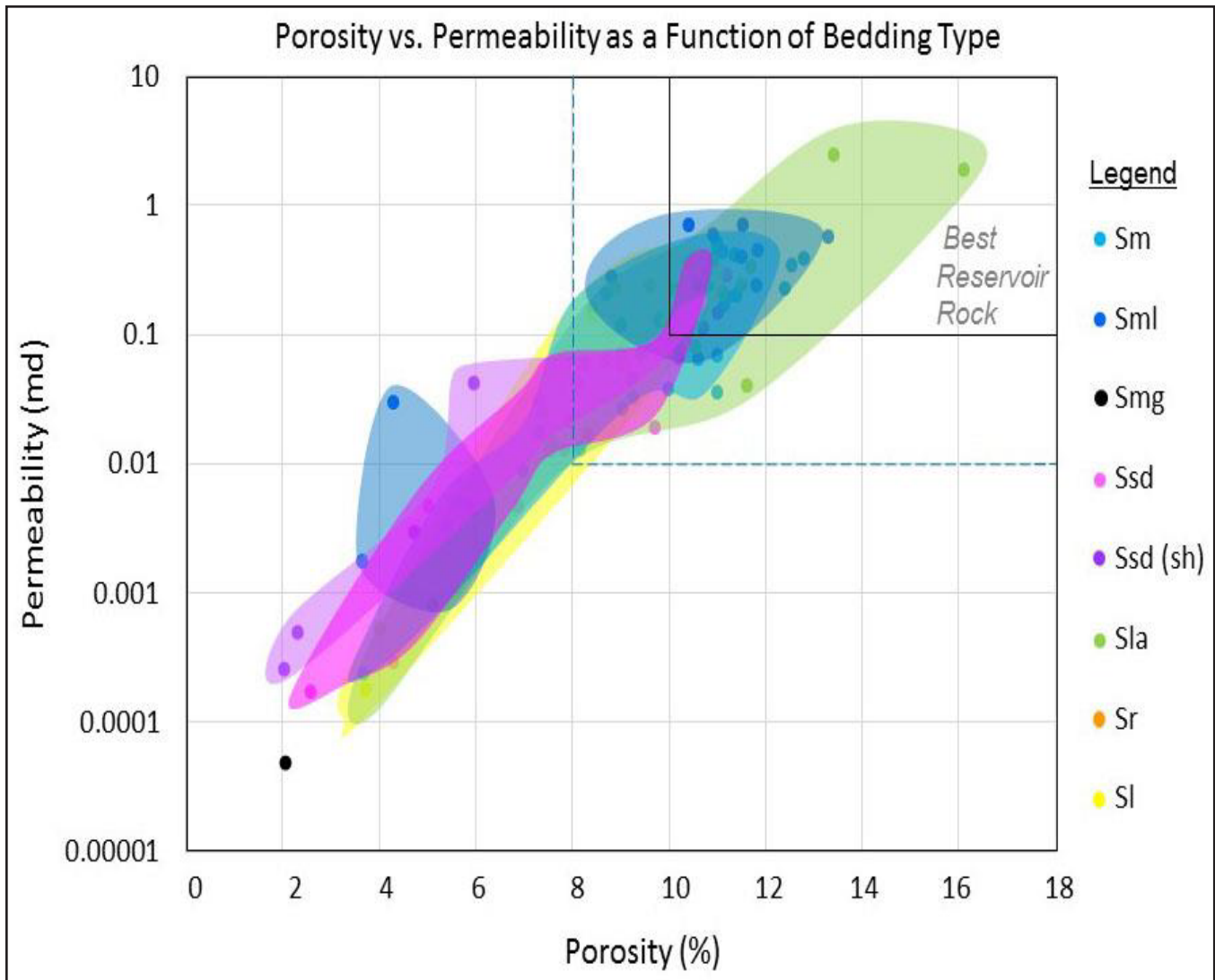


Figure 7-27. Porosity and permeability compared to bedding in cores. Colored fields encompass all points for each bed type. The best reservoir rock field is defined as greater than 0.1 md and greater than 10 percent porosity. The dashed-line box represents a field with greater than 0.01 md permeability and greater than 8 percent porosity. See Table 7-7 for explanation of bed types.

then the best reservoirs have some dolomite rather than no dolomite (Fig. 7-30), and there is a fairly good trend of increasing dolomite percentage with decreasing porosity and permeability. More dolomite cement means less pore space.

Illite and Mica – Silt- and clay-sized illite and mica are difficult to differentiate in thin section and XRD. Hence they are combined in many analyses. XRD analysis of the Berea shows that the amount of illite and mica varies from 2 to 38 percent in 74 samples from the four study cores. In general, increasing illite and mica percentage corresponds to decreasing porosity and permeability, although there is considerable overlap in the data fields

(Figs. 7-31, 7-32). The best reservoir rock (highest porosity and permeability) has less than 10 percent and mostly less than 8 percent illite and mica. The least porous and permeable rock has more than 15 percent illite and mica.

Total Clays – Illite is the dominant clay component in the Berea, but some samples also have significant layered clays (smectite; 0–4.8 percent) and kaolinite (0–12 percent). XRD analysis of the Berea shows that the amount of total clays varies from 7.7 to 55 percent in 74 samples from the four study cores. A comparison of porosity and permeability as a function of total clays shows a relatively good relationship between increasing clay content and

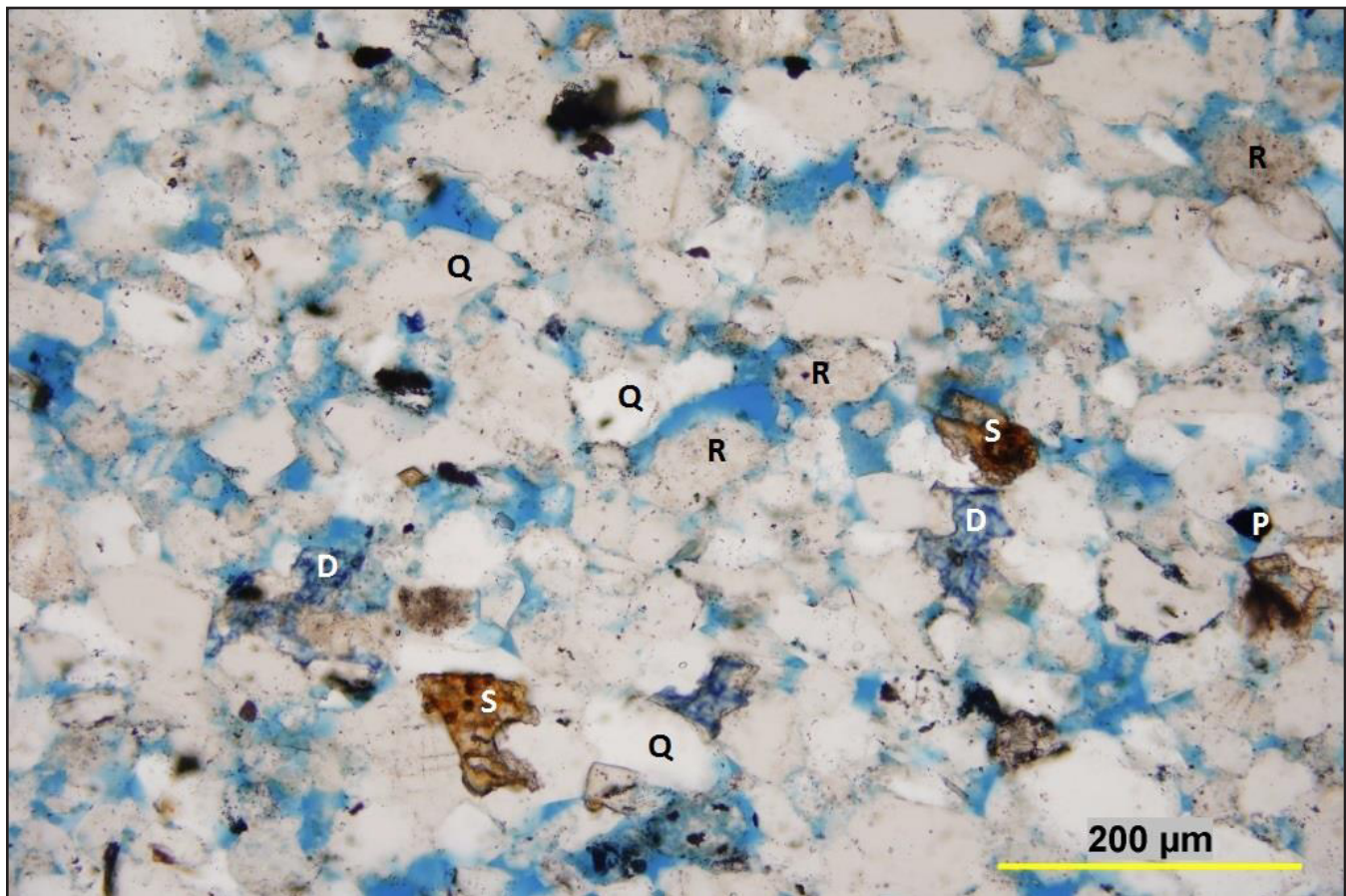


Figure 7-28. Typical porous lithic arenite. Milton Moore #1122 well, 1,269 ft, Lawrence County. Blue areas between grains are open pores. Q = quartz. R = rock fragment. S = siderite. D = ferroan dolomite (stained). P = pyrite. Core porosity = 11.1 percent, permeability = 0.170679 md. Scale in microns.

decreasing porosity and permeability (Fig. 7-33), but with considerable overlap of percentage fields (Fig. 7-34). The best reservoirs (greatest porosity and permeability) generally have less than 15 percent total clays. There are two exceptions, and one of those (17.7 percent) has a relatively high kaolinite percentage (8.6). Kaolinite is a late cement (see petrography section). The least porous and permeable rock has more than 20 percent total clays.

Quartz (Quartz Grains Versus Quartz Overgrowth Cements) – Quartz cement cannot be distinguished from detrital quartz in the XRD data, so graphs were not plotted for quartz versus porosity and permeability. The Berea in Kentucky has very fine grain size (mostly coarse silt), and grains often lack distinctive dust rims, so identifying quartz overgrowths is difficult. The degree of quartz cementation is not high, but quartz overgrowths were observed in many thin sections, and they

likely influence porosity and permeability (see Thin-Section Petrography section).

Siderite – Reddish iron-staining is noted at the top of the Berea in many outcrops. In cores, iron staining also occurs in some deformed beds and in siltstones and sandstones above and below interbedded shales. Shales in some of the lower parts of the Berea and adjacent to parts of the Berea with some oil saturation also may have red or maroon color, presumed to be iron staining. Much of that iron staining appears to be siderite. XRD analysis of the Berea shows that the amount of siderite varies from 0 to 3.8 percent in 74 samples from the four study cores.

Pyrite – Pyrite is pervasive in the Berea. It commonly occurs as pinpoint grains or intergranular cements, but may be concentrated in some layers, especially (1) filling burrows, (2) along fractures, and (3) along shear zones of soft-sediment-defor-

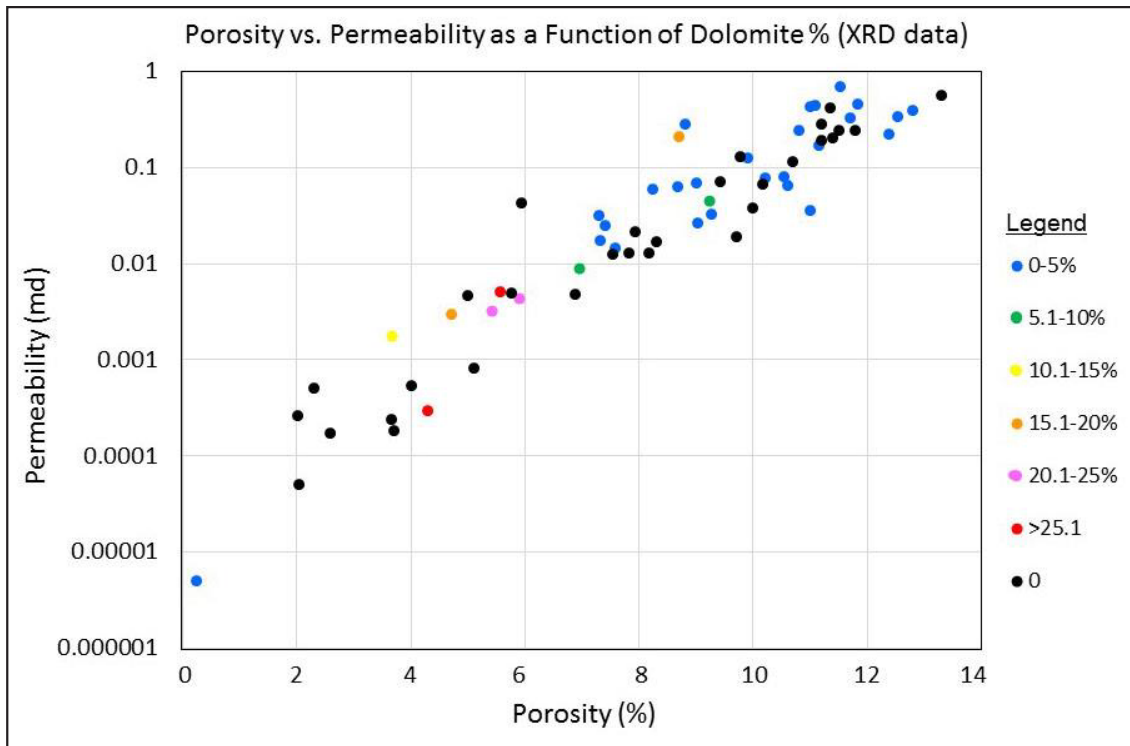


Figure 7-29. Porosity and permeability compared to dolomite content in cores.

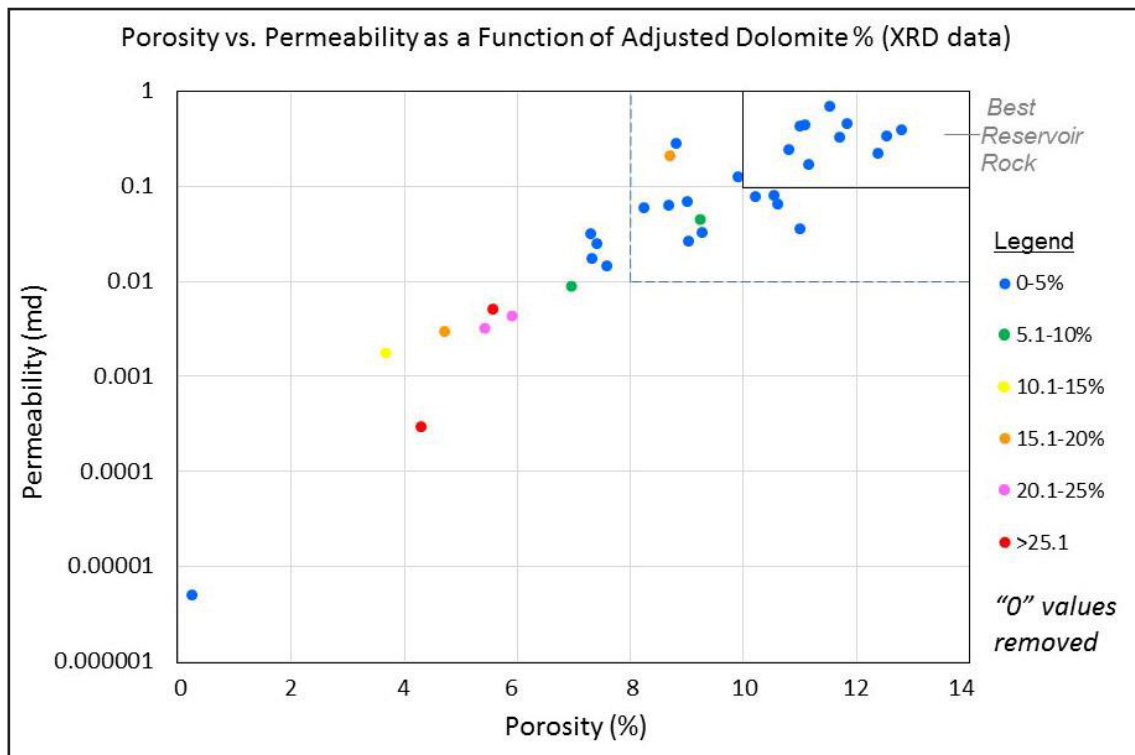


Figure 7-30. Porosity and permeability compared to dolomite content in cores, excluding all "0" values. The best reservoir rock field is defined as greater than 0.1 md and greater than 10 percent porosity. The dashed-line box represents a field with greater than 0.01 md permeability and greater than 8 percent porosity.

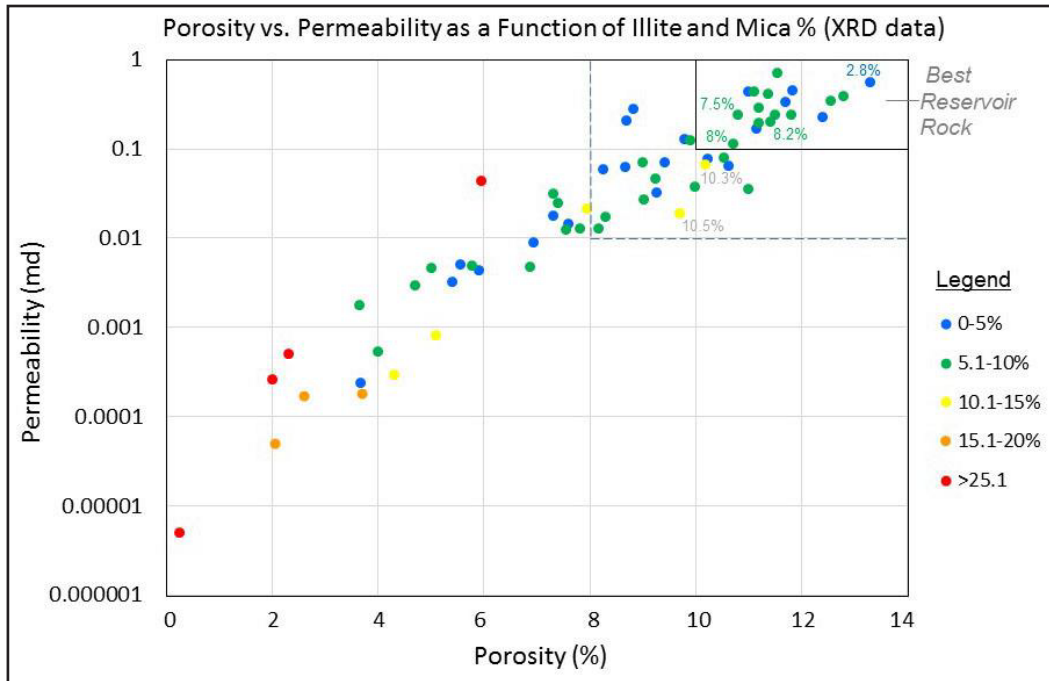


Figure 7-31. Porosity and permeability compared to illite and mica content in cores. The best reservoir rock field is defined as greater than 0.1 md and greater than 10 percent porosity. The dashed-line box represents a field with greater than 0.01 md permeability and greater than 8 percent porosity.

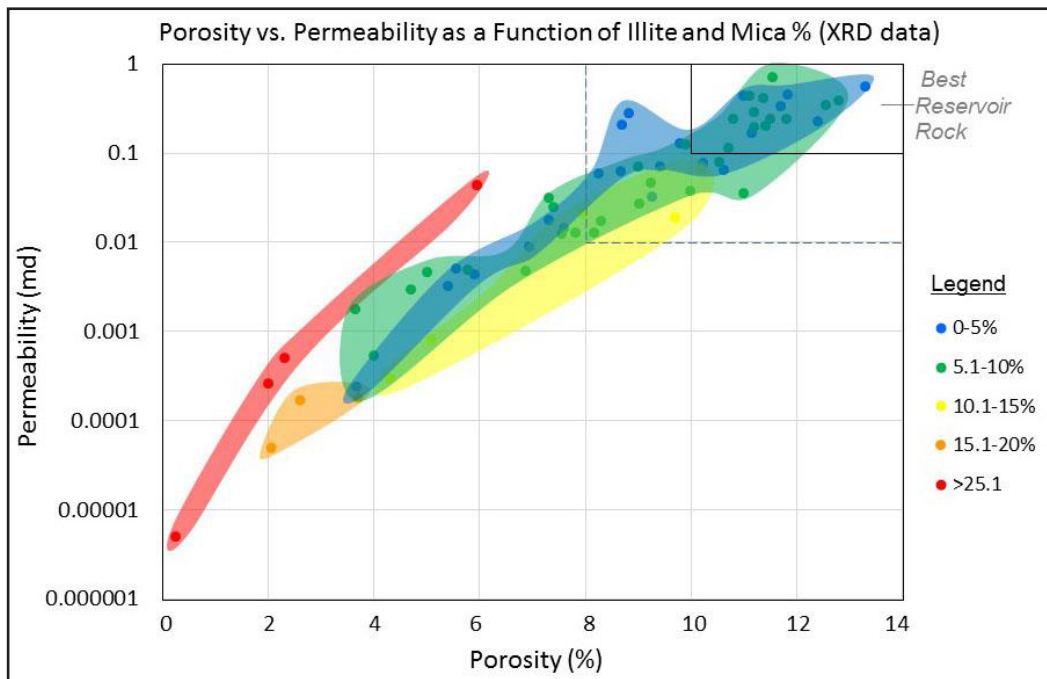


Figure 7-32. Porosity and permeability compared to illite and mica content in cores. Colored fields encompass all points for each percentage range. The best reservoir rock field is defined as having greater than 0.1 md permeability and greater than 10 percent porosity. The dashed-line box represents a field with greater than 0.01 md permeability and greater than 8 percent porosity.

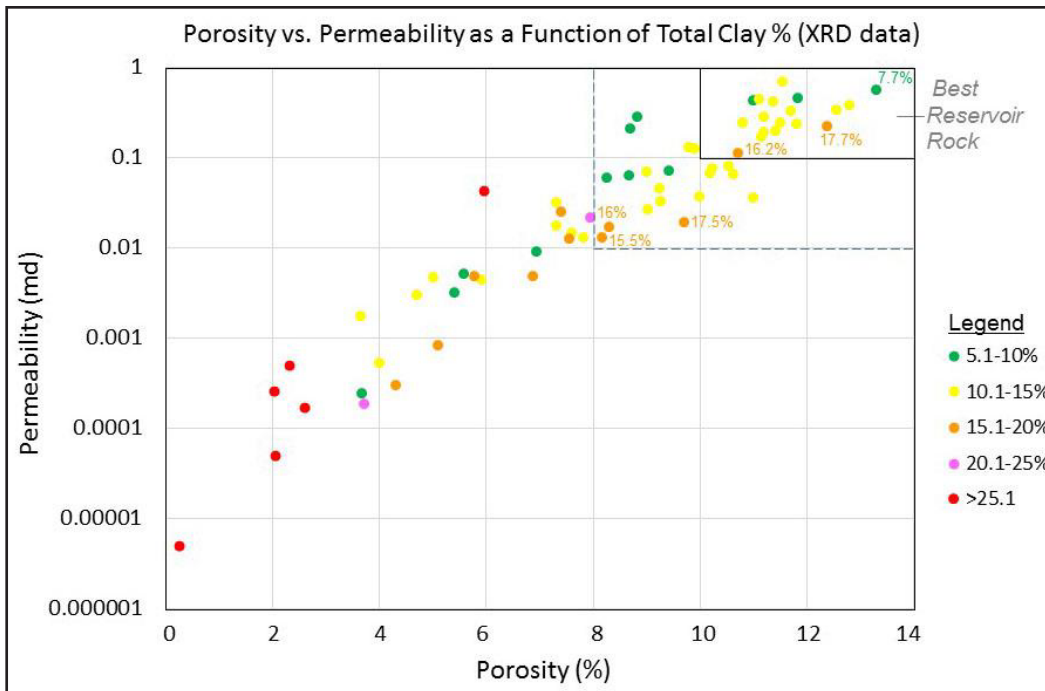


Figure 7-33. Porosity and permeability compared to total clay content in cores. The best reservoir rock field is defined as having greater than 0.1 md permeability and greater than 10 percent porosity. The dashed-line box represents a field with greater than 0.01 md permeability and greater than 8 percent porosity. Values are included for some of the 15–20 percent total clays in the greater than 8 percent permeability and greater than 10 percent porosity fields.

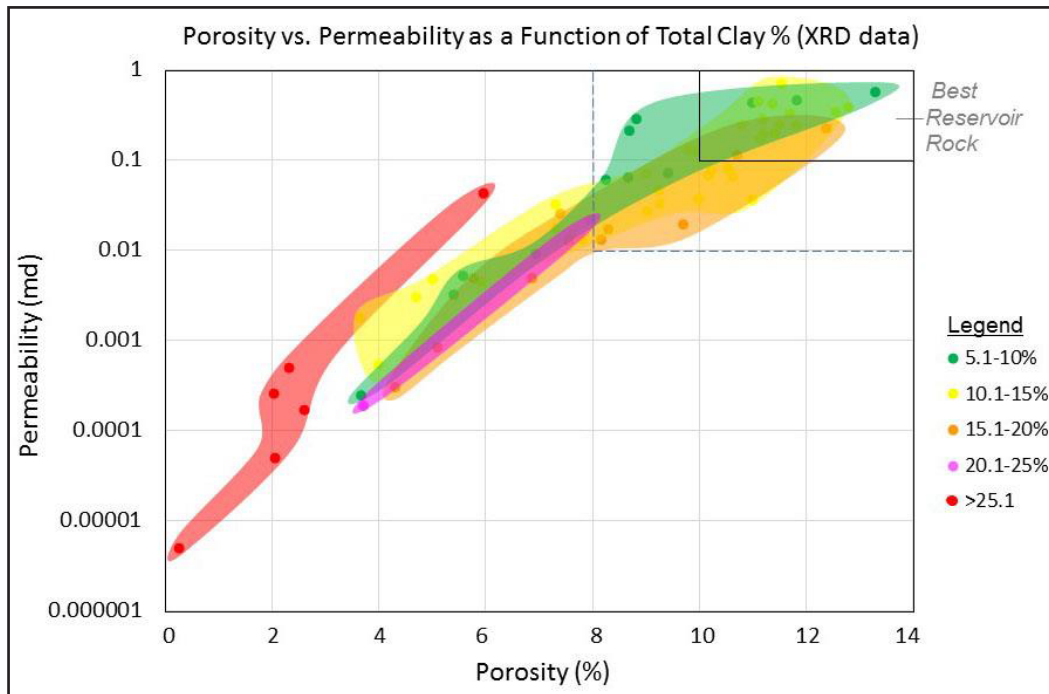


Figure 7-34. Porosity and permeability compared to total clay content in cores. The best reservoir rock field is defined as having greater than 0.1 md permeability and greater than 10 percent porosity. The dashed-line box represents a field with greater than 0.01 md permeability and greater than 8 percent porosity.

mation structures (flow rolls, etc.). XRD analysis of the Berea shows that the amount of pyrite varies from 0 to 5 percent in 74 samples from the four study cores.

Thin-Section Petrography

As part of the reservoir-quality assessment, thin sections from six wells in Lawrence, Johnson, and Pike Counties were prepared and examined (Table 7-8). No core samples were available from Greenup County. The goal of this task was to document the porosity types and diagenetic history that have affected porosity development in these rocks. These results help us understand the variability in porosity, both within the Lawrence County play area and regionally across eastern Kentucky.

Berea Pore Types. The Berea in eastern Kentucky has long been designated a tight reservoir with permeability generally below 1 md (Avila, 1983a, b). Despite the low permeability, porosity is well developed, commonly more than 10 percent of the rock volume. Based on observations of thin sections collected in this study, three general pore types are identified in the Berea in eastern Kentucky: (1) primary intergranular pores, (2) secondary moldic pores, and (3) microporosity. Pore types in Lawrence and Johnson Counties are similar between wells, but differ significantly from the one deeper core examined from Pike County. These pore types are discussed in more detail in the next few pages.

Intergranular Porosity – Intergranular porosity is the most abundant pore type, and occurs in most Berea samples. These pores are remnants of the primary porosity present when the sediment was deposited. It has typically been reduced by various types of cement, detrital clay matrix, and intergranular compaction, but is well connected

with other pores, as evidenced by the excellent impregnation of thin sections with blue-dyed epoxy (Fig. 7-35). Pore sizes were not measured, but grain sizes are in the silt to very fine sand range, so intergranular pores are much smaller, many in the 10 to 25 μ range. Pore size alone partly contributes to the low permeability of these rocks. In the EQT 504353 core from Pike County, some intervals contain only intergranular porosity plugged with bitumen (degraded oil) (Table 7-8). Locations are shown in Figure 7-36). Mercury injection capillary pressure analysis done on six samples gives an idea of the pore-throat size distribution, and is discussed later.

Secondary Moldic Porosity – Secondary porosity that formed after deposition is an important Berea pore type in Lawrence and Johnson Counties. These pores formed by dissolution of framework grains, and are typically larger than intergranular pores (Fig. 7-37). The higher-porosity samples have significant secondary porosity. The immature composition of Berea sandstones makes them particularly susceptible to grain dissolution after burial. Many moldic pores formed by dissolution of plagioclase feldspars, and partly dissolved grains are commonly observed. Potassium feldspars could also form secondary pores, but the sections were not stained for K-spar, making positive identification difficult. Other leached grains are hard to identify, but likely include rock fragments and possibly glauconite or carbonate grains (Fig. 7-38).

It is interesting to note that secondary pores were not observed in the Pike County core samples. Whether this resulted from a different diagenetic history or different original mineralogy is not known.

Table 7-8. List of wells with Berea Sandstone thin sections available for this study. Locations are shown in Figure 7-5.

Well	Permit No.	County	Core Analysis Dates	Logs	Samples
Ashland #1 Neal	43004	Lawrence	2014, 1981	yes	12
Columbia #20505 Simpson	32260	Lawrence	2014	yes	8
Ky.-W.Va. Gas #1122 Moore, M.	773E9	Lawrence	2014, 1959	no	11
EQT Prod. #504353 Equitable Prod.	105494	Pike	none	yes	6
Ashland #KY-4 Kelly-Watt-Bailey-Skaggs Unit	33985	Johnson	none	yes	1
Hay Ex. #H-50 Cassidy	110610	Lawrence	N/A (cuttings)	yes	4
various Berea outcrops	N/A	Lewis	N/A	N/A	10

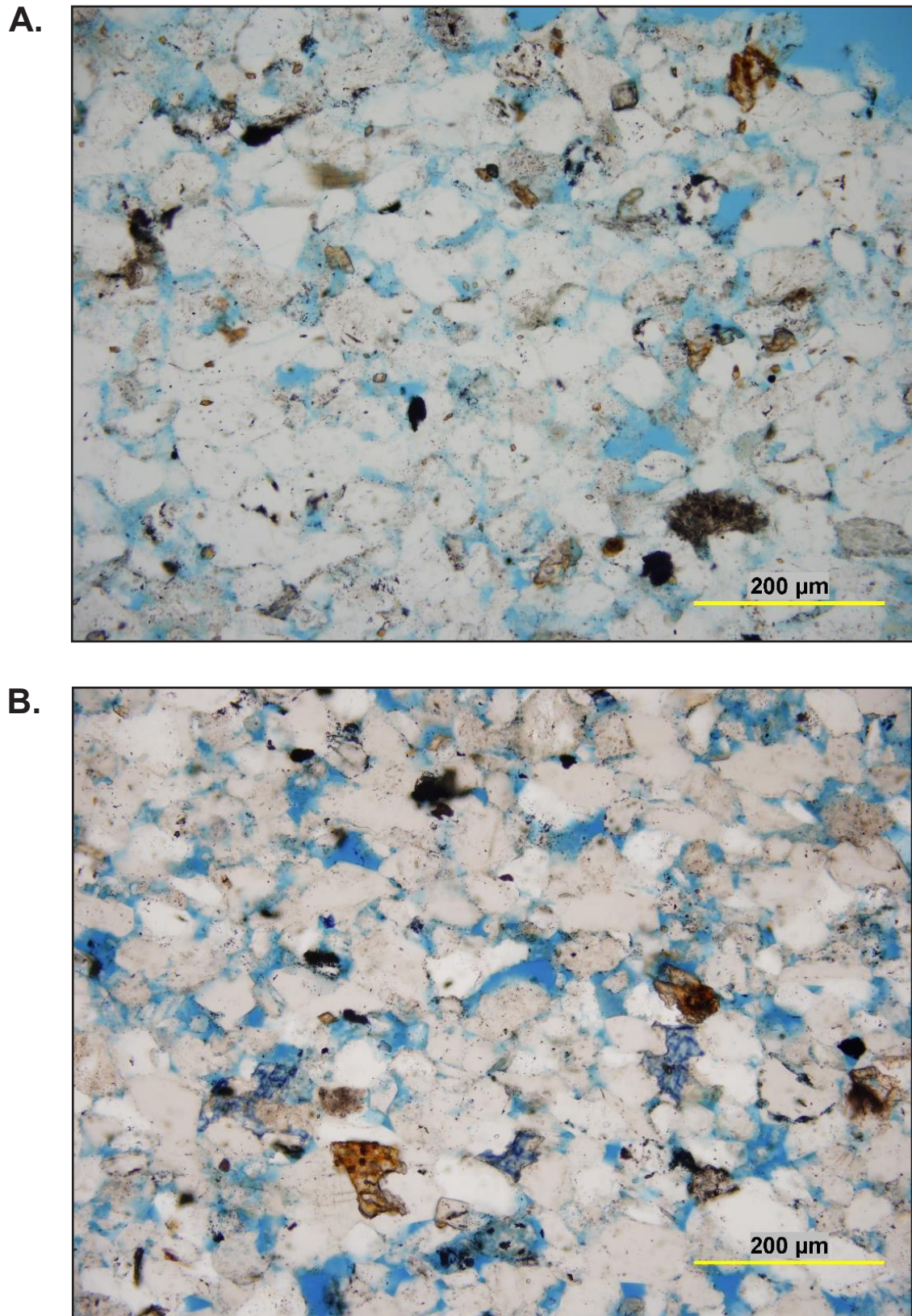


Figure 7-35. Berea Sandstone dominated by intergranular porosity. A. Ashland #1 Neal, Lawrence County, 1,502 ft, porosity=7.3 percent, permeability=0.0319 md. B. Ky.-W.Va. Gas #1122 Moore, M., Lawrence County, 1,269 ft, porosity=11.1 percent, permeability=0.1707 md.

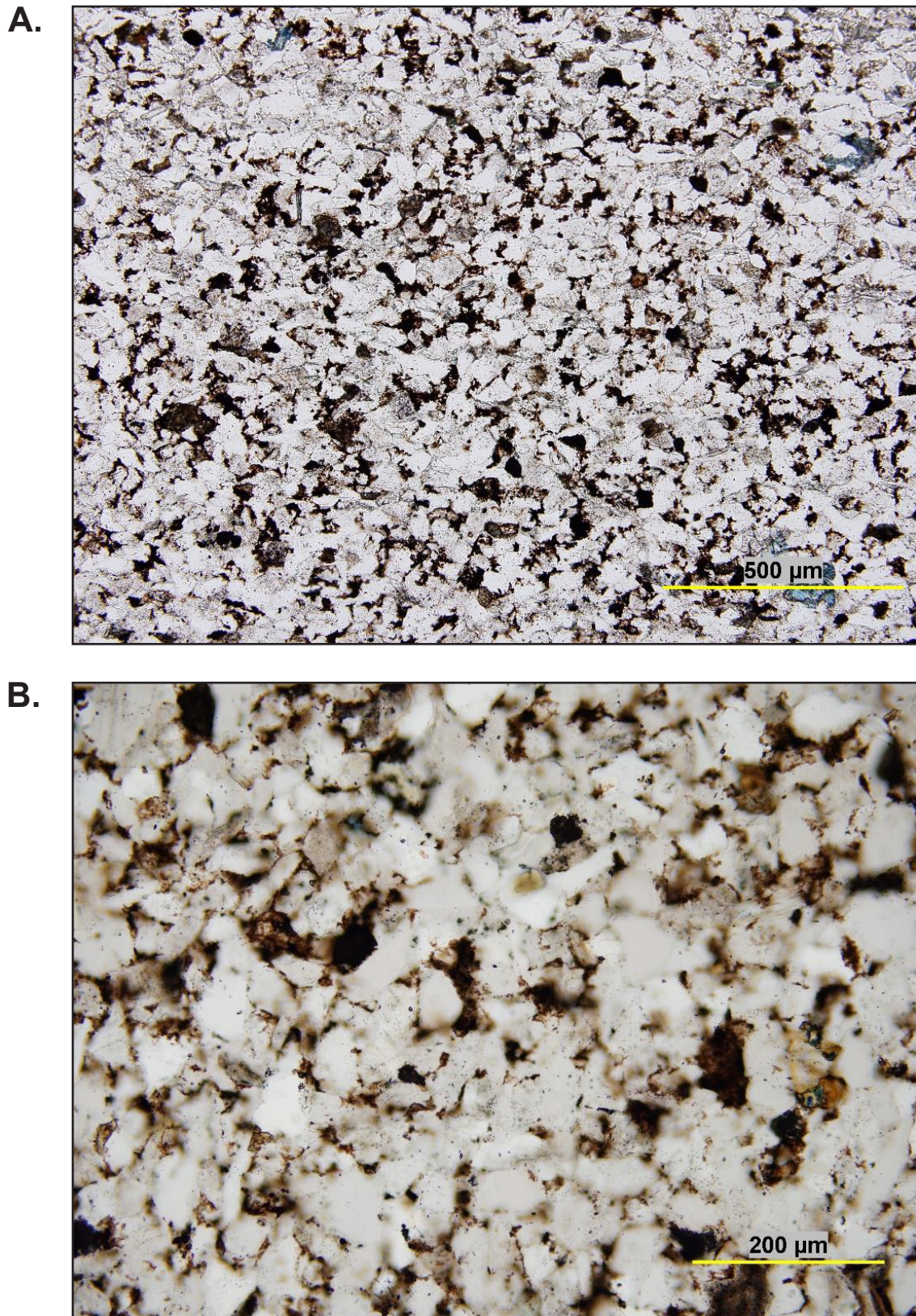


Figure 7-36. Intergranular porosity filled with bitumen (black opaque areas). This oil-filled porosity was only observed in the Pike County core. Intergranular pores have been reduced by quartz overgrowths. A. EQT Prod. #504353 Equitable Prod., 3,909.9 ft, Pike County. B. EQT Prod. #504353 Equitable Prod., 3,859.3 ft, Pike County.

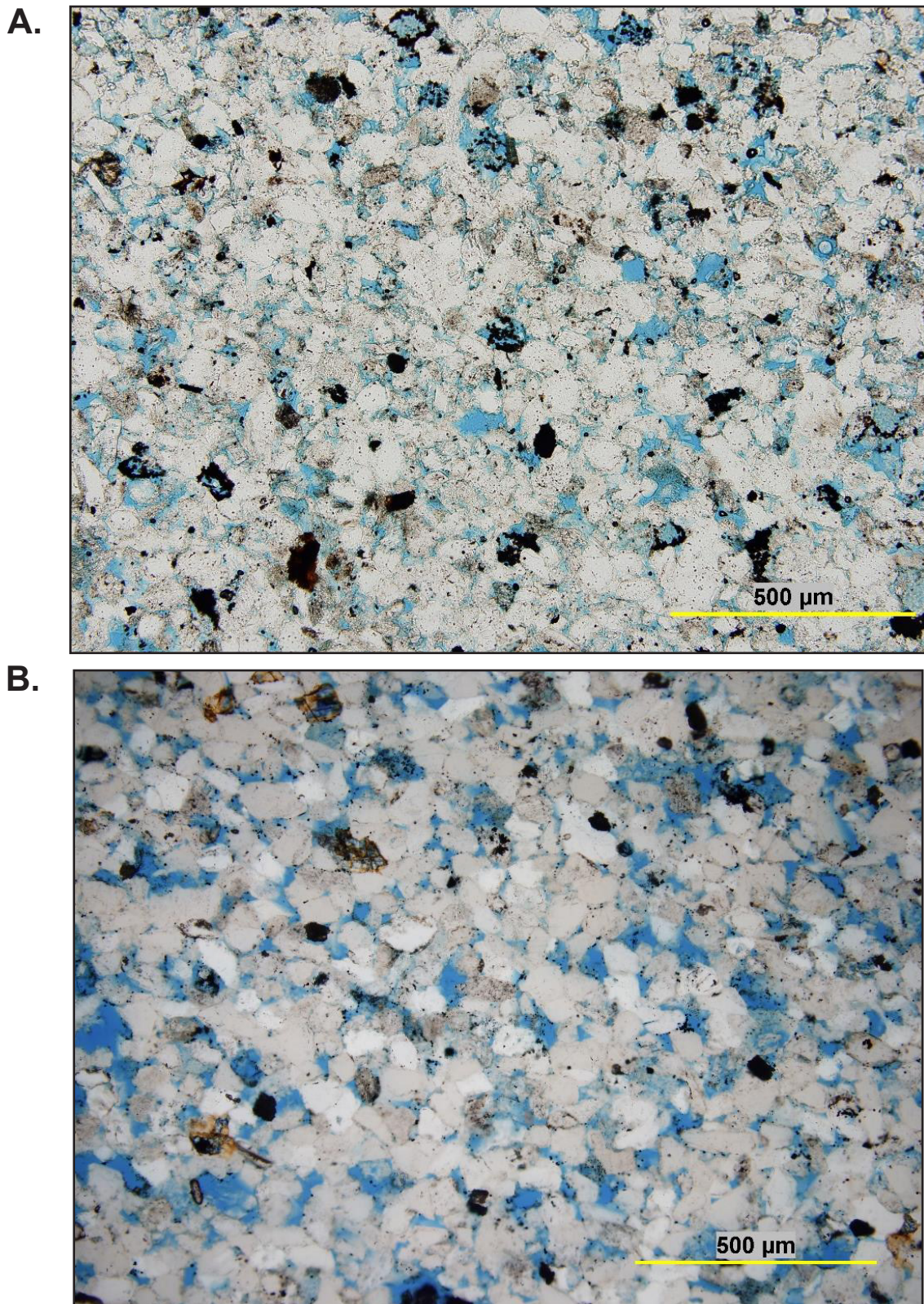


Figure 7-37. Berea sandstone with well-developed secondary (moldic) porosity. Larger, oversized pores are dissolved framework grains, connected by intergranular pores. A. Ky.-W.Va. Gas #1122 Moore, M., 1,231.5 ft, Lawrence County, porosity=13.3 percent, permeability=0.5680 md. B. Ky.-W.Va. Gas #1122 Moore, M., 1,229 ft, Lawrence County, porosity/permeability not measured.

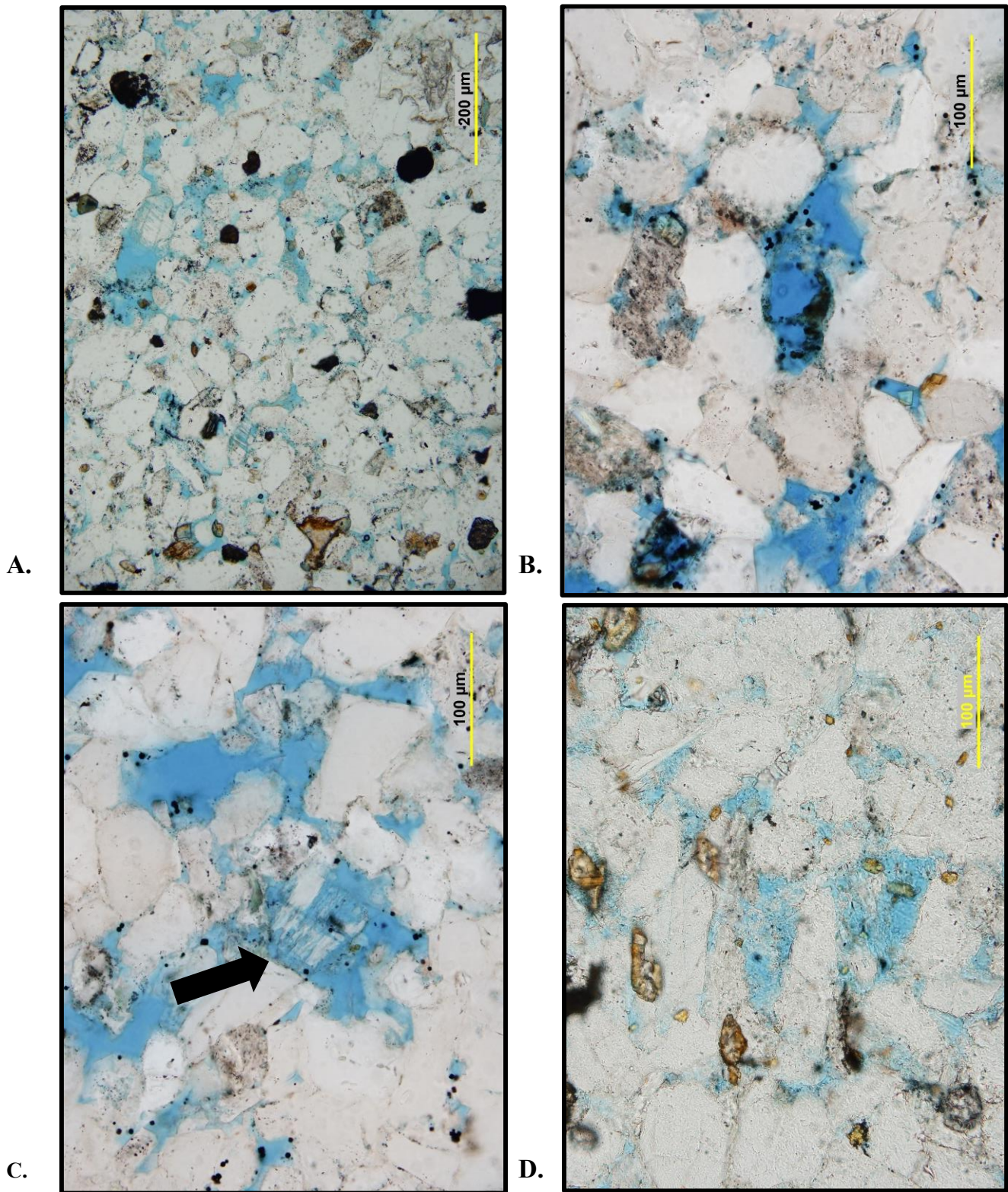


Figure 7-38. Secondary porosity types in Berea sandstones. A, C, and D are partly leached feldspars and B is a partly dissolved glauconite grain. A. Columbia #20505 Simpson, 1,680 ft, Lawrence County, porosity=11.0 percent, permeability=0.4358 md. B. Ky.-W.Va. Gas #1122 Moore, M., 1,229 ft, Lawrence County, no porosity/permeability data. C. Ky.-W.Va. Gas #1122 Moore, M., 1,229 ft, Lawrence County, no porosity/permeability data. D. Ashland #1 Neal, 1,502 ft, Lawrence County, porosity=7.3 percent, permeability=0.0319 md.

Microporosity – Very small pores are common in the Berea, and are classified as microporosity. These pores are impregnated with blue epoxy and connected to larger intergranular or moldic pores, and do form an effective, but lower-permeability, part of the reservoir. Many larger intergranular or moldic pores contain fine-grained material that reduces the permeability of the reservoir.

Microporosity occurs in several ways. Most commonly it occurs in partially dissolved framework grains, such as feldspars or glauconite (Figs. 7-38C, D, 7-39B). Clays in the Berea also have associated microporosity, commonly authigenic clay cements such as kaolinite (Fig. 7-39A). Some low-porosity rocks have been almost completely cemented by quartz or dolomite, and show microporosity along remnant grain or cement contacts (Fig. 7-39C). Many Berea sandstones have fine-grained material in pores, which reduces permeability and increases irreducible water saturations. For example, Figure 7-39D shows a core sample with 10.2 percent porosity, but only 0.0679 md permeability.

Pore-Type Distribution. Relative abundance of the pore types was not quantified in this preliminary study. No obvious differences were observed between the four cores from Lawrence and Johnson Counties. Pore types in the one cored well from Pike County are different than the pores in the cores from Lawrence and Johnson Counties. The EQT #504353 Equitable Production samples have significant dead oil (bitumen) plugging intergranular pores. This dark oil staining was not observed in any of the cores from farther north at shallower depths. The Pike County samples also lack the well-developed secondary porosity seen in the shallower cores. This may reflect the deeper burial history, or a different original grain mineralogy that was less susceptible to dissolution. More information about pore-type size distribution is included in the MICP analyses at the end of this chapter.

Berea Diagenetic History. In addition to characterizing the pore types in Berea siltstones and sandstones, a preliminary attempt to document diagenetic events that have affected these rocks was made. Additional work is necessary to fully establish the Berea diagenetic story, but initial observa-

tions may help us understand porosity preservation and development.

Cements present in the thin sections include quartz overgrowths, ferroan dolomite, siderite, pyrite, and kaolinite. In addition, these rocks were subject to varying degrees of intergranular compaction and secondary porosity formation (grain dissolution). These diagenetic events are briefly discussed below, and summarized in the discussion section (Chapter 8).

Quartz Overgrowths – Quartz overgrowths are present in variable amounts throughout the Berea. The very fine grain size and limited development of quartz cements makes recognition of overgrowths difficult in some samples. Quartz never completely occludes all pore space, but partly fills larger intergranular pores (Fig. 7-40A, B). It is primarily developed on monocrystalline quartz grains, and to a lesser degree on polycrystalline quartz.

The relative timing of quartz cement can be constrained by petrographic relationships. Quartz predates ferroan dolomite cement, which fills intergranular pores (Fig. 7-40D). It also predates pyrite precipitation and siderite cement (discussed below). It also appears to predate secondary porosity development. Grain molds do not contain quartz cements, and quartz cement conforms to the former margin of dissolved grains (Figs. 7-38B, 7-40C).

Ferroan Dolomite – Dolomite cement and replacement is common in the Lawrence and Johnson County cores. Dolomite stains blue with potassium ferricyanide, indicating it is iron-rich or ferroan. Dolomite commonly occurs as small patches of cement filling intergranular pores, and possibly replacing matrix or grains. In rare cases, dolomite completely fills all intergranular pore space, creating nonreservoir intervals (Figs. 7-41A, B). Ferroan dolomite also occurs as a fracture-fill cement (Fig. 7-41C), suggesting it is a late event in the diagenetic history. The sample in which this occurs is from the deeper core in Pike County, so dolomite was observed across the entire study area. In one sample, ferroan dolomite occurs as laminations interbedded with siltstone (Fig. 7-41D). The presence of pure dolomite laminations suggests that dolomite replaced a precursor carbonate sediment, probably carbonate mud.

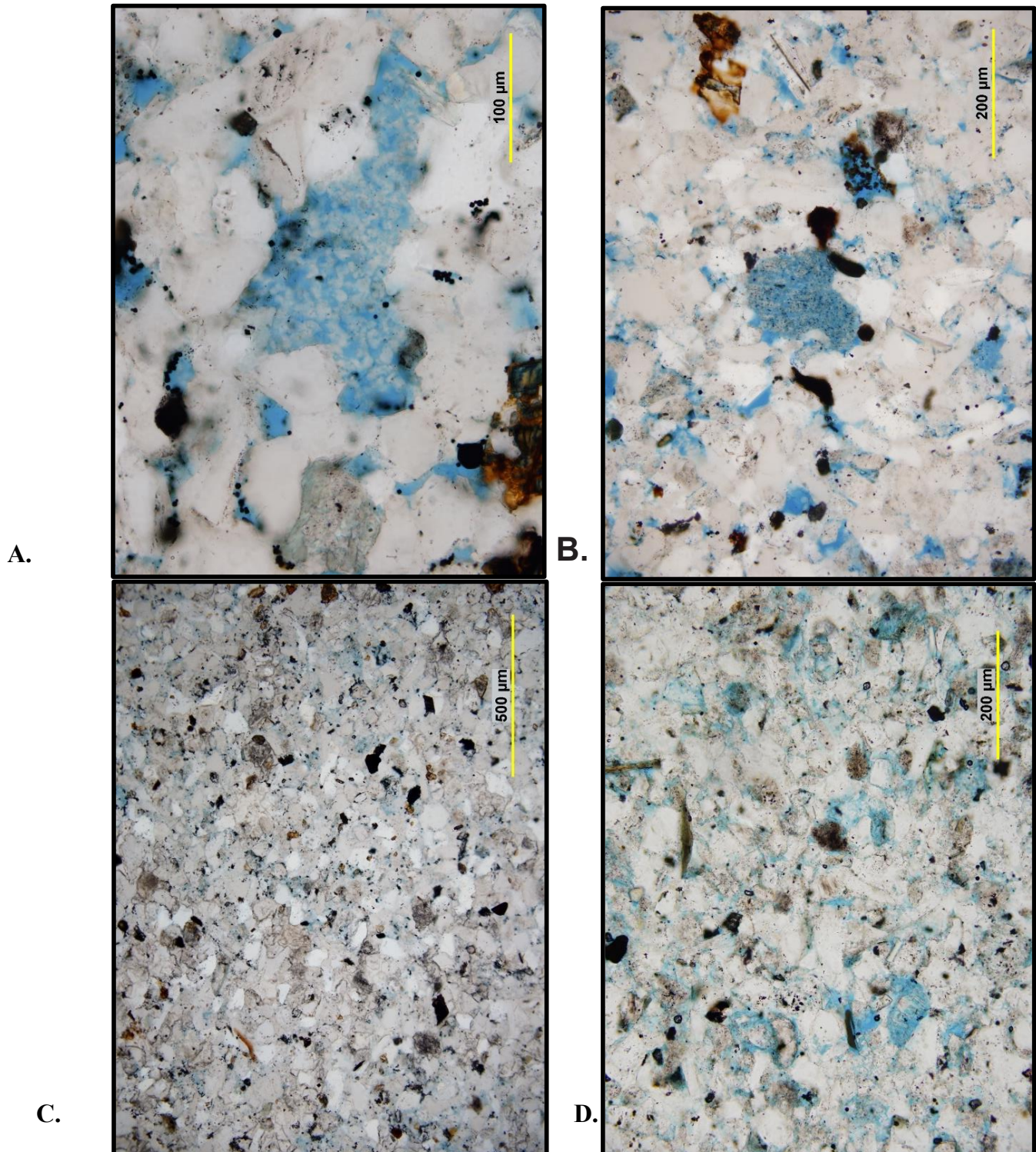


Figure 7-39. Microporosity in Berea sandstones. A. Ky.-W.Va. Gas #1122 Moore, M., 1,229 ft, Lawrence County, porosity/permeability not available. Microporous kaolinite (clay) cement filling secondary pore. B. Ky.-W.Va. Gas #1122 Moore, M., 1,241 ft, Lawrence County, porosity/permeability not available. Microporous glauconite(?) grain. C. Ashland #1 Neal, 1,505 ft, Lawrence County, porosity=4.3 percent, permeability=0.0003 md. Intergranular microporosity (faint blue epoxy), with abundant dolomite and quartz cement. D. Columbia #20505 Simpson, 1,663 ft, Lawrence County, porosity=10.2 percent, permeability=0.0679 md.

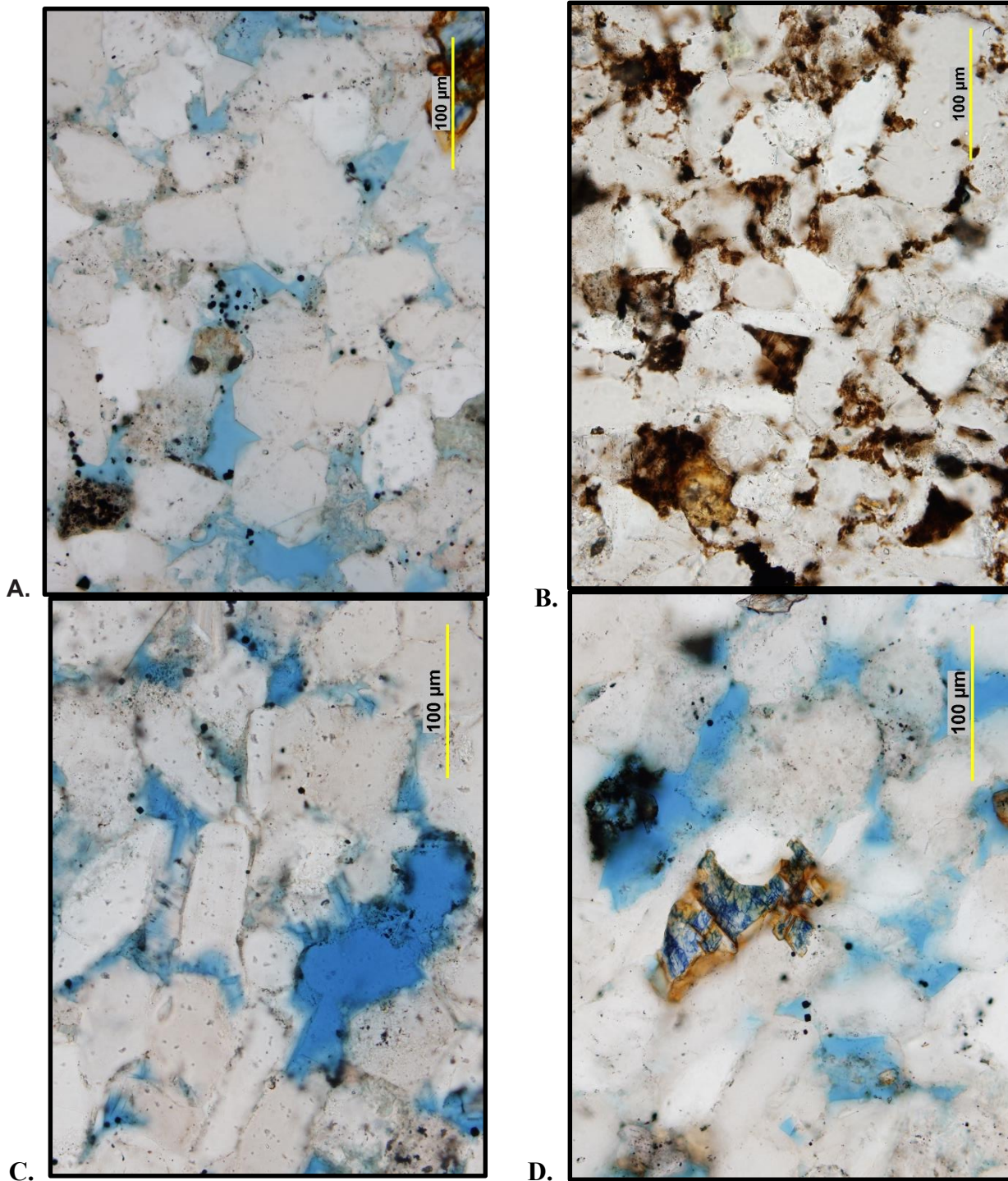


Figure 7-40. Quartz overgrowth cements in Berea sandstone. A. Ky.-W.Va. Gas #1122 Moore, M., 1,229 ft, Lawrence County, porosity/permeability not available. Euhedral quartz overgrowths developed on quartz grains. B. EQT Prod. #504353 Equitable Prod., 3,859.3 ft, Pike County, porosity/permeability not available. Quartz is primary cement in oil-stained pores. C. Ky.-W.Va. Gas #1122 Moore, M., 1,229 ft, Lawrence County, porosity/permeability not available. Quartz overgrowths between grains do not fill moldic pore and predate grain dissolution. D. Ky.-W.Va. Gas #1122 Moore, M., 1,229 ft, Lawrence County, porosity/permeability not available. Euhedral quartz overgrowth is overlain by later pore-filling ferroan dolomite cement (stained blue).

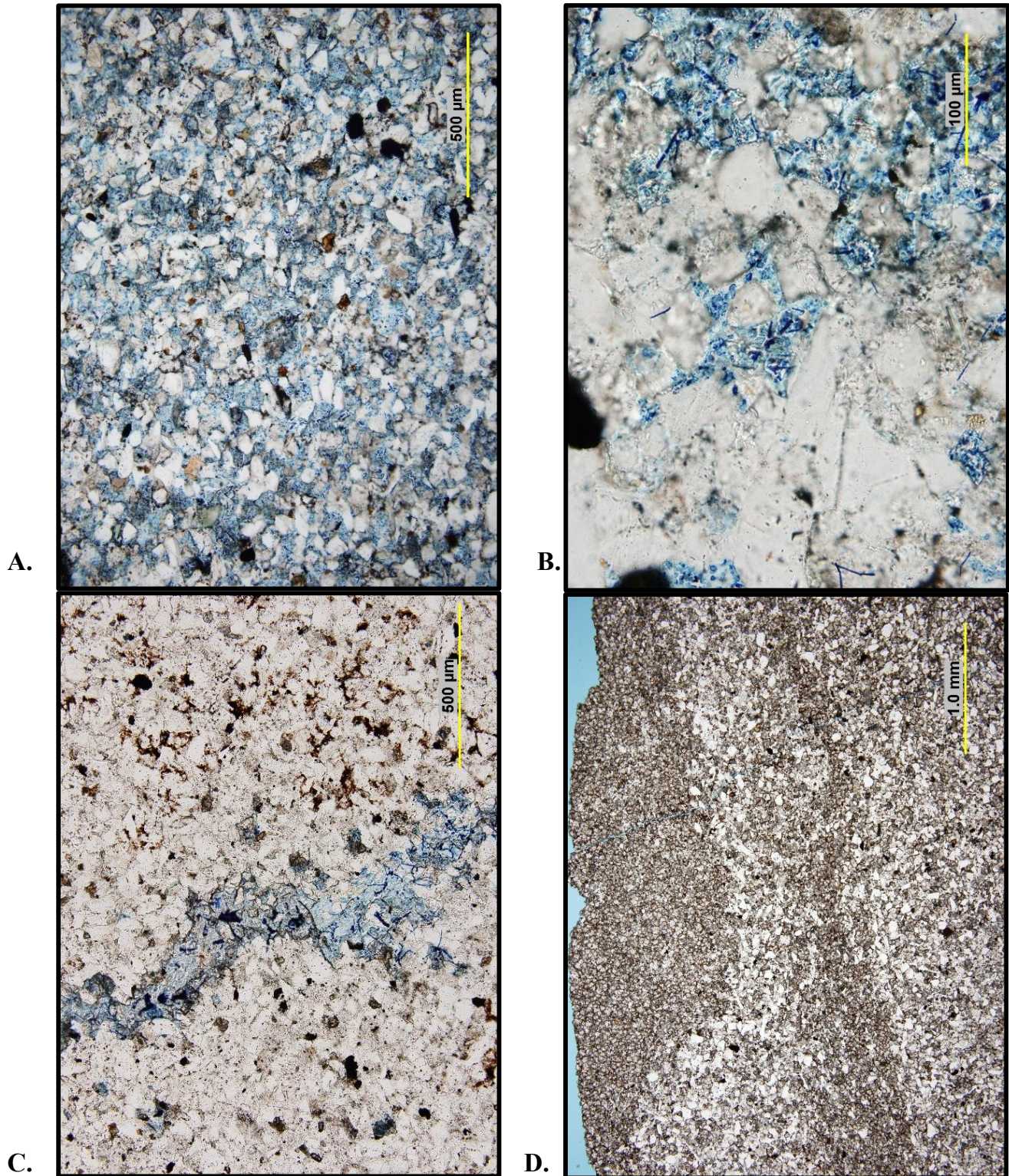


Figure 7-41. Ferroan dolomite occurrence in Berea siltstones/sandstones. A. Ashland #1 Neal, 1,505 ft, Lawrence County. Sample lacks porosity due to ferroan dolomite (blue stain). Note loose quartz-grain packing—due to late timing of dolomite, it possibly replaced a carbonate matrix. B. Ashland #1 Neal, 1,505 ft, Lawrence County. Close-up view of stained ferroan dolomite. C. EQT Prod. #504353 Equitable Prod., 3,896 ft, Pike County. Fracture healed by ferroan dolomite, indicating it is a late event, post-lithification. D. Ashland #1 Neal, 1,505 ft, Lawrence County. Siltstone/dolomite laminations. Pure dolomite laminations (finer layers) suggest dolomite replaced a precursor carbonate matrix.

The timing of ferroan dolomite replacement and cementation is important in interpreting porosity evolution in the Berea. Early carbonate cements can sometimes help to preserve intergranular pores from compaction, and then undergo dissolution to form secondary porosity later in the burial history. Several features observed in these rocks suggest that ferroan dolomite is not an early event. No evidence of partially dissolved or corroded rhombs was seen, indicating dolomite has not been dissolved. The iron content of the dolomite indicates it was formed under reducing conditions, since iron must be in the reduced Fe^{2+} state to substitute for Mg in the dolomite lattice. In addition, dolomite precipitates much more readily at higher temperatures. Both of these conditions are more consistent with deeper burial environments than early shallow conditions. In addition, ferroan dolomite occurs as a fracture-fill cement, indicating it postdates lithification of the sediments.

Pyrite – Pyrite (FeS_2) is very common in the Berea. It occurs as both a pore-filling cement and a replacement of framework grains and matrix. Its distribution is commonly confined to specific laminations, burrows, or other sedimentary structures, suggesting a permeability control (Fig. 7-42A). Pyrite has a patchy distribution in some samples, and larger framboids have replaced entire areas of siltstone (grains, matrix, cements) (Fig. 7-42B).

In a few samples, pyrite occurs as a cement in intergranular pores (Fig. 7-42C). In these instances, pyrite cubes precipitated on top of quartz overgrowths, indicating they postdate quartz cementation. Pyrite could have formed at multiple times in the Berea, but petrographic features suggest that most formed late in the diagenetic sequence.

Siderite – Siderite (FeCO_3) is also very common. It consists of brown, flattened, rhomb-shaped crystals in pores (Fig. 7-43A, B). Siderite does not completely fill pores. Based on X-ray diffraction data, the highest concentration of siderite reaches 3.5 percent in the Columbia Gas #20505 Simpson well in Lawrence County (at 1,720 ft).

Siderite was observed in moldic secondary pores (Fig. 7-43C), which postdates dissolution. Siderite can also be seen replacing ferroan dolomite in some wells (Fig. 7-43D). The brown edges and zones along cleavage planes in the blue-stained dolomite are interpreted to be siderite replacement of

ferroan dolomite. This relationship indicates siderite postdated ferroan dolomite cements.

Siderite has a negative, but minor, effect on reservoir quality since it is a cement, but does not reach a significant percentage of the rock.

Kaolinite – Kaolinite clay cement is also very common in the thin sections examined. Kaolinite (and possibly dickite; $\text{Al}_2\text{Si}_2\text{O}_5(\text{OH})_4$) occurs in pores, particularly late secondary pores (Fig. 7-44A). It was identified by its distinctive crystal habit, which is as stacked vermicular pseudo-hexagonal plates (Fig. 7-44B). Kaolinite also occurs in fractures, as a final cement phase (Fig. 7-44B, C).

Kaolinite is commonly microporous and has a detrimental effect on reservoir permeability where it bridges and fills entire pores. Kaolinite has been interpreted as a byproduct of feldspar dissolution, and this association in the Berea is possible because feldspar dissolution is seen in many samples.

Mercury Injection Capillary Pressure Analysis

Six Berea samples were selected for mercury injection capillary pressure (MICP) analysis in order to better characterize permeability and improve our understanding of fluid production in these tight sandstones (coarse siltstones). The samples covered a range of porosity and permeabilities. Analysis was done by Weatherford Laboratories in Houston, and data were received in April 2016. Methods are summarized in Chapter 3, and original data files are located in Appendix 1. Initial analysis of the data was conducted by Rick Bowserox at KGS. This work is ongoing, but his initial work is included herein in order of increasing sample permeability.

Figures 7-45 through 7-50 show photomicrographs and corresponding graphs of pore-throat-diameter distribution based on MICP analysis for the sample in the thin section. Figure 7-45 is a low-porosity (1.9 percent), low-permeability (0.0004 md) Berea siltstone from Lawrence County. The sample is from an argillaceous siltstone with no visible porosity. Intergranular pores are filled with detrital clay matrix. The large pyrite framboid on the left side of the thin section (Fig. 7-45) has replaced grains and clay matrix. Pore-throat diameters based on MICP analysis are between 0.06 and greater than $0.01\ \mu$, with most pore volume (less

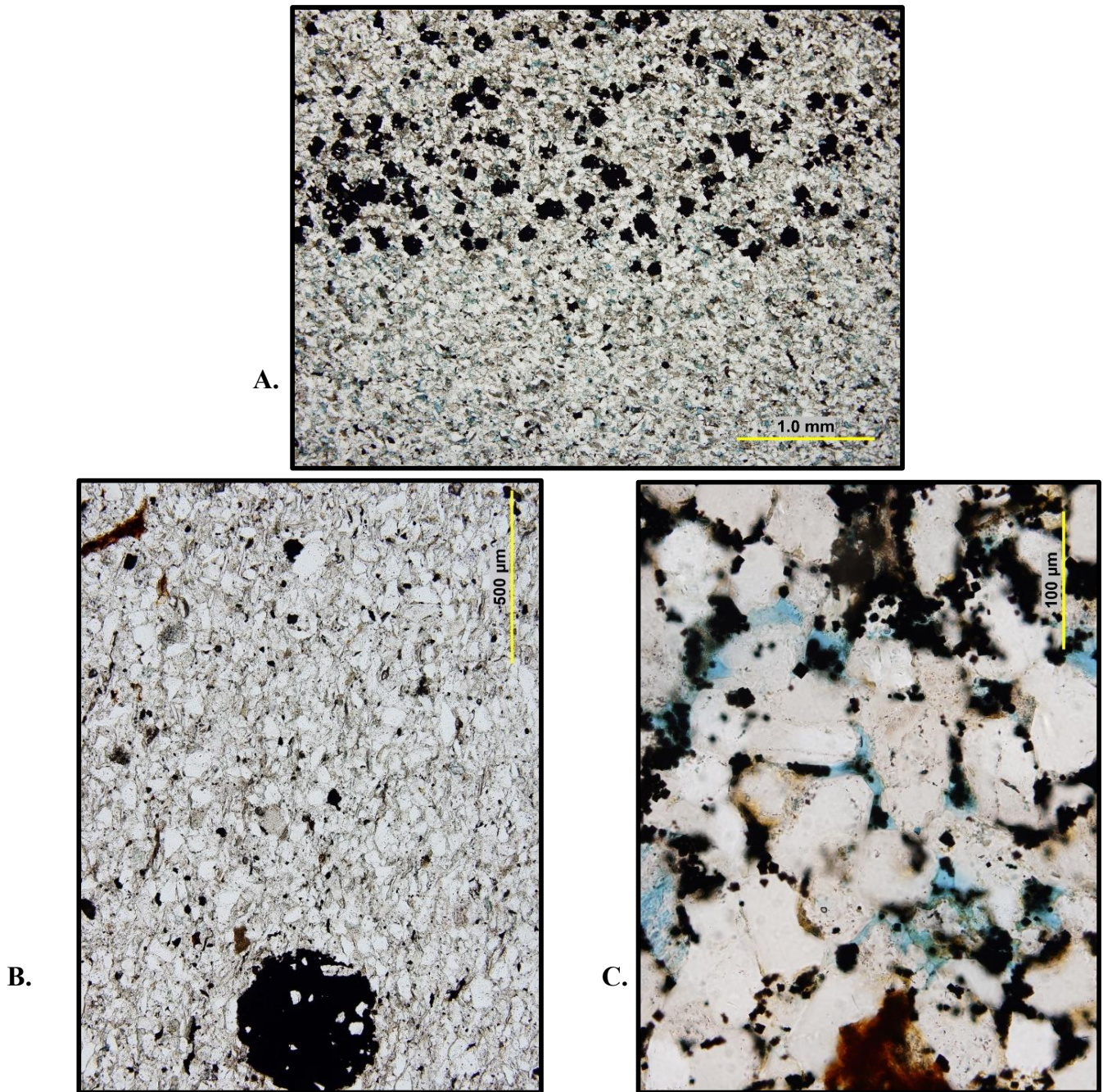


Figure 7-42. Pyrite fabrics in Berea siltstones/sandstones. A. Columbia #20505 Simpson, 1,663 ft, Lawrence County. Pyrite framboids replaced specific lamination in siltstone. B. Columbia #20505 Simpson, 1,672 ft, Lawrence County. Larger (500 μ) pyrite framboid replaced grains and matrix. C. Ky.-W.Va. Gas #1122 Moore, M., 1,229 ft, Lawrence County. Pyrite cement (opaque crystals) occur on top of quartz overgrowths and post-date quartz cementation.

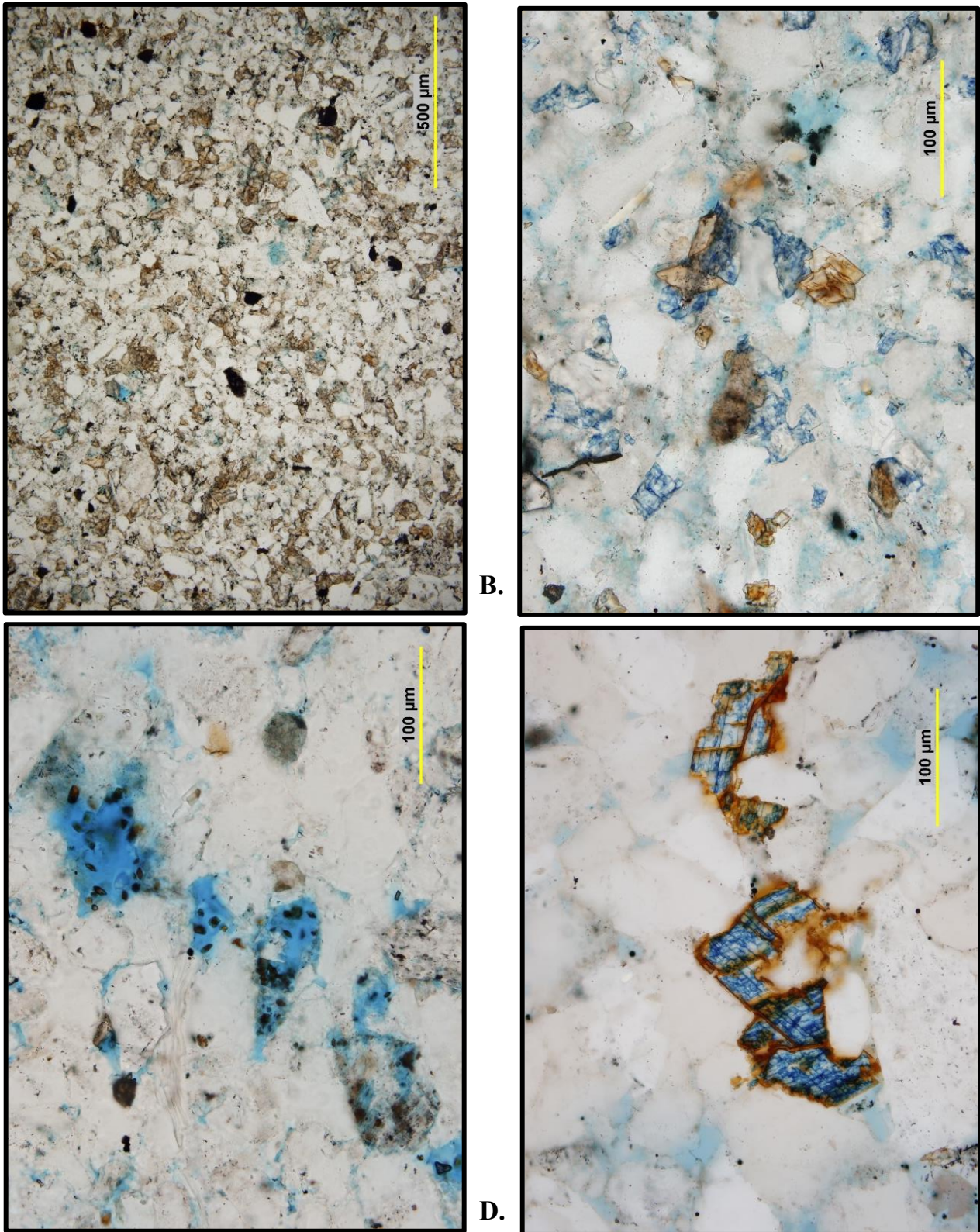


Figure 7-43. Siderite cement and replacement fabrics. A. Ky.-W.Va. Gas #1122 Moore, M., 1,286 ft. Siderite crystals (brown) in siltstone. Siderite is 3.8 percent by XRD. B. Ashland #KY-4 Kelly-Watt-Bailey-Skaggs Unit, 968 ft. Siderite (brown flattened rhombs with ferroan dolomite (stained blue)). C. Ky.-W.Va. Gas #1122 Moore, M., 1,241 ft. Siderite cement crystals in moldic pores. D. Ky.-W.Va. Gas #1122 Moore, M., 1,229 ft. Siderite (brown) replacing ferroan dolomite cement in intergranular pore.

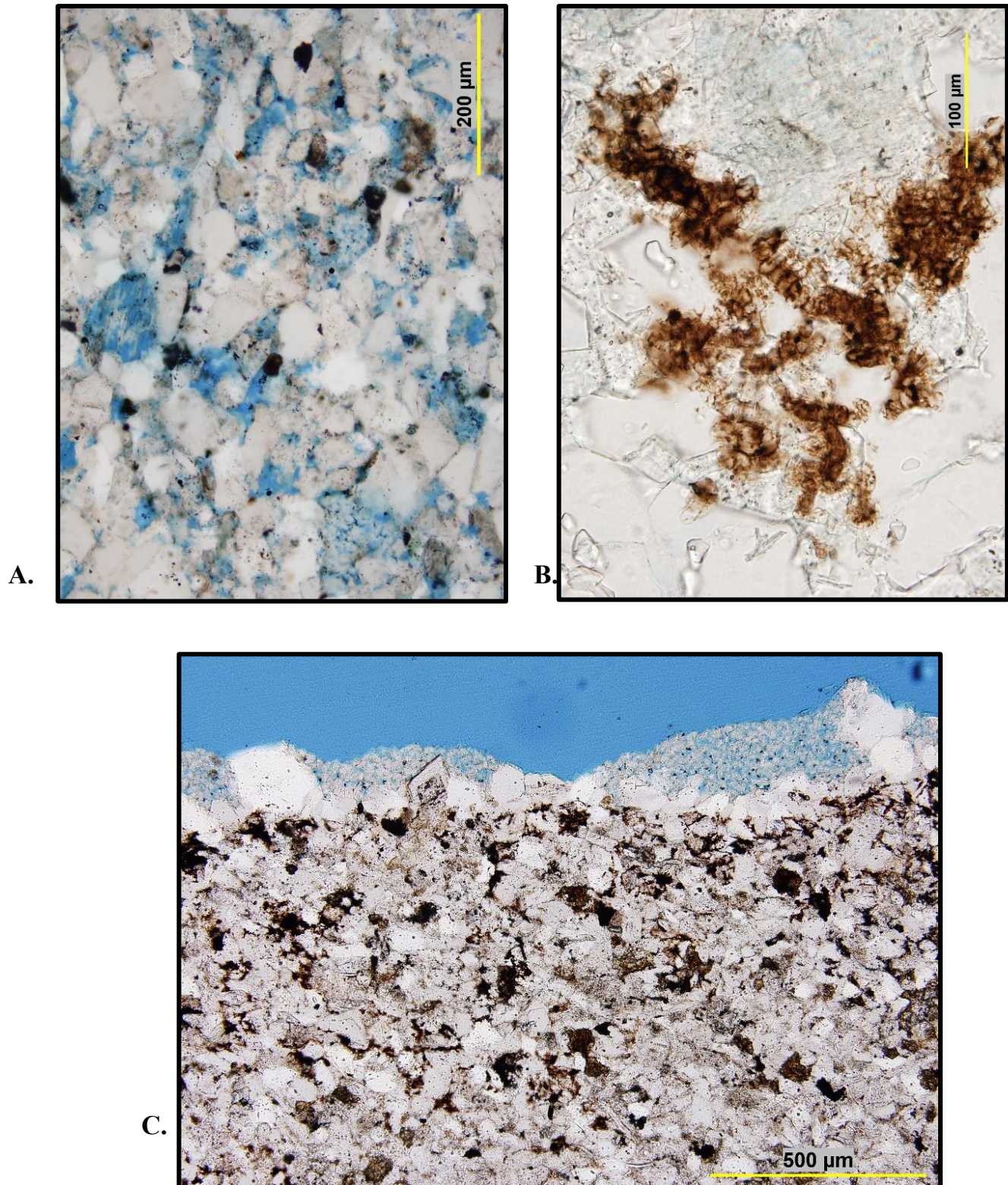


Figure 7-44. Kaolinite (clay) occurrence in Berea siltstones/sandstones. A. Ashland #1 Neal, 1,498 ft, Lawrence County. Microporous kaolinite is a common cement in secondary porosity. B. EQT Prod. #504353 Equitable Prod., 3,896 ft, Pike County. Oil-stained kaolinite cement is the final cement phase in a fracture, indicating it is a late event. C. EQT Prod. #504353 Equitable Prod., 3,912.5 ft, Pike County. Fracture margin with multiple generations of cement: quartz (white), a single dolomite rhomb, and microporous kaolinite cement (impregnated with blue epoxy).

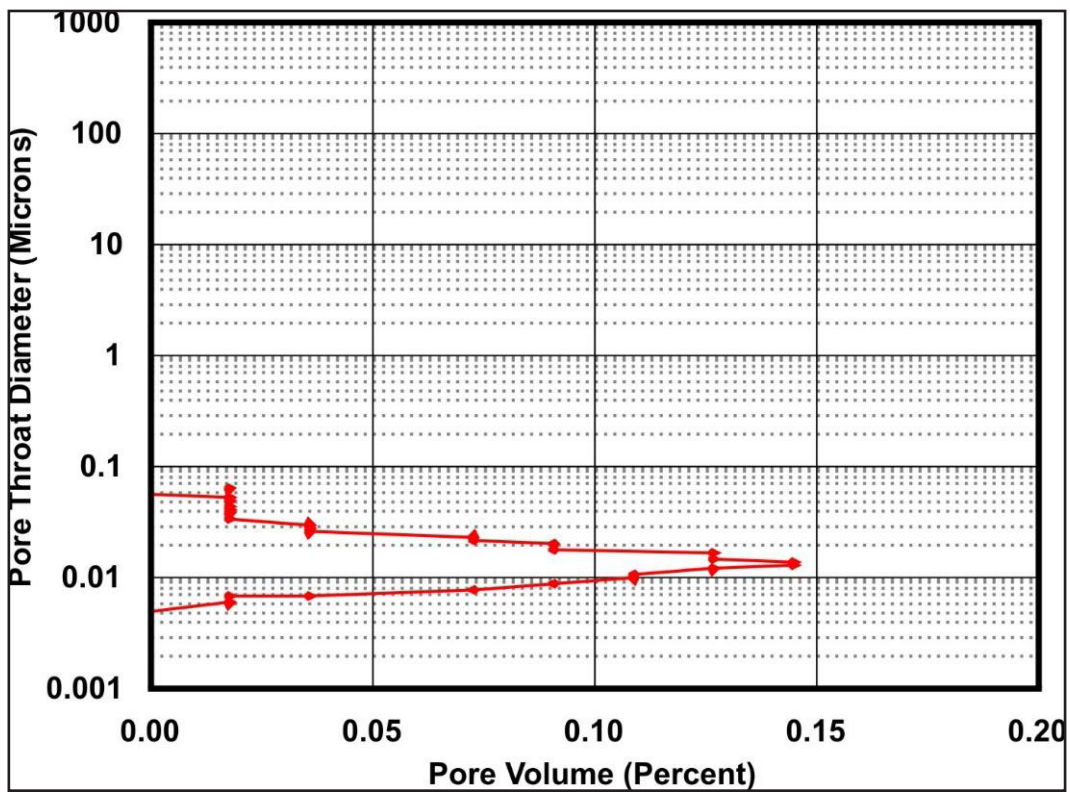
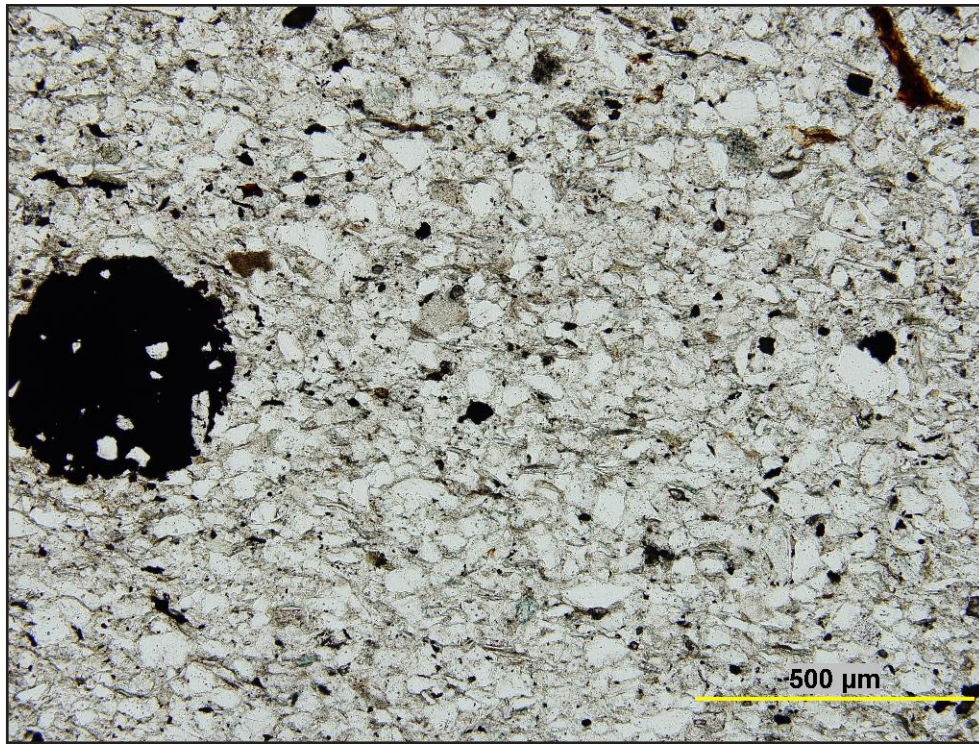


Figure 7-45. Mercury injection capillary pressure plot and photomicrographs for sample MS1672, Columbia Nat. Resc. #20505 Margaret Simpson core, Lawrence County, Ky., 1,672 ft. Porosity = 1.9 percent, permeability = 0.00004 md.

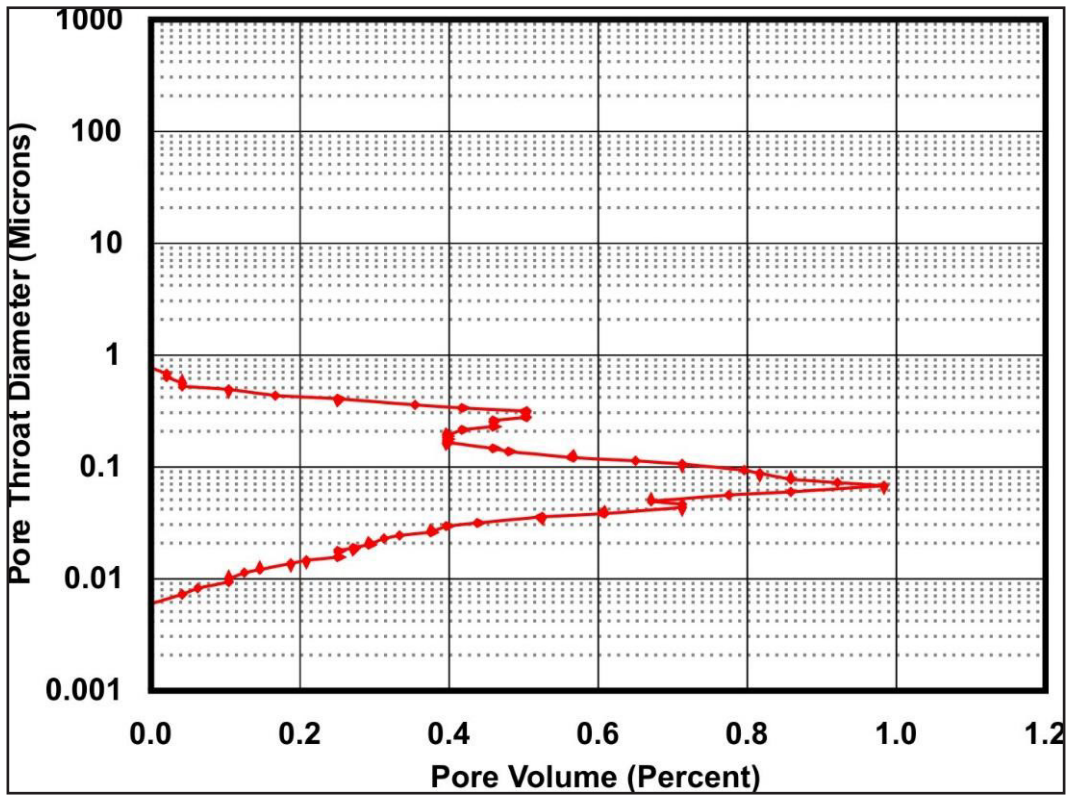
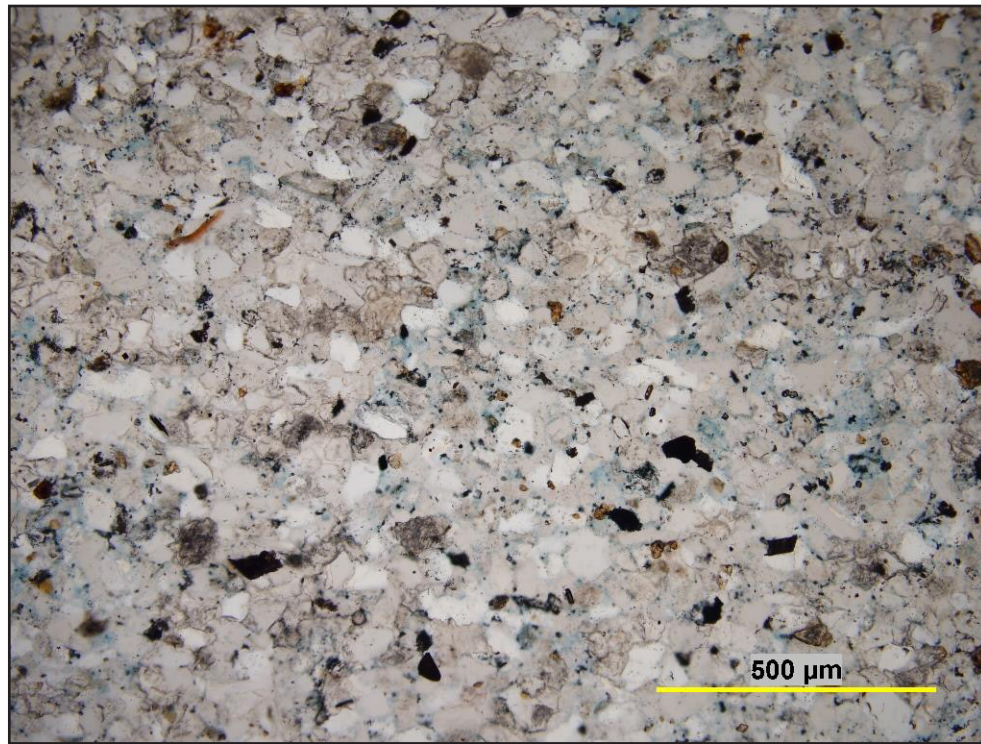


Figure 7-46. Mercury injection capillary pressure plot and photomicrographs for sample HN1505, Ashland No.1 Hattie Neal core, Lawrence County, Ky., 1,505 ft. Porosity=2.6 percent, permeability=0.0009 md.

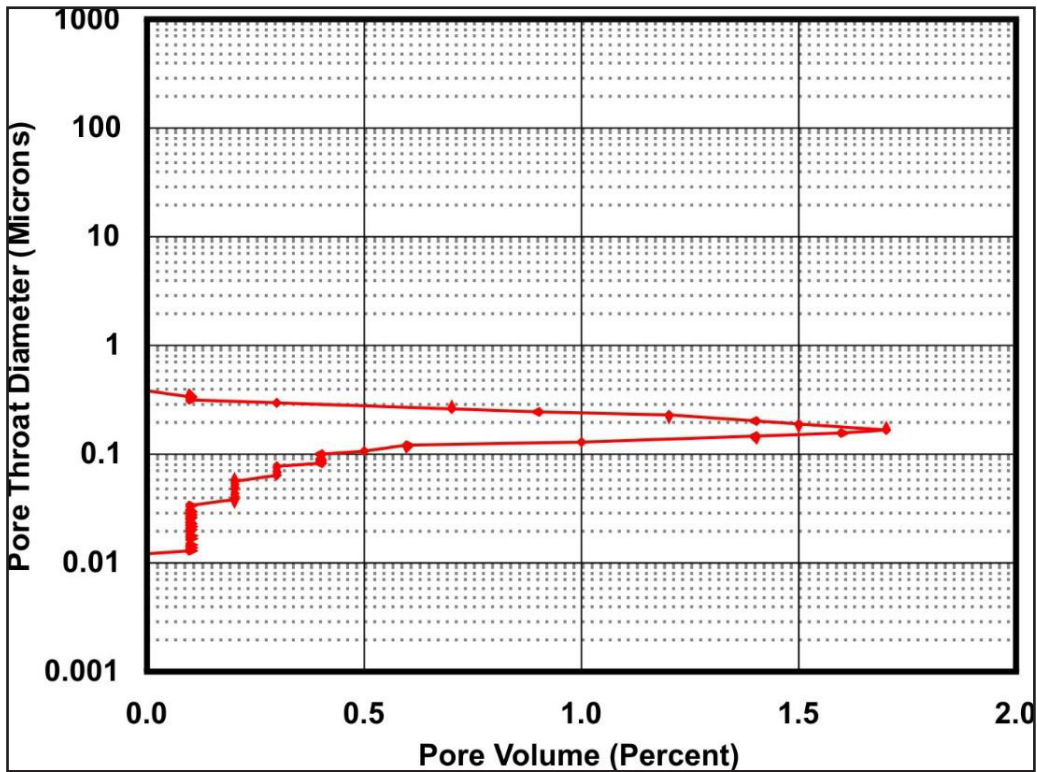
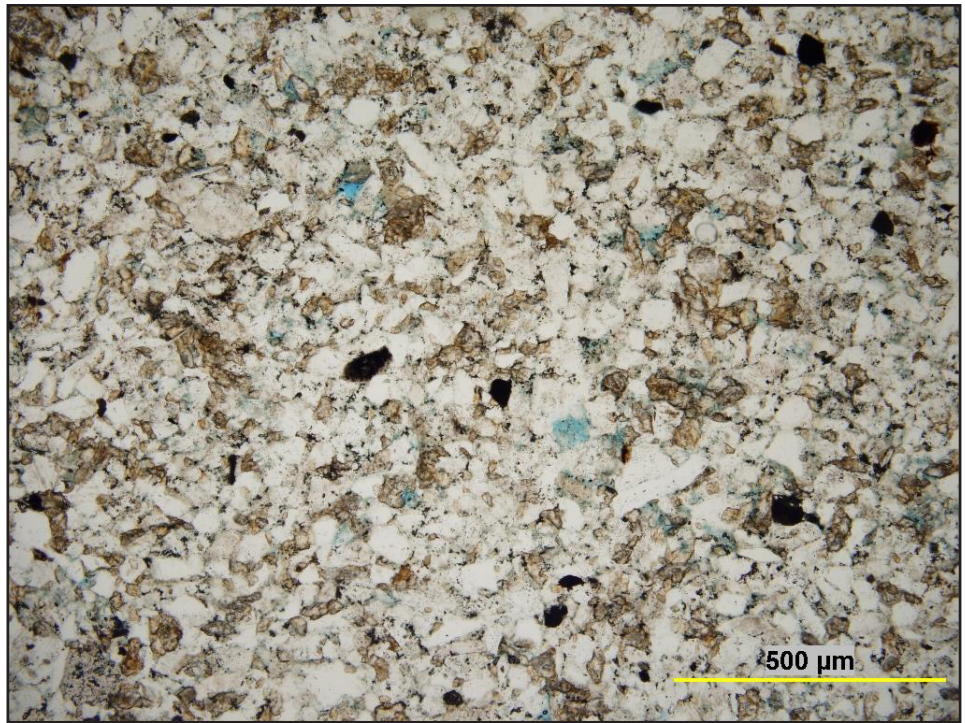


Figure 7-47. Mercury injection capillary pressure plot and photomicrographs for sample MM1286, KY-WV Gas No. 1122 Milton Moore core, Lawrence County, Ky., 1,286 ft. Porosity= 7.1 percent, permeability=0.021 md.

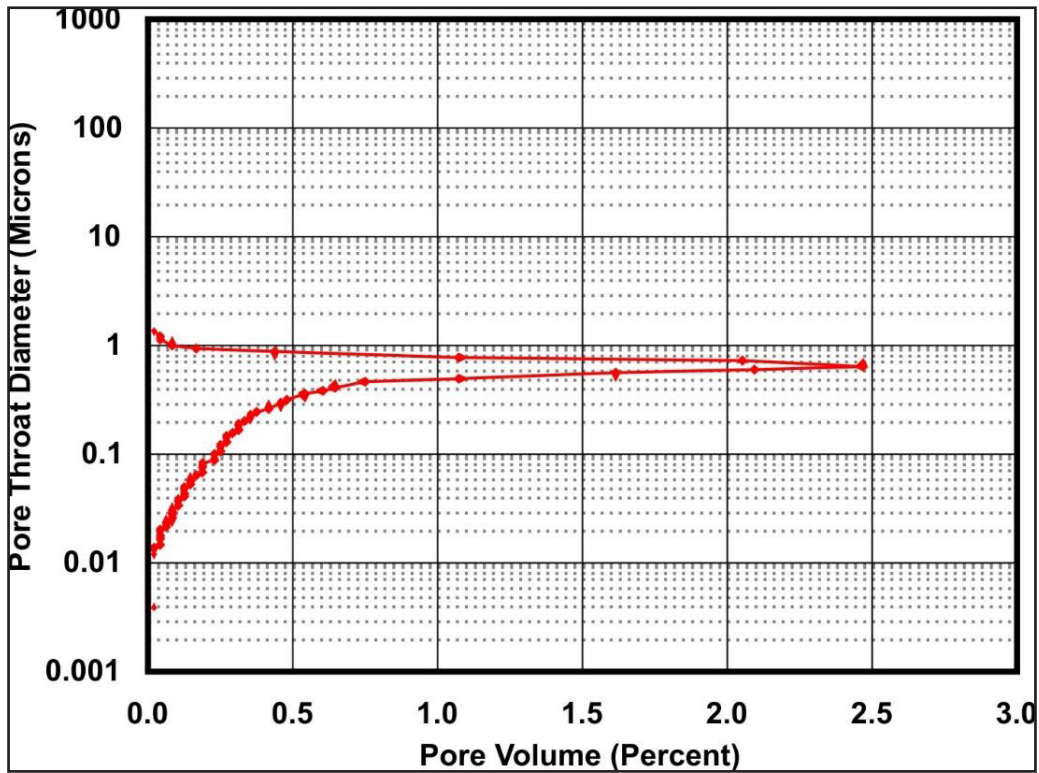
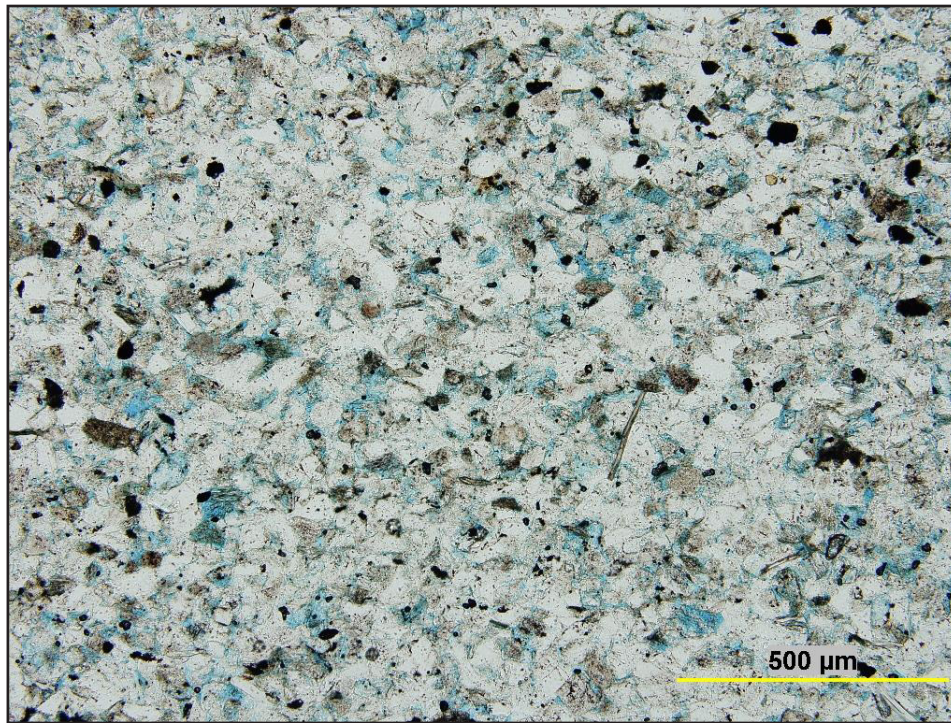


Figure 7-48. Mercury injection capillary pressure plot and photomicrographs for sample MS1663, Columbia Nat. Resc. No. 20505 Margaret Simpson core, Lawrence County, Ky., 1,663 ft. Porosity=9.4 percent, permeability=0.2206 md.

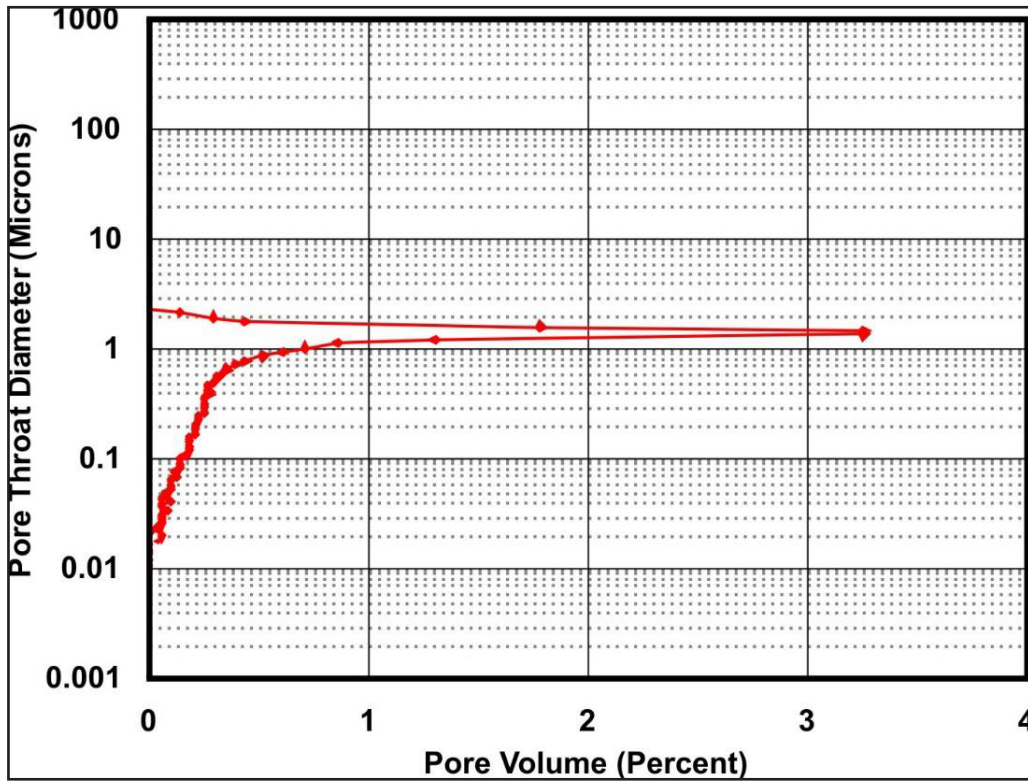
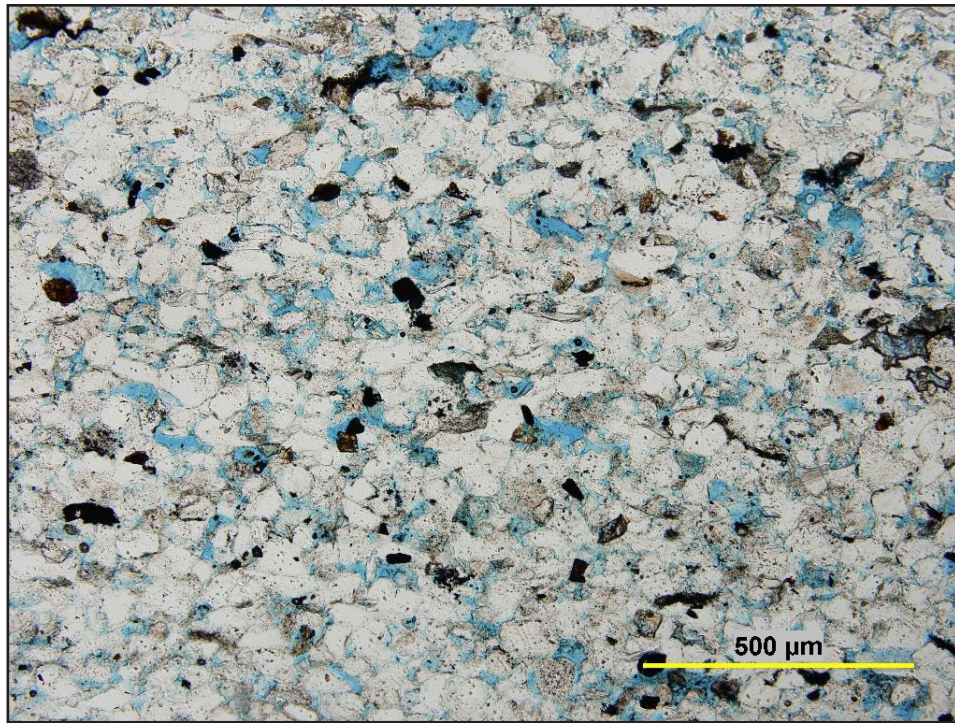


Figure 7-49. Mercury injection capillary pressure plot and photomicrographs for sample HN1516, Ashland No. 1 Hattie Neal core, Lawrence County, Ky., 1,516 ft. Porosity = 11.2 percent, permeability = 1.1874 md.

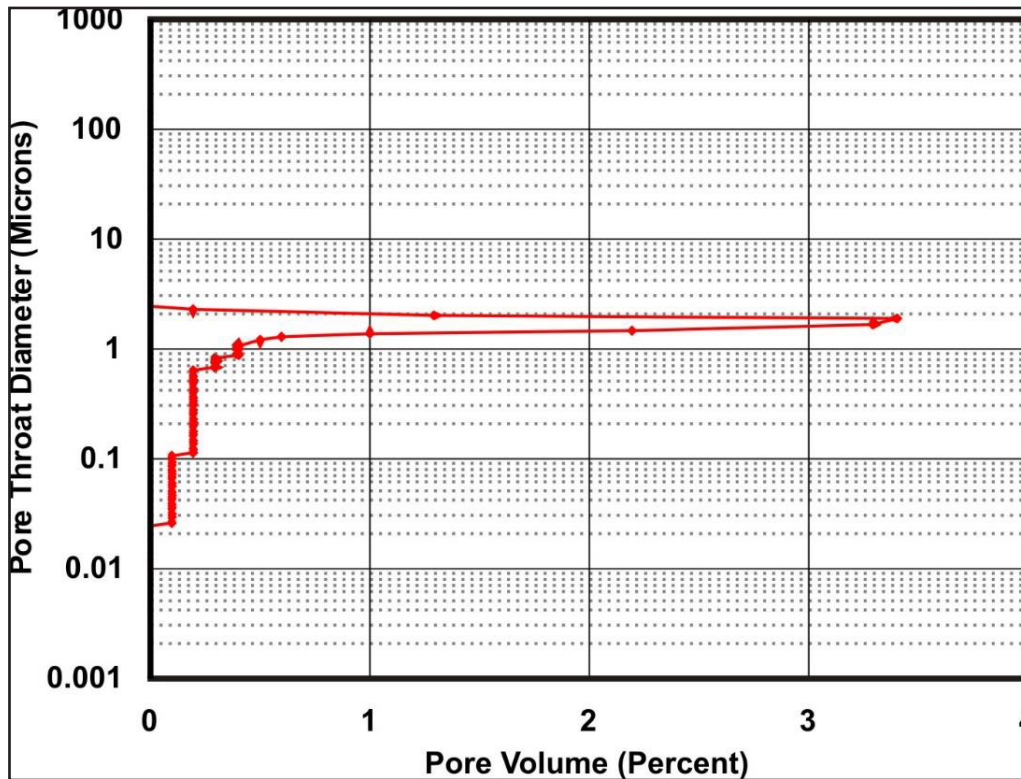
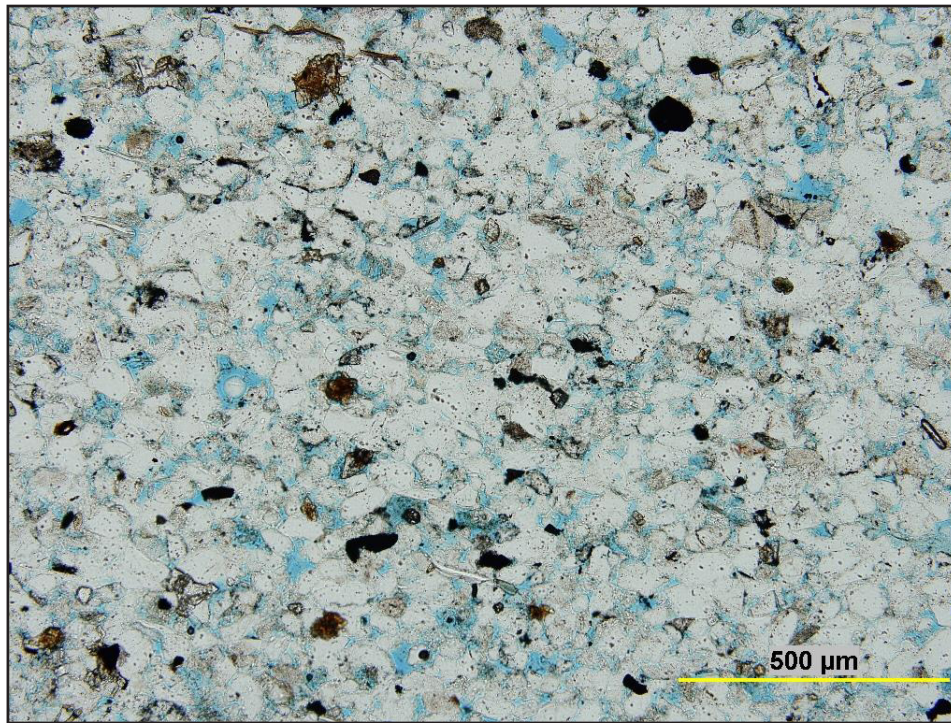


Figure 7-50. Mercury injection capillary pressure plot and photomicrographs for sample MS1683.4, Columbia Nat. Resc. No. 20505 Margaret Simpson core, Lawrence County, Ky., 1,683.4 ft. Porosity=12.3 percent, permeability=2.039md.

than 0.15 pore volume percent) distributed through pore throats less than 0.01 to 0.02 μ , suggesting gas would be the expected production from this reservoir (Sneider and Bolger, 2008). Sneider and Bolger's (2008) interpretations of fluid-phase production based on MICP data are dependent on oil gravity, so the general conclusions below should be considered in light of the high gravity of Berea oils.

Figure 7-46 shows another low-porosity (2.6 percent), low-permeability (0.0009 md) Berea siltstone from Lawrence County. In this sample, intergranular porosity (blue) has been almost completely occluded by quartz and ferroan dolomite cement. Opaque grains are pyrite. MICP analysis for this sample shows that the pore volume (near 1 percent) is 0.8 to greater than 0.1 μ , mostly 0.5 to 0.6 μ . If this were the best reservoir rock, it is likely that only gas would be produced from this reservoir (Sneider and Bolger, 2008).

Figure 7-47 is from a sample with 7.1 percent porosity and 0.021 md permeability. The sample has intergranular porosity (blue), which has been reduced by intergranular compaction and quartz and siderite (brown crystals) cements. Grain-moldic pores are poorly developed. MICP analysis for this sample shows that the pore volume (near 1.75 percent) is 0.4 to 0.1 μ , mostly 0.1 to 0.2 μ . It is likely that gas would be produced from this reservoir (Sneider and Bolger, 2008).

Figure 7-48 is a sample with higher porosity (9.4 percent) and permeability (0.221 md). This is an order of magnitude higher permeability than the preceding sample shown in Figure 7-47. This

sample might be considered more typical of Berea reservoir rock. The sample has intergranular and grain-moldic porosity (blue) and lacks ferroan dolomite cement. Opaque grains are pyrite. The corresponding pore-volume distribution based on MICP analysis shows a pore-throat distribution of 1 to less than 0.1 μ , but mostly from 0.5 to 0.6 μ , which is common in reservoirs that produce gas (Sneider and Bolger, 2008).

Figure 7-49 is from a sample with 11.2 percent porosity and 1.1874 md permeability. This sample would be an example of a good Berea reservoir. Intergranular porosity (blue) is well developed and consists of intergranular and oversized grain-moldic pores. Opaque grains are pyrite. The pore-throat-diameter distribution is 2 to greater than 0.1 μ , with the greatest pore volume (near 3.25 percent) having pore diameters of 1 to 2 μ and characteristic of an oil-producing reservoir (Sneider and Bolger, 2008).

Lastly, Figure 7-50 is from a sample with 12.3 percent porosity and 2.04 md permeability, which is the highest porosity and permeability of the samples analyzed. Well-developed intergranular and grain-moldic porosity (blue) is visible in the thin section. This sample has only a trace of ferroan dolomite cement, and minor siderite. Opaque grains are pyrite. Similar to the previous sample (HN1516), pore-diameter distribution (pore volume near 1.75 percent) is largely from pore throats with diameters from 1 to 2 μ and characteristic of an oil-producing reservoir (Sneider and Bolger, 2008).

8. Reservoir Geology Discussion

Stephen F. Greb and David C. Harris

The goal of the reservoir characterization task was to determine how sand bodies, pay zones, porosity, and permeability are distributed within the Berea. This work has involved interpretation of Berea Sandstone outcrop exposures, Berea core from nine wells, hundreds of well logs, and more than 50 thin sections. Data and observations are documented in Chapter 7; this chapter presents discussion and interpretations of those data.

Berea fields are said to produce from mostly stratigraphic traps (Tomastik, 1996), but there are numerous examples of structural influence on various aspects of petroleum production in the eastern Kentucky fields, including (1) synsedimentary structural influence on sandstone deposition in the Berea, (2) the concentration of fields between the Wallbridge Fault and another subparallel fault in the Irvine-Paint Creek Fault System in Lawrence County, (3) water-oil contacts across fault or up structural dip, and (4) development of oil fields on small, subtle anticlines reported from Martin County and other parts of the coal field. If known structures are near a potential well, cross sections should be made across structure to see if the structure influenced either bed thickness, sandstone/coarse siltstone percentage, or, potentially, the oil-water contact in a field. Changes in bed dip are also common across or off of structures. These can be very important in horizontal wells. Even where the structures themselves do not influence sedimentation, faults and fracturing, especially above arches and along tensional folds in strata associated with bed draping across faults, were potential pathways for hydrocarbon migration to Berea reservoirs. Bed dip may also be influenced by clinoforms through the prograding Bedford-Berea interval. In some of the correlations of cores to surrounding wells, shallow-dipping clinoform-like dip is apparent. In others, bedding appears to be more horizontal. Clinoforms, by their nature, may involve downdip changes, so can be difficult to correlate based on geophysical signatures. In the Berea, where structural influences seem to have been common, clinoforms, where they occur, might change orientation and dip relative to structure. Preliminary correla-

tions in the Bedford-Berea interval suggest possibly north- and northwest-dipping clinoforms in parts of Lawrence County into Greenup County. More work is needed on detailed correlation of bedding in distinct field areas.

Berea reservoirs in eastern Kentucky can be examined at different scales of heterogeneity (Fig. 8-1). The largest scale is the regional variation in thickness and net sandstone/coarse siltstone in the Bedford-Berea interval. There are several areas of increased net coarse siltstone/very fine sandstone: (1) a northern shelf or basin, north of the Kentucky River Fault System in Greenup, Lewis, Carter, and Boyd Counties, (2) an elongate central shelf/slope area in Lawrence and Johnson Counties east of the Paint Creek Uplift and south of the Wallbridge Fault (Irvine-Paint Creek Fault System), (3) central shelf/slope area in eastern Martin County, also associated with faulting on the southern margin of the Rome Trough, and (4) a southern shelf/slope area on the Pike County Uplift along the D'Invilliers Structure. The southern area is mostly associated with gas, although Nuttall (2016) has found that some oil completions have been reported from the Berea in Pike County.

Berea deposits are thickest in the northern Greenup-Boyd County area. This is also the shallowest area of current Berea oil production. Some areas may have north-dipping clinoforms. Thicker Berea-Bedford on a structural high is curious, but denotes persistent loci for coarser (coarse silt to fine sandstone) east of the Waverly Arch and north of the Kentucky River Fault System. The occurrence of thicker Berea on the "up side" of the Kentucky River Fault System suggests the possibility of reverse movement on these faults during Berea deposition. Hence, rather than being a hinge for a shelf slope or ramp to the south, the slope may have been dipping into a depocenter north of the faults. Similarly, the Berea and Berea-Bedford interval thins dramatically westward into Lewis County toward the Waverly Arch. This suggests the arch (1) was a relatively positive feature during deposition, and that the whole interval may have thinned onto its flanks or (2) the arch was uplifted

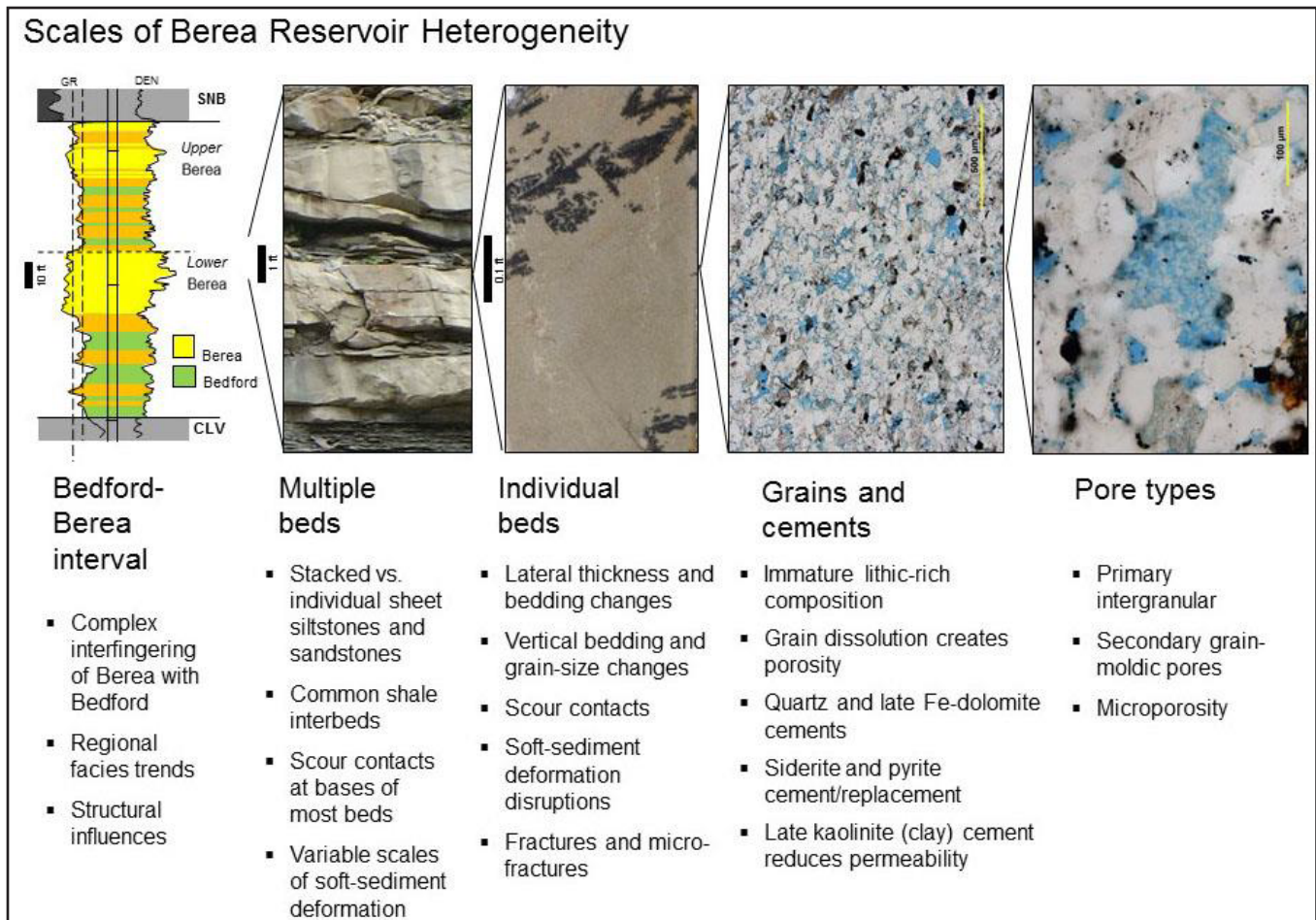


Figure 8-1. Summary of scales of heterogeneity in Berea "tight sandstone" reservoirs.

after deposition and significant sediment was removed at the unconformity at the base of the Sunbury Shale. Another interesting feature is that oil seeps are not noted along the outcrop belt in Lewis County, updip from current Greenup County production. This may indicate a permeability or water barrier between the reservoirs and the outcrop.

Outcrops in the Garrison, Ky., area (field trip guidebook) and the Aristech No. 4 core (core book) are the best approximation of bedding in the subsurface for this northern oil area. In the outcrop area, significant bed dip and small-scale faults seem common, so these might also be expected in the subsurface.

In the central areas south of the Kentucky River Fault System and north of the Pike County Uplift, thicker interbeds of Bedford shales commonly separate two or more distinct Berea inter-

vals. Although these areas are commonly inferred to have an upper and lower Berea "sand" by operators, dipping clinofolds can be seen in correlations of some fields, such that the upper "sand" in one field may be equivalent to a lower "sand" downdip in another field. The Lawrence County cores, especially the KY-WV Milton Moore and Ruben Moore cores, provide good examples of typical bedding and bed stacking in these fields, as well as bed dip between two cores, which are only 1.49 mi apart.

In the southern Pike County area, the upper Berea is very argillaceous, and reservoirs are typically developed in the lower part of the Bedford-Berea interval. The EQT 504353 core provides a good example of bedding and bed stacking in this area. The Pocahontas Mining core from southern Martin County is also very argillaceous, with a better-developed "lower" Berea for comparison.

Within each Berea interval in these different areas there are different pay zones. Historically, wells were commonly completed across the whole interval in order to complete from multiple porosity zones. Current completions are in horizontal wells, attempting to stay within a much narrower pay zone within the interval. These pay zones are composed of multiple beds (Fig. 8-1). Berea pay zones are commonly 12 to 30ft thick, but are composed of thinner porosity zones (10 to 14 percent), each 1 to 6ft thick. Typical coarse siltstone/very fine sandstone beds in outcrop and core are less than 3ft thick and separated by thin shales, so many pay zones are formed from multiple thin beds. Thicker pays occur where beds 3ft thick or less come together without significant intervening shales. This may happen toward the top of coarsening-upward (by gamma inference) intervals within clinof orm bedsets or through stacking of multiple thinner coarsening-upward intervals. Scours at the base of individual storm beds (scour-based, massive to parallel-laminated siltstones), loading, and soft-sediment deformation may all act to locally remove intervening shales and connect "coarser" beds into thicker, combined porosity intervals.

Bedding is relatively continuous in outcrop within sheet-sandstone lithofacies, and many pay zones can be correlated for some distance between wells in producing fields. In outcrop, however, lateral transitions in bedding from typical storm beds into soft-sediment-deformed beds and large flow rolls or ball-and-pillow horizons are common. Soft-sediment deformation is common in all of the cores. This is particularly relevant for horizontal drilling. In horizontal drilling, Berea operators are often trying to stay within a 5- to 10-ft pay zone. A gamma tool is used to record bedding. If the tool leaves the pay zone into an overlying or underlying bounding shale layer, the deflection is indicated by a higher gamma kick on the log. However, in the Berea, a sudden change to higher gamma readings might indicate lateral transition into a flow roll or ball-and-pillow structure rather than a vertical change in elevation out of zone (highlighted in the field-trip guidebook). Also, bit direction may be influenced by undulating or deformed shaly flow rolls, and shaly intrusions between flow rolls.

Within individual beds (Fig. 8-1), there is a fair relationship between permeability and poros-

ity ($R^2=0.75$). The relationship is better for lower-permeability ($R^2=0.81$) than higher-permeability samples ($R^2=0.57$). For permeabilities greater than 0.1 md, porosities are generally greater than 10 percent. All values above 12 percent have permeabilities greater than 0.1 md. A limited comparison of wells with density logs and plug data shows log-derived porosities commonly vary by as much as 2 percent (both high and low) from analytical results, so some caution is needed when predicting permeability from log-based data alone. Berea siltstones with greater than 10 percent porosity and greater than 0.1 md permeability generally have less than 15 percent total clays (mostly illite), dolomite, siderite, and pyrite.

In the EQT 504353 core, bitumen impregnation provides evidence of an in-situ oil reservoir that was thermally cracked and stranded. In that core, internal flow barriers within beds can be seen as unstained core. Some of the internal, small-scale barriers to flow in the reservoir include slickensided shear zones and glide planes along soft-sediment-deformed bedding, fine-grained bedding contacts, scour contacts, microfractures associated with soft-sediment deformation, and cement-filled fractures. These features were noted in all cores, and likely influence all reservoirs.

At the microscopic level (Fig. 8-1), preliminary petrographic examination of Berea reservoir cores has revealed a complex diagenetic history that includes cementation by quartz, ferroan dolomite, siderite, pyrite, and kaolinite. The immature composition of Berea clastics (mostly sublithic and lithic arenites) made them susceptible to secondary porosity development. Framework grain dissolution and moldic porosity are common in Lawrence and Johnson Counties. This pore type was not observed in the single Pike County core, which has lower amounts of intergranular porosity. These regional differences will require more work to determine controls on grain dissolution. Secondary porosity contributes significantly to the reservoir volume in Lawrence and Johnson Counties. It is likely important in Greenup County as well, but no cores were available from Greenup County for this study.

Microporosity is common in many Berea reservoir rocks, and together with the very small grain size accounts for the low permeability of the

interval in general. Microporosity results from clay cements and matrix, and partially dissolved framework grains.

Determination of a complete sequence of diagenetic events will require further petrographic work. Integration of scanning electron microscopy (SEM) with optical petrography would be particularly helpful due to the small grain sizes present. A scanning electron microscope was not available for this study, but KGS will have a new instrument by fall of 2016. The Berea will be perfect for applying this technology. Based on the preliminary work to date, quartz cement is an early event, followed by ferroan dolomite cementation. Later events include framework grain dissolution (secondary porosity) and pyrite and siderite precipitation. Kaolinite (clay) cement is observed in all pore types, including fractures, and is one of the latest events.

Specific intra-well and regional variability in porosity development or preservation was not addressed in this study. In general, presence of porosity is not thought to be a limiting constraint on the Berea play in the study area. The focus of this work has been on macroscopic reservoir heterogeneities, rather than at the pore scale. Additional

diagenetic work, including geochemistry, is certainly warranted. Extending the petrography into Greenup County would provide additional data at even shallower depths. Examining additional cores from the deeper Berea reservoirs might help to identify trends in secondary-porosity development related to burial depth.

Mercury injection capillary pressure data were received late in the project and are still being interpreted. Data show that maximum pore throats for the best-quality reservoir rock are around $1\ \mu$, and range down to approximately $0.01\ \mu$ for very low-permeability rock. These pore-throat sizes lie close to empirically derived cutoffs for oil and gas production, and may help to explain fluid-phase production in the Berea. The work by Sneider and Bolger (2008) indicates that minimum pore-throat diameters of $1\ \mu$ are required for oil production, whereas greater than $0.1\ \mu$ is required for gas production. This is also dependent to some degree on fluid properties. More work is needed to better evaluate the role of pore-throat distribution on petroleum production in the Berea of eastern Kentucky.

References Cited

- Algeo, T.J., Scheckler, S.E., and Maynard, J.B., 2001, Effects of early vascular land plants on weathering processes and global chemical fluxes during the Middle and Late Devonian, *in* Gensel, P.G., and Edwards, D., eds., *Plants invade the land: Evolutionary and Environmental Perspectives*: New York, Columbia University Press, p.213–236.
- Alsharani, S., and Evans, J.E., 2014, Shallow-water origin of a Devonian black shale, Cleveland Shale Member (Ohio Shale), northeastern Ohio, USA: *Open Journal of Geology*, v.4, p.636–653.
- Ammerman, M.L., and Keller, G.R., 1979, Delineation of Rome Trough in eastern Kentucky by gravity and deep drilling data: *American Association of Petroleum Geologists Bulletin*, v.63, p.341–353.
- Andrusevich, V.E., Engel, M.H., and Zumberge, J.E., 2000, Effects of paleolatitude on the stable carbon isotope composition of crude oils: *Geology*, v.28, p.847–850.
- Araujo, C.V., Borrego, A.G., Cardott, B., das Chagas, R.B.A., Flores, D., Gonçalves, P., Hackley, P.C., Hower, J.C., Kern, M.L., Kus, J., Mastalerz, M., Mendonça Filho, J.G., Mendonça, J.O., Menezes, T.R., Newman, J., Suarez-Ruiz, I., Sobrinho da Silva, F., and Viegas de Souza, I., 2014, Petrographic thermal indices of a Devonian shale maturation series, Appalachian Basin, USA: *International Journal of Coal Geology*, v.130, p.89–101.
- ASTM, 2015a, D2797: Standard practice for preparing coal samples for microscopical analysis by reflected light: *Annual book of ASTM standards, petroleum products, lubricants, and fossil fuels; gaseous fuels, coal and coke*, v.5.06, www.astm.org/Standards/D2797.htm [accessed 2/14/2016].
- ASTM, 2015b, D7708: Standard test method for microscopical determination of the reflectance of vitrinite dispersed in sedimentary rocks: *Annual book of ASTM standards, petroleum products, lubricants, and fossil fuels; gaseous fuels, coal and coke*, v.5.06, www.astm.org/Standards/D7708.htm [accessed 2/14/2016].
- ASTM, 2015c, D4239: Standard test method for sulfur in the analysis sample of coal and coke using high-temperature tube furnace combustion: *Annual book of ASTM standards, petroleum products, lubricants, and fossil fuels; gaseous fuels, coal and coke*, v.5.06, www.astm.org/Standards/D4239.htm [accessed 4/18/2016].
- Avila, J., 1983a, Area requested for tight formation designation in the Berea Sandstone, Pike County, Kentucky: *Kentucky Geological Survey, ser.11, Open-File Report 83-01*, 100 p.
- Avila, J., 1983b, Area requested for tight formation designation in the Berea Sandstone, Pike County, Kentucky: *Kentucky Geological Survey, ser.11, Open-File Report 83-02*, 53 p.
- Azevedo, D.A., Aquino Neto, F.R., Simoneit B.R.T., and Pinto, A.C., 1992, Novel series of tricyclic aromatic terpanes characterized in Tasmanian tasmanite: *Organic Geochemistry*, v.18, p.9–16.
- Barker, C.E., 1991, An update on the suppression of vitrinite reflectance: *Society for Organic Petrology Newsletter*, v.8, no.4, p.8–11.
- Barker, C.E., Lewan, M.D., and Pawlewicz, M.J., 2007, The influence of extractable organic matter on vitrinite reflectance suppression: A survey of kerogen and coal types: *International Journal of Coal Geology*, v.70, nos.1–3, p.67–78.
- Barrows, M.N., and Cluff, R.M., 1984, New Albany Shale Group (Devonian-Mississippian) source rocks and hydrocarbon generation in the Illinois Basin, *in* Demaison, G., and Murriss R.J., eds., *Petroleum geochemistry and basin evolution: American Association of Petroleum Geologists Memoir 35*, p.111–138.
- Baskin, D.K., and Jones, R.W., 1993, Prediction of oil gravity prior to drill-stem testing in Monterey Formation reservoirs, offshore California: *American Association of Petroleum Geologists Bulletin*, v.9, p.1749–1487.
- Baskin, D.K., and Peters, K.E., 1992, Early generation characteristics of a sulfur-rich Monterey kerogen: *American Association of Petroleum Geologists Bulletin*, v.76, p.1–3.

- Behar, F., and Jarvie, D.M., 2013, Compositional modeling of gas generation from two shale gas resource systems: Barnett Shale (USA) and Posidonia Shale (Germany), *in* Chatelier, J.Y., and Jarvie, D.M., eds., *Critical assessment of shale resource plays: American Association of Petroleum Geologists Memoir 103*, p.25–44.
- Behar, F., Lorant, F., and Lewan, M., 2008, Role of NSO compounds during primary cracking of a Type II kerogen and a Type III lignite: *Organic Geochemistry*, v. 39, p.1–22.
- Behar, F., Roy, S., and Jarvie, D., 2010, Artificial maturation of a Type I kerogen in closed system: Mass balance and kinetic modelling: *Organic Geochemistry*, v. 41, p.1235–1247.
- Bernard, B.B., Brooks, J.M., and Sackett, W.M., 1976, Natural gas seepage in the Gulf of Mexico: *Earth and Planetary Science Letters*, v. 31, p.48–54.
- Bertrand, R., and Malo, M., 2001, Source rock analysis, thermal maturation and hydrocarbon generation in the Siluro-Devonian rocks of the Gasps Belt Basin, Canada: *Bulletin of Canadian Petroleum Geology*, v. 49, p.238–261.
- Blumer, M., Guillard, R.R.L., and Chase, T., 1971, Hydrocarbons of marine plankton: *Marine Biology*, v. 8, issue 3, p.183–189.
- Boswell, R., 1996, Play UDs: Upper Devonian black shales, *in* Roen, J.B., and Walker, B.J., eds., *The atlas of major Appalachian gas plays: West Virginia Geological and Economic Survey Publication V-25*, p.93–99.
- Bourbonniere, R.A., and Meyers, P.A., 1996, Sedimentary geolipid records of historical changes in the watersheds and productivities of Lakes Ontario and Erie: *Limnology and Oceanography*, v. 41, p.352–359.
- Brown, H.R., Cook, A.C., and Taylor, G.H., 1964, Variations in the properties of vitrinite in iso-metamorphic coal: *Fuel*, v. 34, p.111–124.
- Burruss, R.C., and Laughrey, C.D., 2010, Carbon and hydrogen isotopic reversals in deep basin gas: Evidence for limits to the stability of hydrocarbons: *Organic Geochemistry*, v. 41, p.1285–1296.
- Cable, M.S., and Beardsley, R.W., 1984, Structural controls on Late Cambrian and Early Ordovician carbonate sedimentation in eastern Kentucky: *American Journal of Science*, v.284, no.7, p.797–823.
- Cecil, C.B., Brezinski, D.K., and Dulong, F., 2004, The Paleozoic record of changes in global climate and sea level: Central Appalachian Basin, *in* Southworth, S., and Burton, W., eds., *Geology of the national capital region—Field trip guide book compendium: U.S. Geological Survey Circular 1264*, p.77–133.
- Charpentier, R.R., de Witt, W., Jr., Claypool, G.E., Harris, L.D., Mast, R.F., Megeath, J.D., Roen, J.B., and Schmoker, J.W., 1993, Estimates of unconventional natural gas resources of the Devonian shales of the Appalachian Basin, *in* Roen, J.B., and Kepferle, R.C., eds., *Petroleum geology of the Devonian and Mississippian black shale of eastern North America: U.S. Geological Survey Bulletin 1909-B*, p.N1–N20, pubs.er.usgs.gov/publication/b1909 [accessed 02/05/2019].
- Chung, H.M., Gormly, J.R., and Squires, R.M., 1988, Origin of gaseous hydrocarbons in subsurface environments: Theoretical considerations of carbon isotope distribution: *Chemical Geology*, v. 71, p.97–103.
- Clementz, D.M., 1979, Effects of oil and bitumen saturation on source-rock pyrolysis: *American Association of Petroleum Geologists Bulletin* 63, p.2227–2232.
- Coates, K.P., 1988, Depositional environments of the Bedford and Berea Formations in central Ohio: Columbus, Ohio State University, master's thesis, 199 p.
- Cole, G.A., Drozd, R.J., Sedivy, R.A., and Halpern, H.I., 1987, Organic geochemistry and oil-source correlations, Paleozoic of Ohio: *American Association of Petroleum Geologists Bulletin*, v. 71, p.788–809.
- Coleman, U., and Clayton, G., 1987, Palynostratigraphy and palynofacies of the uppermost Devonian and Lower Mississippian of eastern Kentucky (USA) and correlation with western Europe: *Courier Forschungsinstitute Senckenberg*, v. 98, p.75–93.
- Conant, L.L., and Swanson, V.E., 1961, Chattanooga Shale and related rocks of central Tennessee and nearby areas: *U.S. Geological Survey Professional Paper 357*, 91 p.

- Cooper, J.R., 1943, Flow structures in the Berea Sandstone and Bedford Shale of central Ohio: *Journal of Geology*, v. 51, no. 3, p. 190–203.
- Curtis, J.B., 1988, Well sample/borehole diagnostic methods for tight black shales: Gas Research Institute, final report, GRI-88/0223, 200 p.
- De Graaf, W., Sinninghe Damsté, J.S., and de Leeuw, J.W., 1992 Laboratory simulation of natural sulfurization. I. Formation of monomeric and oligomeric isoprenoid polysulfides by low-temperature reactions of inorganic polysulfides with phytol and phytadienes: *Geochimica et Cosmochimica Acta*, v. 56, p. 4321–4328.
- Delvaux, D., Martin, H., LePlat, P., and Paulet, J., 1990, Comparative Rock-Eval pyrolysis as an improved tool for sedimentary organic matter analysis: *Advances in Organic Chemistry*, v. 16, nos. 4–6, p. 1221–1229.
- Dever, G.R., Jr., 1999, Tectonic implications of erosional and depositional features in upper Meramecian and lower Chesterian (Mississippian) rocks of south-central and east-central Kentucky: Kentucky Geological Survey, ser. 11, Bulletin 5, 67 p.
- DeWitt, W., Jr., Roen, J.B., and Wallace, L.G., 1993, Stratigraphy of the Devonian black shales in the Appalachian Basin, in Roen, J.B., and Kefferle, R.C., eds., *Petroleum geology of the Devonian and Mississippian black shales of eastern North America*: U.S. Geological Survey Bulletin 1909, p. B1–B57.
- Dillman, S.B., and Ettensohn, F.R., 1980, Isopach maps of black-shale units in eastern Kentucky: U.S. Department of Energy, Morgantown Energy Technology Center, Eastern Gas Shales Project, METC/EGSP Series, nos. 507–514, 7 sheets.
- Durand, B., Alpern B., Pittion J.L., and Pradier, B., 1986, Reflectances of vitrinite as a control of thermal history of sediments, in Burris, J., ed., *Thermal modeling in sedimentary basins*: Paris, Editions Technipaper, p. 441–474.
- East, J.A., Swezey, C.S., Repetski, J.E., and Hayba, D.O., 2012, Thermal maturity map of Devonian shale in the Illinois, Michigan, and Appalachian Basins of North America: U.S. Geological Survey Scientific Investigations Map 3214, scale 1:24,000.
- Ekweozor, C.M., Okogun, J.I., Ekong, D.E.U., and Maxwell, J.M., 1979, Preliminary organic geochemical studies of samples from the Niger Delta (Nigeria). I. Analyses of crude oils for triterpanes: *Chemical Geology*, v. 27, p. 11–28.
- Elam, T.D., 1981, Stratigraphy and paleoenvironmental analysis of the Bedford-Berea sequence and the Sunbury Shale in eastern and south-central Kentucky: Lexington, University of Kentucky, master's thesis, 155 p.
- Ettensohn, F.R., 1980, An alternative to the barrier-shoreline model for deposition of Mississippian and Pennsylvanian rocks in northeastern Kentucky: *Geological Society of America Bulletin*, v. 91, no. 3, p. 130–135.
- Ettensohn, F.R., 1985, Controls on development of Catskill Delta complex basin-facies, in Woodrow, D.L., and Sevon, W.D., eds., *The Catskill Delta*: Geological Society of America, Special Paper 201, p. 65–78.
- Ettensohn, F.R., 1994, Tectonic control on the formation and cyclicity of major Appalachian unconformities and associated stratigraphic sequences, in Dennison, J.M., and Ettensohn, F.R., eds., *Tectonic and eustatic controls on sedimentary cycles: SEPM [Society for Sedimentary Geology] Concepts in Sedimentology and Paleontology*, v. 4, p. 217–242.
- Ettensohn, F.R., 2004, Modeling the nature and development of major Paleozoic clastic wedges in the Appalachian Basin, USA: *Journal of Geodynamics*, v. 37, p. 657–681.
- Ettensohn, F.R., and Barron, L.S., 1981, Depositional model for the Devonian-Mississippian black-shale sequence of North America—A tectono-climatic approach: U.S. Department of Energy, Morgantown Energy Technology Center, METC/12040-2, 80 p.
- Ettensohn, F.R., and Elam, T.D., 1985, Defining the nature and location of a Late Devonian-Early Mississippian pycnocline in eastern Kentucky: *Geological Society of America Bulletin*, v. 96, p. 1313–1321.
- Ettensohn, F.R., Lierman, R.T., and Mason, C.E., 2009, Upper Devonian-Lower Mississippian clastic rocks in northeastern Kentucky: Evidence for Acadian alpine glaciation and models for source-rock and reservoir-rock development in the eastern United States:

- American Institute of Petroleum Geologists–Kentucky Chapter, 53 p.
- Ettensohn, F.R., Miller, M.L., Dillman, S.B., Elam, T.D., Geller, K.L., Swager, D.R., Markowitz, G., Woock, R.D., and Barron, L.S., 1988, Characterization and implications of the Devonian–Mississippian black shale sequence, eastern and central Kentucky, U.S.A.: Pycnoclines, transgression, regression, and tectonism, *in* McMillan, N.J., Embry, A.F., and Glass, D.J., eds., *Devonian of the world: Proceedings of the 2nd International Symposium on the Devonian System*: Canadian Society of Petroleum Geologists, Memoir 14, v. 2, p. 323–345.
- Floyd, J., 2015, *Subsurface geological analyses of the Berea petroleum system in eastern Kentucky*: Lexington, University of Kentucky, master's thesis, 153 p.
- GeoMark, 2015, Rock and fluid database: geomarkresearch.com/database-products [accessed 7/20/2015].
- Hackley, P.C., Ryder, R.T., Trippi, M.H., and Alimi, H., 2013, Thermal maturity of northern Appalachian Basin Devonian shales: Insights from sterane and terpane biomarkers: *Fuel*, v. 106, p. 455–462.
- Hackley, P.C., and SanFilipo, J.R., 2016, Organic petrology and geochemistry of Eocene Suzak bituminous marl, north-central Afghanistan: Depositional environment and source rock potential: *Marine and Petroleum Geology*, v. 73, p. 572–589.
- Hackley, P.C., Araujo, C.V., Borrego, A.G., Bouzinos, A., Cardott, B.J., Cook, A.C., Eble, C., Flores, D., Gentzis, T., Gonçalves, P.A., Mendonça Filho, J.G., Hámor-Vidó, M., Jelonek, I., Kommeren, K., Knowles, W., Kus, J., Mastalerz, M., Rêgo Menezes, T., Newman, J., Oikonomopoulos, I.K., Pawlewicz, M., Pickel, W., Potter, J., Ranasinghe, P., Read, H., Reyes, J., De La Rosa Rodriguez, G., Fernandes de Souza, I.V.A., Suárez-Ruiz, I., Sýkorová, I., and Valentine, B.J., 2015, Standardization of reflectance measurements in dispersed organic matter: Results of an exercise to improve interlaboratory agreement: *Marine and Petroleum Geology*, v. 59, p. 22–34.
- Hamilton-Smith, T., 1993, Gas exploration in the Devonian shales of Kentucky: Kentucky Geological Survey, ser. 9, Bulletin 4, 31 p.
- Harris, D.C., Drahovzal, J.A., Hickman, J.G., Nuttall, B.C., Baranoski, M.T., and Avary, K.L., 2004, Rome Trough Consortium final report and data distribution (report submitted to industry partners and to the U.S. Department of Energy in fulfillment of U.S. Department of Energy Contract DE-AF26-98FT02147): Kentucky Geological Survey, Open-File Report 04-06, 1 CD-ROM.
- Hatch, J.R., Jacobson, S.R., Witzke, B.J., Rissati, J.B., Anders, D.E., Watney, W.L., Newell, K.D., and Vuletich, A.K., 1987, Possible late Middle Ordovician organic carbon isotopic excursion: Evidence from Ordovician oil and hydrocarbon source rocks, Mid-continent and east-central United States: *American Association of Petroleum Geologists Bulletin*, v. 71, p. 1342–1354.
- Hoefs, J., 2004, *Stable isotope geochemistry* [5th ed.]: New York, Springer, 244 p.
- Hower, J.C., and Rimmer, S.M., 1991, Coal rank trends in the central Appalachian coalfield: Virginia, West Virginia, and Kentucky: *Organic Geochemistry*, v. 17, p. 161–173.
- Hunt, J.M., 1996, *Petroleum geochemistry and geology*: New York, W.H. Freeman, 743 p.
- Hunter, C.D., and Young, D.M., 1953, Relationship of natural gas occurrence and production in eastern Kentucky (Big Sandy Gas Field) to joints and fractures in Devonian bituminous shale: *American Association of Petroleum Geologists Bulletin*, v. 37, no. 2, p. 282–299.
- Hutcheon, I., and Abercrombie, H.J., 1989, The role of silicate hydrolysis in the origin of CO₂ in sedimentary basins: *Proceedings of the Sixth International Symposium on Water-Rock Interaction*, Rotterdam, p. 321–324.
- Hutton, A.C., 1987, Petrographic classification of oil shales: *International Journal of Coal Geology*, v. 8, no. 3, p. 203–231.
- Hutton, A.C., and Cook, A.S., 1980, Influence of alginite on the reflectance of vitrinite from Joadja, NSW, and some other coals and oil shales containing alginite: *Fuel*, v. 59, p. 711–714.
- Jacob, H., 1989, Classification, structure, genesis, and practical importance of natural solid oil

- bitumen (migrabitumen): *International Journal of Coal Geology*, v. 11, no. 1, p. 65–79.
- James, A.T., 1983, Correlation of natural gas by use of carbon isotopic distribution between hydrocarbon components: *American Association of Petroleum Geologists Bulletin*, v. 67, p. 1176–1191.
- Jarvie, D.M., Claxton, B.L., Henk, F., and Breyer, J.T., 2001, Oil and shale gas from the Barnett Shale, Fort Worth Basin, Texas [abs.]: *American Association of Petroleum Geologists Annual Meeting Program*, v. 10, p. A100.
- Jarvie, D.M., Jarvie, B.M., Weldon, D., and Maende, A., 2015, Geochemical assessment of in situ petroleum in unconventional resource systems: *Unconventional Resource Technology Conference*, 20 p., doi:10.15530/URTEC-2015-2173379.
- Kalkreuth, W., and Macauley, G., 1987, Organic petrology and geochemical (Rock-Eval) studies on oil shales and coals from the Pictou and Antigonish areas, Nova Scotia, Canada: *Bulletin of Canadian Petroleum Geology*, v. 35, p. 263–295.
- Kenig, F., Sinninghe Damsté, J.S., Frewin, N.L., Hayes, J.M., and de Leeuw, J.W., 1995, Molecular indicators for palaeoenvironmental change in a Messinian evaporitic sequence (Vena del Gesso, Italy). II: High-resolution variation in abundances and ^{13}C contents of free and sulphur-bound carbon skeletons in a single marl bed: *Organic Geochemistry*, v. 23, p. 485–526.
- Kepferle, R.C., 1993, A depositional model and basin analysis for gas-bearing black shale (Devonian and Mississippian) in the Appalachian Basin, in Roen, J.B., and Kepferle, R.C., eds., *Petroleum geology of the Devonian and Mississippian black shale of eastern North America*: U.S. Geological Survey Bulletin 1909, p. F1–F23.
- Kepferle, R.C., Wilson, E.N., and Ettensohn, F.R., 1978, Preliminary stratigraphic cross section showing radioactive zones in the Devonian black shales in the southern part of the Appalachian Basin: U.S. Geological Survey Oil and Gas Investigations Chart OC-85, 13 cross sections on 1 sheet.
- Kohnen, M.E.L., Sinninghe Damsté, J.S., and de Leeuw, J.W., 1991, Biases from natural sulphurization in paleoenvironmental reconstruction based on hydrocarbon biomarker distributions: *Nature*, v. 349, p. 775–778.
- Köster, J., Van Kaam-Peters, H.M.E., Koopmans, M.E., de Leeuw, J.W., and Sinninghe Damsté, J.S., 1997, Sulfurization of homohopanooids: Effects on carbon number distribution, speciation and 22S/22R epimer ratios: *Geochimica et Cosmochimica Acta*, v. 61, p. 2431–2452.
- Kroon, J., and Castle, J.W., 2011, Biomarkers in the Upper Devonian Lower Huron Shale as indicators of biological source of organic matter, depositional environment, and thermal maturity: *American Association of Petroleum Geologists Search and Discovery Article #20117*, www.searchanddiscovery.com/pdfz/documents/2011/20117kroon/ndx_kroon.pdf.html [accessed 6/18/2018].
- Kubik, W., 1993, Natural fracturing style on Devonian shale production, Pike County, Kentucky: *Gas Shales Technology Review*, v. 8, no. 2, p. 1–25.
- Landis, C.R., and Castaño, J.R., 1994, Maturation and bulk chemical properties of a suite of solid hydrocarbons: *Organic Geochemistry*, v. 22, p. 137–149.
- Lee, K.D., 1980, Subsurface structure of the eastern Kentucky gas field: Morgantown, West Virginia University, master's thesis, 56 p.
- Lewan, M.D., 1985, Evaluation of petroleum generation by hydrous pyrolysis experimentation: *Philosophical Transactions of the Royal Society, London*, v. 315, p. 123–134.
- Lewan, M.D., 1986, Stable carbon isotopes of amorphous kerogens from Phanerozoic sedimentary rocks: *Geochimica et Cosmochimica Acta*, v. 50, p. 1583–1591.
- Lewan, M.D., 1997, Experiments on the role of water in petroleum formation: *Geochimica et Cosmochimica Acta*, v. 61, p. 3691–3723.
- Lewis, T.L., 1988, Late Devonian and Early Mississippian distal basin-margin sedimentation of northern Ohio: *Ohio Journal of Science*, v. 88, no. 1, p. 23–39.
- Lo, H.B., 1993, Correction criteria for the suppression of vitrinite reflectance in hydrogen-rich

- kerogen: Preliminary guidelines: *Organic Geochemistry*, v. 20, p. 653–657.
- Lowry, P.H., Hamilton-Smith, T., Faleur, J.P., and Peterson, R.M., 1989, Well report: CNG Development Company United Affiliates Corporation No. 2814, GRI Comprehensive Study Well No. 3, Logan County, West Virginia: Gas Research Institute, GRI-89/0199, 31 p.
- Lu, H., Shen, C., Zhang, Z., Liu, M., Sheng, G., Peng, P., and Hsu, C.S., 2015, 2,3,6-/2,3,4-aryl isoprenoids in Paleocene crude oils from Chinese Jiangnan Basin: Constrained by water column stratification: *Energy & Fuels*, v. 29, p. 4690–4700.
- Magoon, L.B., 1988, The petroleum system – A classification scheme for research, exploration, and resource assessment, *in* Magoon, L.B., ed., *Petroleum systems of the United States*: U.S. Geological Survey Bulletin 1870, p. 2–15.
- Maynard, J.B., 1981, Some geochemical properties of the Devonian-Mississippian shale sequence, *in* Kepferle, R.C., and Roen, J.B., eds., *Field trip no. 3, Chattanooga and Ohio Shales of the southern Appalachians*, *in* Roberts, T.G., ed., *Field trip guidebooks for the annual meeting of the Geological Society of America*, 1981, Cincinnati, Ohio, v. 2, *Economic geology, structure*: American Geological Institute, p. 336–343.
- Mausser, H.F., 1982, Stratigraphy and sedimentology of the Cleveland Shale (Devonian) in northeast Ohio: Cleveland, Ohio, Case Western Reserve University, master's thesis, 232 p.
- McCarthy, K., Rojas, K., Niemann, M., Palmowski, D., Peters, K., and Stankiewicz, A., 2011, Basic petroleum geochemistry for source rock evaluation: Schlumberger Oil Field Review, v. 23, no. 22, p. 32–43.
- McDowell, R.C., 1986, The geology of Kentucky; a text to accompany the geologic map of Kentucky: U.S. Geological Survey Professional Paper 1151-H, p. H1–H76.
- Mello, M.R., Telnaes, N., Gaglianone, P.C., Chicarelli, M.I., Brassell, S.C., and Maxwell, J.R., 1988, Organic geochemical characterization of depositional palaeoenvironments of source rocks and oils in Brazilian marginal basins: *Organic Geochemistry*, v. 13, p. 31–45.
- Milici, R.C., Ryder, R.T., Swezey, C.S., Charpentier, R.R., Cook, T.A., Crovell, R.A., Klett, T.R., Pollastro, R.M., and Schenk, C.J., 2003, Assessment of undiscovered oil and gas resources of the Appalachian Basin Province, 2002: U.S. Geological Survey Fact Sheet 009-03, 2 p.
- Moldowan, J.M., Sundararaman, P., and Schoell, M., 1986, Sensitivity of biomarker properties to depositional environment and/or source input in the Lower Toarcian of S.W. Germany: *Organic Geochemistry*, v. 10, p. 915–926.
- Molyneux, S.G., Manger, W.L., and Owens, B., 1984, Preliminary account of Late Devonian palynomorph assemblages from the Bedford Shale and Berea Sandstone formations of central Ohio, U.S.A.: *Journal of Micropaleontology*, v. 3, p. 41–51.
- Morris, R.H., and Pierce, K.L., 1967, Geologic map of the Vanceburg quadrangle, Kentucky-Ohio: U.S. Geological Survey Geologic Quadrangle Map GQ-598, scale 1:24,000.
- Nuttall, B.C., 2016, Summary of publicly available production data for the Devonian Berea Sandstone play, eastern Kentucky: American Association of Petroleum Geologists Search and Discovery Article 10895, 37 p.
- Nuttall, B.C., Drahovzal, J.A., Eble, C.F., and Bustin, R.M., 2006, Analysis of the Devonian black shale in Kentucky for potential carbon dioxide sequestration and enhanced natural gas production: U.S. Department of Energy final report for project DE-FC26-02NT41442, 120 p., www.uky.edu/KGS/emsweb/devsh/final_report.pdf [accessed 10/1/2016].
- Nuttall, B.C., Eble, C.F., Bustin, R.M., and Drahovzal, J.A., 2005, Analysis of Devonian black shales in Kentucky for potential carbon dioxide sequestration and enhanced natural gas production, *in* Wilson, M., Morris, T., Gale, J., and Thambimuthu, K., eds., *Greenhouse gas control technologies*: Amsterdam, Elsevier, p. 2225–2228.
- Ourisson, G., Albrecht, P., and Rohmer, M., 1982, Predictive microbial biochemistry: From molecular fossils to prokaryotic membranes: *Trends in Biochemical Sciences*, v. 7, p. 236–239.
- Pashin, J.C., 1985, Paleoenvironmental analysis of the Bedford-Berea sequence, northeastern

- Kentucky and south-central Ohio: Lexington, University of Kentucky, master's thesis, 105 p.
- Pashin, J.C., and Etensohn, F.R., 1987, An epeiric shelf-to-basin transition; Bedford-Berea sequence, northeastern Kentucky and south-central Ohio: *American Journal of Science*, v. 287, no. 9, p. 893–926.
- Pashin, J.C., and Etensohn, F.R., 1992, Palaeoecology and sedimentology of the dysaerobic Bedford fauna (Late Devonian), Ohio and Kentucky (USA): *Palaeogeography, Palaeoclimatology, Palaeoecology*, v. 91, nos. 1–2, p. 21–34.
- Pashin, J.C., and Etensohn, F.R., 1995, Reevaluation of the Bedford-Berea sequence in Ohio and adjacent states: Forced regression in a foreland basin: *Geological Society of America Special Paper 298*, p. 1–69.
- Pepper, J.F., de Witt, W.J., and Demarest, D.F., 1954, *Geology of the Bedford Shale and Berea Sandstone in the Appalachian Basin*: U.S. Geological Survey Professional Paper 259, 111 p.
- Perkins, R.B., Piper, D.Z., and Mason, C.E., 2008, Trace-element budgets in the Ohio/Sunbury Shales of Kentucky: Constraints on ocean circulation and primary productivity in the Devonian–Mississippian Appalachian Basin: *Palaeogeography, Palaeoclimatology, Palaeoecology*, v. 265, no. 1, p. 14–29.
- Peters, K.E., 1986, Guidelines for evaluating petroleum source rock using programmed pyrolysis: *American Association of Petroleum Geologists Bulletin*, v. 70, no. 3, p. 318–329.
- Peters, K.E., and Cassa, M.R., 1994, Applied source rock geochemistry, in Magoon, L.B., and Dow, W.G., eds., *The petroleum system—From source to trap*: *American Association of Petroleum Geologists Memoir 60*, p. 93–120.
- Peters, K.E., and Moldowan, J.M., 1993, The biomarker guide: Interpreting molecular fossils in petroleum and ancient sediments: Upper Saddle River, N.J., Prentice Hall, 363 p.
- Peters, K.E., Moldowan, J.M., and Sundararaman, P., 1990, Effects of hydrous pyrolysis on biomarker thermal maturity parameters: Monterey phosphatic and siliceous members: *Organic Geochemistry*, v. 15, p. 249–265.
- Peters, K.E., Walters, C.C., and Moldowan, J.M., 2005, *The biomarker guide*, v. 2: Biomarkers and isotopes in petroleum exploration and earth history: Cambridge, Cambridge University Press, 1155 p.
- Petersen, H.I., Schovsbo, N.H., and Nielsen, A.T., 2013, Reflectance measurements of zooclasts and solid bitumen in lower Paleozoic shales, southern Scandinavia: Correlation to vitrinite reflectance: *International Journal of Coal Geology*, v. 114, p. 1–18.
- Pomerantz, A.E., Bake, K.D., Craddock, P.R., Kurzenhauser, K.W., Kodalen, B.G., Mitra-Kirtley, S., and Bolin, T.B., 2014, Sulfur speciation in kerogen and bitumen from gas and oil shales: *Organic Geochemistry*, v. 68, p. 5–12.
- Potter, P.E., Ausich, W.I., Klee, J., Krissek, L.A., Mason, C.E., Schumacher, G.A., Wilson, R.T., and Wright, E.M., 1980, *Geology of the Alexandria-Ashland Highway (Kentucky Highway 546), Maysville to Garrison* (Guidebook, Joint Field Conference of the Geological Society of Kentucky and Ohio Geological Society): Kentucky Geological Survey, ser. 12, 65 p.
- Potter, P.E., Maynard, J.B., Jackson, D., and DeReamer, J., 1983, *Lithologic and environmental atlas of Berea Sandstone (Mississippian) in the Appalachian Basin*: Appalachian Geological Society Special Publication 1, 170 p.
- Price, L.C., and Barker, C.E., 1985, Suppression of vitrinite reflectance in amorphous rich kerogen: A major unrecognized problem: *Journal of Petroleum Geology*, v. 8, p. 59–84.
- Price, L.C., Ging, T., Daws T., Love, A., Pawlewicz, M., and Anders, D., 1984, Organic metamorphism in the Mississippian-Devonian Bakken Shale, North Dakota portion of the Williston Basin, in Woodward, J., Meissner, F.F., and Clayton, J.L., eds., *Hydrocarbon source rocks of the Greater Rocky Mountain Region*: Rocky Mountain Association of Geologists, p. 83–133.
- Provo, L.J., Kepferle, R.C., and Potter, P.E., 1978, Division of black Ohio Shale in eastern Kentucky: *American Association of Petroleum Geologists Bulletin*, v. 62, no. 9, p. 1703–1713.
- Quinlan, G.M., and Beaumont, C., 1984, Appalachian thrusting, lithospheric flexure, and the Paleozoic stratigraphy of the Eastern Interior of North America: *Canadian Journal of Earth Sciences*, v. 21, p. 973–996.

- Radke, M., 1988, Application of aromatic compounds as maturity indicators in source rocks and crude oils: *Marine and Petroleum Geology*, v. 5, p. 224–236.
- Radke, M., and Welte, D.H., 1983, The methylphenanthrene index (MPI): A maturity parameter based on aromatic hydrocarbons, *in* Bjørøy, M., Albrecht, C., and Cornford, C., eds., *Advances in organic geochemistry 1981*: New York, Wiley, p. 504–512.
- Repetski, J.E., Ryder, R.T., Weary, D.J., Harris, A.G., and Trippi, M.H., 2008, Thermal maturity patterns (CAI and % R_o) in Upper Ordovician and Devonian rocks of the Appalachian Basin: A major revision of USGS Map I-917-E using new subsurface collections: U.S. Geological Survey Scientific Investigations Map 3006, 1 CD-ROM, pubs.usgs.gov/sim/3006 [accessed 6/18/2018].
- Rhoads, D.C., and Morse, J.W., 1971, Evolutionary and ecologic significance of oxygen-deficient marine basins: *Lethaia*, v. 4, p. 413–428.
- Riley, R.A., 2016, Mapping source rock and thermal maturity of the Devonian shale interval in eastern Ohio: Columbus, Ohio Department of Natural Resources, Division of Geological Survey Open-File Report 2016-3, 22 p.
- Rimmer, S.M., 2004, Geochemical paleoredox indicators in Devonian–Mississippian black shales, central Appalachian Basin (USA): *Chemical Geology*, v. 206, no. 3, p. 373–391.
- Rimmer, S.M., and Cantrell, D.J., 1989, Organic maturation of the Cleveland Member of the Ohio Shale (eastern Kentucky) [abs.], *in* Lazar, D.J., ed., *Proceedings of the 1988 Eastern Oil Shale Symposium*, November 30–December 2, 1988, Lexington, Kentucky: University of Kentucky Institute for Mining and Minerals Research, IMMR88/101, p. 232.
- Rimmer, S.M., Cantrell, D.J., and Gooding, P.J., 1993, Rock-Eval pyrolysis and vitrinite reflectance trends in the Cleveland Shale Member of the Ohio Shale, eastern Kentucky: *Organic Geochemistry*, v. 20, no. 6, p. 735–745.
- Rimmer, S.M., Hawkins, S.J., Scott, A.C., and Cressler, W.L., 2015, The rise of fire: Fossil charcoal in Late Devonian marine shales as an indicator of expanding terrestrial ecosystems, fire and atmospheric change: *American Journal of Science*, v. 315, p. 713–733.
- Robert, P., 1981, Classification of organic matter by means of fluorescence; application to hydrocarbon source rocks: *International Journal of Coal Geology*, v. 1–2, p. 101–137.
- Robert, P., 1988, Organic metamorphism and geothermal history; microscopic history of organic matter and thermal evolution of sedimentary basins: Norwell, Mass., Elf-Aquitaine and D. Reidel (Kluwer Academic Publishers), 291 p.
- Robl, T.L., Rimmer, S.M., and Barron, L.S., 1991, Organic petrography of Mississippian and Devonian shales in east-central Kentucky, *in* *Proceedings of the 1990 Eastern Oil Shale Symposium*, Lexington, Kentucky: University of Kentucky Institute for Mining and Minerals Research, p. 173–178.
- Robl, T.L., Taulbee, D.N., Barron, L.S., and Jones, W.C., 1987, Petrologic chemistry of a Devonian Type-II kerogen: *Energy Fuels*, v. 1, p. 507–510.
- Roen, J.B., Wallace, L.G., and de Witt, W., Jr., 1978, Preliminary stratigraphic cross section showing radioactive zones in the Devonian black shales in eastern Ohio and west-central Pennsylvania: U.S. Geological Survey, Oil and Gas Investigations Chart OC-82, 1 sheet.
- Roen, J.B., and de Witt, W., Jr., 1984, Stratigraphic framework of the Devonian black shales of the Appalachian Basin: U.S. Geological Survey, Open-File Report 84-111, 71 p., plus 34 plates.
- Root, S., and Onasch, C.M., 1999, Structure and tectonic evolution of the transitional region between the central Appalachian Foreland and Interior Cratonic Basins: *Tectonophysics*, v. 305, no. 1, p. 205–223.
- Ruppert, L.F., Hower, J.C., Ryder, R.T., Levine, J.R., Trippi, M.H., and Grady, W.C., 2010, Geologic controls on thermal maturity patterns in Pennsylvanian coal-bearing rocks in the Appalachian Basin: *International Journal of Coal Geology*, v. 81, p. 169–181.
- Ryder, R.T., Hackley, P.C., Alimi, H., and Trippi, M.H., 2013, Evaluation of thermal maturity in the low maturity Devonian shales of the northern Appalachian Basin: *American Association of Petroleum Geologists Search and Discov-*

- ery Article #10477, www.searchanddiscovery.com/pdfz/documents/2013/10477ryder/ndx_ryder.pdf.html [accessed 6/18/2018].
- Ryder, R.T., Harris, D.C., Gerome, P., Hainsworth, T.J., Burruss, R.C., Lillis, P.G., Jarvie, D.M., and Pawlewicz, M.J., 2014, Evidence for Cambrian petroleum source rocks in the Rome Trough of West Virginia and Kentucky, Appalachian Basin, *in* Ruppert, L.F., and Ryder, R.T., eds., Coal and petroleum resources in the Appalachian Basin; distribution, geologic framework, and geochemical character: U.S. Geological Survey Professional Paper 1708, chapter G.8, 36 p., doi:dx.doi.org/10.3133/pp1708G.8.
- Sageman, B.B., Murphy, A.E., Werne, J.P., Ver Straeten, C.A., Hollander, D.J., and Lyons, T.W., 2003, A tale of shales: The relative roles of production, decomposition, and dilution in the accumulation of organic-rich strata, Middle–Upper Devonian, Appalachian Basin: *Chemical Geology*, v. 195, no. 1, p. 229–273.
- Schieber, J., 1994, Evidence for high-energy events and shallow-water deposition in the Chattanooga Shale, Devonian, central Tennessee, USA: *Sedimentary Geology*, v. 93, no. 3, p. 193–208.
- Schieber, J., 1998, Developing a sequence stratigraphic framework for the Late Devonian Chattanooga Shale of the southeastern USA: Relevance for the Bakken Shale, *in* Christopher, J.E., Gilbo, C.F., Paterson, D.F., and Bend, S.L., eds., Eighth International Williston Basin Symposium: Saskatchewan Geological Society Special Publication 13, p. 58–68.
- Schieber, J., and Riciputi, L., 2004, Pyrite ooids in Devonian black shales record intermittent sea-level drop and shallow-water conditions: *Geology*, v. 32, no. 4, p. 305–308.
- Schmoker, J.W., 1980, Determination of organic-matter content of Appalachian Devonian shales from gamma-ray logs: *American Association of Petroleum Geologists Bulletin*, v. 65, p. 1285–1295.
- Schoell, M., 1983, Genetic characterization of natural gases: *American Association of Petroleum Geologists Bulletin*, v. 67, p. 225–238.
- Schoenherr, J., Littke, R., Urai, J.L., Kukla, P.A., and Rawahi, Z., 2007, Polyphase thermal evolution in the Infra-Cambrian Ara Group (South Oman Salt Basin) as deduced by maturity of solid reservoir bitumen: *Organic Geochemistry*, v. 38, p. 1293–1318.
- Seifert, W.K., and Moldowan, J.M., 1986, Use of biomarkers in petroleum exploration, *in* Johns, R.B., ed., *Methods in geochemistry and geophysics*: Amsterdam, Elsevier, v. 24, p. 261–290.
- Shanmugam, G., 1985, Significance of coniferous rain forests and related organic matter in generating commercial quantities of oil, Gippsland Basin, Australia: *American Association of Petroleum Geologists Bulletin*, v. 69, p. 1241–1254.
- Shumaker, R.C., 1980, Porous fracture facies in the Devonian shales of eastern Kentucky and West Virginia, *in* Wheeler, R.L., and Dean, C.S., eds., *Proceedings, Western Limits of Detachment and Related Structures in the Appalachian Foreland*: Geological Society of America, Southeastern Section, annual meeting, Chattanooga, Tenn.: U.S. Department of Energy, Morgantown Energy Technology Center, DOE/METC/SP-80/23, p. 124–132.
- Shumaker, R.C., 1993, Structural parameters that affect Devonian shale gas production in West Virginia and eastern Kentucky, *in* Roen, J.B., and Kepferle, R.C., eds., *Petroleum geology of the Devonian and Mississippian black shale of eastern North America*: U.S. Geological Survey Bulletin, v. 1909, p. K1–K38.
- Shumaker, R.C., 1996, Structural history of the Appalachian Basin, *in* Roen, J.B., and Walker, B.J., eds., *The atlas of major Appalachian gas plays*: West Virginia Geological and Economic Survey Publication V-25, p. 8–25.
- Sitler, J.A., 1979, Effects of source material on vitrinite reflectance: Morgantown, West Virginia University, master's thesis, 108 p.
- Sneider, J.S., and Bolger, G.W., 2008, Understanding porosity and permeability using high-pressure MICP data: Insights into hydrocarbon recovery: *American Association of Petroleum Geologists Search and Discovery Article 40345*.
- Snowdon, L.R., 1995, Rock-Eval T_{max} suppression: Documentation and amelioration: *American*

- Association of Petroleum Geologists Bulletin, v. 79, no. 9, p. 1337–1348.
- Sofer, Z., 1984, Stable carbon isotope compositions of crude oils: Application to source depositional environments and petroleum alteration: American Association of Petroleum Geologists Bulletin, v. 68, p. 31–49.
- Stach, E., Mackowsky, M.Th., Teichmüller, M., Taylor, G., Chandra, D., and Teichmüller, R., 1982, Stach's text book of coal petrology: Berlin, Gebruder Borntraeger, 535 p.
- Stahl, W.J., 1978, Source rock–crude oil correlation by isotopic type-curves: *Geochimica et Cosmochimica Acta*, v. 42, p. 1573–1577.
- Tang, Y., Perry, J.K., Jenden, P.D., and Schoell, M., 2000, Mathematical modeling of stable carbon isotope ratios in natural gases: *Geochimica et Cosmochimica Acta*, v. 64, p. 2673–2687.
- Tankard, A.J., 1986, Depositional response to foreland deformation in the Carboniferous of eastern Kentucky: American Association of Petroleum Geologists Bulletin, v. 70, p. 853–868.
- Teichmüller, M., 1974, Über neue Macerale der Liptinit-Gruppe und die Entstehung des Micrinit: *Fortschritte Geologisches Rheinland und Eestfalen*, v. 24, p. 37–64.
- Tissot, B.P., Pelet, R., and Ungerer, P.H., 1987, Thermal history of sedimentary basins, maturation indices, and kinetics of oil and gas generation: American Association of Petroleum Geologists Bulletin, v. 71, p. 1446–1466.
- Tissot, B.P., and Welte, D.H., 1984, Petroleum formation and occurrence [2d ed.]: Berlin, Springer, 699 p.
- Tomastik, T., 1996, Play MDe; Lower Mississippian–Upper Devonian Berea and equivalent sandstones, in Roen, J.B., and Walker, B.J., eds., The atlas of major Appalachian gas plays: West Virginia Geological and Economic Survey Publication V-25, p. 56–62.
- Van Beuren, V.V., and Pryor, W.A., 1981, Sunbury Shale of central Appalachian Basin—Depositional model for basinal black shales: American Association of Petroleum Geologists Bulletin, v. 65, p. 1003–1004.
- Volkman, J.K., 1986, A review of sterol markers for marine and terrigenous organic matter: *Organic Geochemistry*, v. 9, p. 83–99.
- Wallace, L.G., Roen, J.B., and de Witt, W., Jr., 1977, Preliminary stratigraphic cross section showing radioactive zone in the Devonian black shales in the western part of the Appalachian Basin: U.S. Geological Survey Oil and Gas Investigations Chart 80, 1 sheet.
- Wenger, L.M., and Baker, D.R., 1987, Variations in vitrinite reflectance with organic facies—Examples from Pennsylvanian cyclothem of the Midcontinent, U.S.A.: *Organic Geochemistry*, v. 11, p. 411–416.
- Woodward, H.P., 1961, Preliminary subsurface study of southeastern Appalachian interior plateau: American Association of Petroleum Geologists Bulletin, v. 45, no. 10, p. 1634–1655.
- Zhu, Y., Shi, B., and Fang, C., 2000, The isotopic compositions of molecular nitrogen: Implications on their origins in natural gas accumulations: *Chemical Geology*, v. 164, p. 321–330.
- Zielinski, R.E., and McIver, R.D., 1982, Resource and exploration assessment of the oil and gas potential in the Devonian shales of the Appalachian Basin: U.S. Department of Energy, Morgantown Energy Technology Center, DOE/DP/0053-1125, MLM-MU-82-61-0002, 423 p.

Field Trip

Petroleum Geology of the Bedford-Berea Petroleum System

Stephen Greb and Cortland Eble



April 26, 2016

Contents

Introduction.....	147
Stop 1 – Distal Petroleum System (Farmers Exit).....	149
Cleveland Shale Member, Ohio Shale.....	149
Bedford Shale.....	151
Sunbury Shale.....	151
Stop 2 – Submarine Channel in Bedford Slope (Ky. 59).....	153
Stop 3 – Margin of the Berea Shelf (Ky. 9 – AA Highway).....	155
Road Between Stops 3 and 4.....	157
Stop 4 – Sheet Sandstones and Bedding of the Berea Shelf (Ky. 9 – AA Highway).....	157
Stop 5 – The Berea-Sunbury Contact (Ky. 10).....	159
Stop 6 – Sheet Sandstones and Vertical Bed Stacking (Ky. 10).....	160
Stop 7 – Sheet Sandstones and Horizontal Continuity (Ky. 10).....	162
References Cited.....	164

Figures

FT-1. Stratigraphic correlation of units in the Berea petroleum system.....	147
FT-2. Diagram of the Berea petroleum system.....	148
FT-3. Interpretation of depositional systems and presumed lateral stratigraphic relationships for elements of the Berea petroleum system.....	149
FT-4. Map of net isopach thickness of the Berea Sandstone in eastern Kentucky showing location of the stops for this field trip.....	150
FT-5. Strike section along the outcrop margin showing the Ohio Shale.....	151
FT-6. Measured section of the Cleveland through Sunbury Shale at the Farmers stop.....	152
FT-7. Photograph illustrating inferred repeated section and thrust positions of dark shale interbedded with gray shale in the lower Bedford Shale at stop 1.....	153
FT-8. A. Photomosaic of channel at the base of the Berea on Ky. 59. B. North end of the outcrop with Cleveland Shale Member beneath Berea channel scour. C. Large shale clasts in lower part of the Berea above the basal scour.....	155
FT-9. Bedding in typical submarine channel and fan facies from proximal to distal position.....	156
FT-10. Examples of logs with a basal fining-upward section, which might be possible channels similar to the one at this stop.....	157
FT-11. Measured section of Bedford-Berea interval at stop 3.....	158
FT-12. Photograph of the Bedford and Berea at stop 3.....	159
FT-13. A. Contact of the Sunbury Shale with the Berea Sandstone at stop 4. B. Berea sheet sandstones beneath the contact. C. Detail of sharp-based hummocky, massive, and deformed beds.....	160
FT-14. A. Sunbury Shale contact with the upper Berea at stop 5. B. Detail of the contact. C. The underlying beds are dominated by hummocky, swaley, and massive, scour-based storm beds.....	161
FT-15. Photograph of large outcrop of Berea on south side of Ky. 10 near Spyrun Cemetery Road.....	163
FT-16. A. Large flow rolls and B. soft-sediment deformation just above road level at stop 7....	164
FT-17. Photographs of bedding in sheet sandstones at stop 7.....	165
FT-18. Photomosaic of lower bench at road level in part of the north end of the outcrop.....	166
FT-19. Geophysical log through the Bedford-Berea interval from a well 2.6 mi east of milepost 15 on Ky. 10.....	167

Figures (Continued)

FT-20. Conceptual models to explain Bedford-Berea thickness trends westward toward Cincinnati Arch.....	168
FT-21. Conceptual models to explain Bedford-Berea thickness trends southward across the Kentucky River Fault System.....	169

Tables

FT-1. Geochemistry and thermal-maturity parameters for shale units at stop 1	154
FT-2. Geochemistry and thermal-maturation parameters for shale units at stop 2	154
FT-3. Geochemistry and thermal-maturity parameters for shale units at stop 2	160
FT-4. Geochemistry and thermal-maturity parameters for the Sunbury Shale at stop 5	162

Field Trip: Petroleum Geology of the Bedford- Berea Petroleum System

Stephen F. Greb and Cortland F. Eble

Introduction

The purpose of this field trip is to show participants regional changes in the Bedford-Berea interval and typical bedding features in the Berea, for comparison to well logs and cores featured in the core workshop.

The Berea Sandstone is the latest Devonian unit in eastern Kentucky (Fig. FT-1). Both the Bedford Shale and Berea Sandstone were once considered part of the lowest Mississippian, but fossil plant spores from the Bedford subsequently indicated a Late Devonian age (Molyneux and others, 1984; Coleman and Clayton, 1987). Although termed "Sandstone," the Berea in eastern Kentucky is actually a siltstone across much of its extent. Berea sandstones and siltstones complexly

intertongue with and grade laterally into the Bedford shales (Pepper and others, 1954; Pashin and Ettensohn, 1987, 1992, 1995), and were mapped together at the surface in many 7.5-minute geologic quadrangle maps (e.g., Morris and Pierce, 1967; McDowell, 1986).

Figure FT-2 shows the general stratigraphic relationships of much of the Berea petroleum system. Members of the Ohio Shale can be divided into black, organic-rich (Lower Huron, Upper Huron, and Cleveland) and still black, but less organic-rich (Middle Huron, Three Lick Bed) shales. The Bedford-Berea is also overlain by the organic-rich Sunbury Shale (Fig. FT-2). As discussed in the core workshop, the high-TOC, high-organic shales are potential sources for Berea reservoirs.

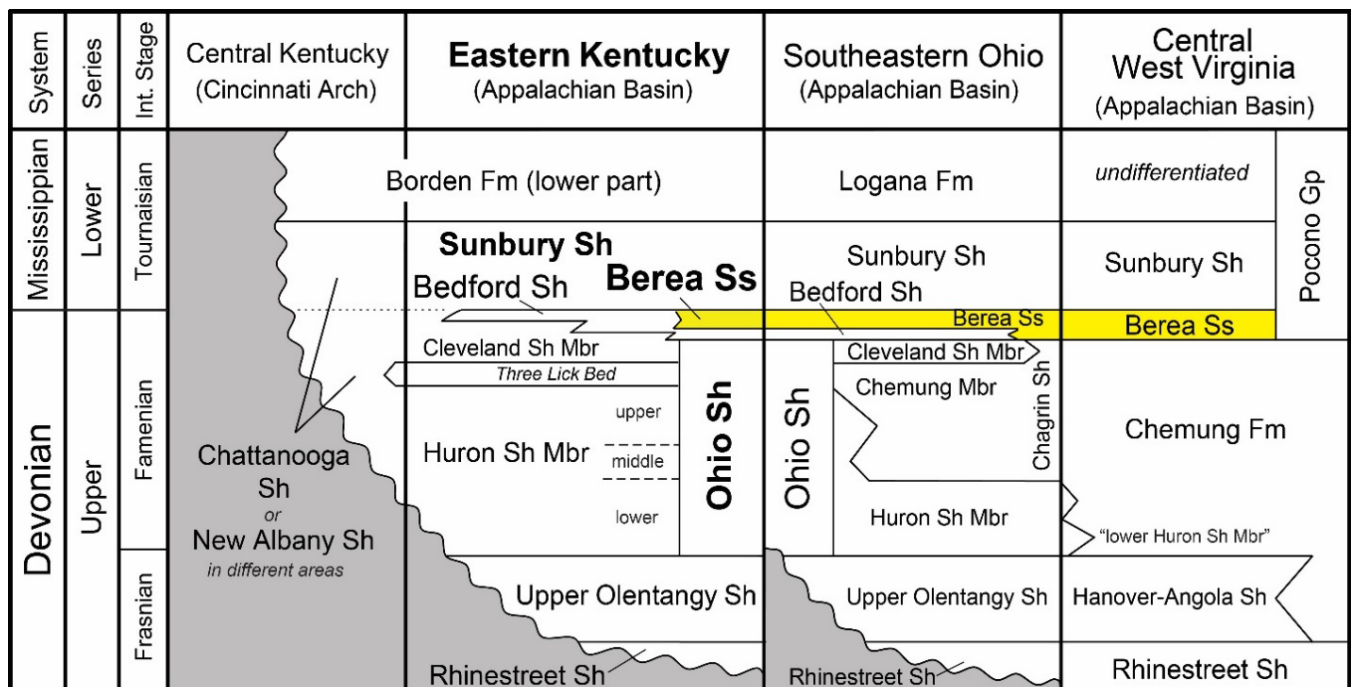


Figure FT-1. Stratigraphic correlation of units in the Berea petroleum system.

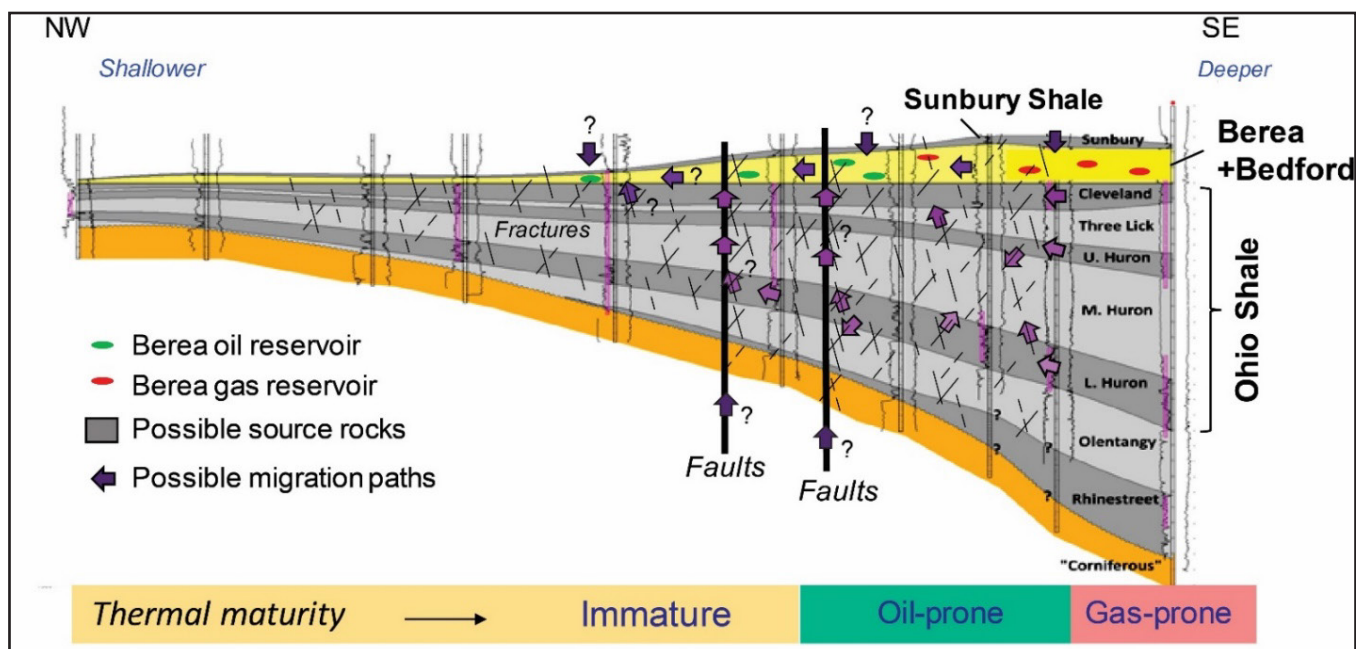


Figure FT-2. Diagram of the Berea petroleum system. Hydrocarbons in Berea reservoirs may be sourced from the Ohio or Sunbury Shales.

Pashin and Ettensohn (1995) have modeled the Bedford-Berea as an outer marine-shelf sand prograding westward and southward (Fig. FT-3). Slope facies are equivalent to the Bedford Shale, which grades downdip into black shales. The black shales of the Ohio and Sunbury Shales were deposited in relatively deep anoxic waters (Rhoads and Morse, 1971; Potter and others, 1980b; Ettensohn and Barron, 1981; Ettensohn and Elam, 1985; Ettensohn and others, 1988; Kepferle, 1993). Each of the organic members pinches out or grades laterally into progressively less organic-rich black and gray silty shales of the Chemung and Chagrin Formations to the east. The Middle Huron and Three Lick Bed represent distal tongues of the Chemung and Chagrin Formations, which are the distal parts of the Catskill Delta Complex or clastic wedge (Provo and others, 1978; Wallace and others, 1977; Kepferle and others, 1978; Roen and others, 1978; Roen, 1984; Kepferle, 1993). The Bedford-Berea interval represents another part of that clastic wedge. In eastern Kentucky, Bedford gray and green-gray shales intertongue with and grade southward and westward into black Bedford shales and then into black, organic-rich shales of the Cleveland Shale Member of the Ohio Shale (Ettensohn and Elam, 1985). The Bedford is interpreted to represent distal deltaic or lower slope deposits seaward of the

Berea marine shelf (Potter and others, 1983; Pashin and Ettensohn, 1987, 1992, 1995; Coats, 1988). It is dominated by shales and siltstones inferred to represent turbidite and distal turbidite fan deposition. The color change from black to gray-green between the Bedford and Cleveland shales, and within the distal parts of the Bedford itself, are interpreted as representing the position of a paleo-pycnocline between relatively deeper, downdip, anoxic water and shallower, updip, dysaerobic waters (Ettensohn and Elam, 1985; Pashin and Ettensohn, 1987, 1992, 1995). Where Bedford gray shales can no longer be detected westward, the underlying Ohio Shale and overlying Sunbury Shale cannot be differentiated and are equivalent to the Upper Devonian-Lower Mississippian New Albany Shale of the Illinois Basin.

The Berea intertongues with and grades laterally into Bedford shales (Fig. FT-3). The combined Bedford-Berea interval is thickest in northeastern Kentucky and thins laterally from an elongate belt extending from Greenup County southwestward into Pike County. The Berea is dominated by sheet-form sandstones and siltstones with hummocky, swaley, and massive bedding in outcrops, suggestive of storm-influenced, shallow marine shelf environments (Pepper and others, 1954; Potter and others, 1983; Pashin and Ettensohn, 1987, 1992,

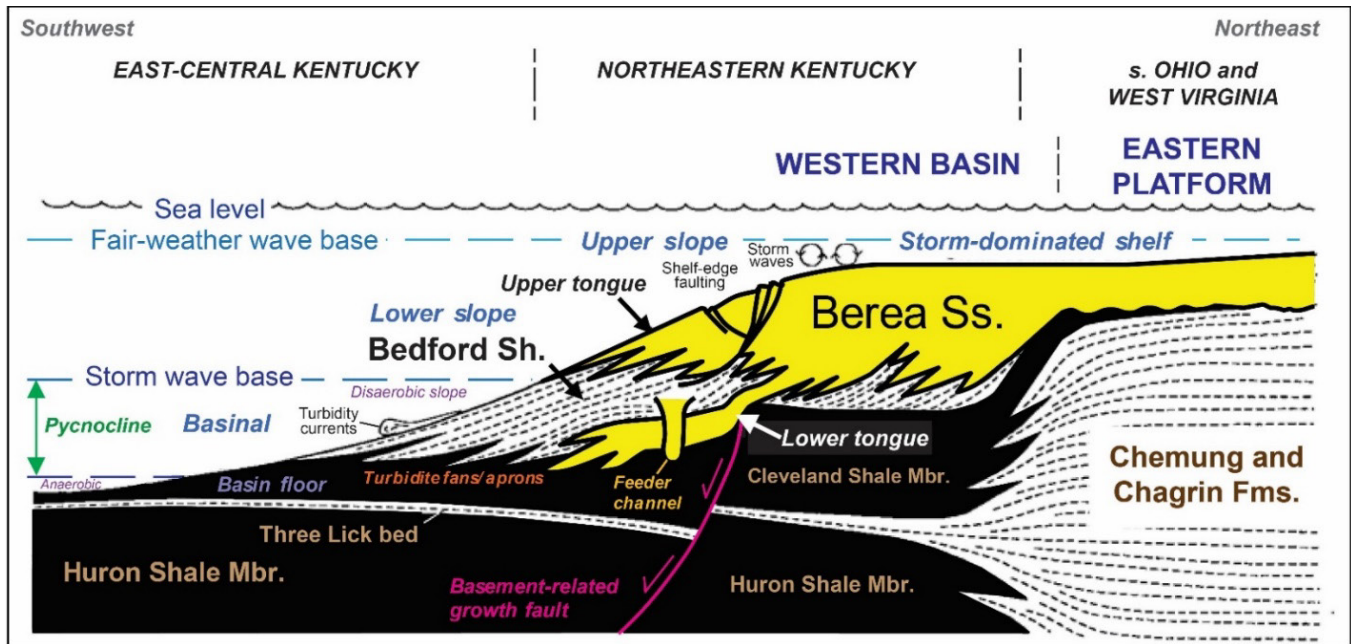


Figure FT-3. Interpretation of depositional systems and presumed lateral stratigraphic relationships for elements of the Berea petroleum system. Modified from Pashin and Ettensohn (1995, Fig. 49); used with permission of the Geological Society of America. The Sunbury Shale would cap the units shown.

1995; Coats, 1988). In parts of the Lewis County outcrop belt, the Berea can be divided into two tongues separated by and underlain by Bedford shales (Morris and Pierce, 1967; McDowell, 1986). Southward, upper and lower tongues of the Berea have also been recognized in some Berea oil fields in Lawrence and Johnson Counties. Pashin and Ettensohn (1987) showed this as a response to faulting (Fig. FT-3), although eustatic and sedimentation changes (including migrating clinofolds) may also have influenced the stratigraphy.

This field trip will highlight roadcut exposures in northeastern Kentucky. The position of the stops relative to net Berea thickness shown in the core workshop yesterday and in the final report are shown in Figure FT-4. Figure FT-5 is a generalized cross section of subsurface logs near the outcrop belt between stops 1 and 2. We will start the trip just southwest of the pinchout of Berea beneath the Sunbury Shale near Farmers, Ky., and end (stop 7) at thick exposures of Berea near Garrison, Ky.

Stop 1—Distal Petroleum System (Farmers Exit)

The Farmers outcrop is located on Ky. 801 at milepost 12.5, 1.9 mi south of Interstate 64 (Farmers exit). The outcrop has been featured in many field

guides. It is a good spot to start a Berea petroleum system field trip because at this one stop we can see the Ohio through Sunbury Shales (and overlying Borden members). Our focus at this stop is to look at the organic-rich black shales bounding the Bedford-Berea interval.

Cleveland Shale Member, Ohio Shale

The base of the outcrop is the Cleveland Shale Member (Upper Devonian). The Cleveland here is 4.25 m thick (Fig. FT-6). This shale is brown-black to black, fissile, and silty, like other underlying Ohio Shale members. The shale contains scattered pyritic nodules (sulfur blooms sometimes in outcrop) with occasional siderite and phosphate nodules. It is a gas producer deeper in the basin and is a potential source of oil and gas for the Berea.

Ettensohn and others (2009) noted several tongues of black shale in the lower part of the Bedford at this location (Fig. FT-7). They noted slickensides along the contacts of the black shales with more typical gray and gray-green shales of the Bedford, and interpreted the tongues as low-angle thrust faults. The inferred thrusts strike at approximately N74°E and dip at an angle of about 5° to the north, and the lower thrust appears to be displaced up and over gray Bedford Shale. Ettensohn and

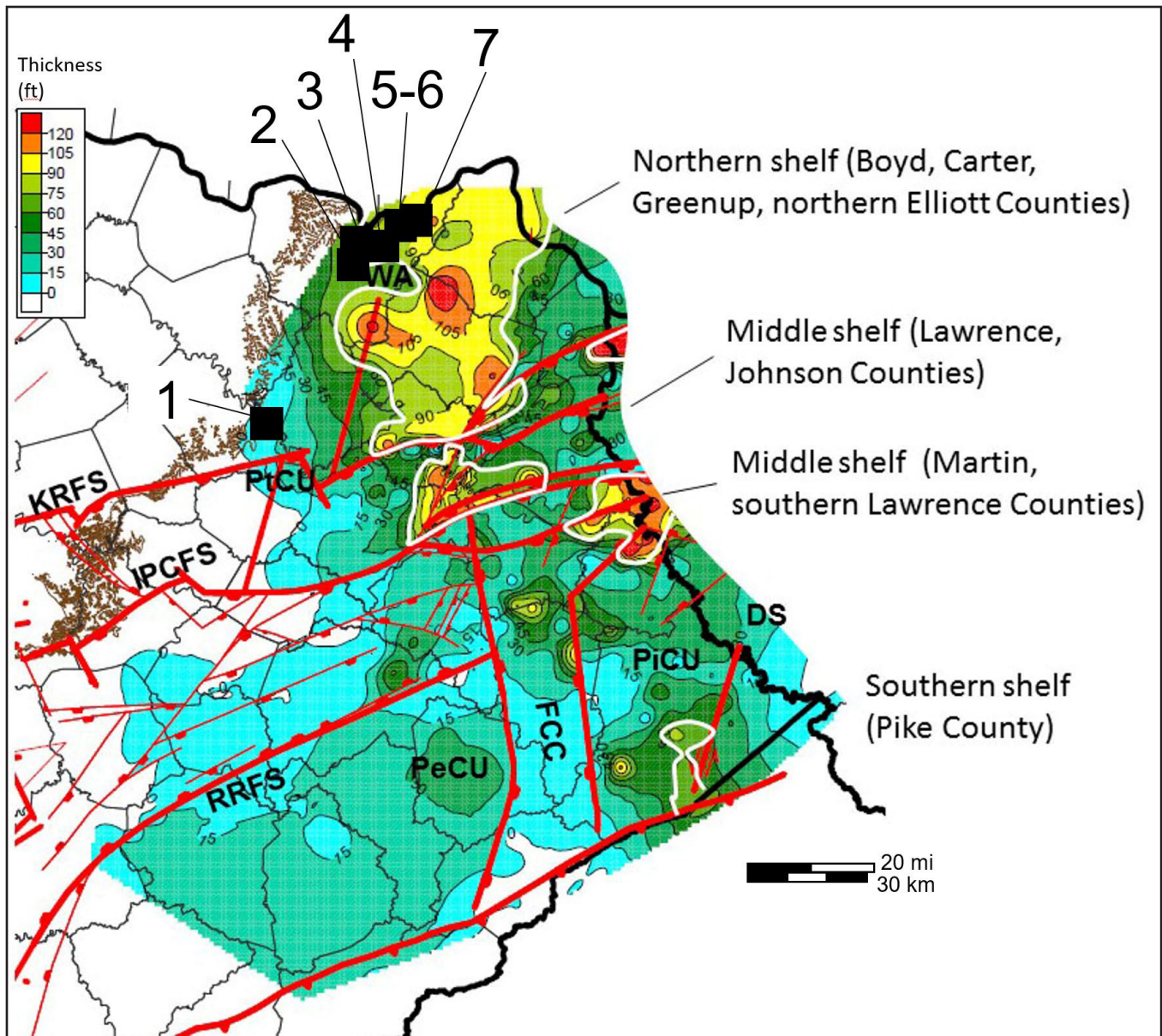


Figure FT-4. Net isopach thickness of the Berea Sandstone in eastern Kentucky (from Floyd, 2015; used with permission) showing location of the stops for this field trip. All of the stops are in the northern shelf area, north of the Kentucky River Fault System. DS=D'Inwilliers Structure. FCC=Floyd County Channel. KRFS=Kentucky River Fault System. IPCFS=Irvine–Paint Creek Fault System. PeCU=Perry County Uplift. PiCU=Pike County Uplift. PtCU=Paint Creek Uplift. RRFS=Rockcastle River Fault System. WA=Waverly Arch.

others (2009) interpreted these structures as a subsurface response to growth faulting along nearby basement structures at depth or mass movement from another dimension. Since tectonic thrusts have not been reported in this area, a mass movement along low-angle beds (possibly clinoforms) and interfingering of the basal Bedford Shale and upper Cleveland Shale Member of the Ohio Shale seems more likely. Apparent thrusting may repre-

sent local post-depositional movement from loading along sedimentary interbeds of black shale.

Ettensohn and Elam (1985) noted regional interfingering of the Bedford gray shale downdip (to the west and south) into black Bedford shales and then into the Cleveland Shale. Similar interfingering was noted in subsurface geophysical logs by Floyd (2015). Along the outcrop belt to the south, typical Bedford gray shales pinch out and only

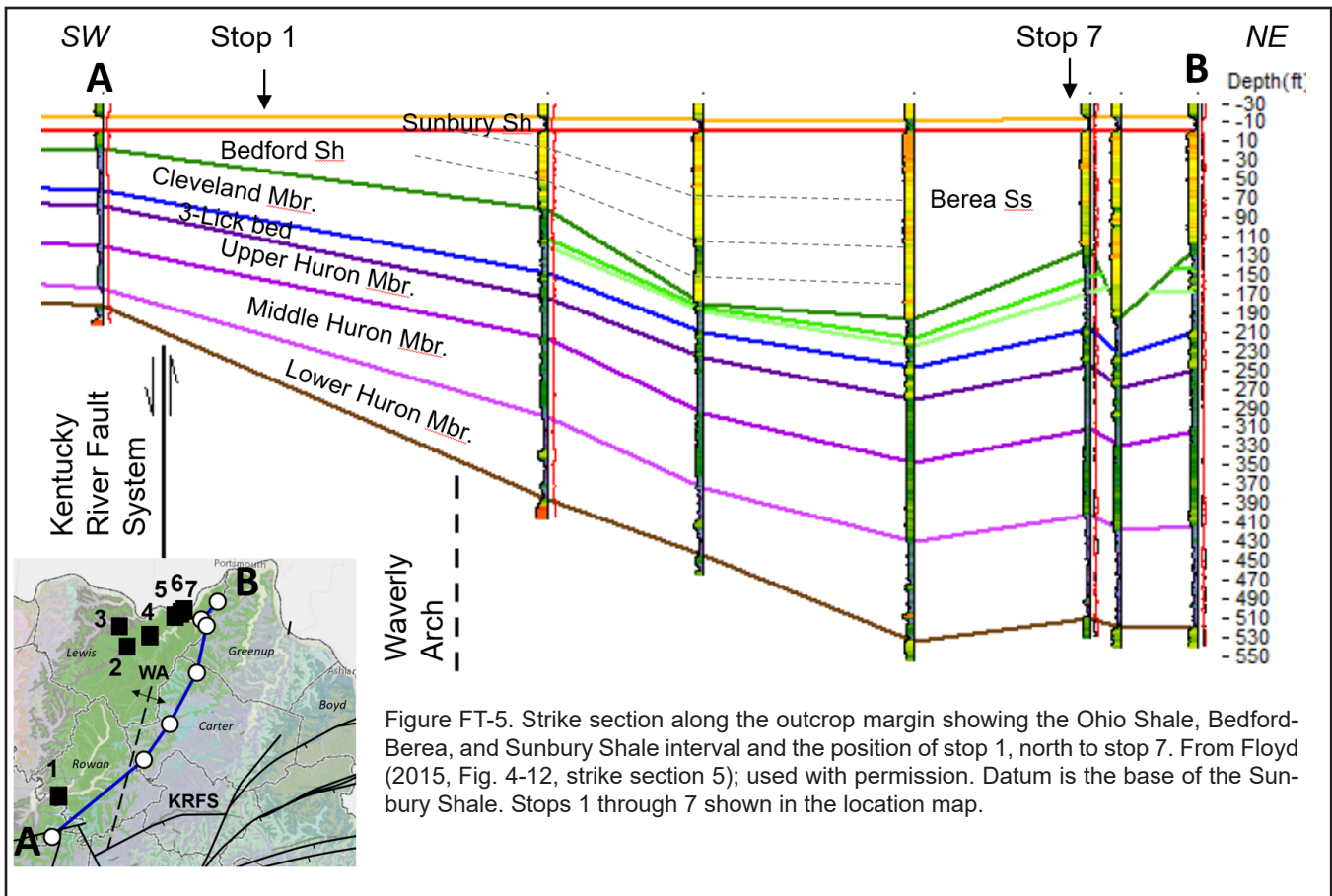


Figure FT-5. Strike section along the outcrop margin showing the Ohio Shale, Bedford-Berea, and Sunbury Shale interval and the position of stop 1, north to stop 7. From Floyd (2015, Fig. 4-12, strike section 5); used with permission. Datum is the base of the Sunbury Shale. Stops 1 through 7 shown in the location map.

“black Bedford” is observed. The black Bedford can be differentiated from the overlying Sunbury and underlying Cleveland Shale Member of the Ohio Shale on gamma logs, but in outcrop or core, it looks very similar to typical black shales. The Somerset Morelandbell well in Leslie County is a good example of this black Bedford facies. Interfingering of the black Bedford or Cleveland Shale with typical gray and black shales of the lower Bedford can be seen in many geophysical logs.

Bedford Shale

The Bedford Shale here is 26ft thick. There is no Berea at this locality because the location is on the margin of the Berea pinchout (Fig. FT-4). The Bedford Shale here is gray to gray-green and similar in appearance to some of the Bedford interbeds seen in Berea cores. As we head north and east today, the Bedford-Berea interval will increase in thickness dramatically (Figs. FT-4, FT-5), but the lithology remains similar. The contact of the Bedford with the Sunbury Shale at this location is marked by a thin, (5.5cm), discontinuous, cone-

in-cone limestone laminae. Stylolites are also associated with these cone-in-cone structures, which indicates that the layer was produced by pressure solution along the contact. Iron-staining and pyrite are also common in the Bedford beneath the Sunbury Shale. We will see this contact later in the day where the Sunbury rests on the Berea.

Sunbury Shale

The Sunbury Shale is the basal Mississippian unit in eastern Kentucky. It is a more tabular unit (regionally) than the underlying members of the Ohio Shale, which dramatically thicken to the east. Here the Sunbury is 4.75m thick. The contact is sharp with the underlying Bedford Shale. A thin (1.5cm) “lag” lies above the contact and contains both pyritized and phosphatic fossil remains, including inarticulate linguloid and orbiculoid brachiopods, a variety of conodonts, as well as phosphatic fish debris including teeth, scales, spines, and broken dermal plates (Ettensohn and others, 2009). The basal lag is common along the outcrop belt (Pepper and others, 1954; Ettensohn and oth-

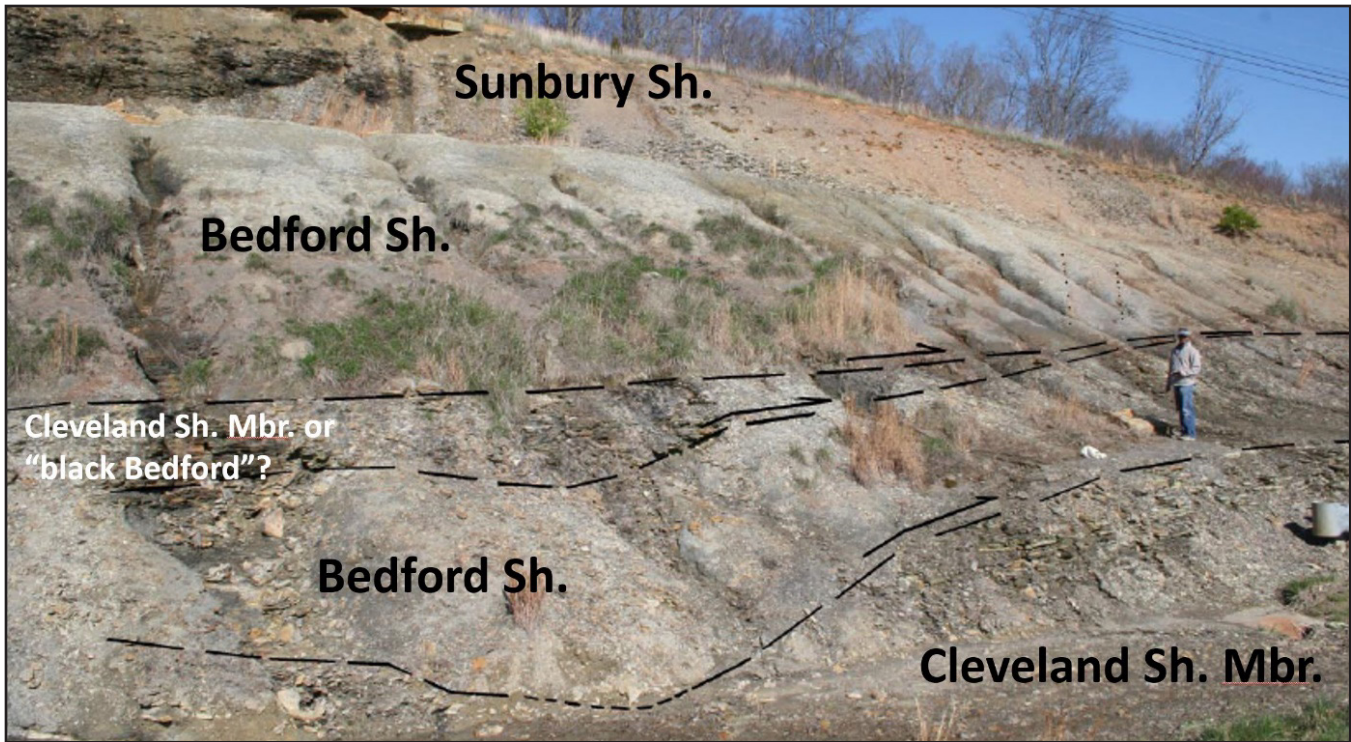


Figure FT-7. Inferred repeated section and thrust positions of dark shale interbedded with gray shale in the lower Bedford Shale at stop 1. Unit names are added to show possible interfingering of basal Bedford Shale with the Cleveland Shale Member. From Ettensohn and others (2009, Fig. 22). American Institute of Professional Geologists–Kentucky Section © 2009; used with permission.

ers, 2009), and can be seen in some cores. Ettensohn (1994) suggested the contact is a major regional unconformity, so there may be considerable erosion along the surface. In most outcrops and cores, however, the lag is very thin and very fine grained (medium to coarse silt).

Another interesting feature noted at this outcrop of the Sunbury is oil-staining along the side of the road. We are wary of assigning oil-staining along the side of a road to an outcrop source, but on several trips, at different times of the year, oil-staining was noted in waters at the base of the Sunbury outcrop. As shown in Table FT-1, the Sunbury Shale has an average total organic carbon of 14.5 percent, an average total sulfur content of 1.6 percent, and an average vitrinite reflectance (VR_o) of 0.52 percent. The underlying Cleveland Shale Member has an average TOC of 14.4 percent, an average total sulfur content of 1.4 percent, and an average VR_o of 0.54 percent. By comparison, the Three Lick Bed, sampled at its type location nearby, has an average TOC of 9.1 percent, an average

total sulfur content of 0.7 percent, and an average vitrinite reflectance of 0.55 percent.

Stop 2—Submarine Channel in Bedford Slope (Ky. 59)

Stop 2 is located on Ky. 59 near Vanceburg, Ky. From stop 1, travel north back to I-64. Take I-64 east to Morehead, Ky. (4 mi). Exit onto Ky. 32 and head north 1.1 mi to Ky. 377 (Cranston Road). Take Ky. 377 to Ky. 344 (23.8 mi). Turn right (north) and drive 4.6 mi to Ky. 59. Travel 1 mi north on Ky. 59 to milepost 19.1 to stop 2.

This stop highlights the only known Berea channel deposit in eastern Kentucky. It has been discussed in several field guides and reports. The base of the Berea here is sharp and scour-form. Black shale can be seen in a “high” along the scour and in rip-up clasts within the lower Berea. The top of the Ohio Shale was mapped in the nearby creek (just below road level) on the Vanceburg 7.5-minute geologic quadrangle map (Morris and Pierce, 1967), although it is not currently visible in the creek. As shown in Table FT-2, a sample of the

Interval ID	Total Carbon	Total Inorganic Carbon	Total Organic Carbon	Total Sulfur	Average VR _o	Standard Deviation
Sunbury Shale (top)	15.01	0.00	15.01	1.61	0.53	0.03
Sunbury Shale (middle)	14.01	0.00	14.01	1.52	0.51	0.03
Sunbury Shale (base)	14.54	0.00	14.54	1.56	0.51	0.03
Average	14.52	0.00	14.52	1.56	0.52	0.03
Cleveland Shale Member (top)	13.14	0.00	13.14	1.73	0.54	0.04
Cleveland Shale Member (middle)	15.72	0.03	15.69	0.96	0.54	0.04
Average	14.43	0.02	14.42	1.35	0.54	0.04
Three Lick Bed (top)	9.80	0.00	9.80	0.56	0.55	0.04
Three Lick Bed (middle)	10.64	0.00	10.64	0.78	0.55	0.04
Three Lick Bed (base)	6.87	0.00	6.87	0.66	0.55	0.03
Average	9.10	0.00	9.10	0.67	0.55	0.04

Interval ID	Total Carbon	Total Inorganic Carbon	Total Organic Carbon	Total Sulfur	Average VR _o	Standard Deviation
Cleveland Shale Member (top)	5.42	0.00	5.42	1.47	0.58	0.04

shale has a TOC of 5.4 percent, a total sulfur content of 1.5 percent, and a VR_o of 0.58 percent. The relatively high TOC and total sulfur content indicate that it is probably the Cleveland Shale Member, at the top of the Ohio Shale.

Pashin (1990) defined two lithofacies of the Berea here, which were subsequently used in several publications (Pashin and Ettensohn, 1987, 1995). The channel fill was termed the "massive siltstone facies." It was defined as a mostly structureless "sandstone." Many units in the Berea are termed "sandstone," but in this case, as in most others in northeastern Kentucky, much of this unit is coarse siltstone. It truncates and is draped by the lower sheet sandstone lithofacies. Figure FT-8A is a photomosaic of the outcrop and an interpretation of bedding within the channel. The channel has two apparent dips in its scour (Figs. FT-8A, FT-8B). Whether this represents a single channel and scour or composite channels is uncertain. Large rip-up clasts of shale are noted above the scours (Fig. FT-8C). The fills contain many internal slumps and soft-sediment-deformation structures.

The channel is approximately 350ft wide. If this is a submarine channel on a slope or ramp,

then it was likely feeding submarine fans in the lower Berea and Bedford. The lateral lower sheet sandstone facies may represent submarine fans truncated by this channel.

Typical submarine fan facies of prograding systems coarsen upward in gamma and density logs and have beds that thicken upward. Channel fills and lateral levee and fan facies are interpreted to show variable bedding proximally to distally relative to slope position (e.g., Walker, 1978; Shanmugam and Moiola, 1988). If we compare the facies at this outcrop with the interpretive diagrams shown in Figure FT-9, what would be the relative position of this channel?

Think about what the gamma signature of this channel might look like. In the center it would likely have a relatively blocky, uniform signature, which would be flanked laterally by interdigitating signatures of the Bedford or lower sheet sandstone facies. In regional subsurface correlations of the Bedford-Berea, the basal Bedford interval tends to coarsen upward, as is typical for prograding slope systems and fan facies. A few well logs, however, have thick, blocky signatures at the base (Fig. FT-10). These likely represent submarine channels. If

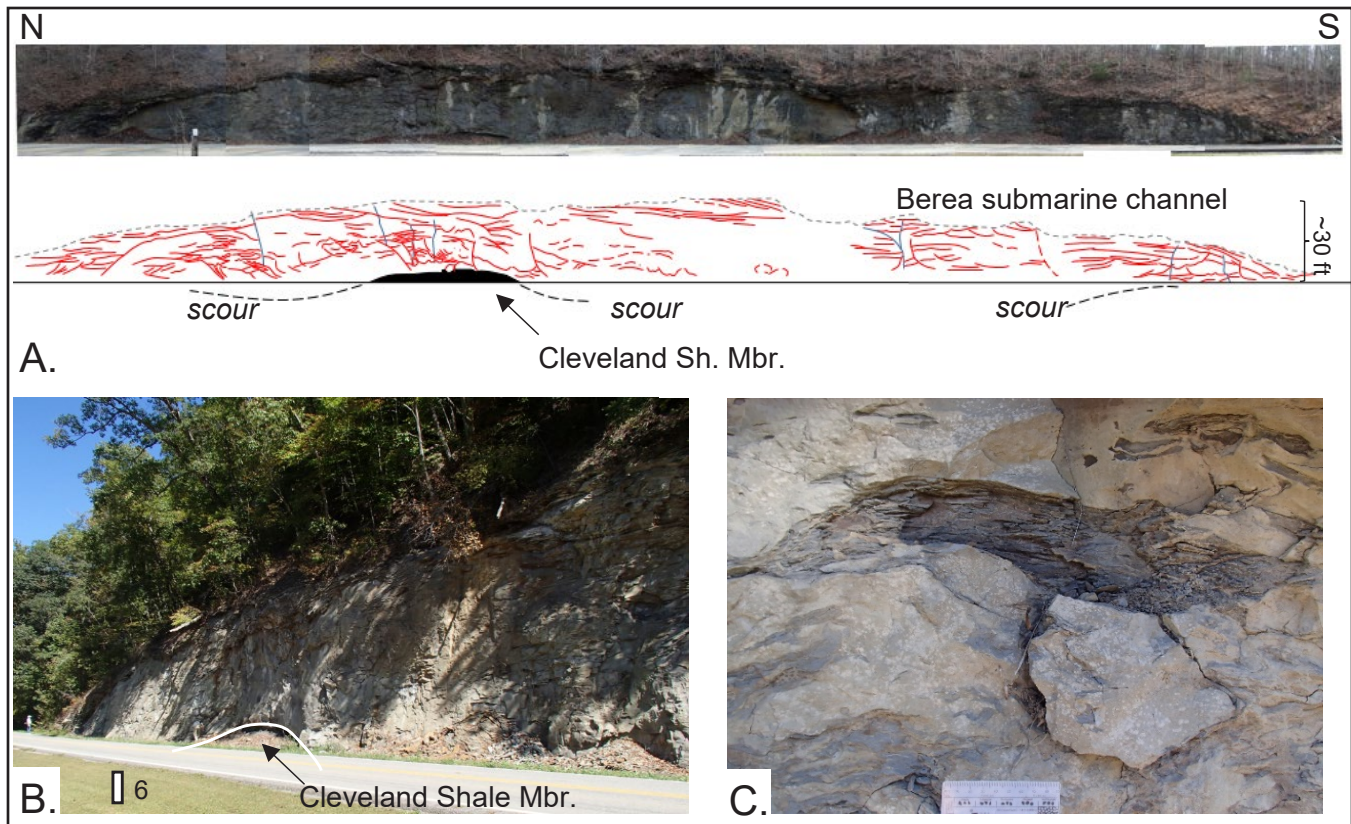


Figure FT-8. A. Photomosaic of channel at the base of the Berea on Ky. 59. Note scour with black shale remnant on north-center part of the panel and southwest-dipping lateral accretion on north end of outcrop. B. North end of the outcrop with Cleveland Shale Member beneath Berea channel scour. C. Large shale clasts in lower part of the Berea above the basal scour.

you look at the width of the channel at stop 2, and consider typical well spacing, channels of this size would commonly be missed.

Stop 3—Margin of the Berea Shelf (Ky. 9—AA Highway)

From stop 2, travel north to Ky. 9 (AA Highway) at Vanceburg. There is a gas station and McDonald's a short distance to the left (west) if anyone needs to use a restroom. From the intersection, travel east 1.5 mi. You will pass several low outcrops of Devonian Ohio Shale; then the road turns uphill. Stop 3 is an exposure of the Bedford and Berea at approximately milepost 9.8 (Figs. FT-11, FT-12).

At this stop, more typical "Berea" sheet sandstones are exposed above the Bedford Shale. The Bedford here has similar thickness as the Bedford we saw at stop 1. The difference here is that the Berea caps the Bedford. The Berea here is part of the upper sheet sandstone lithofacies of Pashin

(1990) and Pashin and Ettensohn (1987, 1995). A lower "dolomite" was reported at the base of the Bedford above the Cleveland (below road level) in the original road plans for the AA Highway. This "dolomite" is not exposed, and may have been a dolomitic sandstone. Dolomite cements are relatively common in the Berea. A lower Berea sandstone was mapped on the Vanceburg 7.5-minute geologic quadrangle map (Morris and Pierce, 1967). The main point to note here is that the Berea is 16 ft thick. It thickens dramatically eastward.

The Berea is exposed above the Bedford Shale (Figs. FT-11, FT-12). Bedding is dominated by scour-based, swaley, and hummocky bedding (HCS) and massive beds. HCS has been interpreted as a type of bedding formed by oscillatory flow (Dott and Bourgeois, 1982; Harms and others, 1982), or from combined flows (Allen, 1985; Nottvedt and Kreisa, 1987). In the Berea, HCS may be capped by combined-flow ripples, so likely represents storm-derived combined flows. Swaley bedding also occurs locally. Swaley beds are thought to

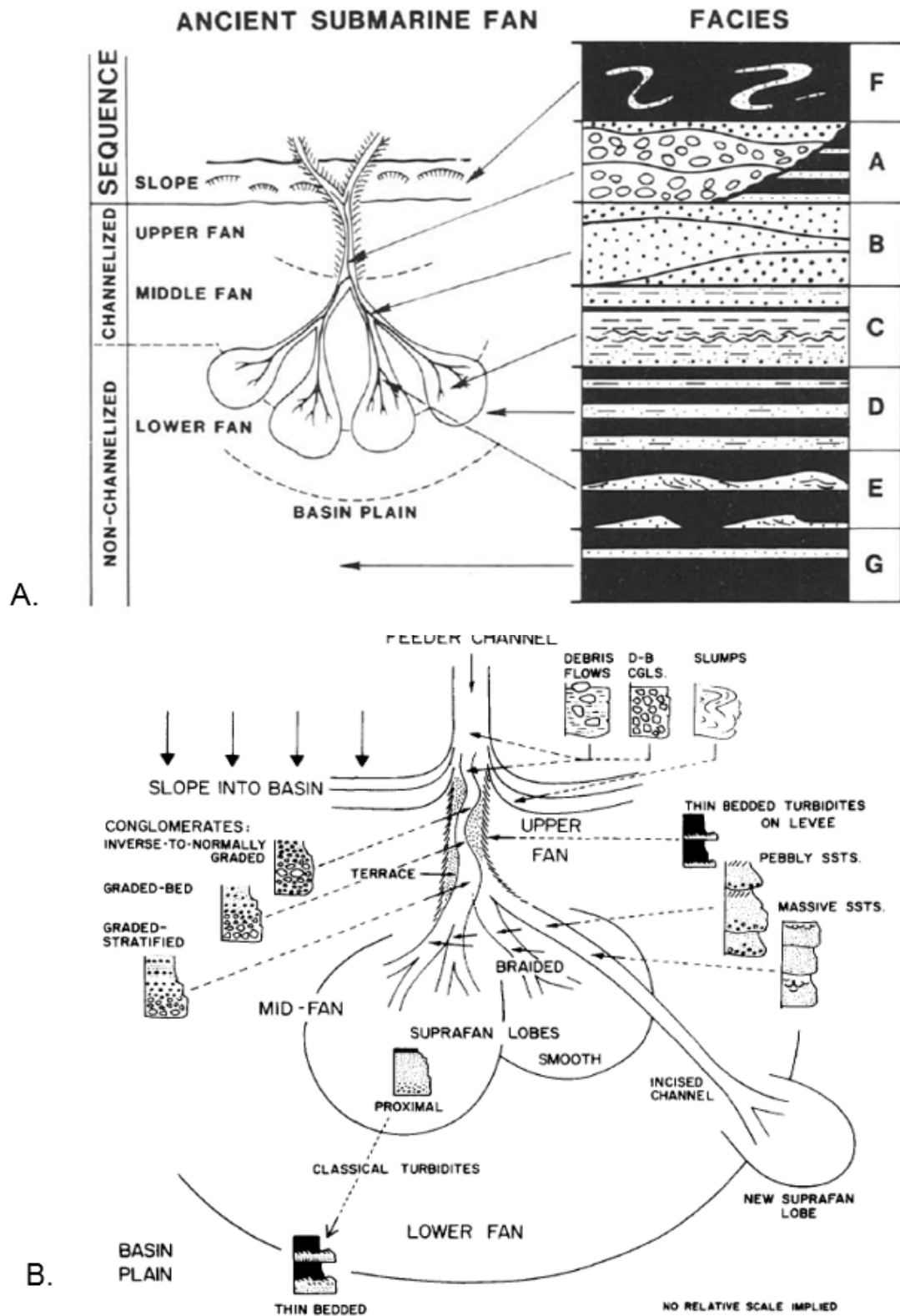


Figure FT-9. Bedding in typical submarine channel and fan facies from proximal to distal position. From (A) Shanmugam and Moiola, (1988); reprinted with permission of Earth-Science Reviews and (B) Walker (1978); American Association of Petroleum Geologists © 1978; reprinted by permission of the AAPG, whose permission is required for further use.

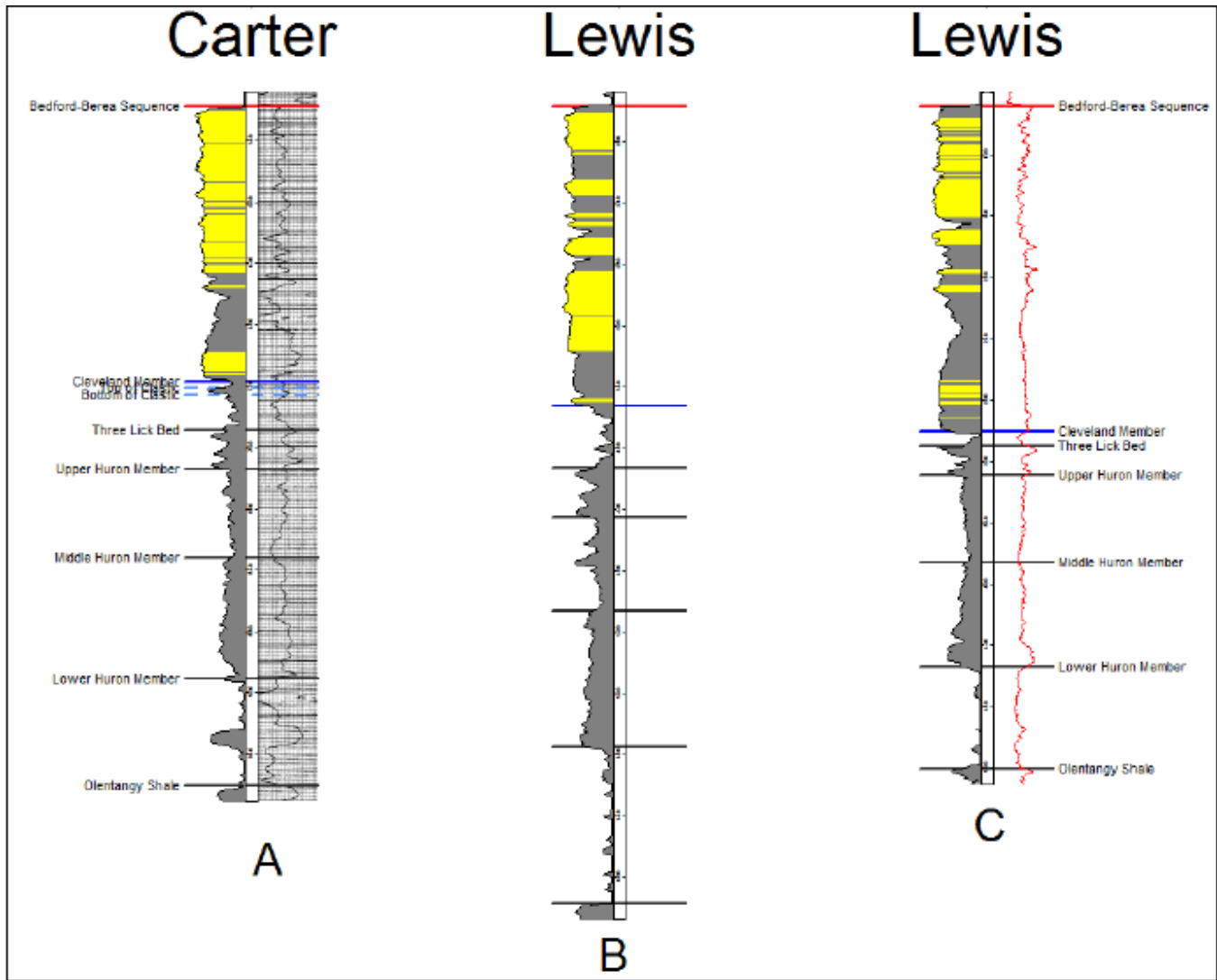


Figure FT-10. Examples of logs with a basal fining-upward section, which might be possible channels similar to the one at this stop. From Floyd (2015, Fig. 5.2); used with permission).

occur in slightly shallower water than HCS (Leckie and Walker, 1982). Pashin (1990) and Pashin and Ettensohn (1995) identified a swaley-bedded sheet sandstone facies on the interpreted Berea shelf in the Vanceburg area.

Road Between Stops 3 and 4

From stop 3 continue eastward to Birchwood Road at milepost 6.7, approximately 3 mi. As we drive between stops 3 and 4 we are generally following the base of the Borden Formation. The Henley Bed at the base of the Borden is well exposed. Note the dip of the bed and changes in bed dip.

Stop 4—Sheet Sandstones and Bedding of the Berea Shelf (Ky. 9—AA Highway)

The Birchwood Road access road is on the north side of the AA Highway. This outcrop is a good exposure for looking at the Sunbury-Berea contact and the upper part of the Berea in the upper sheet sandstone lithofacies (Fig. FT-13). The Berea here is at least 80ft thick (Figs. FT-4, FT-5). This contact is mostly covered at stop 3, but is well exposed here on both sides of the road. At Birchwood Lane you can see the upper Berea Sand-

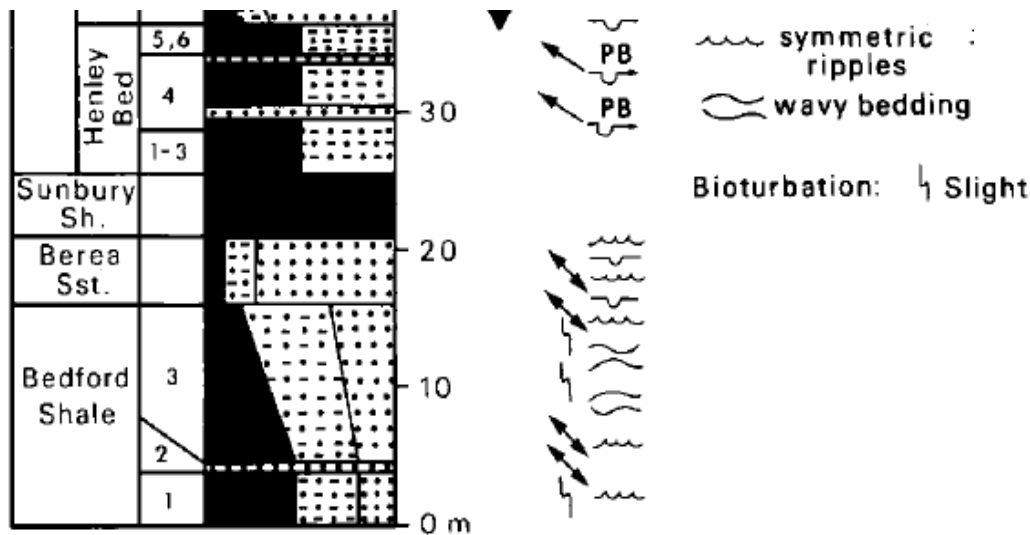
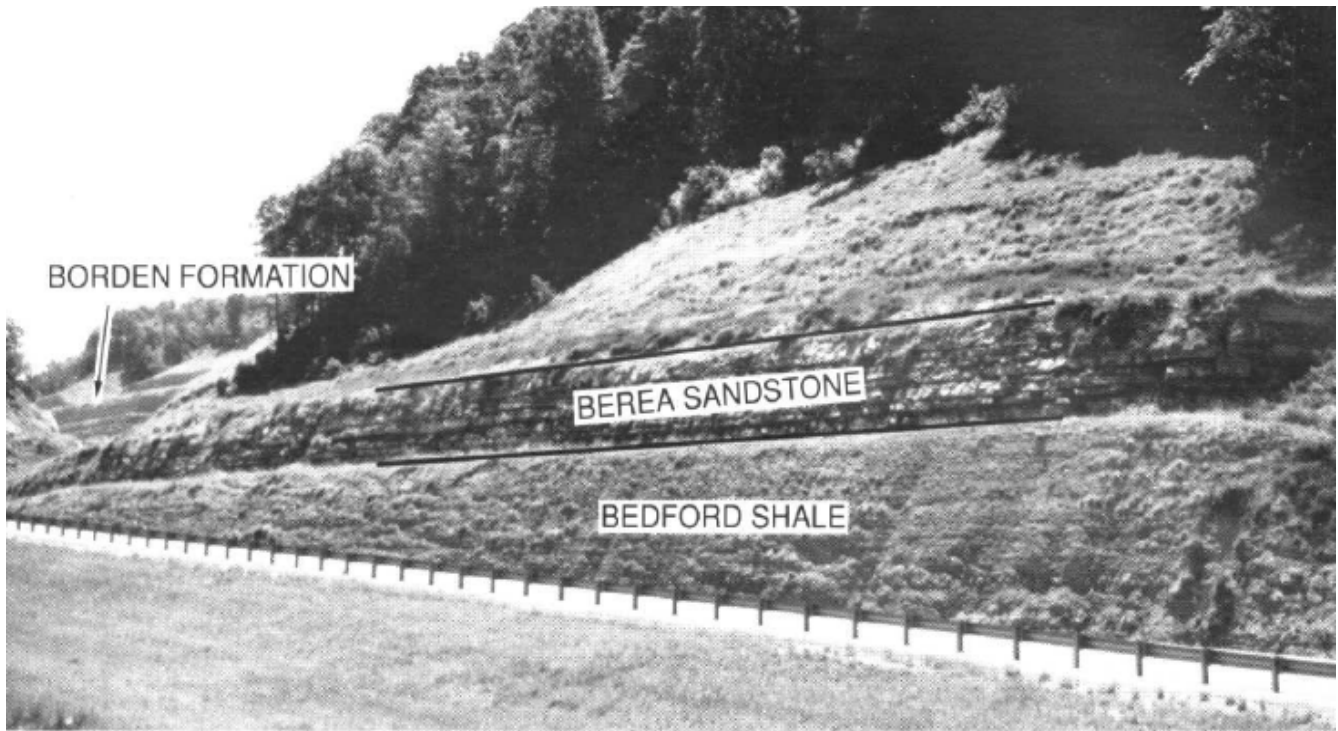


Figure FT-11. Measured section of Bedford-Berea interval at stop 3. The photograph is shown to illustrate what the roadcut looked like prior to vegetation. From Potter and others, 1980a; Geological Society of Kentucky © 1980; used with permission.

stone, Sunbury Shale, and lower Borden Formation (including the basal Henley bed).

The Sunbury Shale is a black, fissile, pyritic shale. Asphalt dripping down the upper Berea on the south side of the road is from roadwork, not in-situ petroleum in the Sunbury. As shown in Table FT-3, the Sunbury Shale at this location has

an average TOC of 21.4 percent, an average total sulfur content of 1.7 percent, and an average VR_0 of 0.53 percent.

The contact of the Sunbury with the Berea is sharp (Fig. FT-13A) and has pyrite- and possibly marcasite-filled burrows. Bedding in the underlying Berea consists of scour-based coarse siltstones/

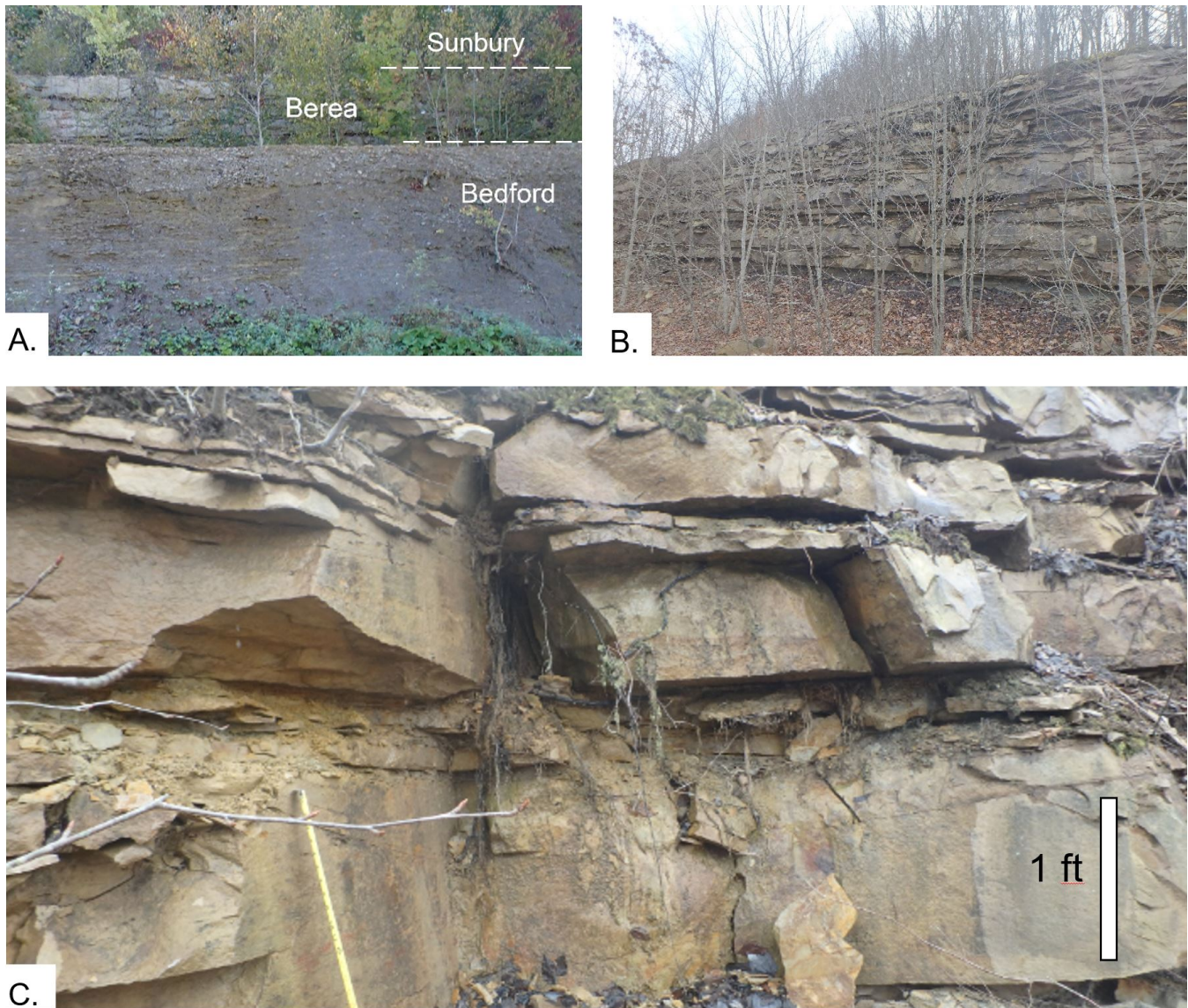


Figure FT-12. Exposure of the Bedford and Berea at stop 3. A. The Bedford Shale is exposed above road level and the Berea is on the second bench (partly covered by vegetation). B. The Berea is 16 ft thick here and consists of sheet sandstones dominated by swaley and hummocky crossbedding (C.).

very fine sandstones with massive, parallel-laminated, hummocky crossbedded, and soft-sediment-deformed beds (Figs. FT-13B, FT-13C). Many of the individual beds are argillaceous at the top. Some beds are separated by thin (inches) gray shales. Laterally, some scour-based beds cut intervening shales. In the core, thin shales and glide planes of flow rolls, and slickensided surfaces, are small flow barriers to oil and gas migration. Imagine that you are putting a horizontal well in some part of this upper unit. What happens laterally within beds? Walk down the access road—What happens to

bedding in the upper Berea? Strata similar to bedding at the base of the road (creek level) are at road level at stop 7.

Stop 5—The Berea-Sunbury Contact (Ky. 10)

From stop 4, head back north on Ky. 9 (AA Highway) to Ky. 10 (1.3 mi). Turn right and head north 3.2 mi to milepost 10. At milepost 10, the Sunbury Shale is exposed above the Berea on both sides of the road. The southside roadcut is benched on the Sunbury-Berea contact (Fig. FT-



Figure FT-13. Stop 4. A. Contact of the Sunbury Shale with the Berea Sandstone. B. Berea sheet sandstones beneath the contact. C. Detail of sharp-based hummocky, massive, and deformed beds. Yellow scales = 3 ft.

Interval ID	Total Carbon	Total Inorganic Carbon	Total Organic Carbon	Total Sulfur	Average VR _o	Standard Deviation
Sunbury Shale (base)	21.39	0.00	21.39	1.68	0.53	0.05

14). The Berea beneath the contact is bioturbated and pyritic. Pyrite occurs as burrow fills (Fig. FT-14B). Bedding consists of sharp-based hummocky, swaley, and massive beds (Fig. FT-14C). As shown in Table FT-4, the Sunbury Shale at this location has an average TOC of 13.3 percent, an average total sulfur content of 1.0 percent, and an average

VR_o of 0.53 percent. The TOC is much lower than at stop 4, which is only a short distance away.

Stop 6—Sheet Sandstones and Vertical Bed Stacking (Ky. 10)

From stop 5, head north to stop 6, 1 mi to milepost 11 at Spyrun Cemetery Road. This stop is



Figure FT-14. Stop 5. A. Sunbury Shale contact with the upper Berea. B. Detail of the contact, showing large phosphate nodules, shale clasts, and pyritized burrows (arrows). C. The underlying beds are dominated by hummocky (HCS), swaley (SCS), and massive, scour-based storm beds. Hammer for scale.

Interval ID	Total Carbon	Total Inorganic Carbon	Total Organic Carbon	Total Sulfur	Average VR _o	Standard Deviation
Sunbury Shale (top)	13.18	0.00	13.18	1.08	0.54	0.04
Sunbury Shale (middle)	10.43	0.00	10.43	0.91	0.52	0.05
Sunbury Shale (base)	16.24	0.02	16.22	1.08	0.53	0.04
Average	13.28	0.01	13.28	1.02	0.53	0.04

mostly a “look at” rather than “climb on” exposure. A large outcrop is exposed south of the creek on the south side of the road (Fig. FT-15). More than 75 ft of Berea is exposed, and the base is not exposed. The outcrop provides a good view of vertical and lateral Berea sheet-sandstone bedding. The top of the Berea would be at the top of the outcrop. Look at the bedding in the upper part of the Berea and compare it to what we saw at stop 4. Look down the outcrop to the section above the creek. Compare that part of the section to creek level at stop 6. Imagine a well log through this exposure. What would it look like? Look at the horizontal continuity of the beds.

Stop 7—Sheet Sandstones and Horizontal Continuity (Ky. 10)

From stop 6, continue 2 mi to three large outcrops in the Berea at Garrison, Ky. (milepost 13). At road level, sheet sandstones are in a shaly interval similar to the shaly interval at creek level at the base of stop 5. Large flow rolls occur in the upper 15 ft of this outcrop and in the shalier interval at road level (Fig. FT-16). Overlying beds include similar storm deposits to what we have seen at other stops, including massive, parallel-laminated, and hummocky beds. Some beds have ripple tops (Figs. FT-17A, FT-17B, FT-17C). The first bench in these outcrops has some extensive ripple surfaces. All ripples are combined-flow types with straight symmetrical crests striking northwest-southeast and foresets dipping to the southwest. Most ripples occur as a single train on the upper bed surface. Bioturbation is mostly limited to horizontal trails on bed tops and small paired holes (*Arenicolites*) on the surface of some beds (Fig. FT-17A).

Let’s walk the outcrop and look at lateral continuity of beds and local discontinuities in bedding, especially in shale interbeds, and imagine a

horizontal wellbore trying to stay in a bed (Fig. FT-18). What types of gamma changes would you see along different discontinuities? Would flow rolls cause the bit to roll or change orientation?

Figure FT-19 is a well log from only a few miles east of stop 7. The combined Bedford-Berea is nearly 200 ft thick. That type of thickness change is difficult to address with facies change and sedimentology. Floyd (2015) and many previous researchers have noted structural influences on Bedford-Berea deposition. There are almost certainly structural influences here, although there are no known faults (major faults). Pashin and Ettensohn (1995) inferred a fault along the Ohio River, and inferred a basement fault below the Waverly Arch. The Waverly Arch is a somewhat enigmatic structure, which has been shown in several different positions through time (Ettensohn, 1980; Cable and Beardsley, 1984; Tankard, 1986). In the Pashin and Ettensohn (1995) model, the Waverly Arch marks the shelf edge with thickening slope rocks to the west. Although the arch may mark a Berea shelf edge, net Bedford-Berea thickness actually decreases to the west off of the flanks of the arch, so both the Bedford and Berea thin.

If we look at the model, three constraints to understanding structural inferences are (1) the underlying Cleveland Shale thickening to the east, (2) the Bedford-Berea being thick in an elongate north-south trend, and (3) the overlying Sunbury Shale being a relatively tabular and widespread deposit. A possible explanation for the westward thinning of the Bedford-Berea interval without thickening of the Sunbury or Cleveland in the accommodation space in front of the prograding Bedford-Berea interval is that the basin margin was farther west, and the clastic wedge pinched out onto the structure (Fig. FT-20). Another possibility is that the base of the Sunbury is an unconformity,



Figure FT-15. Large outcrop of Berea on south side of Ky. 10 near Spyrun Cemetery Road.

as proposed by Ettensohn (2004), and that there was either truncation of the Bedford-Berea package westward or a combination of sedimentary thinning and post-depositional truncation.

The existing model (Fig. FT-21) shows thickening of the Bedford-Berea interval on the downthrown side of basement growth faults. Relative to any possible fault movement here, and more important, southward across known faults in the Kentucky River Fault System and the bounding faults of the Pike County Uplift, the Bedford-Berea is actually thicker on the upthrown side of the faults. This is curious, because structural highs are generally areas of thinner clastic deposition. This inverse thickness association may indicate reverse movements on known normal faults at the end of

the Devonian. Kepferle (1993) noted a single locale with thicker Sunbury Shale on the upthrown side of the Kentucky River Fault System, so reverse movement is possible, but more work is needed. If reverse movement is not the explanation, then the thickness differences in the Bedford-Berea interval across faults need to be explained by differential compaction of muddier (shalier) intervals on the downthrown side of faults, relative to less compactable siltstone on the upthrown side. Again, the Sunbury Shale has local thickness changes across faults, but does not show consistent change either on the up- or downthrown side of faults, suggesting that it was filling any available space at the end of Berea deposition. Therefore, it is a constraint on differential compaction as well.



Figure FT-16. Stop 7. A. Large flow rolls and B. soft-sediment deformation just above road level. Shaly diapirs disrupt many beds in the Berea at these outcrops.

References Cited

- Allen, P.A., 1985, Hummocky cross-stratification is not produced purely under progressive gravity waves: *Nature*, v. 313, p. 562-564.
- Cable, M.S., and Beardsley, R.W., 1984, Structural controls on Late Cambrian and Early Ordovician carbonate sedimentation in eastern Kentucky: *American Journal of Science*, v. 284, no. 7, p. 797-823.
- Coats, K.P., 1988, Depositional environments of the Bedford and Berea Formations in central Ohio: Columbus, Ohio State University, master's thesis, 199 p.
- Coleman, U., and Clayton, G., 1987, Palynostratigraphy and palynofacies of the uppermost Devonian and Lower Mississippian of eastern Kentucky (USA) and correlation with western Europe: *Courier Forschungsinstitute Senckenberg*, v. 98, p. 75-93.
- Dott, R.H., Jr., and Bourgeois, J., 1982, Hummocky stratification: Significance of its variable se-

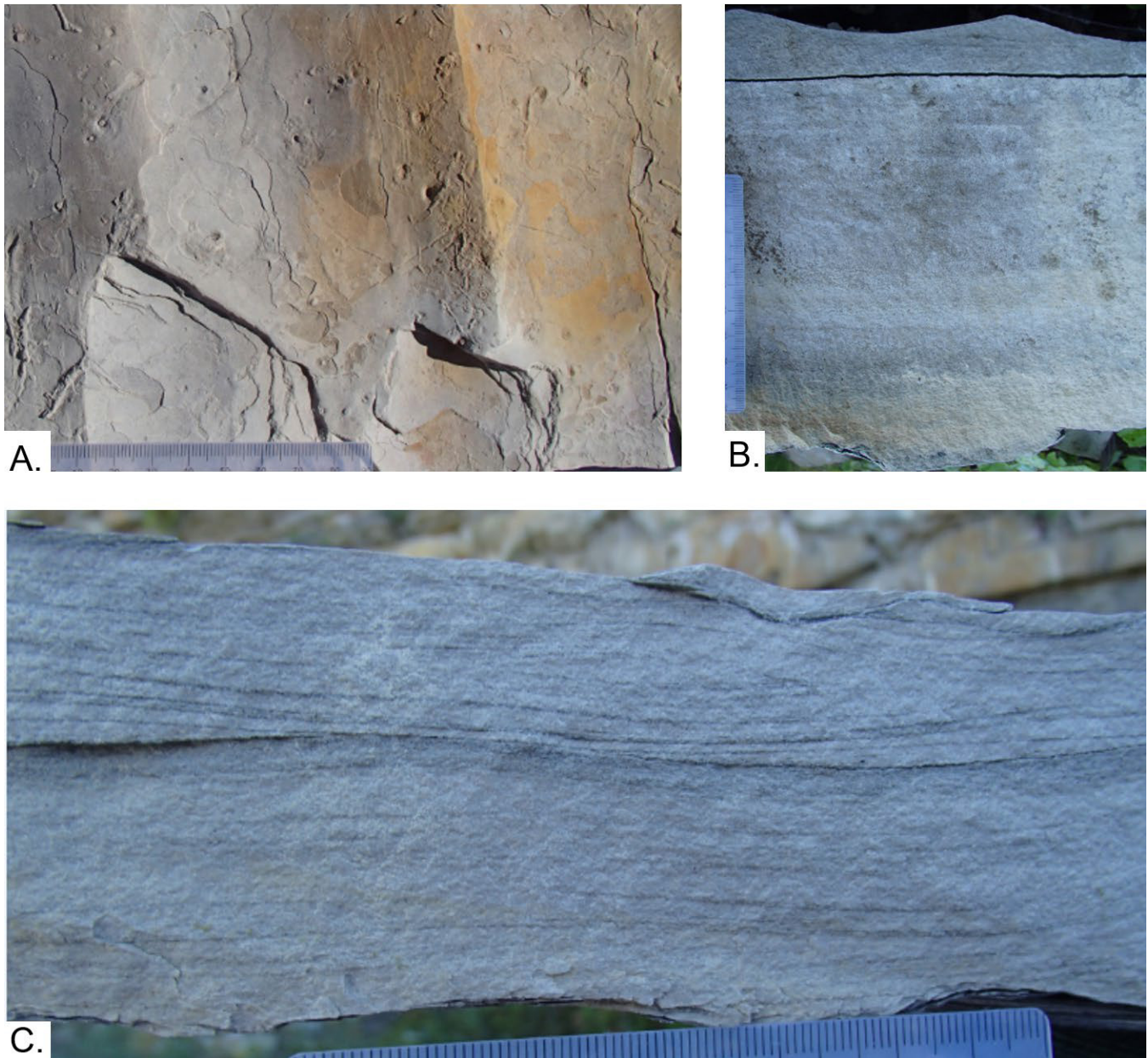


Figure FT-17. Bedding in sheet sandstones at stop 7. A. Bedding plane view of ripple tops and bioturbation. B. Section through thin bed showing scour base, parallel lamination, and rippled top. C. Section through thin bed showing undulating hummocky bedding. Centimeter scales.

quences: *Geological Society of America Bulletin*, v. 93, p. 663–680.

Ettensohn, F.R., 1980, An alternative to the barrier-shoreline model for deposition of Mississippian and Pennsylvanian rocks in northeastern Kentucky: *Geological Society of America Bulletin*, v. 91, no. 3, p. 130–135.

Ettensohn, F.R., 1994, Tectonic control on the formation and cyclicity of major Appalachian

unconformities and associated stratigraphic sequences, *in* Dennison, J.M., and Ettensohn, F.R., eds., *Tectonic and eustatic controls on sedimentary cycles: SEPM [Society for Sedimentary Geology] Concepts in Sedimentology and Paleontology* 4, p. 217–242.

Ettensohn, F.R., 2004, Modeling the nature and development of major Paleozoic clastic wedges in the Appalachian Basin, USA: *Journal of Geodynamics*, v. 37, p. 657–681.

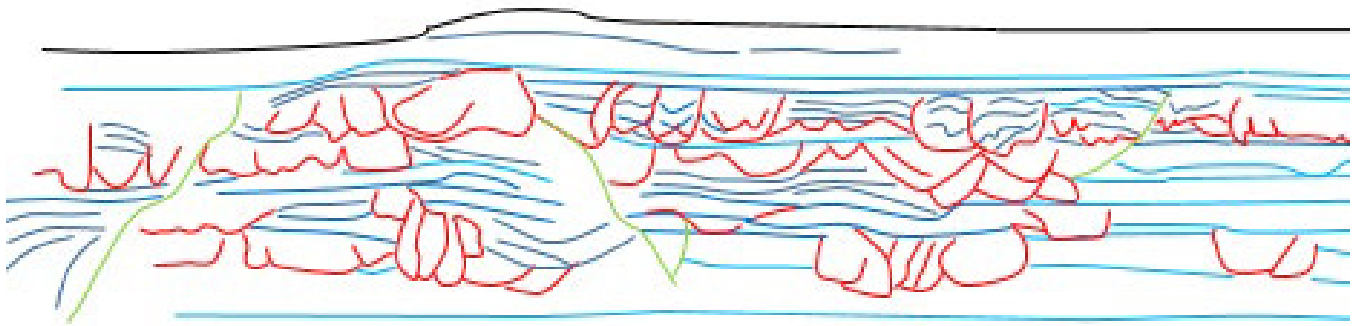


Figure FT-18. Photomosaic of lower bench at road level in part of the north end of the outcrop. Shows traces of bedding (blue lines) and soft-sediment-deformation discontinuities (red lines) and small fault offsets (green).

- Ettensohn, F.R., and Barron, L.S., 1981, Depositional model for the Devonian-Mississippian black-shale sequence of North America – A tectono-climatic approach: U.S. Department of Energy, Morgantown Energy Technology Center, METC/12040-2, 80 p.
- Ettensohn, F.R., and Elam, T.D., 1985, Defining the nature and location of a Late Devonian–Early Mississippian pycnocline in eastern Kentucky: *Geological Society of America Bulletin*, v. 96, p. 1313–1321.
- Ettensohn, F.R., Lierman, R.T., and Mason, C.E., 2009, Upper Devonian–Lower Mississippian clastic rocks in northeastern Kentucky: Evidence for Acadian alpine glaciation and models for source-rock and reservoir-rock development in the eastern United States: *American Institute of Professional Geologists–Kentucky Section spring field trip*, 52 p.
- Ettensohn, F.R., Miller, M.L., Dillman, S.B., Elam, T.D., Geller, K.L., Swager, D.R., Markowitz, G., Woock, R.D., and Barron, L.S., 1988, Characterization and implications of the Devonian-Mississippian black shale sequence, eastern and central Kentucky, U.S.A.: Pycnoclines, transgression, regression, and tectonism, *in* McMillan, N.J., Embry, A.F., and Glass, D.J., eds., *Devonian of the world: Proceedings of the 2nd International Symposium on the Devonian System*: Canadian Society of Petroleum Geologists, *Memoir 14*, v. 2, p. 323–345.
- Floyd, J., 2015, Subsurface geological analyses of the Berea petroleum system in eastern Kentucky: Lexington, University of Kentucky, master's thesis, 153 p.
- Harms, J.C., Southard, J.B., and Walker, R.G., 1982, Structures and sequences in clastic rocks: Calgary, Society of Economic Paleontologists and Mineralogists Short Course No. 9, 249 p.
- Kepferle, R.C., 1993, A depositional model and basin analysis for gas-bearing black shale (Devonian and Mississippian) in the Appalachian Basin, *in* Roen, J.B., and Kepferle, R.C., eds., *Petroleum geology of the Devonian and Mis-*

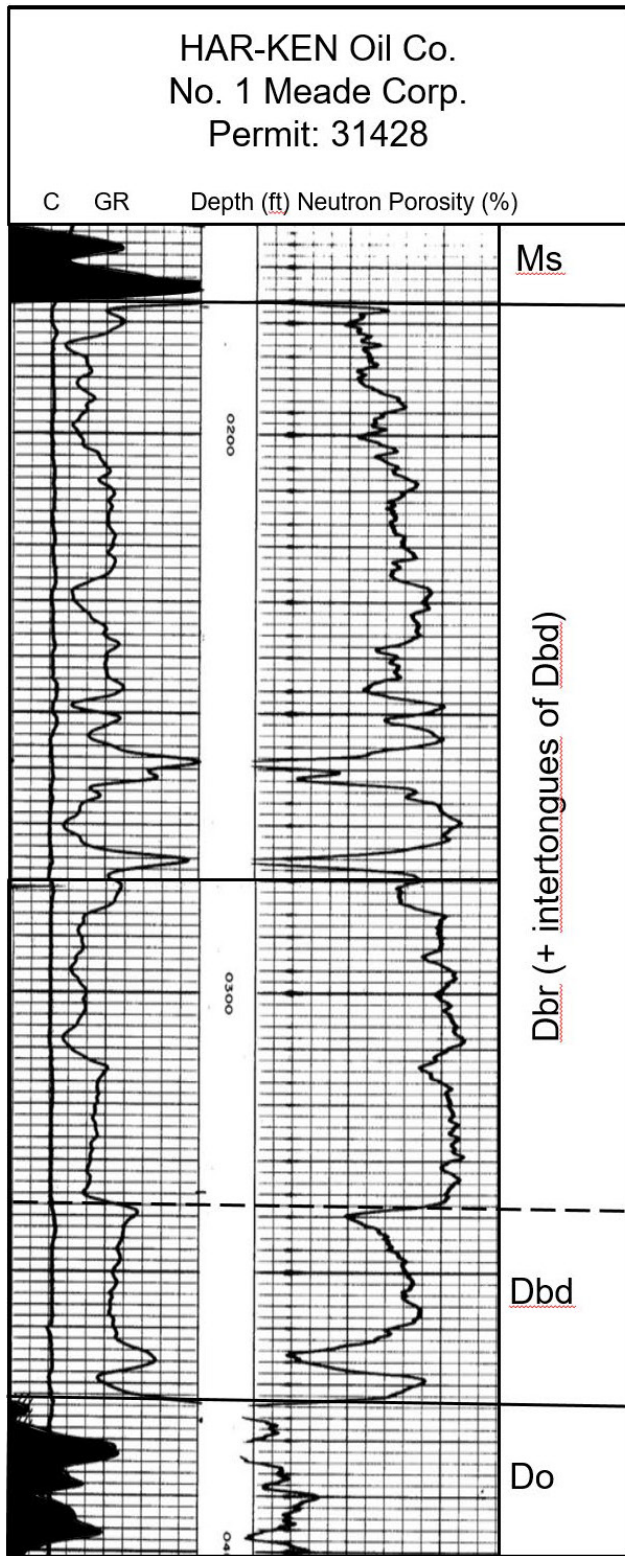
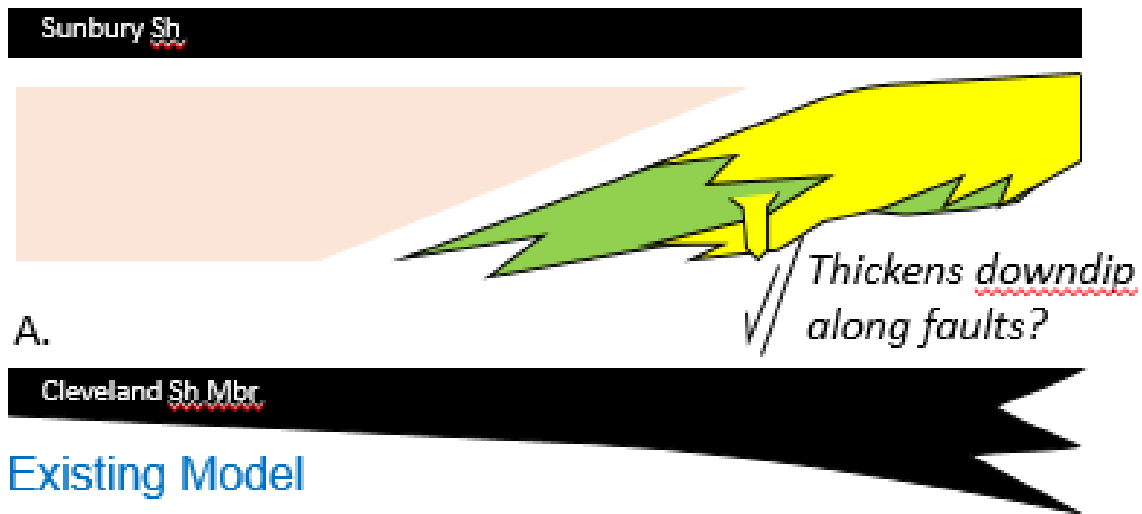


Figure FT-19. Geophysical log through the Bedford-Berea interval from a well 2.6 mi east of milepost 15 (east of Garrison) on Ky. 10. The combined Bedford-Berea interval is 193 ft thick in this well.



Figure FT-20. Conceptual models to explain Bedford-Berea thickness trends westward toward Cincinnati Arch. B-B=Bedford and Berea interval.



Constraints: (1) Upside of faults tends to be coarser and thicker (2) Tabular Sunbury Sh

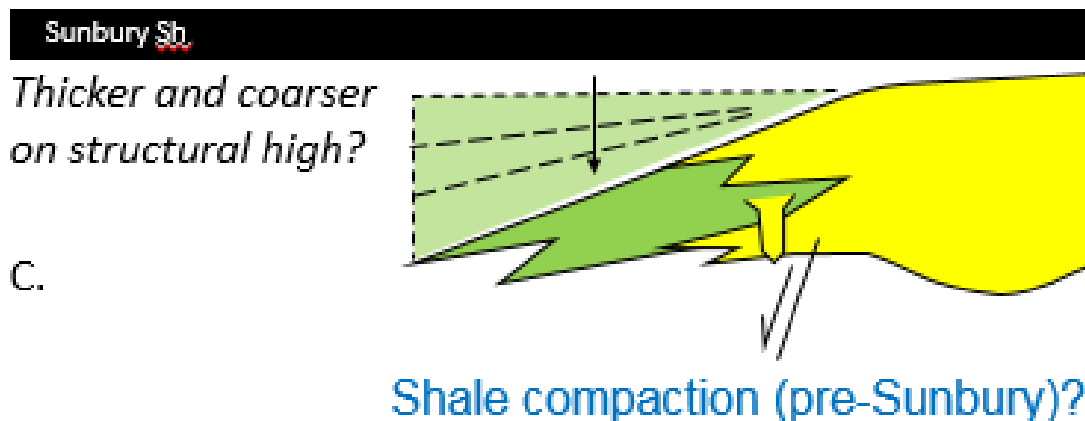
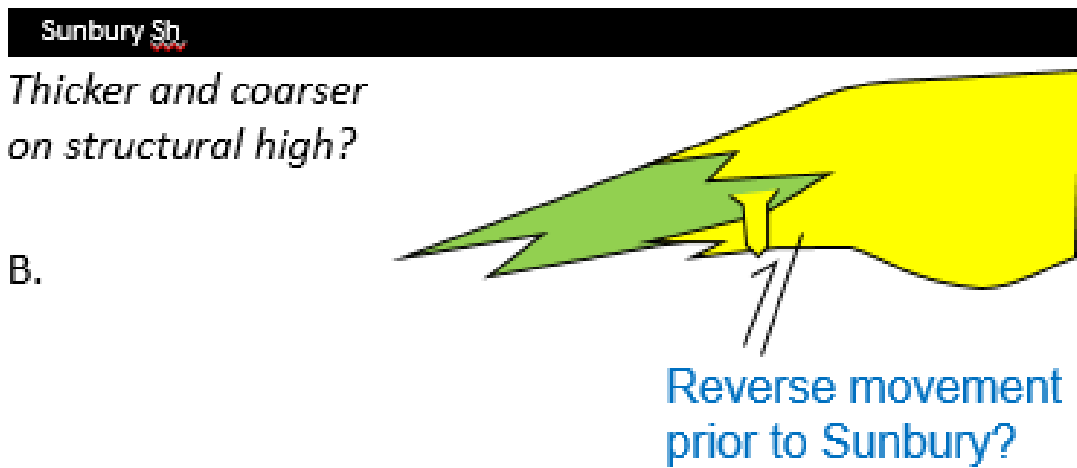
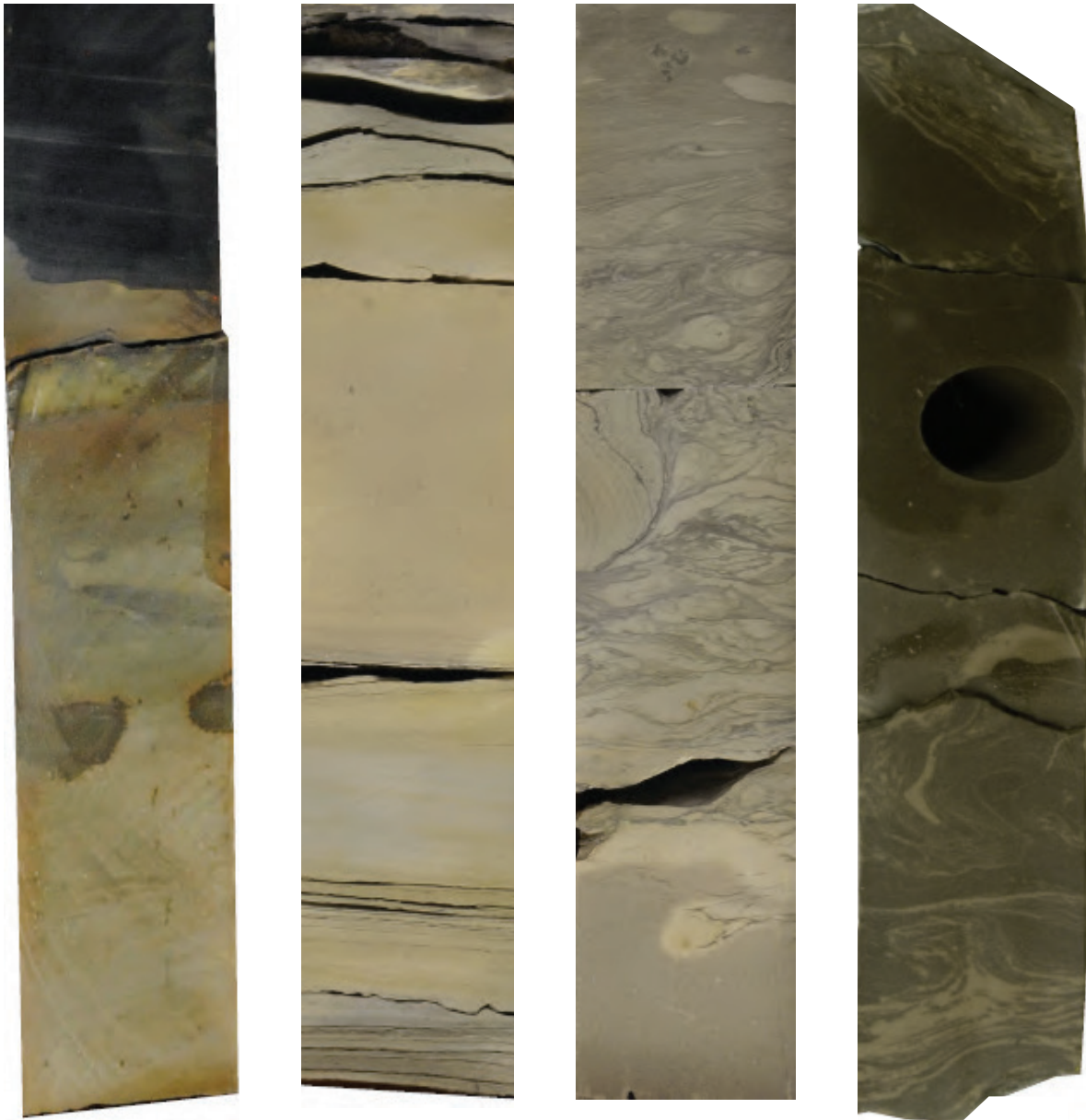


Figure FT-21. Conceptual models to explain Bedford-Berea thickness trends southward across the Kentucky River Fault System.

- Mississippian black shale of eastern North America: U.S. Geological Survey Bulletin 1909, p. F1-F23.
- Kepferle, R.C., Wilson, E.N., and Ettensohn, F.R., 1978, Preliminary stratigraphic cross section showing radioactive zones in the Devonian black shales in the southern part of the Appalachian Basin: U.S. Geological Survey Oil and Gas Investigations Chart OC-85, 13 cross sections on 1 sheet.
- Leckie, D.A., and Walker, R.G., 1982, Storm- and tide-dominated shorelines in Cretaceous Moosebar-Lower Gates interval—Outcrop equivalents of deep basin gas trap in western Canada: American Association of Petroleum Geologists Bulletin, v. 66, p. 138-157.
- McDowell, R.C., 1986, The geology of Kentucky; a text to accompany the geologic map of Kentucky: U.S. Geological Survey Professional Paper 1151-H, 76 p.
- Molyneux, S.G., Manger, W.L., and Owens, B., 1984, Preliminary account of Late Devonian palynomorph assemblages from the Bedford Shale and Berea Sandstone formations of central Ohio, U.S.A.: Journal of Micropaleontology, v. 3, p. 41-51.
- Morris, R.H., and Pierce, K.L., 1967, Geologic map of the Vanceburg quadrangle, Kentucky-Ohio: U.S. Geological Survey Geologic Quadrangle Map GQ-598, scale 1:24,000.
- Nottvedt, A., and Kreisa, R.D., 1987, Model for the combined-flow origin of hummocky cross-stratification: Geology, v. 15, p. 357-361.
- Pashin, J.C., 1990, Reevaluation of the Bedford-Berea sequence in Ohio and adjacent states: New perspectives on sedimentation and tectonics in foreland basins: Lexington, University of Kentucky, doctoral dissertation, 824 p.
- Pashin, J.C., and Ettensohn, F.R., 1987, An epeiric shelf-to-basin transition; Bedford-Berea sequence, northeastern Kentucky and south-central Ohio: American Journal of Science, v. 287, no. 9, p. 893-926.
- Pashin, J.C., and Ettensohn, F.R., 1992, Palaeoecology and sedimentology of the dysaerobic Bedford fauna (Late Devonian), Ohio and Kentucky (USA): Palaeogeography, Palaeoclimatology, Palaeoecology, v. 91, nos. 1-2, p. 21-34.
- Pashin, J.C., and Ettensohn, F.R., 1995, Reevaluation of the Bedford-Berea sequence in Ohio and adjacent states: Forced regression in a foreland basin: Geological Society of America Special Paper 298, p. 1-69.
- Pepper, J.F., de Witt, W., Jr., and Demarest, D.F., 1954, Geology of the Bedford Shale and Berea Sandstone in the Appalachian Basin: U.S. Geological Survey Professional Paper 700-D, 109 p.
- Potter, P.E., Ausich, W.I., Klee, J., Krissek, L.A., Mason, C.E., Schumacher, G.A., Wilson, R.T., and Wright, E.M., 1980a, Geology of the Alexandria-Ashland Highway (Kentucky Highway 546), Maysville to Garrison (field trip guidebook, joint field conference of the Geological Society of Kentucky and Ohio Geological Society): Kentucky Geological Survey, ser. 12, 65 p.
- Potter, P.E., Maynard, J.B., Jackson, D., and DeReamer, J., 1983, Lithologic and environmental atlas of Berea Sandstone (Mississippian) in the Appalachian Basin: Appalachian Geological Society, Special Publication 1, 157 p.
- Potter, P.E., Maynard, J.B., and Pryor, W.A., 1980b, Final report of special geological, geochemical, and petrological studies of the Devonian shales in the Appalachian Basin: University of Cincinnati, H.N. Fisk Laboratory of Sedimentology, final report prepared for U.S. Department of Energy, Eastern Gas Shales Project, 86 p.
- Provo, L.J., Kepferle, R.C., and Potter, P.E., 1978, Division of black Ohio Shale in eastern Kentucky: American Association of Petroleum Geologists Bulletin, v. 62, no. 9, p. 1703-1713.
- Rhoads, D.C., and Morse, J.W., 1971, Evolutionary and ecologic significance of oxygen-deficient marine basins: Lethaia, v. 4, p. 413-428.
- Roen, J.B., 1984, Geology of the Devonian black shales of the Appalachian Basin: Organic Geochemistry, v. 5, no. 4, p. 241-254.
- Roen, J.B., Wallace, L.G., and de Witt, W., Jr., 1978, Preliminary stratigraphic cross section showing radioactive zones in the Devonian black shales in the central part of the Appalachian Basin: U.S. Geological Survey Oil and Gas Investigations Chart OC-87, 1 sheet.

- Shanmugam, G., and Moiola, R.J., 1988, Submarine fans: Characteristics, models, classification, and reservoir potential: *Earth-Science Reviews*, v. 24, p.383-428.
- Tankard, A.J., 1986, Depositional response to foreland deformation in the Carboniferous of eastern Kentucky: *American Association of Petroleum Geologists Bulletin*, v. 70, p.853-868.
- Walker, R.G., 1978, Deep-water sandstone facies and ancient submarine fans: Models for exploration for stratigraphic traps: *American Association of Petroleum Geologists Bulletin*, v. 62, no. 6, p.932-966.
- Wallace, L.G., Roen, J.B., and de Witt, W., Jr., 1977, Preliminary stratigraphic cross section showing radioactive zones in the Devonian black shales in the western part of the Appalachian Basin: U.S. Geological Survey Oil and Gas Investigations Chart OC-80, 2 sheets.

Berea Sandstone (Late Devonian) Core in Eastern Kentucky (and Adjoining Southern Ohio)



Stephen F. Greb
With the Assistance of Ryan Pinkston and Ethan Davis
(Kentucky Geological Survey)
and Jeffrey Deisher (Ohio Geological Survey)

Contents

Introduction.....	173
Stratigraphy and Deposition.....	173
Core Descriptions and Photographs	174
Grain Size on Graphic Sections.....	176
Core Bedding on Graphic Sections.....	178
Aristech Chemical Corp. #4 Aristech.....	182
Background and Distance to Recent Berea Oil Wells.....	182
Key Features	182
Data and Analysis.....	182
Graphic Sections and Photographs	183
Description from slabbed core.....	183
Description from slabbed core.....	184
Description from slabbed core.....	185
Aristech Chem. No. 4 Aristech, box 63.....	186
Aristech Chem. No. 4 Aristech, box 64.....	187
Aristech Chem. No. 4 Aristech, box 65.....	188
Aristech Chem. No. 4 Aristech, box 66.....	189
Aristech Chem. No. 4 Aristech, box 67.....	190
Aristech Chem. No. 4 Aristech, box 68.....	191
Aristech Chem. No. 4 Aristech, box 69.....	192
Aristech Chem. No. 4 Aristech, box 70.....	193
Aristech Chem. No. 4 Aristech, box 71.....	194
Aristech Chem. No. 4 Aristech, box 72.....	195
Aristech Chem. No. 4 Aristech, box 73.....	196
Aristech Chem. No. 4 Aristech, box 74.....	197
Aristech Chem. No. 4 Aristech, box 75.....	198
Ashland Exploration #1 Hattie Neal.....	199
Background and Distance to Recent Berea Oil Wells.....	199
Key Features	199
Data and Analysis.....	199
Graphic Sections and Photographs	201
Description from slabbed core.....	201
Ashland Exploration No. 1 Hattie Neal, box 1	202
Ashland Exploration No. 1 Hattie Neal, box 2.....	203
Ashland Exploration No. 1 Hattie Neal, box 3.....	204
Ashland Exploration No. 1 Hattie Neal, box 4.....	205
Ashland Exploration No. 1 Hattie Neal, box 5.....	206
Columbia Natural Resources #20505 Margaret Simpson	207
Background and Distance to Recent Berea Oil Wells.....	207
Key Features	207
Data and Analysis.....	207
Graphic Sections and Photographs	209
Description from slabbed core.....	209
Description from slabbed core.....	210
Columbia No. 20505 Margaret Simpson, core 1, box 1.....	211
Columbia No. 20505 Margaret Simpson, core 1, box 2.....	212
Columbia No. 20505 Margaret Simpson, core 1, box 3.....	213
Columbia No. 20505 Margaret Simpson, core 1, box 4.....	214

Contents (Continued)

Columbia No. 20505 Margaret Simpson, core 2, box 1.....	215
Columbia No. 20505 Margaret Simpson, core 2, box 2.....	216
Columbia No. 20505 Margaret Simpson, core 2, box 3.....	217
Columbia No. 20505 Margaret Simpson, core 2, box 4.....	218
Columbia No. 20505 Margaret Simpson, core 2, box 5.....	219
Kentucky-West Virginia Gas #1122 Milton Moore.....	220
Background and Distance to Recent Berea Oil Wells.....	220
Key Features.....	220
Data and Analysis.....	221
Graphic Sections and Photographs.....	222
Description from mostly unslabbed core.....	222
Description from mostly unslabbed core.....	223
KY WV Gas No. 1122 Milton Moore, KGS C-268, box 1.....	224
KY WV Gas No. 1122 Milton Moore, KGS C-268, box 2.....	225
KY WV Gas No. 1122 Milton Moore, KGS C-268, box 3.....	226
KY WV Gas No. 1122 Milton Moore, KGS C-268, box 4.....	227
KY WV Gas No. 1122 Milton Moore, KGS C-268, box 5.....	228
KY WV Gas No. 1122 Milton Moore, KGS C-268, box 6.....	229
KY WV Gas No. 1122 Milton Moore, KGS C-268, box 7.....	230
KY WV Gas No. 1122 Milton Moore, KGS C-268, box 8.....	231
KY WV Gas No. 1122 Milton Moore, KGS C-268, box 9.....	232
KY WV Gas No. 1122 Milton Moore, KGS C-268, box 10.....	233
KY WV Gas No. 1122 Milton Moore, KGS C-268, box 11.....	234
Kentucky-West Virginia Gas #1087 Ruben Moore.....	235
Background and Distance to Recent Berea Oil Wells.....	235
Key Features.....	235
Data and Analysis.....	235
Graphic Sections and Photographs.....	236
Description from mostly unslabbed core.....	236
Description from mostly unslabbed core.....	237
KY-WV Gas No. 1087 Ruben Moore, KGS core no. 270, box 1.....	238
KY-WV Gas No. 1087 Ruben Moore, KGS core no. 270, box 2.....	239
KY-WV Gas No. 1087 Ruben Moore, KGS core no. 270, box 3.....	240
KY-WV Gas No. 1087 Ruben Moore, KGS core no. 270, box 4.....	241
KY-WV Gas No. 1087 Ruben Moore, KGS core no. 270, box 5.....	242
KY-WV Gas No. 1087 Ruben Moore, KGS core no. 270, box 6.....	243
KY-WV Gas No. 1087 Ruben Moore, KGS core no. 270, box 7.....	244
Ashland Oil #KY-4 Kelly-Watt-Bailey-Skaggs.....	245
Background and Distance to Recent Berea Oil Wells.....	245
Key Features.....	245
Data and Analysis.....	245
Graphic Sections and Photographs.....	246
Description from oriented core.....	246
Ashland No. 3RS Kelly-Watt-Bailey-Skaggs, KGS C-1186, box 1.....	247
Ashland No. 3RS Kelly-Watt-Bailey-Skaggs, KGS C-1186, box 2.....	248
Ashland No. 3RS Kelly-Watt-Bailey-Skaggs, KGS C-1186, box 3.....	249

Contents (Continued)

Ashland No. 3RS Kelly-Watt-Bailey-Skaggs, KGS C-1186, box 4.....	250
Ashland No. 3RS Kelly-Watt-Bailey-Skaggs, KGS C-1186, box 5.....	251
Ashland No. 3RS Kelly-Watt-Bailey-Skaggs, KGS C-1186, box 6.....	252
Ashland No. 3RS Kelly-Watt-Bailey-Skaggs, KGS C-1186, box 7.....	253
Gillespie #1 Lowell Bailey	254
Background and Distance to Recent Berea Oil Wells.....	254
Key Features	254
Data and Analysis.....	254
Photographs.....	255
Gillespie No. 1 Lowell Bailey, KGS C-859, box 1	255
Gillespie No. 1 Lowell Bailey, KGS C-859, box 2	256
Columbia Natural Resources #20456 Pocahontas Land Co. (Pocahontas Mining).....	257
Background and Distance to Recent Berea Oil Wells.....	257
Key Features	257
Data and Analysis.....	257
Graphic Sections and Photographs	259
Description: siltstones are slabbed, shales are not.....	259
Description: siltstones are slabbed, shales are not.....	260
Description: siltstones are slabbed, shales are not.....	261
Columbia Gas Trans. (TCO) No. 1 Pocahontas Mining, core box 1 [1A]	262
Columbia Gas Trans. (TCO) No. 1 Pocahontas Mining, core 1, box 2 [1B] ...	263
Columbia Gas Trans. (TCO) No. 1 Pocahontas Mining, core 1, box 3	264
Columbia Gas Trans. (TCO) No. 1 Pocahontas Mining, core 1, box 4	265
Columbia Gas Trans. (TCO) No. 1 Pocahontas Mining, core 1, box 5	266
Columbia Gas Trans. (TCO) No. 1 Pocahontas Mining, core 2, box 1	267
Columbia Gas Trans. (TCO) No. 1 Pocahontas Mining, core 2, box 2	268
Columbia Gas Trans. (TCO) No. 1 Pocahontas Mining, core 2, box 3	269
Columbia Gas Trans. (TCO) No. 1 Pocahontas Mining, core 2, box 4	270
Columbia Gas Trans. (TCO) No. 1 Pocahontas Mining, core 3, box 1	271
Columbia Gas Trans. (TCO) No. 1 Pocahontas Mining, core 3, box 2	272
Columbia Gas Trans. (TCO) No. 1 Pocahontas Mining, core 3, box 3	273
Columbia Gas Trans. (TCO) No. 1 Pocahontas Mining, core 3, box 4	274
Columbia Gas Trans. (TCO) No. 1 Pocahontas Mining, core 3, box 5	275
Columbia Gas Trans. (TCO) No. 1 Pocahontas Mining, core 3, box 6	276
Columbia Gas Trans. (TCO) No. 1 Pocahontas Mining, core 3, box 7	277
Columbia Gas Trans. (TCO) No. 1 Pocahontas Mining, core 4, box 1	278
Columbia Gas Trans. (TCO) No. 1 Pocahontas Mining, core 4, box 2	279
Columbia Gas Trans. (TCO) No. 1 Pocahontas Mining, core 4, box 3	280
Equitable Production Company #504353 EQT.....	281
Background and Distance to Recent Berea Oil Wells.....	281
Key Features	281
Data and Analysis.....	282
Graphic Sections and Photographs	283
Described from slabbed core.....	283
Described from slabbed core.....	284
Described from slabbed core.....	285

Contents (Continued)

EQT No. 504353, core 1, box 13, and core 2, box 1	286
EQT No. 504353, core 2, boxes 2-3	287
EQT No. 504353, core 2, box 4, and core 3, box 1	288
EQT No. 504353, core 3, boxes 2-3	289
EQT No. 504353, core 4, boxes 1-2	290
EQT No. 504353, core 4, boxes 3-4	291
EQT No. 504353, core 4, boxes 5-6	292
EQT No. 504353, core 4, box 7.....	293
EQT No. 504353, core 5, boxes 1-2	294
EQT No. 504353, core 6, boxes 1-2	295
EQT No. 504353, core 6, boxes 3-4	296
EQT No. 504353, core 6, boxes 5-6	297
EQT No. 504353, core 6, boxes 7-8	298
EQT No. 504353, core 6, boxes 9-10	299
EQT No. 504353, core 6, boxes 11-12	300
EQT No. 504353, core 7, boxes 1-2	301
EQT No. 504353, core 7, boxes 3-4	302
EQT No. 504353, core 7, box 7 and boxes 5-6.....	303
Somerset Gas Service Company #1 Morlandbell Inc.	304
Background and Distance to Recent Berea Oil Wells	304
Key Features	304
Data and Analysis.....	304
Graphic Sections and Photographs	305
Description from slabbed core.....	305
Somerset No. 1 Morlandbell, box 5	306
Somerset No. 1 Morlandbell, box 6	307
Somerset No. 1 Morlandbell, box 7	308
Somerset No. 1 Morlandbell, box 8	309
Somerset No. 1 Morlandbell, box 9	310
References Cited.....	311

Figures

CB-1. Map showing location of publicly available Bedford-Berea cores in the Kentucky Geological Survey Earth Analysis Research Library, and of a single core in southern Ohio available at the Ohio Geological Survey core repository	174
CB-2. Map showing locations of the 10 cores studied relative to the thickness of the Bedford-Berea interval and major tectonic structures	175
CB-3. Map showing locations of the 10 cores studied relative to producing gas and oil wells	175
CB-4. Diagram showing relative position of the studied cores in the Bedford-Berea interval and geophysical logs of the cored holes	176
CB-5. Stratigraphic correlation of units in the Berea petroleum system	179

Figures (Continued)

CB-6. Interpretation of depositional systems and presumed lateral stratigraphic relationships for elements of the Berea petroleum system.....	179
CB-7. Legend for graphic core logs.....	180

Tables

CB-1. Bedford-Berea cores in Kentucky and adjacent to Kentucky	177
CB-2. Bedford-Berea stratigraphic cores at the outcrop margin.....	178

Berea Sandstone (Late Devonian) Core in Eastern Kentucky (and Adjoining Southern Ohio)

Stephen F. Greb

With the Assistance of

**Ryan Pinkston and Ethan Davis (Kentucky Geological Survey) and
Jeffrey Deisher (Ohio Geological Survey)**

Introduction

The Berea Sandstone in eastern Kentucky has long been a producing oil and gas horizon, but production has increased in recent years with the advent of horizontal drilling. Because of interest in Berea reservoirs, there has also been renewed interest in Berea cores and core analyses. This core book was put together to provide information on publicly available Berea cores and analyses for eastern Kentucky for use by operators, researchers, and students.

Potter and others (1983) first summarized core and outcrop data on the Berea in the region in their "Lithologic and Environmental Atlas of the Berea Sandstone." That booklet contained descriptions of 22 cores and 16 outcrops of the Berea in the Appalachian Basin. Two of the outcrops and eight cores were from Kentucky, and one was from an adjacent well in southern Ohio. Of the eight cores described from the Berea in eastern Kentucky, five were near-surface, 1-in.-diameter cores drilled by the University of Kentucky's Kentucky Geological Survey and Institute for Mining and Minerals Research along the outcrop margin of the Bedford-Berea. A total of 18 cores was drilled along the Bedford-Berea outcrop margin by KGS and IMMR, and the five described by Potter and others (1983) include those cores that had Berea. In the other IMMR cores, the Berea is absent and the Sunbury rests directly on the Bedford Shale. Core descriptions for the KGS and IMMR cores are included in Elam (1981). Pashin (1985) also has descriptions of 11 outcrops in southern Ohio and northern Kentucky, six of which include the Berea.

Figure CB-1 is a map showing the locations of Berea cores in Kentucky. The 10 numbered cores are summarized herein. Figure CB-2 shows the locations of the 10 cores relative to the thickness of the Bedford-Berea interval. Figure CB-3 shows the core locations relative to oil and gas production from the Bedford-Berea interval. Many of the gas wells shown, especially those in southeastern Kentucky, commingle Berea and deeper Ohio Shale gas. Figure CB-4 is a graphic comparison of the cores studied, showing the relative parts of the interval each core contains. Table CB-1 is a list of the cores and their locations. Descriptions and photographs of the IMMR cores from the shallow outcrop margin are not included, but the locations of the wells these cores came from are shown in Figure CB-1 and Table CB-2, in case readers are interested in further study of these cores. All of the Kentucky cores shown in this core book are held in the Kentucky Geological Survey Earth Analysis Research Library in Lexington, Ky. The Aristech No.4 core in southern Ohio, across the river from Greenup County, Ky., is in the Ohio Geological Survey's H.R. Collins Lab and Core Repository in Columbus, Ohio. These cores are available for study, and researchers can make arrangements with the core facilities to view cores or sample cores. For rules and regulations regarding sampling, contact the geological surveys.

Stratigraphy and Deposition

The Berea Sandstone is the uppermost Devonian unit in eastern Kentucky (Fig. CB-5). It is underlain by, interbeds with, and pinches out into the Bedford Shale. The Bedford is underlain by the

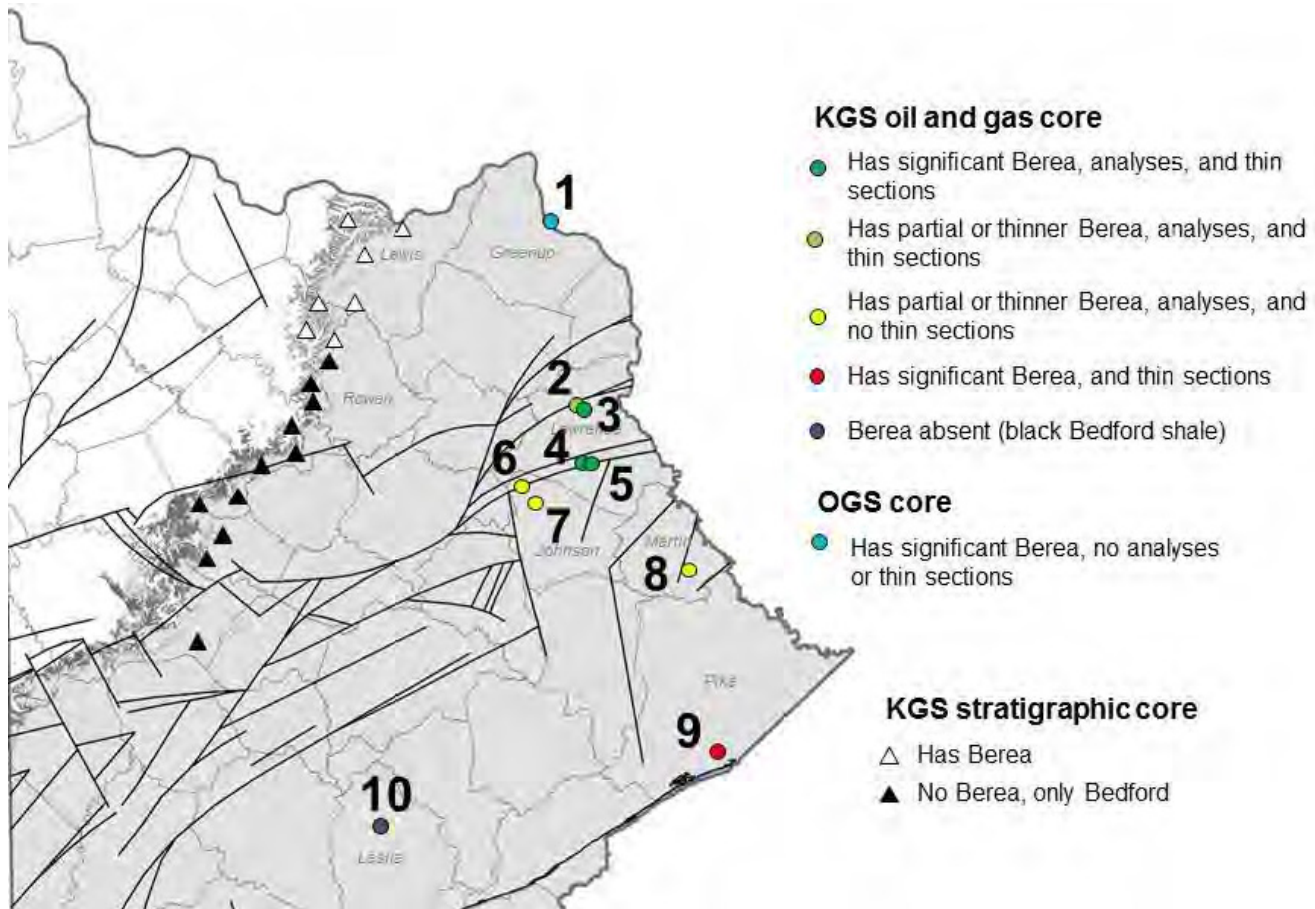


Figure CB-1. Location of publicly available Bedford-Berea cores in the Kentucky Geological Survey Earth Analysis Research Library, and of a single core in southern Ohio available at the Ohio Geological Survey core repository. The 10 numbered cores are summarized herein (see Table CB-1 for core names). Gray shaded area has Devonian strata.

Cleveland Member of the Ohio Shale. The Berea and Bedford (where the Berea is absent) are overlain by the Lower Mississippian Sunbury Shale. The contact with the Sunbury may be unconformable (Ettensohn, 2004). Cleveland and Sunbury shales are organic-rich black shales. The Berea pinches out to the west and southwest beneath the Sunbury, such that the Sunbury Shale overlies the Bedford Shale in much of the southwestern part of the Appalachian Basin in eastern Kentucky.

The Berea is interpreted as having been deposited on a storm-influenced, shallow marine shelf (Fig. CB-6) (Potter and others, 1983; Pashin and Ettensohn, 1987, 1992, 1995). Good examples of typical storm-shelf bedding can be seen in the cores. Berea sandstones and siltstones complexly intertongue with and grade laterally into Bedford shales. The Bedford is interpreted to represent distal deltaic slope deposits seaward of the prograd-

ing Berea marine shelf (Fig. CB-6) (Potter and others, 1983; Pashin and Ettensohn, 1987, 1992, 1995). The Bedford may contain gray, green, or black shales. The color change from black shale to gray-green shales is interpreted to represent the position of a paleopycnocline between relatively deeper, downdip, anoxic water and shallower, updip, dysaerobic water (Ettensohn and Elam, 1985; Pashin and Ettensohn, 1987, 1992).

Core Descriptions and Photographs

For each of the cores studied in this report we include (1) a brief summary of the core relative to its location to the recent oil play, key features, and available data, (2) a graphic log description of the core, and (3) photographic plates of the Bedford-Berea interval in the core. Data and analyses are in Appendix 1. Additional information on the origi-

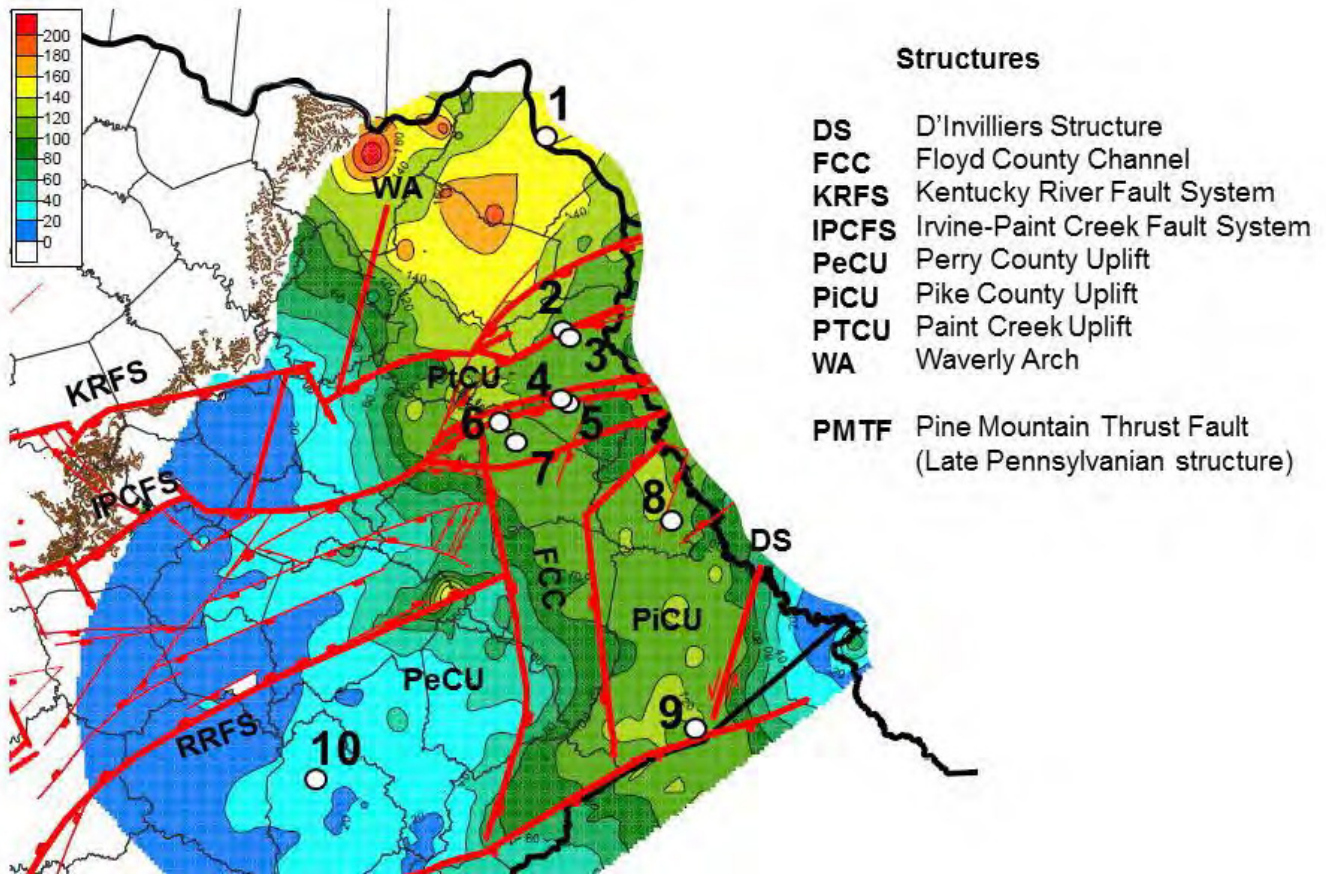


Figure CB-2. Locations of the 10 cores studied relative to the thickness of the Bedford-Berea interval and major tectonic structures. See Figure CB-1 and Table CB-1 for well and location information. Bedford-Berea isopach map modified from Floyd (2015); used with permission. See Table CB-1 for core well names.

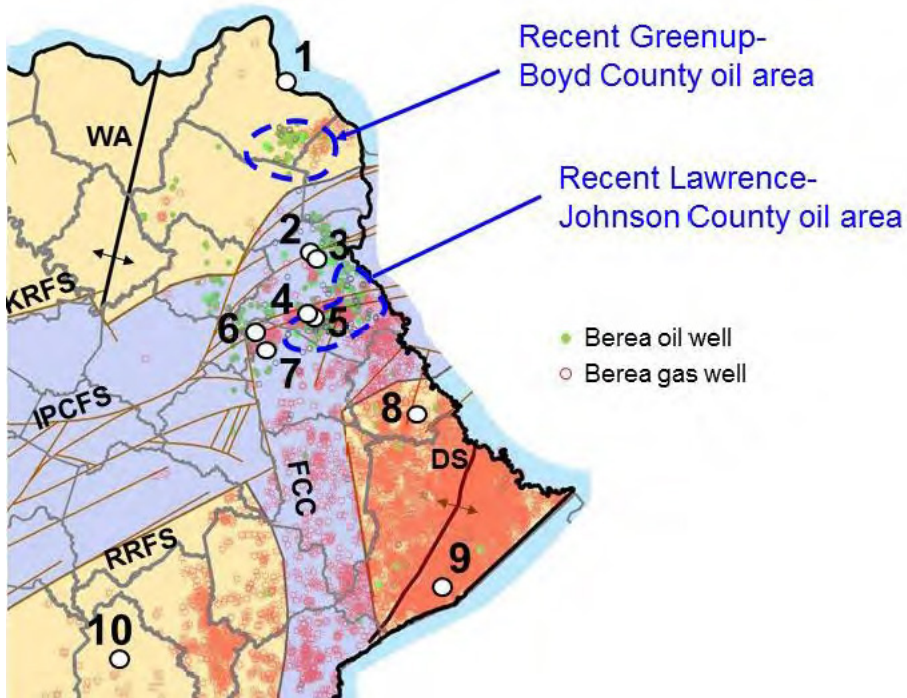


Figure CB-3. Locations of the 10 cores studied relative to producing gas (red) and oil (green) wells. See Table CB-1 for well names and information. The current horizontal oil play areas are shown by blue dashed lines.

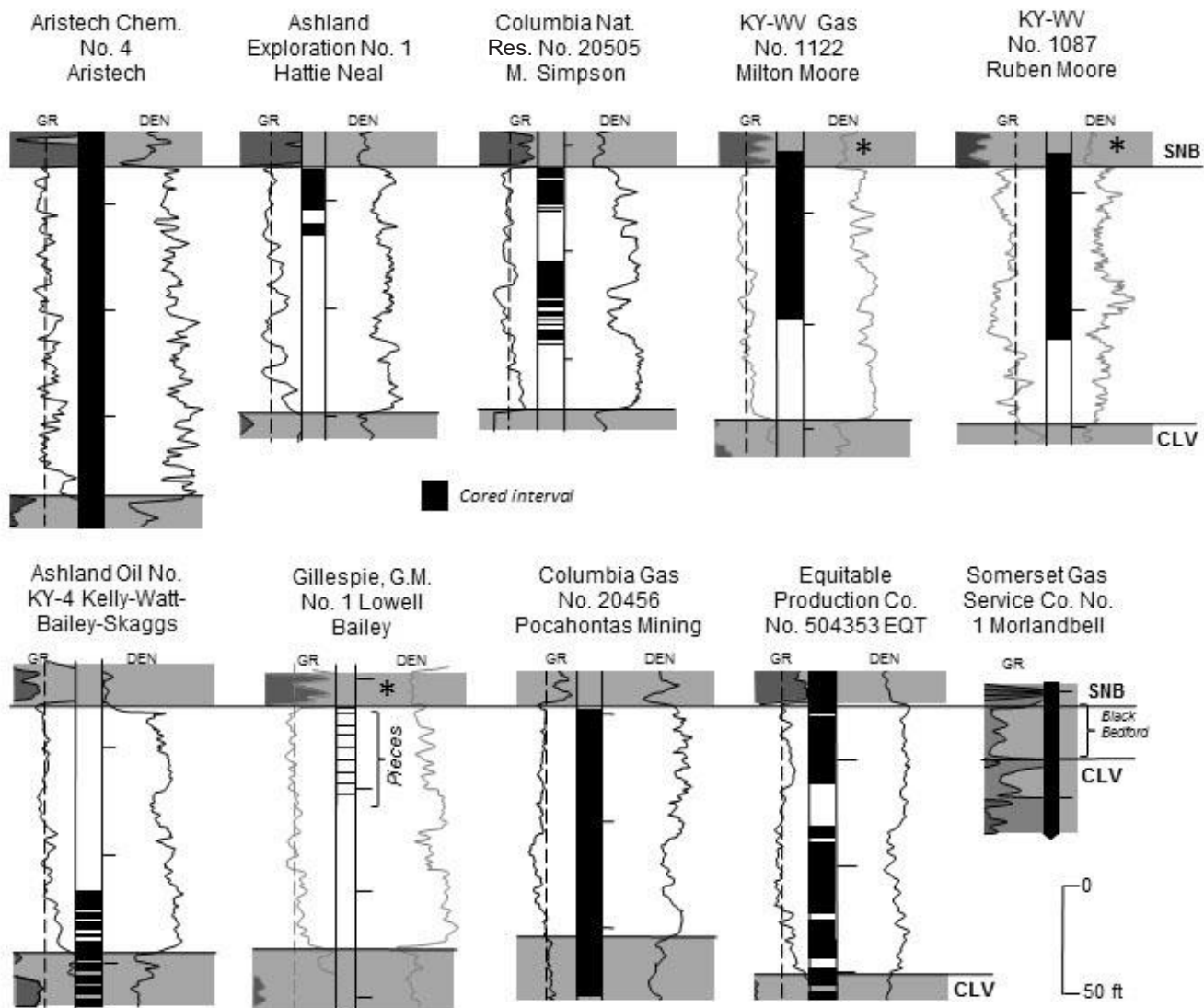


Figure CB-4. Relative position of the studied cores in the Bedford-Berea interval and geophysical logs of the cored holes. Wells are shown in the order of their appearance in this core book, essentially from north to south. See Figures CB-1, CB-2, CB-3 and Table CB-1 for core locations. Where geophysical logs are not available for cored holes (*), logs from nearby wells were used to show the relative position of the core. Organic-rich, high-gamma shales are shaded. CLV = Cleveland Shale Member of the Ohio Shale. SNB = Sunbury Shale. GR = gamma ray. DEN = density. The Morlandbell well does not have a density log.

nal well, completion report, etc., can be found at the geological survey websites. Cores are presented from north to south (Fig. CB-1).

Grain Size on Graphic Sections

Although the Berea is called a sandstone in eastern Kentucky, grain-size analysis shows it is mostly a coarse siltstone to very fine sandstone. Differentiating coarse siltstone from very fine sandstone in core is difficult and requires microscopic evaluation. Hence, the widths of the graphic

logs made in this report are subdivided into four recognizable divisions, which could be delineated in hand specimen, rather than the grain-size divisions used in standard graphic logs. The coarsest division is for typical gray (or iron-stained) Berea coarse siltstone to very fine sandstone. The next division is for slightly darker, argillaceous, medium to dark gray siltstones. The third division is for mixed thin-bedded siltstones and shales in which beds are very thin. The fourth and narrowest di-

Table CB-1. Bedford-Berea cores in Kentucky and adjacent to Kentucky. All except for the Aristech core in Ohio are oil and gas exploration cores. BDFD = Bedford Shale. BREA = Berea Sandstone. SNB = Sunbury Shale. OHIO = Ohio Shale.

No. on Figures	KGS Core Call No.	County	GQ	KGS Oil and Gas Record No.	Carter Coordinate Location	Operator	Hole	Farm	North Latitude (83)	West Longitude (83)	Cored Interval
2	5691	Lawrence	Webbville	11647	2-T-81	Ashland Exploration	1	Hattie Neal	38.156891	-82.768127	BREA
3	5906	Lawrence	Fallsburg	101940	6-T-82	Columbia Natural Resources	20505	Simpson, Margaret	38.142397	-82.748492	BREA
4	268	Lawrence	Blaine	37673	21-S-81	KY-West Virginia Gas	1122	Moore, Milton	38.015056	-82.756648	SNB-BREA
5	270	Lawrence	Adams	52302	25-S-82	KY-West Virginia Gas	1087	Moore, Ruben	38.011127	-82.735469	BREA
6	1186	Johnson	Redbush	42373	12-R-79	Ashland Oil	KY-4	Kelly-Watt-Bailey-Skaggs unit	37.961779	-82.937911	BDFD-OHIO
7	859	Johnson	Redbush	45797	25-R-80	Gillespie, G.M.	1	Bailey, Lowell	37.92037	-82.903467	BREA
8	5907	Martin	Varney	66348	3-O-85	Columbia Gas Transmission (TCO)	20456	Pocahontas Mining	37.746665	-82.450993	BREA-OHIO
9	6591	Pike	Hellier	137835	7-J-86	Equitable Production Co. (EQT)	504353	EQT	37.312666	-83.388906	SNB-BDFD-BREA-OHIO
10	6588	Leslie	Hyden West	32289	4-H-74	Somerset Gas Service	1	Morlandbell Inc.	37.15606	-83.388906	SNB-BDFD-OHIO
No. on Figures	Ohio GS Call No.	County				Operator	Hole	Farm	North Latitude (83)	West Longitude (83)	Cored Interval
1	3409	Scioto				Aristech Chemical Corp	4	Aristech Chemical Corp.	38.59427853	-82.82200781	SNB-BREA-BDFD-OHIO

Table CB-2. Bedford-Berea stratigraphic cores at the outcrop margin. These are 1-in.-diameter, shallow cores drilled along the outcrop belt in eastern Kentucky. Descriptions of cores are in Elam (1981). Shaded cores have Berea Sandstone. In unshaded cores, the Sunbury rests directly on the Bedford Shale, with no Berea present. BDFD = Bedford Shale. BREA = Berea Sandstone. SNB = Sunbury Shale. OHIO = Ohio Shale.

Berea cores (KGS-IMMR) near the outcrop in Kentucky							
KGS Core Call No.	County	GQ	Carter Coordination Location	Hole	North Latitude (83)	West Longitude (83)	Cored Interval
1544	Bath	Olympia	14-T-71	D-2	38.120866	-83.638634	SNB-BDFD-OHIO
1545	Bath	Salt Lick	8-S-71	D-3	38.056397	-83.620746	SNB-BDFD-OHIO
1546	Bath	Olympia	17-S-70	D-4	38.027114	-83.728038	SNB-BDFD-OHIO
1552	Estill	Leighton	20-N-67	D-10	37.612492	-83.9328	SNB-BDFD-OHIO
5673	Fleming	Farmers	15-U-72	D-11	38.214359	-83.576149	SNB-BDFD-OHIO
5665	Fleming	Burtonville	3-W-72	KEP-4	38.408041	-83.538829	SNB-BREA-BDFD-OHIO
811	Fleming	Plummers Landing	1-V-72	KEP-5	38.324984	-83.502175	SNB-BDFD-OHIO
5671	Fleming	Plummers Landing	21-W-71	KEP-6	38.34824	-83.584031	SNB-BDFD-OHIO
812	Fleming	Plummers Landing	19-V-72	KEP-7	38.27471	-83.519189	SNB-BDFD-OHIO
6387	Lewis	Stricklett	2-W-73	KEP-3	38.409002	-83.437255	SNB-BREA-BDFD-OHIO
813	Lewis	Vanceburg	3-Y-75	KEP-8	38.582669	-83.288835	SNB-BREA-BDFD-OHIO
814	Lewis	Tollesboro	18-Z-73	KEP-9	38.610029	-83.452448	SNB-BREA-BDFD-OHIO
6386	Lewis	Charters	17-Y-74	KEP-2	38.52435	-83.395545	SNB-BREA-BDFD-OHIO
1547	Montgomery	Means	13-R-69	D-5	37.955847	-83.797123	SNB-BDFD-OHIO
1548	Montgomery	Levee	20-R-67	D-6	37.938082	-83.917107	SNB-BDFD-OHIO
1543	Rowan	Farmers	25-U-72	D-1	38.175397	-83.568404	SNB-BDFD-OHIO
1549	Powell	Stanton	20-Q-68	D-7	37.864636	-83.848664	SNB-BDFD-OHIO
1550	Powell	Clay City	6-P-68	D-8	37.807616	-83.901377	SNB-BDFD-OHIO

vision is for shales. Shales may contain thin, silty laminae.

Core Bedding on Graphic Sections

Bedding in the Bedford-Berea is characteristic of marine and slope (or ramp) deposits. Because of the Berea and Bedford's fine grain size, large-scale crossbeds do not occur. Figure CB-7 is a legend for the measured sections in the core book. The most common bedding in the cores is massive, parallel laminated, and soft-sediment deformed. Massive beds were subdivided into massive beds, massive beds with faint parallel laminae or texture, and massive beds with faint low-angle textures or laminae.

Distinct low-angle laminated beds occur in some cores and may represent several bed types in outcrop, including hummocky bedding, swaley bedding, and soft-sediment-deformed (convo-

luted, flow rolls, ball-and-pillow structures) beds. Both hummocky and swaley bedding have been identified in outcrop exposures, and likely occur in cores. Some low-angle bedding may also represent soft-sediment deformation, which is also pervasive in this interval.

A wide variety of soft-sediment deformation structures can be seen in all of the cores. Larger disruptions are shown as flow rolls on the graphic logs. A distinction is made between soft-sediment deformation in silty beds (little grain-size variation visible) and deformed beds with appreciable shale (significant shale interbeds). For smaller-scale deformations, a symbol for convolute laminae was used where laminae are disrupted or significantly folded, and a symbol for undulatory laminae was used where bedding or laminae were mostly intact but undulating or mounding.

System	Series	Int. Stage	Central Kentucky (Cincinnati Arch)	Eastern Kentucky (Appalachian Basin)	Southeastern Ohio (Appalachian Basin)	Central West Virginia (Appalachian Basin)		
Mississippian	Lower	Tournaisian	[Stratigraphic column with Chattanooga Sh, New Albany Sh, etc.]	Borden Fm (lower part)	Logana Fm	<i>undifferentiated</i>		
				Sunbury Sh Bedford Sh Berea Ss	Sunbury Sh Bedford Sh Berea Ss	Sunbury Sh		
Devonian	Upper	Famennian	[Stratigraphic column with Chattanooga Sh, New Albany Sh, etc.]	Cleveland Sh Mbr <i>Three Lick Bed</i>	Cleveland Sh Mbr	Berea Ss		
				Huron Sh Mbr upper	Ohio Sh	Ohio Sh	Chemung Mbr Chagrin Sh	Chemung Fm
				Huron Sh Mbr middle	Ohio Sh	Ohio Sh	Huron Sh Mbr	
Frasnian	Huron Sh Mbr lower	Ohio Sh	Ohio Sh	Huron Sh Mbr	"lower Huron Sh Mbr"			
			Upper Oolentangy Sh	Upper Oolentangy Sh	Upper Oolentangy Sh	Hanover-Angola Sh		
			Rhinestreet Sh	Rhinestreet Sh	Rhinestreet Sh	Rhinestreet Sh		

Figure CB-5. Stratigraphic correlation of units in the Berea petroleum system.

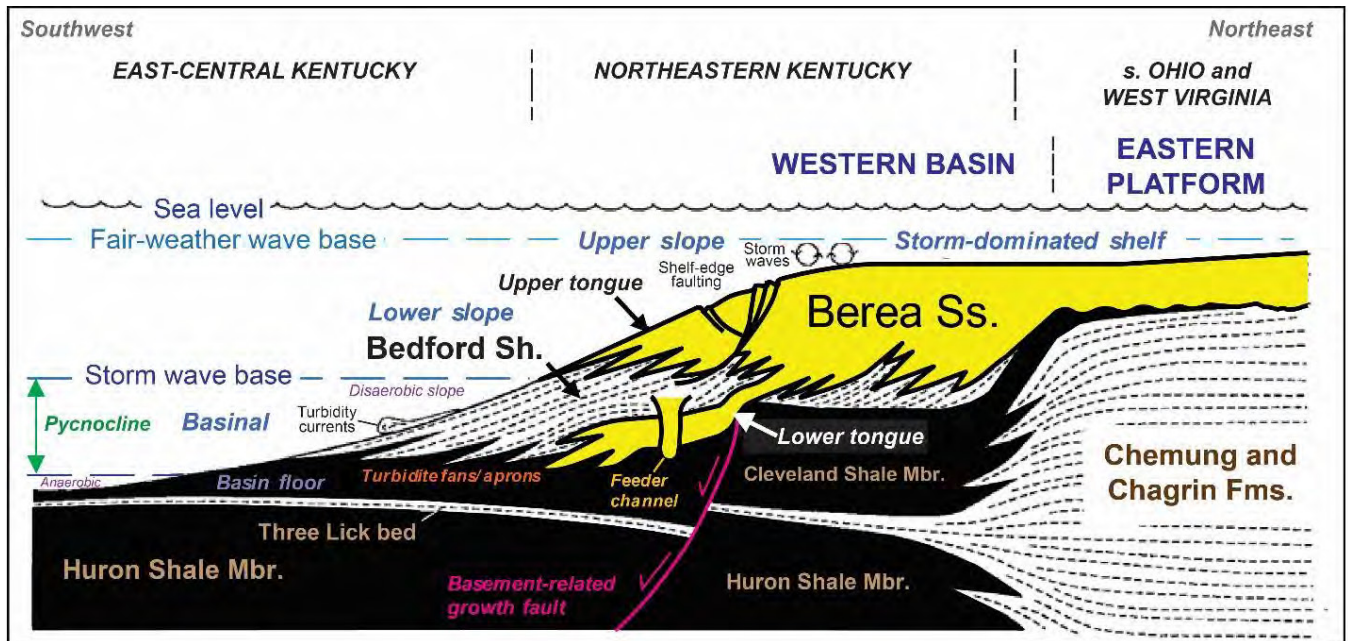


Figure CB-6. Interpretation of depositional systems and presumed lateral stratigraphic relationships for elements of the Berea petroleum system. Modified from Pashin and Ettensohn (1995, Fig. 9); used with permission of the Geological Society of America. The Sunbury Shale would cap the units shown.

Ripple laminae are common on the tops of some bedding surfaces in outcrop, but are relatively rare to uncommon in core. Ripples in core are generally single trains at the tops of beds or within thin laminae in interbedded shales and sandstones (especially in those cores that contain the lower

Bedford interval). All ripples observed in core are asymmetric (have inclined foresets) and likely represent combined-flow ripples, similar to outcrop occurrence. In some of the gray shales and interbedded shales and siltstones, there are also small lenticular to wavy intervals that look like ripples,

Legend

 Massive bedding	 Interlaminated siltstone (or sandstone) and shale
 Massive bedding (with faint parallel lamination or texture)	 Gray shale
 Massive bedding (with faint inclined low-angle lamination or texture)	 Gray shale with thin silty laminae (mostly shale)
 Graded bedding	 Very dark gray shale
 Parallel lamination	 Black shale
 Low-to moderate-angle lamination (likely HCS or SCS)	 Thin, silty to shaly interval at top or bottom of bed (often gradational)
 Shale-clast lag	 Bioturbation (mostly small vertical burrows, <i>Arenicolites</i> , or isolated <i>Planolites</i>)
 Undulatory lamination	 Offset bedding (minor compactional faulting)
 Ripple bedding or lamination	 F Fracture
 Pseudo-ripple or silty lenticular bedding (with indistinct foresets)	 S Slickensides
 Convoluted or contorted laminae	 • p Pyrite
 Flow roll or other soft-sediment deformation	 r Red (maroon, orange) color
 Flow roll or other soft-sediment deformation (with significant shale)	 dg Dark gray color (highlighting core that is darker than the normal light gray siltstone of the Berea)
 Load casts	 ← Sample plug (horizontal)
 Pillows, detached load casts, and pseudo-nodules in shale	 ↑ Sample plug (vertical)
 Dish structures	 X Missing core

C1B2 Core no., Box no. (multiple core runs)
 1674.3 Bottom depth in core box

B2 Box no.
 1674.3 Bottom depth in core box

Figure CB-7. Legend for graphic core logs.

but do not exhibit foresets. These are marked as pseudo-ripples on the graphic logs.

Bioturbation is rare in the core, and is uncommon in outcrop. Horizontal traces are most common on the tops of bedsets in outcrop exposures of the Berea, which would be difficult to see in cores. A single symbol was used for bioturbation in the graphic logs. Most of the features are very small. Also, many tiny oval siltstones in shales are shown as questionable bioturbation, because in some cases they may represent isolated load structures.

List of cores described and photographed:

1. Aristech Chemical Corp. #4 Aristech, p.182-198
2. Ashland Exploration #1 Hattie Neal, p. 199-206
3. Columbia Natural Resources #20505 Margaret Simpson, p. 207-219
4. Kentucky-West Virginia Gas #1122 Milton Moore, p. 220-234
5. Kentucky-West Virginia Gas #1087 Ruben Moore, p. 235-244
6. Ashland Oil #KY-4 Kelly-Watt-Bailey-Skaggs, p. 245-253
7. Gillespie #1 Lowell Bailey, p. 254-256
8. Columbia Gas Transmission #18120456 Pocahontas Mining, p. 257-280
9. Equitable Production Co. #18150353 EQT, p. 281-303
10. Somerset Gas Service #1 Morlandbell Inc., p. 304-310

Aristech Chemical Corp. #4 Aristech

Location: Scioto County, Ohio (see Figure CB-1, Table CB-1)

OGS Core Call No.: 3409

Oil and Gas API No.: 341456014100000

Geophysical Logs: Caliper, gamma-ray, induction, neutron

Well Completion Date: 1998

Core Depth: Top of Berea at 679.2 ft

Bedford-Berea Core Interval Thickness: 157.8 ft

Field: None

Completion: None; well was drilled for monitoring

Background and Distance to Recent Berea Oil Wells

The Aristech core is the northernmost core examined in the study. Additional Berea cores northward into Ohio are publicly available from the Ohio Geological Survey. This is the closest core to the outcrops in northeastern Kentucky and to the recent Greenup County Berea oil play. The core is from 8 mi north of the unnamed recent oil field operated by Nytis Exploration in Greenup County, Ky., and 9 mi northwest of the old Ashland gas field, which also had local Berea production. It is from 19 mi east and down-dip of the Berea outcrops in Garrison, Ky. This core is one of several from the Aristech property that extend down to the base of the Cambrian.

Key Features

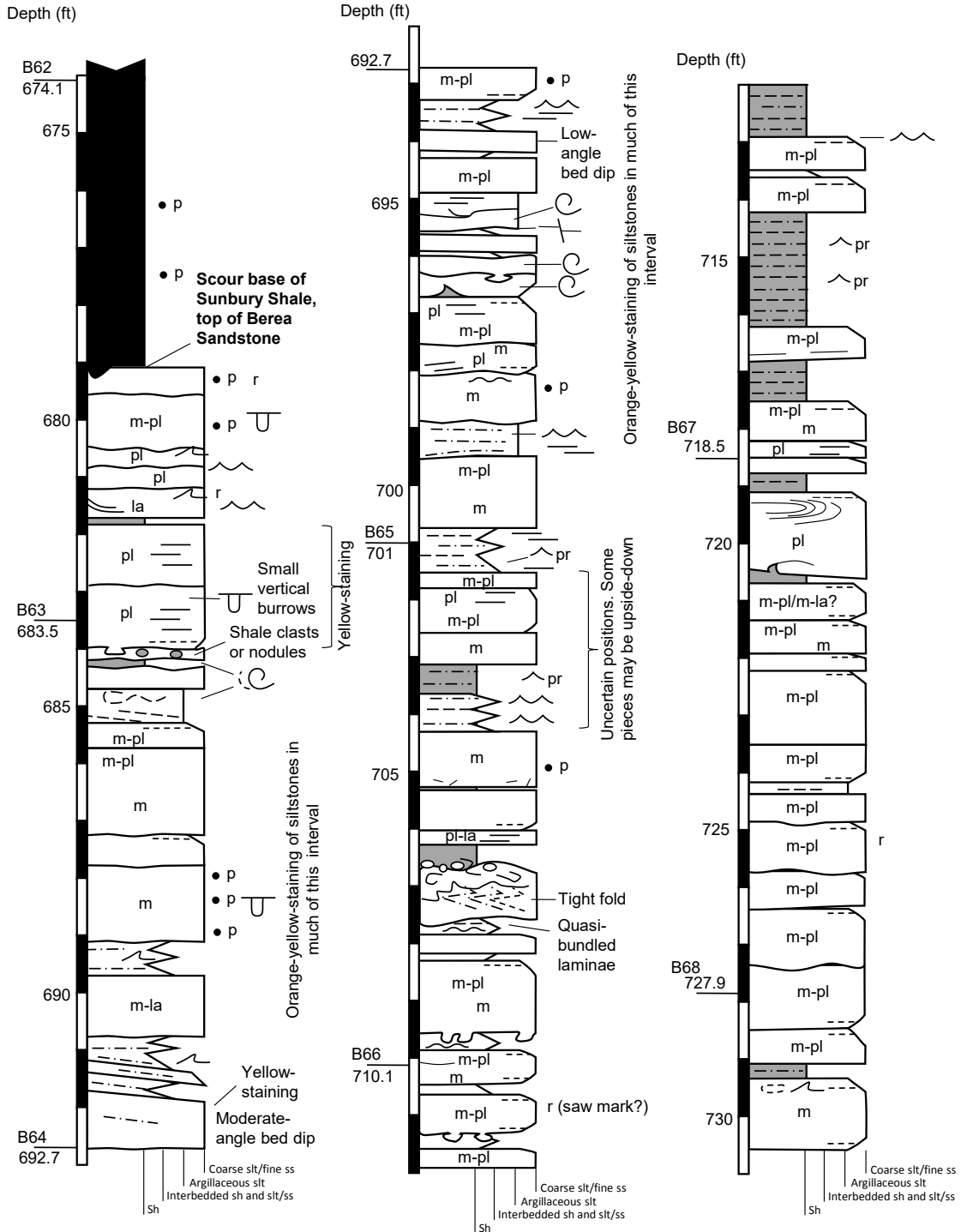
This is a complete core from the northern part of the study area (Figs. CB-3, CB-4). It is the thickest Berea core studied, and has a greater percentage of Berea siltstones/sandstones to Bedford shales than the other cores examined. Bedding is dominated by thin storm-shelf beds (sharp-based, massive to parallel-laminated beds), as in other cores, but beds tend to have more ripple caps and less soft-sediment deformation than do cores to the south.

Data and Analysis

None (for Berea). No new samples collected for this project.

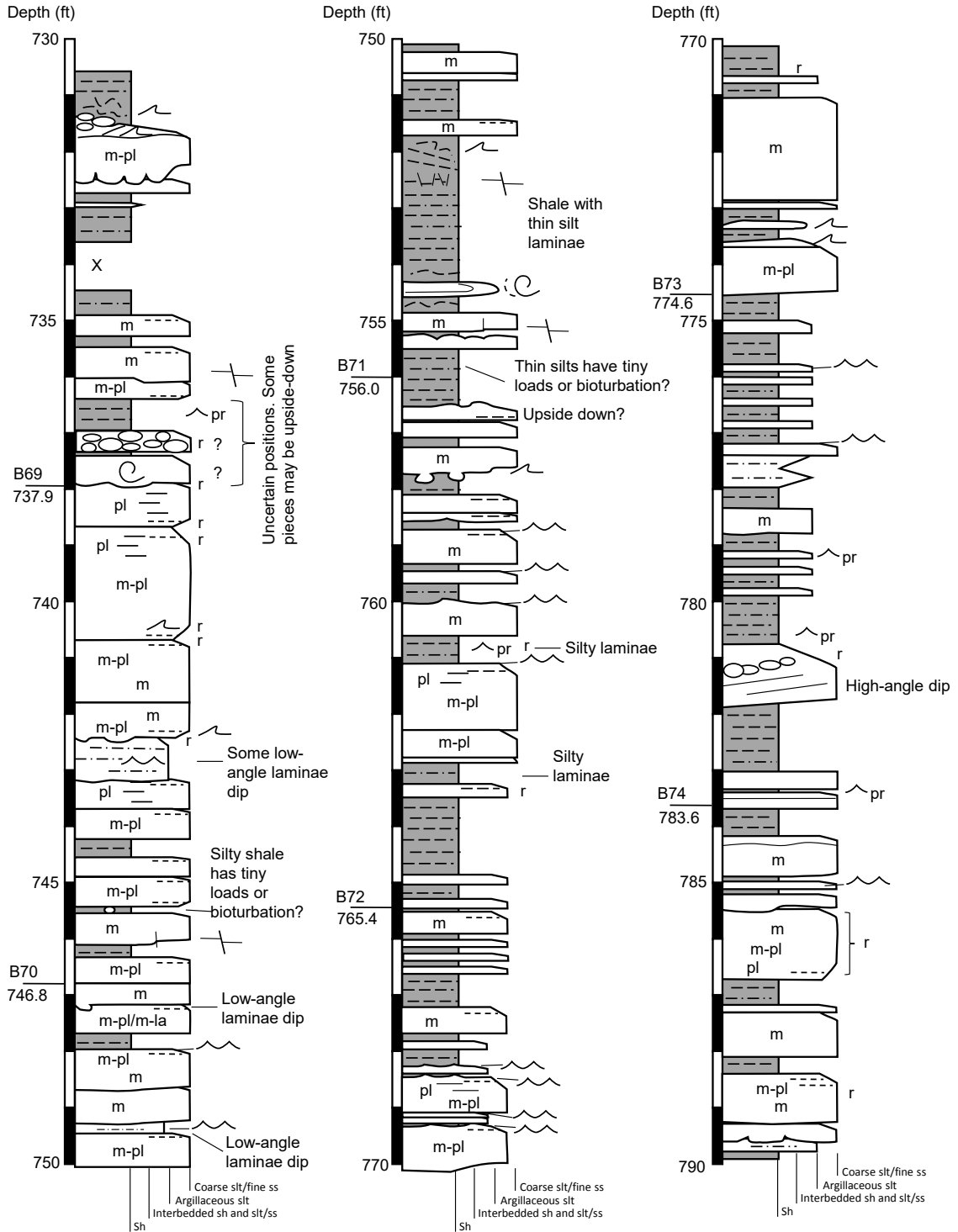
Aristech Chemical Corp. No. 4 Aristech

Description from slabbed core



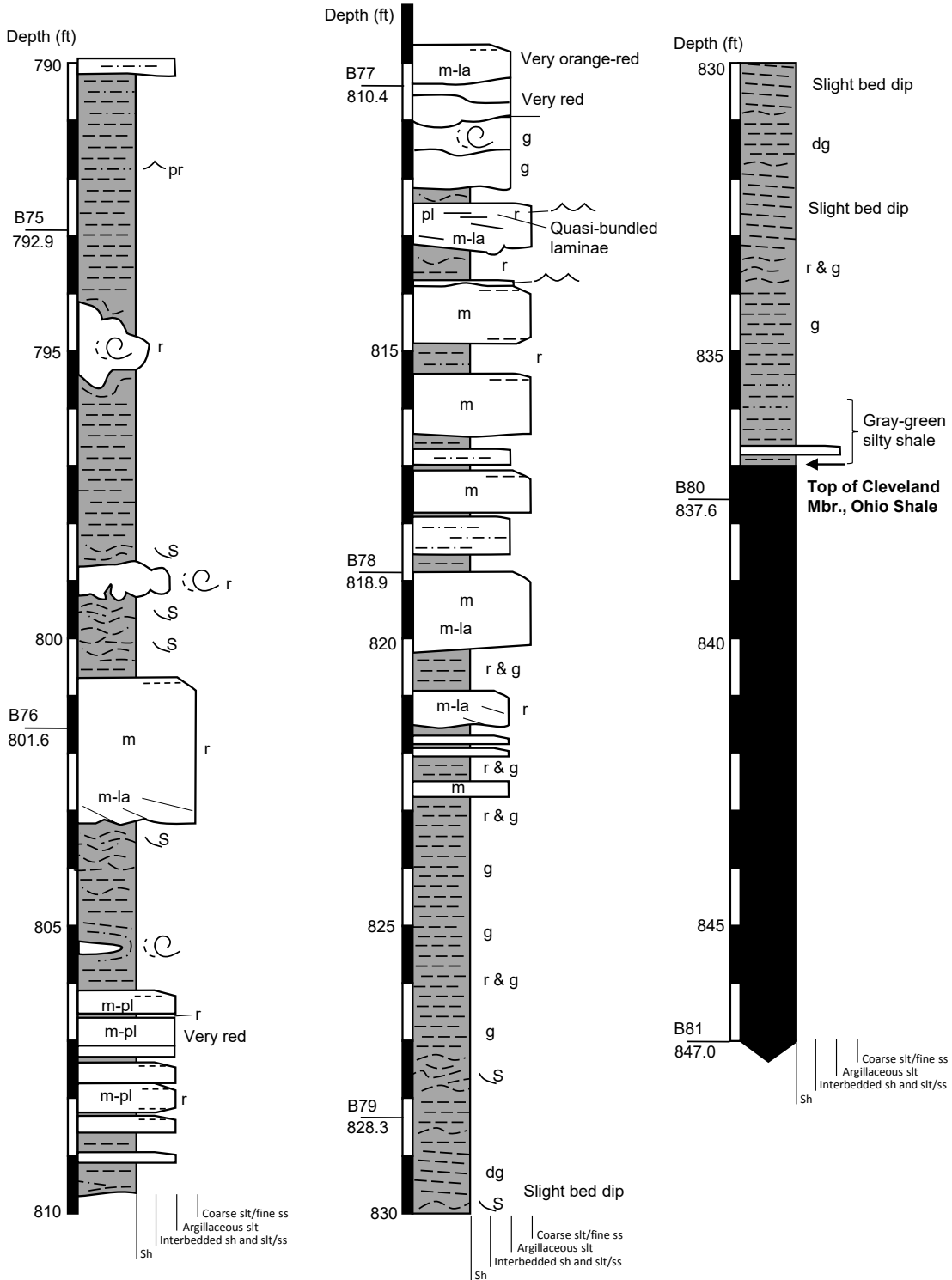
Aristech Chemical Corp. No. 4 Aristech

Description from slabbed core

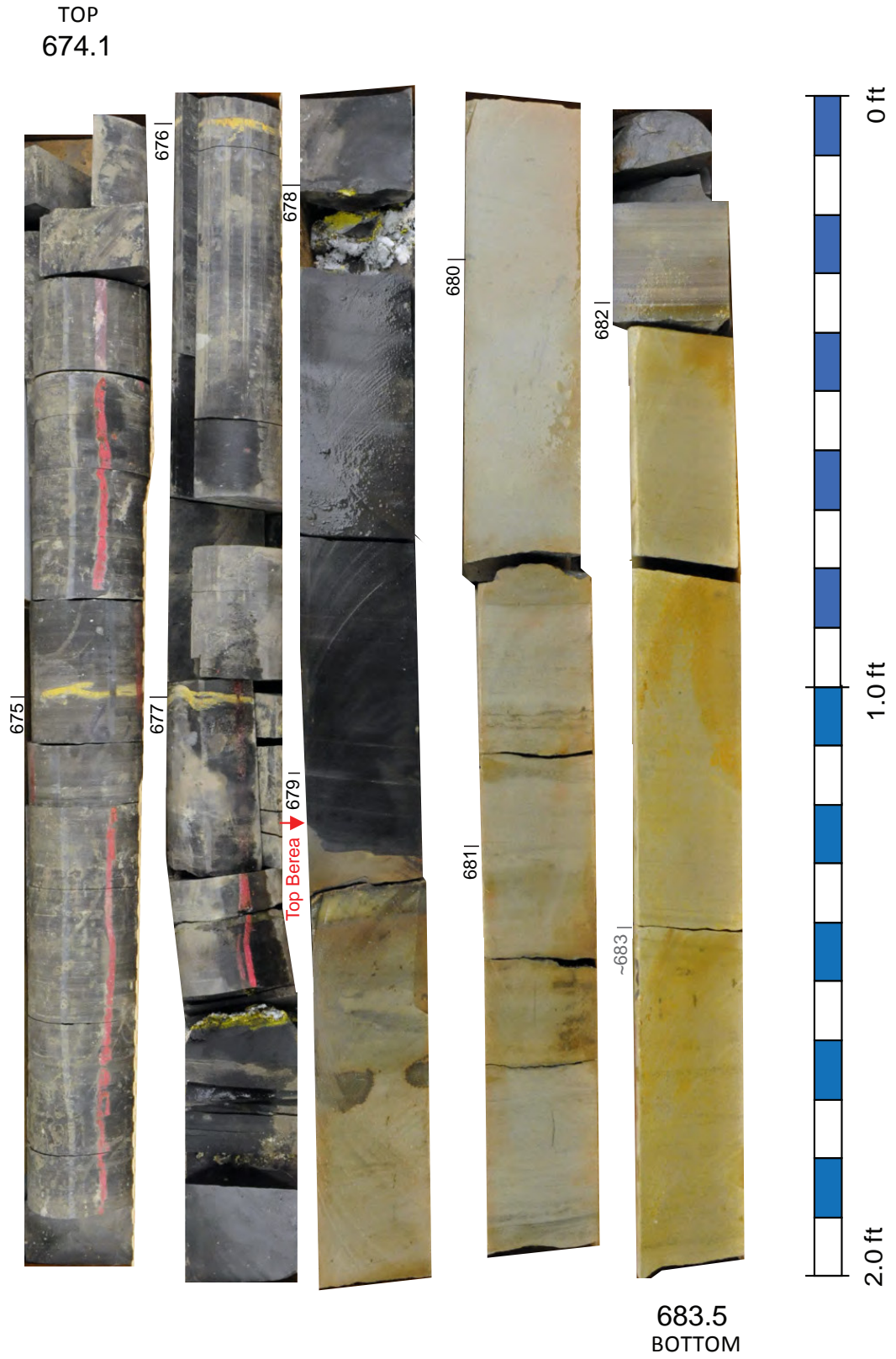


Aristech Chemical Corp. No. 4 Aristech

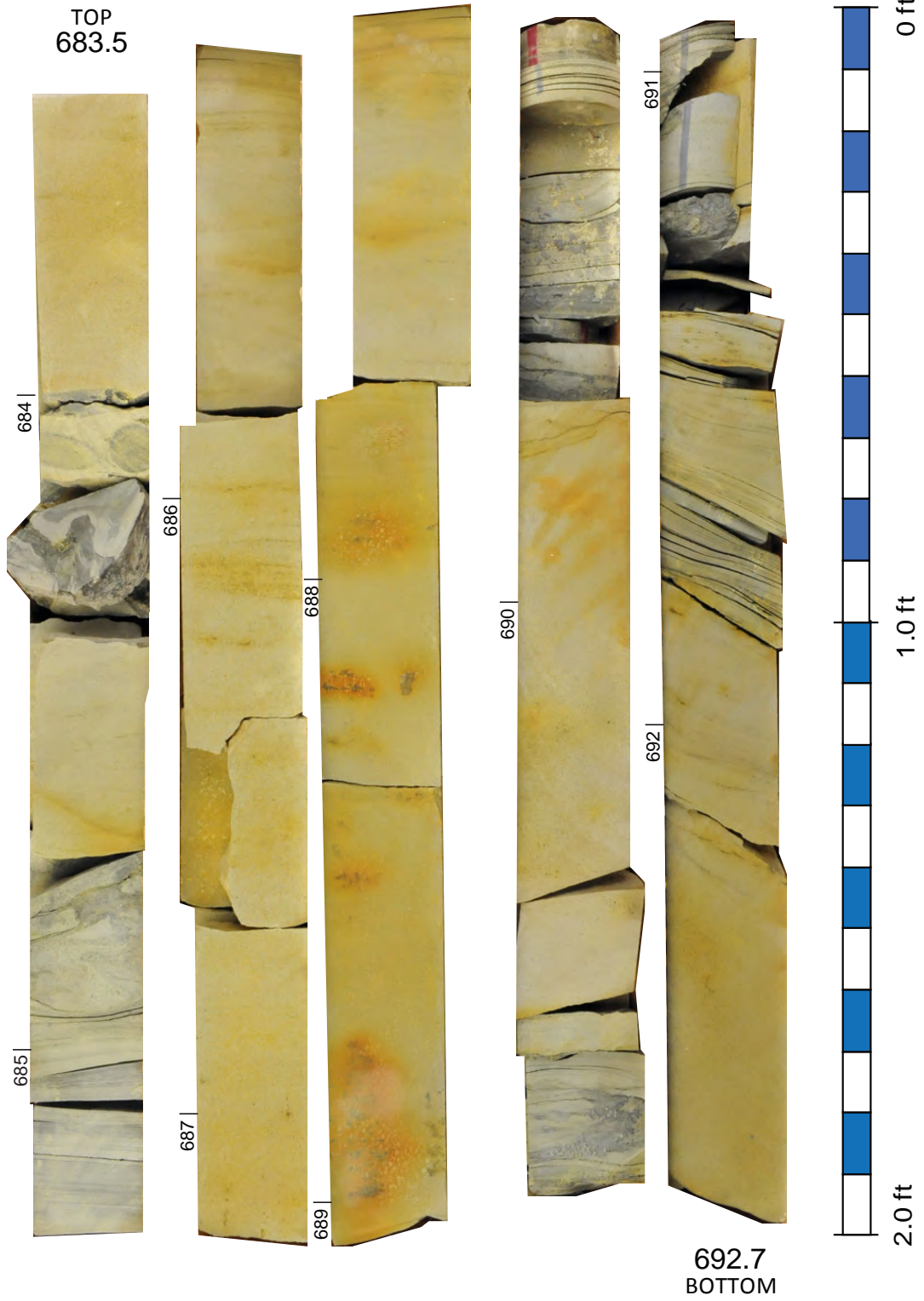
Description from slabbed core



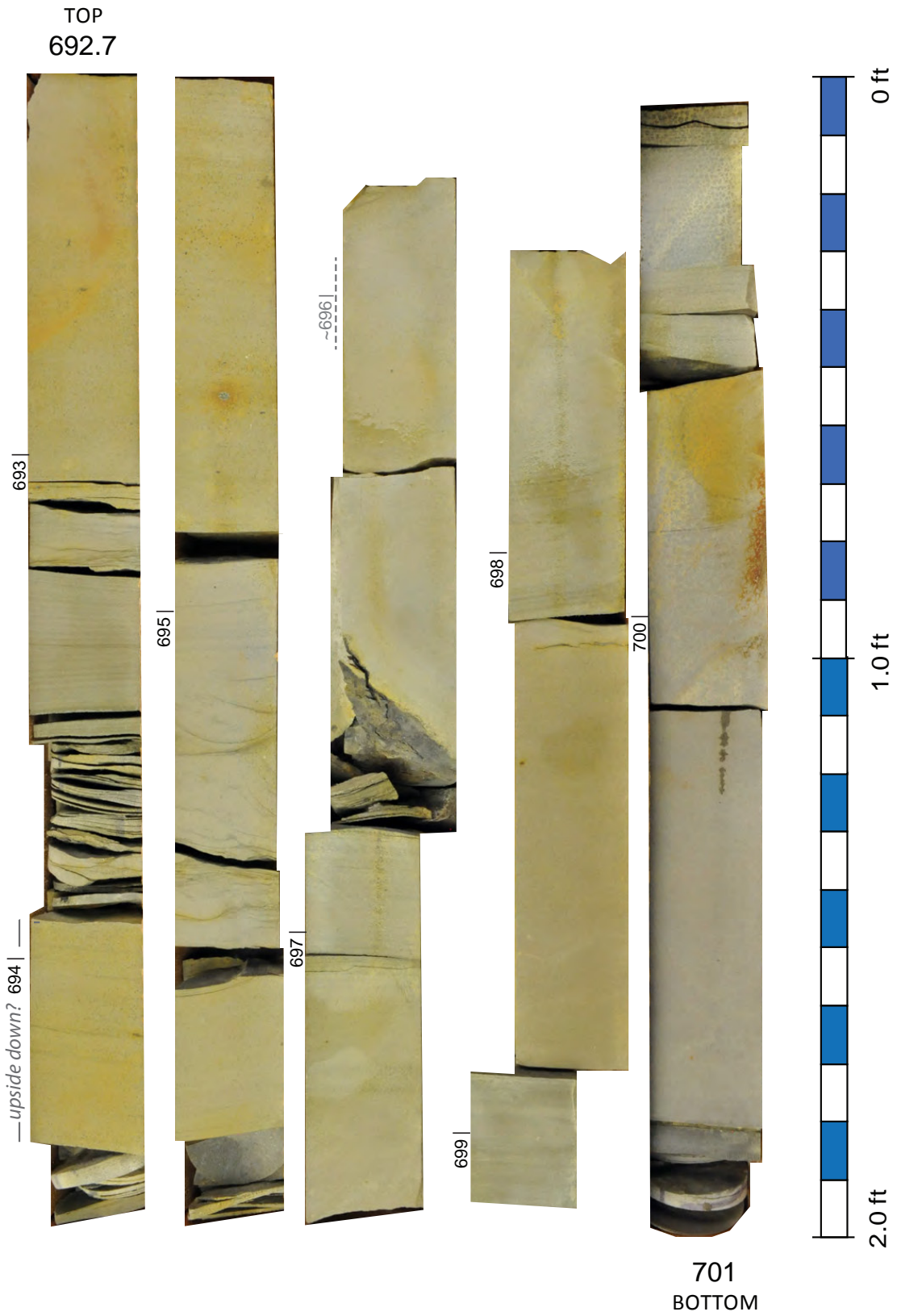
Aristech Chem. No. 4 Aristech, Box 63



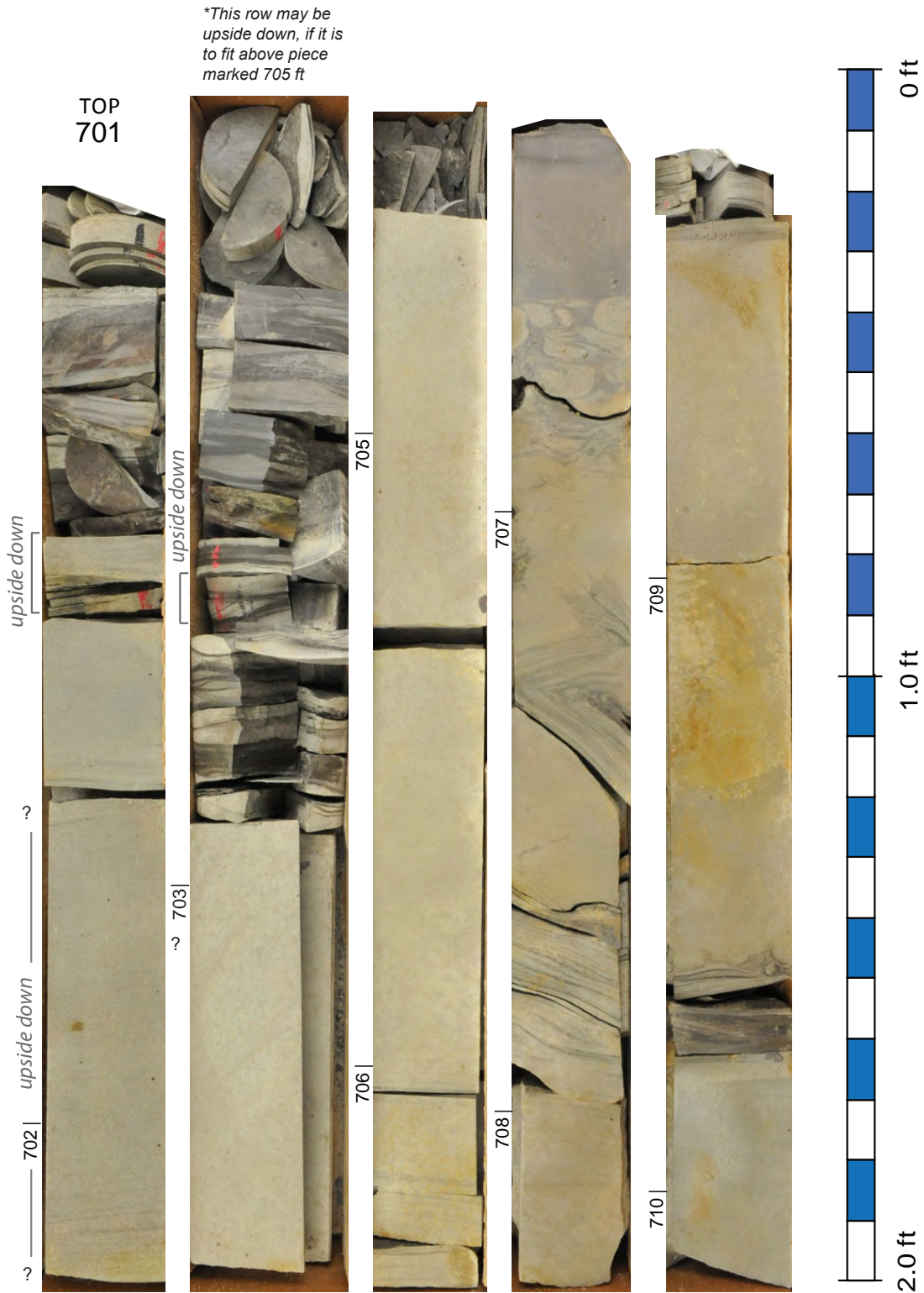
Aristech Chem. No. 4 Aristech, Box 64



Aristech Chem. No. 4 Aristech, Box 65

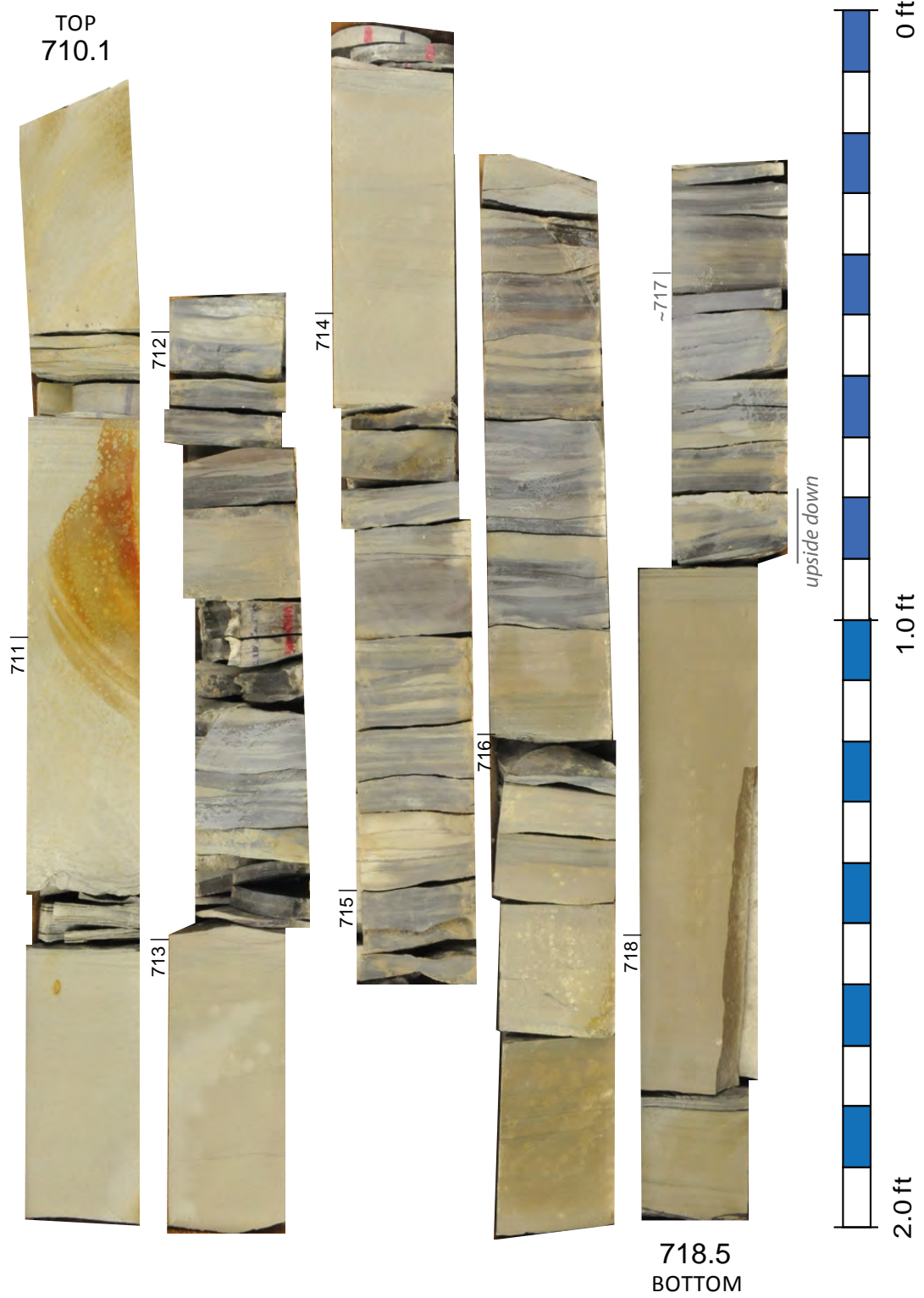


Aristech Chem. No. 4 Aristech, Box 66

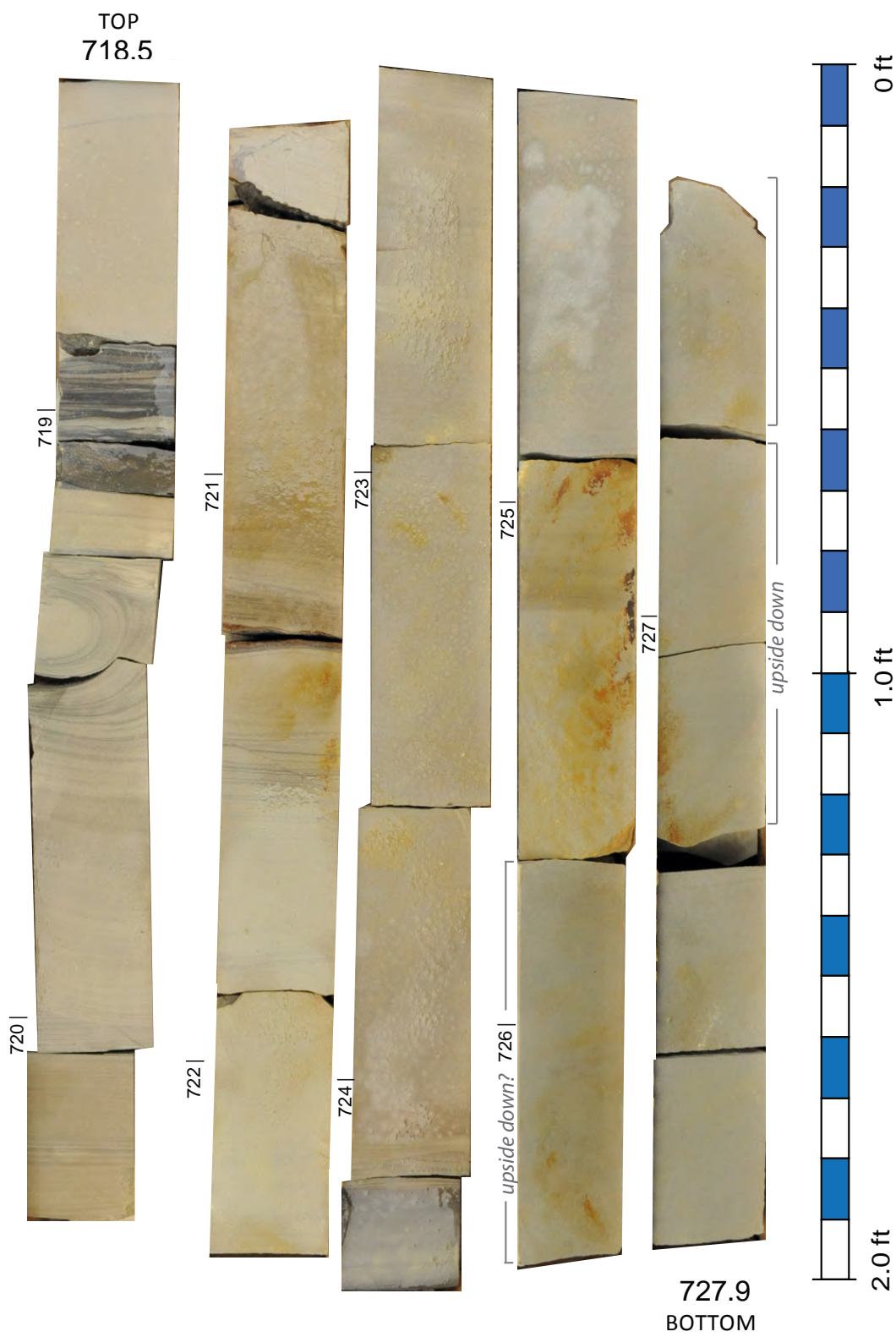


Position of marked 702 ft depth is 1.5 ft beneath 701 ft. Marked depth 703 in second row. is 1.6 ft beneath 702 and is closer to where the 704 ft position should be. No core is marked "704", although it might be in the broken shaly interval above, in which case the entire row may be upside down.

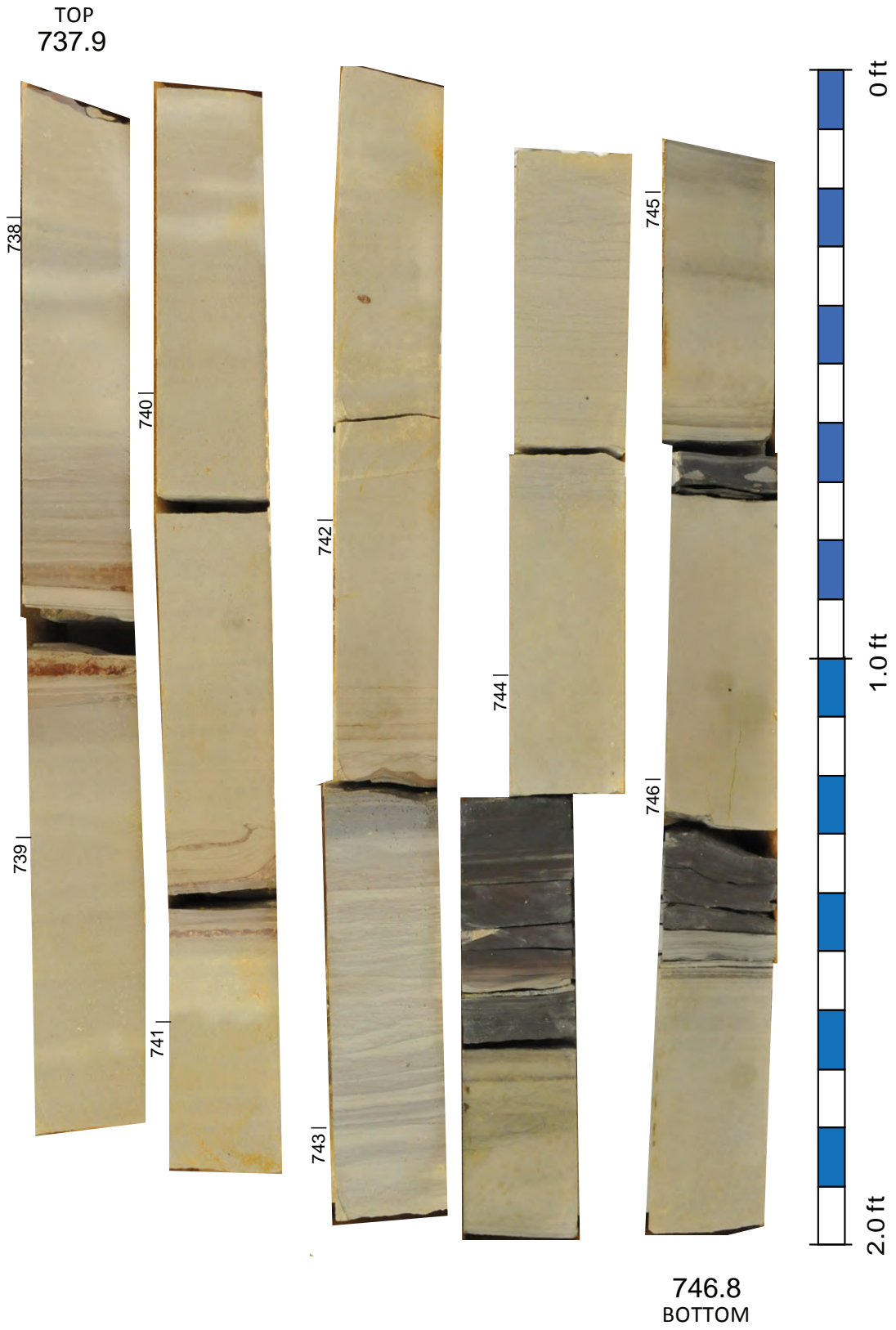
Aristech Chem. No. 4 Aristech, Box 67

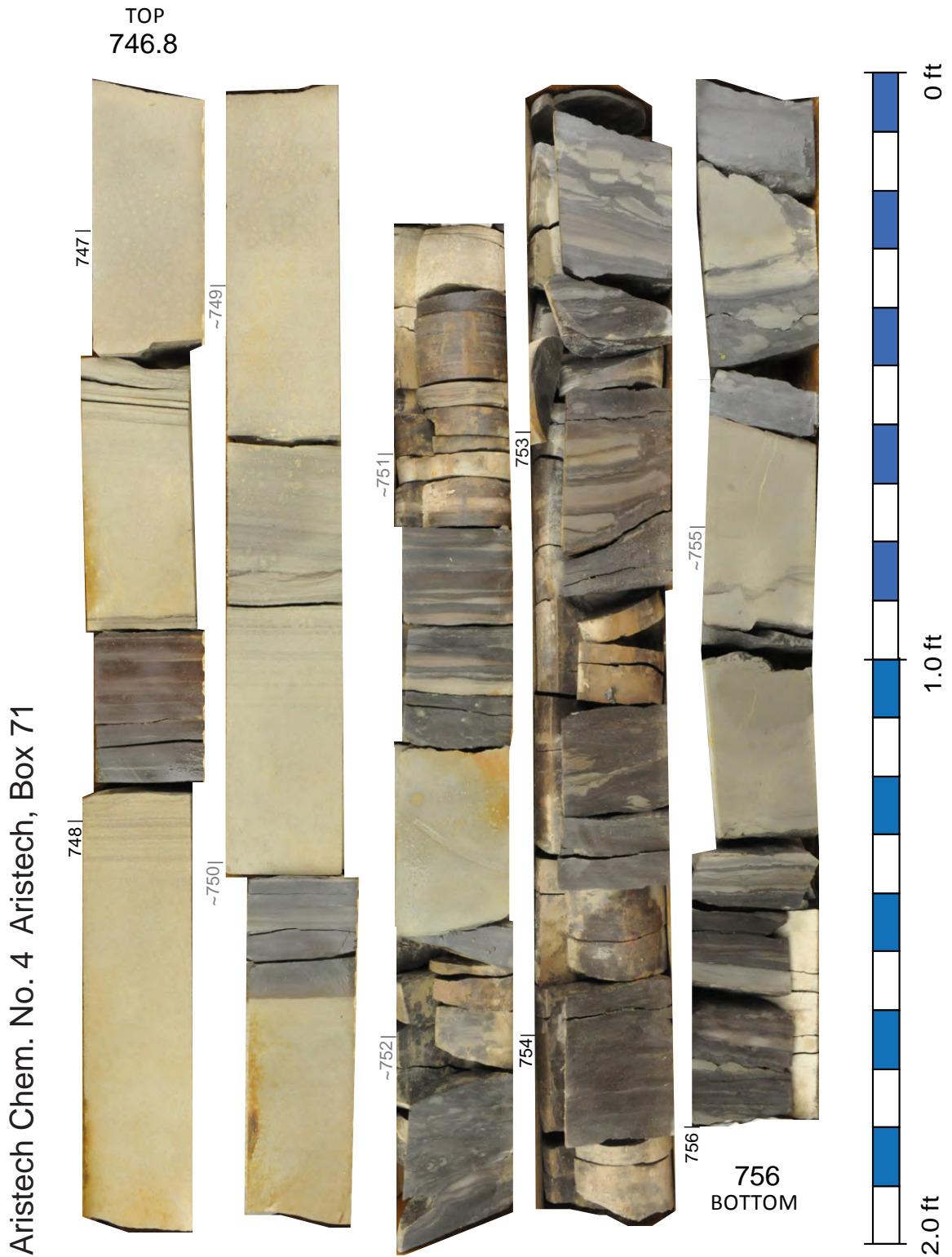


Aristech Chem. No. 4 Aristech, Box 68



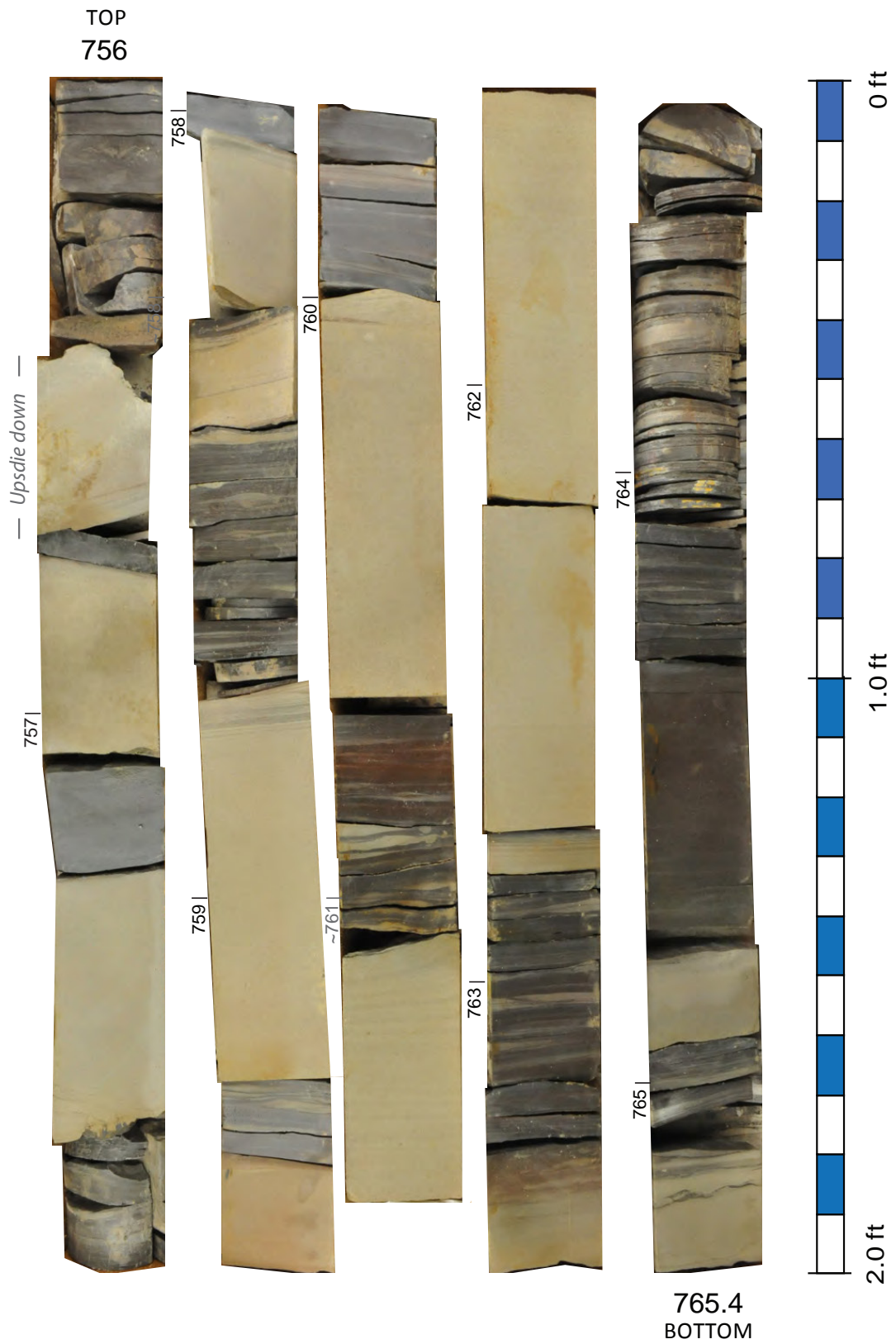
Aristech Chem. No. 4 Aristech, Box 70



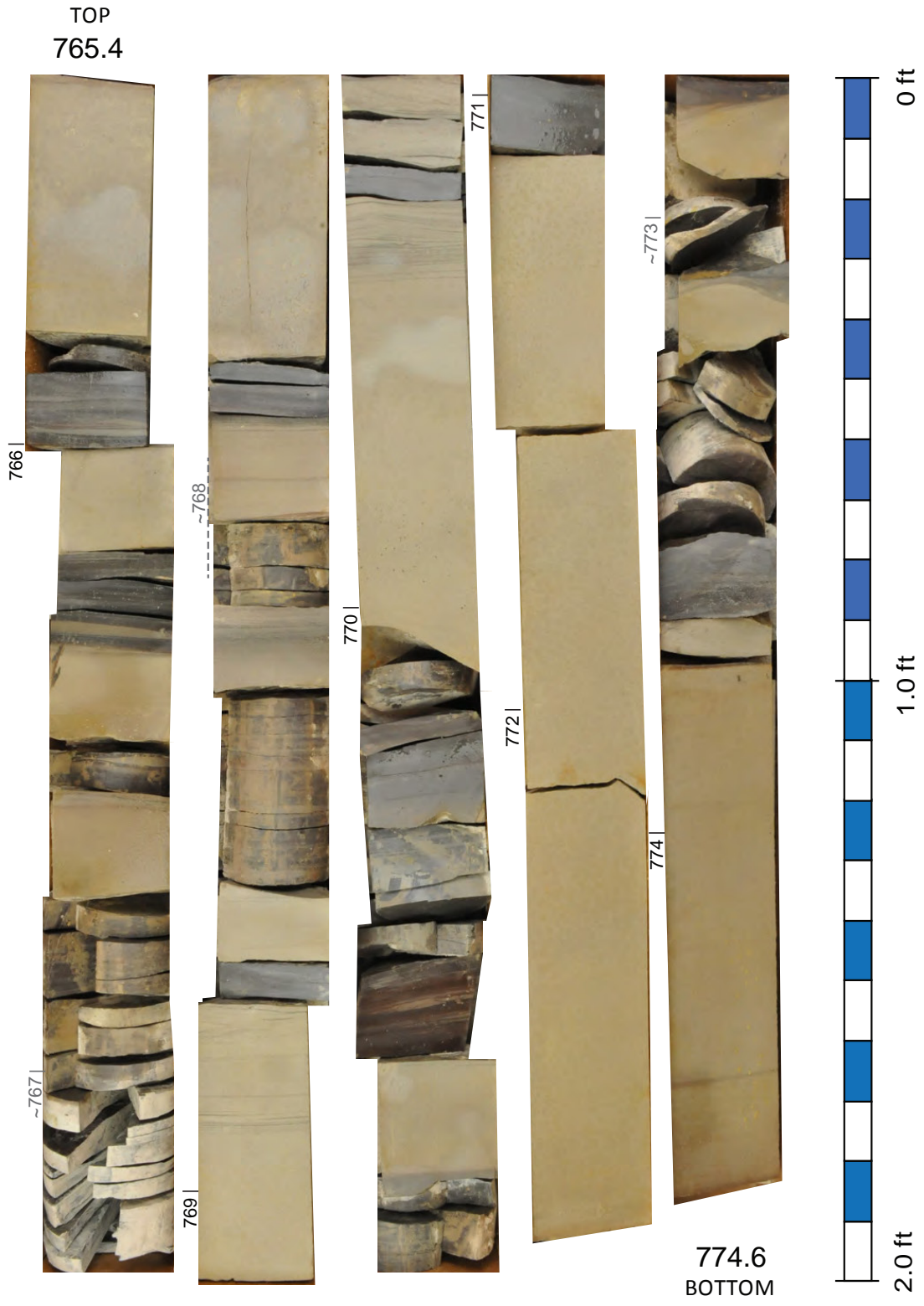


Depths are not marked (or have worn off) on the core between 748 - 753 ft, so depths shown in gray on this page are measured below the marked depth of 748 ft and shown as approximate depths.

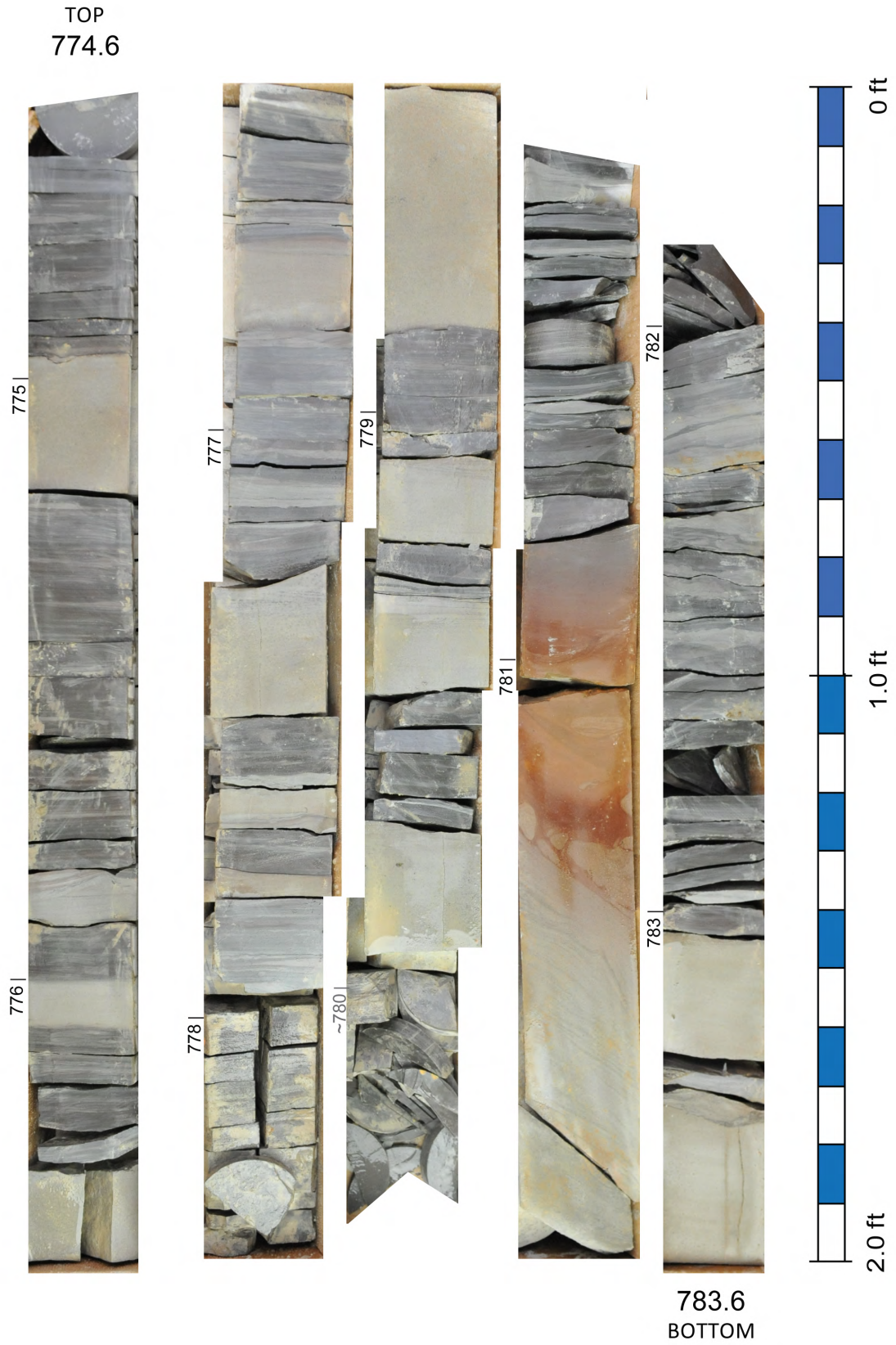
Aristech Chem. No. 4 Aristech, Box 72



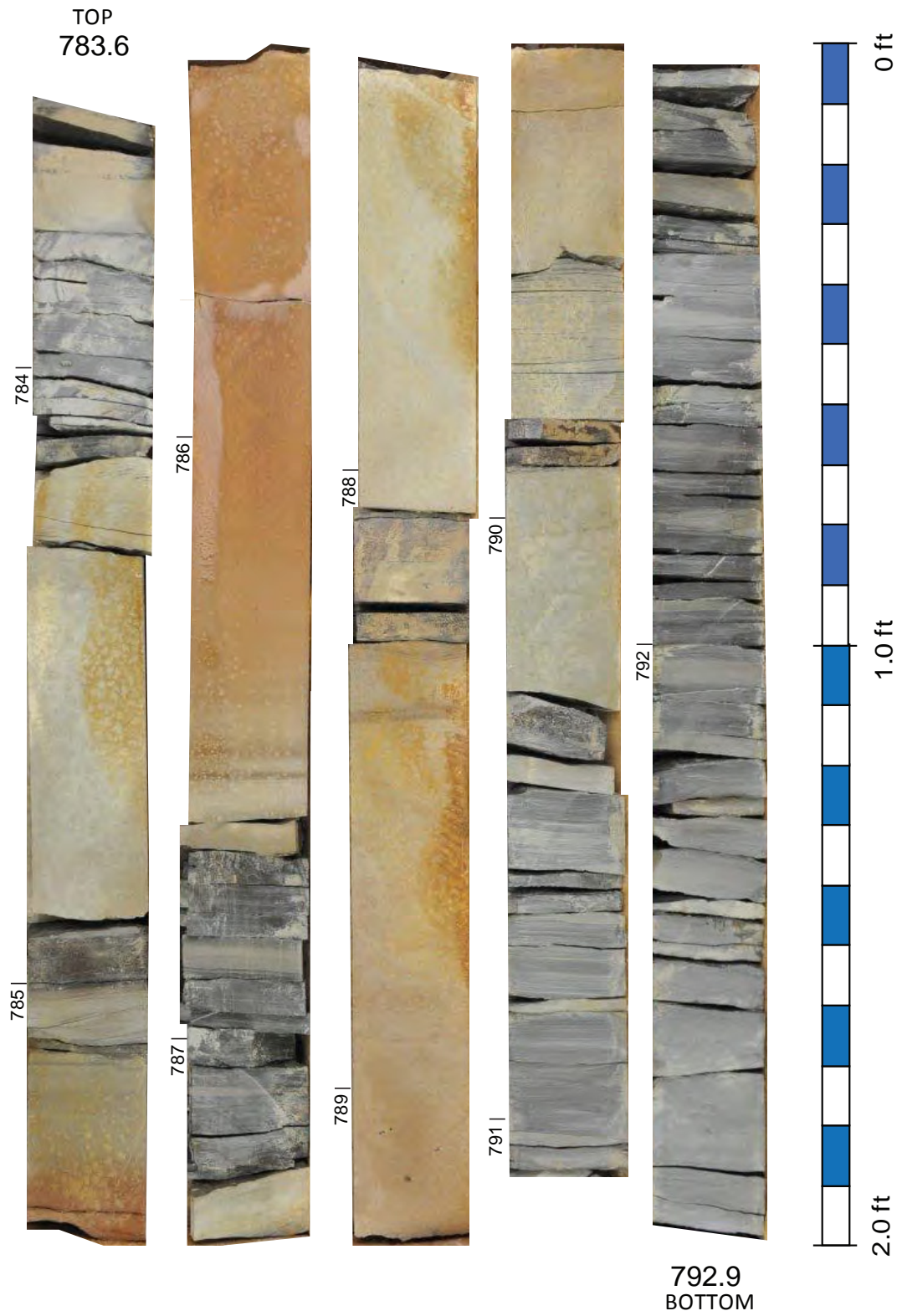
Aristech Chem. No. 4 Aristech, Box 73



Aristech Chem. No. 4 Aristech, Box 74



Aristech Chem. No. 4 Aristech, Box 75



Ashland Exploration #1 Hattie Neal

Location: Lawrence County, Ky. (see Figure CB-1, Table CB-1)

KGS Core Call No.: C-5691

KGS Oil and Gas Record No.: 11647

Geophysical Logs: Compensated formation density (caliper, gamma-ray, compensated density porosity, bulk density), induction (spontaneous potential, resistivity), radioactivity (gamma-ray, neutron), temperature

Well Completion Date: 8/7/1981

Core Depth: Top of Berea at 1,484.5(?) ft

Bedford-Berea Core Interval Thickness: 33.5 ft (with gaps)

Bedford-Berea Total Thickness: 113 ft

Field: None (no name); 4.1 mi west of Fallsburg oil field

Completion: Oil and gas from Berea (1,499–1,510, 1,514–1,520, 1,552–1,564 ft). Initial production after treatment was 3 bbl oil/day–2 bbl water/day, 11 MCF gas/day

Background and Distance to Recent Berea Oil Wells

One slabbed half of the Hattie Neal core was donated to KGS, and the other was apparently given to the University of Cincinnati to study. Potter and others (1983) used the Cincinnati core in their Berea core atlas. In 2015, the Cincinnati half of the core was donated to KGS. Over the years, pieces have been mixed up and removed from both cores, but with most of both halves, pieces can be rearranged into their correct positions. Several unmarked pieces still have uncertain depths.

The Ashland Hattie Neal core is one of four cores from Lawrence County. The core well is 1 to 5.2 mi west of several recent horizontal Berea oil wells drilled by Hay Exploration, and 2.8 to 4.6 mi southwest of an unnamed field of horizontal Berea oil wells drilled by Nytis Exploration and Quality Natural Gas. The Hattie Neal well is 1.48 mi northwest of the location of the Columbia Margaret Simpson core, which is a more complete Berea core from the area.

Key Features

The Hattie Neal core preserves only the upper 33 ft of the Berea, and there are many gaps (Fig. CB-4). The top of the core is beneath the base of the Sunbury Shale, but is iron-stained and bioturbated, so is likely from near the top of the Berea. The core is dominated (approximately 70 percent) by massive bedding or massive bedding with faint low-angle lamination (possibly hummocky stratification) and faint parallel laminae. Most beds are scour-based and often have a thin, argillaceous top, which is typical of inferred outer-shelf storm beds. Soft-sediment-deformed beds (flow rolls, ball-and-pillow structures, etc.) account for approximately 25 percent of the core. Many soft-sediment-deformed beds are truncated by the overlying bed. Some flow rolls are offset by small, presumably compaction or loading microfaults.

Potter and others' (1983) graphic log of this core noted convolute laminae, some horizontal laminae, and a few ripples. The ripples are shown at approximately 1,512–1,513 ft depth. The ripples do not appear to be present in the core now, so may be from a piece that is no longer in the boxes. Potter and others (1983) also noted stylolites in the core, one of which was shown on their graphic log at approximately 1,506 ft. There is a gap in the preserved core from 1,506–1,511 ft depth, so that footage also appears to be missing.

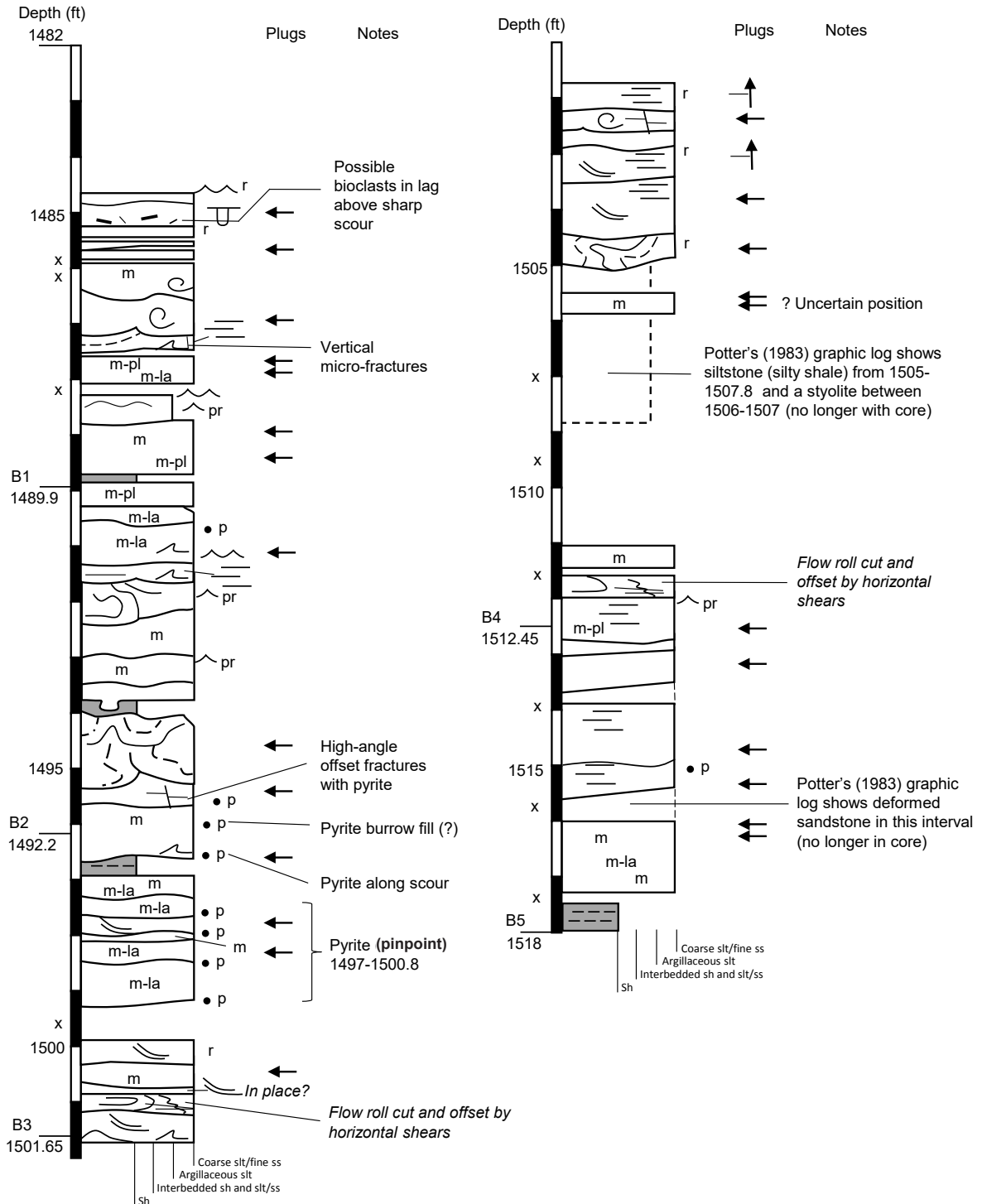
Data and Analysis

The Ashland Hattie Neal core has porosity, permeability, oil and water percentage data (n=33) from an Oil Field Research core analysis report. These data are available online from the KGS Oil and Gas Database. The core was previously studied by Potter and others (1983), who included grain-size analysis and a graphic log. Modal grain-size measurements (n=30) indicated a maximum grain size of approximately 0.65 μm (which is very fine sandstone, near the border with coarse siltstone), a minimum grain size of approximately 0.3 μm (near the coarse siltstone–medium siltstone border), and average grain size between 0.5 and 0.6 μm (coarse siltstone). Potter and others (1983) noted a slight coarsening-

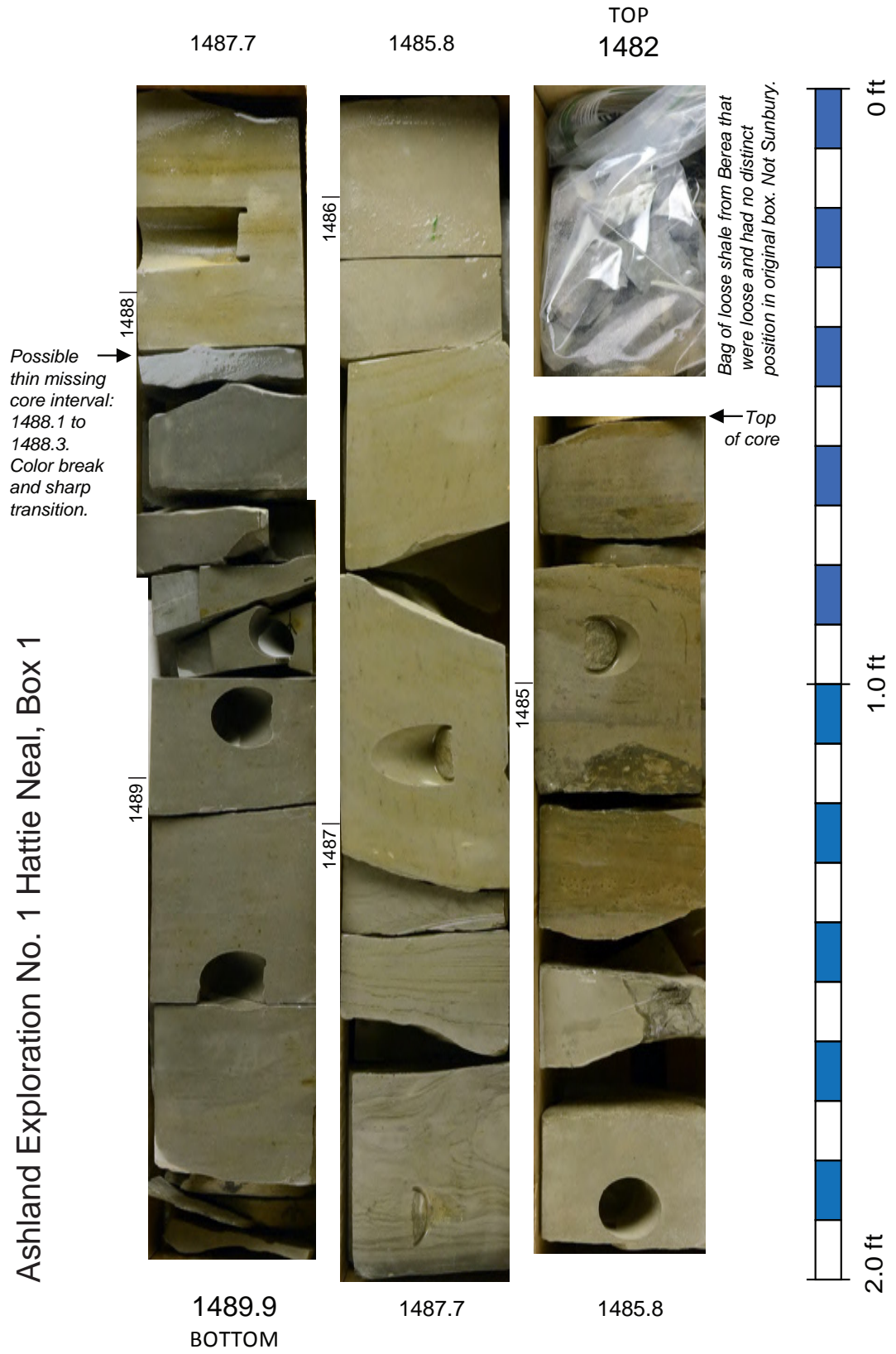
upward trend in the upper part of the core. More recently, additional porosity and permeability data, as well as XRD data, were collected by Chesapeake Energy. Thin sections were made from several of the Chesapeake sample plugs as part of the present Berea Consortium study.

Ashland Exploration No. 1 Hattie Neal

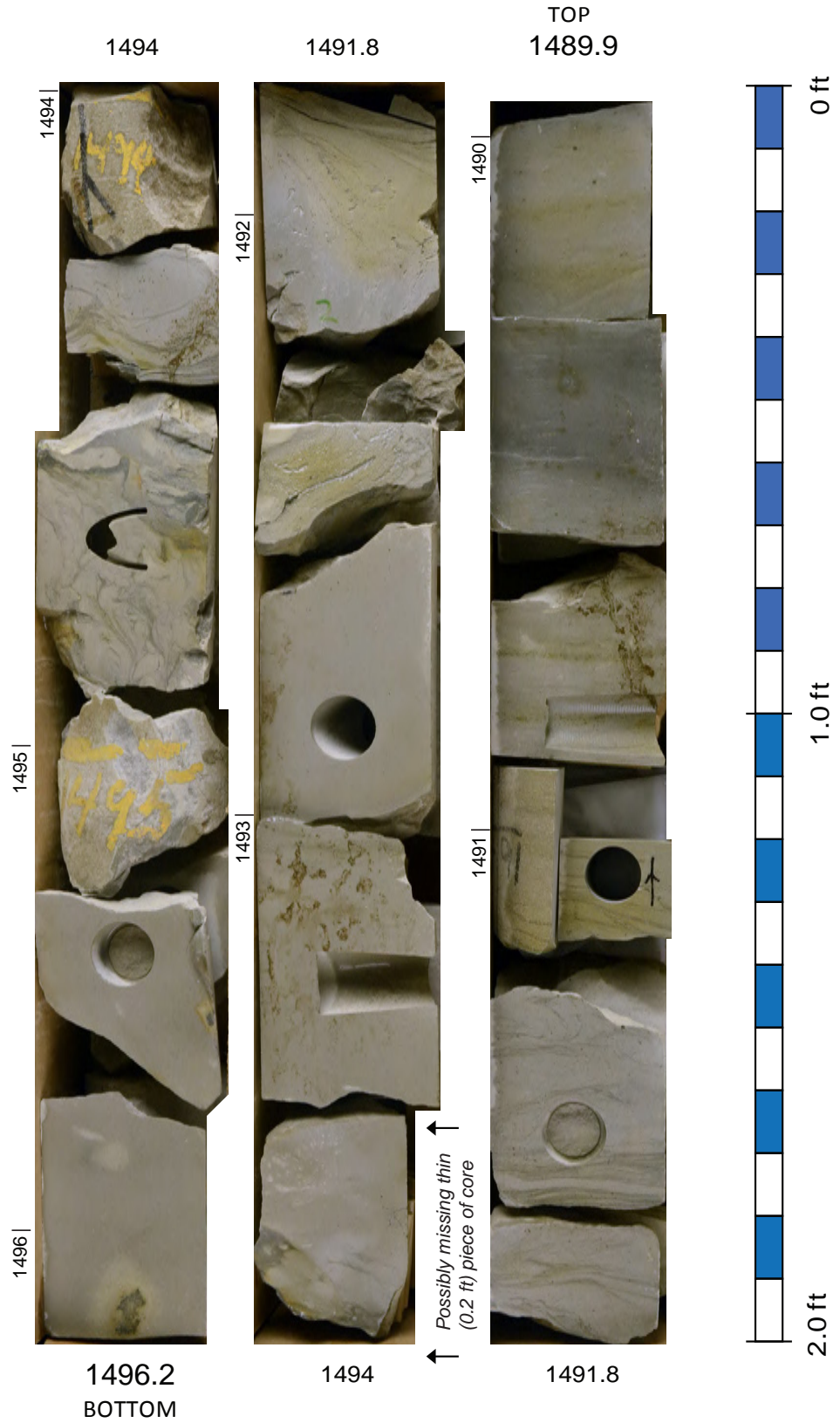
Description from slabbed core

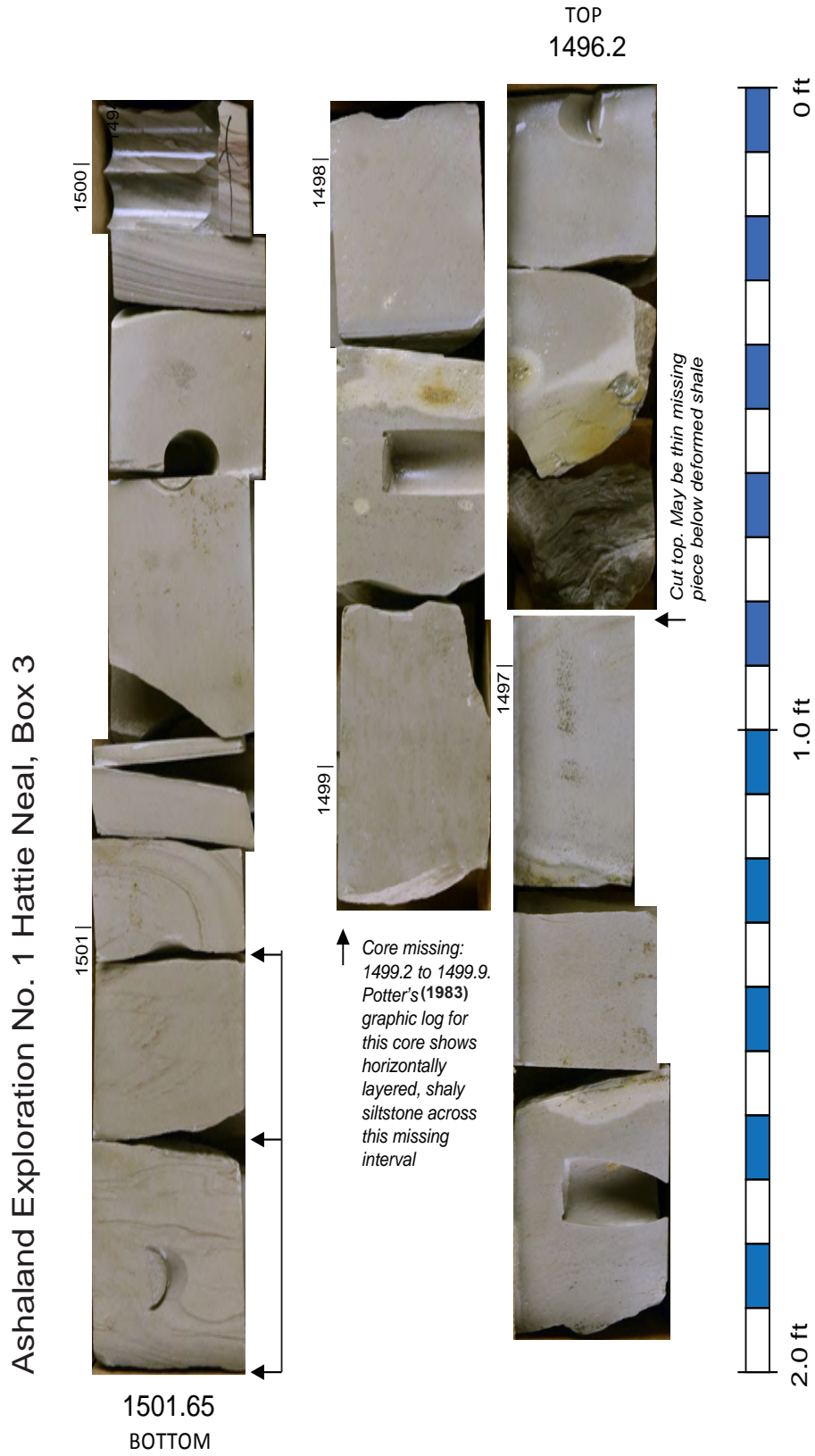


Ashland Exploration No. 1 Hattie Neal, Box 1

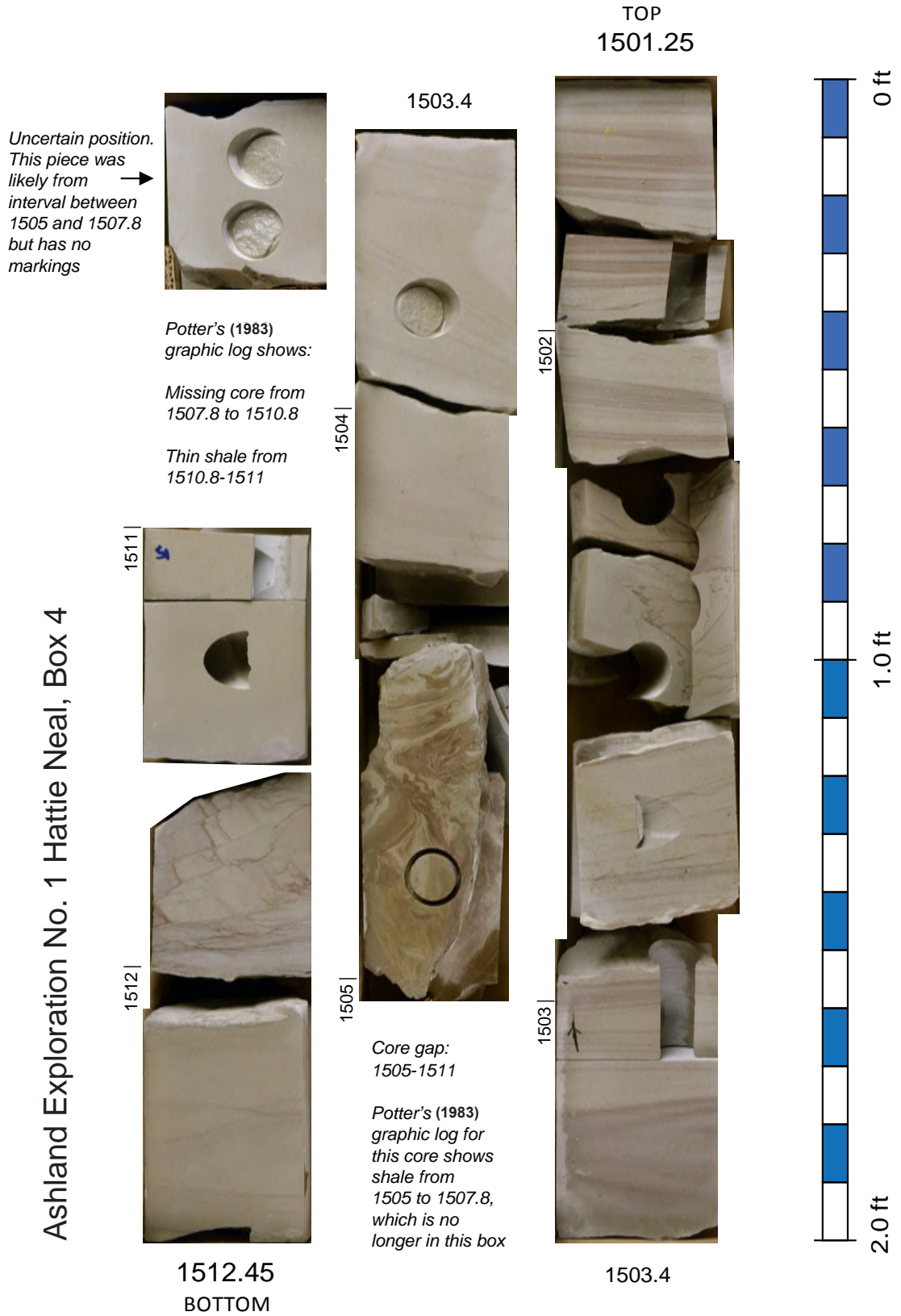


Ashland Exploration No. 1 Hattie Neal, Box 2





Ashland Exploration No. 1 Hattie Neal, Box 4



Ashland Exploration No. 1 Hattie Neal, Box 5

Core has 1516 written on it, but appears to fit below 1517

Sharp transition at base; possibly thin missing piece



1518
BOTTOM

1516.6

1517

1516

1515

1516.6

1514.5

1514

1513

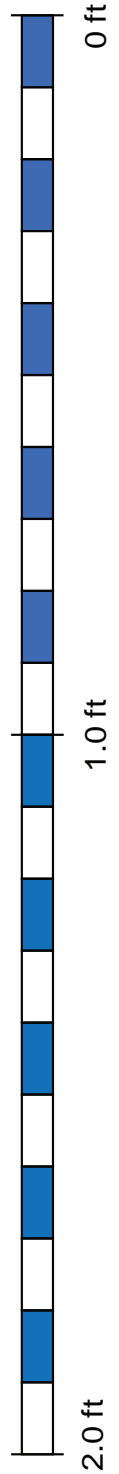
TOP
1512.45



1514.5

Core gap:
1515.65-
1516

Thin
core gap:
1513.75
1513.9



Columbia Natural Resources #20505 Margaret Simpson

Location: Lawrence County, Ky. (see Figure CB-1, Table CB-1)

KGS Core Call No.: C-5906

KGS Oil and Gas Record No.: 101940

Geophysical Logs: Compensated formation density (caliper, gamma-ray, compensated density porosity, bulk density)

Well Completion Date: 8/7/1977

Core Depth: Top of Berea at 1,660 ft

Bedford-Berea Core Interval Thickness: 82.7 ft (with gaps)

Bedford-Berea Total Thickness: 116 ft

Field: None (no name); 2.4 mi west of Yatesville gas field, 2 mi north of Midwest Church gas field, and 3.4 mi west of Fallsburg oil field

Completion: Shut-in gas well in Berea (1,718–1,720, 1,729–1,736 ft)

Background and Distance to Recent Berea Oil Wells

This core from the Columbia Margaret Simpson well is one of four cores from Lawrence County. The core is from 1.4 to 1.5 mi south of several recent horizontal Berea oil wells drilled by Hay Exploration and 1.48 mi northwest of the location of the Ashland Hattie Neal core (see previous core description), so the two cores can be compared to wells in the general vicinity. The Margaret Simpson core is thicker than the Hattie Neal core.

Key Features

The Margaret Simpson core preserves an 83-ft interval of the Berea, but there are many gaps (Fig. CB-4). Similar to the Hattie Neal core, the top of this core is below the base of the Sunbury Shale, but is iron-stained and likely near the top of the Berea. The core contains the upper part of the Berea and the upper part of the lower Berea at this location. A significant part of the middle Berea is missing. The core is dominated by thin-bedded siltstones and contains few interbedded shales. The most common beds are sharp-based and thin, massive to parallel-laminated to low-angle laminated. Approximately 20 percent of the massive beds show faint low-angle or parallel texture or lamination. Low-angle texture and bedding (approximately 5 percent of the core) may represent hummocky crossbedding, but could result from soft-sediment deformation and bed loading. Pyrite, especially as small (pinpoint) black flecks, is common in the upper part of the core. Red staining (presumably iron-siderite) is common in the lower parts of the core.

Potter and others (1983), in their summary of the core, noted some bioturbation throughout the core. Our analysis found distinct bioturbation in the uppermost beds of the core, but otherwise only a few intervals of possible bioturbation lower in the core. Many small siltstone nodules and bedding irregularities could be bioturbation, but could also be the result of soft-sediment deformation, which is abundant in the core. Potter and others (1983) also noted a clay-filled fracture at approximately 1,682 ft in their graphic log. This red-stained, shaly, vertical feature near the base of core 1 of box 2 (see photo plates) may be a fracture fill, but could also be a dewatering pipe between ball-and-pillow structures.

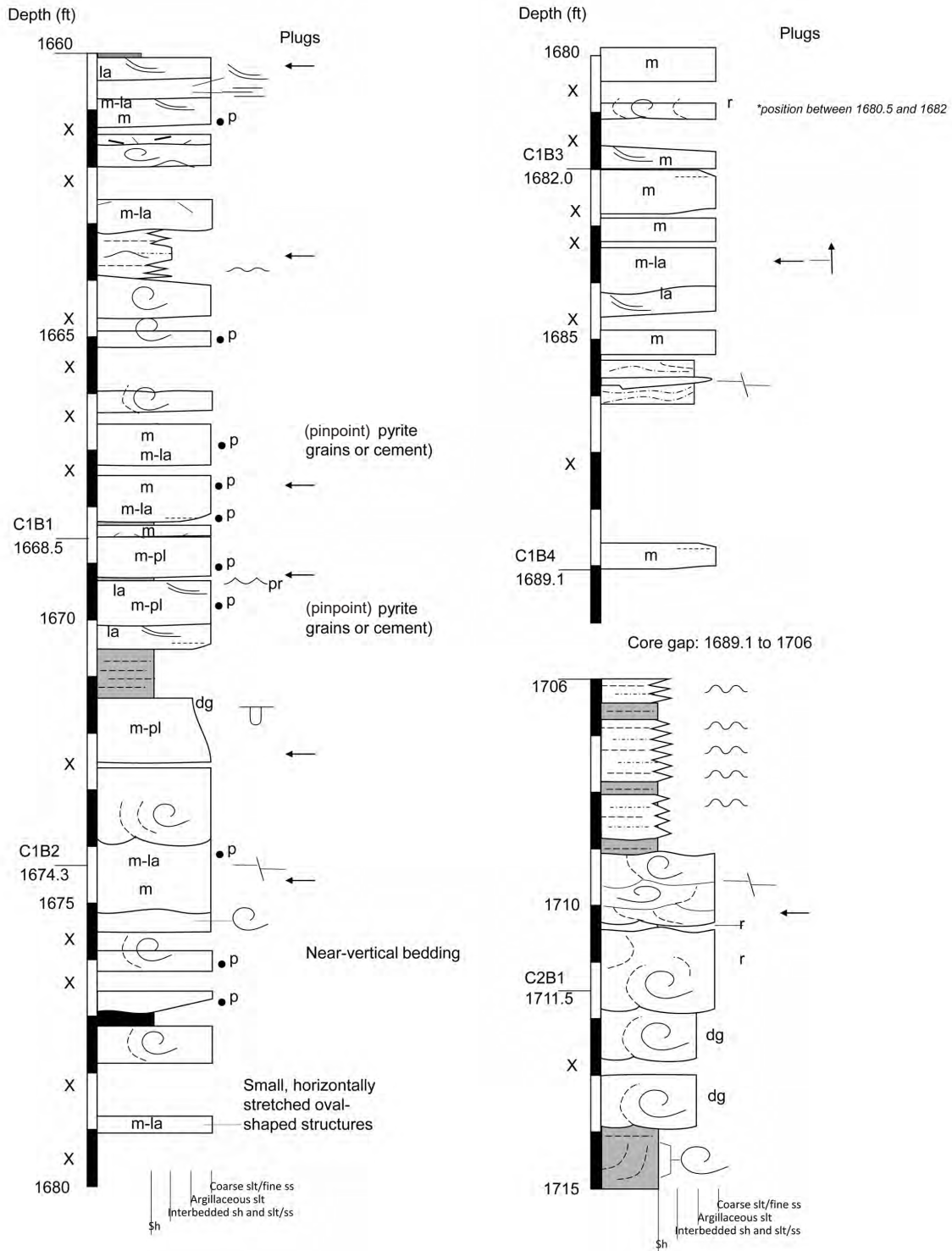
Data and Analysis

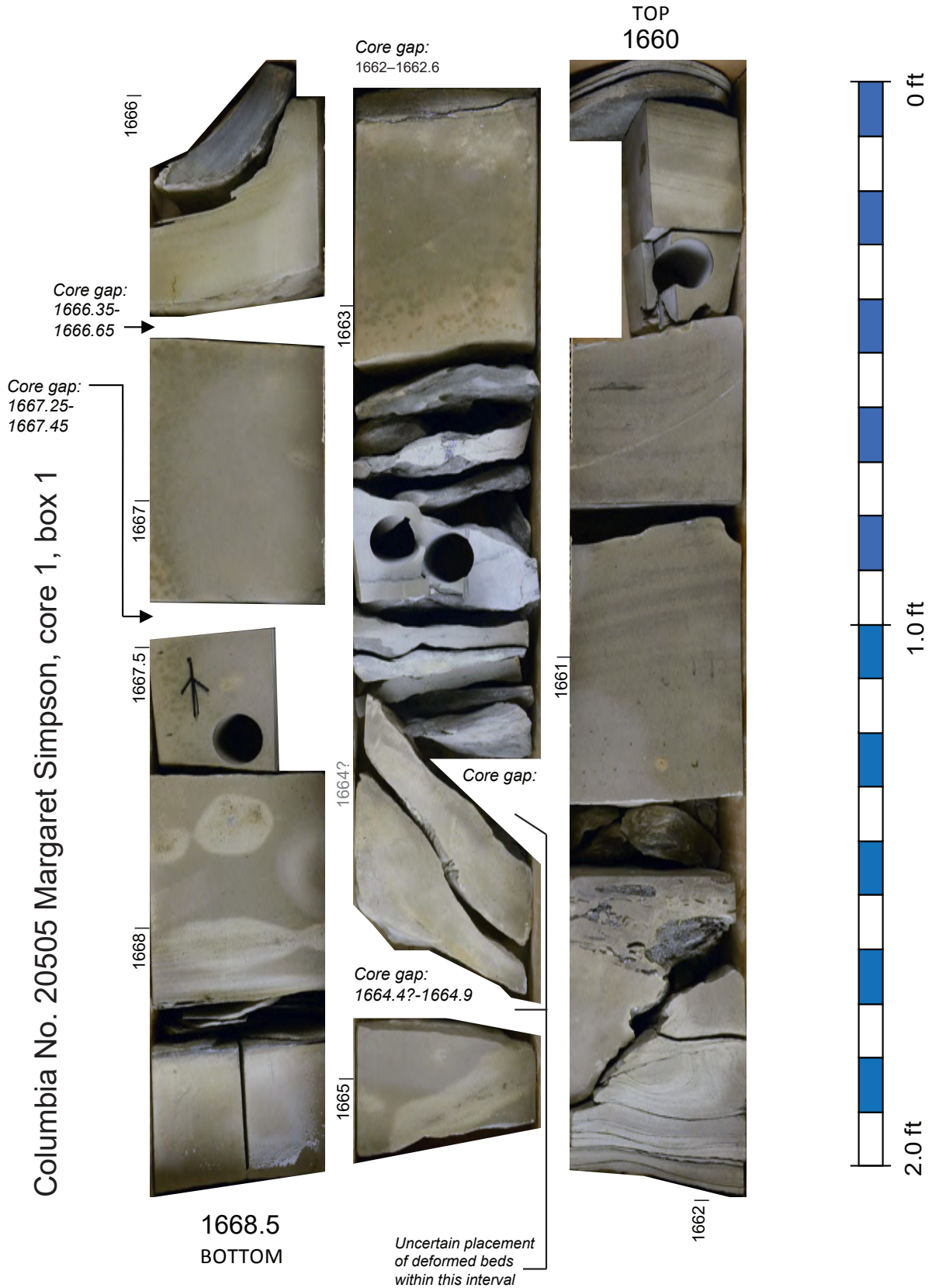
The Columbia Margaret Simpson core had no original data or analysis provided with the core donation or well record. Potter and others (1983) showed five porosity and permeability samples graphically for the core, but no record remains of the numerical data. Potter and others (1983) also included modal grain-size analysis for the core. Nineteen samples were measured from the upper core (approximately 1,660–1,689 ft) and 16 were taken from the lower core (approximately 1,718–1,742 ft). The maximum grain size was approximately 75 μm (very fine sandstone), minimum grain size was approximately 30 μm (coarse to medium siltstone), and average grain size was 50–60 μm (coarse siltstone). In general, vertical trends in grain size are more variable than in the Hattie Neal core, but that may be because the Hattie Neal core is thinner.

More recently, additional porosity and permeability data, as well as XRD data, were collected by Chesapeake Energy. Thin sections were made from several of the Chesapeake sample plugs as part of the present Berea Consortium study.

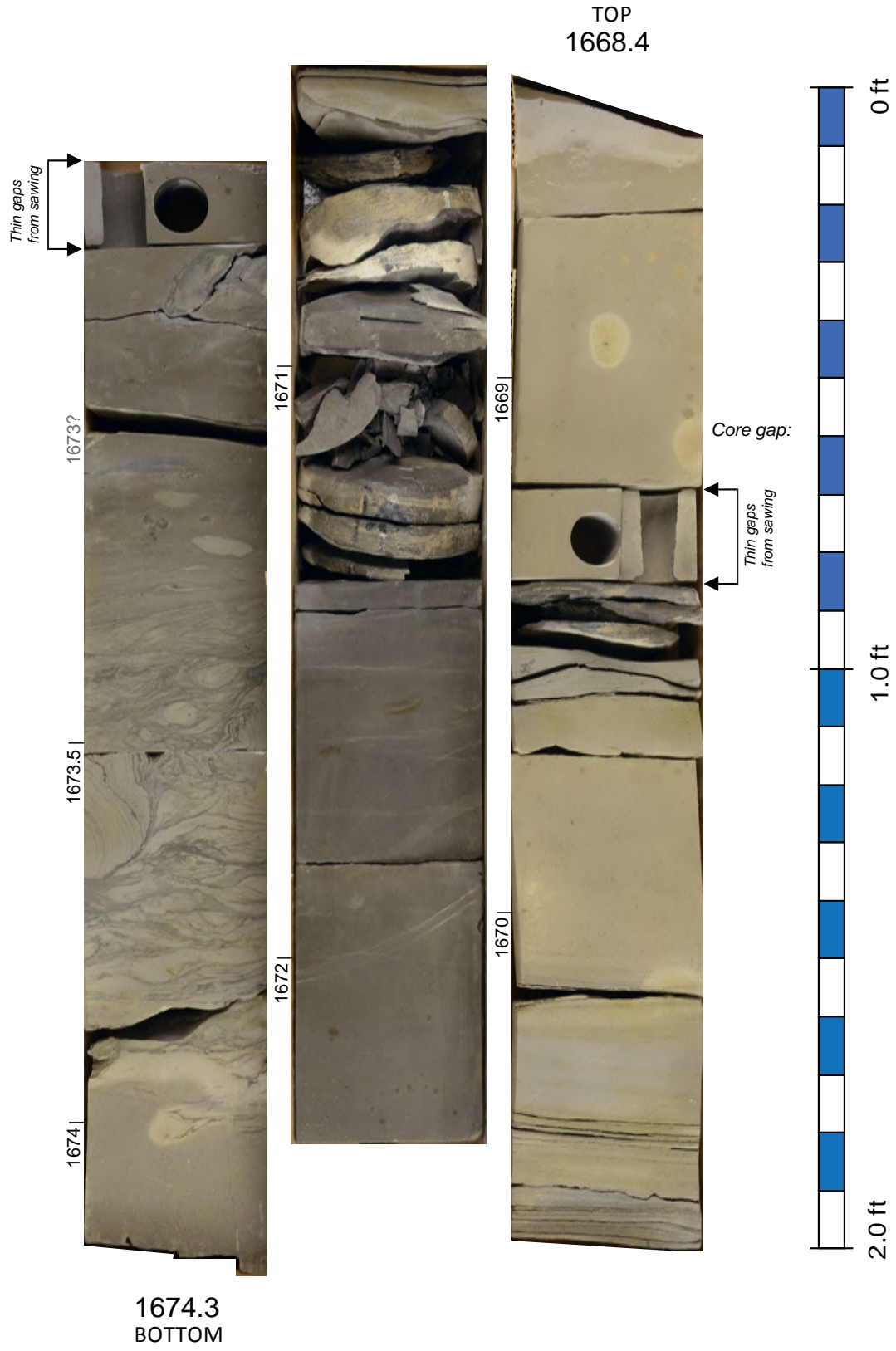
Columbia Natural Resources No. 20505 Margaret Simpson

Described from slabbed core

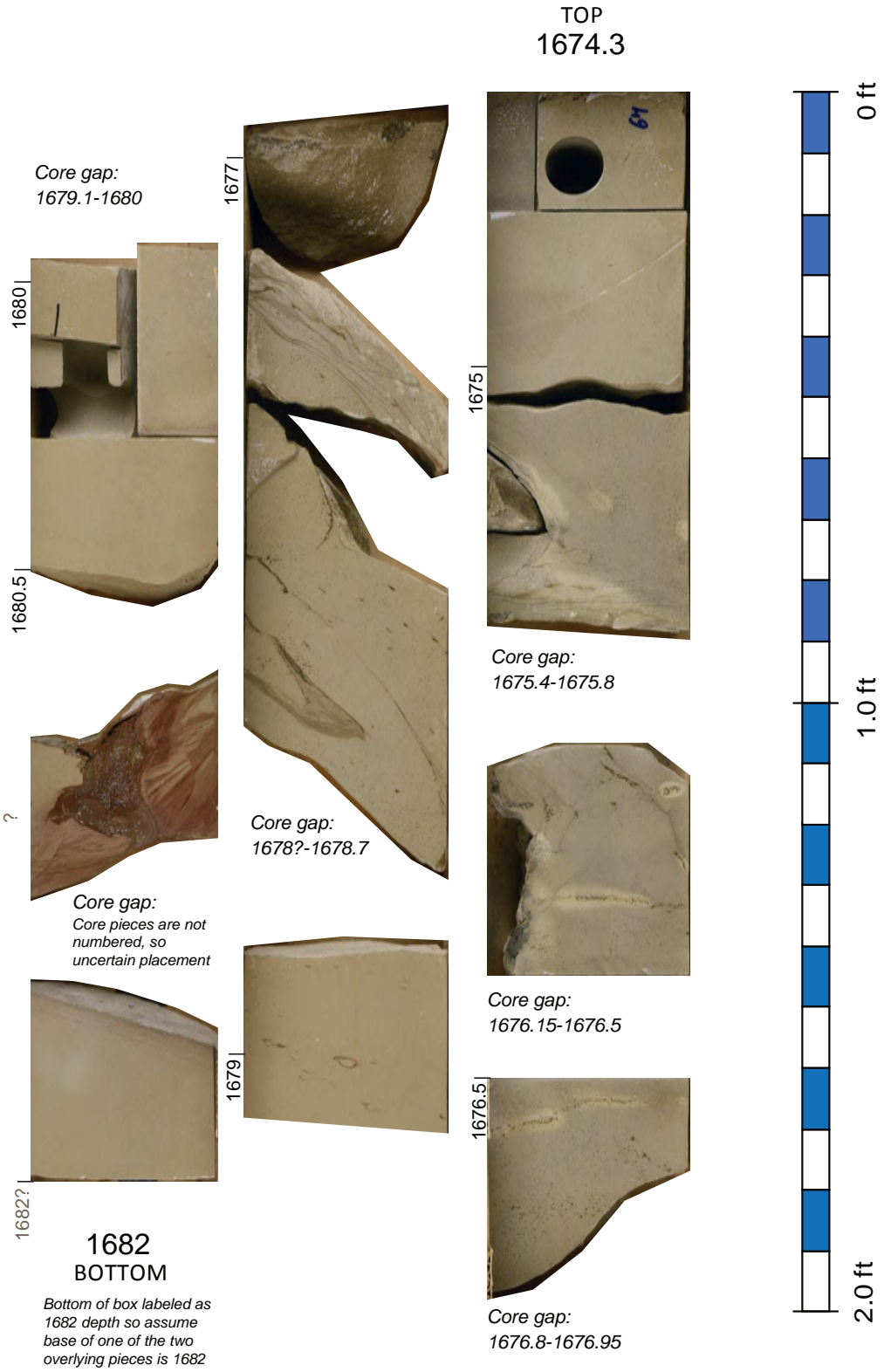




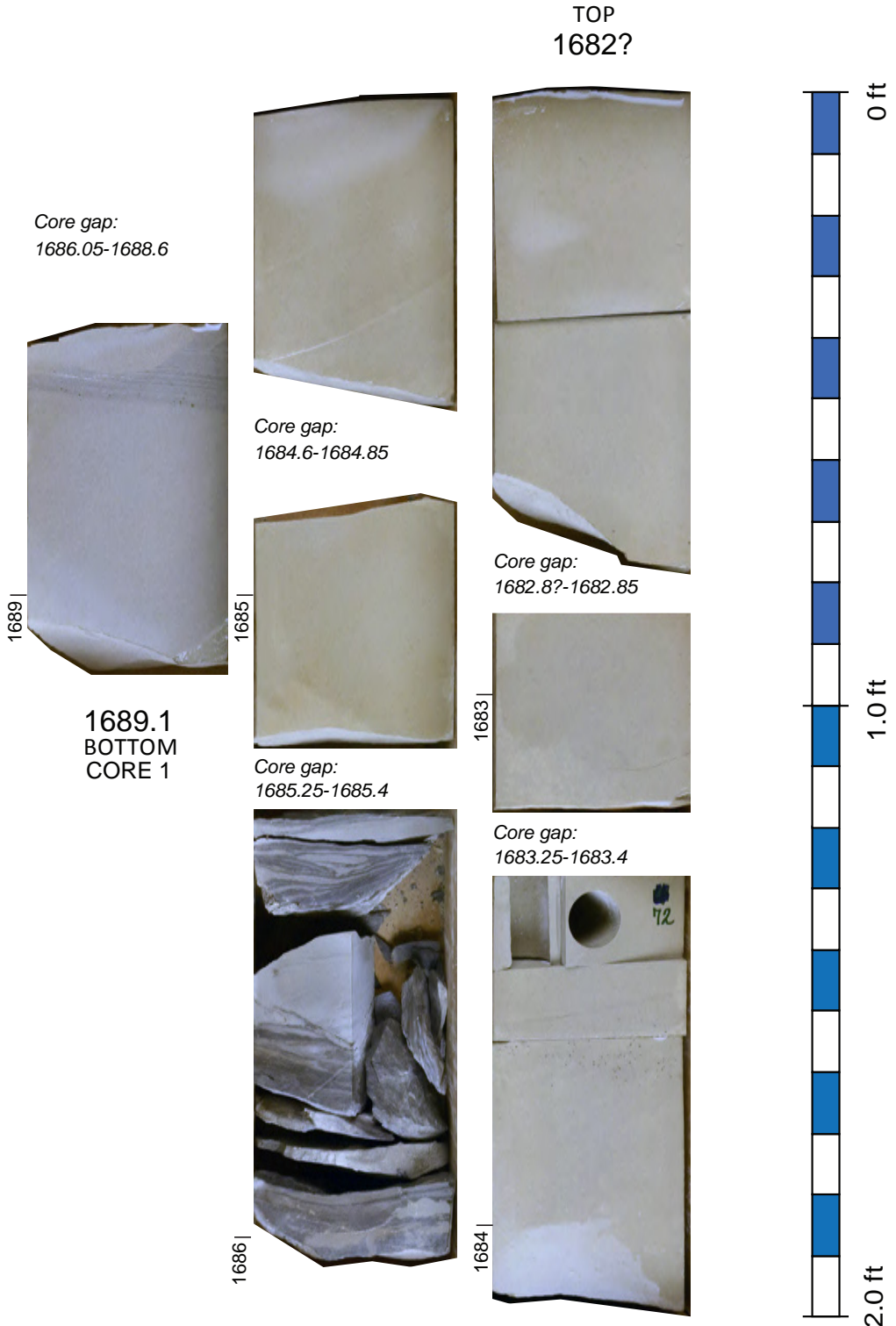
Columbia No. 20505 Margaret Simpson, core 1, box 2 :



Columbia No. 20505 Margaret Simpson, core 1, box 3



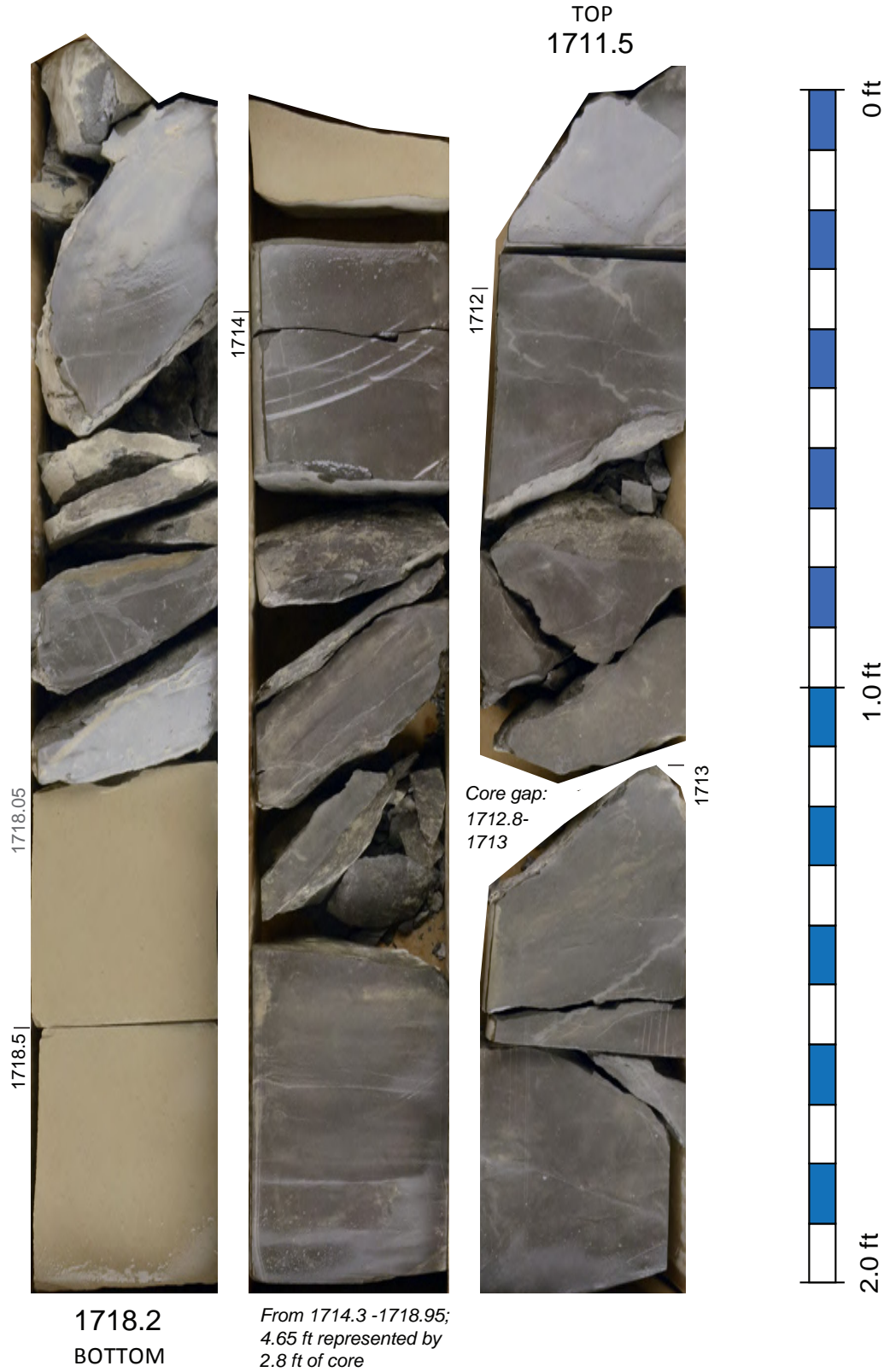
Columbia No. 20505 Margaret Simpson, core 1 ,box 4



Columbia No. 20505 Margaret Simpson, core 2, box 1



Columbia No. 20505 Margaret Simpson, core 2, box 2



1718.2
BOTTOM

From 1714.3 -1718.95;
4.65 ft represented by
2.8 ft of core

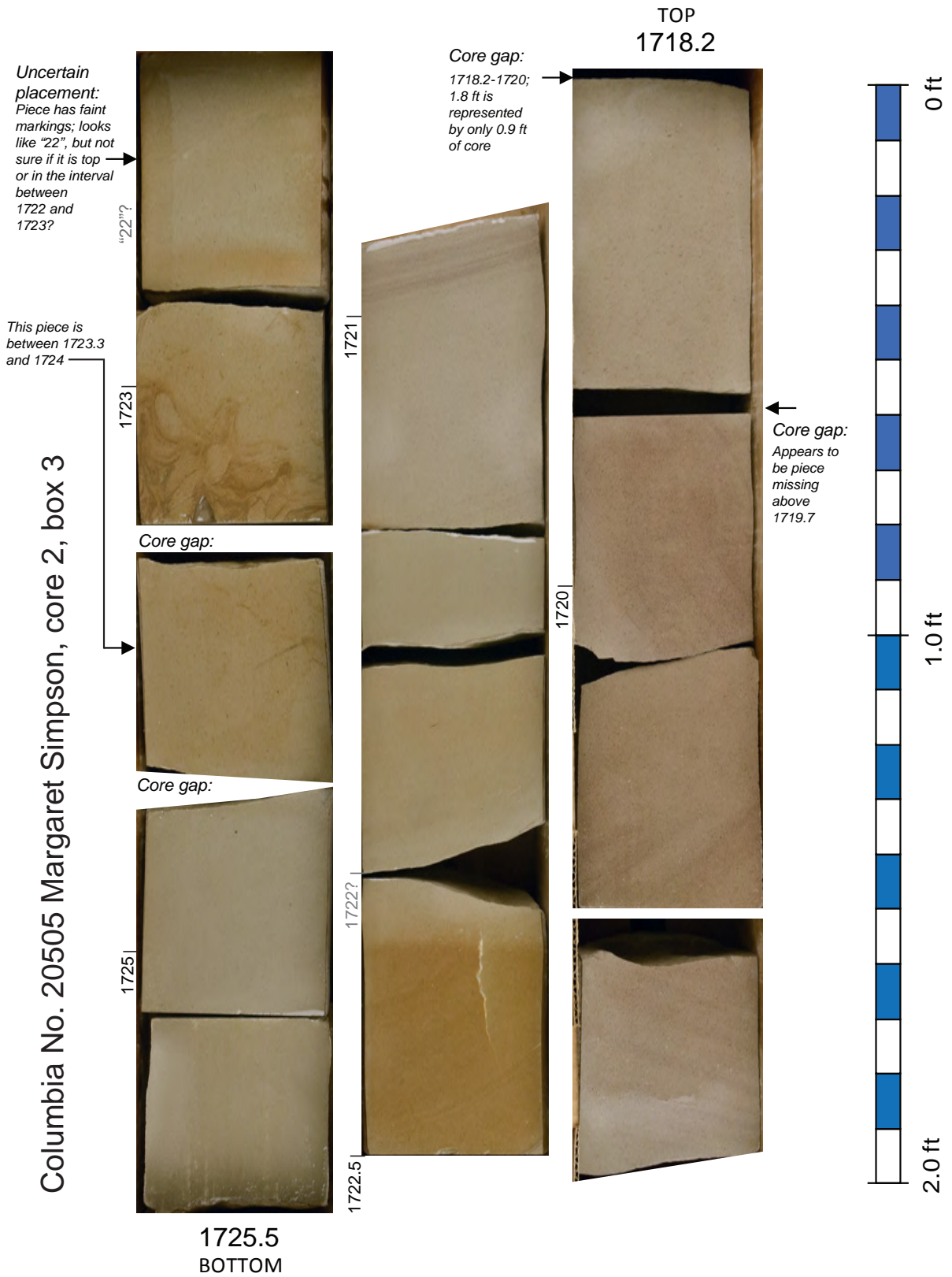
Core gap:
1712.8-
1713

TOP
1711.5

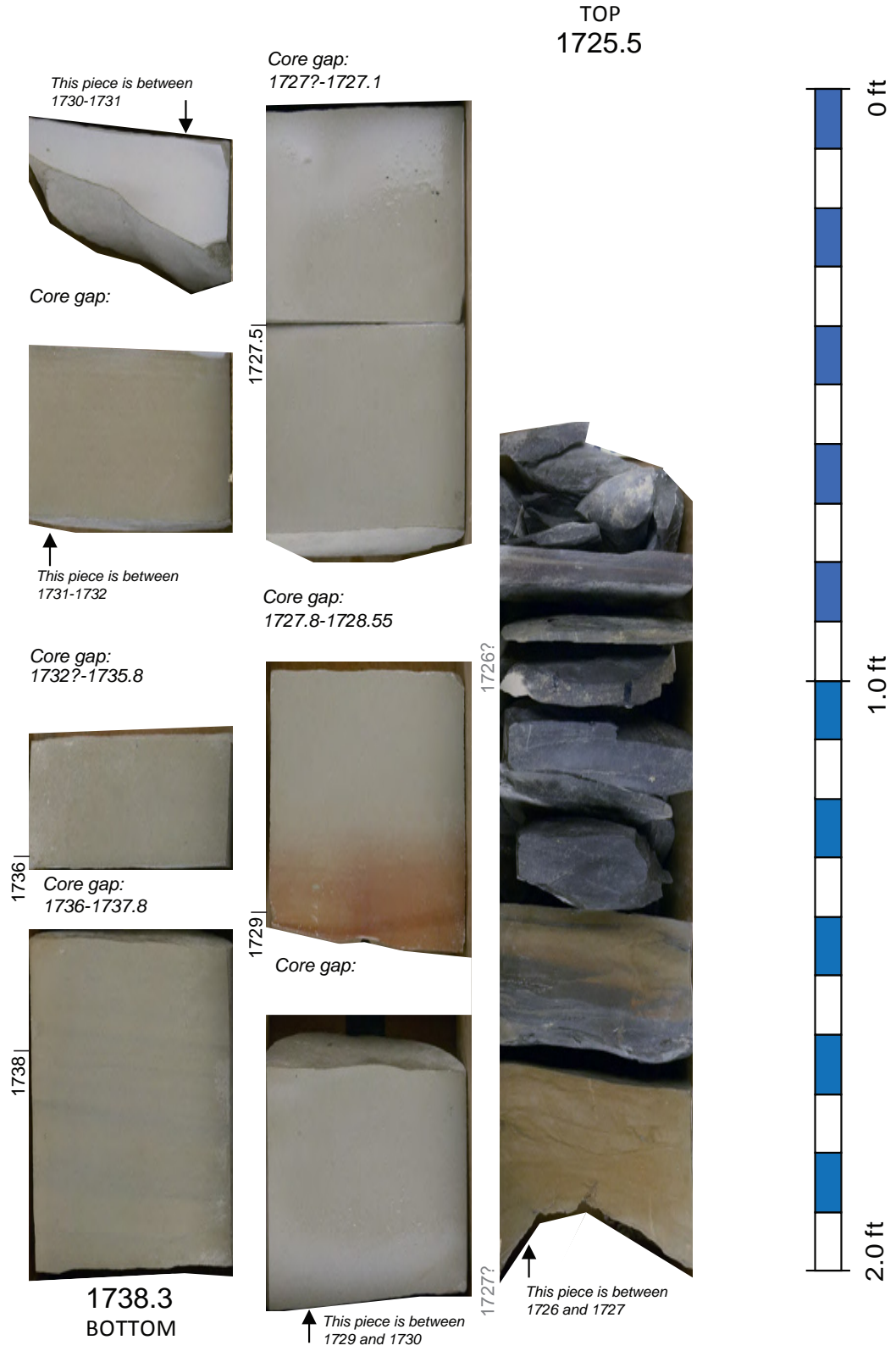
2.0 ft

1.0 ft

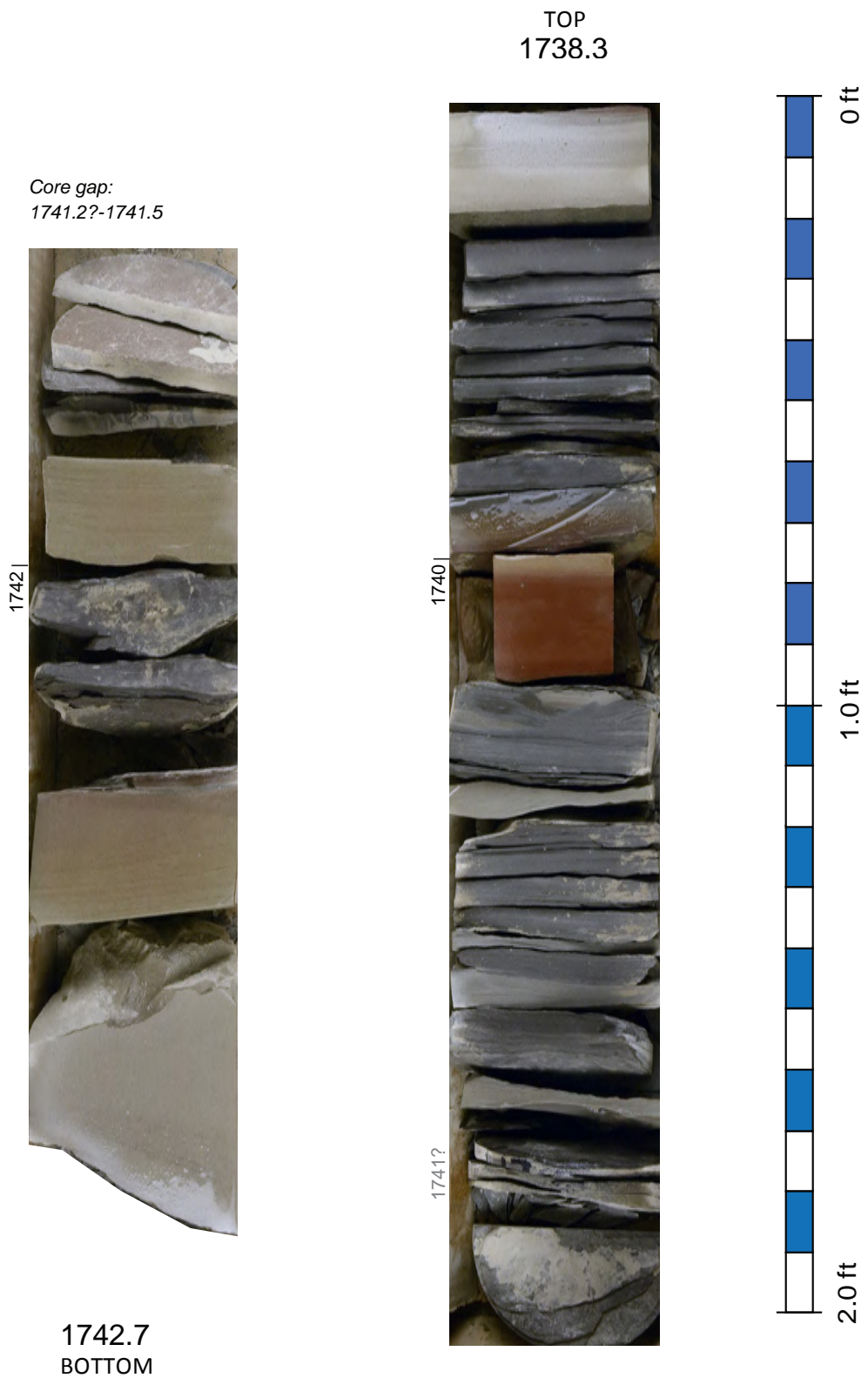
0 ft



Columbia No. 20505 Margaret Simpson, core 2, box 4



Columbia No. 20505 Margaret Simpson, core 2, box 5



Kentucky-West Virginia Gas #1122 Milton Moore

Location: Lawrence County, Ky. (see Figure CB-1, Table CB-1)

KGS Core Call No.: C-268

KGS Oil and Gas Record No.: 37673

Geophysical Logs: None

Well Completion Date: 1/20/1960

Core Depth: Top Berea at 1,226.8 ft

Bedford-Berea Core Interval Thickness: 76 ft

Bedford-Berea Total Thickness: 109 ft from driller's log; 114 ft from nearest geophysical log (KGS record no. 37586)

Field: Cordell

Completion: Gas well in Berea (1,220 [1,227]-1,316 ft) commingled with Ohio Shale (1,585-1,595 ft)

Background and Distance to Recent Berea Oil Wells

The Kentucky-West Virginia Milton Moore core is one of four Lawrence County cores. The KY-WV Milton Moore core is from 1.49 mi east of the KY-WV Ruben Moore core (see next core description). Stratigraphic intervals in the two cores correlate well. Both cores are in the northern, gas-producing part of the Cordell Field. The Milton Moore core is from 0.43 mi south of a recent horizontal well in the Berea drilled by Eagle Well Service and 1.7 to 6 mi north of a large number of recent horizontal oil wells on the southern end of the Cordell Field drilled by APP Energy LLC. The core does not have a corresponding well log. The nearest well with a log is the Weaver Oil and Gas #1 Hayes-Daugirda well (KGS record no. 37586), 0.38 mi away.

Key Features

The Milton Moore core preserves 7 ft of the Sunbury Shale and approximately 76 ft continuous interval of the upper through part of the lower Berea (Fig. CB-4). The core exhibits a thin capping sandstone/siltstone (6.4 ft) separated from a thicker upper coarse siltstone/sandstone by 5 ft of shale and interbedded shale and siltstone. The main, upper Berea is approximately 34 ft thick and is separated from a lower Berea coarse siltstone/sandstone by approximately 16 ft of shale. If the shale is correlated to the Ruben Moore core, it is evident that the Milton Moore core is in a relatively down-dip position to the Ruben Moore core.

The upper main Berea coarse siltstone/sandstone package is thicker in the Milton Moore core than in the Ruben Moore well. It is dominated by thin beds (average 1-2 ft) of massive, parallel-laminated, and soft-sediment-deformed beds, but several beds are more than 3 ft thick. Soft-sediment deformation is more common in the upper and middle parts of the interval. The Ruben Moore core shows the same pattern.

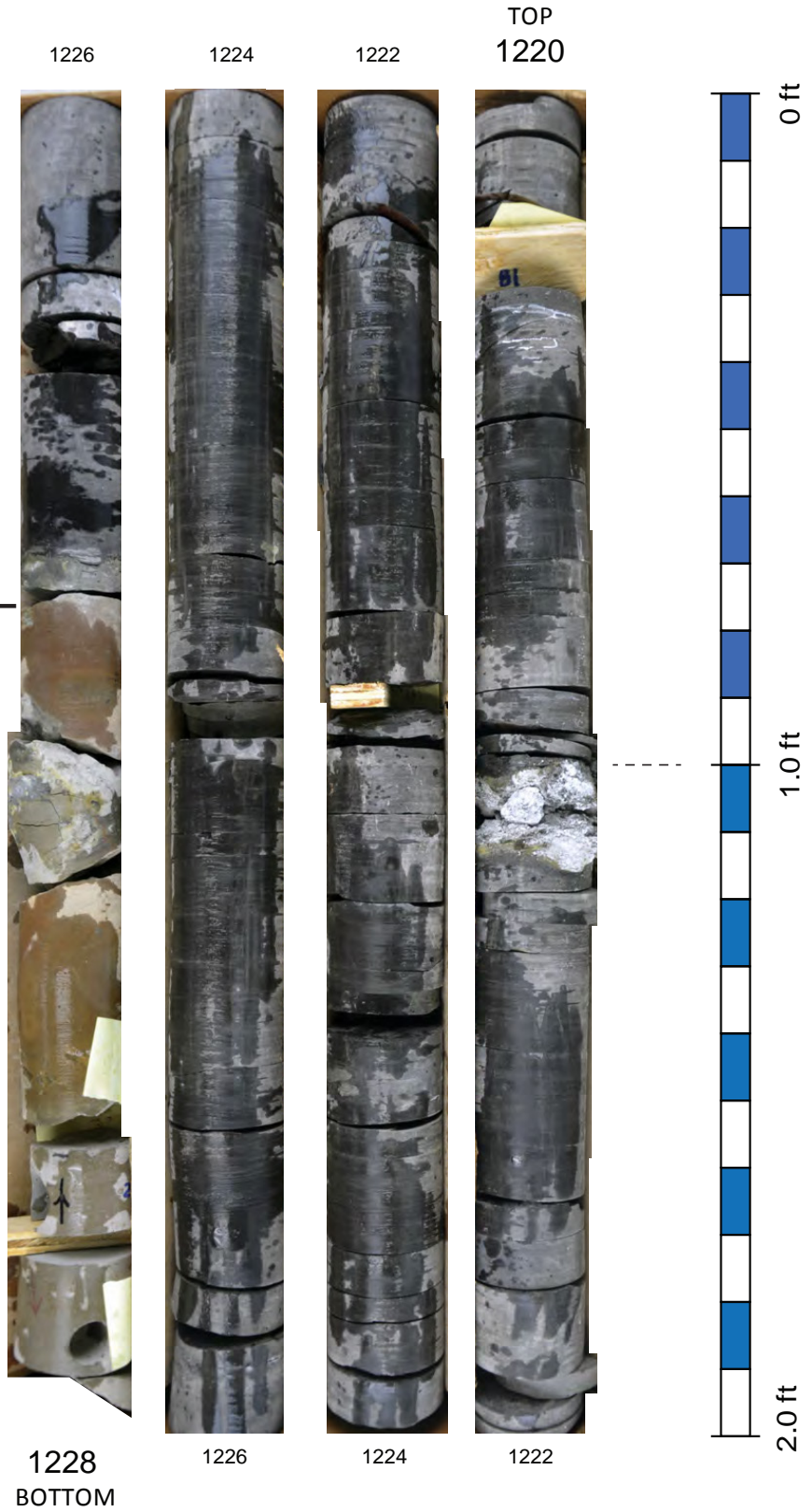
The upper Berea is separated from a lower interval of Berea coarse siltstones/sandstones by 16 ft of gray shale with several zones of isolated and highly contorted siltstone lenses, loads, and stringers. The lower part of the core contains two coarse siltstone/sandstone packages (6 ft and 5 ft thick) dominated by sharp-based, massive sandstones/coarse siltstones. These intervals are separated by gray shales with isolated and contorted siltstones, similar to the overlying shale.

A complicating factor in the Milton Moore core is that the core boxes each contain 8 ft of core, but were not marked in 8-ft intervals. Also, no depths were marked directly on the core, so the depths marked on the boxes are the only data from the drillers on core depths. This leads to several cumulative depth errors in the core. Also, most of the plugs that were taken for analysis were identified and measured based on the footages marked on the box, rather than the cumulative depths on measured 8-ft intervals from the top of the core. Because plug depths appear to have used the depths noted on the core boxes, those depths are shown on the photographic plates and as one measurement on the graphic logs. A cumulative footage from the top of the core (based on 8-ft increments) is shown in parentheses beneath the box depths.

Data and Analysis

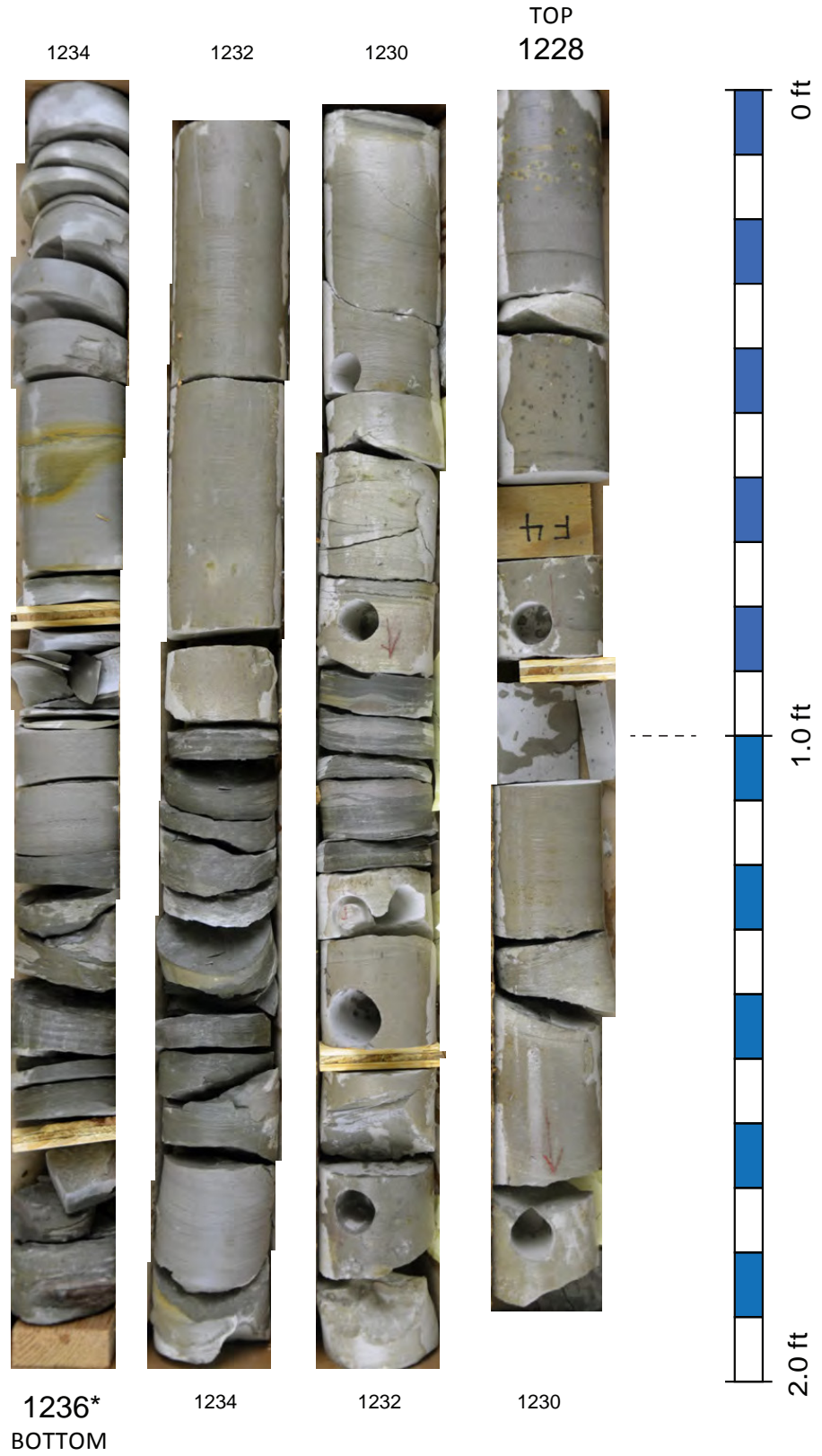
The Columbia Milton Moore core had some porosity and permeability data (n=9) provided with the core donation or well record, which can be viewed online through the Kentucky Geological Survey Oil and Gas Database. Additional porosity and permeability data, as well as XRD data, were collected by Chesapeake Energy. Thin sections were made from several of the Chesapeake sample plugs as part of the present Berea Consortium study. The core is mostly unslabbed (see photo plates), so additional plugs can be taken in the future, if needed.

KY WV Gas No. 1122 Milton Moore, KGS C-268, Box 1



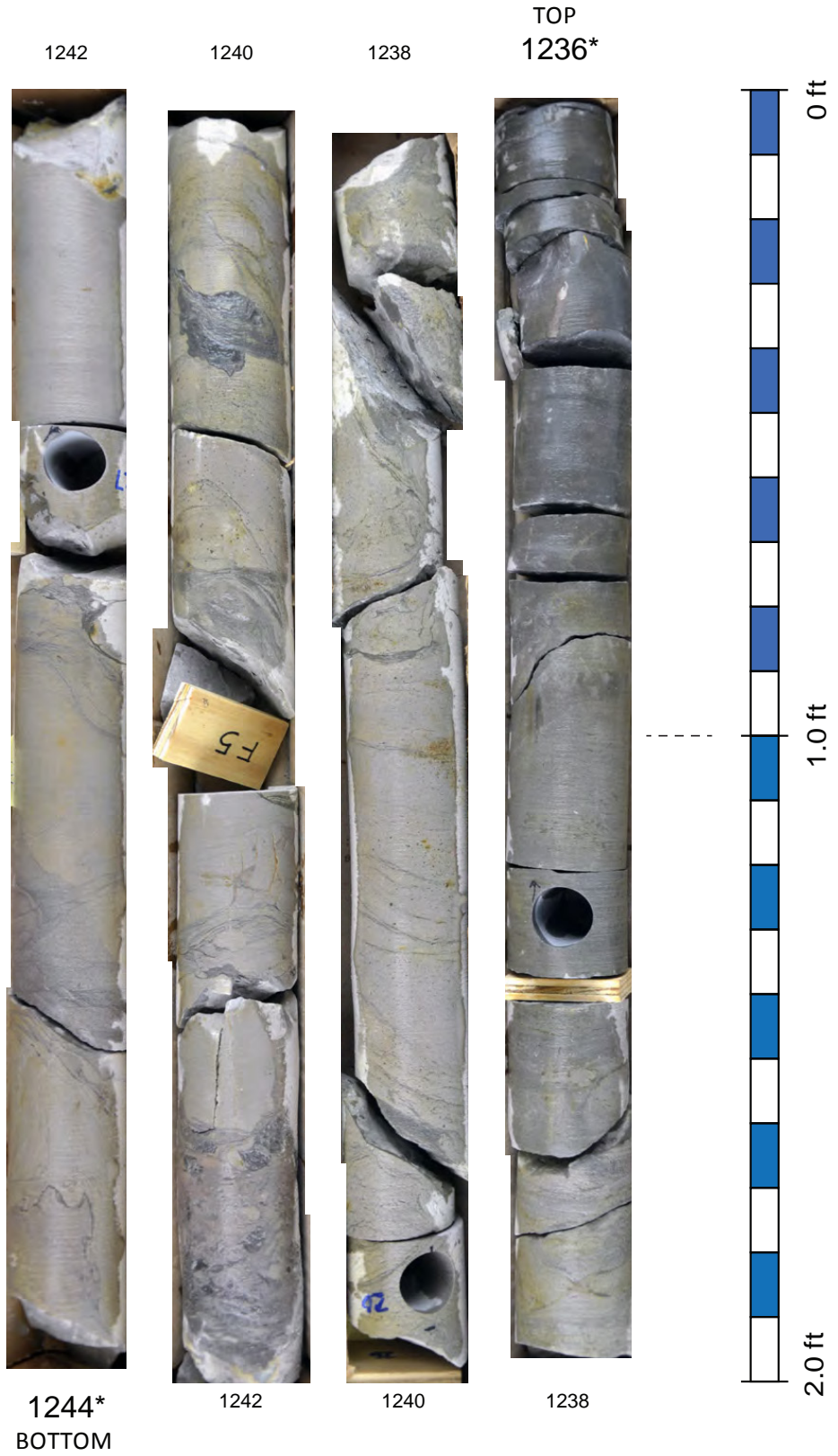
*The labeled footage on box 2 is 1228-1235, which would be 7 ft of core, but there are 8 ft of core in the box, so the depths for this box should be 1228-1236. There are no markings on the core itself to aid in calibration.

KY WV Gas No. 1122 Milton Moore, KGS C-268, Box 2



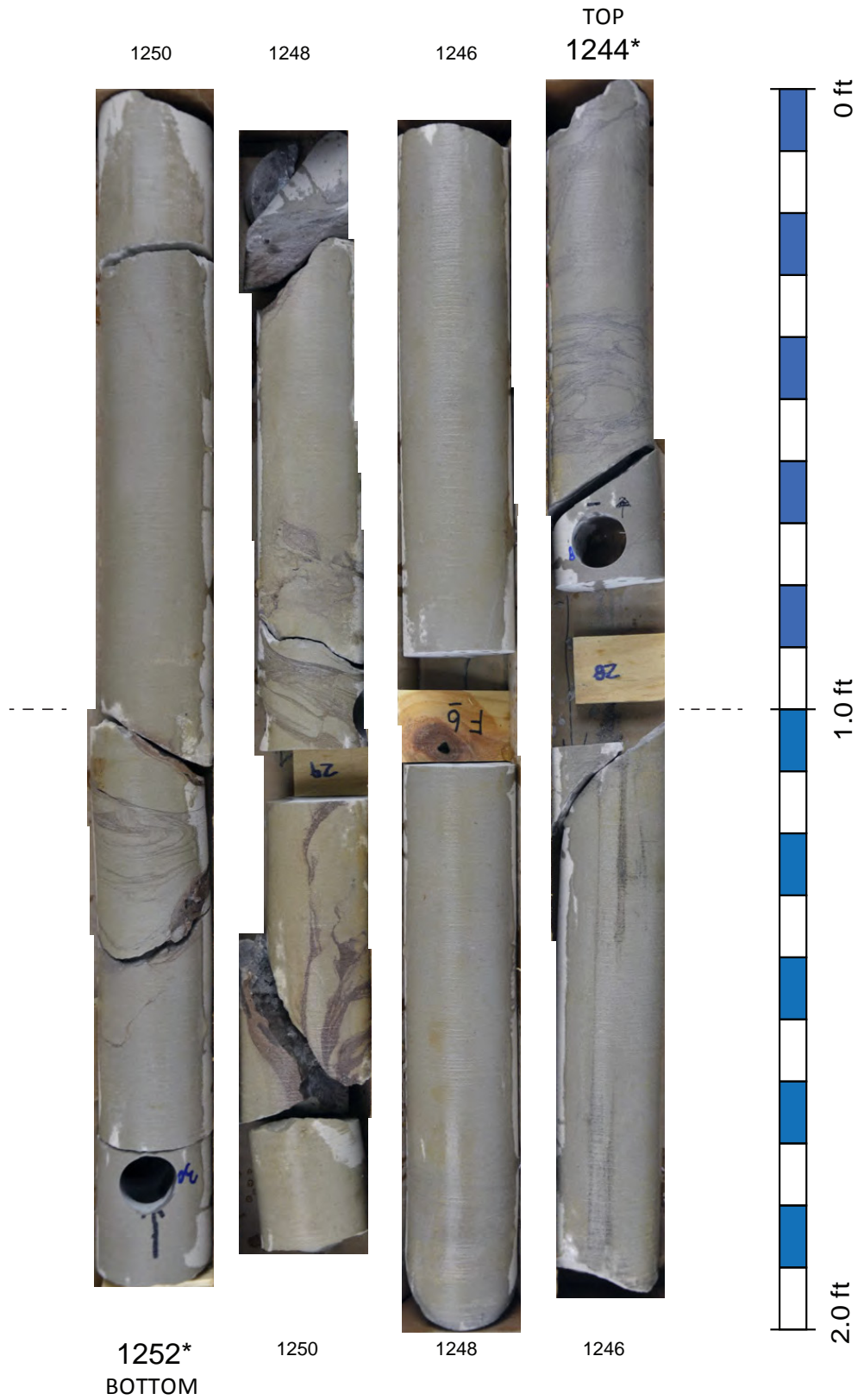
*The labeled footage on box 3 is 1235-1243, but there are 8 ft of core in each box, and counting down from box 1 the depths for this box should be 1236-1244. There are no markings on the core itself to aid in calibration.

KY WV Gas No. 1122 Milton Moore, KGS C-268, Box 3



*The labeled footage on box 4 is 1243-1250, but there are 8 ft of core in each box, and counting down from box 1 the depths for this box should be 1244-1252. There are no markings on the core itself to aid in calibration.

KY-WV Gas No. 1122 Milton Moore, KGS C-268, Box 4



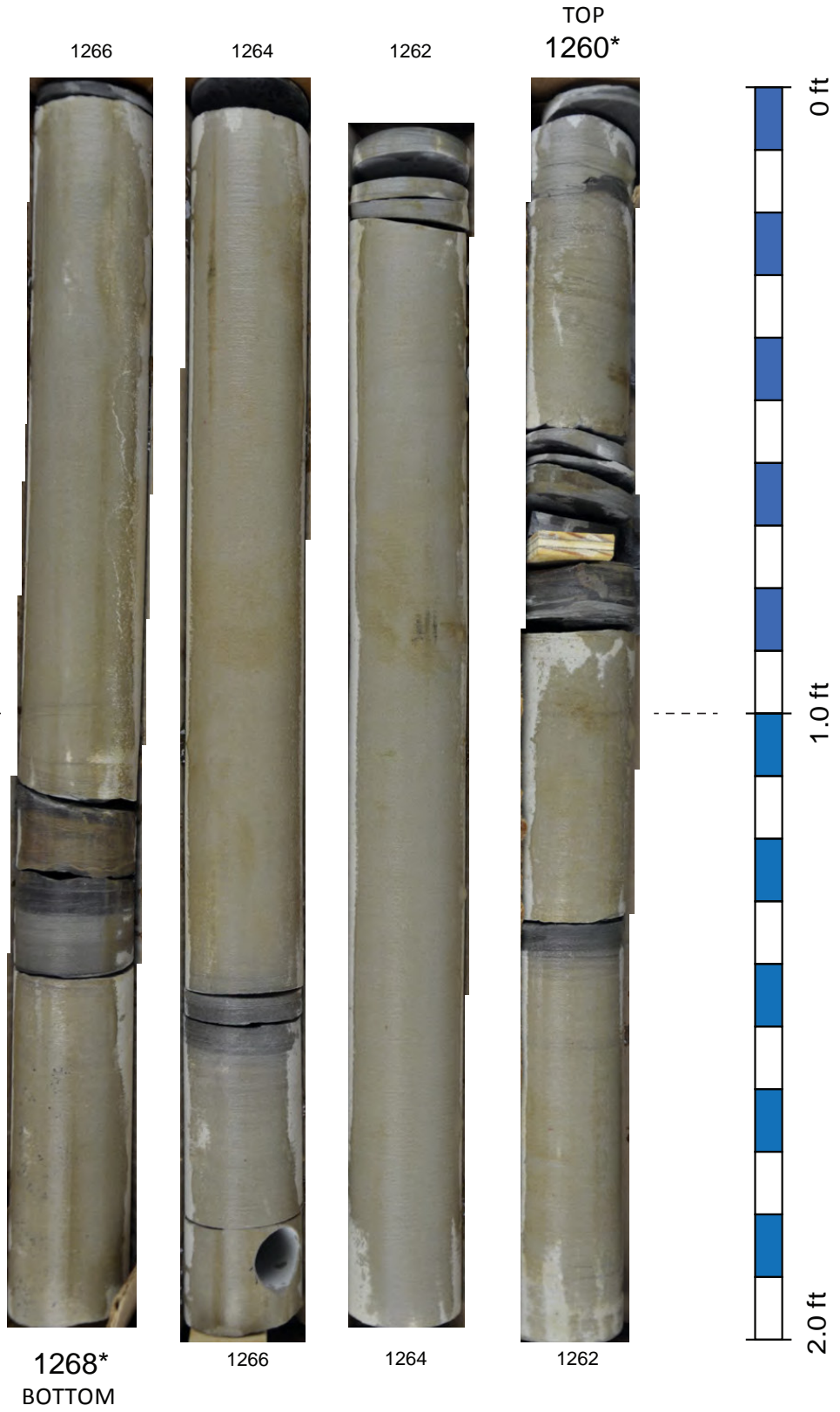
*The labeled footage on box 5 is 1250-1258 but there are 8 ft of core in each box, and counting down from box 1 the depths for this box should be 1252-1260. There are no markings on the core itself to aid in calibration.

KY-WV Gas No. 1122 Milton Moore, KGS C-268, Box 5



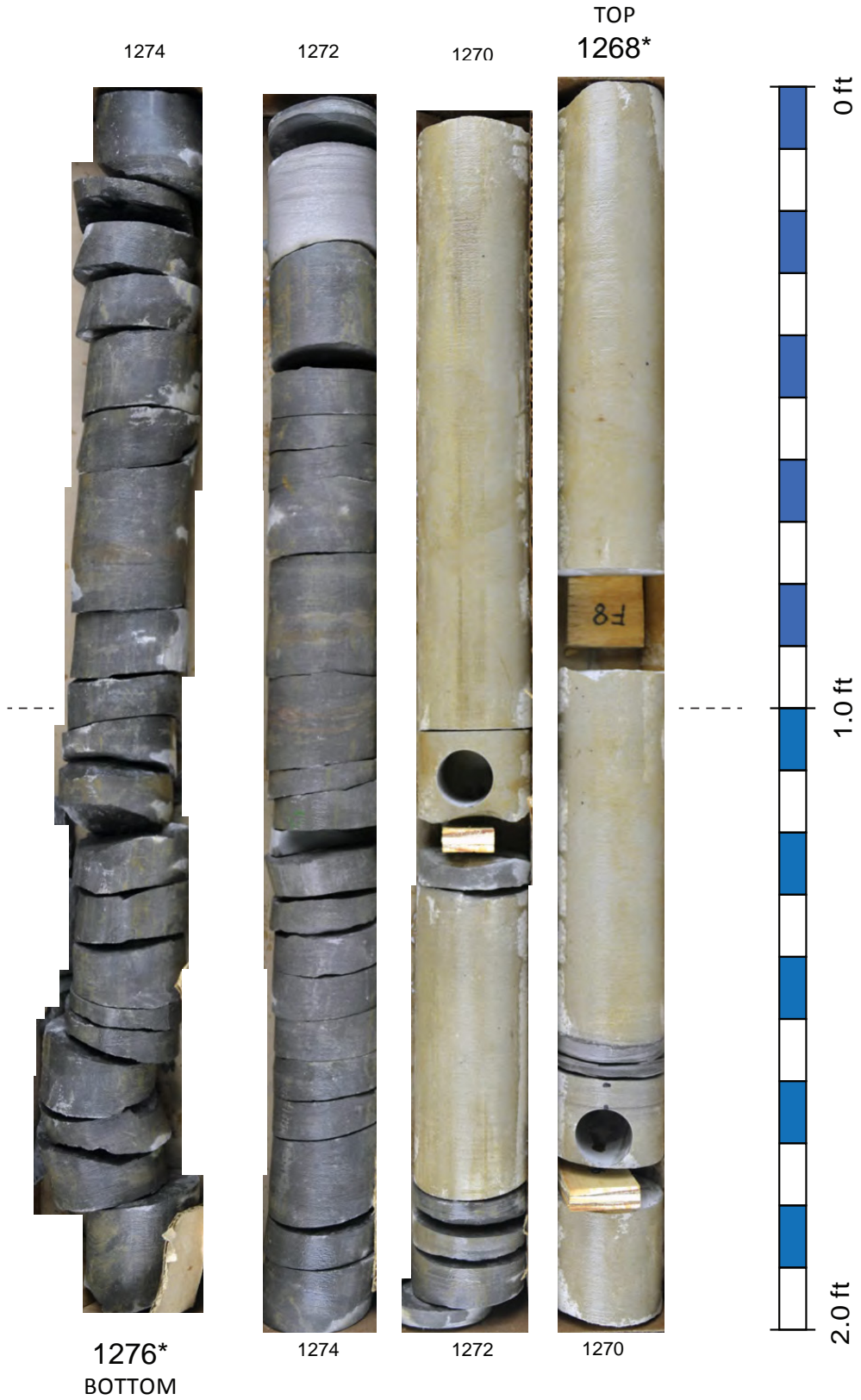
*The labeled footage on box 6 is 1258-1266 but there are 8 ft of core in each box, and counting down from box 1 the depths for this box should be 1260-1268. There are no markings on the core itself to aid in calibration.

KY-WV Gas No. 1122 Milton Moore, KGS C-268, Box 6



*The labeled footage on box 7 is 1266-1273 but there are 8 ft of core in each box, and counting down from box 1 the depths for this box should be 1268-1276. There are no markings on the core itself to aid in calibration.

KY-WV Gas No. 1122 Milton Moore, KGS C-268, Box 7



*The labeled footage on box 8 is 1273-1281 but there are 8 ft of core in each box, and counting down from box 1 the depths for this box should be 1276-1284. There are no markings on the core itself to aid in calibration.

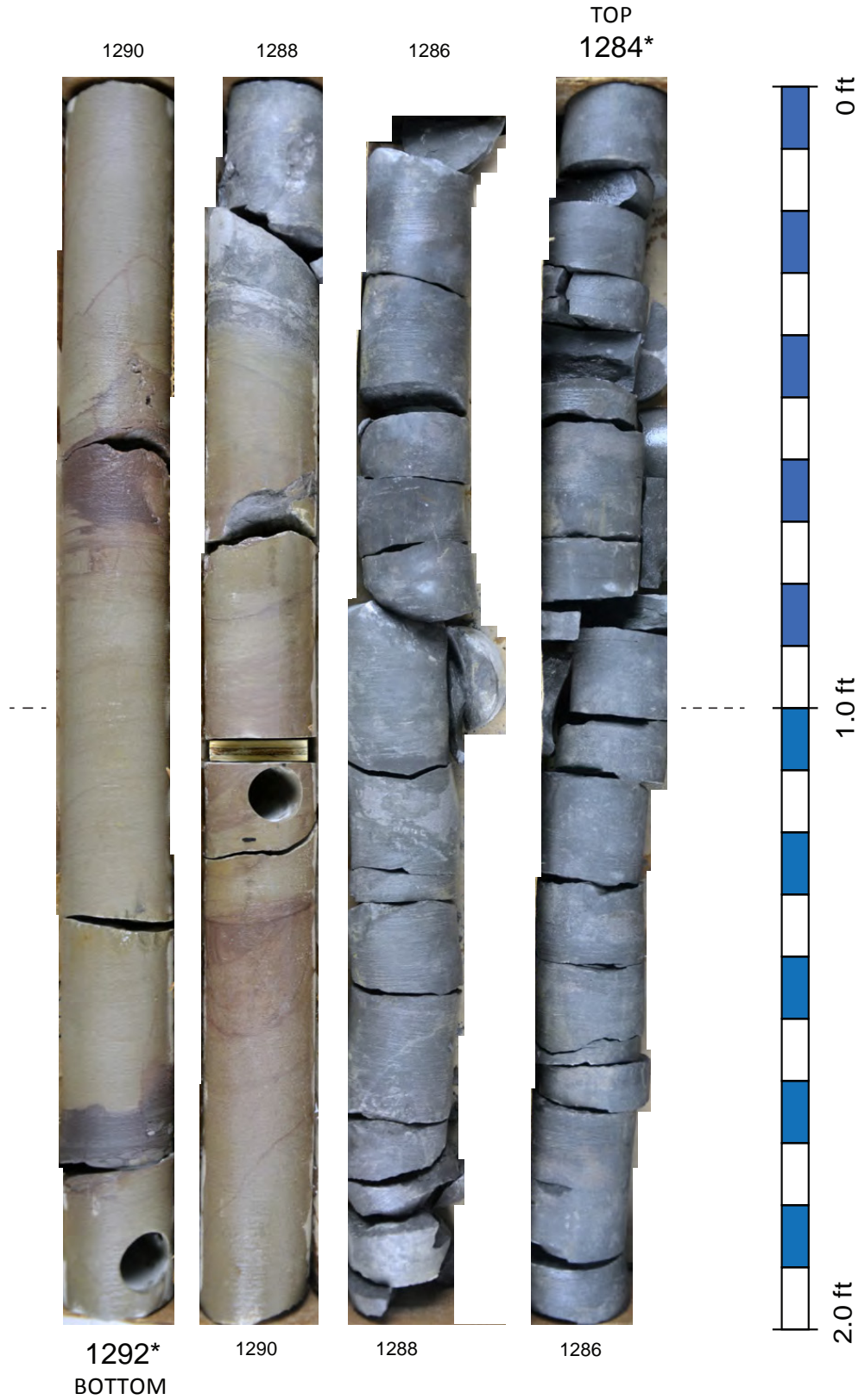
KY-WV Gas No. 1122 Milton Moore, KGS C-268, Box 8



1284*
BOTTOM

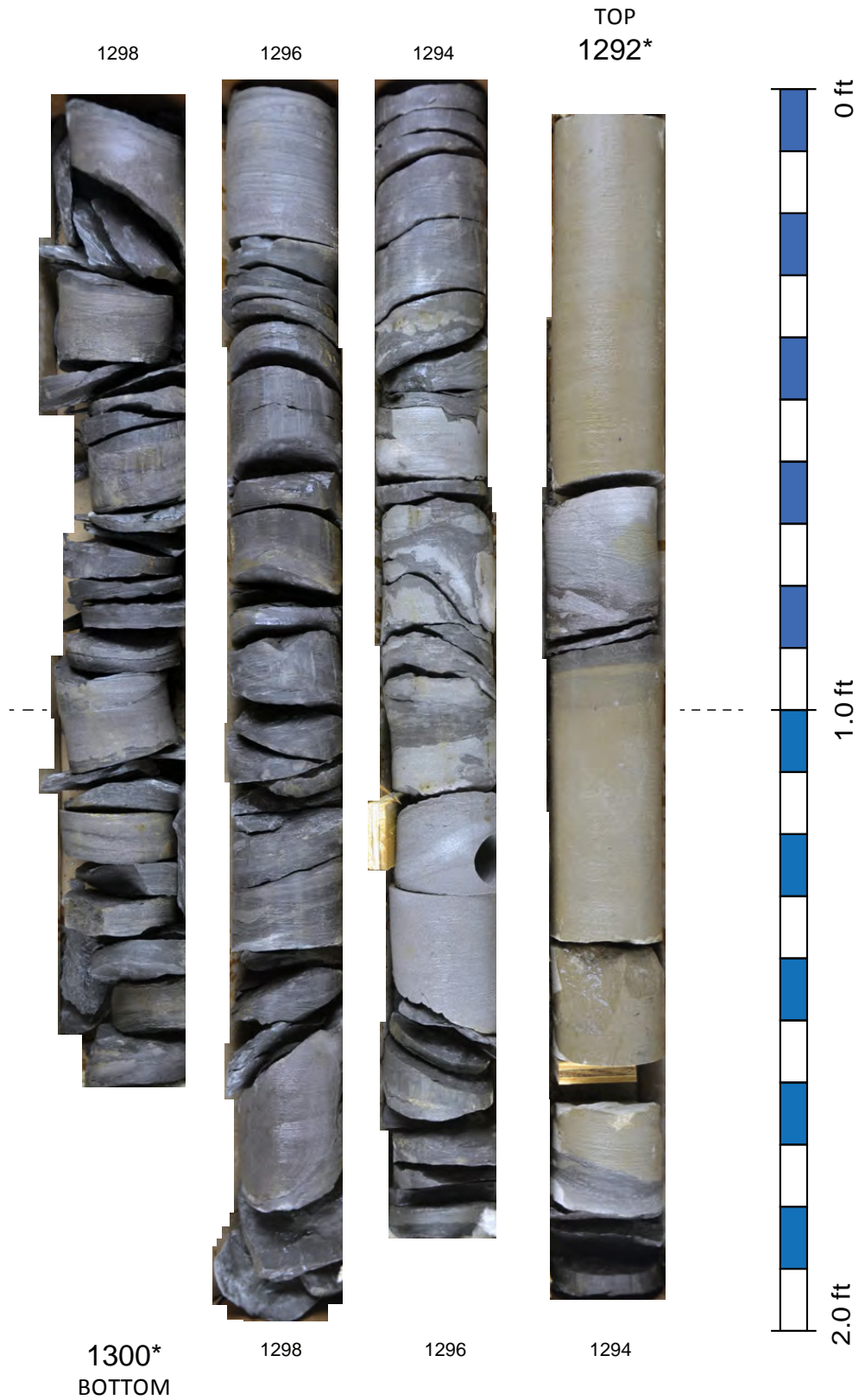
*The labeled footage on box 9 is 1281-1289 but there are 8 ft of core in each box, and counting down from box 1 the depths for this box should be 1284-1292. There are no markings on the core itself to aid in calibration.

KY-WV Gas No. 1122 Milton Moore, KGS C-268, Box 9



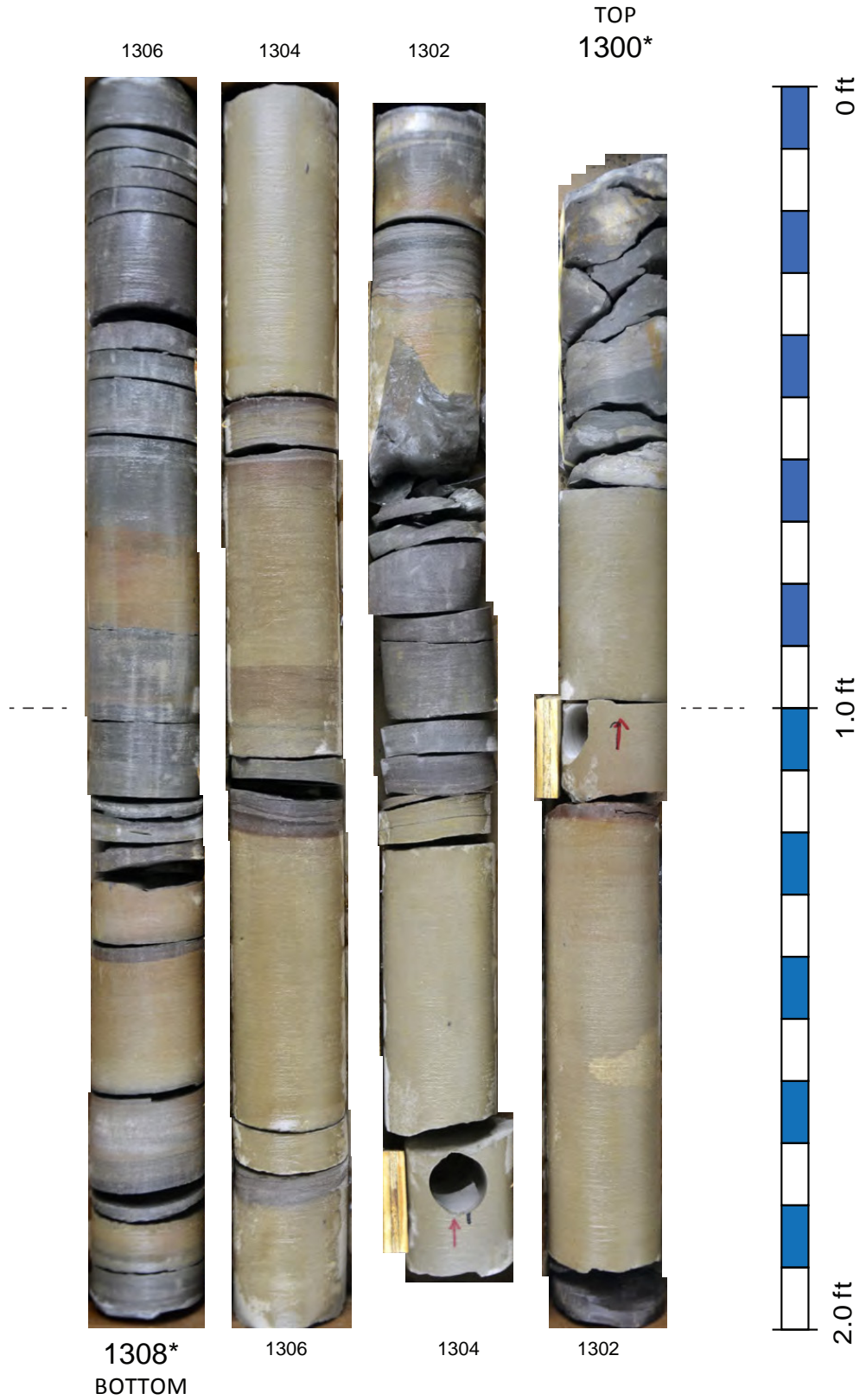
*The labeled footage on box 10 is 1289-1295 but there are 8 ft of core in each box, and counting down from box 1 the depths for this box should be 1292-1300. There are no markings on the core itself to aid in calibration.

KY-WV Gas No. 1122 Milton Moore, KGS C-268, Box 10



1300*
BOTTOM

*The labeled footage on box 11 is 1295-1303 but there are 8 ft of core in each box, and counting down from box 1 the depths for this box should be 1300-1308. There are no markings on the core itself to aid in calibration.
KY-WV Gas No. 1122 Milton Moore, KGS C-268, Box 11



Kentucky-West Virginia Gas #1087 Ruben Moore

Location: Lawrence County, Ky. (see Figure CB-1, Table CB-1)

KGS Core Call No.: C-268

KGS Oil and Gas Record No.: 52302

Geophysical Logs: None

Well Completion Date: 1/3/1958

Core Depth: 1,220–1,227 (Sunbury), 1,227–1,322 (Berea) ft

Bedford-Berea Core Interval Thickness: 95 ft

Bedford-Berea Total Thickness: No drillers' or geophysical logs for cored well. Interval is 113 ft thick in a nearby well.

Field: Cordell

Completion: Gas well in Berea (1,213–1,274 ft)

Background and Distance to Recent Berea Oil Wells

The Kentucky-West Virginia Ruben Moore core is one of four Lawrence County cores. The KY-WV Ruben Moore core is from 1.49 mi west of the KY-WV Milton Moore core (see previous core description). Stratigraphic intervals are easily correlated between the two cores. Both cores are in the northern, gas-producing part of the Cordell Field. The Ruben Moore core is from 1.8 mi southeast of a recent horizontal well in the Berea drilled by Eagle Well Service and 1.5–5 mi north of a large number of recent horizontal oil wells on the southern end of the Cordell Field drilled by APP Energy LLC. The southern part of the Cordell Field has historically produced oil. The core does not have a corresponding well log. The nearest well with a log is Gas Acquisition Corp. #GAC-3 Robert and Julia Moore (KGS record no. 115164), 0.57 mi away, but the Robert and Julia Moore well did not reach the Cleveland Shale Member of the Ohio Shale.

Key Features

The Ruben Moore core preserves a 95-ft continuous interval of the upper Berea and upper part of the lower Berea (Fig. CB-4). The Sunbury Shale–Berea contact is preserved in the core. The core exhibits a thin capping coarse siltstone/sandstone (2.5 ft) separated from a thicker, upper coarse siltstone/sandstone by 5.5 ft of soft-sediment-deformed argillaceous siltstone. The upper main Berea coarse siltstone/sandstone is approximately 23 ft thick. Similar to the Milton Moore core, soft-sediment deformation dominates beds in the upper and part of the middle of the upper unit. The other part of the middle and lower part of the unit are dominated by sharp-based, mostly massive beds.

The upper Berea is separated from coarse siltstone/sandstone intervals in the lower part of the core by 13 ft of gray shale with slickensides and highly contorted, isolated lenses, loads, and stringers of siltstones, and by 7.5 ft of gray shale with thin beds of moderately dipping siltstone. If the shaly interval is correlated to the Ruben Moore core, it is evident that the Ruben Moore core is in a relatively updip position to the Milton Moore core.

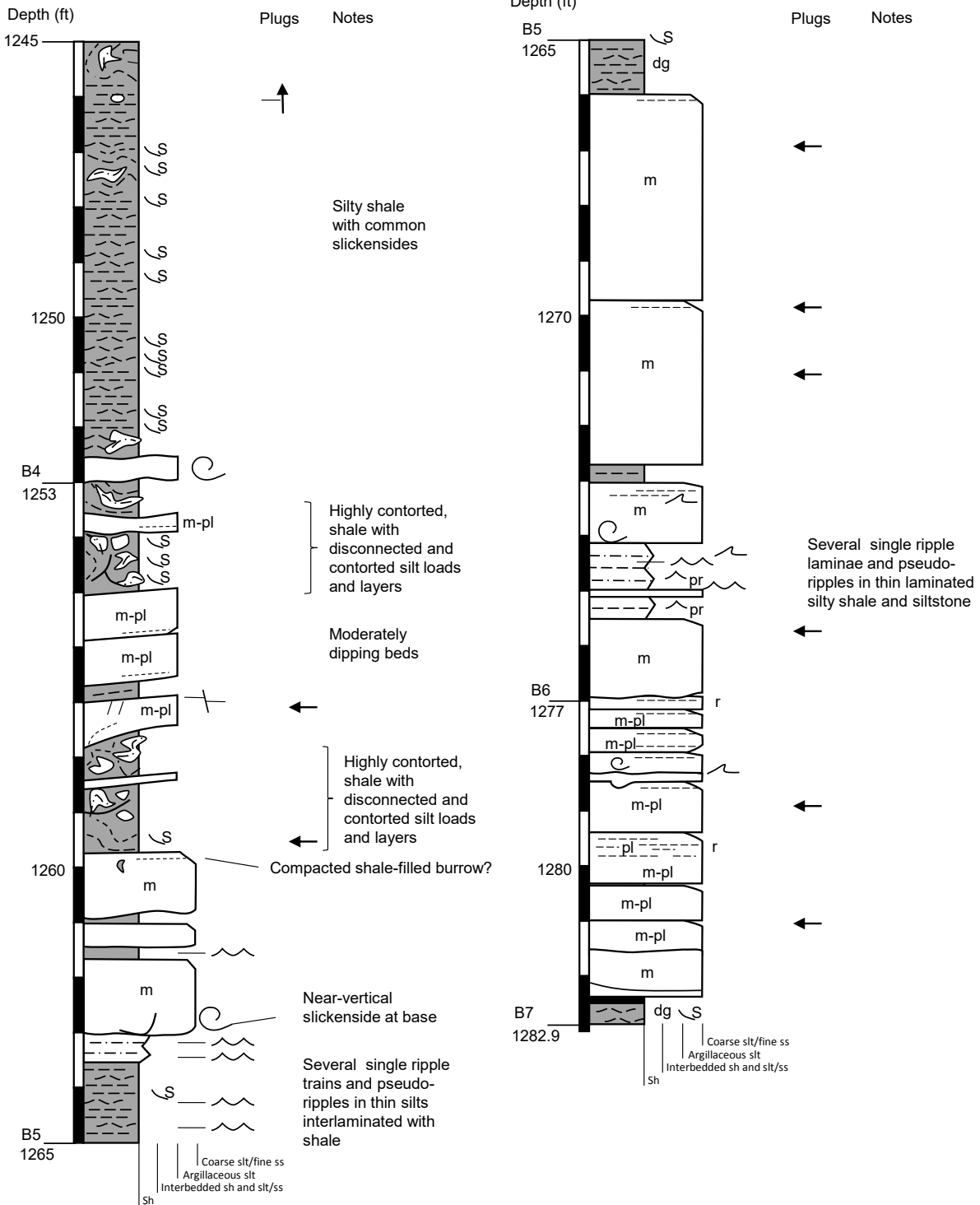
The lower Berea coarse siltstone/sandstone in the core (1,266–1,282.3 ft depth) is thicker and contains more coarse siltstone/sandstone beds than in the Milton Moore core. Bedding generally thickens upward from beds less than 1 ft thick to a bed 3.7 ft thick at the top of the interval. Beds are sharp-based, massive to massive with parallel lamination, and generally grade sharply upward into a thin, argillaceous cap. Some beds have a thin, argillaceous base. Some intervening shales and interbedded shales and siltstones contain lenticular bedding with ripple-like mounding but exhibiting no discernable foresets, which are shown as pseudo-ripples on the graphic log.

Data and Analysis

The Columbia Ruben Moore core had no original porosity or permeability data with the core donation or well record. Additional porosity and permeability data, as well as XRD data, were collected by Chesapeake Energy. Thin sections were made from several of the Chesapeake sample plugs as part of the present Berea Consortium study. The core is mostly unslabbed (see photo plates), so additional plugs can be taken in the future, if needed.

KY-WV Gas No. 1087 Ruben Moore

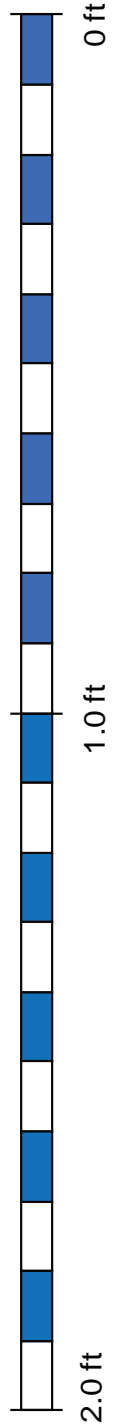
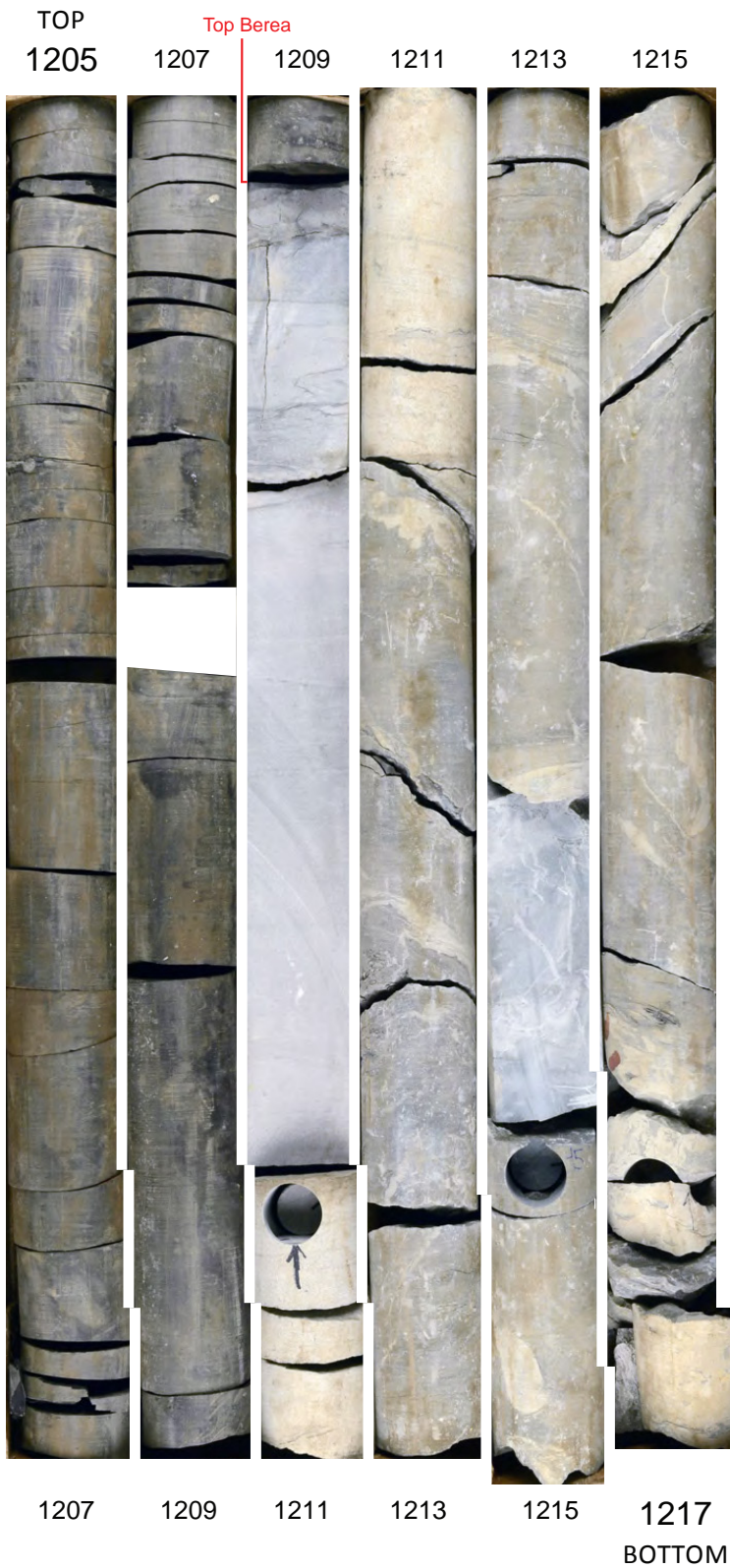
Described from mostly unslabbed core



Dry core images
Only 1209.1-
1202.6 and 1214-
1214.5 slabbed

KGS Core No. 270

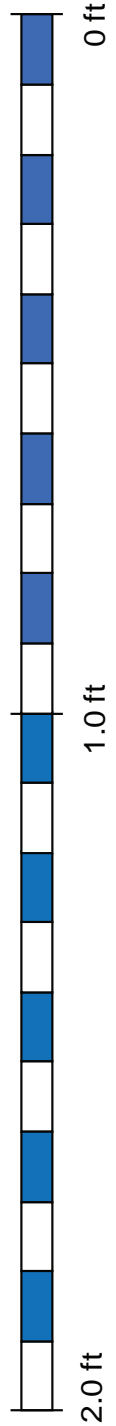
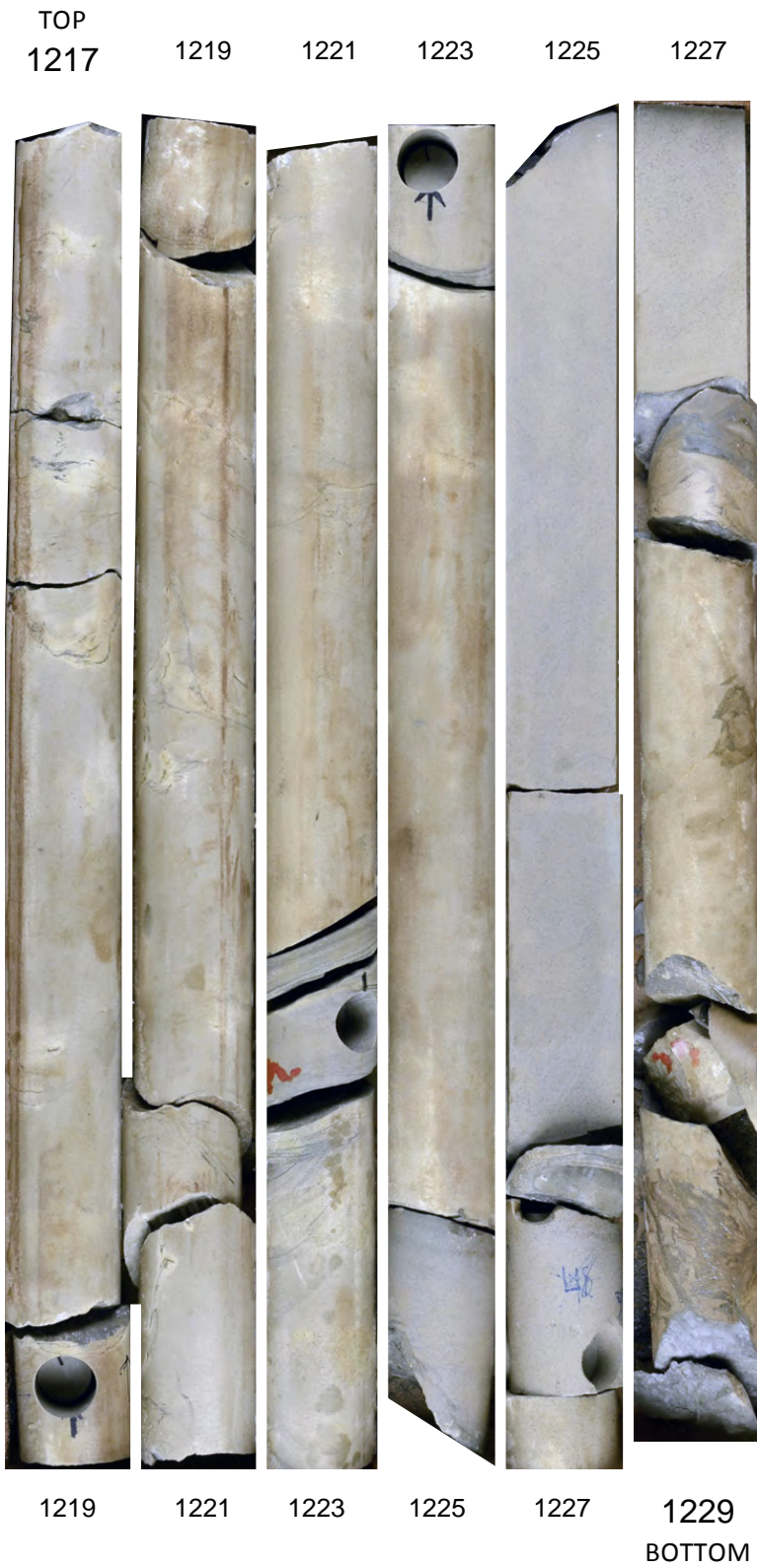
KY-WV Gas No. 1087 Ruben Moore Box 1



Wet core images
Only 1225-1226.5
and 1227-1227.4
slabbed

KGS Core No. 270

KY-WV Gas No. 1087 Ruben Moore Box 2



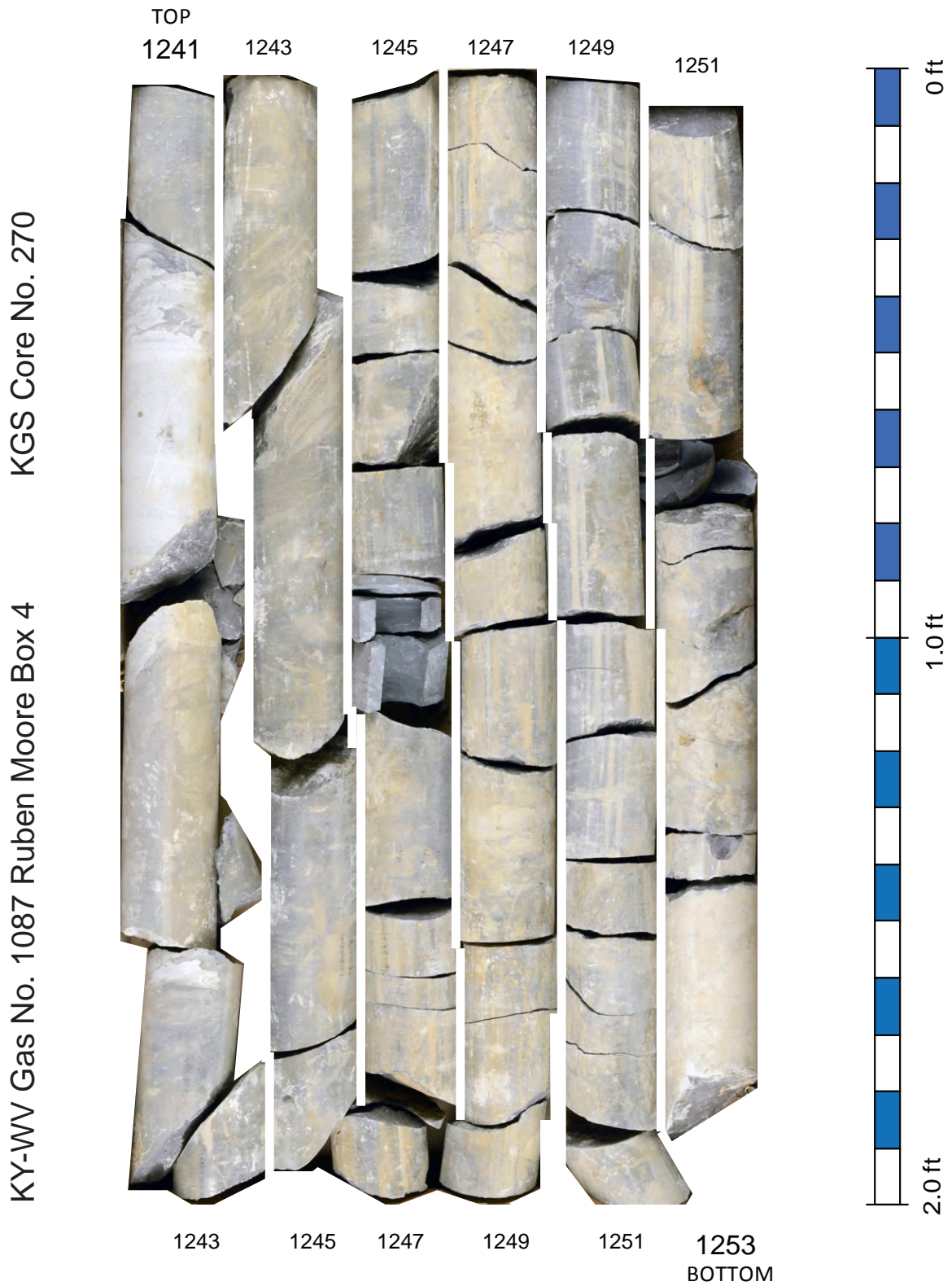
Wet core images
Only 1235-1237
slabbed

KGS Core No. 270

KY-WV Gas No. 1087 Ruben Moore Box 3



Dry core images
Unslabbed



Dry core images
Unslabbed core

KGS Core No. 270

KY-WV Gas No. 1087 Ruben Moore Box 5



Wet core images
Only 1266-1266.8
and 1273-1274.1
slabbed

KGS Core No. 270

KY-WV Gas No. 1087 Ruben Moore Box 6



Wet core images

Only 1277.15-
1277.95 and 1281.5-
1282.4 slabbed

KGS Core No. 270

KY-WV Gas No. 1087 Ruben Moore Box 7

TOP
1277

1279

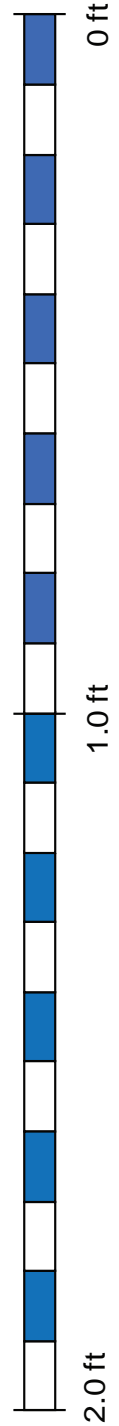
1281



1279

1281

1282.9
BOTTOM



Ashland Oil #KY-4 Kelly-Watt-Bailey-Skaggs

Location: Johnson County, Ky. (see Figure CB-1, Table CB-1)

KGS Core Call No.: C-1186

KGS Oil and Gas Record No.: 42373

Geophysical Logs: Compensated formation density (caliper, gamma-ray, compensated density porosity, bulk density), gamma-ray, gamma-ray after frac, sibilation (sonic), synergetic (gamma-ray, secondary porosity interpretation, water saturation interpretation, porosity and fluid volume interpretation, formation analysis interpretation), temperature

Well Completion Date: 12/18/1978

Core Depth: 967–1,006 (Berea, mostly Bedford), 1,006–1,510 (Ohio Shale) ft

Bedford-Berea Core Interval Thickness: 39 ft (with gaps)

Bedford-Berea Total Thickness: 116 ft

Field: Redbush

Completion: Gas well in Ohio Shale

Background and Distance to Recent Berea Oil Wells

The Ashland Kelly-Watt-Bailey-Skaggs core is from 3.4 mi northwest of the Gillespie Bailey core well (next core herein). The Kelly-Watt-Bailey-Skaggs contains the lower part of the Berea and underlying Bedford Shale. The Gillespie core contains pieces of the upper Berea. The two cores can be compared to the more complete Milton Moore and Ruben Moore cores, from 10 to 12 mi to the east in Lawrence County. The Kelly-Watt-Bailey-Skaggs and Gillespie-Bailey cores are the two closest cores to recent Berea horizontal wells in Johnson County. The Ashland Kelly-Watt-Bailey-Skaggs core is from 1.9 to 3.2 mi northwest of two clusters of recent horizontal oil wells drilled in the Berea by ABARTA Oil and Gas Inc. and 4 mi west of another cluster of recent ABARTA horizontal wells.

Key Features

The Kelly-Watt-Bailey-Skaggs core includes only the lower part of the Berea (Fig. CB-4). It is dominated by soft-sediment-deformed siltstones. It is a good core for examining the lower Berea-Bedford and Bedford-Cleveland contacts. The lower part of the Bedford is dark gray and likely partly transitional with the underlying Cleveland Shale Member of the Ohio Shale. In the core report that accompanies the well record on the Kentucky Geological Survey website, the top of the Cleveland is picked at 1,006 ft. The geophysical log for the well shows the base of Bedford silty shale at 996 ft and the top of the Cleveland shale (where gamma is off-scale at greater than 200 API units) at 1,006 ft, however. A DOE report (Zielinski and Nance, 1980) on the Devonian shale in this core placed the top of the Cleveland at 992 ft. Herein, the top of the Cleveland is shown on the graphic log at 997 ft, which is the uppermost relatively thick interval of black shale in the core. The contact is transitional from 992–1,006 ft.

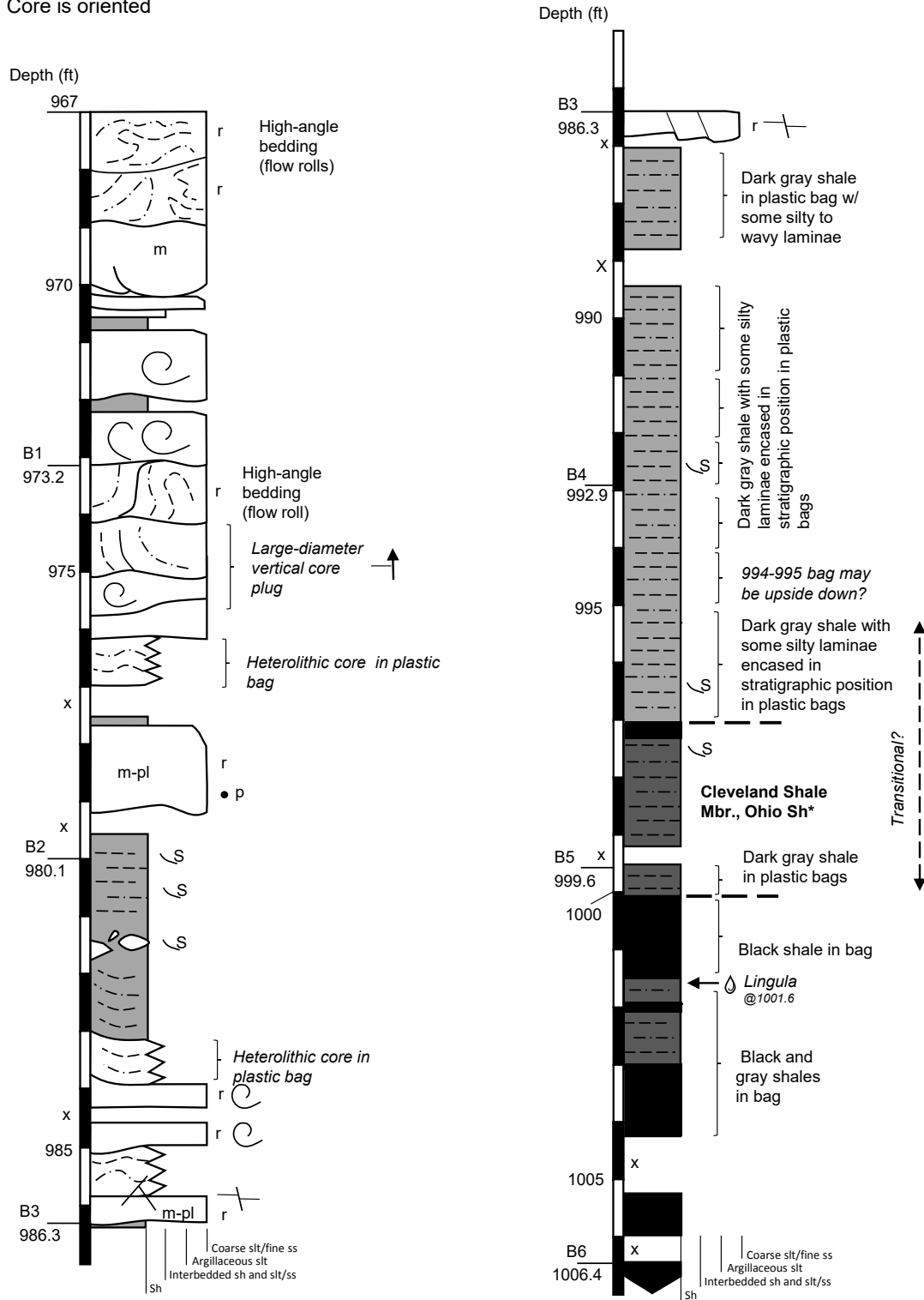
Data and Analysis

The Ashland Kelly-Watt-Bailey-Skaggs core had no original porosity or permeability data with the core donation or well record for the Berea part of the core, and no additional data were collected from the Berea in this study. The core is unslabbed, so plugs can be taken in the future, if needed.

Three Bedford samples were collected at 974.16, 984.32, and 994.05 ft, and many additional Ohio Shale samples were collected from deeper parts of the core for a previous DOE report (Zielinski and Nance, 1980). The sample at 984.32 ft (KY-4-2), which would be in the Bedford Shale, had permeability of 7.4×10^{-10} darcys. Major-element and kerogen-element analyses, and material balance assays for carbon and ash from the report are available from the well record through the Kentucky Geological Survey Oil and Gas Database.

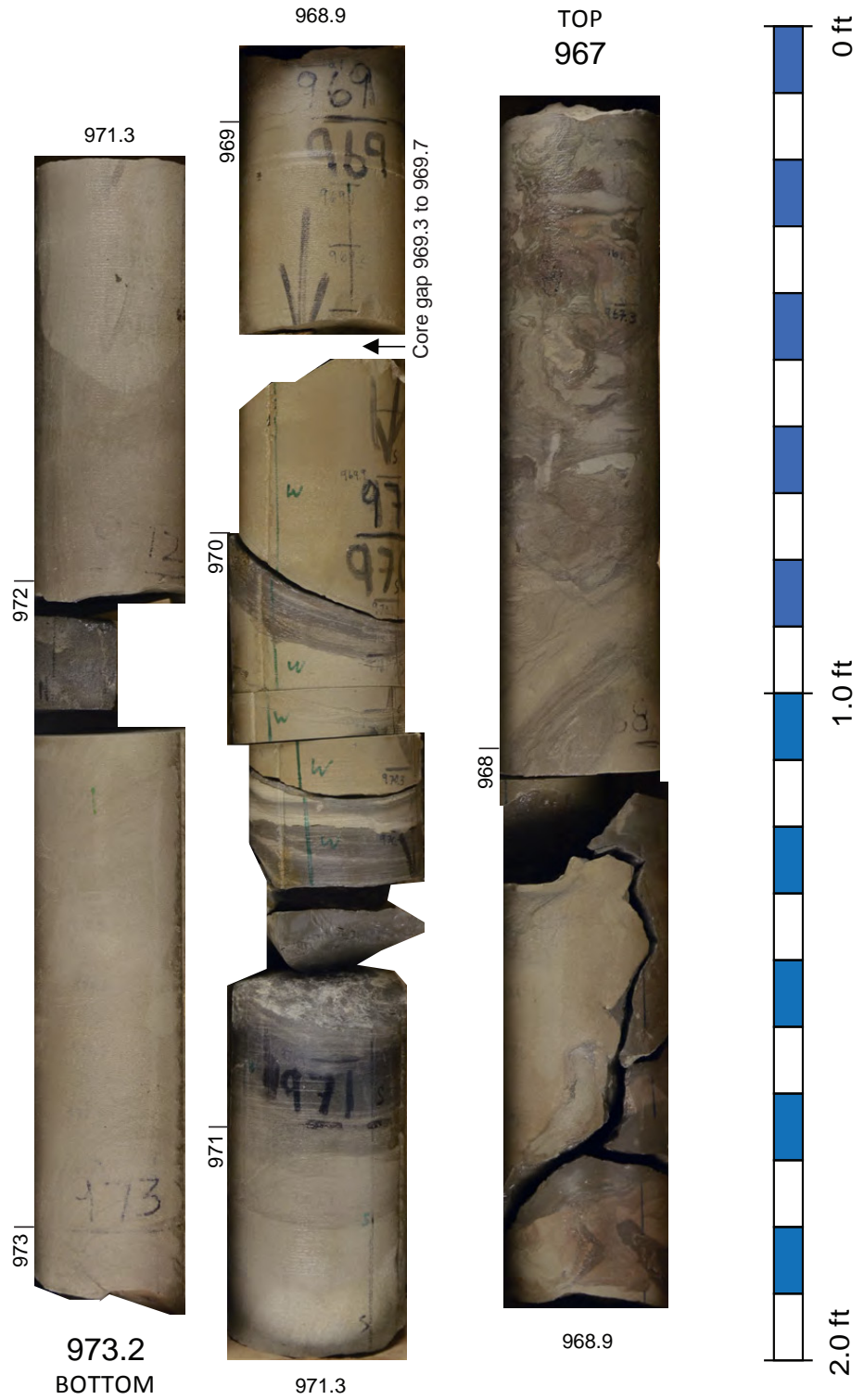
Ashland Oil No. 3RS Kelly-Watt-Bailey-Skaggs

Core is oriented

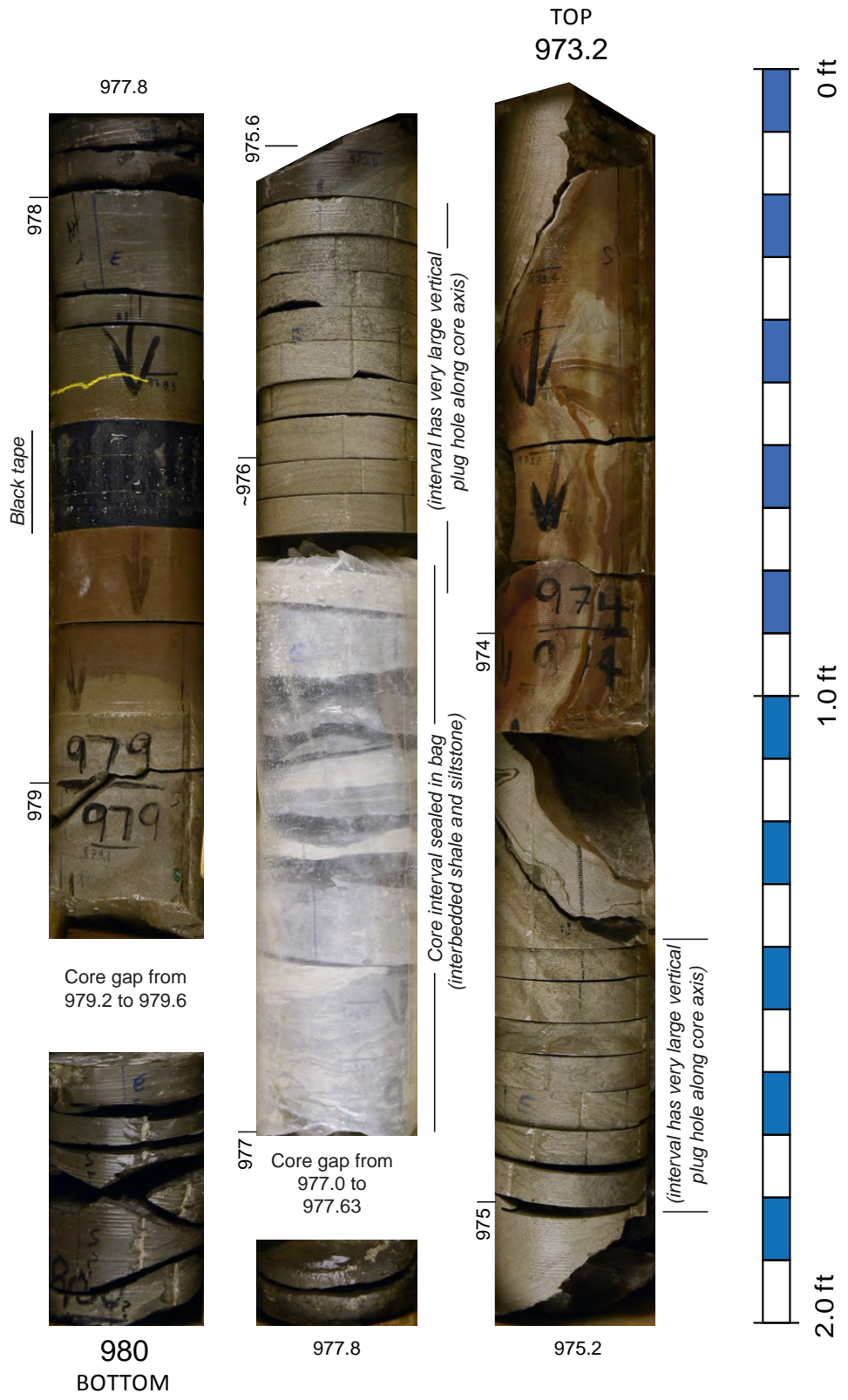


* In core report, top of Cleveland is 1006 ft, but geophysical log shows base of Bedford silts at 996, and top of Cleveland shale, where gamma is off-scale (>200 API units) at 1006 ft. DOE report (Zielinski and Nance, 1980) on the Devonian Shale in this core placed top at 992 ft. Top is shown here at 997 ft, although the top is transitional.

Ashland No. 3RS Kelley-Watt-Bailey-Skaggs, KGS C-1186, Box 1



Ashland No. 3RS Kelley-Watt-Bailey-Skaggs, KGS C-1186, Box 2

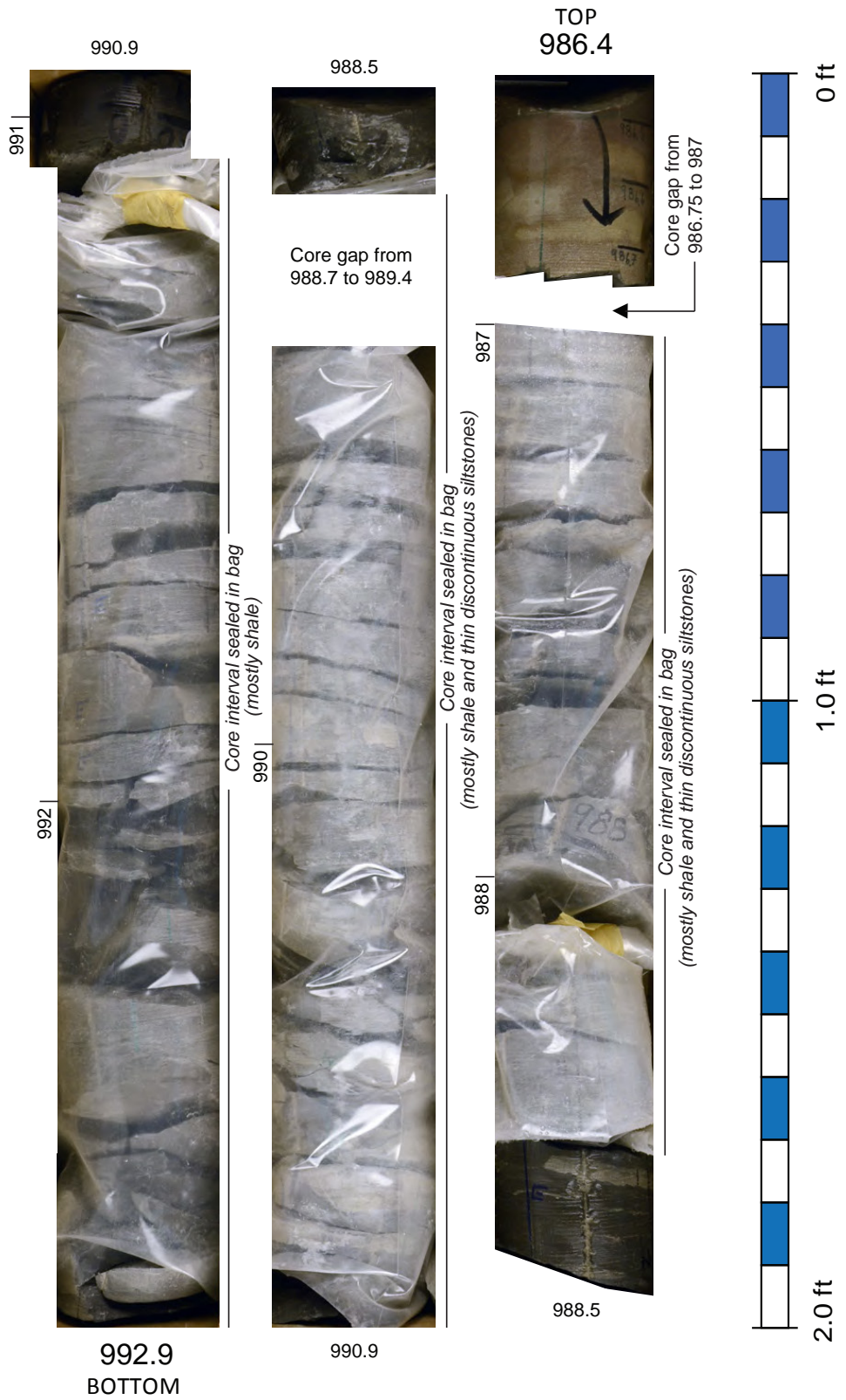


Ashland No. 3RS Kelley-Watt-Bailey-Skaggs, KGS C-1186, Box 3



Ashland No. 3RS Kelley-Watt-Bailey-Skaggs, KGS C-1186, Box 4

Base of Berea siltstones is 986.75



Several black to dark gray shales (Cleveland Mbr.) interfinger with medium gray shales (Cleveland or Bedford shales)

Ashland No. 3RS Kelley-Watt-Bailey-Skaggs, KGS C-1186, Box 5

Broken shale pieces from 997 to 991.15 (may be some gaps)



Core gap
999.15 to 999.4



999.6
BOTTOM



Core interval sealed in bag
(mostly shale)

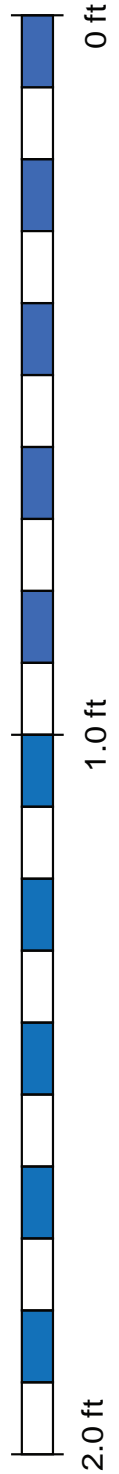
997



Core interval sealed in bag
(mostly shale)

TOP
992.9

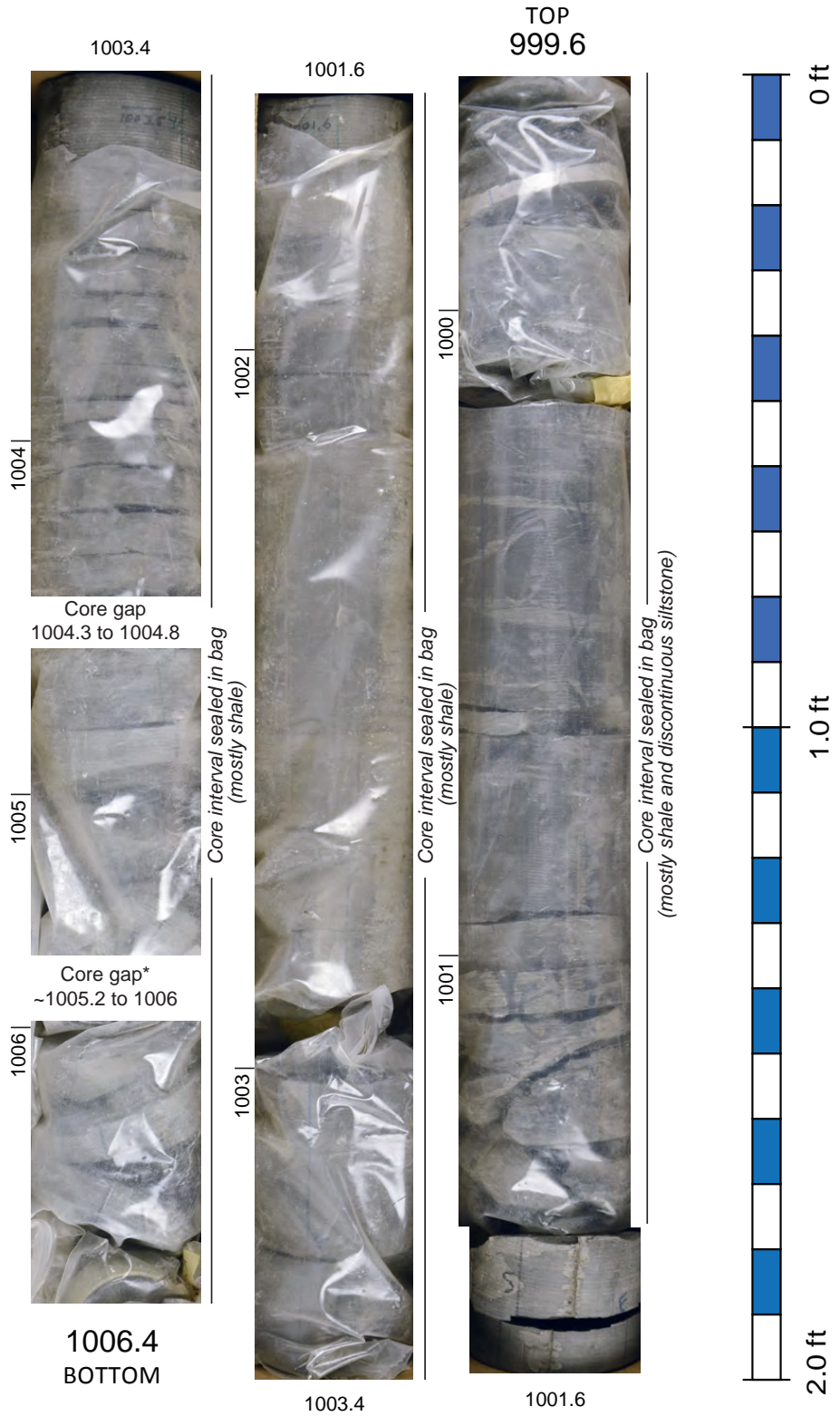
995



Several black to dark gray shales (Cleveland Mbr.) interfinger with medium gray shales (Cleveland or Bedford shales)

**Spacer at 1005.2 is mislabeled with much lower footage, so gap is inferred from base of box*

Ashland No. 3RS Kelley-Watt-Bailey-Skaggs, KGS C-1186, Box 6



Ashland No. 3RS Kelley-Watt-Bailey-Skaggs, KGS C-1186, Box 7



Gillespie #1 Lowell Bailey

Location: Johnson County, Ky. (see Figure CB-1, Table CB-1)

KGS Core Call No.: C-859

KGS Oil and Gas Record No.: 45797

Geophysical Logs: None

Well Completion Date: 8/1/1961

Core Depth: Top of Berea at 787 ft

Bedford-Berea Core Interval Thickness: 16 ft of core representing 96 ft of Bedford-Berea interval

Bedford-Berea Total Thickness: 107 ft in nearby well

Field: Redbush

Completion: Oil well in Berea (786–871 ft); initial production, 20 bbl/day

Background and Distance to Recent Berea Oil Wells

The Gillespie Bailey core is from 3.4 mi southeast of the Kelly-Watt-Bailey-Skaggs core well (previous core herein). The Gillespie Bailey core represents the upper 46 ft of the Berea, whereas the Kelly-Watt-Bailey-Skaggs core represents the lower part of the Berea and underlying Bedford Shale. The two cores can be compared to the more complete Milton Moore and Ruben Moore cores, from 10 to 12 mi to the east in Lawrence County. The Bailey well is less than 0.4 mi west of several recent horizontal oil wells drilled by ABARTA Oil and Gas Co.

Key Features

Only two boxes of the Gillespie Bailey core are preserved. These boxes contain small pieces of core, each 1 to 5 in. long, each representative of 1-ft intervals in the original core. The core presumably began near the top of the Berea, and footages suggest it represents the uppermost Berea in the well. In general, bedding is similar to that in the more complete Milton and Ruben Moore cores to the east, but bedding successions and relative abundance are difficult to infer because of the lack of continuous section and absence of a corresponding well log. Few of the surrounding wells have logs. For comparison, the log shown in Figure CB-3 is from a well (KGS record no. 121949) 1.1 mi south of the Bailey well.

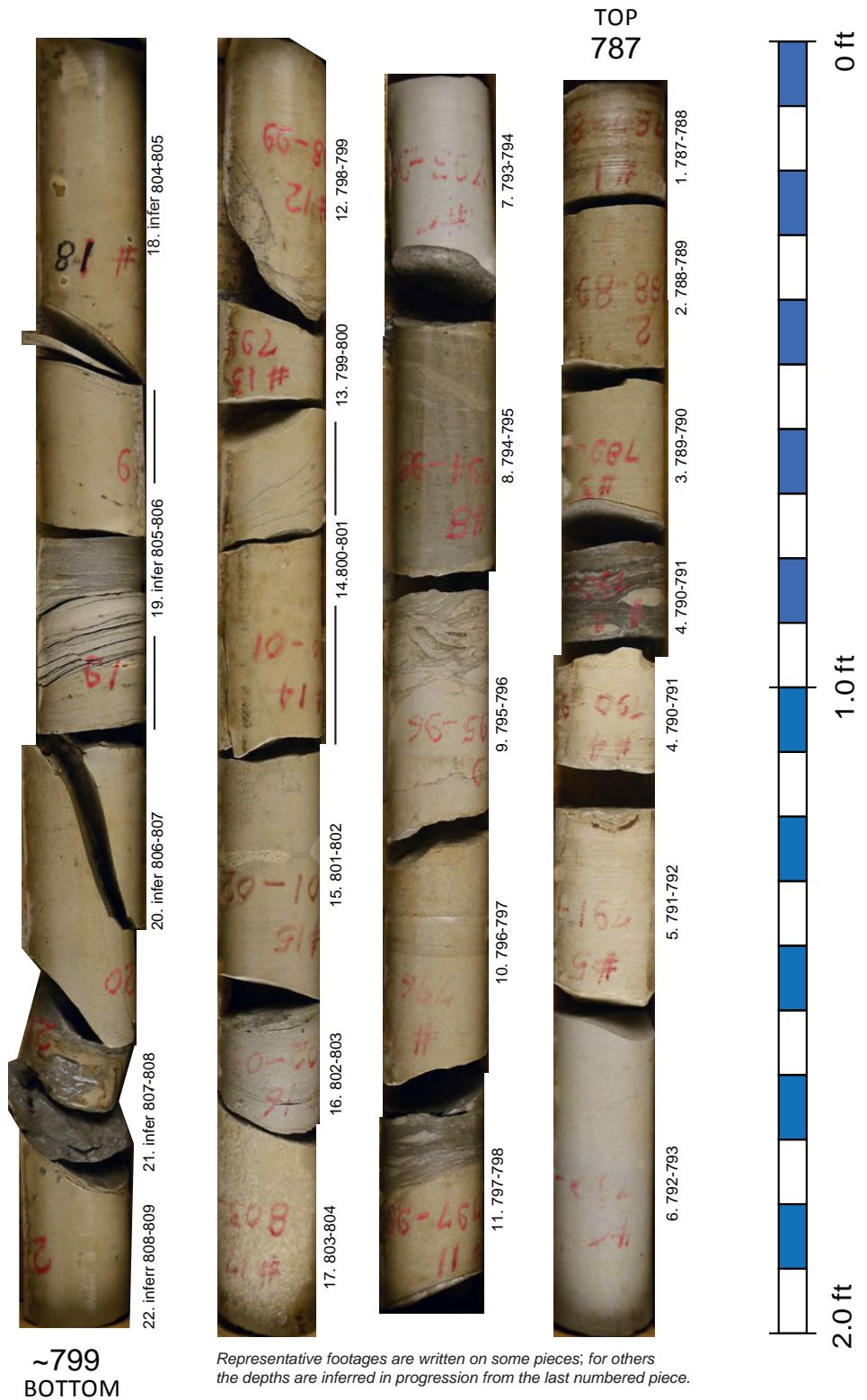
Data and Analysis

The Gillespie Bailey core had 32 original porosity, permeability, oil saturation, and water-content measurements in a core analysis report from Oilfields Research Inc., which were included with the well record. None of the pieces of core (small pieces supposedly representative of larger intervals) have plug holes, however, so it is difficult to compare the porosity and permeability data to the core. The available data can be viewed online through the Kentucky Geological Survey Oil and Gas Database. Because of the fragmentary nature of the core, and because the core was from west of the main thermal-maturity trend, no additional samples were taken for analysis for this report. Core pieces remain unslabbed in case future plugs need to be taken for analysis.

This is not continuous core.

Box contains samples of core (each 0.1 to 0.5 feet) representing one-foot core intervals in the original core.

Gillespie No. 1 Lowell Bailey, KGS C-859, Box 1

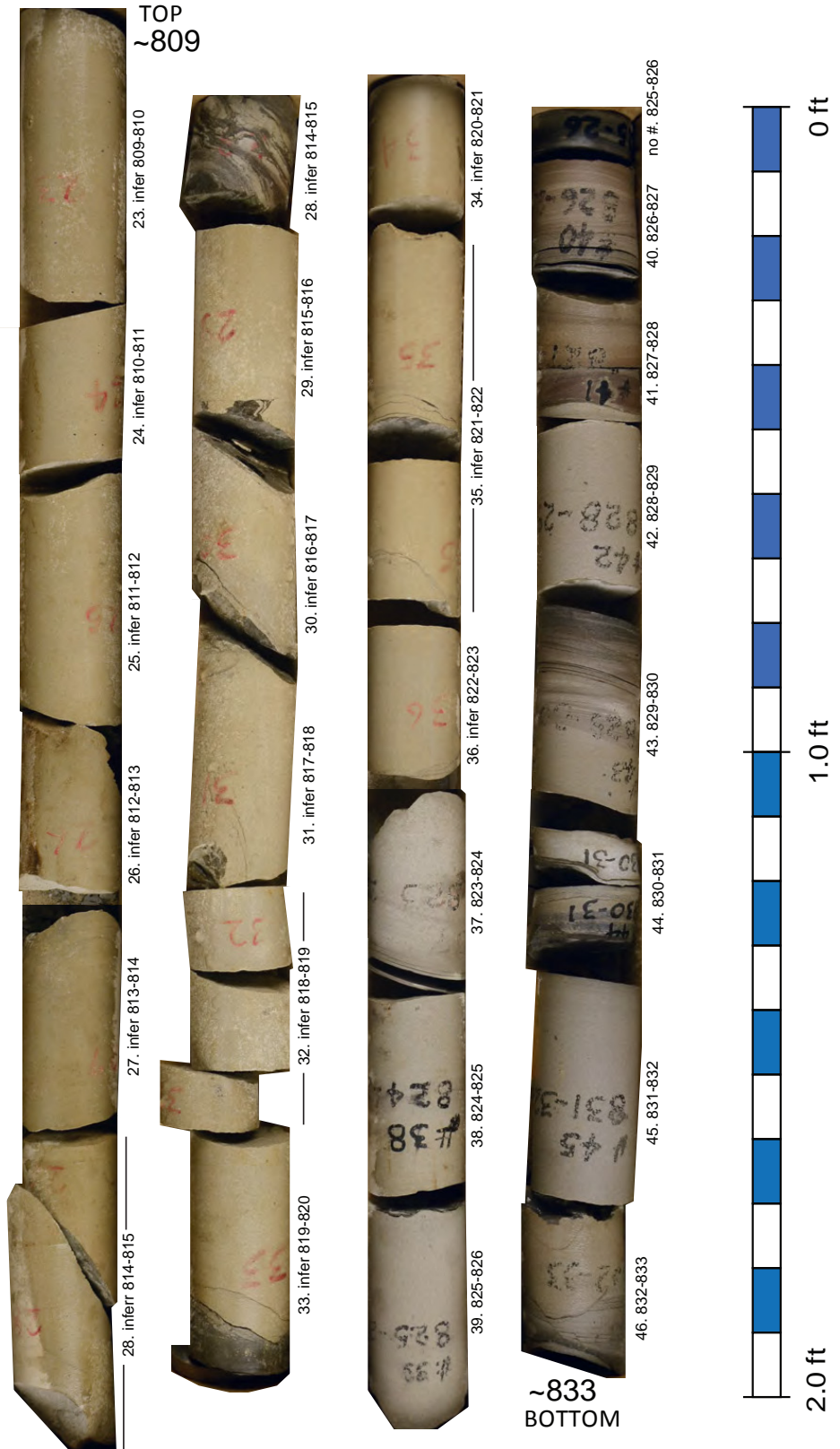


Gillespie No. 1 Lowell Bailey, KGS C-859, Box 2

This is not continuous core.

Box contains samples of core (each 0.1 to 0.5 feet) representing one-foot core intervals in the original core.

Pieces are numbered, 1-46.



Representative footages are written on some pieces; for others the depths are inferred in progression from the last numbered piece.

Columbia Natural Resources #20456 Pocahontas Land Co. (Pocahontas Mining)

Location: Martin County, Ky. (see Figure CB-1, Table CB-1)

KGS Core Call No.: C-5907 KGS

Oil and Gas Record No.: 66348

Geophysical Logs: Compensated density (gamma-ray, caliper, density), spontaneous potential, resistivity

Well Completion Date: 10/4/1977

Core Depth: Top of Berea at 2,298 ft (may originally have been 2,296 ft; piece may be missing)

Bedford-Berea Core Interval Thickness: 107 ft

Bedford-Berea Total Thickness: 112 ft

Field: Big Sandy

Completion: Gas well (shut in), completed in Big Lime and Ohio Shale; not Berea

Background and Distance to Recent Berea Oil Wells

The Columbia Pocahontas core is from south of the current Berea oil play, in a region where the Berea has produced gas. It is from 6.4 mi south of the Warfield Fault, which marks the southern margin of the Rome Trough and the northern margin of the Pike County Uplift. Both the Pocahontas core and the EQT core (from 30 mi to the south) contain substantial thicknesses of shales and very argillaceous siltstones, which can be compared.

Key Features

The top of the Bedford-Berea on the geophysical log is at 2,294 ft. The original top of the interval in core was designated as 2,296 ft with a 3- to 4-ft-thick, fine sandstone at the top of the interval (Potter and others, 1983). Currently, only 1 ft of siltstone remains at the top of the Berea core, so an upper piece of core may be missing. The present top of the core is near 2,298 ft depth.

The upper half of the Pocahontas core is shaly. Siltstone interbeds in the upper half of the core contain a wide variety of convolute laminae and soft-sediment deformation features. Berea siltstones/sandstones dominate the lower half of the Bedford-Berea interval in the core. Several beds between 2,357 and 2,363 ft exhibit overturned folds or flow rolls, which are offset along multiple thin, horizontal shear planes. Most coarse siltstone/sandstone beds below 2,363 ft are thin, sharp-based, massive to faintly laminated, with thin argillaceous tops. Many beds have moderately dipping bases, likely from loading into interbedded shales. Small-scale compactional microfaults are common at the base of beds, and sometimes at the top of beds. These are more common in this core (and possibly the EQT 504353 core) than in the other cores examined. Red staining (presumably from siderite) is common in shaly or argillaceous laminae in the siltstones. Some beds in the lower part of the Berea interval contain dish structures (2,373.2 ft), which suggest fluidization or liquefaction.

This is a good core for examining the Bedford-Cleveland contact. A thin black shale occurs from 2,404.1–2,404.2 ft, and the top of thicker black shale occurs at 2,404.8 ft. Either could be the top of the Cleveland Shale Member. The top of the shale on the geophysical log is at 2,406 ft, and appears to represent the top of the thick black shale at 2,404.8 ft in the core. Neither the overlying or underlying black shales have very high gamma signatures, likely because this location is near the eastern pinchout of the shales.

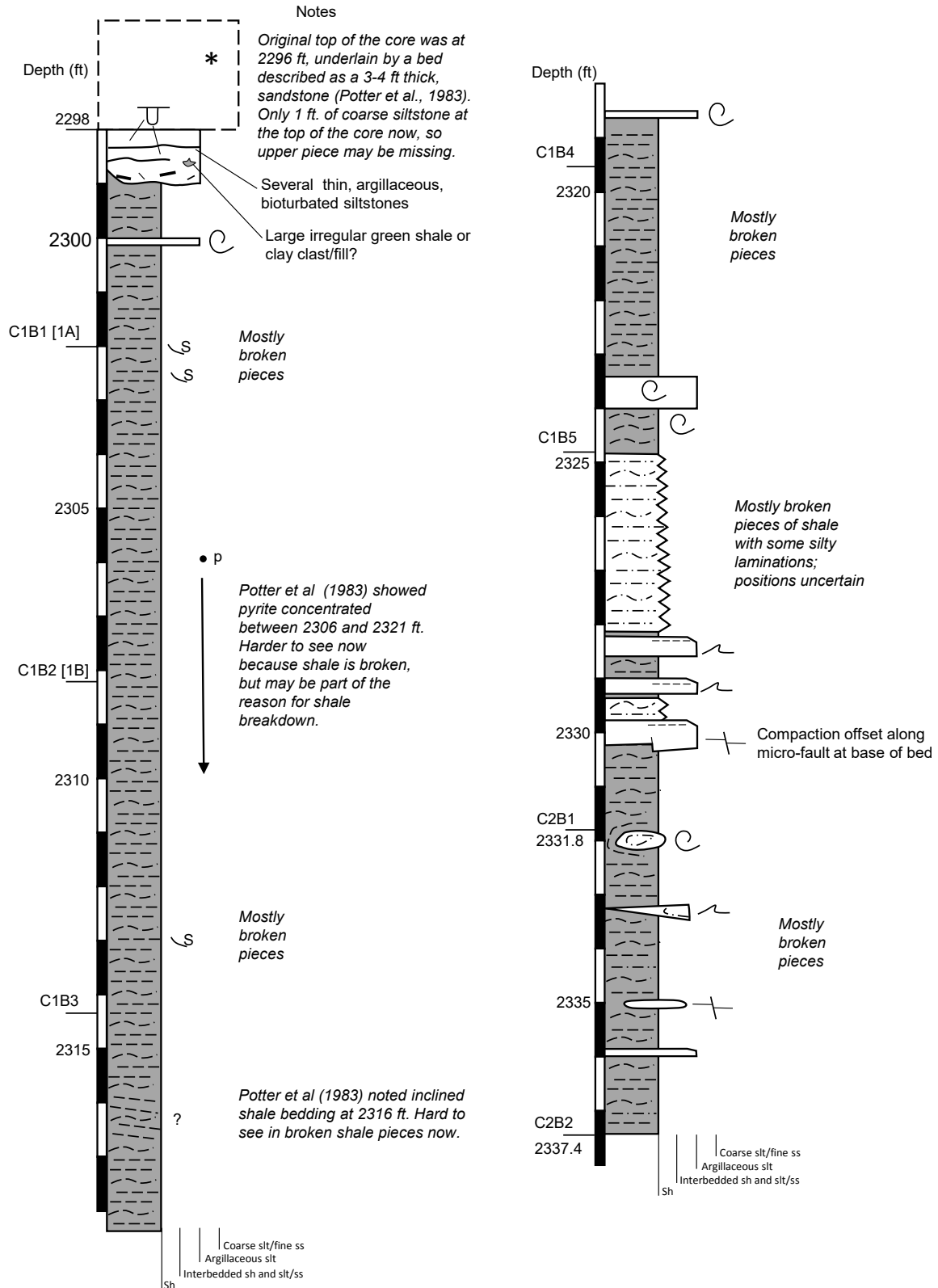
Data and Analysis

The Columbia Pocahontas core has 43 porosity, permeability, oil and water saturation measurements from an Oil Field Research core analysis report. These data are available through the KGS Oil and Gas Database. Plug holes are not visible in the core slab in the KGS repository (see photographic plates), so an exact match of plug analysis to bedding cannot be determined. Presumably, plugs were taken from the other half of the core. Potter and others (1983) summarized this core in a graphic log.

They noted a fining-upward interval from a scour near 2,376 ft upward to approximately 2,337 ft. Scours were also noted at approximately 2,299 ft and approximately 2,410 ft. Potter and others (1983) made 44 modal grain-size measurements. The maximum grain size was at the top of the core (likely a piece now apparently missing), from one sample, at 70 μm (very fine sandstone). Most of the core has grain sizes of 40–50 μm , which would be coarse siltstone. No additional Berea data were collected for this study, although samples were collected from the underlying Ohio Shale.

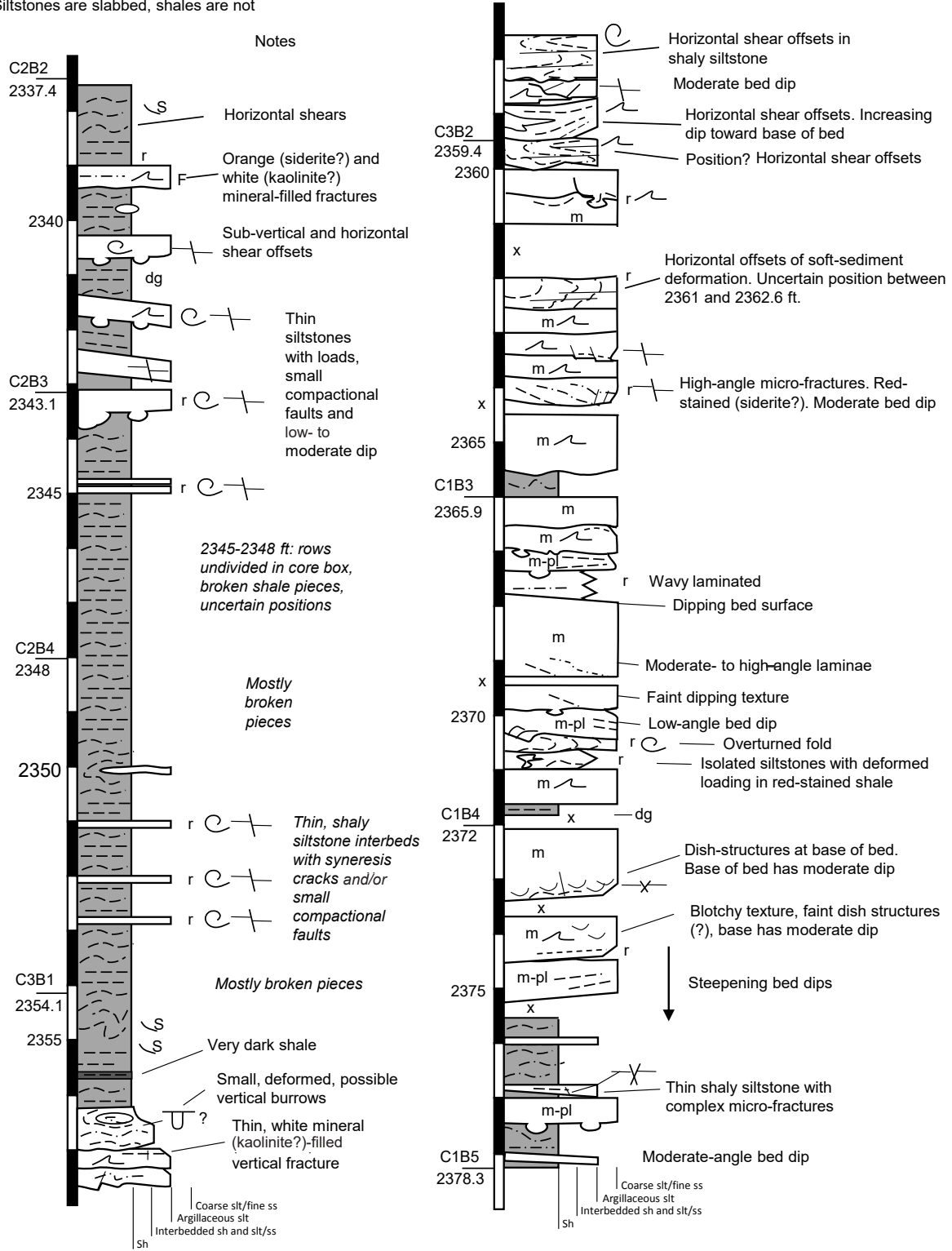
Columbia Gas Transmission No. 1 Pocahontas Land Co. (Mining)

Siltstones are slabbed, shales are not



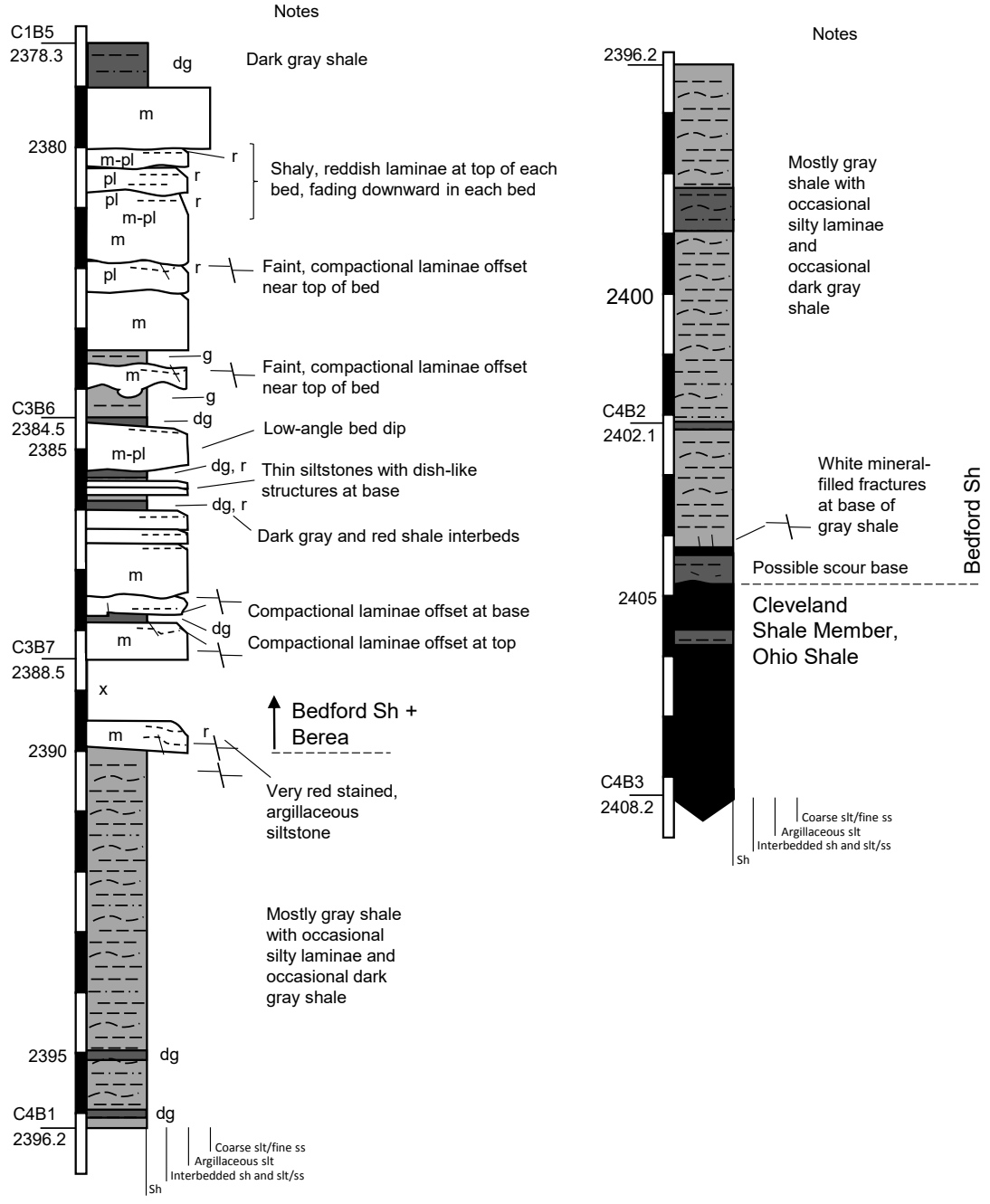
Columbia Gas Transmission No. 1 Pocahontas Land Co. (Mining)

Siltstones are slabbed, shales are not



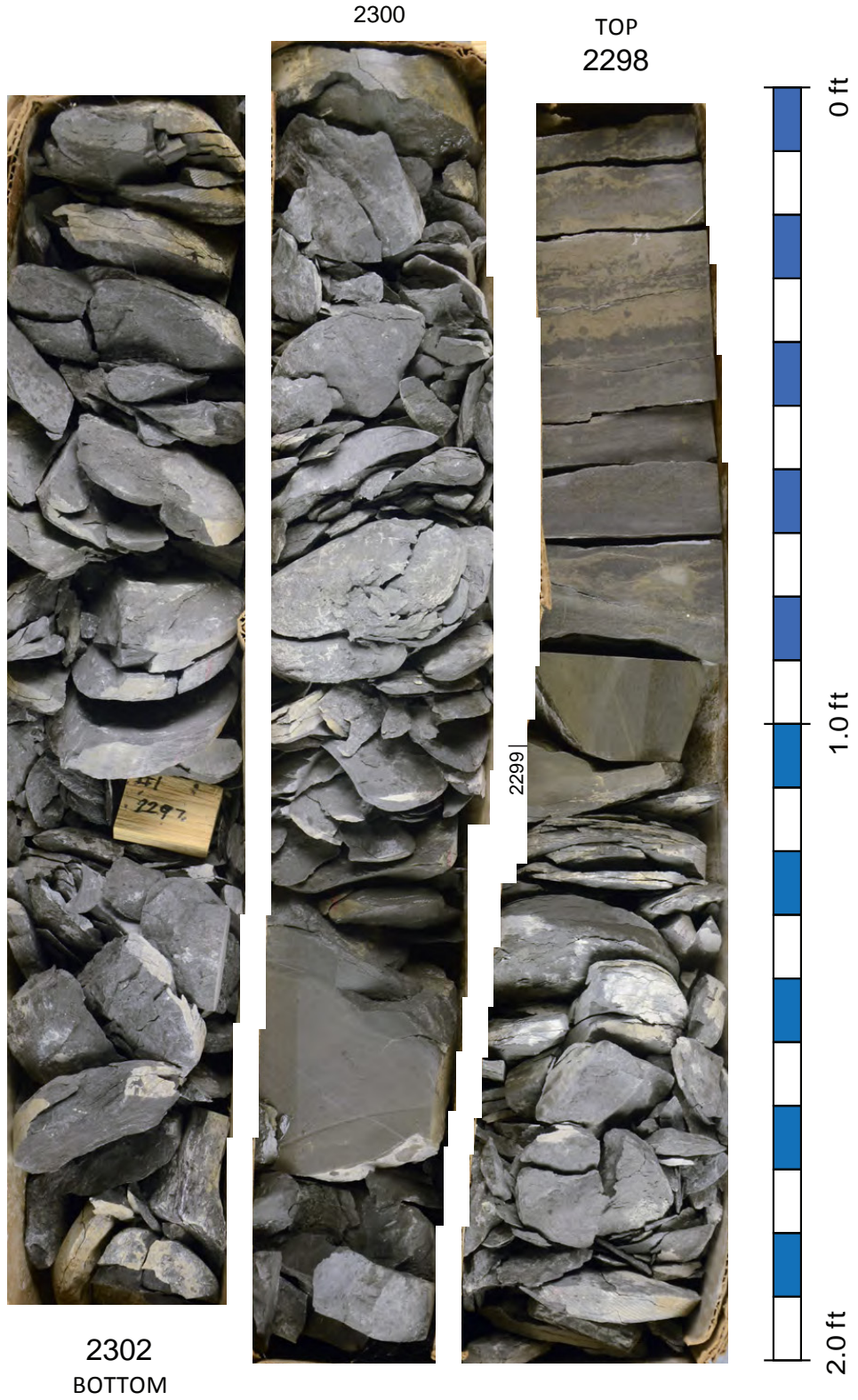
Columbia Gas Transmission No. 1 Pocahontas Land Co. (Mining)

Siltstones are slabbed, shales are not



Slabbed siltstones
wet, shale left dry

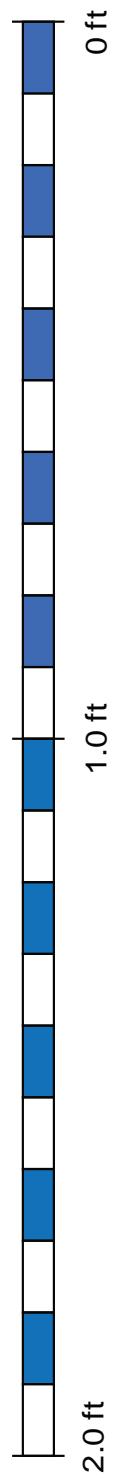
Columbia Gas Trans.(TCO) No. 1 Pocahontas Mining, Core 1 Box 1 [1A]



Dry core

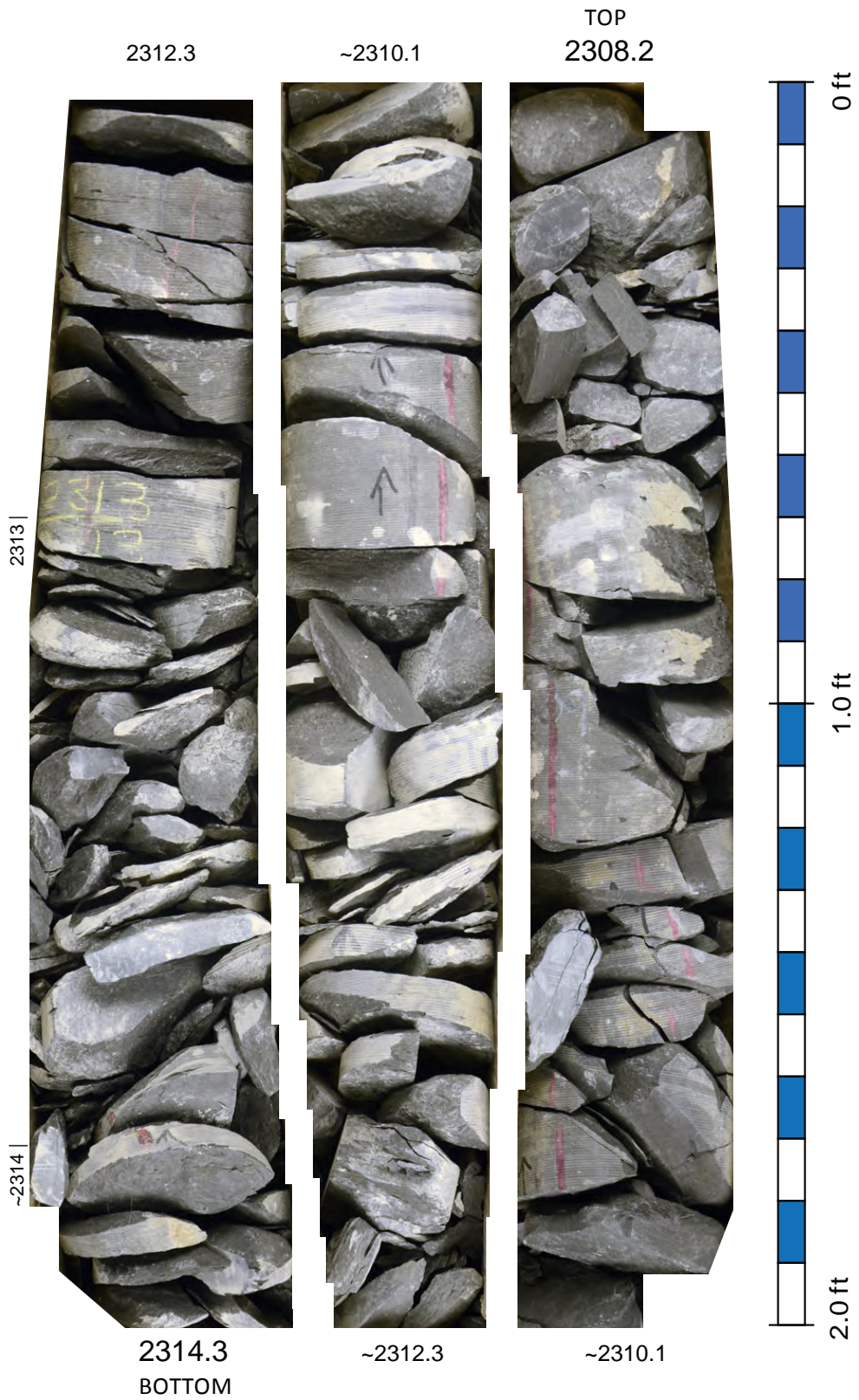
2305 is likely out of place in the box

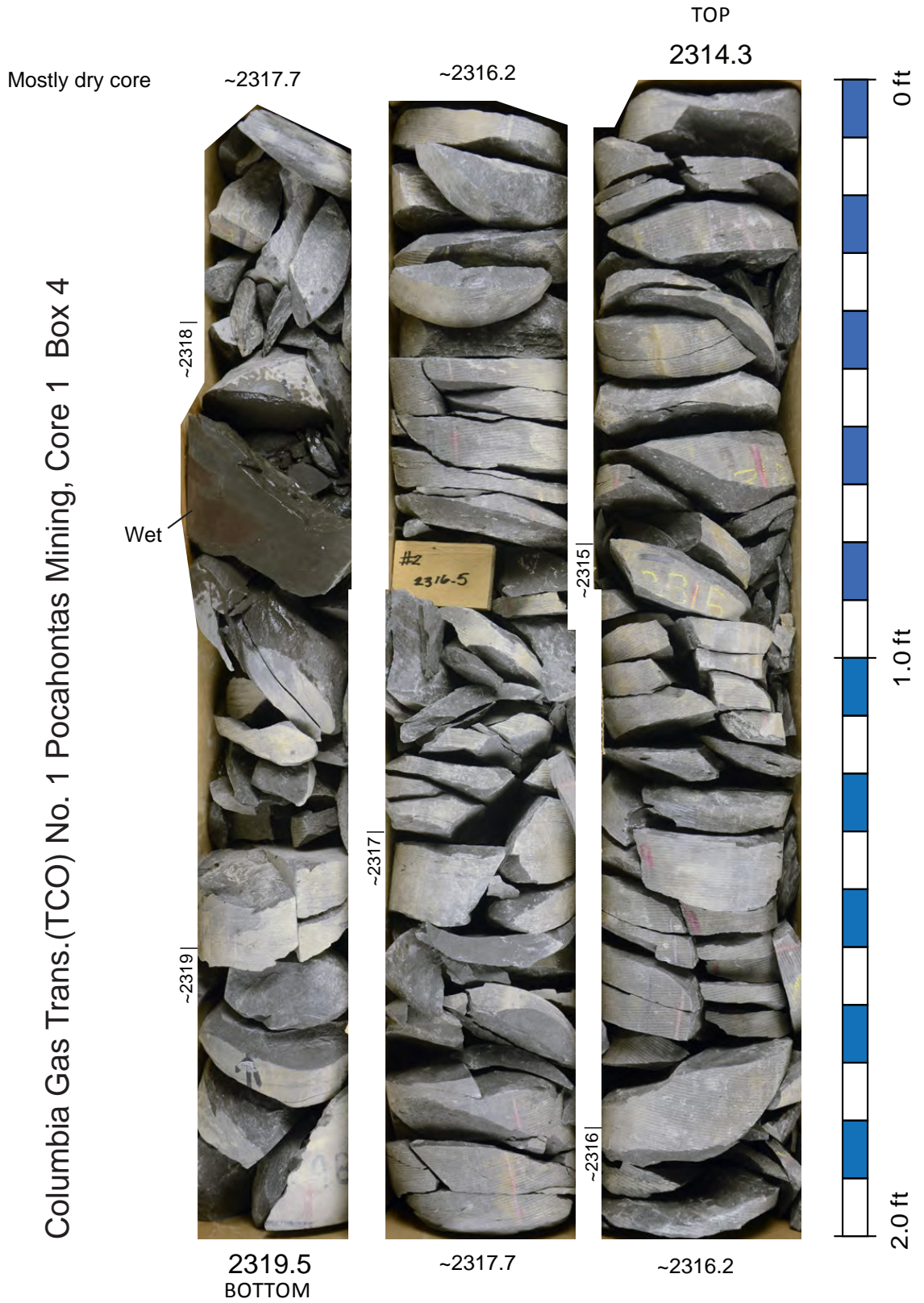
Columbia Gas Trans.(TCO) No. 1 Pocahontas Mining, Core 1 Box 2 [1B]



Dry core

Columbia Gas Trans.(TCO) No. 1 Pocahontas Mining, Core 1 Box 3





Mostly dry core

Columbia Gas Trans.(TCO) No. 1 Pocahontas Mining, Core 1 Box 5

Wet



2324.8
BOTTOM

~2323.4

~2321.5

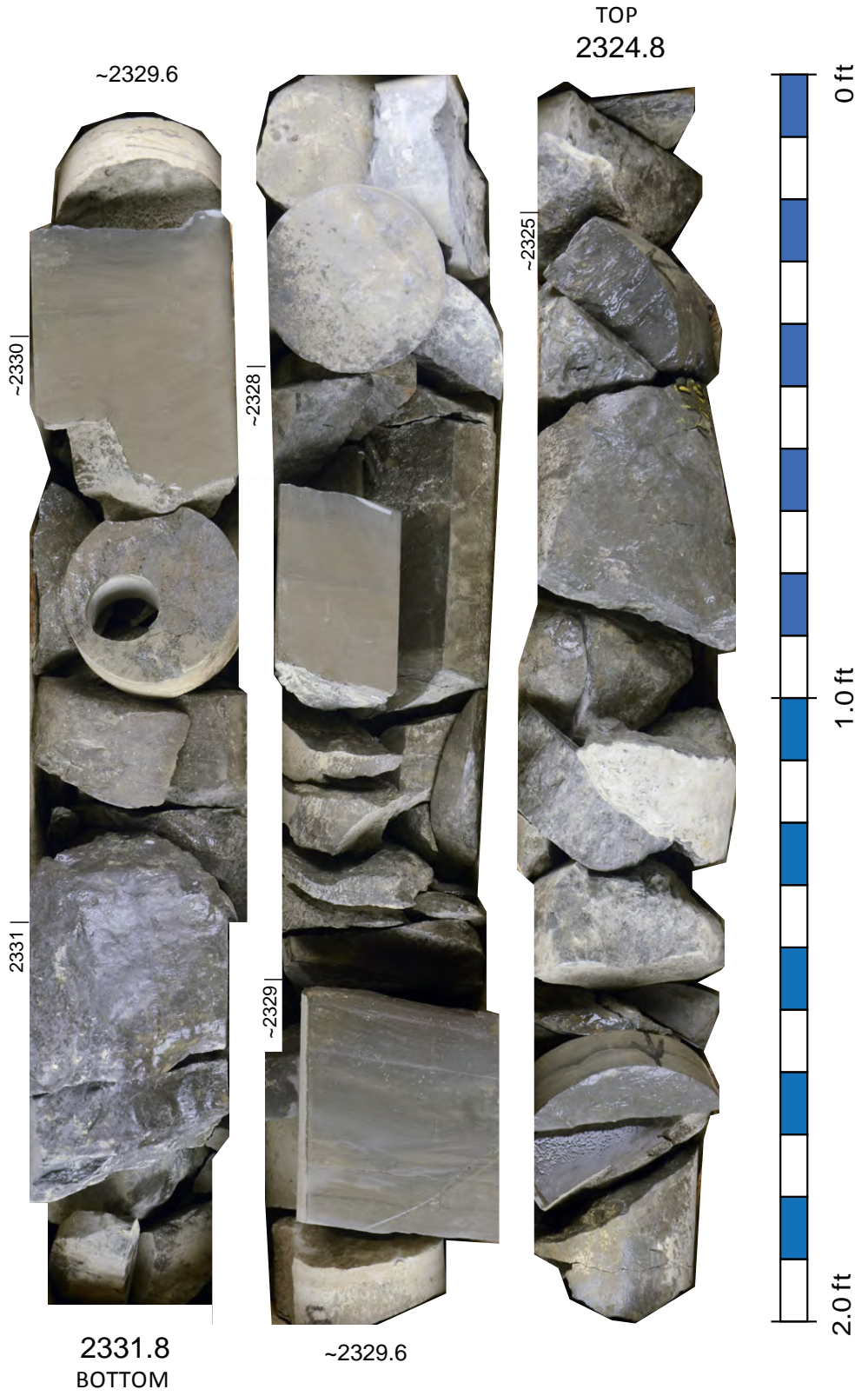
2.0 ft

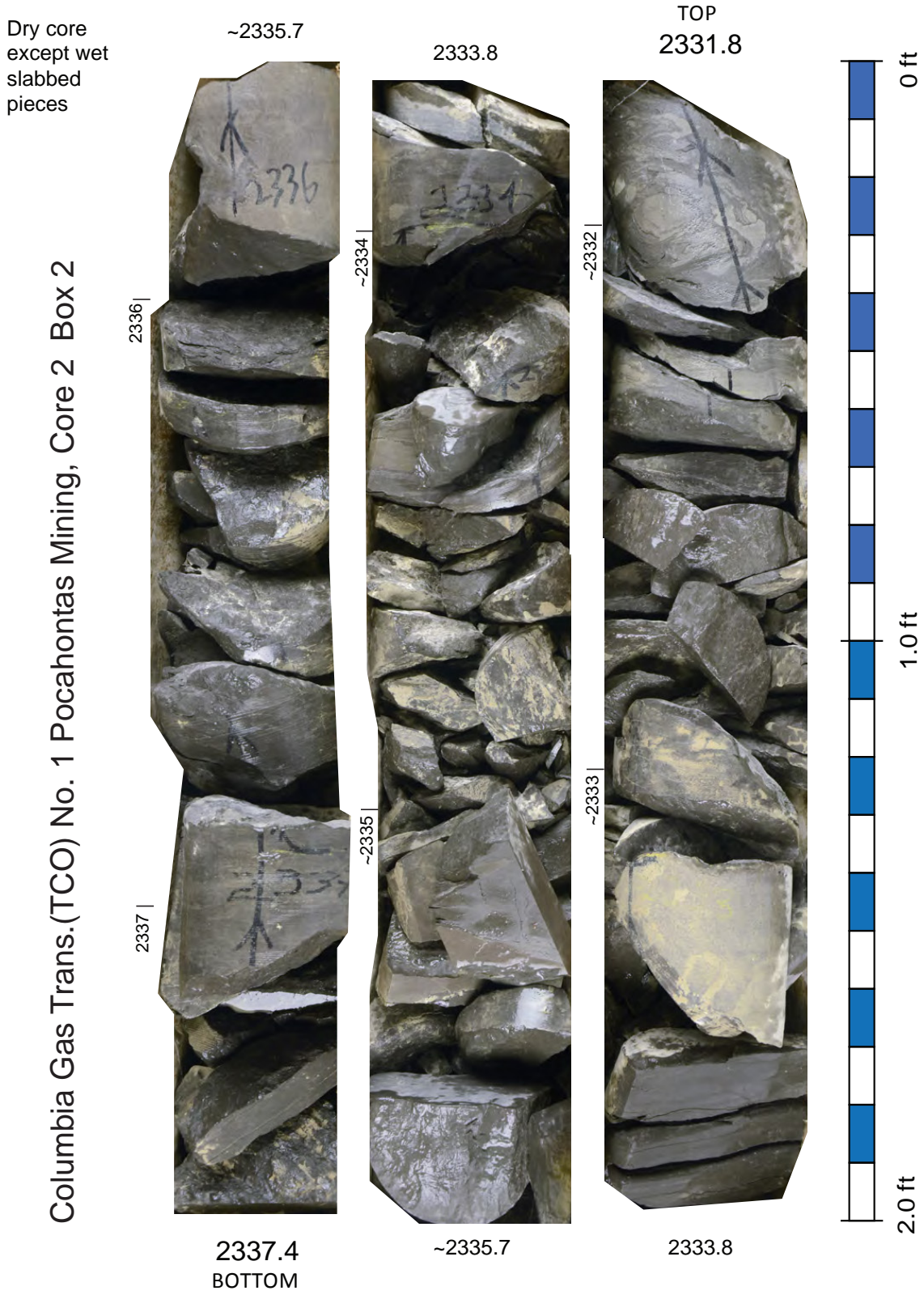
1.0 ft

0 ft

Dry core
except wet
slabbed
pieces

Columbia Gas Trans.(TCO) No. 1 Pocahontas Mining, Core 2 Box 1

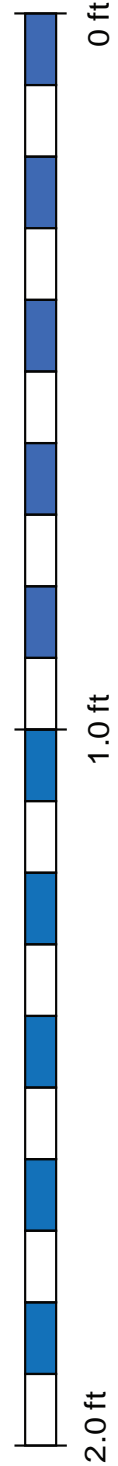




Dry core
except wet
slabbed
pieces

Columbia Gas Trans.(TCO) No. 1 Pocahontas Mining, Core 2 Box 3

Likely slightly
out of place



Dry core
except wet
slabbed
pieces

Columbia Gas Trans.(TCO) No. 1 Pocahontas Mining, Core 2 Box 4



2348
BOTTOM

*Two rows mixed
~shale; 2345-2348*

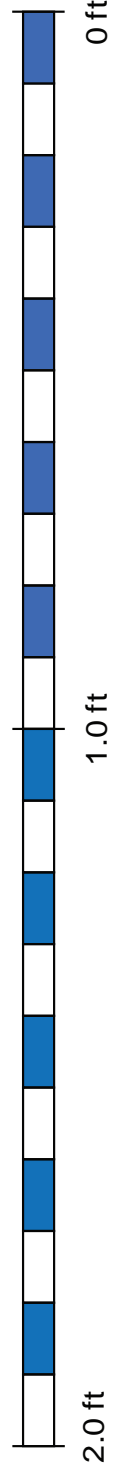
*Two rows mixed
~shale; 2345-2348*



TOP
2343.1

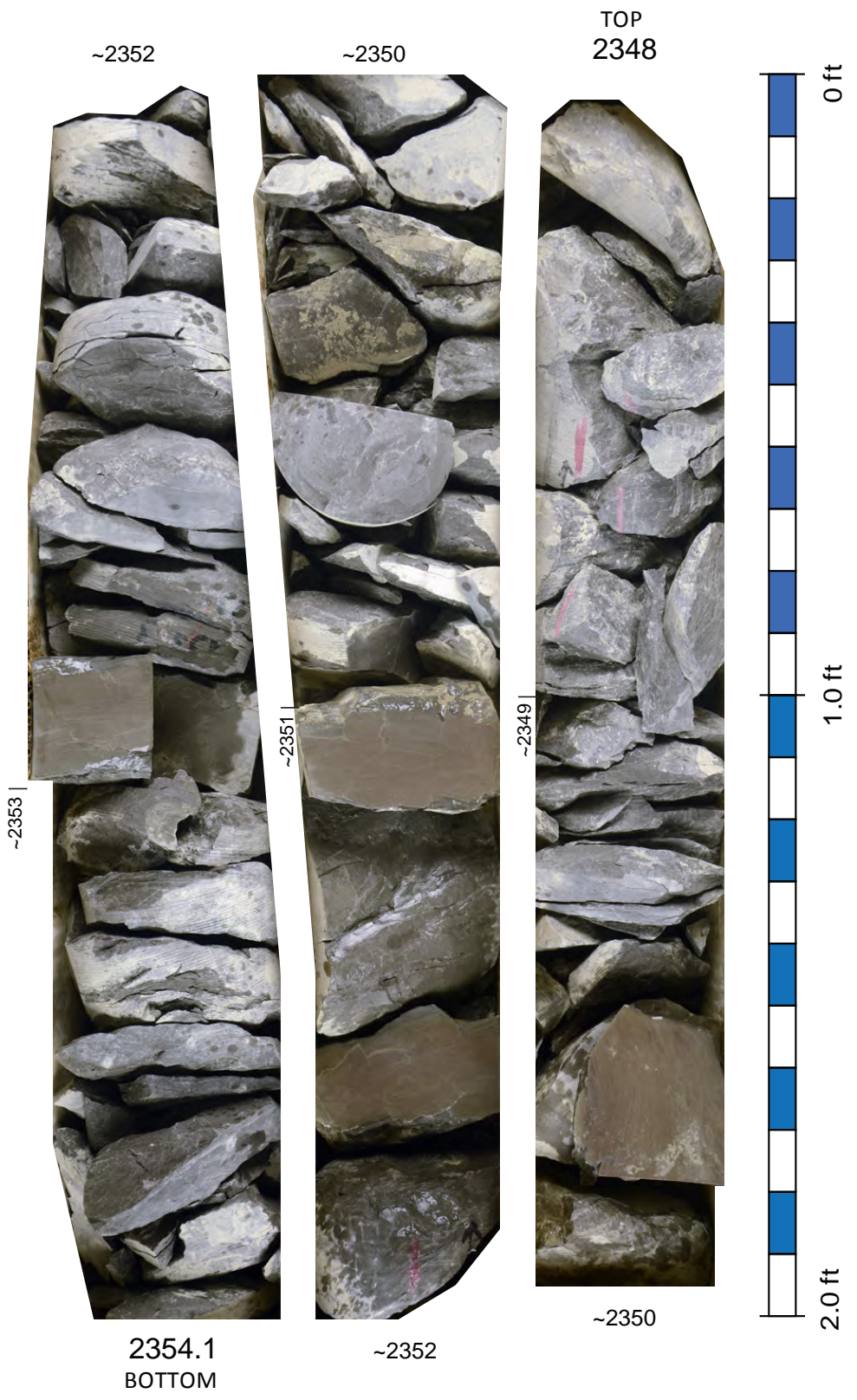
~2344 |

~2345



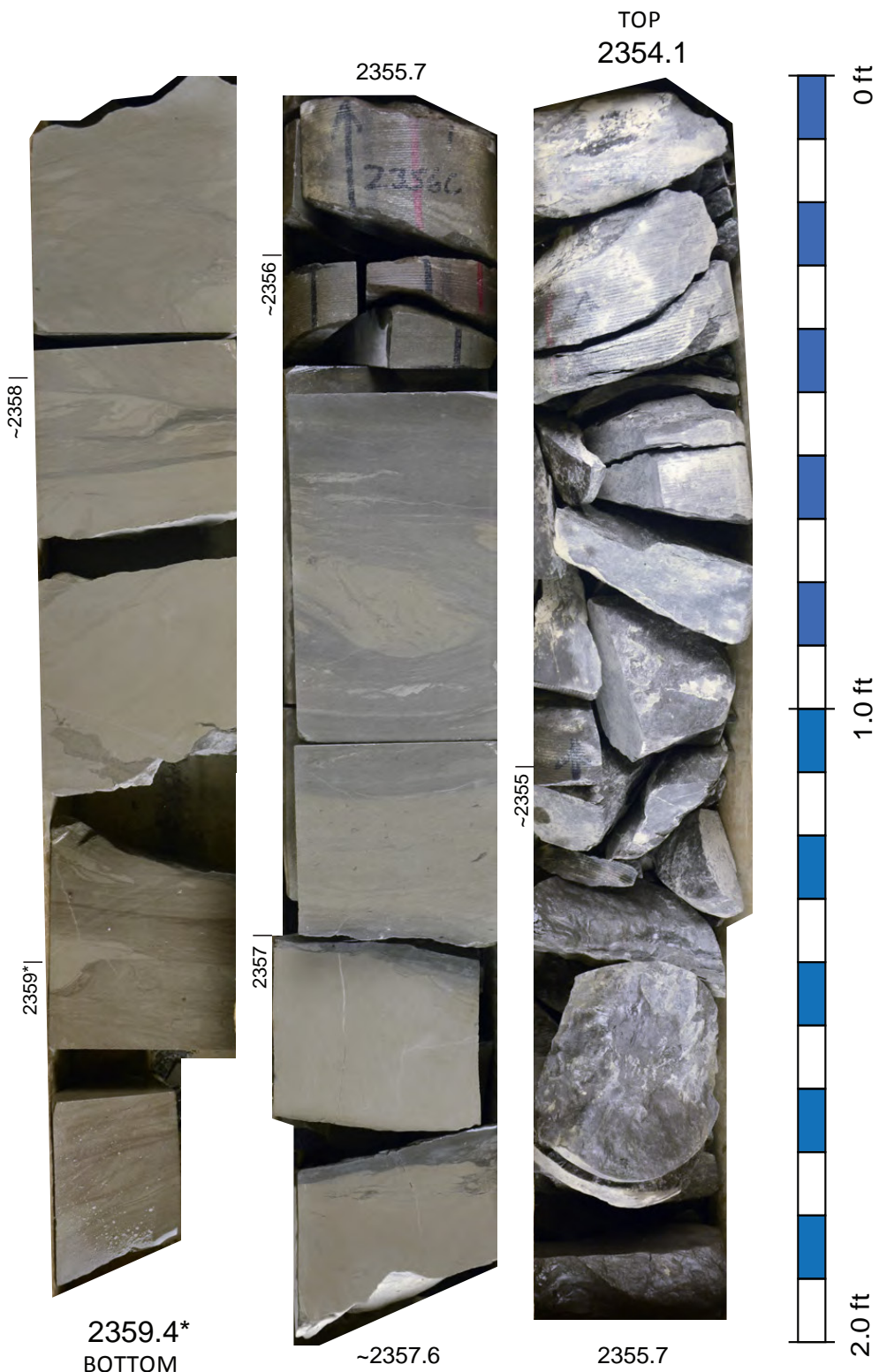
Dry core
except wet
slabbed
pieces

Columbia Gas Trans.(TCO) No. 1 Pocahontas Mining, Core 3 Box 1



Dry core
except wet
slabbed
pieces

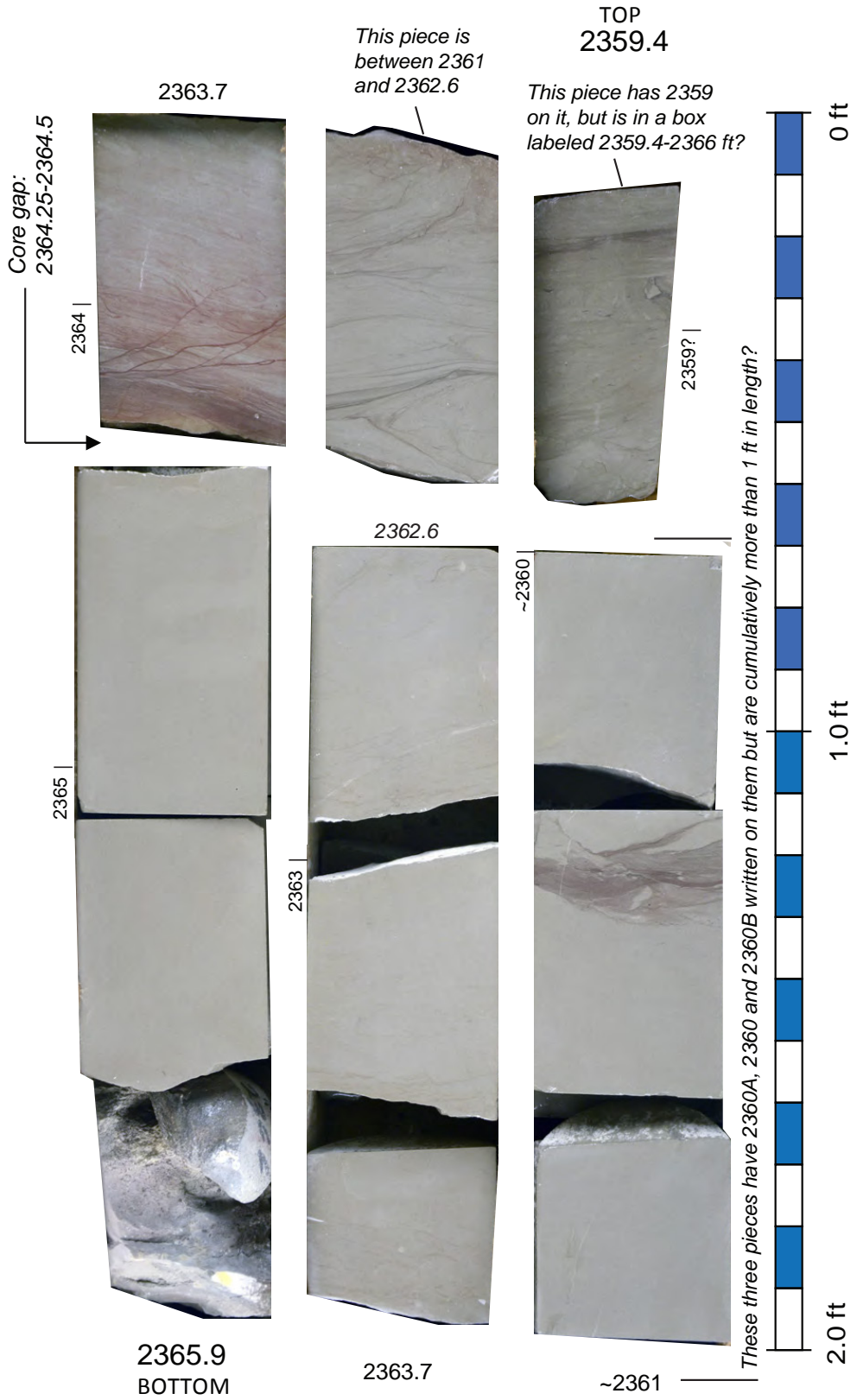
Columbia Gas Trans.(TCO) No. 1 Pocahontas Mining, Core 3 Box 2



* A piece of core in Box 3 also has 2359 written on it, but the base of this box says 2359.4ft, so assume these are correct footages

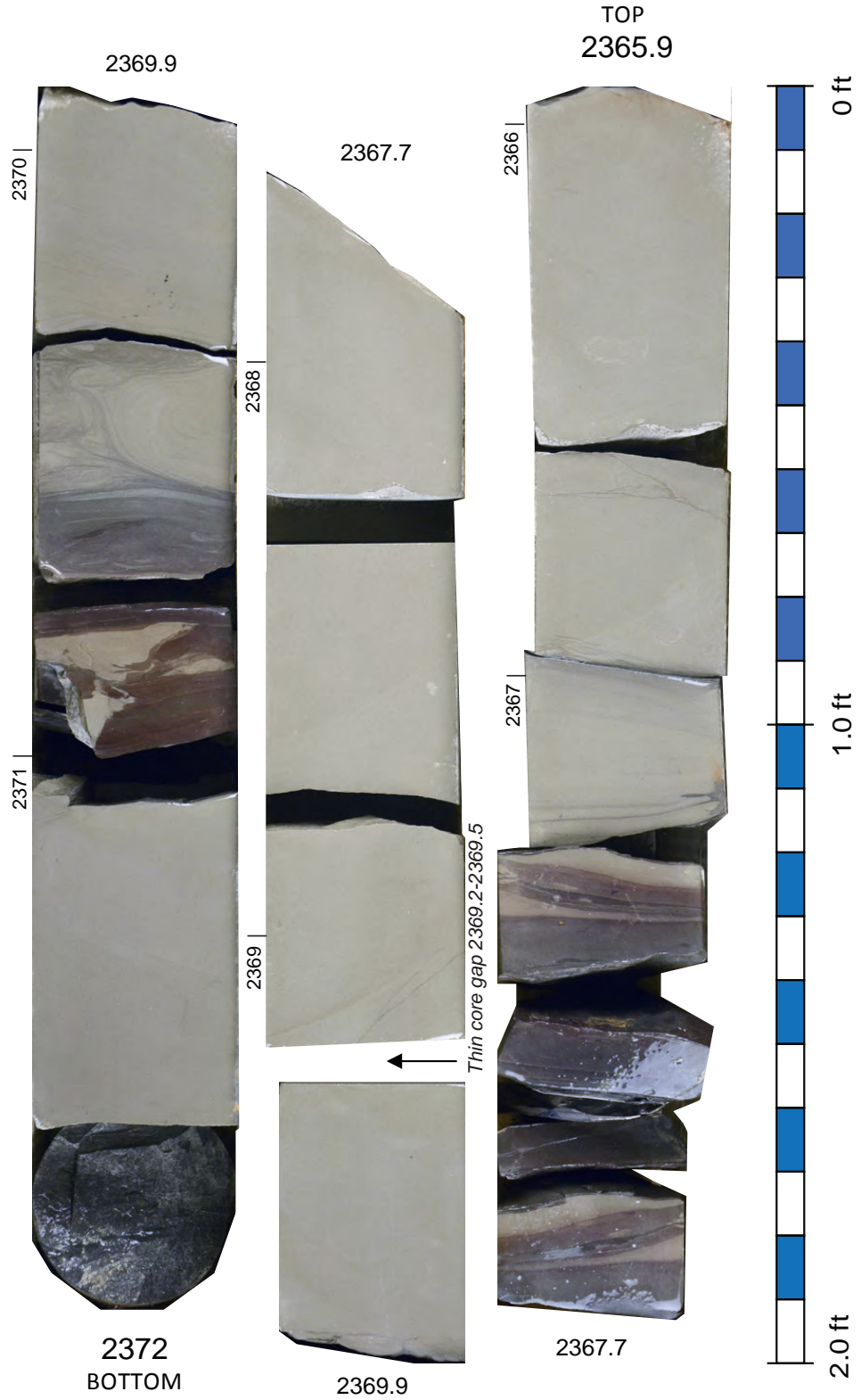
Wet core

Columbia Gas Trans.(TCO) No. 1 Pocahontas Mining, Core 3 Box 3



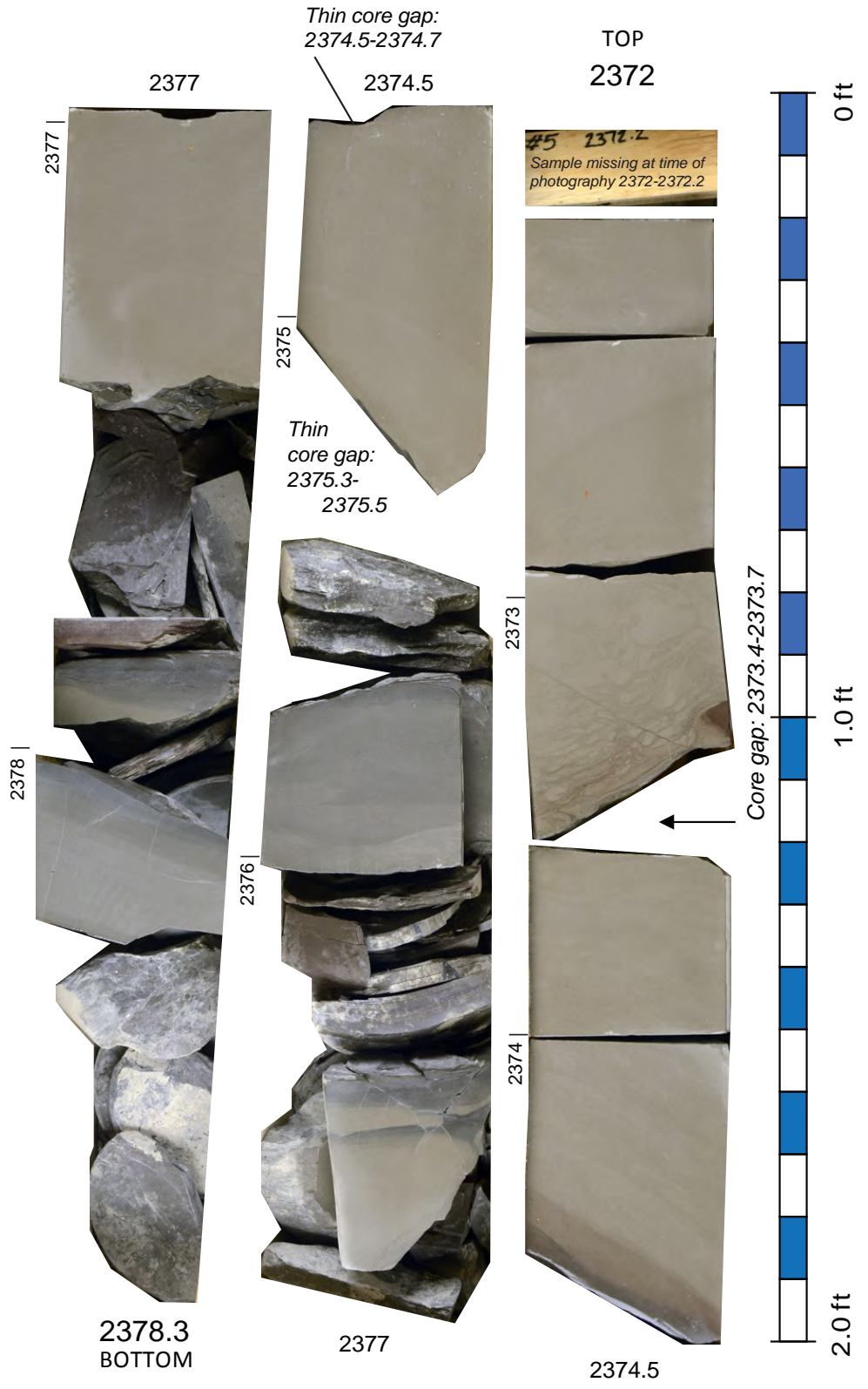
Wet core

Columbia Gas Trans.(TCO) No. 1 Pocahontas Mining, Core 3 Box 4



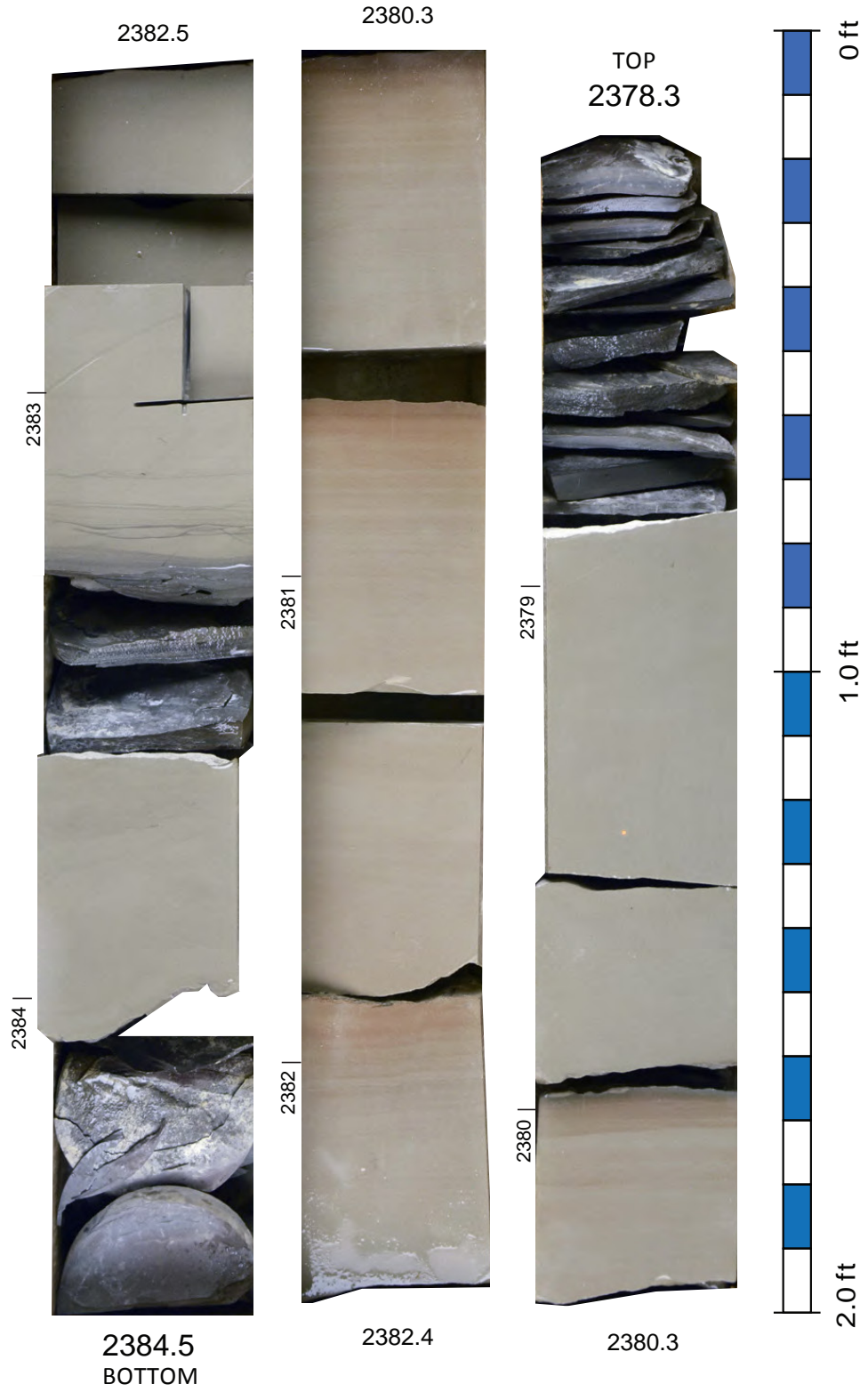
Wet core

Columbia Gas Trans.(TCO) No. 1 Pocahontas Mining, Core 3 Box 5



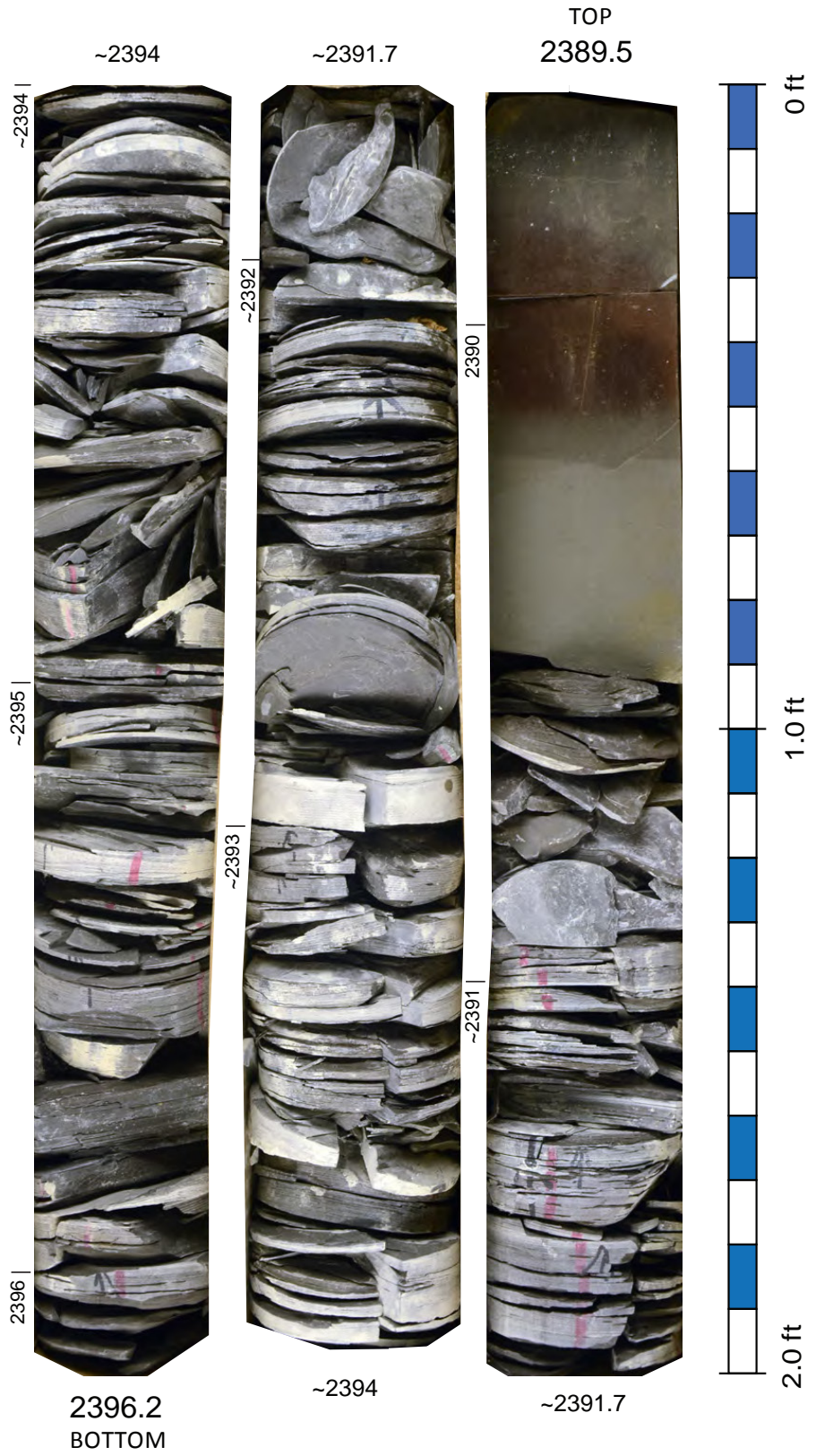
Wet core

Columbia Gas Trans.(TCO) No. 1 Pocahontas Mining, Core 3 Box 6



Mostly dry core;
wet slabbed piece
from 2389.5-
2390.5

Columbia Gas Trans.(TCO) No. 1 Pocahontas Mining, Core 4 Box 1

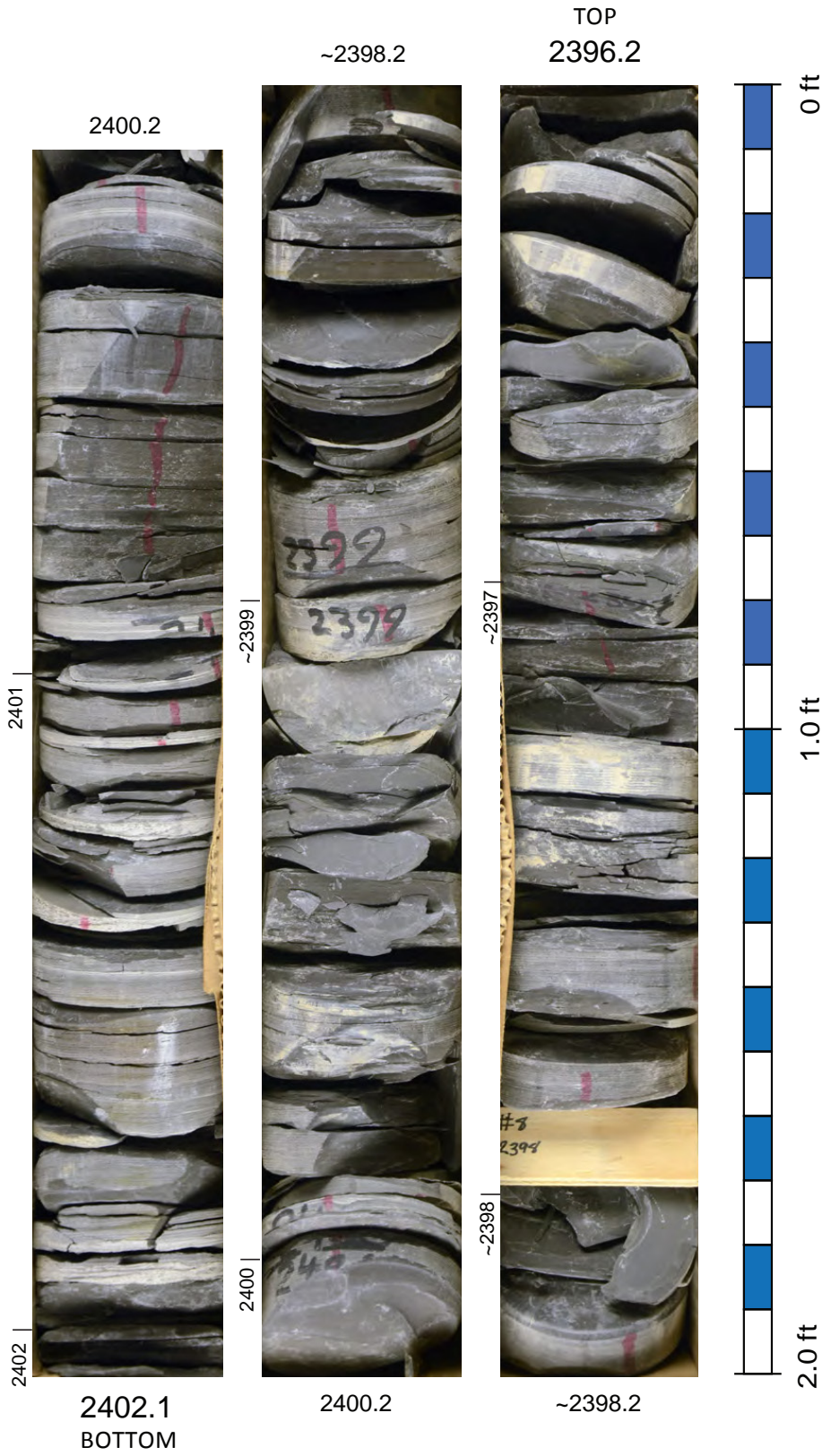


2396.2
BOTTOM

~2394

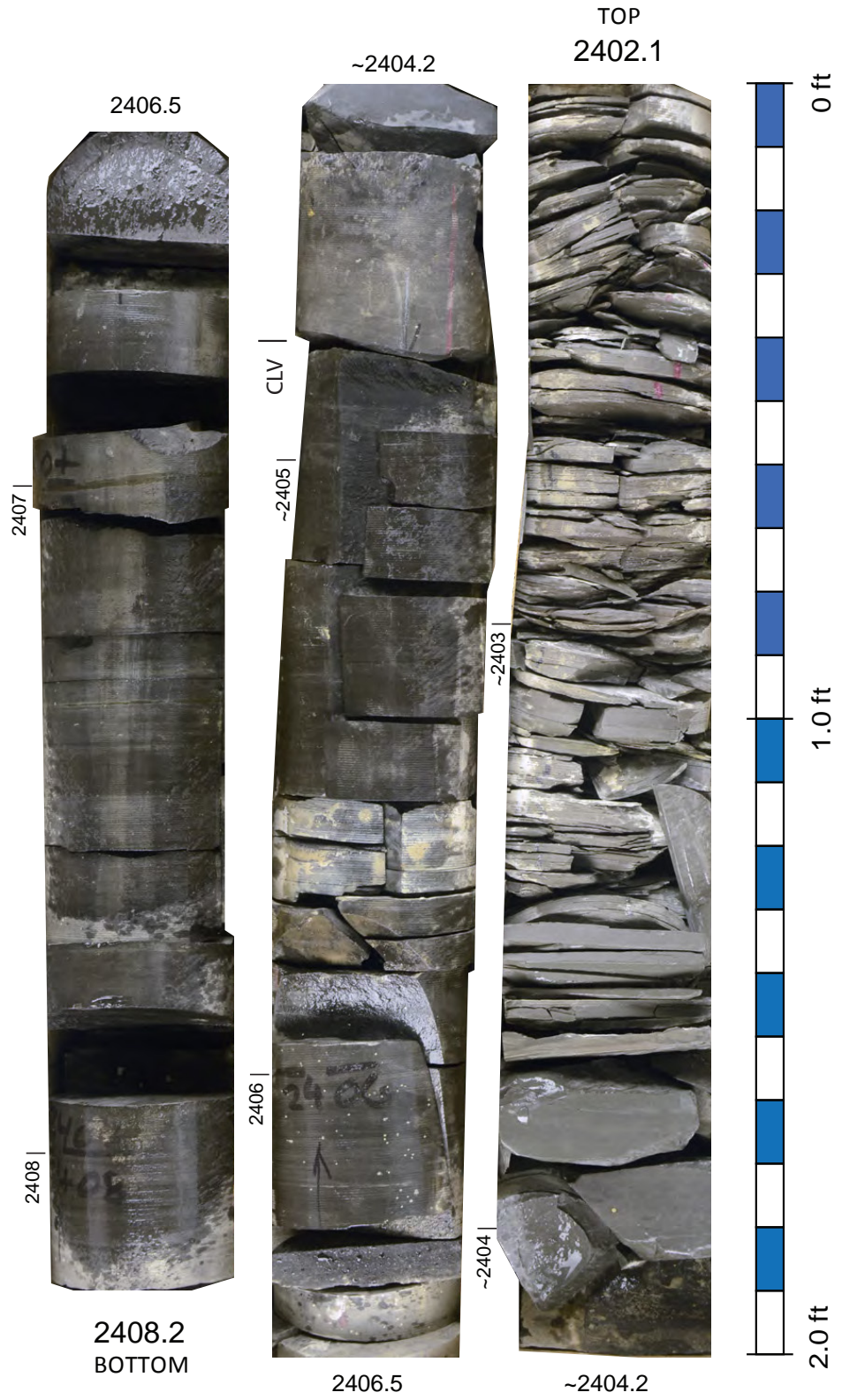
~2391.7

Columbia Gas Trans.(TCO) No. 1 Pocahontas Mining, Core 4 Box 2



Wet core

Columbia Gas Trans.(TCO) No. 1 Pocahontas Mining, Core 4 Box 3



Equitable Production Company #504353 EQT

Location: Pike County, Ky. (see Figure CB-1, Table CB-1)

KGS Core Call No.: C-6591

KGS Oil and Gas Record No.: 137835

Geophysical Logs: Caliper, compensated density, density, density porosity, gamma-ray, gas detector, induction, matrix density, neutron porosity, photoelectric index, temperature

Well Completion Date: 3/24/2009

Core Depth: 3,782–3,824 (Sunbury), 3,824–3,949 (Berea), 3,949–4,758.4 (Ohio Shale) ft [only Berea shown here]

Bedford-Berea Core Interval Thickness: 93 ft (with gaps) representing 114 ft

Bedford-Berea Total Thickness: 114 ft

Field: Elkhorn City DBS

Completion: Horizontal gas well in Lower Huron Member of Ohio Shale

Background and Distance to Recent Berea Oil Wells

The EQT core is from well south of the current Berea oil play, in a region in which the Berea has only produced gas. It is the only Berea core from the southeastern part of eastern Kentucky for comparison to gas-producing Berea fields in southern Pike County. The well is 2.8 mi north of the Pine Mountain Thrust Fault and situated along the flank of the D'Invilliers Structure. It is most similar to the Columbia Pocahontas Mining core.

Key Features

The EQT core is a near-continuous (several gaps) core through the Berea in southernmost Pike County. The upper part of the core is very argillaceous and contains a wide variety of convolute laminae and soft-sediment-deformation features, including some with horizontal, cross-cutting microfaults. A fracture at 3,860 ft exhibited siderite (orange), and kaolinite (white) was examined in thin section. Several cement-filled fractures occur in the core.

The most interesting feature of the EQT core, and the feature that sets it apart from the other cores studied, is that it contains in-situ bitumen in the Berea, representing cracked oil. The bitumen is the dark-brown-stained sections of core. If you rub your finger over the stained portion of core, no oil or smudge will appear on your finger, which is how you can tell bitumen from oil in the field. The bitumen impregnation provides insight into the initial oil migration into Berea reservoirs, and potential flow barriers within this tight "sandstone" (coarse siltstone). The graphic log shows the parts of the core that contain bitumen. In parts of the core, bedding is difficult to interpret because the beds are completely uniform in staining; in other parts of the core, staining highlights bedding that would otherwise appear massive without the staining.

Good examples of stained-unstained transitions within the core can be seen toward the upper part of the stained interval from 3,887–3,893 ft (core 6, boxes 1 and 2) and in the lower part of the stained interval from 3,911–3,916 ft (core 6, box 9). Vertical gradational contacts within beds between stained and unstained core are apparent from 3,893–3,899 ft (core 6, boxes 3 and 4) and 3,899–3,905 ft (core 6, boxes 5 and 6). Good examples of staining contrast along parallel laminae, and low-angle dipping laminae within beds can be observed from 3,905–3,911 ft (core 6, boxes 7 and 8). A good example of staining along cross-cutting microfractures is at 3,844.5 ft. Very good examples of staining along flow rolls or ball-and-pillow-like structures, and dewatering pipes between pillows, can be seen at 3,883, 3,889.7, 3,889.9, and 3,912.5 ft.

This core is also interesting for examining the Bedford-Cleveland contact. On the geophysical log, the base of the Bedford would be placed at 3,848 ft depth. The top of the Berea is at 3,824 ft depth on the log and is 3,820 ft in the core, so there is a -4-ft correction between the core and log. This means the top of the Cleveland Shale should be at or near 3,844 ft in the core (which is in a missing, sampled section of the core). Interestingly, black shales begin 10 ft higher (3,834 ft) in the core. The interval between 3,834 and

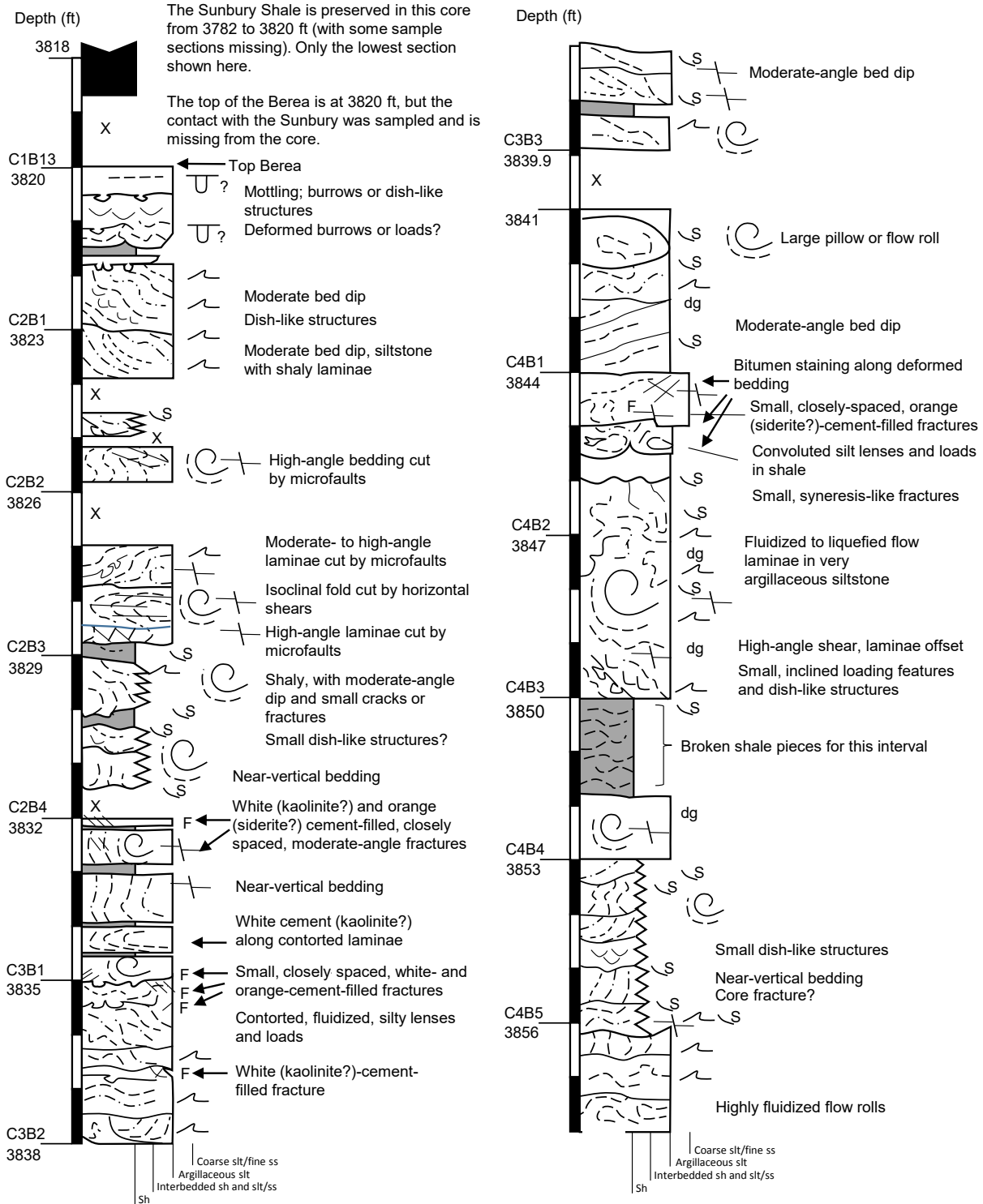
3,844 ft is an example of “black” Bedford shale. See the Somerset Morlandbell core for another example of black Bedford shale.

Data and Analysis

The EQT core has numerous plugs through the Berea, but those data are confidential with EQT and not available to the public or for this study. No additional plugs were collected from the Berea or Bedford in this study, although several thin sections were made to examine bitumen impregnation and a fracture fill in the Berea. These are discussed in the Thin-Section Petrography section of Chapter 7 in the main report.

Equitable Production Company No. 504353 EQT

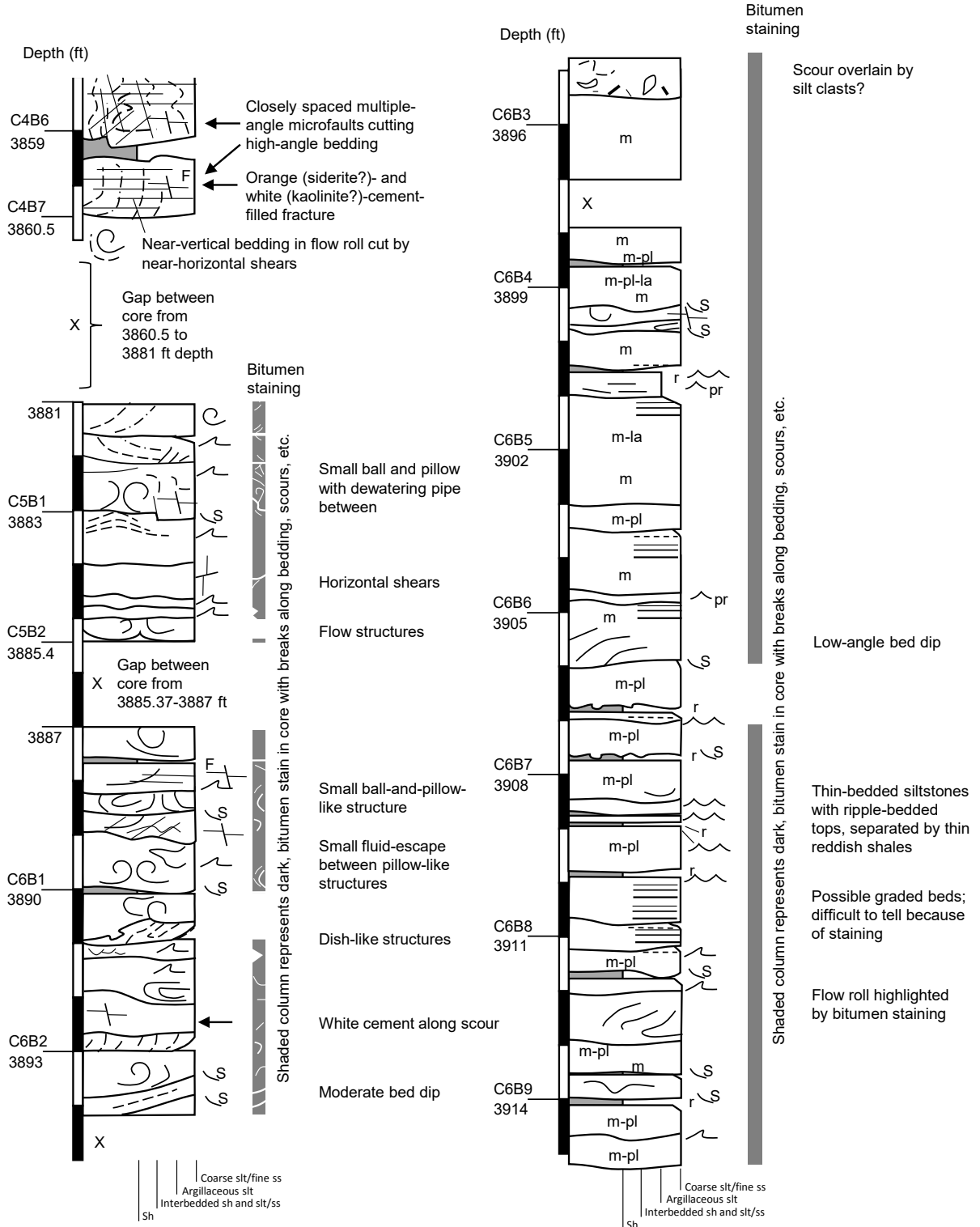
Description from slabbed core



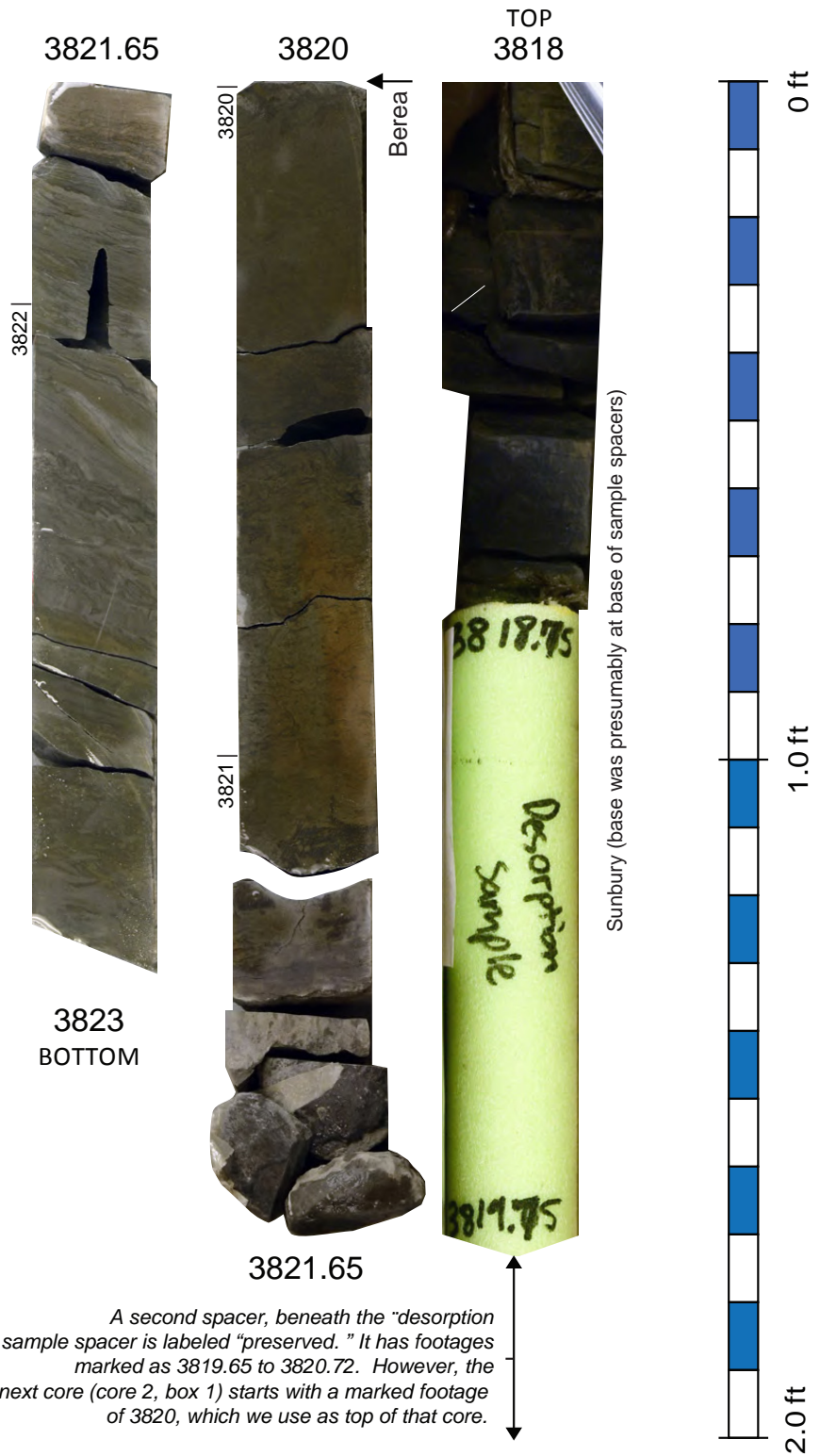
*Core was extensively plugged and sampled prior to being donated to KGS, but the data were not donated with the core, so plug positions are not shown.

Equitable Production Company No. 504353 EQT

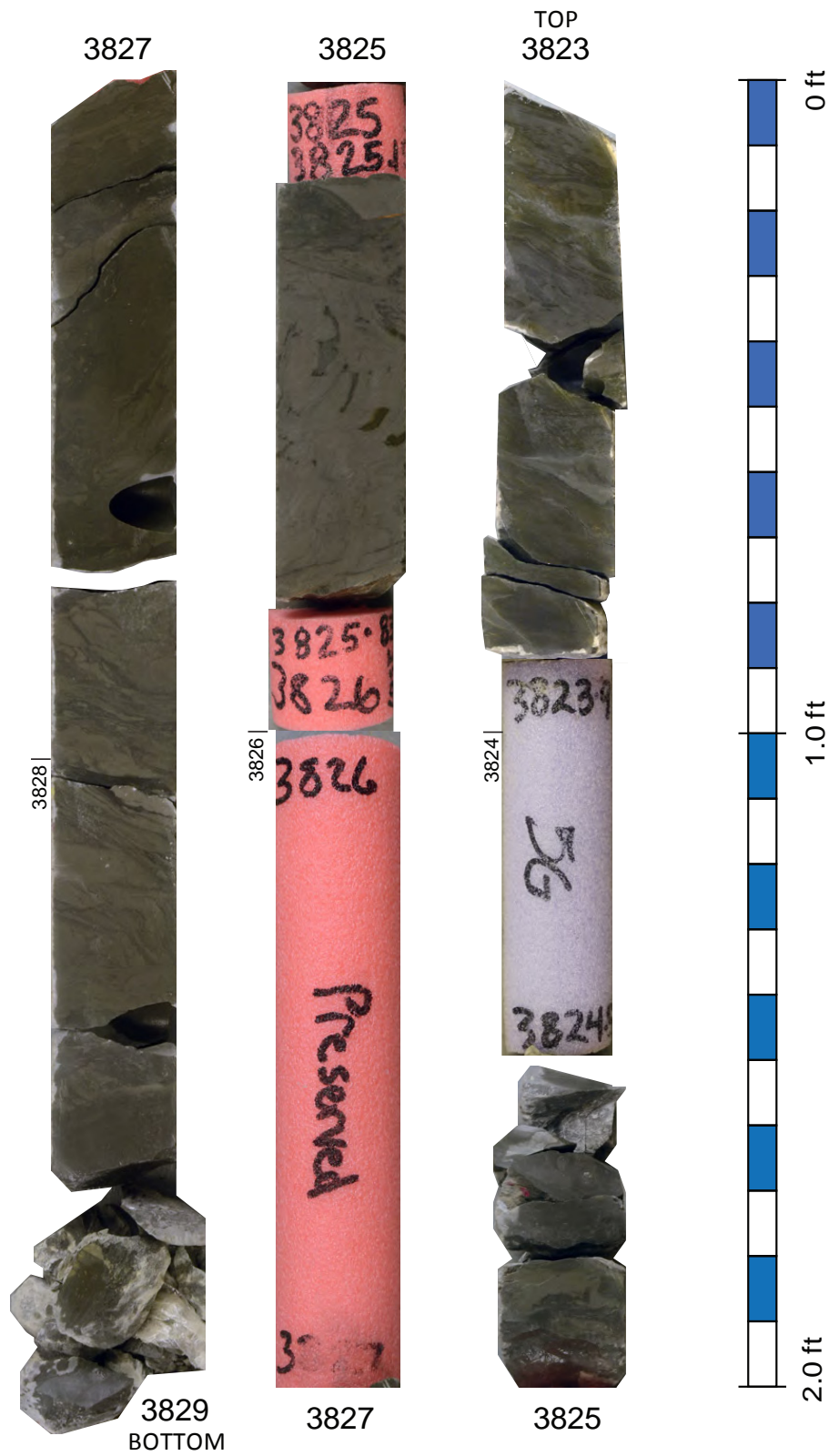
Description from slabbed core



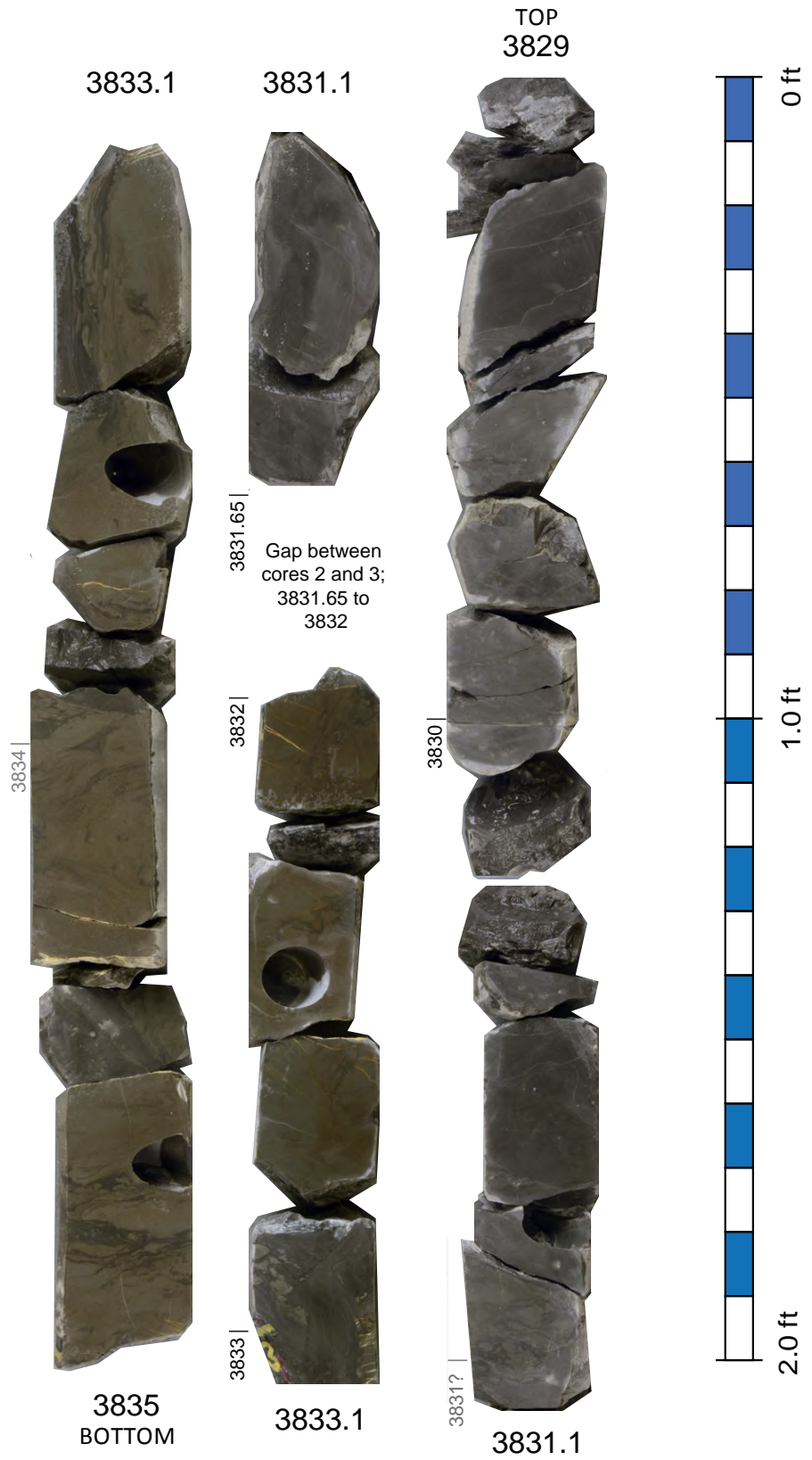
EQT No. 504353, Core 1, Box 13 and Core 2, Box 1



EQT No. 504353, Core 2, Box 2-3



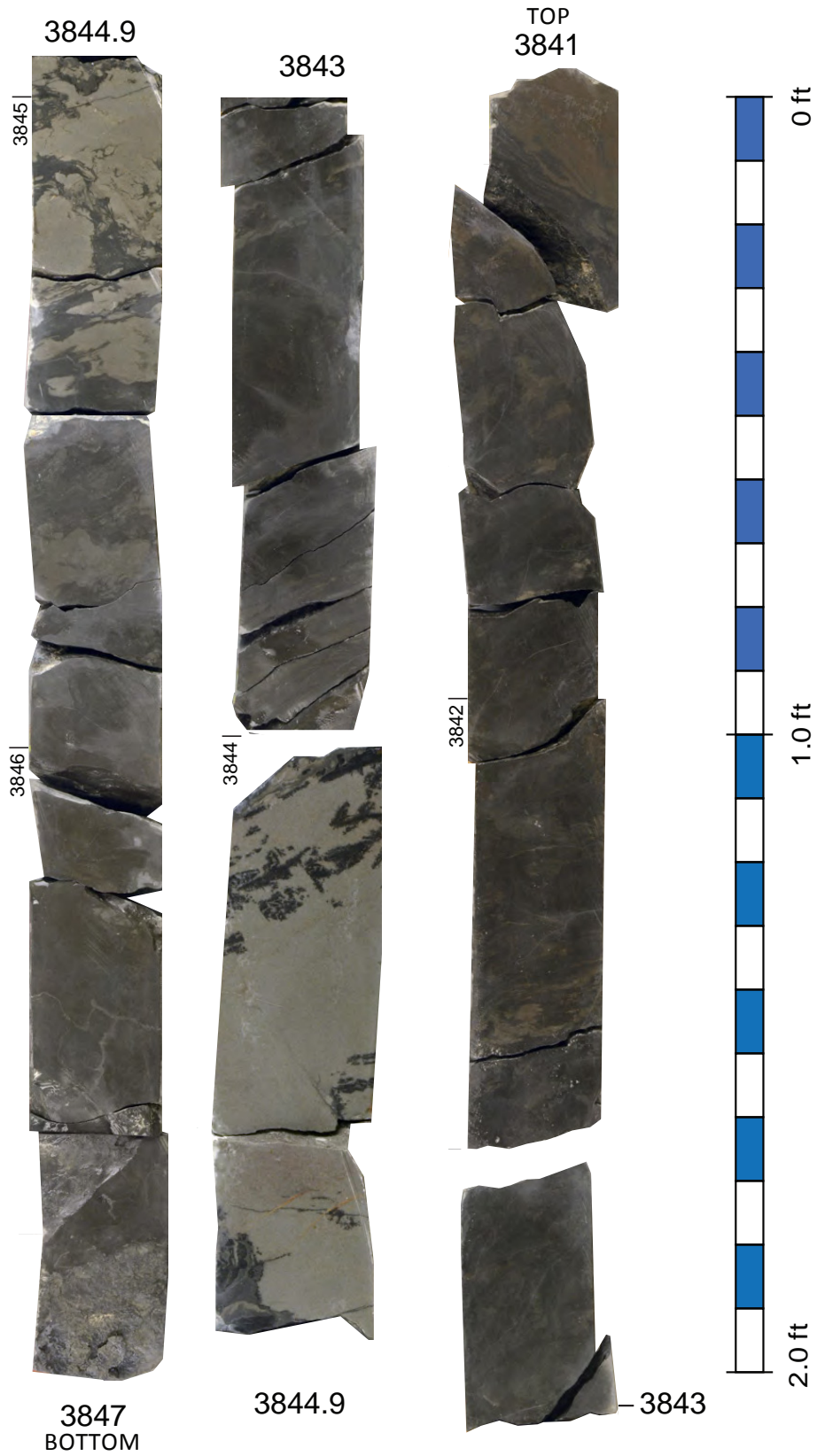
EQT No. 504353, Core 2, Box 4 and Core 3, Box 1



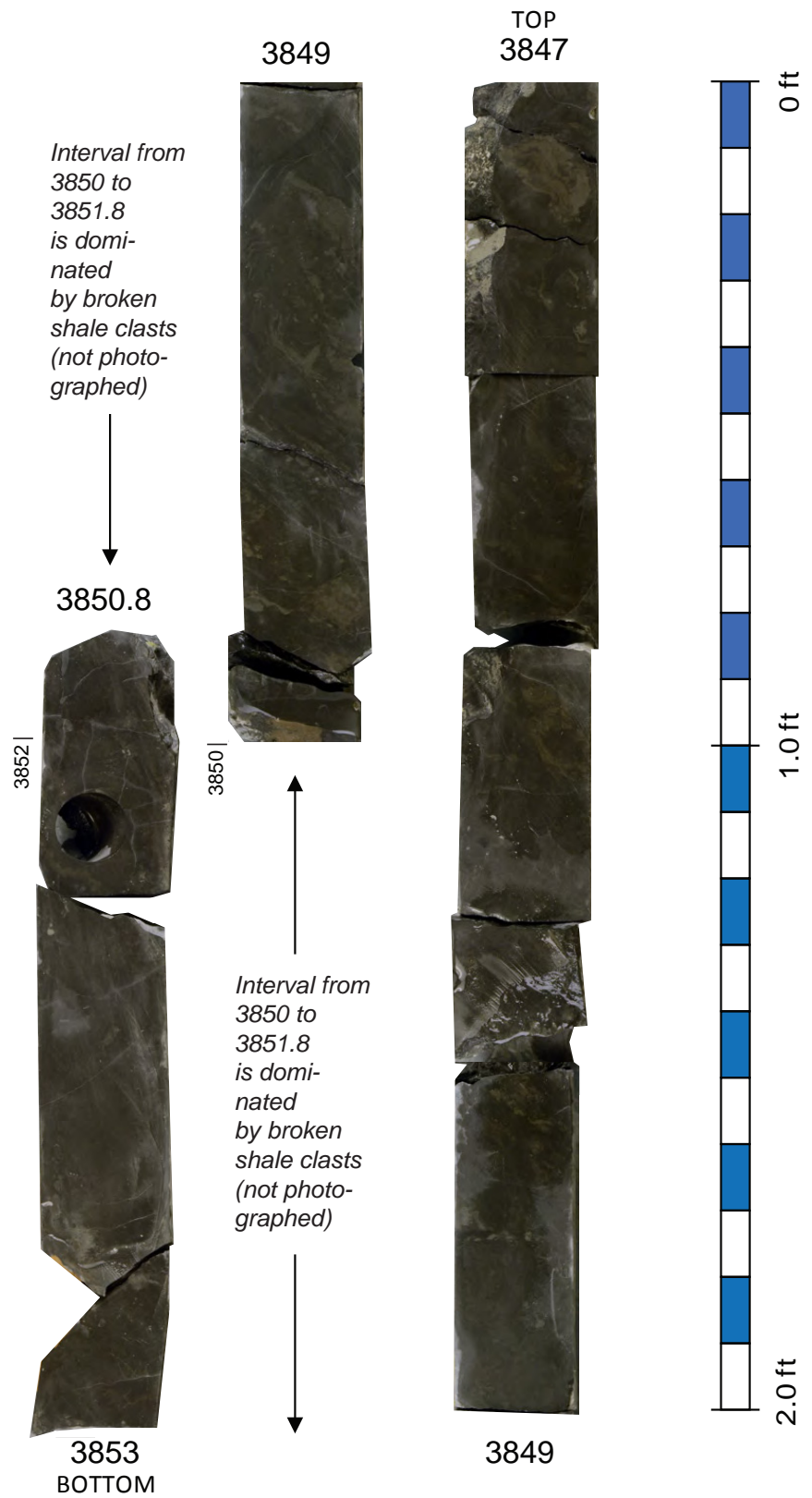
EQT No. 504353, Core 3, Box 2-3



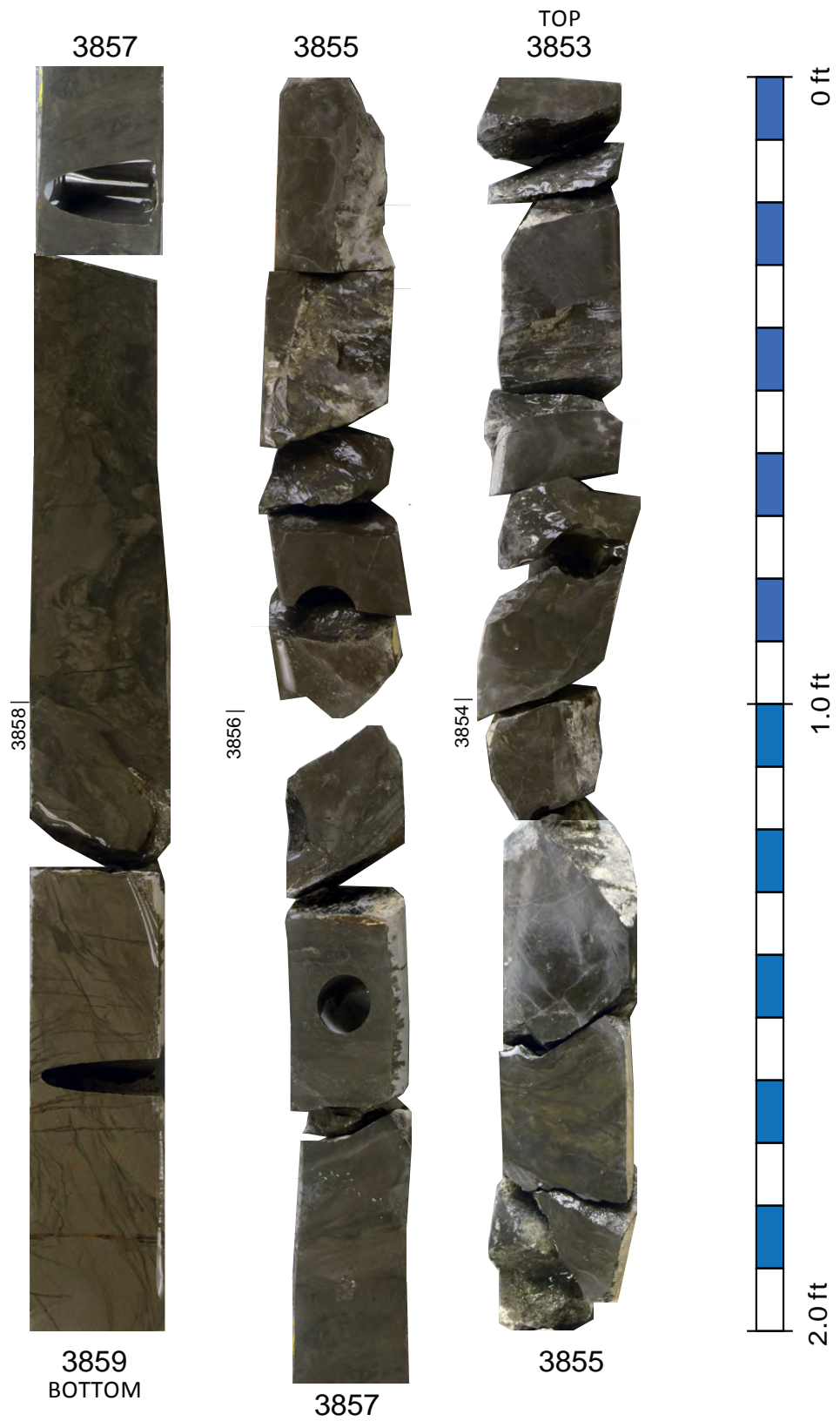
EQT No. 504353, Core 4, Box 1-2



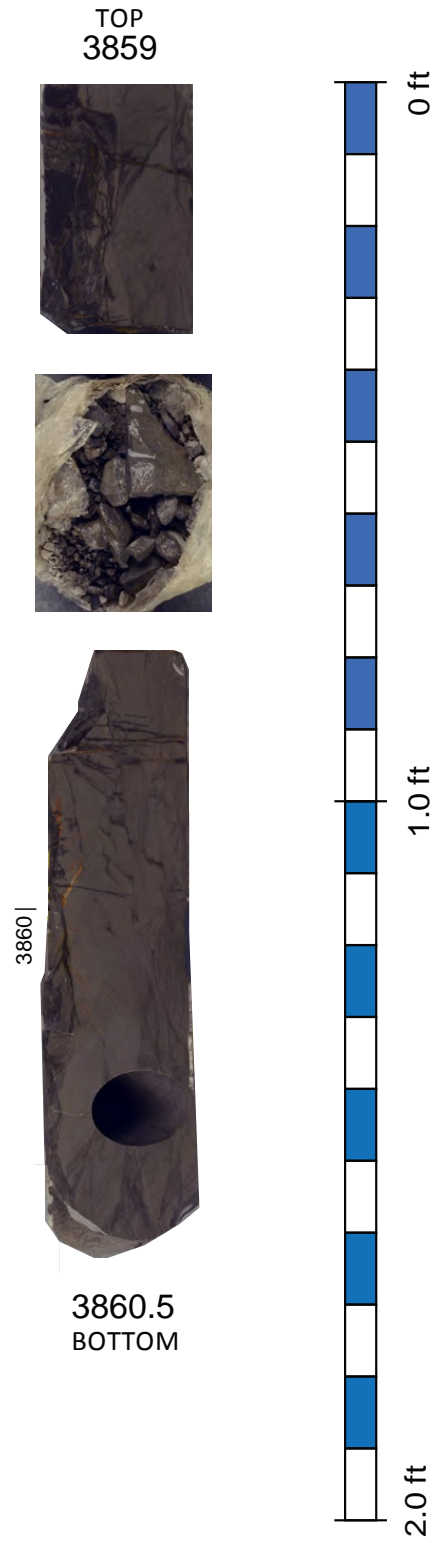
EQT No. 504353, Core 4, Box 3-4



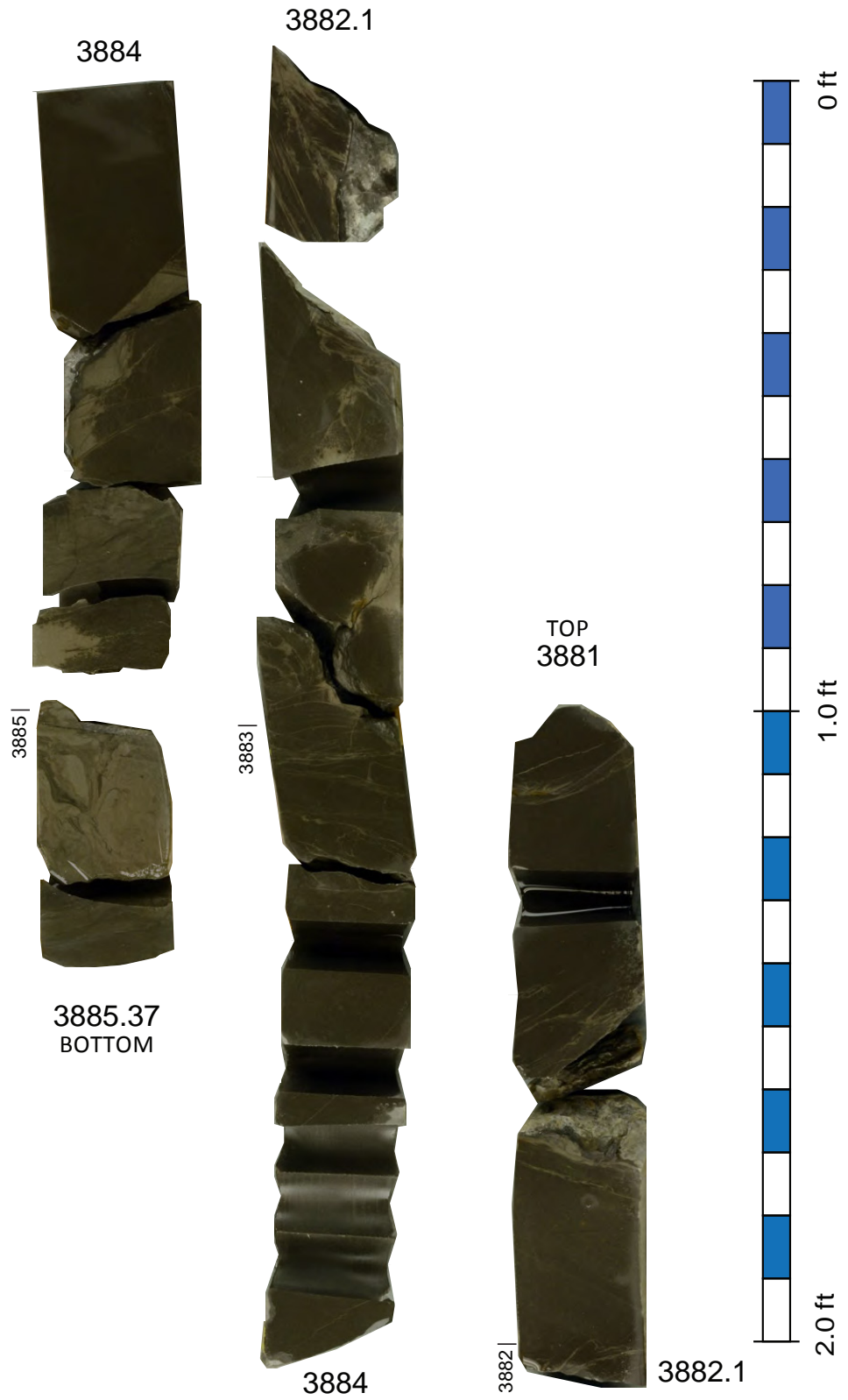
EQT No. 504353, Core 4, Box 5-6



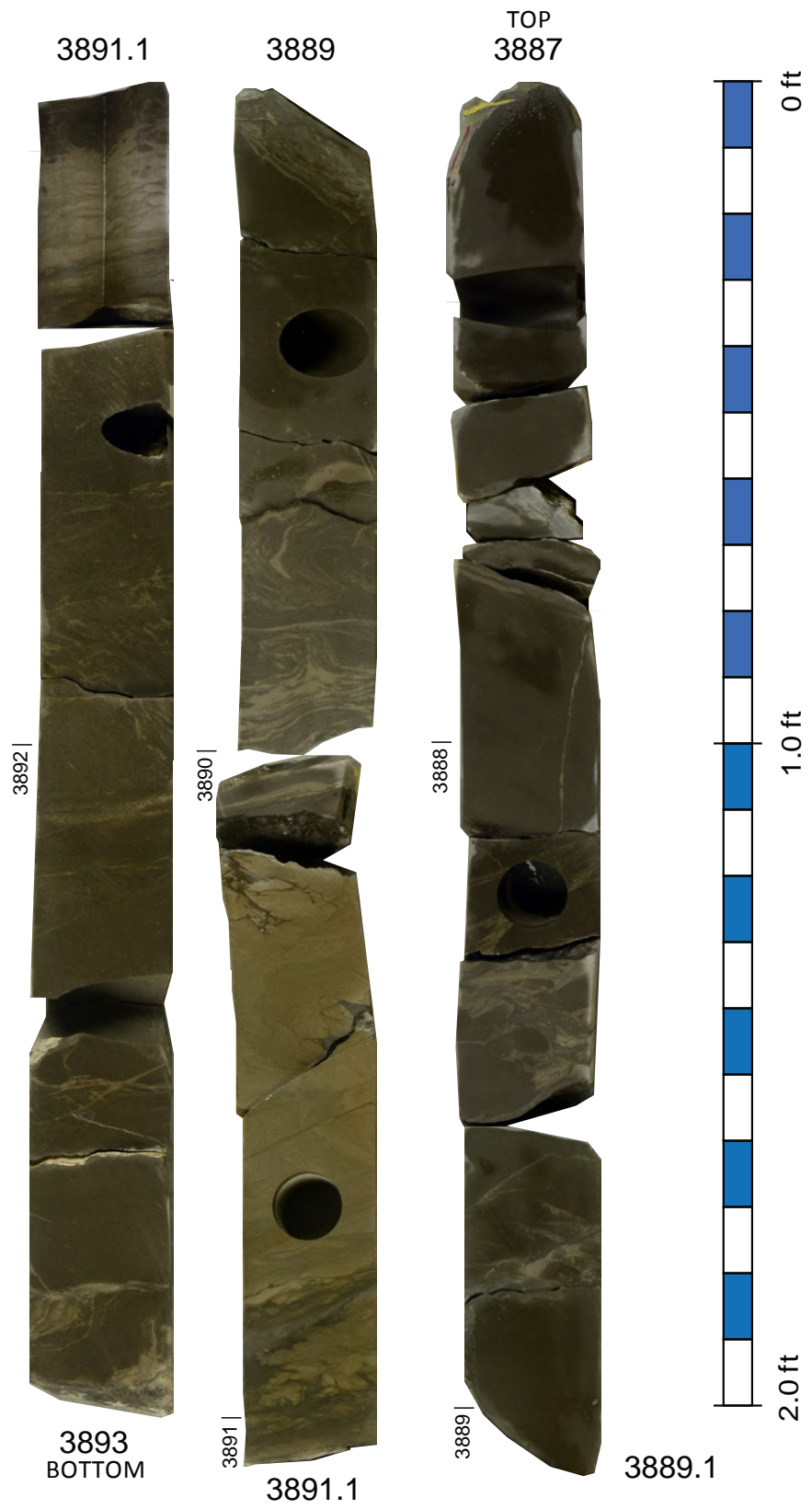
EQT No. 504353, Core 4, Box 7



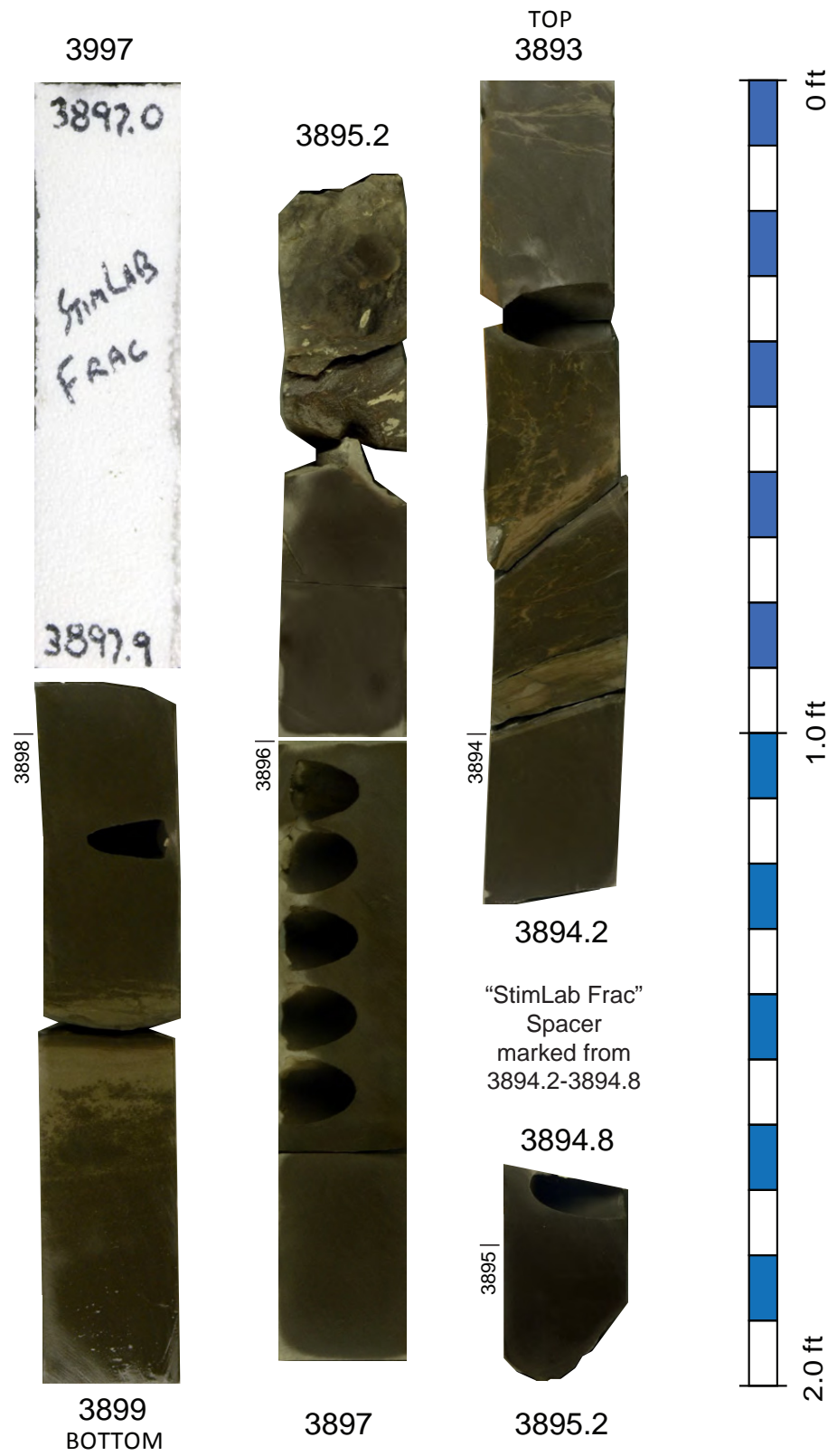
EQT No. 504353, Core 5, Box 1-2



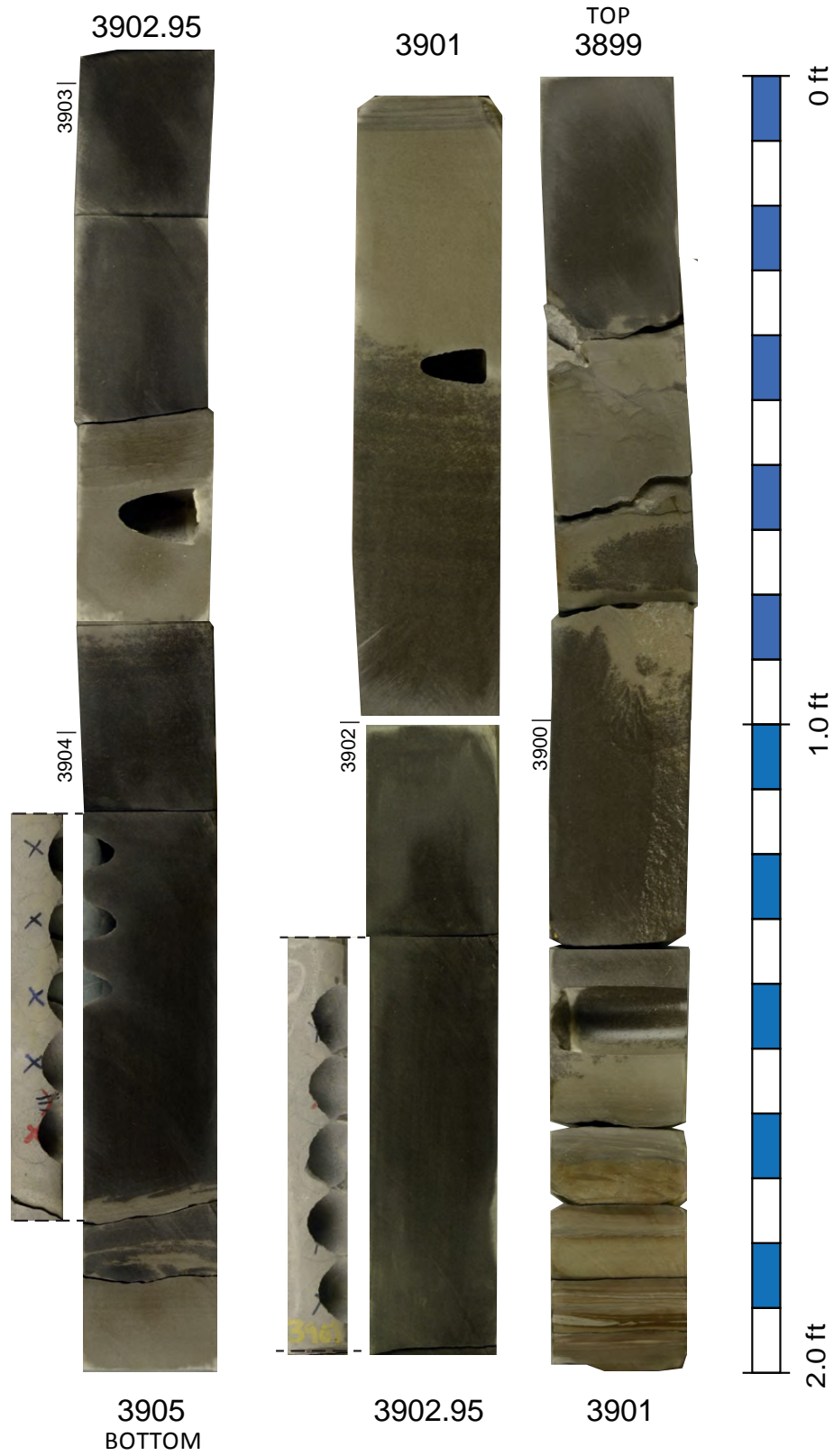
EQT No. 504353, Core 6, Box 1-2

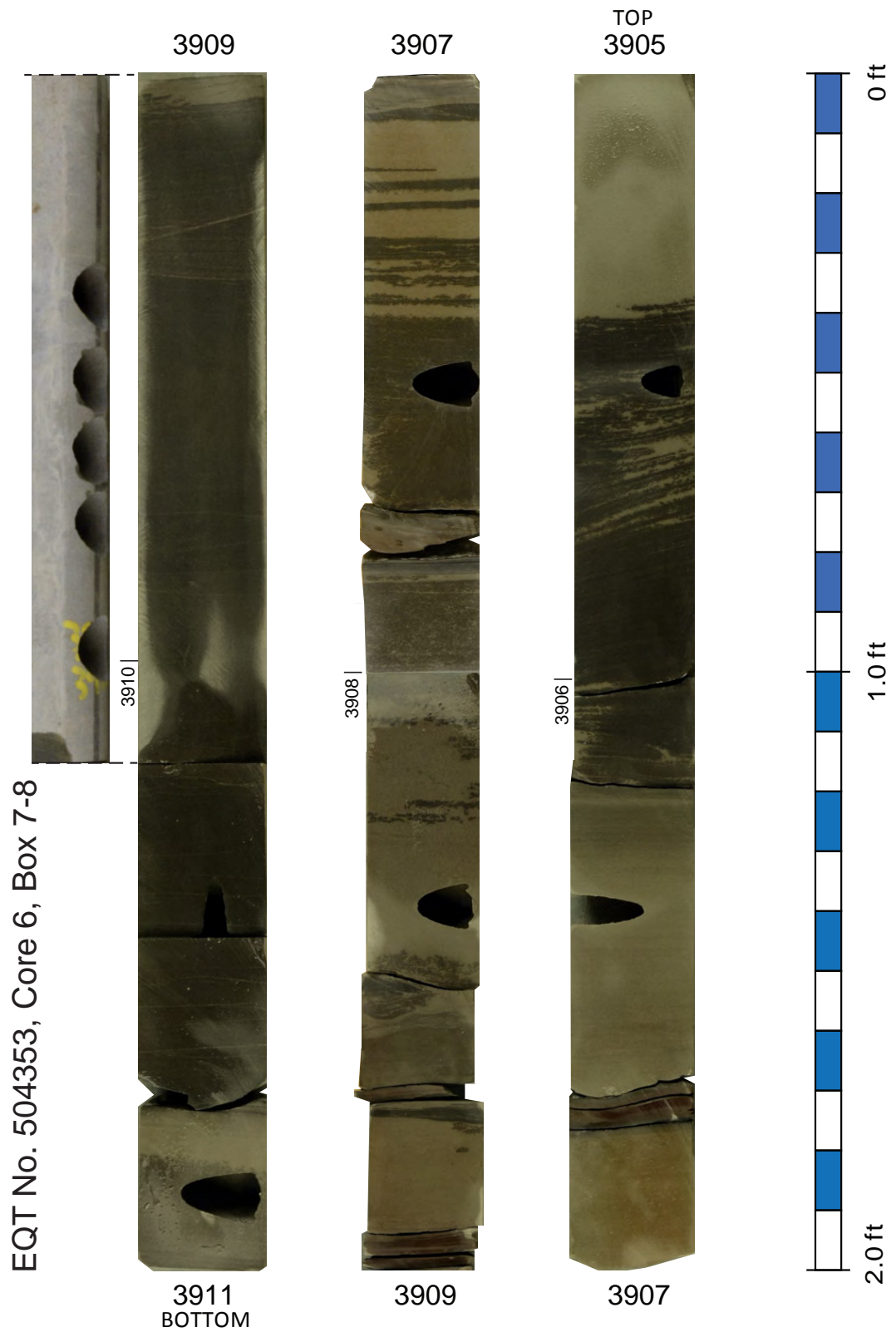


EQT No. 504353, Core 6, Box 3-4

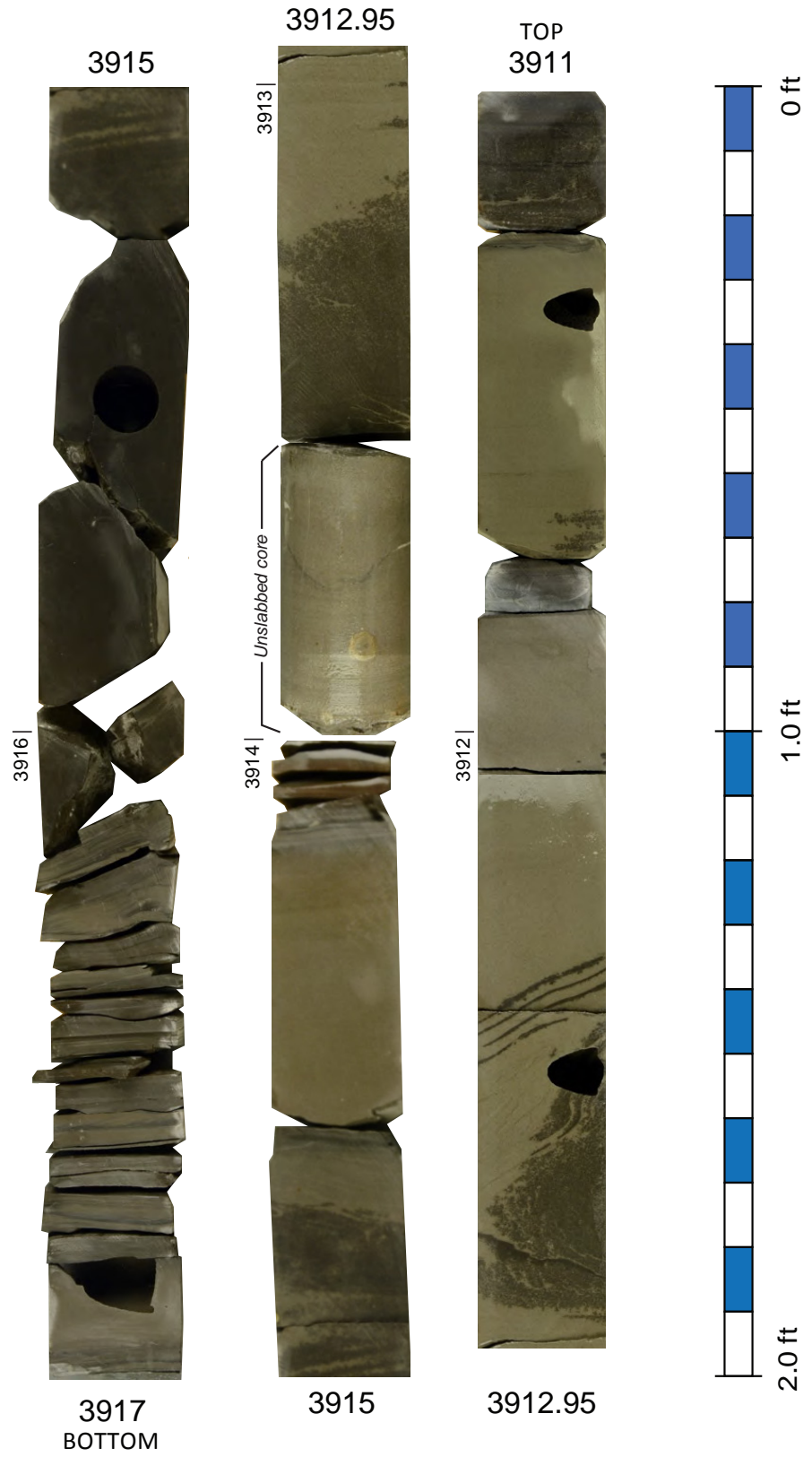


EQT No. 504353, Core 6, Box 5-6

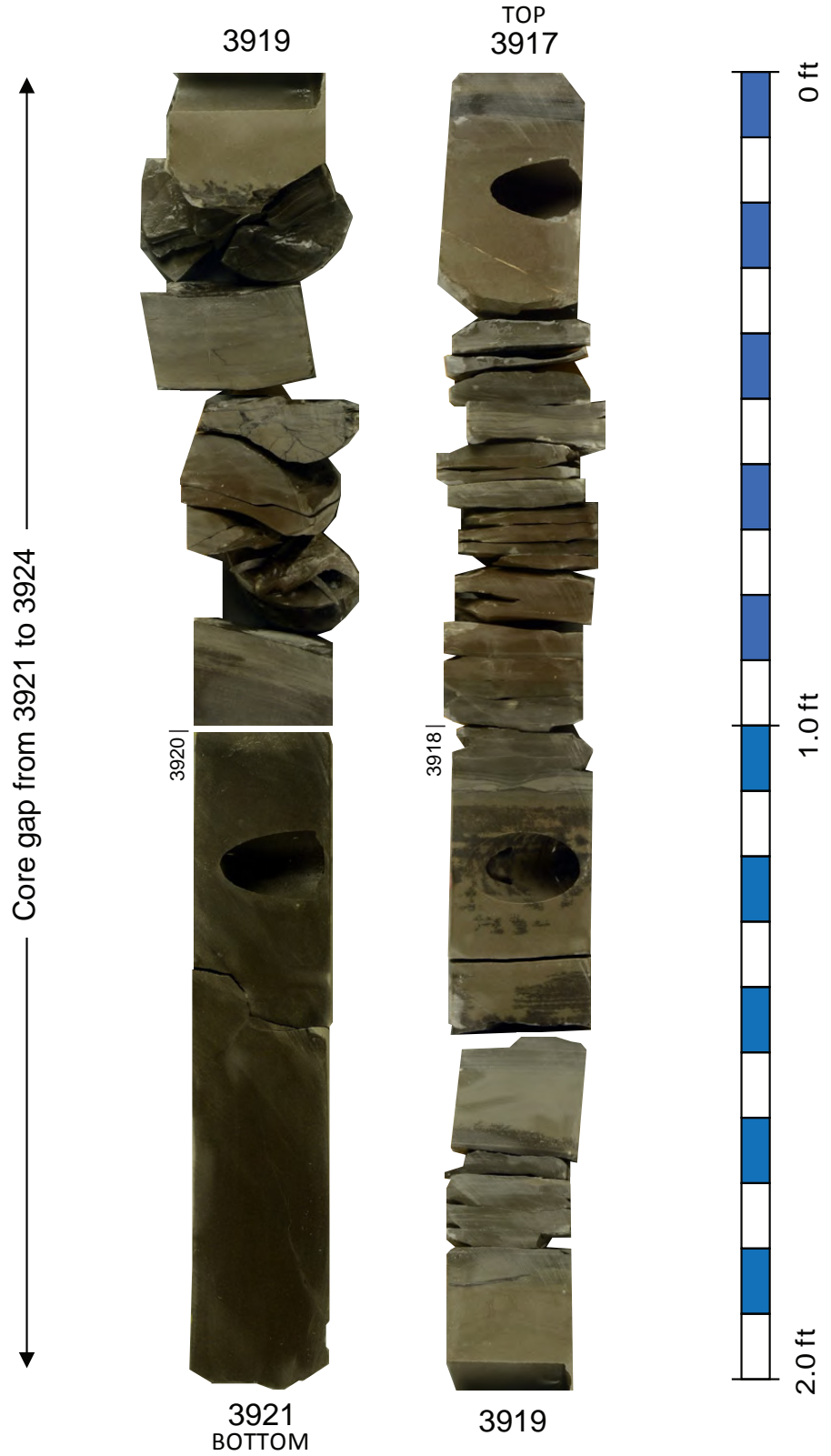




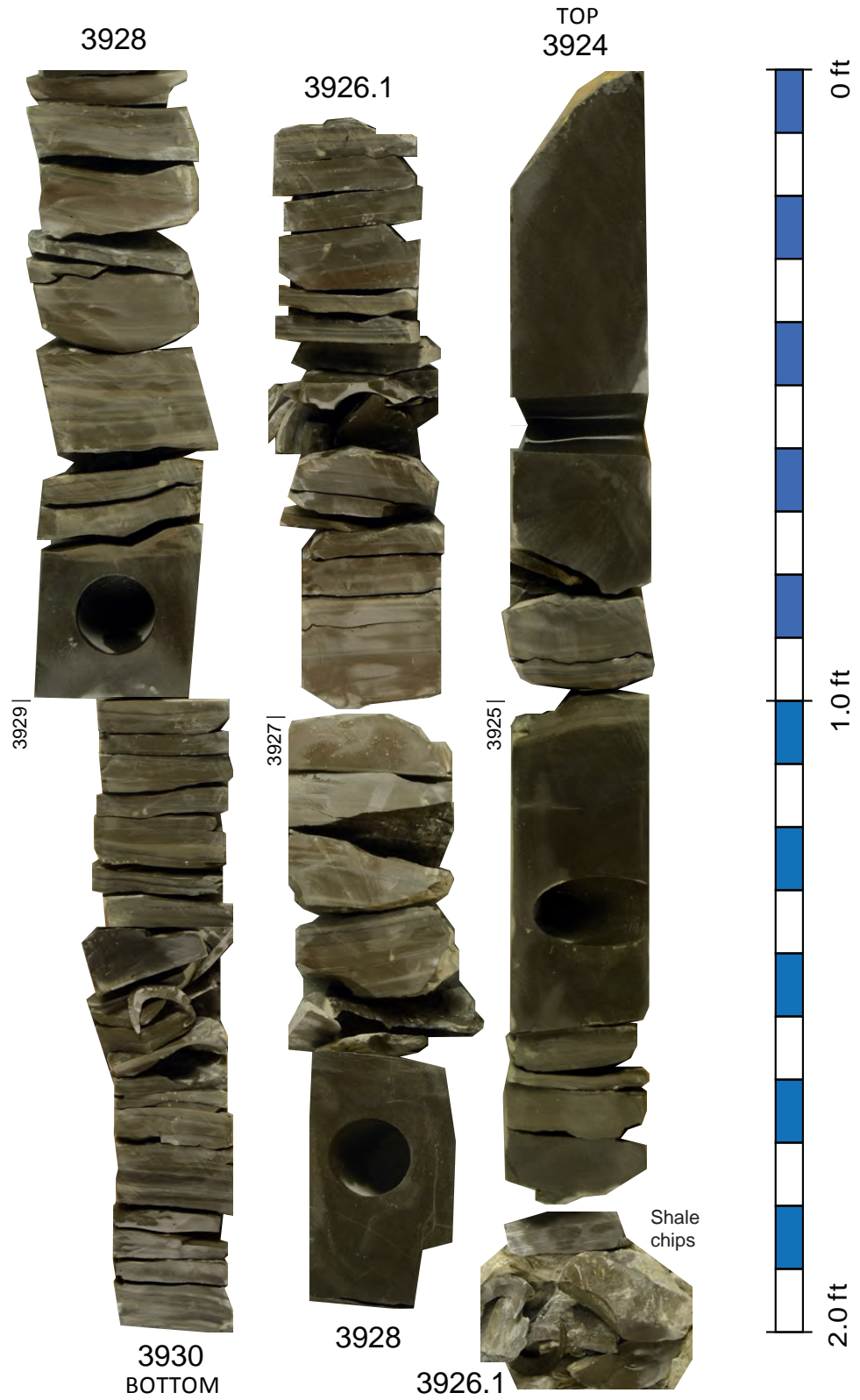
EQT No. 504353, Core 6, Box 9-10



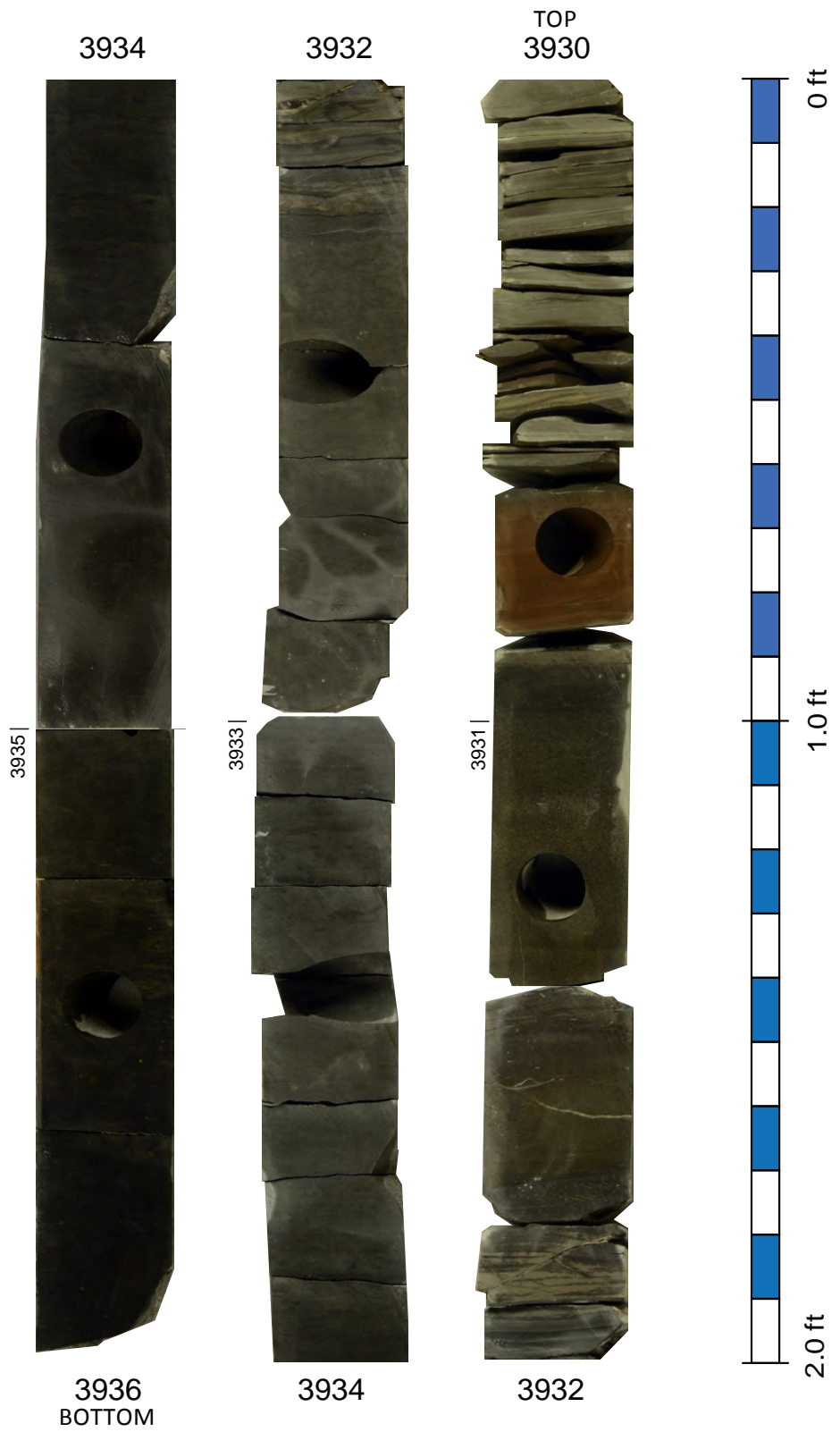
EQT No. 504353, Core 6, Box 11-12



EQT No. 504353, Core 7, Box 1-2



EQT No. 504353, Core 7, Box 3-4



EQT No. 504353, Core 7, Box 7

3942



Sample spacer
from
3947.7 to
3942

3940



3938



TOP
3936



EQT No. 504353, Core 7, Box 5 and 6

3941



3942

3939

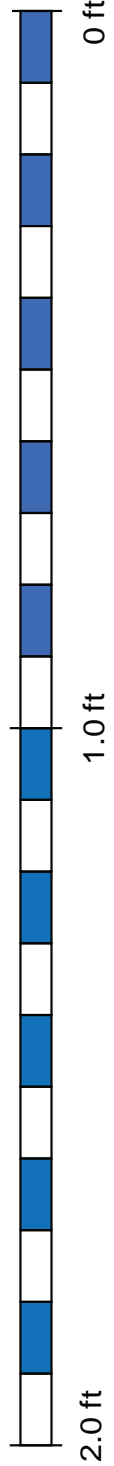


3940

3937



3938



Somerset Gas Service Company #1 Morlandbell Inc.

Location: Leslie County, Ky. (see Figure CB-1, Table CB-1)

KGS Core Call No.: C-6588

KGS Oil and Gas Record No.: 32289

Geophysical Logs: Caliper, computer-processed, conductivity, density porosity, gamma-ray, neutron porosity, sibilation (sonic)

Well Completion Date: 6/23/83

Core Depth: 2,682–2,709 (Sunbury), 2,709–2,735 (Bedford/no Berea), 2,735–2,967 (Ohio Shale) ft [only Berea shown here]

Bedford-Berea Core Interval Thickness: 26 ft (with gaps)

Bedford-Berea Total Thickness: 26 ft (Bedford only)

Field: None; 2.4 mi east of Hyden East Field

Completion: Shut-in gas well in the Ohio Shale and Corniferous

Background and Distance to Recent Berea Oil Wells

The Somerset Morelandbell core is from far west of the current Berea oil play, and is west of the Berea pinchout.

Key Features

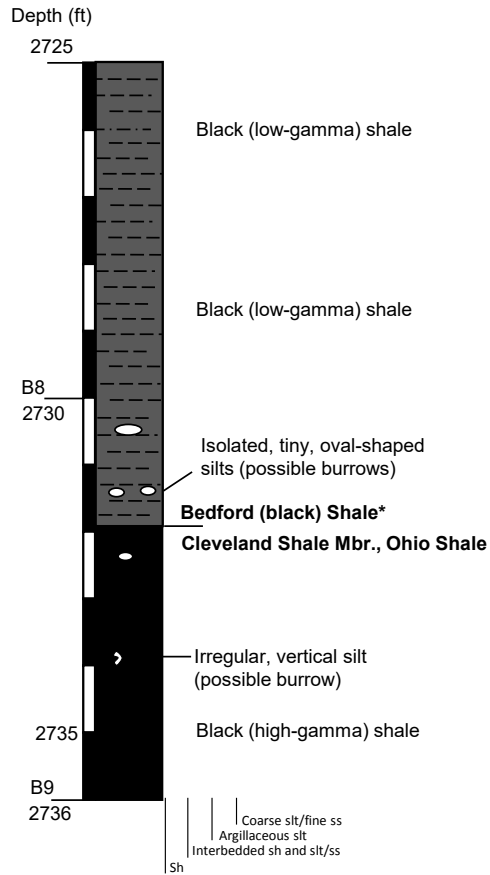
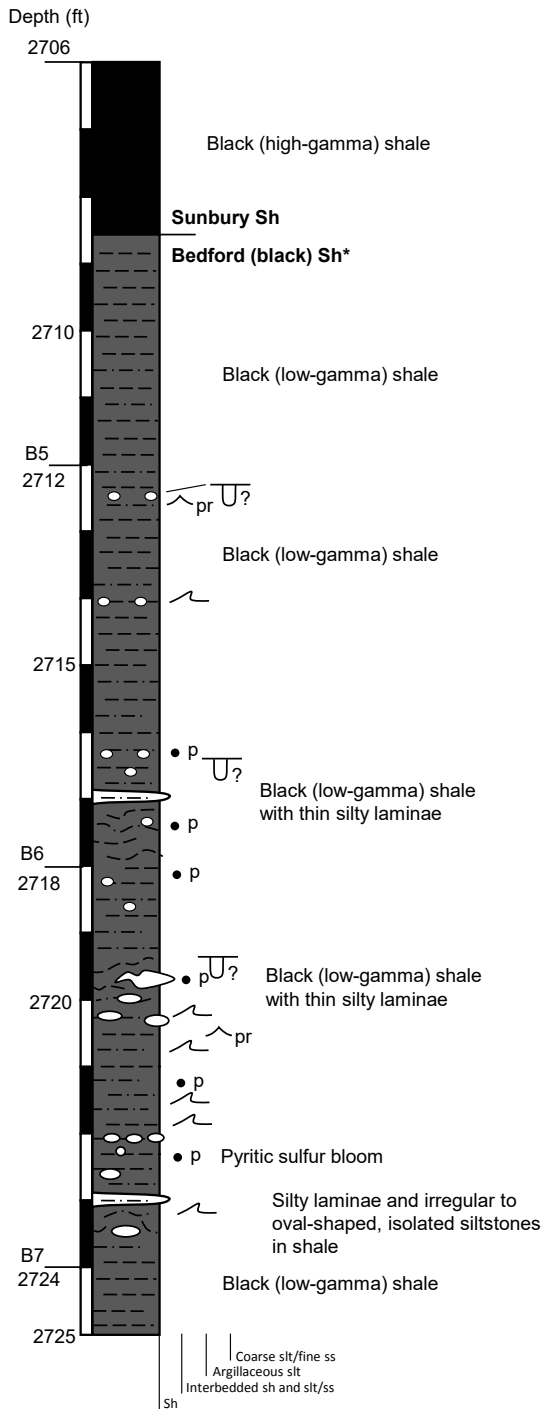
This core is composed of “black” Bedford shale, with no Berea coarse siltstones/sandstones. This is what the Bedford-Berea interval looks like in much of the southwestern part of eastern Kentucky. It is a continuous core through a thin Bedford interval. This is a good core from which to examine the difference between relatively organic-poor black Bedford shales and overlying and underlying organic-rich Sunbury and Cleveland black shales. The black Bedford in this core can be compared to black Bedford shales at the base of the EQT 504353 core.

Data and Analysis

There is no Berea in the core, so no analysis is available.

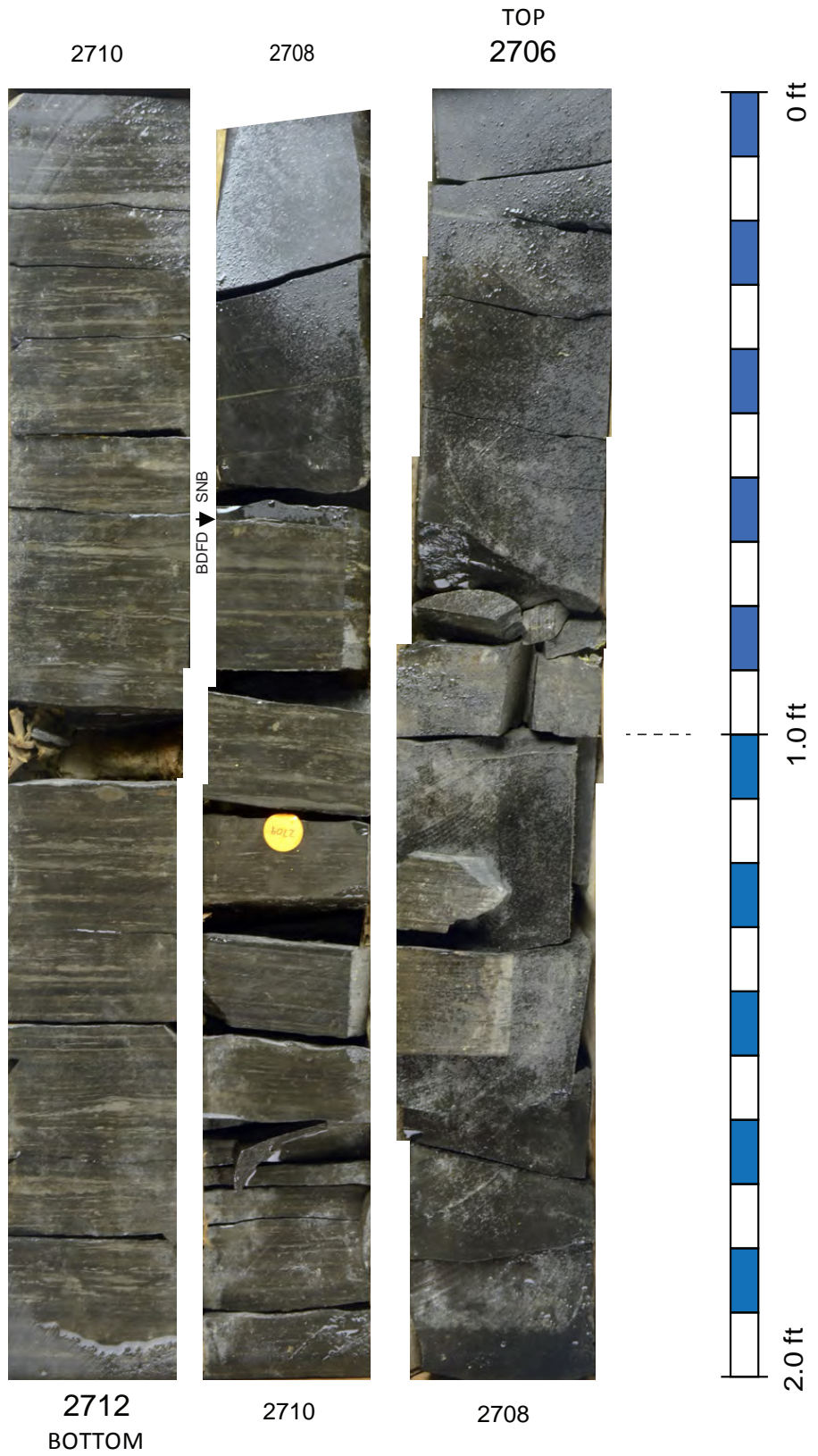
Somerset Gas Service No. 1 Morlandbell Inc.

Description from slabbed core

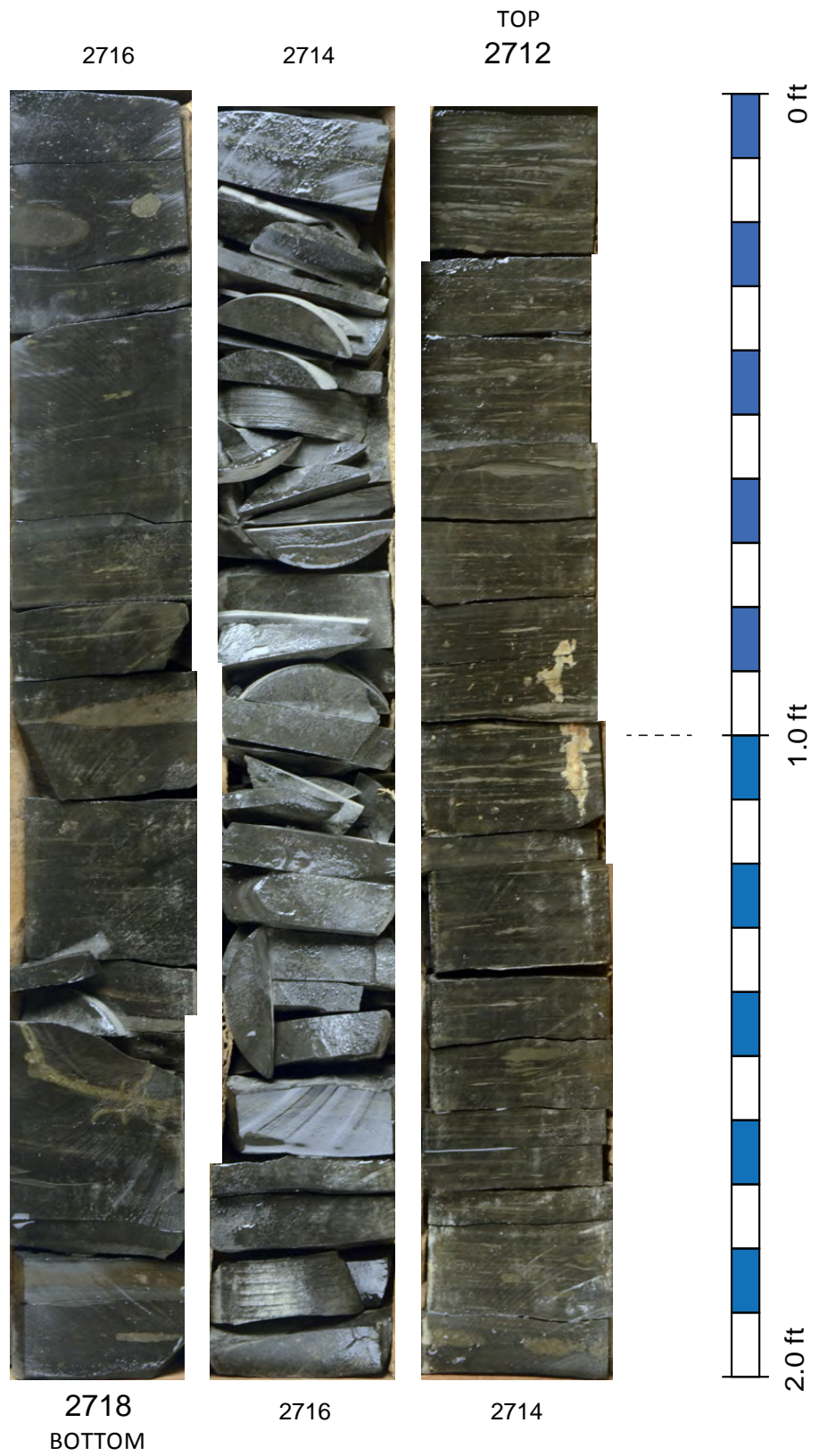


**The Bedford in this core is a black shale. Much of it is similar in appearance to the overlying and underlying black shales, but its gamma-ray reading is less than 100 units (does not go off scale). It is shown with dark gray shading here to differentiate it from the overlying and underlying high-gamma black shales.*

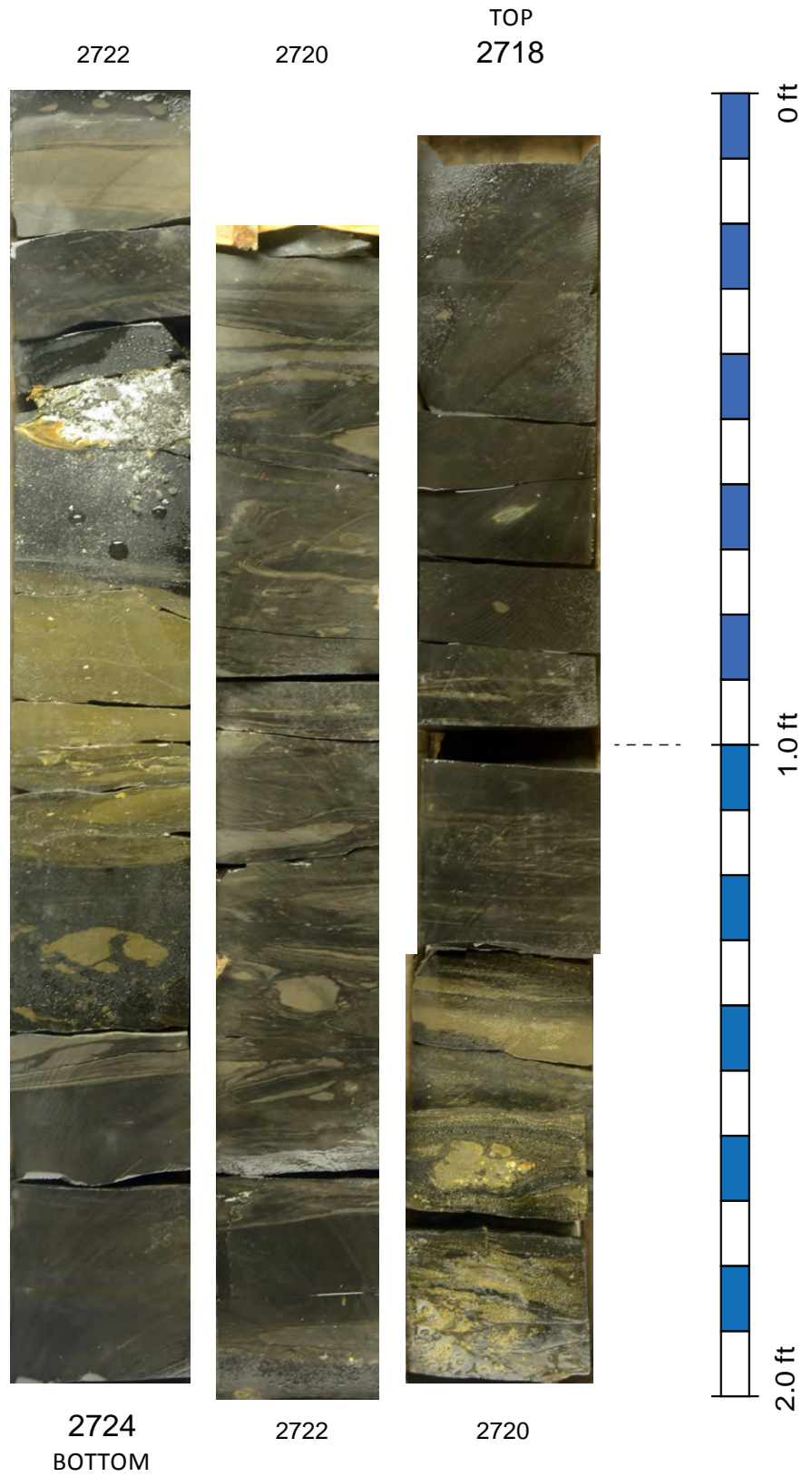
Somerset No. 1 Morlandbell, Box 5



Somerset No. 1 Morlandbell, Box 6



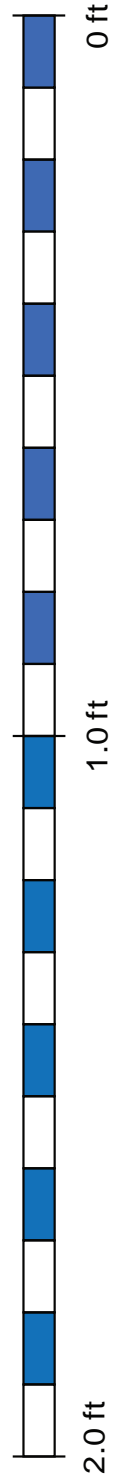
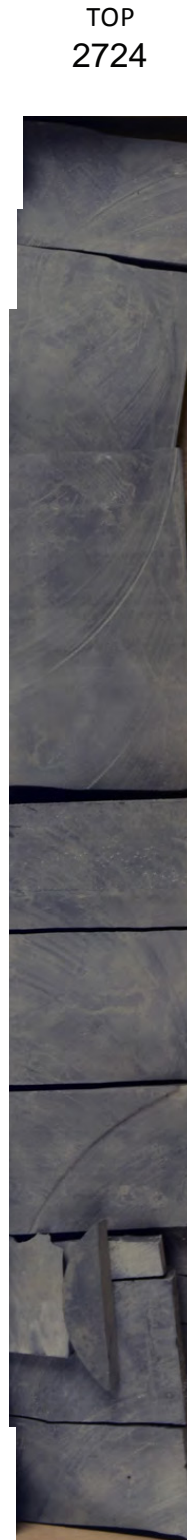
Somerset No. 1 Morlandbell, Box 7



Somerset No. 1 Morlandbell, Box 8

Dry core photo.
All dark shale

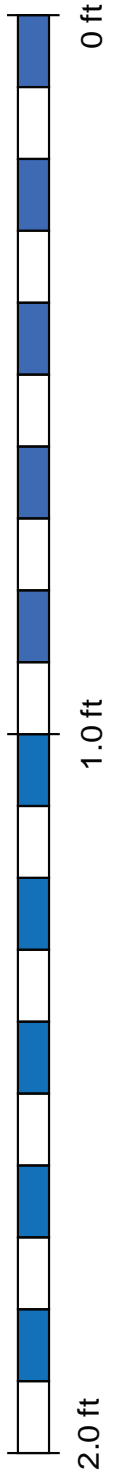
Gradational contact with CLVD



Somerset No. 1 Morlandbell, Box 9

Dry core photo.
All dark shale.

Dark intervals
have been
coated with
acetate?



References Cited

- Elam, T.D., 1981, Stratigraphy and paleoenvironmental analysis of the Bedford-Berea sequence and the Sunbury Shale in eastern and south-central Kentucky: Lexington, University of Kentucky, master's thesis, 155 p.
- Ettensohn, F.R., 2004, Modeling the nature and development of major Paleozoic clastic wedges in the Appalachian Basin, USA: *Journal of Geodynamics*, v. 37, p. 657–681.
- Ettensohn, F.R., and Elam, T.D., 1985, Defining the nature and location of a Late Devonian–Early Mississippian pycnocline in eastern Kentucky: *Geological Society of America Bulletin*, v. 96, p. 1313–1321.
- Floyd, J., 2015, Subsurface geological analyses of the Berea petroleum system in eastern Kentucky: Lexington, University of Kentucky, master's thesis, 153 p.
- Pashin, J.C., 1985, Paleoenvironmental analysis of the Bedford-Berea sequence (Devonian–Mississippian), northeastern Kentucky and south-central Ohio: Lexington, University of Kentucky, master's thesis, 105 p.
- Pashin, J.C., and Ettensohn, F.R., 1987, An epeiric shelf-to-basin transition; Bedford-Berea sequence, northeastern Kentucky and south-central Ohio: *American Journal of Science*, v. 287, no. 9, p. 893–926.
- Pashin, J.C., and Ettensohn, F.R., 1992, Palaeoecology and sedimentology of the dysaerobic Bedford fauna (Late Devonian), Ohio and Kentucky (USA): *Palaeogeography, Palaeoclimatology, Palaeoecology*, v. 91, nos. 1-2, p. 21–34.
- Pashin, J.C., and Ettensohn, F.R., 1995, Reevaluation of the Bedford-Berea sequence in Ohio and adjacent states: Forced regression in a foreland basin: *Geological Society of America Special Paper 298*, 69 p.
- Potter, P.E., Maynard, J.B., Jackson, D., and DeReamer, J., 1983, Lithologic and environmental atlas of Berea Sandstone (Mississippian) in the Appalachian Basin: *Appalachian Geological Society Special Publication 1*, 157 p.
- Zielinski, R.E., and Nance, S.W., 1980, Physical and chemical characterization of Devonian gas shale: Contract report to U.S. Department of Energy, DE-AC04-76-DP00053, 148 p. [data and analyses from this well available from the KGS Oil and Gas Database, record no. 42373.]

Appendix 1

Chapters 7 and 8

Chesapeake XRD Data

- HattieNeal1XRDresultsTTformat.xlsm
- HattieNeal1_14-0201RE6TOC.xlsm
- MooreMilton1122_14-0202RE6TOC.xlsm
- MooreMilton1122XRDresultsTTformat.xlsm
- MooreRubenET_UX1087_14-0203RE6TOC.xlsm
- MooreRubenET_UX-1087XRDresultsTTformat.xlsm
- SimpsonMargaretD20505_14-0204RE6TOC.xlsm
- SimpsonMargaretD20505XRDresultsTTformat.xlsm

MICP Data

- HH91435MICPcombo.xlsx
- HH91435MICPsample1ET.xlsx
- HH91435MICPsample2ET.xlsx
- HH91435MICPsample3ET.xlsx
- HH91435MICPsample4ET.xlsx
- HH-91435MICPsample5ET.xlsx
- HH91435MICPsample6ET.xlsx

Porosity and Permeability Data

- BereaPorosityPermNewDataFromChesapeake.xlsx
- BereaPorosityPermReadMe.docx
- BereaPorosityPermData.xlsx

Geochemistry

Bitumen Extracts Data

- GCextractSummaryRounds1-2.xlsx
- GeoMarkBiomarkerIDsAndCodeDescriptions.xls
- GeomarkRFDbaseGlossaryOfTerms.pdf

Round 1 Measurements

- AromaticsRound1.xlsx
- BulkRound1.xlsx
- ExtractsQuantitativeBiomarkersRound1.xlsx
- GasChromatographyRound1.xlsx
- GCextractSummaryRound1.xlsx
- InterpretationRound1.xlsx
- LocationRound1.xlsx
- Project2057BulkResultsIRMSround1.xlsx
- QuantitativeBiomarkersRound1.xlsx
- RKGS141201-150502-150504QuantExtExtGCEOMround1.XLS
- RKGS151002-150505QuantExtExtGCEOMround1.XLS
- Round1ExtractGeochemicalSummarySheets.pdf

HP Data

Aromatics

- XKY0003SAdata.ms
- XKY0004SAdata.ms
- XKY0005SAdata.ms

- XKY0006SAdata.ms
- XKY0007SAdata.ms
- XKY0008SAdata.ms
- XKY0009SAdata.ms
- XKY0010SAdata.ms
- XKY0011SAdata.ms

Aromatics Clips

- XKY0003A133.CLP
- XKY0003A178-192.CLP
- XKY0003A184-198.CLP
- XKY0003A231.CLP
- XKY0003A245.CLP
- XKY0004A133.CLP
- XKY0004A178-192.CLP
- XKY0004A184-198.CLP
- XKY0004A231.CLP
- XKY0004A245.CLP
- XKY0005A133.CLP
- XKY0005A178-192.CLP
- XKY0005A184_198.CLP
- XKY0005A231.CLP
- XKY0005A245.CLP
- XKY0006A133.CLP
- XKY0006A178-192.CLP
- XKY0006A184-198.CLP
- XKY0006A231.CLP
- XKY0006A245.CLP
- XKY0007A133.CLP
- XKY0007A178-192.CLP
- XKY0007A184-198.CLP
- XKY0007A231.CLP
- XKY0007A245.CLP
- XKY0008A133.CLP
- XKY0008A178-192.CLP
- XKY0008A184-198.CLP
- XKY0008A231.CLP
- XKY0008A245.CLP
- XKY0009A133.CLP
- XKY0009A178-192.CLP
- XKY0009A184-198.CLP
- XKY0009A231.CLP
- XKY0009A245.CLP
- XKY0010A133.CLP
- XKY0010A178-192.CLP
- XKY0010A184-198.CLP
- XKY0010A231.CLP
- XKY0010A245.CLP
- XKY0011A133.CLP
- XKY0011A178-192.CLP

- XKY0011A184-198.CLP
- XKY0011A231.CLP
- XKY0011A245.CLP

Extracts Biomarker Quantitation Summaries

- KY0003QbioSummary.xlsx
- KY0004QbioSummary.xlsx
- KY0005QbioSummary.xlsx
- KY0006QbioSummary.xlsx
- KY0007QbioSummary.xlsx
- KY0008QbioSummary.xlsx
- KY0009QbioSummary.xlsx
- KY0010QbioSummary.xlsx
- KY0011QbioSummary.xlsx

Gas Chromatograms

- C15ExtractGCAristech4_1432ftRKGS-141201-011.xls
- C15ExtractGCAristech4_86380ftRKGS-141201-004.xls
- C15ExtractGCColumbia20336_2449ftRKGS-150505-001.xls
- C15ExtractGCColumbia20336_3400ftRKGS-150505-008.xls
- C15ExtractGCGRoberts1420_1558-1563ftRKGS-151002-002.xls
- C15ExtractGCGRoberts1420_1740-1763ftRKGS-151002-004.xls
- C15ExtractGCGRoberts1420_2339-2358ftRKGS-151002-005.xls
- C15ExtractGCInterstate10_2460-2470RKGS-150502-001.xls
- C15ExtractGCMoore1122_1225ftRKGS-150504-002.xls

Raw Gas Chromatogram Files

- RKGS141201RawGCFiles.zip
- RKGS150502RawGCFile.zip
- RKGS150504RawGCFiles.zip
- RKGS150505RawGCFiles.zip
- RKGS151002RawGCFiles.zip

Saturates

- XKY0003SDdata.ms
- XKY0004SDdata.ms
- XKY0005SDdata.ms
- XKY0006SDdata.ms
- XKY0007SDdata.ms
- XKY0008SDdata.ms
- XKY0009SDdata.ms
- XKY0010SDdata.ms
- XKY0011SDdata.ms

Sat Clips

- XKY0003S.CLP
- XKY0003T.CLP
- XKY0004S.CLP
- XKY0004T.CLP
- XKY0005S.CLP
- XKY0005T.CLP
- XKY0006S.CLP
- XKY0006T.CLP
- XKY0007S.CLP

- XKY0007T.CLP
- XKY0008S.CLP
- XKY0008T.CLP
- XKY0009S.CLP
- XKY0009T.CLP
- XKY0010S.CLP
- XKY0010T.CLP
- XKY0011S.CLP
- XKY0011T.CLP

Round 2 Measurements

- AromaticsRound2.xlsx
- BulkRound2.xlsx
- GasChromatographyRound2.xlsx
- InterpretationRound2.xlsx
- LocationRound2.xlsx
- MassChromatogramsRound2.xlsx
- QuantitativeBiomarkersRound2.xlsx
- RKGS-160301-04QuantExt-ExtGCRound2.xls
- XKY0012-0022GeochemicalSummarySheetsRound2.pdf

HP Data

Aromatics

- XKY0012SADdata.MS
- XKY0013SADdata.MS
- XKY0014SADdata.MS
- XKY0015SADdata.MS
- XKY0016SADdata.MS
- XKY0017SADdata.MS
- XKY0018SADdata.MS
- XKY0019SADdata.MS
- XKY0020SADdata.MS
- XKY0021SADdata.MS
- XKY0022SADdata.MS

Aromatics Clips

- XKY0012A133.CLP
- XKY0012A178-192.CLP
- XKY0012A184-198.CLP
- XKY0012A231.CLP
- XKY0012A245.CLP
- XKY0013A133.CLP
- XKY0013A178-192.CLP
- XKY0013A184-198.CLP
- XKY0013A231.CLP
- XKY0013A245.CLP
- XKY0014A133.CLP
- XKY0014A178-192.CLP
- XKY0014A184-198.CLP

- XKY0014A231.CLP
- XKY0014A245.CLP
- XKY0015A133.CLP
- XKY0015A178-192.CLP
- XKY0015A184-198.CLP
- XKY0015A231.CLP
- XKY0015A245.CLP
- XKY0016A133.CLP
- XKY0016A178-192.CLP
- XKY0016A184-198.CLP
- XKY0016A231.CLP
- XKY0016A245.CLP
- XKY0017A133.CLP
- XKY0017A178-192.CLP
- XKY0017A184-198.CLP
- XKY0017A231.CLP
- XKY0017A245.CLP
- XKY0018A133.CLP
- XKY0018A178-192.CLP
- XKY0018A184-198.CLP
- XKY0018A231.CLP
- XKY0018A245.CLP
- XKY0019A133.CLP
- XKY0019A178-192.CLP
- XKY0019A184-198.CLP
- XKY0019A231.CLP
- XKY0019A245.CLP
- XKY0020A133.CLP
- XKY0020A178-192.CLP
- XKY0020A184-198.CLP
- XKY0020A231.CLP
- XKY0020A245.CLP
- XKY0021A133.CLP
- XKY0021A178-192.CLP
- XKY0021A184-198.CLP
- XKY0021A231.CLP
- XKY0021A245.CLP
- XKY0022A133.CLP
- XKY0022A178-192.CLP
- XKY0022A184-198.CLP
- XKY0022A231.CLP
- XKY0022A245.CLP

Gas Chromatograms

- C15ExtractGCAristech1025ftRKGS-160301-002XKY0013.xls
- C15ExtractGCAristech1035ftRKGS-160301-003XKY0014.xls
- C15ExtractGCAristech678ftRKGS-160301-001XKY0012.xls
- C15ExtractGCAshland3RS1017ftRKGS-160302-001XKY0015.xls
- C15ExtractGCAshland3RS1181ftRKGS-160302-002XKY0016.xls
- C15ExtractGCAshland3RS1183ftRKGS-160302-003XKY0017.xls

- C15ExtractGCashland3RS1402ftRKGS-160302-004XKY0018.xls
- C15ExtractGCColumbia20336_2704ftRKGS-160303-001XKY0019.xls
- C15ExtractGCEQT504353_3810ftRKGS-160304-001XKY0020.xls
- C15ExtractGCEQT504353_4560ftRKGS-160304-002XKY0021.xls
- C15ExtractGCEQT504353_4566ftRKGS-160304-003XKY0022.xls

Extracts Biomarker Quantitation Summary

- XKY0012QbioSummary.xlsx
- XKY0013QbioSummary.xlsx
- XKY0014QbioSummary.xlsx
- XKY0015QbioSummary.xlsx
- XKY0016QbioSummary.xlsx
- XKY0017QbioSummary.xlsx
- XKY0018QbioSummary.xlsx
- XKY0019QbioSummary.xlsx
- XKY0020QbioSummary.xlsx
- XKY0021QbioSummary.xlsx
- XKY0022QbioSummary.xlsx

Saturates

- XKY0012SDdata.ms
- XKY0013SDdata.ms
- XKY0014SDdata.ms
- XKY0015SDdata.ms
- XKY0016SDdata.ms
- XKY0017SDdata.ms
- XKY0018SDdata.ms
- XKY0019SDdata.ms
- XKY0020SDdata.ms
- XKY0021SDdata.ms
- XKY0022SDdata.ms

Saturates Clips

- XKY0012S.CLP
- XKY0012T.CLP
- XKY0013S.CLP
- XKY0013T.CLP
- XKY0014S.CLP
- XKY0014T.CLP
- XKY0015S.CLP
- XKY0015T.CLP
- XKY0016S.CLP
- XKY0016T.CLP
- XKY0017S.CLP
- XKY0017T.CLP
- XKY0018S.CLP
- XKY0018T.CLP
- XKY0019S.CLP
- XKY0019T.CLP
- XKY0020S.CLP
- XKY0020T.CLP
- XKY0021S.CLP

- XKY0021T.CLP
- XKY0022S.CLP
- XKY0022T.CLP

Gases

- Job31348AllIsotopes.pdf
- Job31348AllIsotopes.xls

Oils**Oil Data**

- Aromatics.xlsx
- Bulk.xlsx
- Interpretation.xlsx
- KY0049-0054BulkResults.xlsx
- KY0049-0054GeochemicalSummarySheets.pdf
- Location.xlsx
- OilSamplesQuantitativeBiomarkers.xlsx

HP Data**Aromatics**

- KY0049SADdata.MS
- KY0050SADdata.MS
- KY0051SADdata.MS
- KY0052SADdata.MS
- KY0053SADdata.MS
- KY0054SADdata.MS

Aromatics Clips

- KY0049A133.CLP
- KY0049A178-192.CLP
- KY0049A184-198.CLP
- KY0049A231.CLP
- KY0049A245.CLP
- KY0050A133.CLP
- KY0050A178-192.CLP
- KY0050A184-198.CLP
- KY0050A231.CLP
- KY0050A245.CLP
- KY0051A133.CLP
- KY0051A178-192.CLP
- KY0051A184-198.CLP
- KY0051A245.CLP
- KY0052A133.CLP
- KY0052A178-192.CLP
- KY0052A184-198.CLP
- KY0052A231.CLP
- KY0052A245.CLP
- KY0053A133.CLP
- KY0053A178-192.CLP
- KY0053A184-198.CLP

- KY0053A231.CLP
- KY0053A245.CLP
- KY0054A133.CLP
- KY0054A178-192.CLP
- KY0054A184-198.CLP
- KY0054A231.CLP
- KY0054A245.CLP

Gas Chromatograms

- KY0049GC.xls
- KY0050GC.xls
- KY0051GC.xls
- KY0052GC.xls
- KY0053GC.xls
- KY0054GC.xls
- KY0049Dreport01.xls
- KY0050Dreport01.xls
- KY0051Dreport01.xls
- KY0052Dreport01.xls
- KY0053Dreport01.xls
- KY0054Dreport01.xls

Biomarker Quantitation

- KY0049QbioSummary.xlsx
- KY0050QbioSummary.xlsx
- KY0051QbioSummary.xlsx
- KY0052QbioSummary.xlsx
- KY0053QbioSummary.xlsx
- KY0054QbioSummary.xlsx

Saturates

- KY0049SDdata.ms
- KY0050SDdata.ms
- KY0051SDdata.ms
- KY0052SDdata.ms
- KY0053SDdata.ms
- KY0054SDdata.ms

Saturates Clips

- KY0049S.CLP
- KY0049T.CLP

- KY0050S.CLP
- KY0050T.CLP
- KY0051S.CLP
- KY0051T.CLP
- KY0052S.CLP
- KY0052T.CLP
- KY0053S.CLP
- KY0053T.CLP
- KY0054S.CLP
- KY0054T.CLP

Programmed Pyrolysis

- RockEvalAnalysis01-07-2016.xlsx

Pyrograms Results

- Aristech4RE2pyrograms.pdf
- Aristech4SourceRockAnalyses.xls
- Columbia20336RE2pyrograms.pdf
- EQT504353pyrograms.pdf
- EQT504353SourceRockAnalyses.xls
- GRoberts1420SourceRockAnalyses.xls
- GRoberts1420RE2pyrograms.pdf
- RKGS-150501Hanson1SourceRockAnalyses.xls
- RKGS-150501pyrograms.pdf
- RKGS-150502Interstate10SourceRockAnalyses.xls
- RKGS-150502pyrograms.pdf
- RKGS-150503Moore1087SourceRockAnalyses.xls
- RKGS-150503pyrograms.pdf
- RKGS-150504Moore1122SourceRockAnalyses.xls
- RKGS-150504pyrograms.pdf
- RKGS-150505Columbia20336SourceRockAnalyses.xls
- RKGS-150505pyrograms.pdf
- RKGS-150701Skaggs-Kelley3RSsourceRockAnalyses.xls
- Skaggs-Kelley3RSpyrograms.pdf